

66TH HIGHWAY GEOLOGY SYMPOSIUM SEPTEMBER 14-17, 2015

Sturbridge Host Hotel and Conference Center
STURBRIDGE, MASSACHUSETTS



2015 Proceedings

Hosted By:

*Massachusetts Department of Transportation
and
University of Massachusetts Amherst*

Dedication

*The Proceedings of the 66th Highway Geology Symposium
are dedicated to*

Michael Hager

Mike was born and raised in Delaware and grew up in the town of Hockessin. He earned a Bachelor's Degree in Geology from the University of Wyoming in 1973 and then worked for Texaco Oil Company in Colorado and Utah. Mike returned to Delaware where he attained his Master's Degree in Geology at the University of Delaware in 1976. In 1978, he returned to Wyoming to take a job with Cooper Clark, a geotechnical firm where he performed materials testing and site inspection. One of the more interesting projects he worked on at Cooper Clark was the construction for two of the first large experimental wind energy generators in the country.

In 1981, he began his career with the Wyoming Highway Department Geology Program (now WYDOT). He quickly moved upward at WYDOT, and became the Chief Geologist in 1993. Wyoming has a varied geology with geotechnical issues, including expansive and collapsing soils, rockfall problems, and an abundance of active landslides. During his time as the Chief Geologist, roadway reconstruction in high mountainous terrain, like the Snake River Canyon and a road adjacent to Yellowstone Park, provided many geotechnical challenges. Mike exemplified a transportation geologist who was able to take his knowledge of local geology, construction, and industry innovations and apply it to highway design and construction.

Many of the innovative ideas he applied on these Wyoming Projects were acquired at Highway Geology Symposium (HGS) Conferences. Some of these techniques included dynamic compaction, tieback

anchors, horizontal drains, and geosynthetics. For example, in the 1980s, Mike took the lead using impermeable membrane to mitigate expansive soils, which had previously only been done in a few other states.

Mike is a registered Professional Geologist in Wyoming and was a member of several Transportation Research Board Committees. He was also actively involved with the annual Northwest Geotechnical Workshop Conference where he gave presentations and received several awards. Mike attended his first HGS in Vail, Colorado in 1982 and was a member of the HGS Steering Committee from 1995 to 2008. He served as the Steering Committee Secretary in 1999, Vice Chairman from 2001 to 2003, and Chairman from 2004 to 2006. He was Chairman of the 47th HGS in Cody, Wyoming from September 6 to 9, 1996, and received the prestigious HGS Medallion Award in 2005. Mike was influential in providing educational and networking opportunities to WYDOT Geologists by supporting and promoting their attendance at the HGS Conference.

Mike's leadership extended well beyond Wyoming's borders, serving as a mentor to geologists in transportation departments from other states. He acted as a sounding board for many, sharing his knowledge and cultivating a strong community of professionals along the way.

Mike retired from WYDOT in 2008 and lives in Cheyenne, Wyoming with his wife, Cindy. They have four boys and six grandchildren.



Mike and Cindy Hager

Contents

Dedication	iii
66th HGS Local Organizing Committee	5
Grateful Acknowledgments.	5
At-A-Glance Schedule of Events	6
Transportation Research Board Midyear Session 2015.	11
Sturbridge Host Hotel Floorplan	12
Booth Locations in Exhibit Hall and Commons Foyer	12
Highway Geology Symposium: History, Organization, and Function.	13
HGS Medallion Award Winners	17
Young Author Award Winners	17
Emeritus Members of the Steering Committee	17
HGS National Steering Committee	18
HGS Symposium Contact List	19
Banquet Keynote Address	20
Symposium Sponsors and Exhibitors	21
Paper and Presentation Schedule	Abstracts-1
Abstracts and Notes	Abstracts-4

66TH HIGHWAY GEOLOGY SYMPOSIUM

SEPTEMBER 14-17, 2015

Sturbridge Host Hotel and Conference Center
STURBRIDGE, MASSACHUSETTS



66th HGS Local Organizing Committee

Pete Ingraham (Chair)
Steve Sweeney
Ginny Sweeney
Mike Vierling
Krystle Pelham
Steve Mabee
Tom Eliassen
Linda Hutchins
Don Wise
Chris Condit

Pete Connors
Mike Yako
Kristi White
Jessica Anderson
Shawnie Gruber
Kathryn Haines
Lisa Krugh
Jay Smerekanicz
Jeff Lloyd

Grateful Acknowledgments

HGS Steering Committee
HGS Local Organizing Committee
Isodoro DeJesus Perez
MassDOT District 1 Crew (traffic control)
Massachusetts State Police
Barton Cove
Bub's BBQ
Warfield House

Berkshire Brewery
Specialty Minerals
Brian Rock and the folks at
Old Sturbridge Village
Lizak Bus Service
The Beering Committee
Our Sponsors and Exhibitors
Golder Associates Inc.

On the cover: Fall reflection of one of two covered bridges at Old Sturbridge Village, an 1830s New England Living History Museum. Photograph courtesy Old Sturbridge Village Fall Foliage photo gallery, www.osv.org.

At-A-Glance Schedule of Events

Monday, September 14 – Thursday, September 17, 2015

Monday, September 14th

8:00 AM – 12:00 PM

GeoHazard Professionals Committee Meeting

Location: Executive Room

Non-members welcome

11:00 AM – 5:00 PM

Highway Geology Symposium Registration OPEN

12:00 PM – 5:00 PM

Transportation Research Board Midyear Session 2015

“Geotechnical Risk: Assessment and Performance Management”

Location: Brookfield/Abbingdon

5:00 PM – 8:30 PM

Highway Geology Symposium Exhibitor Area OPEN

5:15 PM – 6:30 PM

HGS Steering Committee Meeting

Location: American Grille

6:30 PM – 8:30 PM

Ice Breaker Social—Sponsored by HITECH Rockfall

Location: Exhibitor Area and Commons Foyer

Tuesday, September 15th

6:30 AM – 9:00 AM

Breakfast—Sponsored by Geokon

Location: Next to Greenhouse

6:30 AM – 5:00 PM

Highway Geology Symposium Registration OPEN

8:00 AM – 5:00 PM

Highway Geology Symposium Exhibitor Area OPEN

7:30 AM – 8:30 AM

Welcome and Opening Remarks

Pete Ingraham, HGS Organizing Committee Chair

Isidoro DeJesus Perez, MassDOT Highway Deputy Administrator, Project Controls & Performance Oversight

Steve Mabee, PhD, PG, UMass/Massachusetts State Geologist

Location: Brookfield/Abbingdon

Highway Geology Symposium Guest Field Trip to Old Sturbridge Village

9:00 AM – 3:00 PM

Transportation sponsored by Geokon

Pick-up Location: Commons Foyer (Side Entrance)

Tuesday, September 15th cont.

Technical Sessions I – Young Authors

Location: Brookfield/Abbingdon

Chris Ruppen, Moderator

8:30 AM – 8:55 AM

High Quality H₂O: Utilizing Horizontal Drains for Landslide Stabilization

Author(s): Cory B. Rinehart

8:55 AM – 9:20 AM

A New Simplified Methodology to Design Flexible Debris Flow Barrier

Author(s): Marco Cerro, Giorgio Giacchetti, Ghislain Brunet, Alessio Savioli, and Alberto Grimod

9:20 AM – 9:45 AM

Estimation of Cambridge Argillite Strength Based on Drilling Parameters

Author(s): Evan Lonstein, Jean Benoit, Stanley Sadkowski, and Kevin Stetson

9:45 AM – 10:05 AM

Red Mountain Pass Rockfall – Multiphase Mitigation of a Unique Rockfall Source Area

Author(s): Nicole Oester (*presentation only*)

10:05 AM – 10:40 AM

Morning Coffee Break—Sponsored by Ameritech Slope Constructors

Location: Exhibit Area

Technical Sessions II

Location: Brookfield/Abbingdon

Tom Eliassen, Moderator

10:40 AM – 11:00 AM

Geotechnical Solutions for Widening of Interstate 95

Author(s): Sarah McInnes, Michael Yang, and Robert Crawford

11:00 AM – 11:20 AM

A Challenging Emergency Rockfall Project Along the North Cascades Highway, Washington

Author(s): Marc Fish and Michael Mulhern

11:20 AM – 11:40 AM

Evaluation of D-cracking Durability of Indiana Carbonate Aggregates for Use in Pavement Concrete

Author(s): Belayneh Desta, Terry West, Jan Olek, and Nancy Whiting

11:40 AM – 12 PM

Soil and Rock Slope Stabilization for Bridge and Highway Reconstruction, State Routes 9 and 125, Lisbon-Durham, Maine

Author(s): Andrew R. Blaisdell and Christopher L. Snow

12:00 PM – 1:00 PM

Lunch—Sponsored by BGC Engineering

Location: Through Commons, next to Greenhouse

Location: Seminar Theatre

John Szturo, Moderator

10:40 AM – 11:00 AM

Telegraph Hill Rock Slope Improvement Project: Construction Challenges and Value Engineering Proposals

Author(s): Martin Woodard

11:00 AM – 11:20 AM

Proactive Interferometry and Point Data Integration – Budge Slide Monitoring

Author(s): John S. Metzger, Enrico Boi, Cliff Preston, and Jason Rolfe

11:20 – 11:40 AM

Sources of Nitrate in Groundwater Near Roadway Rock Blasting Sites

Author(s): Krystle Pelham and David M. Langlais

11:40 AM – 12 PM

A Summary of Technical Safety Training for Slope Access Technicians

Author(s): Jon Tierney (*presentation only*)

Tuesday, September 15th cont.

Technical Sessions II

Location: Brookfield/Abbingdon

Krystle Pelham, Moderator

1:00 PM – 1:20 PM

Slope Stabilization and Scour Protection Using Small Diameter Reticulated Micropiles Along Minisceongo Creek

Author(s): Nathan Beard

1:20 PM – 1:40 PM

Remediation of Slope Instability in Presumpscot Marine Clay Using Steel H Piles, Mile Brook Bridge Over Outlet Stream, Winslow, Maine

Author(s): Erin A. Force and Wayne A. Chadbourne

1:40 PM – 2:00 PM

Stabilizing a Slope Using a High Strength Wicking Geotextile

Author(s): John C. Folts

2:00 PM – 2:20 PM

Stabilization of Paleo Stream Deposits Using High Tensile Steel Mesh

Author(s): Scott D. Neely

2:20 PM – 2:50 PM

Afternoon Break—Sponsored by Ameritech Slope Constructors

Location: Brookfield/Abbingdon

Tom Eliassen, Moderator

2:50 PM – 3:10 PM

Geotechnical Designs to Build on Liquefiable and Compressible Soil in Salem, Massachusetts

Author(s): Tulin Fuselier, Zia Zafir, Jennifer MacGregor, and Stefanie Bridges

3:10 PM – 3:30 PM

Old Problem Requires Innovative Investigation—Geotechnical Investigations of the Chippewa Power Canal Culvert Foundation

Author(s): Gabrielle Mellies, Mark Telesnicki, and Tony Sanguiliano

3:30 PM – 3:50 PM

Bridges in Appalachian-Type Karst: Geotechnical and Design Concerns

Author(s): Joseph A. Fischer, William Kochanov, and Joseph J. Fischer

3:50 PM – 4:10 PM

Louisville Bridges: Then and Now from a Geotechnical Perspective, Louisville, Kentucky

Author(s): Mark A. Litkenhus

Location: Seminar Theatre

Jim Coffin, Moderator

1:00 PM – 1:20 PM

US-12, Greer to Kamiah, Idaho, Rock Slope Assessment and Design

Author(s): William C.B. Gates and Brian Bannan

1:20 PM – 1:40 PM

Installation of Flexible Snow Net Structures for Avalanche Control

Author(s): Chris G. Ingram

1:40 PM – 2:00 PM

Icefall Hazards Along U.S. Transportation Corridors—Are Rockfall Catchment Ditches Sufficient?

Author(s): David J. Scarpato

2:00 PM – 2:20 PM

Rock Slope Stability in Karst Terrain

Author(s): Vanessa C. Bateman

Location: Seminar Theatre

Krystle Pelham, Moderator

2:50 PM – 3:10 PM

Rock Slope Monitoring Using Oblique Aerial Photogrammetry Along Interstate 70 in DeBeque Canyon, Colorado: A CDOT Geotechnical Asset Management Pilot Project

Author(s): Ty Ortiz, Dave Gauthier, Nicole Oester, and Robert Group

3:10 PM – 3:30 PM

Debris Flood Assessment and Mitigation Design: Trans-Canada Highway, Alberta

Author(s): Alex Strouth, Joe Gartner, Kris Holm, and Matthias Jakob

3:30 PM – 3:50 PM

Attenuators for Controlling Rockfalls: Do We Know How They Work? Can We Specify What They Should Do?

Author(s): Duncan Wyllie and Tim Shevlin

3:50 PM – 4:10 PM

Trout Brook Landslide Repairs Following Tropical Storm Irene

Author(s): Mike Yako, Peter Connors, and Jeanne Lefebvre (*presentation only*)

Tuesday, September 15th cont.

4:15 PM – 4:30 PM

Highway Geology Symposium Field Trip Briefing

Presenters: Steve Mabee and Pete Ingraham

Location: Brookfield/Abbingdon

5:30 PM

Optional Tuesday Dinner—Drink tickets and keg sponsored by BGC Engineering

Location: Hotel – Lakeside

Wednesday, September 16th

6:00 AM – 7:30 AM

Breakfast – To-Go Continental Breakfast—Sponsored by Ameritech Slope Constructors

Location: The Commons Foyer

Highway Geology Symposium Field Trip

7:00 AM

Load buses for Field Trip

Pick-up Location: Side Entrance Next to Commons Foyer

7:30 AM – 5:00 PM

Field Trip

Lunch sponsored by GeoBrugg, afternoon beverages sponsored by Golder Associates

NO GLASS ALLOWED INSIDE BUSES

5:30 PM – 6:30 PM

Highway Geology Symposium Social Hour—Sponsored by Access Limited Construction

Location: Grand Ballroom

Highway Geology Symposium Banquet Dinner

6:30 PM – 9:30 PM

Keynote Address by Clif Read, Quabbin Reservoir Historian

Location: Grand Ballroom

Thursday, September 17th

6:30 AM – 9:00 AM

Breakfast—Sponsored by Geokon

Location: Next to Greenhouse

8:00 AM – 11:00 AM

Highway Geology Symposium Exhibitor Area OPEN

Exhibitors need to break down after morning coffee break

Thursday, September 17th cont.

Technical Sessions III

Location: Brookfield/Abbingdon

Steve Sweeney, Moderator

8:00 AM – 8:20 AM

The Importance of Residual Shear Testing in Evaluation of Landslides in Glaciolacustrine Deposits

Author(s): Andrew J. Smithmyer, Frank Namatka, and Richard Bohr

8:20 AM – 8:40 AM

Investigation, Design, and Mitigation of a Landslide in Newport, Vermont

Author(s): Jay R. Smerekanicz, Jeffrey D. Lloyd, Mark S. Peterson, Peter C. Ingraham, and Christopher C. Benda

8:40 AM – 9:00 AM

Stream Restoration to Improve Slope Stability along Park Road at Gibsonville, Letchworth State Park, New York

Author(s): James J. Janora, Mark D. Kenward, and Paula L. Smith

9:00 AM – 9:20 AM

Natural Geologic Controls on Rockfall Hazard and Mitigation on the Niagara Escarpment, King's Highway 403 at Hamilton, ON, Canada

Author(s): Dave Gauthier, David F Wood, D. Jean Hutchinson, and Stephen Senior

9:20 AM – 9:40 AM

An Innovative Case Study on the Use of Test Section/Design-Build Construction on the Sea-to-Sky Highway Improvement Project, Vancouver, BC, Canada

Author(s): Grant A. Lachmuth

9:40 AM – 10:00 AM

Development of Grading Requirements for Drought Weather Conditions

Author(s): James B. Nevels, Jr.

10:00 AM – 10:40 AM

Morning Coffee Break—Sponsored by Ameritech Slope Constructors

Location: Intermingled throughout the Sponsors and Exhibitors

Location: Brookfield/Abbingdon

Pete Ingraham, Moderator

10:40 AM – 11:00 AM

Micropiles in Karst – The New Central Utility Plant at Shippensburg University

Author(s): Jason M. Gardner

11:00 AM – 11:20 AM

An Improved Calculation Method to Design Flexible Facing System for Soil Nailing

Author(s): Marco Cerro, Giorgio Giacchetti, Ghislain Brunet, Alessio Savioli, and Alberto Grimod

11:20 AM – 11:45 AM

The 66-Year Legacy and Why it Matters – Closing Remarks/Adjournment

Pete Ingraham

Transportation Research Board Midyear Session 2015

Engineering Geology and Exploration and Classification of Earth Materials Committees

“Geotechnical Risk: Assessment and Performance Management”

Monday, September 14, 2015 | Brookfield/Abbingdon

Agenda

12:00 PM – 12:05 PM

Opening Remarks – Ty Ortiz

12:05 PM – 12:30 PM

Oso Landslide and Risk – Joe Wartman

12:30 PM – 12:55 PM

SR-530 Landslide, Oso WA, from the Perspective of a DOT – Tom Badger

12:55 PM – 1:15 PM

Oso Landslide Q and A

1:15 PM – 1:30 PM

GAM Background and Status – Dave Stanley

1:30 PM – 1:40 PM

Break

1:40 PM – 2:00 PM

GAM State of Practice: Alaska DOT – Darren Beckstrand and Barry Benko

2:00 PM – 2:20 PM

GAM State of Practice: Colorado DOT – Mark Vessely and Ty Ortiz

2:20 PM – 2:50 PM

Connecting Performance and Risk Management – Chad Allan

2:50 PM – 3:20 PM

Determining Risk for Geotechnical Assets – Herbert H. Einstein

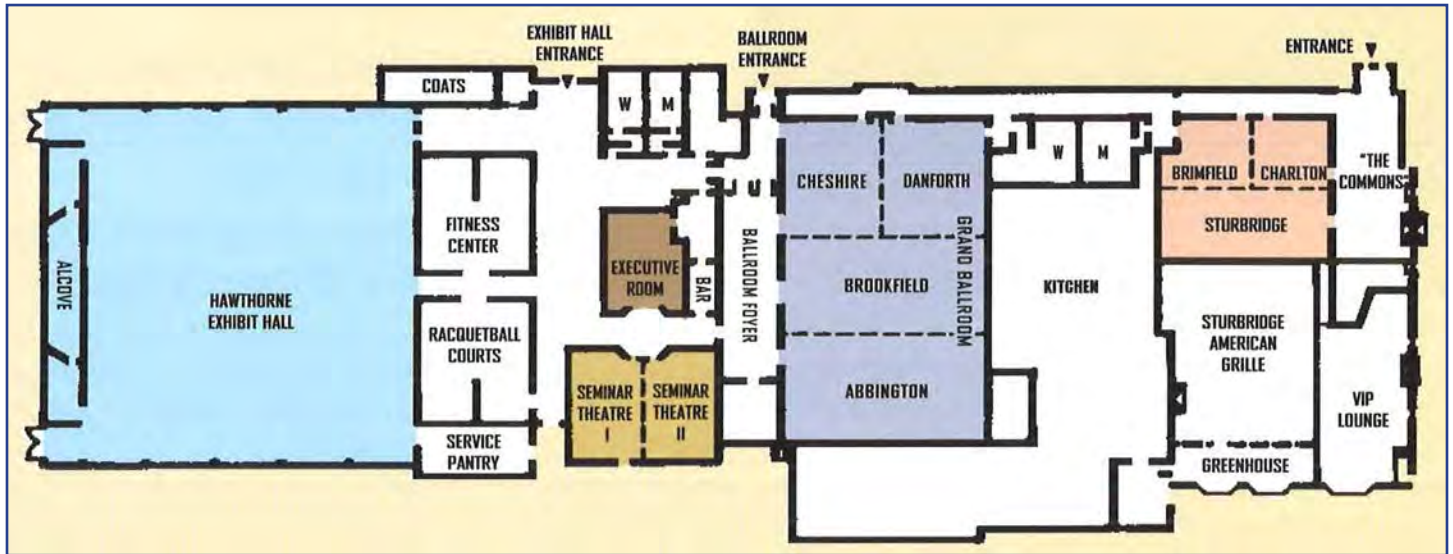
3:20 PM – 3:30 PM

Break

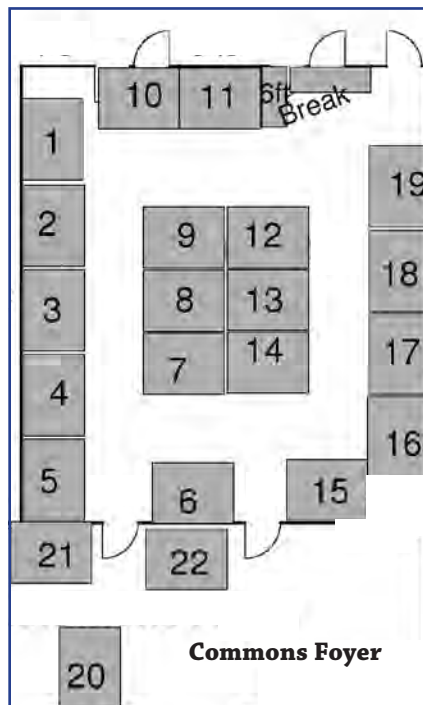
3:30 PM – 5:00 PM

Panel Q&A with Discussion

Sturbridge Host Hotel Floorplan



Booth Locations in Exhibit Hall and Commons Foyer



Booth No	Exhibitor
1	Access Limited Construction
2	Hager Richter Geoscience
3	GeoStabilization International
4	67th Highway Geology Symposium
5	Atlas Pipe Piles
6	Association of Geohazard Professionals
7	Chama Valley Products
8	Berkel
9	Tencate
10	Maccaferri
11	Ameritech
12	Bentley
13	Simco
14	Geokon
15	BGC
16	Trumer
17	Scarptec
18	High-Tec Rockfall Construction
19	GeoBrugg
20	Golder Associates Inc
21	Hager Geoscience
22	USGS/UMass Geosciences

Highway Geology Symposium: History, Organization, and Function

Inaugural Meeting

Established to foster a better understanding and closer cooperation between geologists and civil engineers in the highway industry, the Highway Geology Symposium (HGS) was organized and held its first meeting on March 14, 1950, in Richmond, Virginia. Attending the inaugural meeting were representatives from state highway departments (as referred to at that time) from Georgia, South Carolina, North Carolina, Virginia, Kentucky, West Virginia, Maryland, and Pennsylvania. In addition, a number of federal agencies and universities were represented. A total of nine technical papers were presented.

W.T. Parrott, an engineering geologist with the Virginia Department of Highways, chaired the first meeting. It was Mr. Parrott who originated the Highway Geology Symposium.

It was at the 1956 meeting that future HGS leader, A.C. Dodson, began his active role in participating in the Symposium. Mr. Dodson was the Chief Geologist for the North Carolina State Highway and Public Works Commission, which sponsored the 7th HGS meeting.

East and West

Since the initial meeting, 64 consecutive annual meetings have been held in 33 different states. Between 1950 and 1962, the meetings were east of the Mississippi River, with Virginia, West Virginia, Ohio, Maryland, North Carolina, Pennsylvania, Georgia, Florida, and Tennessee serving as host state. In 1962, the symposium moved west for the first time to Phoenix, Arizona, where the 13th annual HGS meeting was held. Since then, it has alternated, for the most part, back and forth from the east to the west.

The Annual Symposium has moved to different locations as listed on the next page.

Organization

Unlike most groups and organizations that meet on a regular basis, the Highway Geology Symposium has no central headquarters, no annual dues, and no formal membership requirements. The governing body of the Symposium is a steering committee composed of approximately 20 – 25 engineering geologists and geotechnical engineers from state and federal agencies, colleges and universities, as well as private service companies and consulting firms throughout the country. Steering committee members are elected for three-year terms, with their elections and re-elections being determined principally by their interests and participation in and contribution to the Symposium. The officers include a chairman, vice chairman, secretary, and treasurer, all of whom are elected for a two-year term. Officers, except for the treasurer, may only succeed themselves for one additional term.

A number of three-member standing committees conduct the affairs of the organization. The lack of rigid requirements, routing, and relatively relaxed overall functioning of the organization is what attracts many participants.

Meeting sites are chosen two to four years in advance and are selected by the Steering Committee following presentations made by representatives of potential host states. These presentations are usually made at the steering committee meeting, which is held during the Annual Symposium.

Upon selection, the state representative becomes the state chairman and a member pro-tem of the Steering Committee.

List of Highway Geology Symposium Meetings

No.	Year	HGS Location	No.	Year	HGS Location
1st	1950	Richmond, VA	2nd	1951	Richmond, VA
3rd	1952	Lexington, VA	4th	1953	Charleston, WV
5th	1954	Columbus, OH	6th	1955	Baltimore, MD
7th	1956	Raleigh, NC	8th	1957	State College, PA
9th	1958	Charlottesville, VA	10th	1959	Atlanta, GA
11th	1960	Tallahassee, FL	12th	1961	Knoxville, TN
13th	1962	Phoenix, AZ	14th	1963	College Station, TX
15th	1964	Rolla, MO	16th	1965	Lexington, KY
17th	1966	Ames, IA	18th	1967	Lafayette, IN
19th	1968	Morgantown, WV	20th	1969	Urbana, IL
21st	1970	Lawrence, KS	22nd	1971	Norman, OK
23rd	1972	Old Point Comfort, VA	24th	1973	Sheridan, WY
25th	1974	Raleigh, NC	26th	1975	Coeur d'Alene, ID
27th	1976	Orlando, FL	28th	1977	Rapid City, SD
29th	1978	Annapolis, MD	30th	1979	Portland, OR
31st	1980	Austin, TX	32nd	1981	Gatlinburg, TN
33rd	1982	Vail, CO	34th	1983	Stone Mountain, GA
35th	1984	San Jose, CA	36th	1985	Clarksville, TN
37th	1986	Helena, MT	38th	1987	Pittsburgh, PA
39th	1988	Park City, UT	40th	1989	Birmingham, AL
41st	1990	Albuquerque, NM	41st	1991	Albany, NY
43rd	1992	Fayetteville, AR	44rd	1993	Tampa, FL
45th	1994	Portland, OR	46th	1995	Charleston, WV
47th	1996	Cody, WY	48th	1997	Knoxville, TN
49th	1998	Prescott, AZ	50th	1999	Roanoke, VA
51st	2000	Seattle, WA	52nd	2001	Cumberland, MD
53rd	2002	San Luis Obispo, CA	54th	2003	Burlington, VT
55th	2004	Kansas City, MO	56th	2005	Wilmington, NC
57th	2006	Breckinridge, CO	58th	2007	Pocono Manor, PA
59th	2008	Santa Fe, NM	60th	2009	Buffalo, NY
61st	2010	Oklahoma City, OK	62nd	2011	Lexington, KY
63rd	2012	Redding, CA	64th	2013	North Conway, NH
65th	2014	Laramie, WY	66th	2015	Sturbridge, MA
67th	2016	Colorado	68th	2017	West Virginia (tent.)

HGS History, Organization, and Function *cont.*

The symposia are generally scheduled for two and one-half days, with a day-and-a-half for technical papers plus a full day for the field trip. The Symposium usually begins on Wednesday morning. The field trip is usually Thursday, followed by the annual banquet that evening. The final technical session generally ends by noon on Friday. In recent years, this schedule has been modified to better accommodate climate conditions and tourism benefits.

The Field Trip

The field trip is the focus of the meeting. In most cases, the trips cover approximately 150 to 200 miles, provide for six to eight scheduled stops, and require about eight hours. Occasionally, cultural stops are scheduled around geological and geotechnical points of interests.

To cite a few examples: in Wyoming (1973), the group viewed landslides in the Big Horn Mountains; Florida's trip (1976) included a tour of Cape Canaveral and the NASA space installation; the Idaho and South Dakota trips dealt principally with mining activities; North Carolina provided stops at a quarry site, a dam construction site, and a nuclear generation site; in Maryland, the group visited the Chesapeake Bay hydraulic model and the Goddard Space Center. The Oregon trip included visits to the Columbia River Gorge and Mount Hood; the Central mine region was visited in Texas; and the Tennessee meeting in 1981 provided stops at several repaired landslide in Appalachia regions of East Tennessee.

In Utah (1988), the field trip visited sites in Provo Canyon and stopped at the famous Thistle Landslide, while in New Mexico, in 1990, the emphasis was on rockfall treatments in the Rio Grande River canyon and included a stop at the Brugg Wire Rope headquarters in Santa Fe.

Mount St. Helens was visited by the field trip in 1994 when the meeting was in Portland, Oregon, while in 1995 the West Virginia meeting took us to the New River Gorge Bridge that has a deck elevation of 876 feet above the water.

In Cody, Wyoming, the 1996 field trip visited the Chief Joseph Scenic Highway and the Beartooth Uplift in northwest Wyoming. In 1997, the meeting in Tennessee visited the newly constructed future I-26 highway in the Blue Ridge of East Tennessee. The Arizona meeting in 1998 visited the Oak Creek Canyon near Sedona and a mining ghost town at Jerome, Arizona. The Virginia meeting in 1999 visited the "Smart Road" Project that was un-

der construction. This was a joint research project of the Virginia Department of Transportation and Virginia Tech University. The Seattle Washington meeting in 2000 visited the Mount Rainier area. A stop during the Maryland meeting in 2001 was the Sideling Hill road cut for I-68 which displayed a tightly folded syncline in the Allegheny Mountains.

The California field trip in 2002 provided a field demonstration of the effectiveness of rock netting against rock falls along the Pacific Coast Highway. The Kansas City meeting in 2004 visited the Hunt Subtropolis, which is said to be the "world's largest underground business complex," created through the mining of limestone using the room and pillar method. The Rocky Point Quarry provided an opportunity to search for fossils at the North Carolina meeting in 2005. The group also visited the US-17 Wilmington Bypass Bridge, which was under construction. Among the stops at the Pennsylvania meeting, were the Hickory Run Boulder Field, the No. 9 Mine and Wash Shanty Museum, and the Lehigh Tunnel.

The New Mexico field trip in 2008 included stops at a soil nailed wall along US-285/84 north of Santa Fe, and a road cut through the Bandelier Tuff on highway 502 near Los Alamos, where rockfall mesh was used to protect against rockfall. The New York field trip in 2009 visited the Niagara Falls Gorge and the Devil's Hole Trail. The Oklahoma field trip in 2010 toured through the complex geology of the Arbuckle Mountains in the southern part of the state along with stops at Tucker's Tower and Turner Falls.

In the bluegrass region of Kentucky, the 2011 HGS field trip included stops at Camp Nelson which is the site of the oldest exposed rocks in Kentucky near the Lexington and Kentucky River Fault Zones. Additional stops at the Darby Dan Farm and the Woodford Reserve Distillery illustrated how the local geology has played such a large part in the success of breeding prized Thoroughbred horses and made Kentucky the "Birthplace of Bourbon."

In Redding, California, the 2012 field trip included stops at the Whiskeytown Lake, which is one in a series of lakes that provide water and power to northern California. Additional stops included Rocky Point, a roadway construction site containing Naturally Occurring Asbestos (NOA), and Oregon Mountain where the geology and high rainfall amounts have caused Hwy 299 to experience local and global instabilities since first constructed in 1920.

HGS History, Organization, and Function *cont.*

The 2013 field trip of New Hampshire highlighted the topography and geologic remnants left by the Pleistocene glaciations that fully retreated approximately 12,000 years ago. The field trip included stops at various overlooks of glacially-carved valleys and ranges; the Old Man of The Mountain Memorial Plaza, which is a tribute to the famous cantilevered rock mass in the Franconia Notch that collapsed on May 3, 2003; lacustrine deposits and features of the Glacial Lake Ammonoosuc; views of the Presidential Range; bridges damaged during Tropical Storm Irene in August 2011; and the Willey Slide, located in the Crawford Notch where all members of the Willey family homestead were buried by a landslide in 1826.

2014 presented a breathtaking tour of the geology and history of southeast Wyoming, ascending from the high plains surrounding Laramie at 7,000 feet to the Medicine Bow Mountains along the Snowy Range Scenic Byway. Visible along the way were a Precambrian shear zone, and glacial deposits and features. From the glacially carved Mirror Lake and the Snowy Range Ski Area, the path wound east to the Laramie Mountains and the Vedauwoo Recreational Area, a popular rock climbing and hiking area, before returning to Laramie.

Technical Sessions and Speakers

At the technical sessions, case histories and state-of-the-art papers are most common; with highly theoretical papers the exception. The papers presented at the technical sessions are published in the annual proceedings. Some of the more recent papers may be obtained from the Treasurer of the Symposium. Banquet speakers are also a highlight and have been varied through the years.

Member Recognition

Medallion Award. A Medallion Award was initiated in 1970 to honor those persons who have made significant contributions to the Highway Geology Symposium over many years. The award is a 3.5 inch medallion mounted on a walnut shield and appropriately inscribed. The award is presented during the banquet at the annual Symposium. The selection was and is currently made from the members of the national steering committee of the HGS.

Emeritus Members. A number of past members of the national steering committee have been granted Emeritus status. These individuals, usually retired, resigned from the HGS Steering Committee, or are deceased, have made significant contributions to the Highway Geology Symposium. Emeritus status is granted by the Steering Committee. A total of 34 persons have been granted Emeritus status. Fourteen are now deceased.

Dedications. Several Proceedings volumes have been dedicated to past HGS Steering Committee members or others who have made outstanding contributions to HGS. The 36th HGS Proceedings were dedicated to David L. Royster (1931 - 1985, Tennessee) at the Clarksville, Indiana meeting in 1985. In 1991, the Proceedings of the 42nd HGS held in Albany, New York were dedicated to Burrell S. Whitlow (1929 - 1990, Virginia). In 2013, the Proceedings of the 64th HGS held in North Conway, New Hampshire were dedicated to Earl Wright and Bill Lovell. The 2014 Proceedings of the 65th HGS held in Laramie, Wyoming were dedicated to Nicholas Michiel Priznar, and the 2015 Proceedings of the 66th HGS are dedicated to Michael Hager.

HGS Medallion Award Winners

Hugh Chase*	1970	W.A. "Bill" Wisner	1991
Tom Parrott*	1970	David Mitchell	1993
Paul Price*	1970	Harry Moore	1996
K.B. Woods*	1971	Earl Wright*	1997
R.J. Edmondson*	1972	Russell Glass	1998
C.S. Mullin*	1974	Harry Ludowise*	2000
A.C. Dodson*	1975	Sam Thornton	2000
Burrell Whitlow*	1978	Bob Henthorne	2004
Bill Sherman	1980	Mike Hager	2005
Virgil Burgat*	1981	Joseph A. Fischer	2007
Henry Mathis	1982	Ken Ashton	2008
David Royster*	1982	A. David Martin	2008
Terry West	1983	Michael Vierling	2009
Dave Bingham	1984	Richard Cross	2009
Vernon Bump	1986	John F. Szturo	2010
C.W. "Bill" Lovell*	1989	Christopher Ruppen	2012
Joseph A. Gutierrez	1990	Jeff Dean	2012
Willard McCasland	1990		

** Deceased*

Young Author Award Winners

2014 Simon Boone, "Performance of Flexible Debris Flow Barriers in a Narrow Canyon"

Emeritus Members of the Steering Committee

R.F. Baker*	Richard Humphries	Willard L. Sitz
John Baldwin	Charles T. Janik	Mitchell Smith
David Bingham	John Lemish	Steve Sweeney
Virgil E. Burgat*	Bill Lovell*	Sam Thornton
Robert G. Charboneau*	George S. Meadors, Jr.*	Berke Thompson*
Hugh Chase*	Willard McCasland	Burrell Whitlow*
Richard Cross	David Mitchell	W.A. "Bill" Wisner
A.C. Dodson*	Harry Moore	Earl Wright*
Walter F. Fredericksen	W.T. Parrot*	Ed J. Zeigler
Brandy Gilmore*	Paul Price*	Harry Moore
Robert Goddard	David L. Royster*	
Joseph Gutierrez	Bill Sherman	<i>* Deceased</i>

HGS National Steering Committee

Jeff Dean (Medallion)

CHAIRMAN

Oklahoma Department of Transportation
200 NE 21st St.
Oklahoma City, OK 73105
Phone: (405) 522-0988
Fax: (405) 522-4519
Email: jdean@odot.org

Tom Eliassen

SECRETARY

State of Vermont, Agency of Transportation
Materials & Research Section
National Life Building, Drawer 33
Montpelier, VT 05633
Phone: (802) 828-6916
Fax: (802) 828-2792
Email: tom.eliassen@state.vt.us

Vanessa Bateman

VICE-CHAIRMAN

U.S. Army Corps of Engineers
Nashville District
Email: vanessa.c.bateman@usace.army.mil

Russell Glass (Medallion)

TREASURER

(Publications & Proceedings) NCDOT (Retired)
100 Wolf Cove
Asheville, NC 28804
Phone: (828) 252-2260
Email: frgeol@aol.com

Ken Ashton (Medallion)
(Membership)

West VA Geological Survey
P.O. Box 879
Morgantown, WV 26507-0879
Phone: (304) 594-233
Fax: (304) 594-2575
Email: ashton@geosrv.wvnet.edu

Robert Thommen

Rotec International, LLC
P.O. Box 31536
Sante Fe, NM 87594-1536
Phone: (505) 989-3353
Fax: (505) 984-8868
Email: thommen@swcp.com

Richard Lane

NHDOT, Bureau of Materials and Research (Retired)
5 Hazen Drive
Concord, NH 03301
Phone: (603) 271-3151
Email: lanetrisbr@hotmail.com

Jim Coffin

Wyoming Department of Transportation
Geology Program
5300 Bishop Blvd.
Cheyenne, WY 82009-3340
Phone: (307) 777-4205
Fax: (307) 777-3994
Email: jim.coffin@wyo.gov

Victoria Porto

PA DOT Bureau of Construction and Materials (Retired)
1080 Creek Road
Carlisle, PA 17015
Phone: (717) 805-5941
Email: vamporto@aol.com

John F. Szturo (Medallion)

HNTB Corporation
715 Kirk Drive
Kansas City, MO 64105
Phone: (816) 527-2275 (Direct Line)
Cell: (913) 530-2579
Fax: (816) 472-5013
Email: jszturo@hntb.com

Bob Henthorne (Medallion)

Materials and Research Center
2300 Van Buren
Topeka, KS 66611-1195
Phone: (785) 291-3860
Fax: (785) 296-2526
Email: roberth@ksdot.org

John D. Duffy

Caltrans
50 Higuera St.
San Luis Obispo, CA 93401
Phone: (805) 527-2275
Fax: (805) 549-3297
Email: John_D_Duffy@dot.ca.gov

John Pilipchuk

NCDOT Geotechnical Engineering Unit
1589 Mail Service Center
Raleigh, NC 27699-1589
Phone: (919) 707-6851
Fax: (919) 250-4237
Email: jpilipchuk@ncdot.gov

Henry Mathis (By-Laws)

Terracon
561 Marblerock Way
Lexington, KY 40503
Cell: (859) 361-8362
Fax: (859) 455-8630
Email: hmathis@iglou.com

Peter Ingraham

Golder Associates Inc.
670 North Commercial Street, Suite 103
Manchester, NH 03101-1146
Phone: (603) 668-0880
Fax: (603) 668-1199
Email: pingraham@golder.com

Christopher A. Ruppen (Medallion)
(Connections) (YAA)

Michael Baker Jr., Inc.
4301 Dutch Ridge Rd.
Beaver, PA 15009-9600
Phone: (724) 495-4079
Cell: (412) 848-2305
Fax: (724) 495-4017
Email: cruppen@mbakercorp.com

HGS National Steering Committee *cont.*

Deana Sneyd

Golder Associates Inc.
3730 Chamblee Tucker Road
Atlanta, GA 30341
Phone: (770) 496-1893
Fax: (770) 934-9476
Email: Deana_Sneyd@golder.com

Randy Jones

Tennessee Department of
Transportation Geotechnical
Engineering Section
6601 Centennial Blvd.
Nashville, TN 37243
Phone: (615) 350-4150
Fax: (615) 350-4128
Email: Randy.J.Jones@tn.gov

Michael P. Vierling (Medallion) (YAA)

Canal Design Bureau
New York State Thruway Authority
(Retired)
323 Boght Road
Watervliet, NY 12189-1106
Email: rocdoc1956@gmail.com

Erik Rorem

Geobrugg North America, LLC
22 Centro Algodones
Algodones, NM 87001
Phone: (505) 771-4080
Fax: (505) 771-4081
Email: erik.rorem@geobrugg.com

Stephen Senior

Ministry of Transportation, Ontario
1201 Wilson Ave.
Rm 220, Building C
Downsview, ON M3M 1J6 Canada
Phone: (416) 235-3734
Fax: (416) 235-4101
Email: stephen.senior@ontario.ca

Jim Stroud (Appt.)

Vice President
Subhorizon Geologic Resources LLC
(SGR) 4541 Araby Lane
East Bend, NC 27018
Phone: (336) 699-2217
Cell: (336) 416-3656
Email: gemsjims@hotmail.com

Steven Sweeney (Emeritus)

New York State Canal Corporation
(Retired)
105 Albert Rd
Delanson, NY 12053
Email: ssweeney2@nycap.rr.com

Bill Webster

CalTrans
5900 Folsom Blvd.
Sacramento, CA 95819
Phone: (916) 662-1183
Fax: (916) 227-1082
Email: bill_webster@dot.ca.gov

Terry West (Medallion)

Earth and Atmospheric Science Dept.
Purdue University
West Lafayette, IN 47907-1297
Phone: (765) 494-3296
Fax: (765) 496-1210
Email: trwest@purdue.edu

HGS Symposium Contact List

2009	New York	Mike Vierling		Rocdoc1959@gmail.com
2010	Oklahoma	Jeff Dean		jdean@odot.org
2011	Kentucky	Henry Mathis	859-455-8530	hmathis@iglou.com
2012	California	Bill Webster	916-277-1041	Bill_webster@dot.ca.gov
2013	New Hampshire	Krystle Pelham	603-271-1657	Kpelham@dot.state.nh.us
2014	Wyoming	Jim Coffin	307-777-4205	Jim.coffin@wyo.go
2015	Massachusetts	Peter Ingraham	603-688-0880	pingraham@golder.com
2016	Colorado	Ty Ortiz	303-921-2634	Ty.ortiz@state.co.us

Banquet Keynote Address

“Quabbin Reservoir—The Meeting of Many Waters”

Clif Read, Massachusetts Dept. of Conservation and Recreation

The Reservoir

In the 1920s, the Swift River Valley in central Massachusetts was chosen as the site for a massive reservoir, expanding drinking water supplies for the Boston metropolitan area to meet increasing demands. It is a familiar story for large population centers to seek water supplies of sufficient quality and quantity well beyond their municipal boundaries.

The 25,000-acre Quabbin Reservoir created the largest drinking water reservoir in the world at the time and displaced 2,500 residents from four valley towns. Additional watershed land was also purchased to protect the reservoir’s water quality, forming the greatest contiguous tract of protected open space in southern New England. As a result, the reservoir is part of an unfiltered water supply and is one of only a handful of larger metropolitan water systems that meet this stringent requirement.

The presentation will discuss the historical development of the water system, the process for selecting the Quabbin Reservoir site, the engineering and

construction of the Quabbin Project, and current DCR watershed management programs.

About the Speaker

Clif Read was born and raised in Philadelphia, PA, before heading to college at the University of New Hampshire where he received his BS in Environmental Conservation. His interest in environmental issues and education led him to Antioch – New England Graduate School where he earned a Masters in Science Teaching. Moving to Amherst, MA, he spent six years as Public Programs Coordinator at the Hitchcock Center for the Environment. Following a two year stint at the Kellogg Environmental Center in Connecticut, he was offered and he accepted the position of Supervisor of Interpretive Services at Quabbin Reservoir in central Massachusetts.

Twenty seven years later he still works for the MA Department of Conservation and Recreation at the job he loves, teaching people of all ages and interests about the Reservoir, watershed management programs, and the importance of drinking water quality.



Quabbin Reservoir

Symposium Sponsors and Exhibitors

The following companies have graciously contributed toward the sponsorship of the Symposium. The HGS relies on sponsor contributions for refreshment breaks, field trip lunches, and other activities. We gratefully appreciate the contributions made by these generous sponsors.

Platinum Sponsor



Swiss company Geobrugg is the global leader in the supply of safety nets and meshes made of high-tensile steel wire. Many years of experience and intensive collaboration with universities and research institutes have made Geobrugg a reliable partner when it comes to protection and safety solutions.

A global network with branches and partners in over 50 countries ensures fast, thorough, and cost-effective solutions for customer requirements. With production facilities on four continents and more than 300 employees worldwide, Geobrugg combines short delivery times with local support for customers. We are partners, consultants, developers, and project managers for our customers.

**Geobrugg North America, LLC
22 Centro Algodones
Algodones, NM 87001 USA**

**Phone: +1 505 771 4080
Mobile: +1 505 228 6425
geobrugg.com**



TECCO® SYSTEM³ – Your slope made stable

- **TECCO® SYSTEM³**
can be optimized depending on the subsoil
- **High-tensile steel meshes**
made of 2 mm, 3 mm and 4 mm diameter
- **Efficient optimization**
of anchor spacing with two different spike plates
- **Rhomboid-shape**
offers ideal force transmission plus slope adaptation
- **Easy dimensioning**
with the RUVOLUM® tool based on large-scale field tests
- **Environmentally friendly**
light-weight mesh with small CO² footprint,
virtually invisible after vegetation regrowth

Scan and watch our movie on:

www.geobrugg.com/youtube/TECCO-fullscale



Geobrugg AG
Geohazard Solutions
Aachstrasse 11 • CH-8590 Romanshorn • Switzerland
Phone: +41 71 466 81 55 • Fax: +41 71 466 81 50
www.geobrugg.com • info@geobrugg.com



Gold Sponsors



BGC Engineering Inc. (BGC) is an international consulting firm that provides professional services in applied earth sciences. Our practice was established in 1990, based on a specialized appreciation of the impacts of geology on engineered structures. This continues to be our foundation today, enabling us to address a broad spectrum of engineering and environmental issues related to development in challenging terrain. BGC's more than 300 professional engineers, geoscientists, technicians, and support staff operate from eight Canadian offices in British Columbia, Alberta, Ontario, New Brunswick, and Nova Scotia; one US office in Colorado; and one South American office in Chile.

BGC Engineering Inc.
Suite 500, 980 Howe Street
Vancouver, BC
Canada V6Z 0C8

Phone: (604) 684-5900
Fax: (604) 684-5909
info@bgcengineering.ca
bgcengineering.ca



Ameritech Slope Constructors, Inc. is a multi-state licensed, specialty geotechnical construction firm located in Asheville, North Carolina. Our services include: manual rock scaling, high angle drilling, installation of rockfall barriers and rockfall drapes, as well as slope stabilization systems using soil nails and high strength mesh. Ameritech also installs rock bolts, cable anchors, rock dowels, and rock drains. Whether it is a rock face with loose debris or an unstable soil slope, we can install the system that is necessary to provide protection for people and property. The company is proud to offer a team of highly skilled professionals with over 100 years of combined experience in the rockfall and slope stabilization industry.

Ameritech Slope Constructors, Inc.
P.O. Box 2702
Asheville, NC 28802

Phone: (828) 633-6352
Fax: (828) 633-6353
ameritech.pro

BGC

Transportation Services

Common Sense Solutions

BGC Engineering Inc.

Vancouver | Kamloops | Calgary | Edmonton | Toronto | Halifax | Fredericton | Denver | Santiago

bgcengineering.com



Geological Solutions for Slope Stability; Rockfalls, Landslides, and Debris Flows

Silver Sponsors

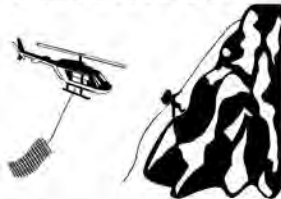


Located in San Luis Obispo, CA, Access Limited Construction is a General Contractor specializing in rockfall mitigation and slope stabilization systems, and is considered to be an industry leader in designing and installing rockfall protection, slope stabilization systems, and performing difficult access drilling throughout the United States.

Access Limited Construction Co.
225 Suburban Rd
San Luis Obispo, CA 93401

Phone: (805) 592-2230
Email: info@accesslimitedconstruction.com
accesslimitedconstruction.com

HI-TECH ROCKFALL CONSTRUCTION



"The Rockfall Specialist"

HI-TECH Rockfall Construction, Inc., founded in 1996, is located in Forest Grove, Oregon, USA. HI-TECH is a General Contractor who specializes in rockfall mitigation and is considered to be the industry leader in designing and installing rockfall protection systems throughout the United States. HI-TECH constructs a vast array of rockfall mitigation systems in a variety of locations such as highways, railroads, dams, quarries, mines, construction sites, commercial and residential properties.

HI-TECH Rockfall Construction, Inc.
2328 Hawthorne St
Forest Grove, OR 97116

Phone: (503) 357-6508
hitechrockfall.com

Bronze Sponsors



Geokon, Incorporated has emerged as The World Leader in Vibrating Wire Technology™ due to our quality, responsive customer service, and industry-leading designs. Our broad range of geotechnical instrumentation is manufactured at our factory in the USA, by a staff of trained, qualified and experienced machinists and assemblers.

Geokon, Inc.
48 Spencer Street
Lebanon, NH 03766

Phone: (603) 448-1562
Fax: 603) 448-3216
info@geokon.com
geokon.com



Golder Associates provides a wide range of independent consulting, design, and construction services in our specialist areas of earth, environment, and energy. Founded by geotechnical engineers in 1960, Golder is recognized as a leading provider of geotechnical services, with particular expertise in soils and rock engineering for transportation systems.

Golder Associates Inc.
670 North Commercial Street, Suite 103
Manchester, NH 03101

Phone: (603) 668-0880
solutions@golder.com
golder.com



Golder Won't Leave You Hanging...

Golder Associates can help solve the challenges of transportation and highway projects from design through construction. Whether designing or constructing a new road or responding to an emergency to keep traffic flowing, we understand the risks associated with geotechnical engineering, environmental permitting, and geologic hazards. With local offices around the US, we are here to support you.

Achieve your goals with Golder.
www.golder.com



Geotechnical and Structural Instrumentation



36 YEARS OF INNOVATION AND QUALITY



geokon.com




Specialized in Rockfall Mitigation, Slope Stabilization, & Difficult Access Drilling

(805) 592-2230
info@accesslimitedconstruction.com

Hi-Tech Rockfall Construction, Inc.



HI-TECH Rockfall is a General Contractor that specializes in Rockfall Mitigation and has been the leader in the field for over 16 years. We service all industries including mines, quarries, railroads and highways.

Products and Services:

- High Wall Stabilization
- Wire Mesh Drapery
- Rock Scaling
- High Wall Monitoring
- Rock Bolts
- Rock Dowels
- Shotcrete
- Rockfall Barriers
- Rope Access Work



Our highly trained and skilled employees have earned us the highest safety record in the industry.

All hold the following certifications:

- MSHA
- First-Aid
- Forklift
- Sprat/Irata
- Asbestos/Lead
- Railroad Access
- LOTO
- Blue Stake
- Confined Space
- Pit Driving




503-357-6508, P.O. Box 674, Forest Grove, OR 97116
www.hitechrockfall.com

"The Rockfall Specialist"

Exhibitors



Access Limited Construction Co.
225 Suburban Rd
San Luis Obispo, CA 93401
Phone: (805) 592-2230
accesslimitedconstruction.com



Ameritech Slope Constructors, Inc.
P.O. Box 2702
Asheville, NC 28802
Phone: (828) 633-6352
Fax: (828) 633-6353
ameritech.pro



Association of Geohazard Professionals
1934 Commerce Lane, Suite 4
Jupiter FL 33458
Phone: (561) 768-9487
GeohazardAssociation.org



Atlas Pipe Piles
1855 E 122nd St
Chicago, IL 60633
(312) 262-1962
atlaspipepiles.com



Bentley Systems
685 Stockton Drive
Exton, PA 19341
Phone: (800) 236-8539
bentley.com



Berkel and Co.
7300 Marks Lane
Austell, GA 30168
Phone: (770) 941-5100
berkelandcompany.com



BGC Engineering Inc.
Suite 500, 980 Howe Street
Vancouver, BC Canada V6Z 0C8
Phone: (604) 684-5900
Fax: (604) 684-5909
bgcengineering.ca



Chama Valley Productions
HC75 Box 1317
Rutheron, NM, 87551
Phone: (575) 588-0332
Fax: (575) 588-0336 www.
chamaproducts.com



Geobrugg North America, LLC
22 Centro Algodones
Algodones, NM 87001 USA
Phone: +1 505 771 4080
Mobile: +1 505 228 6425
geobrugg.com



Geokon, Inc.
48 Spencer Street
Lebanon, NH 03766
Phone: (603) 448-1562
Fax: 603) 448-3216
geokon.com



GeoStabilization International
P.O. Box 4709
Grand Junction, CO 81502
Phone: (970) 210-6170
Fax: (970) 245-7737
geostabilization.com



Golder Associates Inc.
670 North Commercial St.
Suite 103
Manchester, NH 03101
Phone: (603) 668-0880
golder.com

Exhibitors



HAGER GEOSCIENCE, INC.

Hager GeoScience, Inc.
596 Main Street
Woburn, MA 01801
Phone: (781) 935-8111
Fax: (781) 935-2717
Email: hgi@hagergeoscience.com

HAGER-RICHTER GEOSCIENCE, INC.

Hager-Richter Geoscience, Inc.
8 Industrial Way D-10
Salem, NH 03079
Phone: (603) 893-9944

**HI-TECH
ROCKFALL
CONSTRUCTION**



"The Rockfall Specialist"

HI-TECH Rockfall Construction, Inc.
2328 Hawthorne St
Forest Grove, OR 97116
Phone: (503) 357-6508
hitechrockfall.com

MACCAFERRI

Engineering a better solution

Maccaferri, Inc.
10303 Governo Lane Blvd
Williamsport, MD 21795
Phone: (301) 233-6910
maccaferri-usa.com



Scarptec, Inc.
P.O. Box 326
Monument Beach, MA 02553
Phone: (603) 361-0397
dave@scarptec.com
scarptec.com



SIMCO Drilling Equipment
802 Furmas Dr
Osceola, IA 50213
Phone: (800) 338-9925
simocodrill.com

TENCATE
Mirafi®

TenCate
PO Box 1955
Burlington, CT 06613
Phone: (860) 305-4441
tencate.com



TRUMER
Schutzbauten

Trumer Schutzbauten North America
14900 Interurban Ave S.
Suite 271 #19
Seattle, WA 98168
Phone: (855) 732-0325
trumer.cc



The Massachusetts Geological Survey
University of Massachusetts Department of Geosciences
611 North Pleasant Street
Amherst, MA 01003-9297
Phone: (413) 545-4814
mgs.geo.umass.edu

Paper and Presentation Schedule

Tuesday, September 15—Morning Sessions

8:30 AM – 8:55 AM

High Quality H₂O: Utilizing Horizontal Drains for Landslide Stabilization

Author(s): Cory B. Rinehart

8:55 AM – 9:20 AM

A New Simplified Methodology to Design Flexible Debris Flow Barrier

Author(s): Marco Cerro, Giorgio Giacchetti, Ghislain Brunet, Alessio Savioli, and Alberto Grimod

9:20 AM – 9:45 AM

Estimation of Cambridge Argillite Strength Based on Drilling Parameters

Author(s): Evan Lonstein, Jean Benoit, Stanley Sadkowski, and Kevin Stetson

9:45 AM – 10:05 AM

Red Mountain Pass Rockfall – Multiphase Mitigation of a Unique Rockfall Source Area

Author(s): Nicole Oester (*presentation only*)

Tuesday, September 15—Late Morning Sessions (split sessions)

10:40 AM – 11:00 AM

Geotechnical Solutions for Widening of Interstate 95

Author(s): Sarah McInnes, Michael Yang, and Robert Crawford

10:40 AM – 11:00 AM

Telegraph Hill Rock Slope Improvement Project: Construction Challenges and Value Engineering Proposals

Author(s): Martin Woodard

11:00 AM – 11:20 AM

A Challenging Emergency Rockfall Project Along the North Cascades Highway, Washington

Author(s): Marc Fish and Michael Mulhern

11:00 AM – 11:20 AM

Proactive Interferometry and Point Data Integration – Budge Slide Monitoring

Author(s): John S. Metzger, Enrico Boi, Cliff Preston, and Jason Rolfe

11:20 AM – 11:40 AM

Evaluation of D-cracking Durability of Indiana Carbonate Aggregates for Use in Pavement Concrete

Author(s): Belayneh Desta, Terry West, Jan Olek, and Nancy Whiting

11:20 – 11:40 AM

Sources of Nitrate in Groundwater Near Roadway Rock Blasting Sites

Author(s): Krystle Pelham and David M. Langlais

11:40 AM – 12 PM

Soil and Rock Slope Stabilization for Bridge and Highway Reconstruction, State Routes 9 and 125, Lisbon-Durham, Maine

Author(s): Andrew R. Blaisdell and Christopher L. Snow

11:40 AM – 12 PM

A Summary of Technical Safety Training for Slope Access Technicians

Author(s): Jon Tierney (*presentation only*)

Tuesday, September 15—Afternoon Sessions (split sessions)

1:00 PM – 1:20 PM

Slope Stabilization and Scour Protection Using Small Diameter Reticulated Micropiles Along Minisceongo Creek

Author(s): Nathan Beard

1:00 PM – 1:20 PM

US-12, Greer to Kamiah, Idaho, Rock Slope Assessment and Design

Author(s): William C.B. Gates and Brian Bannan

1:20 PM – 1:40 PM

Remediation of Slope Instability in Presumpscot Marine Clay Using Steel H Piles, Mile Brook Bridge Over Outlet Stream, Winslow, Maine

Author(s): Erin A. Force and Wayne A. Chadbourne

1:20 PM – 1:40 PM

Installation of Flexible Snow Net Structures for Avalanche Control

Author(s): Chris G. Ingram

1:40 PM – 2:00 PM

Stabilizing a Slope Using a High Strength Wicking Geotextile

Author(s): John C. Folts

1:40 PM – 2:00 PM

Icefall Hazards Along U.S. Transportation Corridors—Are Rockfall Catchment Ditches Sufficient?

Author(s): David J. Scarpato

2:00 PM – 2:20 PM

Stabilization of Paleo Stream Deposits Using High Tensile Steel Mesh

Author(s): Scott D. Neely

2:00 PM – 2:20 PM

Rock Slope Stability in Karst Terrain

Author(s): Vanessa C. Bateman

Tuesday, September 15—Late Afternoon Sessions (split sessions)

2:50 PM – 3:10 PM

Geotechnical Designs to Build on Liquefiable and Compressible Soil in Salem, Massachusetts

Author(s): Tulin Fuselier, Zia Zafir, Jennifer MacGregor, and Stefanie Bridges

2:50 PM – 3:10 PM

Rock Slope Monitoring Using Oblique Aerial Photogrammetry Along Interstate 70 in DeBeque Canyon, Colorado: A CDOT Geotechnical Asset Management Pilot Project

Author(s): Ty Ortiz, Dave Gauthier, Nicole Oester, and Robert Group

3:10 PM – 3:30 PM

Old Problem Requires Innovative Investigation—Geotechnical Investigations of the Chippewa Power Canal Culvert Foundation

Author(s): Gabrielle Mellies, Mark Telesnicki, and Tony Sanguiliano

3:10 PM – 3:30 PM

Debris Flood Assessment and Mitigation Design: Trans-Canada Highway, Alberta

Author(s): Alex Strouth, Joe Gartner, Kris Holm, and Matthias Jakob

Tuesday, September 15—Late Afternoon Sessions (split sessions) cont.

3:30 PM – 3:50 PM

Bridges in Appalachian-Type Karst: Geotechnical and Design Concerns

Author(s): Joseph A. Fischer, William Kochanov, and Joseph J. Fischer

3:30 PM – 3:50 PM

Attenuators for Controlling Rockfalls: Do We Know How They Work? Can We Specify What They Should Do?

Author(s): Duncan Wyllie and Tim Shevlin

3:50 PM – 4:10 PM

Louisville Bridges: Then and Now from a Geotechnical Perspective, Louisville, Kentucky

Author(s): Mark A. Litkenhus

3:50 PM – 4:10 PM

Trout Brook Landslide Repairs following Tropical Storm Irene

Author(s): Mike Yako, Peter Connors, and Jeanne Lefebvre (*presentation only*)

Thursday, September 17—Morning Sessions

8:00 AM – 8:20 AM

The Importance of Residual Shear Testing in Evaluation of Landslides in Glaciolacustrine Deposits

Author(s): Andrew J. Smithmyer, Frank Namatka, and Richard Bohr

8:20 AM – 8:40 AM

Investigation, Design, and Mitigation of a Landslide in Newport, Vermont

Author(s): Jay R. Smerekanicz, Jeffrey D. Lloyd, Mark S. Peterson, Peter C. Ingraham, and Christopher C. Benda

8:40 AM - 9:00 AM

Stream Restoration to Improve Slope Stability Along Park Road at Gibsonville, Letchworth State Park, New York

Author(s): James J. Janora, Mark D Kenward, and Paula L. Smith

9:00 AM – 9:20 AM

Natural Geologic Controls on Rockfall Hazard and Mitigation on the Niagara Escarpment, King's Highway 403 at Hamilton, ON, Canada

Author(s): Dave Gauthier, David F. Wood, D. Jean Hutchinson, and Stephen Senior

9:20 AM – 9:40 AM

An Innovative Case Study on the Use of Test Section/Design-Build Construction on the Sea-to-Sky Highway Improvement Project, Vancouver, BC, Canada

Author(s): Grant A. Lachmuth

9:40 AM – 10:00 AM

Development of Grading Requirements for Drought Weather Conditions

Author(s): James B. Nevels, Jr.

10:40 AM – 11:00 AM

Micropiles in Karst – The New Central Utility Plant at Shippensburg University

Author(s): Jason M. Gardner

11:00 AM – 11:20 AM

An Improved Calculation Method to Design Flexible Facing System for Soil Nailing

Author(s): Marco Cerro, Giorgio Giacchetti, Ghislain Brunet, Alessio Savioli, and Alberto Grimod

High Quality H₂O, Utilizing Horizontal Drains for Landslide Stabilization

Cory B. Rinehart, P.G.

Wyoming Department of Transportation

5300 Bishop Boulevard

Cheyenne, WY 82009

307-777-4782

cory.rinehart@wyo.gov

Prepared for the 66th Highway Geology Symposium, September 2015

ACKNOWLEDGEMENTS

The author would like to thank the following individuals for their contributions:

George Machan, P.E. - Senior Associate, Landslide Technology

James Dahill, P.G. - Geology Supervisor, WYDOT Geology

Holly Daniels - Administrative Assistant, WYDOT Geology

Disclaimer

Statements and views presented in this paper are strictly those of the author(s), and do not necessarily reflect positions held by their affiliations, the Highway Geology Symposium (HGS), or others acknowledged above. The mention of trade names for commercial products does not imply the approval or endorsements by HGS.

Copyright Notice

Copyright © 2015 Highway Geology Symposium (HGS)

All Rights Reserved. Printed in the United States of America. No part of this publication may be reproduced or copied in any form or by any means - graphic, electronic, or mechanical, including photocopying, taping, or information storage and retrieval systems - without prior written permission of the HGS. This excludes the original author(s).

ABSTRACT

Utilizing horizontal drains for landslides is a relatively new concept in the geotechnical field. Thousands of horizontal drains have been installed throughout the nation and the world, yet a good number of Engineers and Geologists have limited to no experience with this method for landslide stabilization. This was the case for WYDOT in 2009 when several key factors forced us to take a hard look at horizontal drains to help stabilize landslides.

Since 2010, WYDOT has installed horizontal drains on 6 different landslides, primarily on the Togwotee Pass Corridor near Yellowstone National Park, but most recently west of Buffalo, Wyoming at the Caribou Landslide. Most drain sights have been a success, with only a few showing poor performance, but all sites presented distinct challenges from design and construction to the completed product. Design concepts of horizontal drains are relatively simple and straight forward, yet the nature of each landslide and subsequent placement of drain pad sites is critical for a successful product.

WYDOT Geology faced a significant challenge to attempt to stabilize several key landslides with numerous constraints. The new concept of utilizing horizontal drains provided additional factors of safety and proved to be worthwhile, from slide stabilization to dollars saved. So much so, horizontal drains are being considered to be incorporated into three more upcoming landslide contracts. Regardless of whether horizontal drains are utilized in any of these landslides, WYDOT Geology now has the experience and a sound track record to justify use of this method of slide stabilization for projects in the future.

INTRODUCTION

The utilization of horizontal drains (HD's), Figure 1, is just one of many methods that can be considered by designers in the geotechnical field for landslide remediation. Horizontal drains have the potential to completely stop a landslide or more commonly can be incorporated with other landslide remediation methods to raise the Factor of Safety (FOS) to an acceptable value. Thousands of horizontal drains have been installed and used as a method for landslide remediation around the world, yet many organizations and the professionals within have little to no experience with this concept for landslide remediation. This was the case for WYDOT Geology in 2009 when they were tasked with fixing 13 known landslides for complete reconstruction of the Togwotee Pass Corridor leading to Yellowstone National Park. Several key factors during construction of the project limited the ability to utilize other more accepted practices for landslide remediation and left little choice but to consider the use of horizontal drains on some of the landslides. This can also be said for fixing the Caribou Landslide on Powder River Pass in 2012, west of Buffalo, Wyoming.

WYDOT Geology soon found that the advantages of HD's greatly outweighed the disadvantages, with the most obvious advantage being that the concept is relatively simple, "get rid of the water and get rid of the problem". For an ideal low cost, good performing horizontal drain design, you must have room for a permanent drain pad, sloped topography and an abundant amount of water. Picking ideal sites was made easier because if one of these three scenarios wasn't present, there was high potential that cost would go up and performance would go down, which led to HD's quickly being ruled out at some sites. Horizontal drains generally cost less than most other remediation methods due to simple design concepts, which in turn significantly increased the potential for projects to be let to contract in a short time frame. The most obvious disadvantages were slides with less than ideal site conditions, a very limited amount of HD contractors and drains typically require periodic maintenance. Fortunately, for WYDOT Geology, there was significant potential for low cost, good performing drains that would allow for an expedited contract letting on three landslides on Togwotee Pass, as well as, the Caribou Slide on Powder River Pass.



Figure 1 - Construction of horizontal drain pad on Continental Divide Landslide, Togwotee Pass, June 2010.

BACKGROUND

Both projects, Togwotee Pass and Caribou Slide, needed to be constructed in a very short amount of time from a design standpoint. Horizontal drains provided for a quick design and a net increase in the Factor of Safety for all slide areas.

The 37.5 mile-long project corridor on US 26/287 between Dubois and Moran Junction was planned for complete reconstruction and broken into five sections to be let to contract during the years of 2005 to 2012. The start of the 2009 construction season saw the largest and most complex of the five sections let to contract, the 16.28 mile Togwotee/Four-Mile Section. This section proved very challenging for construction due to its extreme elevation and weather. Much of the section is located at or above 8,000 feet in elevation, peaking at the Continental Divide at 9,648 feet. Adding to the challenges, WYDOT was faced with remediating five specific landslides within this section, most notably Continental Divide Landslide located at milepost 25.4 and County Line Landslide located at milepost 26.5. The designed remediation for County Line Landslide began in the fall of 2008 and involved the installation of an upslope tieback wall and a downslope soldier pile/tieback wall. Construction of the upper tieback wall commenced

after snowmelt allowed access in June of 2009, however just down the road at milepost 26.9 a rather disturbing bump was appearing on the highway. Upon further review, the bump in the highway was getting larger and showed up to 1 foot of lateral displacement on the highway centerline. A reconnaissance team was sent out to search for the cause of the displacement in the road, which revealed another major landslide, later named East Boundary Landslide, located 600 feet off the highway.

The addition of the new East Boundary Landslide was of great concern especially given that the Togwotee/Four-Mile Section was under contract. Further research showed that survey points taken in 1999 on both the Continental Divide Landslide and County Line landslide had moved up to two feet, yet survey points outside of those slide masses showed no movement. Surveyed information and a look at the WSGS landslide hazard map led all parties to the acceptable conclusion that all three landslides were a part of one massive landslide approximately 1.5 miles long and a mile wide later named the Mega Slide, Figure 2.

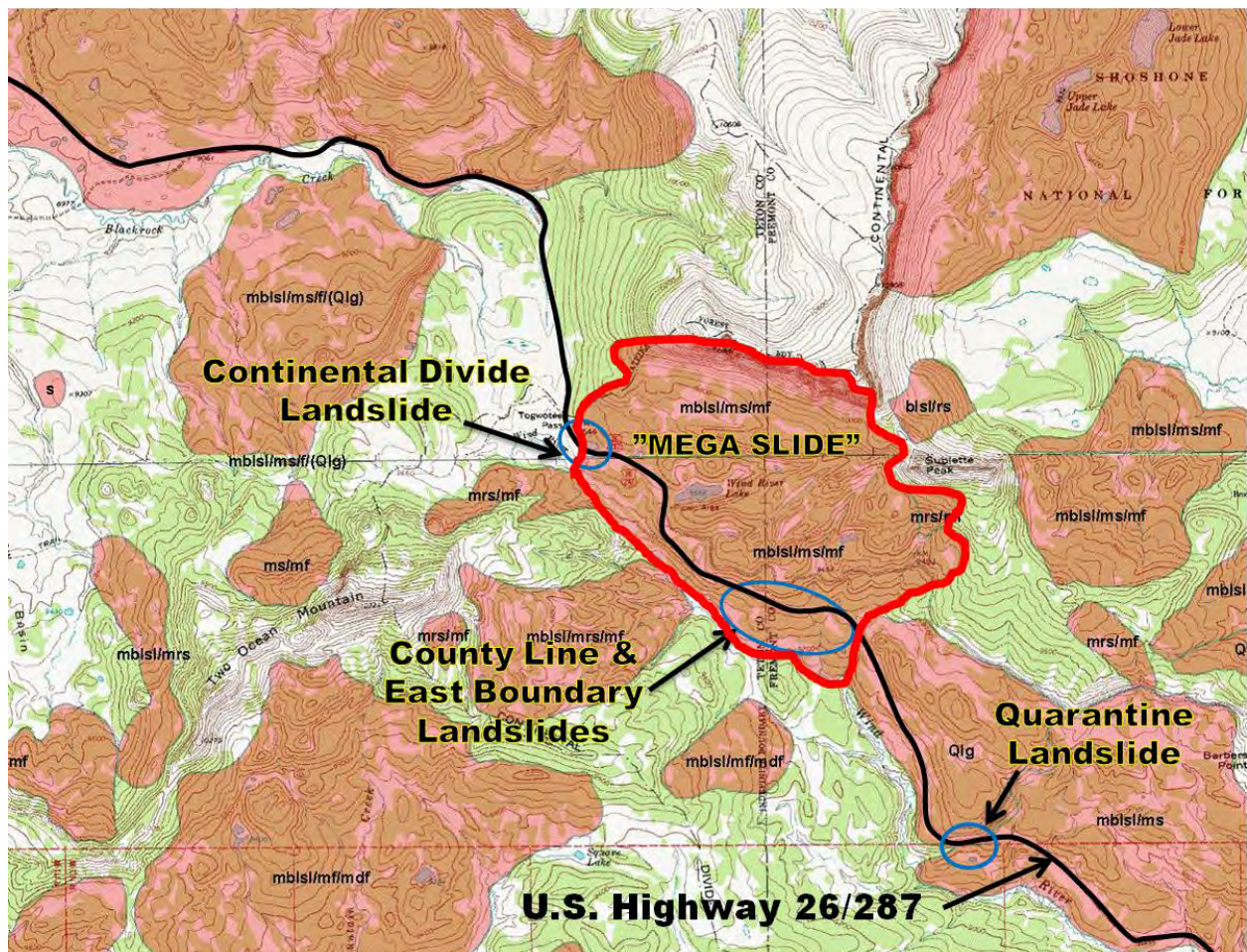


Figure 2 - WSGS Landslide Hazard Map depicting known landslide hazards affecting the Togwotee Pass Corridor.

This meant that the \$6 million tieback anchor project to stabilize the localized County Line Slide could potentially fail due to the massive driving forces generated by the Mega Slide. The decision was made to "tread lightly" and to find ways to increase the Factor of Safety for the localized landslides, which had now increased to another landslide. During the winter of 2009-2010 WYDOT needed to come up with all new concepts for remediating not two, but three landslides before the start of construction in June 2010. Horizontal drains were used in all three localized landslides, as the sole remediation method or as an additional remediation method, for a dewatering change order to the original contract. County Line Landslide was remediated with tie back anchors, EPS lightweight fill and horizontal drains. Continental Divide and East Boundary Landslides were remediated predominantly by horizontal drains, with minor shifts of the road alignment to limit cut/fill transitions to minimize impact in the active slide areas. At each location, most or all landslide instrumentation had been destroyed by construction equipment due to the footprint of the remediation plans from the original contract, or did not exist due to the recent slide activity at East Boundary that occurred during the 2009 construction season. Additional instrumentation was hastily installed in June of 2010 at each site prior to HD construction.

The Caribou Landslide is located on Powder River Pass, between Buffalo and Ten Sleep, Wyoming on US 16. Over the winter of 2010-2011, many of the mountain ranges of Wyoming were at record levels for snow pack, up to 150 percent+ of normal. Furthermore, the spring of 2011 experienced very warm temperatures and numerous rainfall events at high elevations. This combination created excessive amounts of spring runoff water spilling to lower elevations in a very short time period. Hundreds of bridges, box culverts and other structures were severely damaged and over 30 landslides or major failures affected the highways. Many of these areas qualified for Federal Emergency Damage Funding. The Caribou landslide had a long history within the Department and qualified for Federal Emergency Damage Funding. Although the slide had never catastrophically failed, it was a constant mover requiring local maintenance crews to patch and repair the road surface annually. Caribou Landslide was no exception to the high water events in the spring of 2011 and the roadway had dropped significantly that spring. Topography was steep and there was an abundance of groundwater within the slide mass, artesian at times, recorded from a nearby abandoned water well. To satisfy deadlines for Federal Emergency Funding, WYDOT was on an accelerated schedule to let a contract for remediation. The intent for remediation was proposed in two phases, first dewater with horizontal drains and monitor effects of dewatering. If dewatering by horizontal drains did not have the desired effect, an additional remediation concept would be designed in the second phase and constructed in the future. Geotechnical drill investigations were conducted in April and May of 2012 and a horizontal drain contract was granted three months later in September 2012. A horizontal drain gallery consisting of 40 horizontal drains ranging from 400 to 600 feet in length was completed in January 2013, Figure 3.



Figure 3 - Damage to US 16 on Powder River Pass by the Caribou Landslide. Excessive moisture due to winter snowpack accelerated slide movement. A horizontal drain pad was constructed near Crazy Woman Creek to the left of the photo.

GEOLOGY

Geology within the Togwotee Pass area consisted predominantly of Quaternary Landslide Debris consisting of clays of low permeability with gravel atop Tertiary Aycross Formation, a brightly variegated bentonitic claystone to tuffaceous sandstone or Tertiary Thorofare Creek Group consisting of volcanoclastic strata, andesite lava flows and dark brown breccia. Both bedrock formations belong to the Absaroka Volcanic Supergroup. The andesite lava flows and breccia made for problematic, difficult drilling for all parties from geotechnical to contract drill rigs.

Geology within the Caribou Landslide consisted predominantly of Quaternary Landslide Debris consisting of clays and silts of low permeability. Below the landslide debris is a green to variegated micaceous soft shale of the Middle Cambrian Period atop Early Archean Oldest Gneiss Complex. The oldest rock found in Wyoming with metamorphism dating back to 3000+ Ma. As predicted, drilling was very difficult when the Archean Gneiss was encountered.

DESIGN METHODOLOGY

All the landslides proposed for horizontal drains met our minimum criteria in that all sites had enough room for one or more permanent pads, they had ample vertical relief and all were full of water. Another important aspect of each slide area was that each site could accommodate one or more drain pads at or near the toe of the landslide. This was helpful because diversion of drain water to prevent saturating the remaining slide mass was not as critical. Due to the accelerated circumstances of each slide area, adequate time was not available to monitor groundwater conditions by means of thorough piezometric data or groundwater monitoring studies. However, local groundwater conditions were confirmed through visual evidence at the sites, drill data and open groundwater standpipes. Typically, mountainous regions of Wyoming do not show rapid fluctuations in groundwater elevation in response to precipitation and is not the main source for water. Rather, rapid fluctuations in groundwater elevation are in response to the melting of winter snowpack. This is represented in little to no movement of the landslide

during the dry portions of the year and accelerated movement in the spring months from May to July, Figure 4 and 5. The intent for horizontal drains in these areas was to lower groundwater elevations as much as possible within the slide mass, provide drainage for any perched water and maintain a consistent lowered groundwater elevation by providing an outlet for the rapid groundwater fluctuations seen in the spring runoff months.

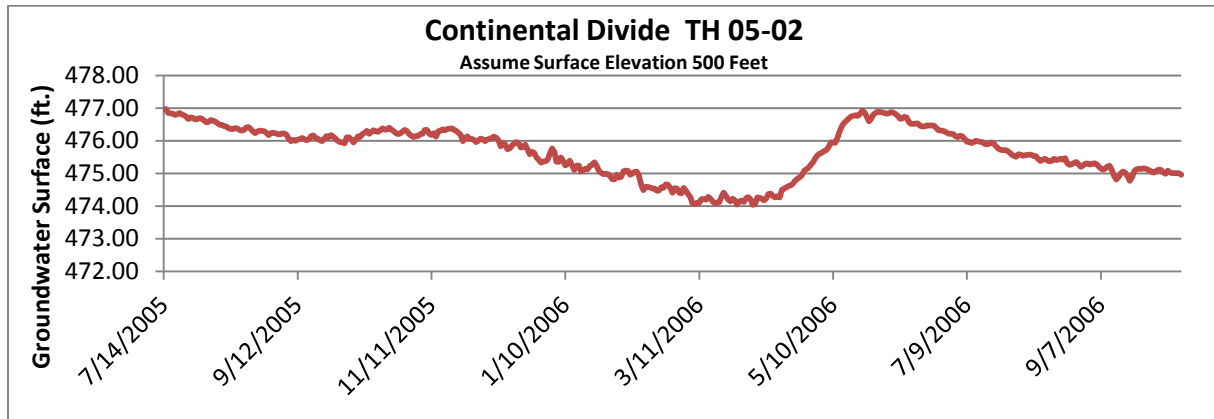


Figure 4 - Single channel piezometer data for Continental Divide Landslide depicting rapid increase in groundwater elevation during spring runoff.

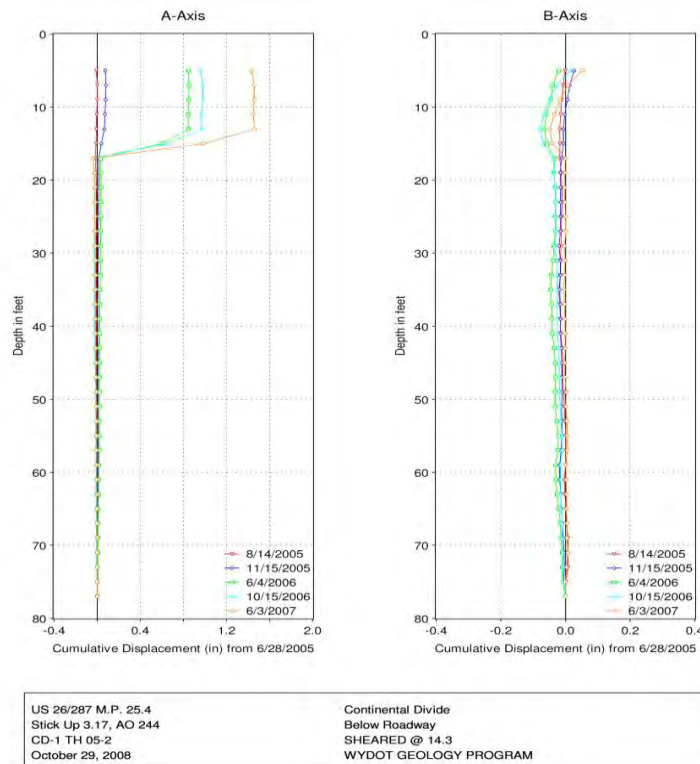


Figure 5 - Inclinometer Plot for Continental Divide Landslide. Bulk of slide movement is occurring during the months of May-July during spring runoff.

Subsurface conditions attained from drill data along with groundwater conditions were then modeled in cross section. Drain pads were then placed where topography would allow for an ample vertical temporary excavation for horizontal drilling and enough horizontal area for a drill rig, circulation/settlement pond, placement of a rock buttress and access space for future drain maintenance. This was typically defined by a 10 to 12 foot near vertical temporary excavation and approximately 40 feet of pad width sloped at a 1 to 2 percent grade away from the pad face to ensure optimum drainage. Lengths of drain pads were typically determined by topography of the area and graded at 1 to 2 percent parallel to the pad face for optimal drainage. Pads were oriented so that the vertical pad face was as close to perpendicular to the planned drain azimuth as possible to accommodate drilling and drain installation. If the site topography would allow and additional drains were desired, a second drain pad was designed under the same criteria. Number of drains for each specific pad were then limited to the maximum number of drains that could fit in each pad area at an 8 to 10 foot spacing, which equated to no more than 40 drains per pad. Up to five contingency drains were added to pad sites in the contract to allow for additional footage for areas of high production during drilling. Once location and number of pads were determined, drain arrays were placed at each pad. Drains were placed at the aforementioned 8 to 10 foot spacing to allow rig access and drains were given an azimuth that would accommodate maximum "fanning" of the slide mass for dewatering purposes. Angle of drains were generally low angle between 1 to 7 percent. Elevation, angle and length of drains were positioned to allow the maximum anticipated potential for a drop in groundwater elevation with respect to site topography, slide mass and geological constraints, Figure 6.

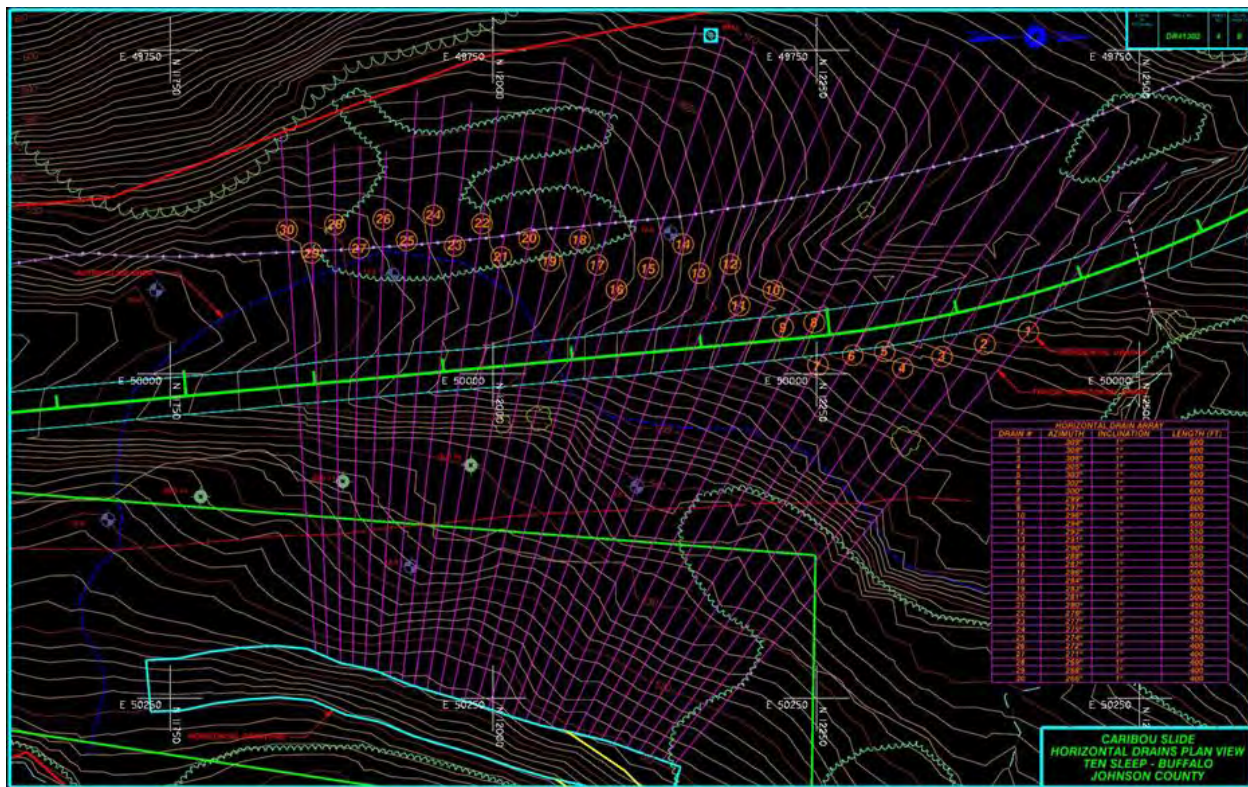


Figure 6 - Design Plan View of North drainage gallery for Caribou Landslide on Powder River Pass.

Once location and dimensions of pad sites were established, they were incorporated and modeled in the accepted slide stability model. Due to the lack of an elaborate groundwater monitoring study being conducted at any site, a definitive estimate of drop in groundwater elevation was unknown. The general consensus was that all sites proposed for horizontal drains would produce a good quantity of water, however if drains as a whole did not produce as expected we were still guaranteed to achieve a higher FOS. This was rationalized by the fact that even a dripping drain over the course of one year's time would produce a significant amount of water, provide a potential outlet for excess water during spring runoff and decrease pore water pressures on the slide mass. Therefore, several elevations and drain angles that would be practical for each pad site were then modeled in the slide stability program as a percentage of increase in FOS for every one foot drop in groundwater elevation.

DRILLING CONCEPTS/CONSTRUCTION

Remediation of many landslides involves the use of innovative ideas and therefore specialty contractors. This was the case for WYDOT during the design and bidding phase of the dewatering contracts, as most if not all the slide remediation involved a specialty horizontal drain contractor. At the time of contract bidding in the spring of 2010 for the Togwotee Slides and again in the fall of 2012 for the Caribou Slide, bids were accepted from the limited number of experienced and qualified horizontal drain contractors available in the nation. The majority of the expense for the horizontal drain contract was in the drilling and installation of the drains themselves. For all contracts let, drilling and installation accounted for approximately 60 to 80 percent of the total bid price, with cost for drilling ranging at a moderate \$14 to \$25 per lineal foot. The horizontal drain contractor was on site and ready to drill in June of 2010 and 2011 for the Togwotee Slides and September of 2012 for the Caribou Landslide.

Once pads were constructed to planned specifications, drilling was set in motion. Drilling began by marking 6 to 8 planned drain locations on the pad face followed by installation of 20 feet of steel surface casing. Prior to surface case installation the inspector on site would align the drill rig at the planned azimuth and inclination of the drain. Once surface casing was set, drilling commenced to planned length of each drain. During drilling, drain angles could be checked by using a monometer and calculating hydraulic water pressures recorded at a known depth. This was a very crude way to determine drain inclination and many times pressures were assumed inaccurate. Generally, once surface casing was set to the planned azimuth and inclination, gravity and geology determined the path of the drilling especially at depth, Figure 7.



Figure 7 - Care should be taken for correct azimuth and angle of a drain. However, the photo above proves when horizontal drilling, bits tend to have a mind of their own.

The stereotypical path seen during horizontal drilling is for the bit to start at the set inclination, then raise, and go to the right with depth until gravity takes over and the bit begins to fall. Completed drilling orientation of the horizontal drain typically rested in a concave manner when viewed in cross section and many times was confirmed through Pajari testing discussed below. In many cases, although a significant portion of the completed drain was drilled at a negative angle, it was assumed pore water pressures were high enough to promote enough head to allow good flowing drains seen at the pad face. Once final planned depth was achieved, the bit was removed from the drill stem using a very unique method in horizontal drilling through the use of a "knock off bit", Figure 8. This is achieved by backing the bit and turning the drill stem counter clockwise Figure 9.



Figure 8 - View of "knock off" bit assembly.

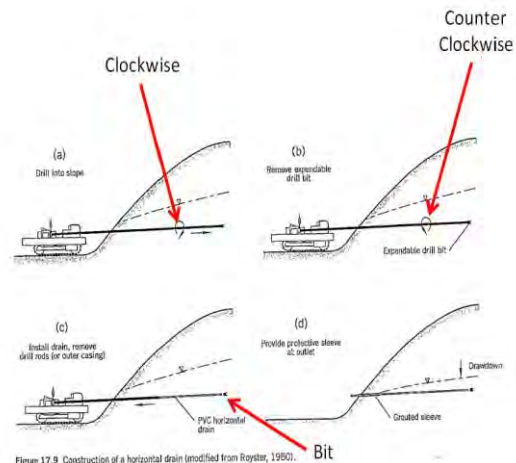


Figure 17.9 Construction of a horizontal drain (modified from Royster, 1980).

Figure 9 - Schematic of HD drilling and drain installation procedure.

Once the bit was removed, the drill head was detached from the drill steel and 1½ inch ID, schedule 80, perforated PVC drain pipe was installed to full drilled depth. A secondary method for determining orientation of drains was by the use of a Pajari borehole survey instrument, which operates through the use of a clockwork mechanism which simultaneously locks a plumb device and a magnetic compass to give the inclination and azimuth of the borehole. This device worked quite well, but was rather tedious and time consuming because it required several measurements to be taken under a set amount of time to be able to plot the entire borehole orientation, Figure 10. Due to reasons discussed above and the cost required to conduct the testing, only a handful of these tests were conducted per drain pad. It is also important to note that Pajari testing could only be conducted through an installed horizontal drain, Figure 11. Therefore, the orientation of that drain was permanent, but it would allow for adjustments to drilling of the remaining drains. Drilling and installation continued in this fashion until drain pads were completed.



Figure 10 - View of Pajari borehole survey instrument.



Figure 11 - Pajari assembled in protective casing for preparation to survey HD.

The final step for drain pad installation involved a rock buttress being placed around the outlet of all drains and adjacent to the temporary vertical excavation. This required a minimum of four feet of rock cover above the drain outlets and matching the grade of the existing slope. Rock was extended the full length of the drain extensions, 20 feet nominal, and tapered at a 1.5H:1V slope to the base of the pad. This required rock to be placed to the bottom elevation of all drains, and then drains were extended to daylight at the proposed rock buttress slope and encased in 4 inch perforated polyurethane pipe at which time the remaining rock was placed to planned specifications outlined above. The rock buttress served many purposes in that it retained the temporary vertical excavation at the pad face, protected and insulated the drain outlets from damage and freezing temperatures and the buttress provided a free draining outlet source for production water to satisfy environmental concerns. Lastly, all drains were cleaned the full length with a high-pressure jetting device to flush of any debris and clear perforations, Figure 12.



Figure 12 - Jetting of HD's on County Line Landslide, Togwotee Pass, November 2010. Preliminary jetting was conducted prior to placement of rock buttress. Drains were producing enough water to supply jetting device with clean water indicated by PVC pipe supplying storage tank to the left of the frame.

PERFORMANCE

Horizontal drain galleries were completed by the contractor well before the contract deadline for all sites. All pad sites experienced variable drain rates, as expected, with flow rates ranging from an initial release of 200+ GPM to a perpetual "dripper" where some eventually went dry. Groundwater elevations during horizontal drilling dropped substantially in three of the landslides. An average overall drop in groundwater elevation was achieved at each slide area with good results seen at Continental Divide, East Boundary and Caribou Slides and moderate results were seen at County Line Slide, Table 1 and Figures 13 through 18.

Table 1 - Horizontal Drain Groundwater Data*			
Landslide	Change in Groundwater Elevation (Feet)		
	Maximum	Minimum	Average
Continental Divide	33.9	0.8	17.5
County Line	20.9	2.0	7.6
East Boundary	32.9	22.1	28.4
Caribou	32.7	10.0	31.1

*Data collected from open standpipe monitoring wells with water tape or single channel piezometer during horizontal drain construction in 2010 and 2012.

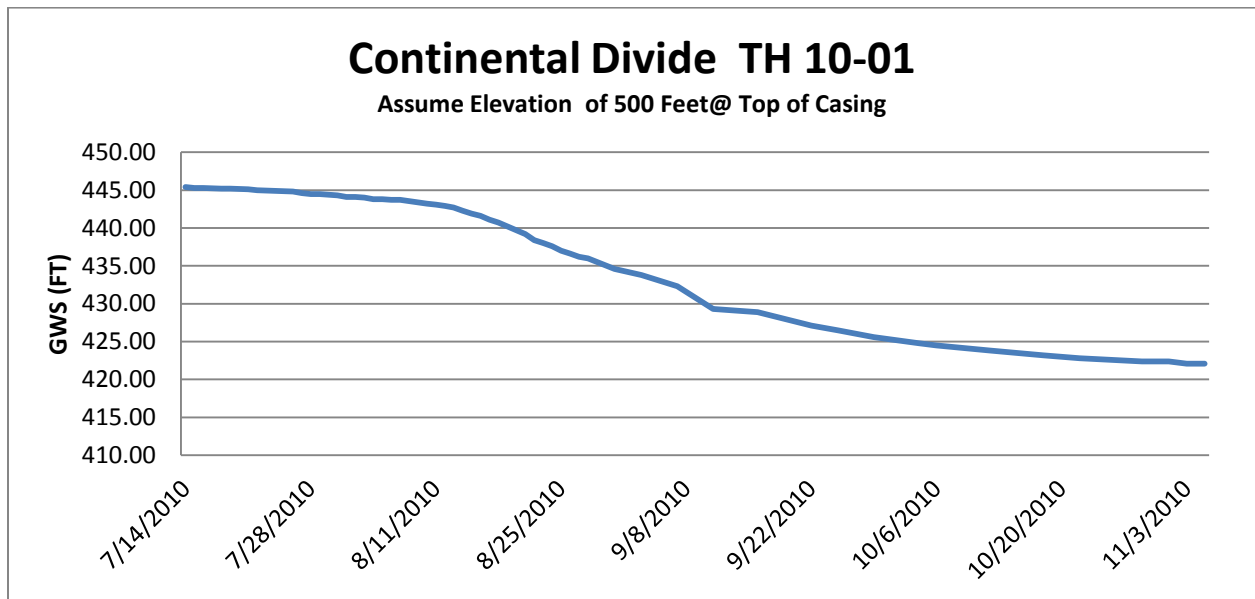


Figure 13 - Gradual drops were seen in some areas of Continental Divide during installation, yet the overall drop in groundwater elevation was impressive.

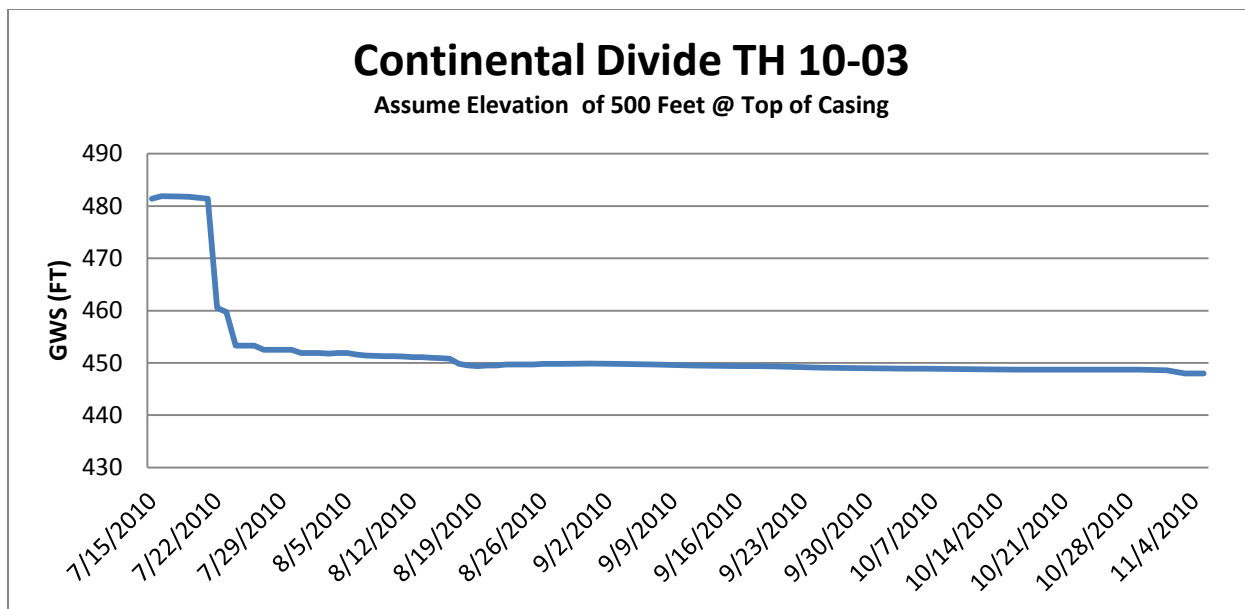


Figure 14 - Significant, nearly instantaneous drops were seen in most areas of Continental Divide.

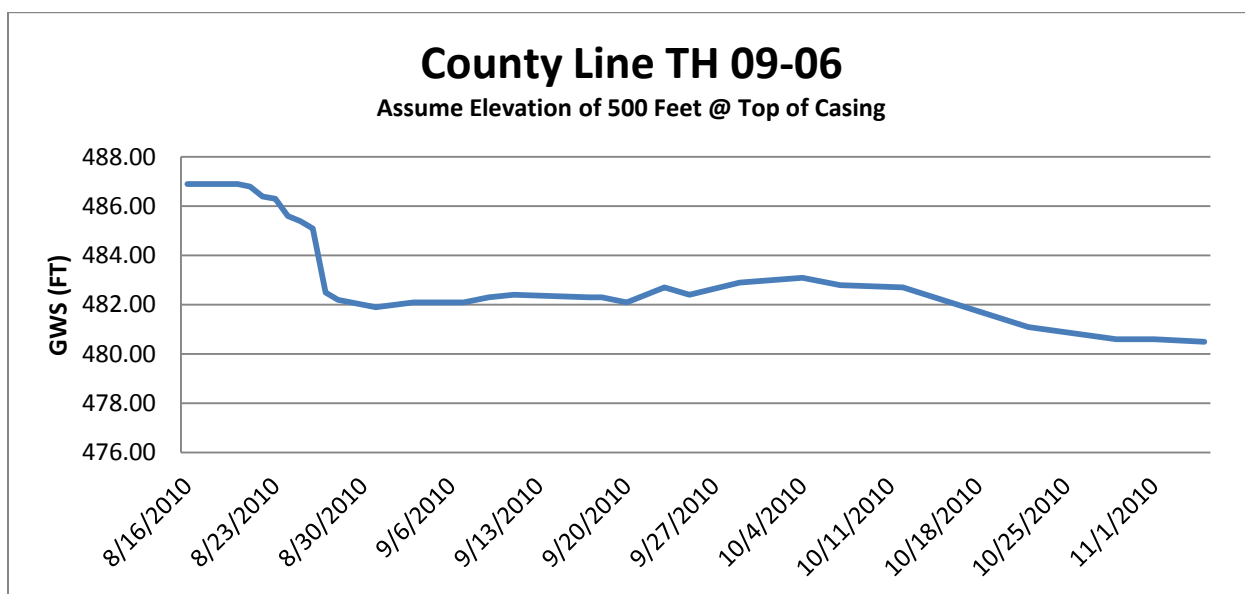


Figure 15 - County Line showed positive signs of drainage to the slide mass, but not nearly to the extent seen at the other slides. County Line groundwater elevations in response to HD installation were much more sporadic than the other slides. This may be attributed to the fractured volcanic breccia bedrock.

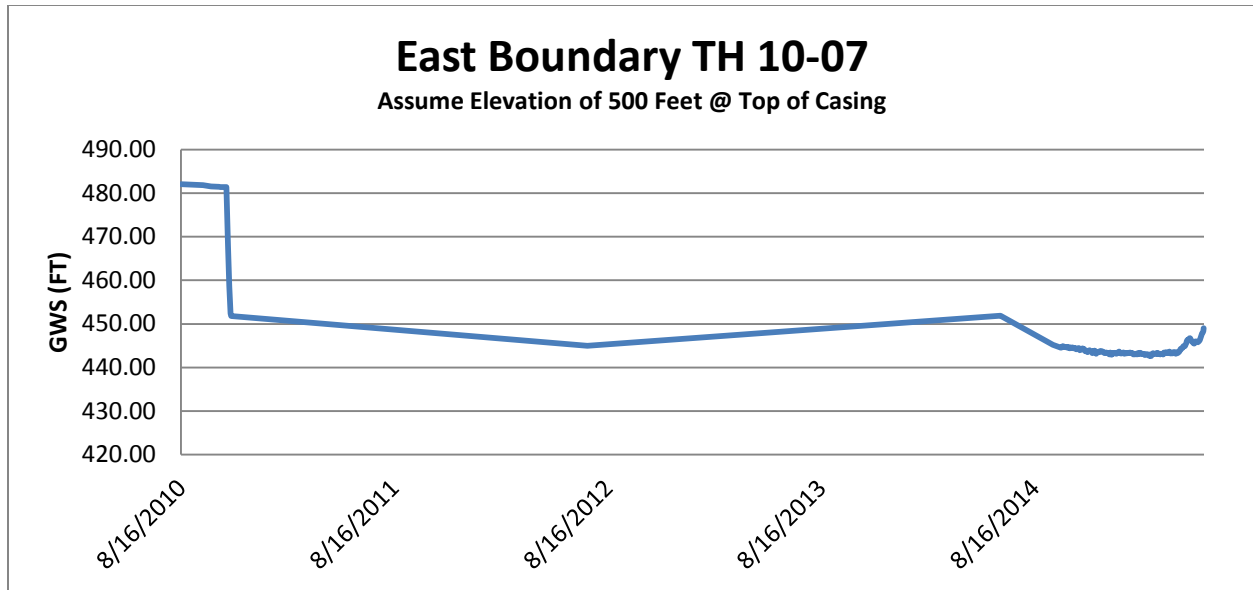


Figure 16 - Initial drop in groundwater elevation seen to the left during HD construction. Piezometer data to the right indicates water elevations are at or below post construction levels even after drains were sheared near the pad face.

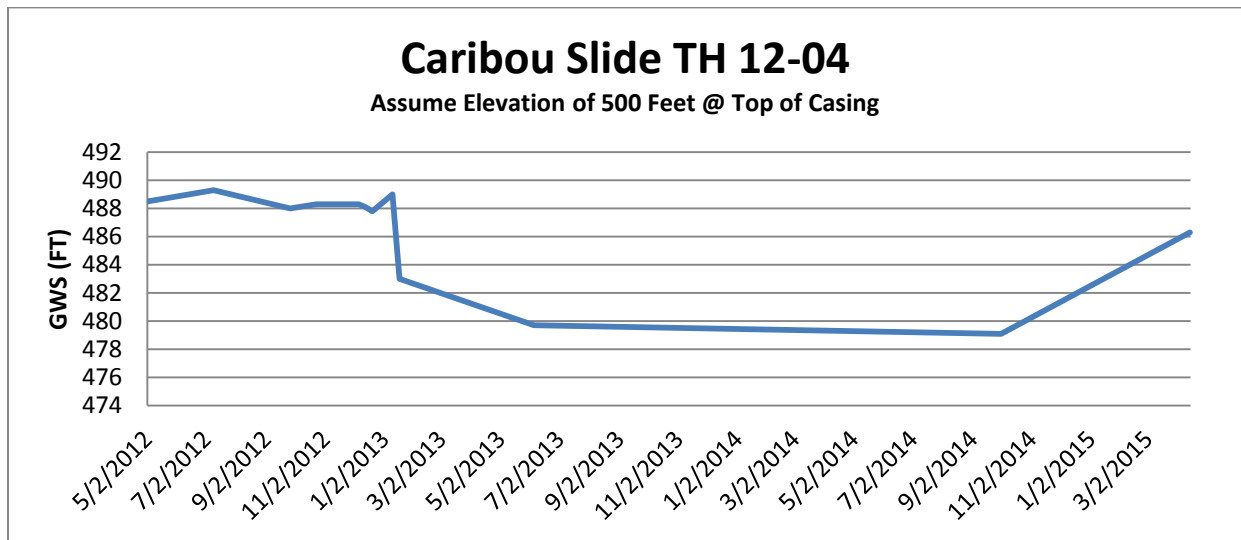


Figure 17 - Initial drop in groundwater elevation seen to the left during HD construction. Raise in groundwater elevation in recent months may indicate a dirty drain or high spring runoff in 2015.

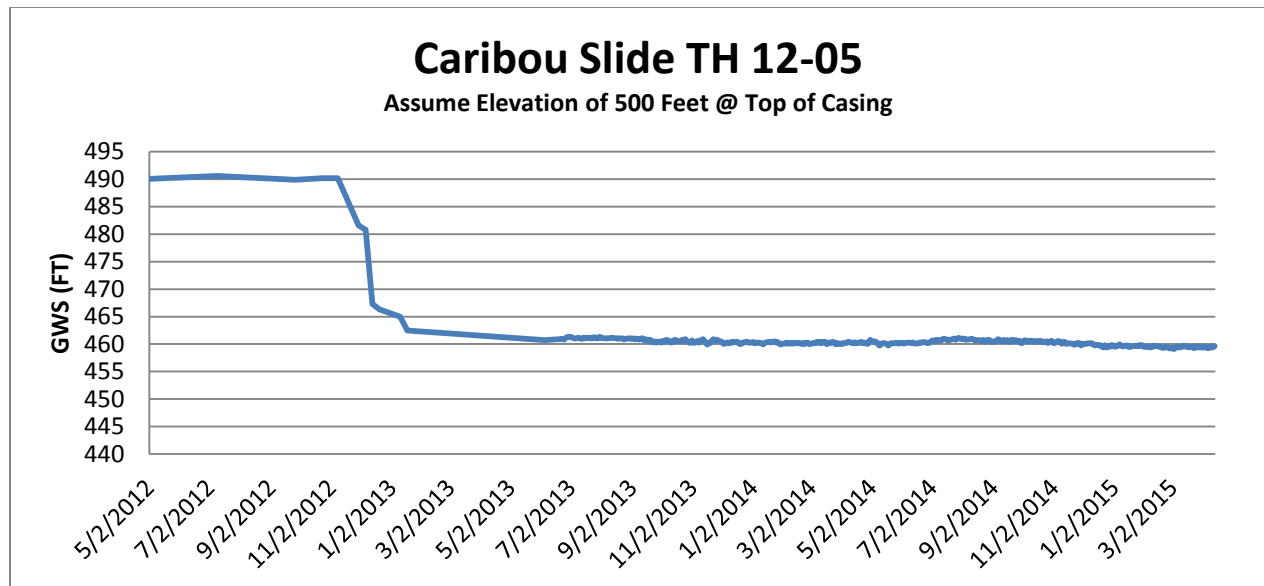


Figure 18 - This graph is indicative of the performance seen at Caribou landslide. Piezometer data post construction indicates drains are continuing to maintain lower elevations.

The integrity of the drainage galleries at all locations remain intact, with the exception of East Boundary Landslide, and continue to produce a significant amount of water. Given that the occurrence of East Boundary was the catalyst for the horizontal drain change order on Togwotee Pass, there was very little time to install and monitor the site. East Boundary landslide experienced significant movement the following spring after drain construction. Many of the drains were sheared 20 to 30 feet into the pad face and are unable to be maintained or cleaned. Yet a significant amount of water is still evident draining out of the buttress rock. Currently, every drain gallery contains a handful of drains that consistently run throughout the year at rates of 5 to 10 GPM with several more drains increasing production or producing water during the months of spring runoff. To date, all landslides have shown very minimal slide movement resulting in no damage or disturbance to the road surface.

Worth noting is that the experience gained with horizontal drains on the previous Togwotee Pass Corridor played an integral part in the design and successful implementation of the Caribou HD contract. This was all encompassing from field resonance and instrumentation to final placement of the rock buttress, Figure 19. In the summer of 2013, to maintain the integrity of the drainage galleries on Togwotee Pass, maintenance personnel flushed the drains and the Caribou Landslide is planned to be flushed in the summer of 2015.



Figure 19 - Completed drainage gallery at Caribou Landslide, Powder River Pass. Drain pipes are exposed at face of rock buttress for future maintenance.

CONCLUSION

WYDOT was successful in meeting the challenge of a condensed time schedule because horizontal drains allowed for a quick design and expedited production of construction plans. Horizontal drains proved to be a very favorable remediation alternative at the sites discussed, given the circumstances, by dropping the overall groundwater surface within the slide masses and gaining a net raise in the Factor of Safety. Dewatering from horizontal drains did not increase the FOS to the desired value of 1.3 on any landslide. Using an average post construction groundwater elevation drop, Caribou Landslide was close with a FOS between 1.25 and 1.3. Although the preference may be to have an extensive groundwater monitoring study and analysis, it is possible to have a successful horizontal drain design with minor groundwater information and analysis under a very tight time frame. Simply put, horizontal drains worked well for WYDOT and the Department is currently considering the incorporation of horizontal drains for the remediation of three upcoming landslide projects. By doing a simple field investigation to determine, room for a permanent drain pad, sloped topography and an abundant amount of water, horizontal drains may prove to be a quick and successful design alternative to consider.

REFERENCES

Cornforth, Derek H., (2005) Landslides in Practice: *Investigation, Analysis, and Remedial/Preventative Options in Soils*, John Wiley & Sons, Hoboken, New Jersey, pp. 315-362.

Turner, A.K., R.L. Schuster (Editors). Landslides Investigation and Mitigation, Special Report 247, Transportation Research Board, National Research Council, National Academy Press, Washington D.C., 1996

Wyoming State Geologic Survey. *Hazards, Mapping and Water Resources*.
<http://www.wsgs.wyo.gov>

Durham Geo-Enterprises, Inc. A Nova Metrix Company, *DigiPro Software for Inclinometers*, Seattle Washington, 2015.

A New Simplified Methodology to Design Flexible Debris Flow Barrier

Marco Cerro

OFFICINE MACCAFERRI S.p.A.

Via Kennedy 10

40069 Zola Predosa

Ph: 01139051646000

m.cerro@maccaferri.com

Giorgio Giacchetti

OFFICINE MACCAFERRI S.p.A.

Via Kennedy 10

40069 Zola Predosa

Ph: 01139051646000

giorgio.giacchetti@maccaferri.com

Ghislain Brunet

Maccaferri, Inc

10303 Governor Lane Blvd.,

Williamsport, MD 21795-3116

Ph: 301-223-6910

gbrunet@maccaferri-usa.com

Alessio Savioli

OFFICINE MACCAFERRI S.p.A.

Via Kennedy 10

40069 Zola Predosa

Ph: 01139051646000

alsessio.savioli@maccaferri.com

Alberto Grimod

France MACCAFERRI SAS

8, rue Pierre Mechain

26901 Valence Cedex 9

Ph: 330475860919

agrimod@maccaferri.fr

Disclaimer

Statements and views presented in this paper are strictly those of the author(s), and do not necessarily reflect positions held by their affiliations, the Highway Geology Symposium (HGS), or others acknowledged above. The mention of trade names for commercial products does not imply the approval or endorsement by HGS.

Copyright Notice

Copyright © 2011 Highway Geology Symposium (HGS)

All Rights Reserved. Printed in the United States of America. No part of this publication may be reproduced or copied in any form or by any means – graphic, electronic, or mechanical, including photocopying, taping, or information storage and retrieval systems – without prior written permission of the HGS. This excludes the original author(s).

ABSTRACT

Since the debris flow can travel at high speeds and transport huge volumes of material, they pose a high risk to human life and infrastructures; roads and railways are particularly exposed to the risk as they cannot avoid crossing gullies and channels. In these situations the deformable debris flow barriers are one of the more often used remedial solutions because they can be easily installed within the path of the debris flow (or shallow landslide). Such barriers are composed by a ring-net interception structure, which restrained to the channel sides by means of longitudinal cables generally coupled with energy dissipaters.

The interaction between barrier and flow is quite difficult to describe, since it changes both in the space and in the time: upon the impact by the debris flow from the bottom to the top, the barrier progressively deforms with the compression brakes and systems absorbing the energy. The hydrostatic pressure within the flow rapidly dissipates once the debris flow has been arrested, leaving the accumulated volume within the fence. If on one hand the debris flow barriers mitigate the risk, on the other one they pose severe problems for the maintenance. Therefore the designer has to face two basic problems: first of all the global design strategy aimed at getting a cost effective remedial barrier and then the calculation of the structure.

The paper recaps a simplified model to design the structure based on the experiences and the research carried out by Officine Maccaferri with the University of Parma; it allows designing all the components of the fence. The model returns restraining forces and cable stresses that can be used for an appropriate barrier design.

INTRODUCTION

The kinetics of a landslide (how movements are distributed through the displaced mass) is one of the main criteria to classifying landslides (Cruden & Varnes, 1996). According to Cruden & Varnes (1996) it is possible to define five distinct landslides, characterized by a different kinetic: fall, topple, slide, spread and flow.

Flow

A flow is a spatially continuous movement in which surfaces of shear are short-lived, closely spaced, and usually not preserved. The distribution of velocities in the displacing mass resembles that in a viscous liquid. The lower boundary of displaced mass may be a surface along which appreciable differential movement has taken place or a thick zone of distributed shear (Cruden & Varnes, 1996). Flows are often activated by heavy rainfall. Thus, the material slides downslope increasing its volume. The dimension of the transported solid particles may reach metric dimensions. The velocity of the flow can vary depending on the water ratio content, grain size and slope gradient. According to Hungr et al. (2001) the following main categories of flows may be distinguished: debris flow, earth flow, debris avalanches and mud flow.

The movement expands along preferential ways, such as natural draining systems, creeks, etc., that allow the flow to travel for miles, therefore their negative effect can be perceived far away from the starting zone (Figure 1).

Debris flow

The category “debris flows” includes the most common flow types that are capable to transport a large amount of material with different sizes. During an event, the total amount of material moving toward the accumulation zone may be defined as the magnitude of the debris flow. The magnitude is rarely related to the volume of the initial mass movement. Often, the initiating slide is small and the bulk of the volume transported to the deposition area results from entrainment of material along the path. Thus, it is the flow mechanism that primarily determines the total volume of a debris flow. Such aspect is extremely important to scale the event and allow correlating it to the run-out distance and maximum discharge (Hungr et al., 2005).

The rheology of the debris flow varies with the time. When the amount of debris is increasing on the front of the flow, the discharge that drives the flow downstream is also increasing. Thus, the peak discharge rises as well. Generally the biggest particles constitute the forward-face of the debris flow, whereas the small ones create the central core. The tail of the flow is basically composed of water and very small material (Figure 2).

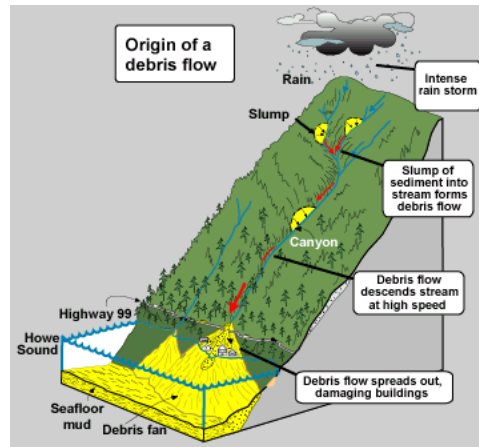


Figure 1 – Origin and evolution of a debris flow (Source: natural Resource Canada)

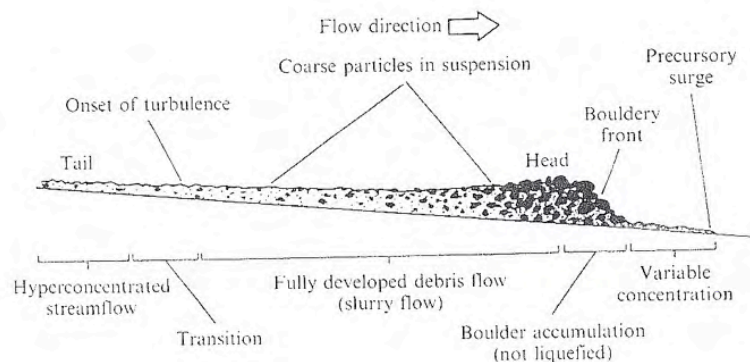


Figure 2 – Evolution of the debris flow (Source: Pierson, 1986)

The mass of the flow can also contain bushes, trees and other elements intercepted during its motion downslope.

Once the debris flow reaches slopes with low gradients (10 to 20 degrees), the deposition of the material starts.

Debris flow mitigation system

As the debris flow develops with features while running down the slope, a different remedial strategy should be adopted to face the problem. Considering the typical section of the debris flow (Figure 3) the following remedial measures can be adopted:

- Starting zone: characterized by erosion and landslide movements. The protection measures must be able to prevent the triggering of the phenomena. Thus, in this zone, erosion control systems, drainages, bio-engineering techniques, soil nailing and superficial stabilizations may be adopted;
- Transit zone: characterized by the passage of the flow with different velocity and volumes. The protection measures must be able to control the flow by reducing its speed and contain

its solid transportation in order to limit the erosion. Therefore, in this area, erosion control systems, channel lining, weirs, selective check dams and channel debris flow barriers may be designed;

- Deposition zone: characterized by the accumulation of the material transported by the flow. The protection measure must be able to mitigate the negative effects of the event. Thus, deviation (i.e. embankments, channeling) and/or accumulation (i.e. selective check dam, embankments, accumulation dam, and open-slope debris flow barriers) structures should be designed.

It should be clear that flexible barriers hereby discussed should represent one among the solutions, because they can only mitigate the consequences of the flow. In these terms, and considering the required maintenance, the best use of these structures should be as ultimate defense, especially for emergency situations.

DEBRIS FLOW BARRIER

Debris flow barriers are positioned within the path of the debris flow or shallow landslide, often in natural gullies, channels, creek or chutes on the slope.

Depending on the type of debris flow these structures can be divided in:

- Channel debris flow barriers, without (Figure 4) or with intermediate posts (Figure 5);
- Open-hill (or open-slope) debris flow barriers (Figure 6).
- Debris flow fences are generally comprised of a number of components, such as:
- Transversal longitudinal ropes: steel ropes that transversally run to the debris flow. These ropes are able to transfer the forces developed by the event from the interception structure to the lateral anchors;
- Interception structure, which is a “rockfall mesh” (generally ring nets panels) held up by the upper longitudinal ropes and fixed to the lower longitudinal and lateral ropes;
- Energy dissipater devices (brakes), which are inserted into the longitudinal ropes in order to dissipate the impact energy of the debris flow, by deformation. The deformation of the brakes allows the extension of the ropes and consequently the forces acting on the anchors are reduced (Figure 7);
- Lateral anchors, which are composed of a double-leg flexible rope. They are installed in a drilled hole and fully grouted. They transfer the forces from the barrier to the ground.

In case of open-slope barriers or channel barriers with intermediate posts (section often larger than 12-17 m), the following elements compose the barrier:

- Posts: constituted by steel beams (H profile). They are connected to the upper longitudinal rope, and to the footplate at the base. This second connection is made with a pin that allows the rotation of the post downstream;
- Post anchoring system: constituted of a small concrete plinth, with a micropile and/or rod steel bars;
- Upslope bracing ropes, which connect the head of the posts to the upslope anchors;

- Upslope anchors: which are composed of a double-leg flexible rope. They are installed in a drilled hole and fully grouted. They transfer the forces from the post to the ground.

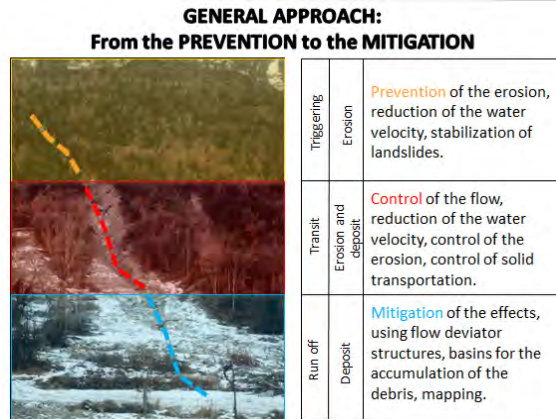


Figure 3 – Areas characterizing a debris flow. Example of a channelized flow. 3-areas can be identified: starting zone (orange), transit zone (red), and deposition zone (blue)



Figure 4 – Channel debris flow barrier with no posts (Italy)



Figure 5 – Channel debris flow barrier with intermediate posts (California - USA)

DEBRIS FLOW BARRIER DEIGN CRITERIA

Designers should take into account the following aspects based on laboratory and field experience:

- Generally the maximum span should not exceed 15-17 m. Larger spans require stronger ropes and deep anchors, thus the introduction of one or more intermediate post may be more cost-effective;
- Transversal ropes should not exceed 22 mm (7/8 inch) in diameter. Larger diameters are strongly unadvisable because their installation is difficult;



Figure 6 – Impacted open slope debris flow barrier (Italy)



Figure 7 – Example of Maccaferri energy dissipater device (brake). Before the test (top) and after the test (bottom). The deformation of the device allows absorbing the impact energy of the debris flow.

- Debris flow barrier should always be intended as emergency remedial solutions, aimed to reduce the peak of the sediments carried by the flow (Figure 8). The followings implications come out accordingly:

1. The riverbed should always be free, so that the ordinary flow and solid transportation can pass without filling the barrier. In these terms a gap should be preserved at the bottom (i.e. lower rope placed 1 m or more above the river bed level);
2. The primary mesh (ring net) is able to catch the debris flow, thus a secondary mesh (i.e. double twist) is unnecessary. The goal of the interception structure is to allow the passage of the water and small particles, and contain the debris;
3. As soon as the barrier screen is filled with the material carried by the event, maintenance works must be foreseen.

If the gap between the lower longitudinal steel rope and the creek bed (or slope) is properly designed, the barrier can be self-cleaned if the sediments do not include boulders. The concept of “self cleaning” is analogous in the slit dams (Shun et al., 1997) where the gaps in the screen are aimed at allowing harmless non-flood sediments to descend rather than accumulate necessarily, and restoring the flood deposition level by discharging the debris after the flood period thanks to progressive erosion throughout the large ring net of the screen and the bottom gap.

Debris flow barrier forms a small dam on the channel. The maximum volume retained by the dam depends upon the geometry of the channel/slope (i.e. stream cross section, riverbed inclination), rheological features of the flow and the amount of material accumulated. Due to the deformable behavior of the sliding mass, it is not possible to correlate the forces developed by the impact with the total volume of the debris flow;

- Once the debris flow volume exceeds the maximum capacity of the barrier, the material starts to overcome the top of the fence and it continues its motion downstream.
- The maximum force developed on the barrier varies with the height of debris deposits. Stresses developed by boulders are greater than the ones developed by fluids. Therefore, the debris flow barrier must be able to withstand the impact of big blocks, especially in creeks where large size debris are present (Figure 9);
- The higher the flow velocity is, the greater the impact force is. Moreover, the smaller the grain size is, the higher the velocity is.

SIMPLIFIED METHODOLOGY TO DESIGN FLEXIBLE DEBRIS FLOW BARRIER

Debris flow modeling

In order to design a debris flow barrier all the morphological, geotechnical, hydrological and hydraulic parameters of the analyzed area must be known. Numerical models can be used to analyze and describe the phenomena (Lo, 2000). Several mechanisms suitable to describe the impact and the accumulation of the debris, as well as the procedures to estimate the effect of the debris flow impact, can be found in literature. Therefore designers can use different approaches (Canelli et al., 2012; Sun et al., 2012; Ferrero et al., 2010). According to the experience of the authors, the most reliable model seems to be the “run up” mechanism defined by Geo Hong Kong Office (Sun et al., 2011) (Figure 8). According to this model, the loads acting on the debris flow barrier can be divided in:

1. Dynamic load: due to the force of the flow wave that impacts against the fence (Figure 10.i);
2. Static load: due to the debris accumulated against the barrier (Figure 10.ii);
3. Drag load: due to the motion of the flow passing over the top of the structure once this one is completely filled of material upstream (Figure 10.iii).

Preliminary assumptions

The debris flow barrier can be designed using a simplified method based on the following hypothesis:

- The barrier is placed on a vertical plane perpendicular to the flow direction;
- Longitudinal ropes absorb all the forces developed by the debris flow (expressed in: Pressure x Screen surface);
- During the calculation, the plastic and elastic behavior of the ropes is neglected in order to increase the overall safety factor of the structure;
- The brakes are able to dissipate a considerable part of the energy developed by the impact. Thanks to these additional elements it is possible to reduce the stress acting on the ropes;
- The energy dissipation due to the deformation of the interception structure (ring net) is neglected;
- The interferences between longitudinal ropes due to the stiffness of the interception structure is neglected (Canelli et al., 2012);
- The interception structure (ring net) is fit to withstand the impact of the debris, as demonstrated by the behavior of deformable rockfall barriers (Cantarelli et al., 2008; Grimod et al., 2013);
- Ropes are stressed by homogenous distributed loads;
- Longitudinal ropes are modeled considering an arch deformation shape (Figure 13).

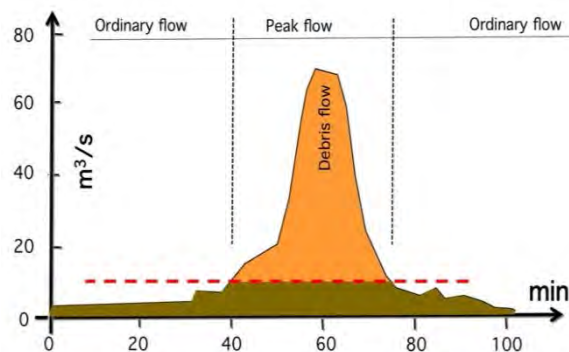


Figure 8 – Correlation between the flow-discharge vs. the duration of the debris flow event. Debris flow barriers should mainly cut the peak of the solid transportation



Figure 9 – Example of a creek subjected to debris flow composed of big boulders (Ciamosseretto torrent, Italy)

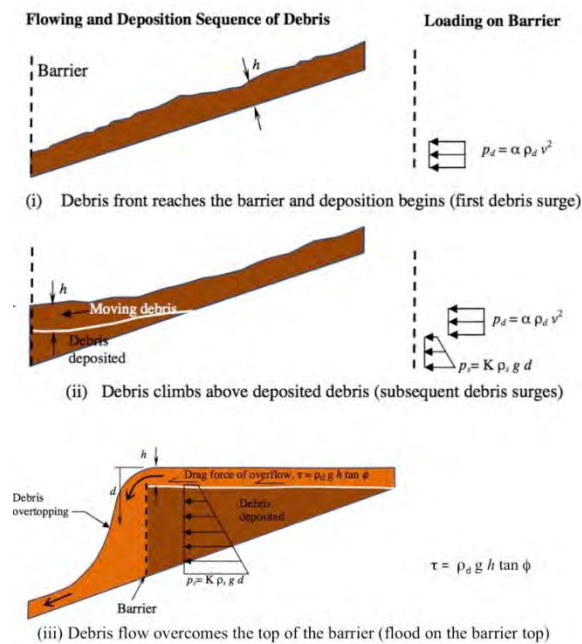


Figure 10 – Flowing and deposition sequence of debris and loads acting on the debris flow barrier (after Sun et al., 2011). The symbols have the following: d = distance between the top surface of the accumulated material against the barrier and the analyzed point; v = velocity of the debris flow at the impact; h = constant height of the debris flow surge; k = coefficient of earth pressure (typical range 0.5 to 1.0); g = gravity acceleration; α = empirical coefficient of dynamic load (according to GEO, 2011: $\alpha = 2$); ρ_d = density of the debris flow; ϕ : friction angle of the debris flow surge.

Calculation approach

The calculation of a debris flow barrier is related to:

1. The action (pressure) acting against the barrier;
2. The resistance of the structure.

The pressure acting against the barrier can be estimated in accordance with the principles previously described. This part of the design is the most uncertain, and it may introduce several errors in the calculation.

The barrier resistance can be estimated according to structural principles, which are totally independent from the rheological and hydraulic aspects of the debris flow. The barrier is designed considering the dynamic, the static and the drag load acting on it (Figure 10). These loads can be developed by any kind of body as long as the body is deformable. Such consideration on one hand clarifies that the full scale tests on these fences could be carried out with any deformable body with or without water; on the other one, it evidences that these structures are suitable to withstand the motion of bodies constituted by debris, shallow landslide, mud flow, debris flow and so on. On the contrary, the impact of a rigid body (as per ETAG 027 guideline) that develops higher stress than the deformable body being equal the energy level, cannot help to predict the deformations of the barriers.

However, the structural design has to consider that the pressure is not uniformly distributed on the screen, because it depends on the history of the static and dynamic loads moving from the bottom to the top of the barrier (GEO, 2011; Huang et al, 2007; Lo, 2000; Sun et al., 2011; Sun et al., 2012). In other terms, the calculation must assume that each longitudinal rope is subjected to a distributed load that varies its intensity during the time of the debris flow event. Therefore, the calculation process results to be quite complex.

The conceptual solution is represented by the flow chart of figure Figure 11, where the results obtained for each rope level are stored and processed in order to define the maximum axial load acting on each transversal rope.

The solution considers that each longitudinal transversal rope of the barrier is composed by coupling one deformable element (energy dissipaters) and one non-deformable element (steel ropes). Due to the deformation of the brake, the stress on the ropes is reduced. According to the graph of figure 12, the energy dissipater device constantly deforms until the axial force on the rope reaches the maximum force applied on the energy dissipater. The maximum load T_{max} acting on the generic rope i^{th} can be calculated:

$$T_{\max(i)} = (V_{(i)}^2 + H_{(i)}^2)^{1/2} \quad [1]$$

Where: V_i and H_i are the maximum loads acting on the generic rope i^{th} respectively in the directions parallel and transversal to flow direction (Figure 13). They are defined as following:

$$V_{(i)} = q_{d(i)} \cdot L_{(i)} / 2 \quad [2]$$

$$H_{(i)} = q_{d(i)} \cdot L_{(i)}^2 / (8 \cdot f_{\max(i)}) \quad [3]$$

A non-linear analysis must be performed in order to define the axial force developed on the different longitudinal rope levels.

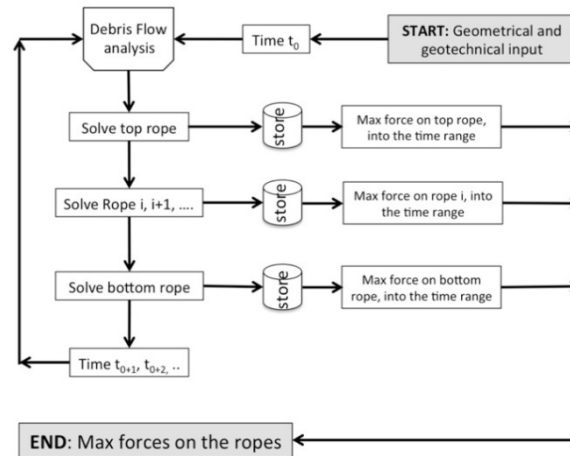


Figure 11 – Conceptual solution to calculate the forces acting on the transversal ropes

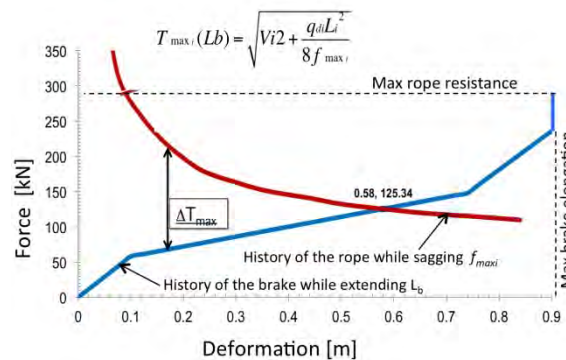


Figure 12 – Load VS deformation on the transversal rope. The calculation has to minimize force-gap ΔT_{\max} , between the dissipater (blu line) and the rope (red line). The value of T_{\max} depends on f_{\max} , which is a function of T_{\max} . Therefore an iterative process is needed to solve the problem. When the elongation of the brake reaches the maximum elongation, the force grows vertically up to the max rope resistance.

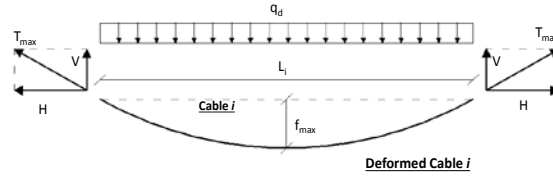


Figure 13 – Plan view with the forces acting on the generic deformed rope-*i*th; q_d = pressure of the debris flow; L_i = width of the generic rope before deforming; f_{max} = maximum sag of the generic rope.

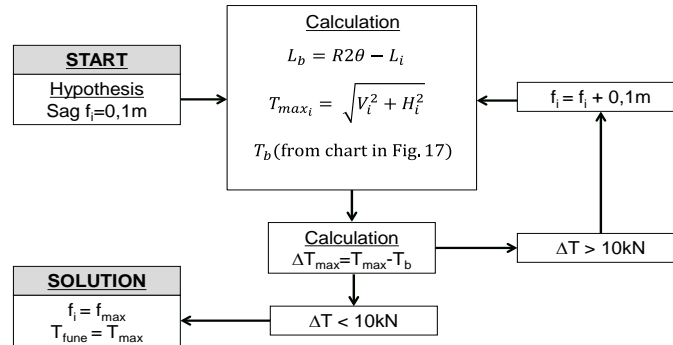
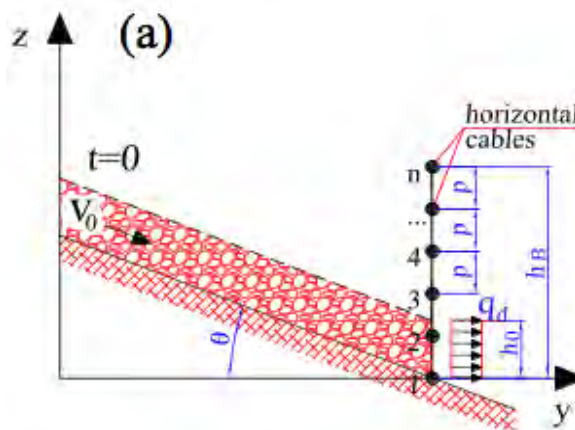


Figure 14 – Conceptual solution solving the non-linear problem of the equilibrium between forces of rope and energy dissipater. R is the curvature radius of the sag (see also figure 13). symbols: $\theta = \arcsin(L_i/2R)$, L_b = brake elongation (see also figure 17).

At each stage of the run-up mechanism, an interactive model evaluates the axial force acting on the rope-brake system (Figure 14). The process ends when the force acting in the rope reaches the equilibrium with the deformation of the energy dissipater.



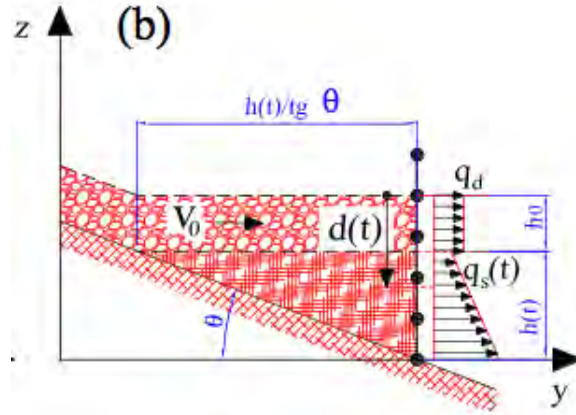


Figure 15 – Debris accumulation against the debris flow barrier and corresponding loads at the generic instant time (Segalini et al., 2012; Canelli et al., 2012)

At any time of the event (t), the static pressure acting at the depth d , measured from to the top free surface of the debris flow, can be assessed through the following relation (Figure 15) (Segalini et al., 2013; Canelli et al., 2012):

$$q_s(d) = k \cdot d(t) \cdot \rho_d \cdot g = k \cdot (h_0 + h(t) - z) \cdot \rho_d \cdot g \quad [4]$$

The spacing between the ropes can be described as:

$$q_s(d) = k \cdot d(t) \cdot \rho_d \cdot g = k \cdot (h_0 + h(t) - z) \cdot \rho_d \cdot g \quad [5]$$

Where h_B is the height of the debris flow barrier and n is the number of rope levels.

Furthermore, the pressure load acting on the i -th longitudinal rope depends on the load sequence according to figures 10 and 15:

$$z_i = h_B \cdot (i - 1) / (n - 1) \geq h_0 \quad [5]$$

Where (figure 15) i = number of analyzed level; z_i = level of the generic rope, h_0 = constant height of the debris flow, h_b = total height of the barrier. Therefore, it is possible to define the distributed load (q_d) acting against the barrier

$$q_t(z_i, t) = q_t(d, t) = \begin{cases} p \cdot q(z_i, t) / 2 & i = 1, n \\ p \cdot q(z_i, t) & 2 \leq i \leq n-1 \end{cases} \quad [7]$$

Where p = vertical distance between the horizontal cables according to figure 15 (a). Once the distributed load (q_d) for each rope (i) has been calculated, the resulting maximum tensile load (T_{max}) has to be assessed for each rope level. This value strictly depends on the length of the longitudinal rope (L_i) and its maximum displacement (f_{max}) (Figures 13 and 15).

In conclusion, the different level of ropes and lateral anchors can be designed using the force $T_{max}(i)$. The elements of the debris flow barrier must be fit to guarantee a defined minimum safety factor.



Figure 16 – Lateral view of the flexible debris flow barrier impacted during the full scale test carried out by the University of Parma in cooperation with Maccaferri

Calculation of the calculation model

The calculation model has been calibrated based on the research carried out by the University of Parma and Maccaferri (Segalini et al., 2013; Canelli et al., 2012; Ferrero et al., 2010). These studies were based on laboratory and full-scale tests (Figure 16), as well as analytical and numerical models.

It was possible to underline the following aspects:

- The energy dissipaters assume a basic function for efficiency of the debris flow barrier. In fact, they are suitable to: maintain the longitudinal ropes properly aligned, reduce the stresses acting on the ropes, and allow the barrier deforming during the event. The functionality of these elements can be taken into account through the design process only if there is a proper knowledge of their behavior. Therefore, the brakes must be always manufactured and tested in order to guarantee high performances (Figure 7) and be able to describe their behavior with Force - Displacement diagrams (an example in Figure 17).
- The barrier does not homogeneously deform along its height (Figure 18). During the history of the loading process different displacement can occur depending on the rope level analyzed (Figure 19). The intensity of these deformations are related to structural factors (length of longitudinal transversal ropes, properties of the energy dissipaters devices) and to the debris flow history (Figure 2), which is basically described by the height of the debris flow waves, and by the rheological properties.
- According to the previous point, it is not possible to define a direct proportion between the load acting on the barrier and its deformation (Figure 18).
- The dynamic load is almost always greater than the static one (Figure 20). A small increasing of the debris flow velocity gives a large increase of the load on the ropes.

- According to the previous point, it is not possible to define a direct proportion between the load acting on the barrier and its deformation (Figure 18).
- The dynamic load is almost always greater than the static one (Figure 20). A small increasing of the debris flow velocity gives large increasing of the load on the ropes.

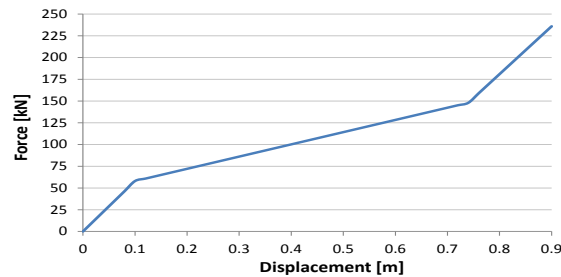


Figure 17 – Example of a typical diagram force – displacement of an energy dissipater device. The elongation of the brake L_b represents the elongation of the rope

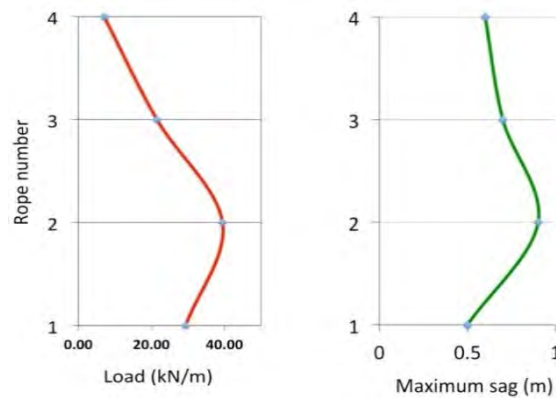


Figure 18 – Results of an impact analysis. Left: maximum load acting on the longitudinal transversal ropes, in terms of kN/m. Right: maximum sag (displacement) of the screen, in terms of m

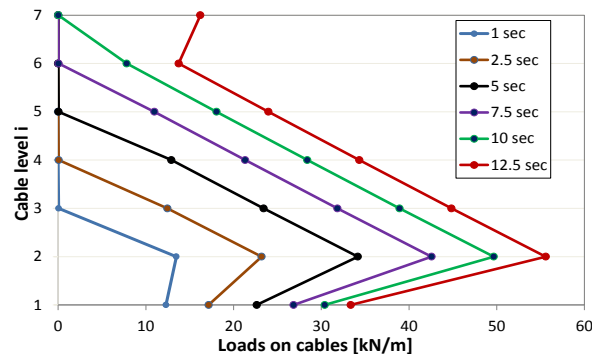


Figure 19 – Maximum distributed load (kN/m) acting on different levels of the transversal ropes while the debris flow is rising up, from the first impact (left line) to the filling of the barrier (right line)

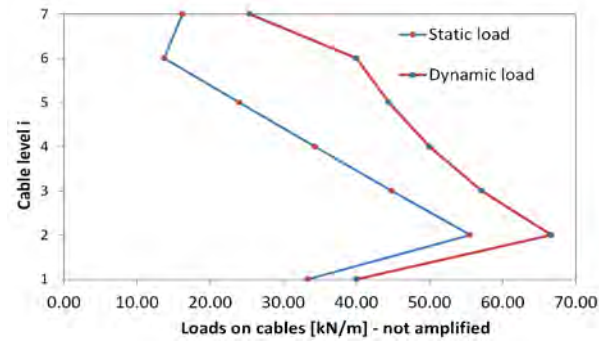


Figure 20 – Maximum distributed load (kN/m) acting on different levels of the transversal ropes related to the static load (left - blue line) and the dynamic (right - red line)

CONCLUSION

The simplified analytical solution presented to design flexible debris flow barrier synthesizes the pragmatic approach developed by the Geological Office of Hong Kong and the accurate researches carried out by the University of Parma in cooperation with Maccaferri. These studies, based on laboratory and full-scale tests, as well as analytical and numerical models, were performed in order to understand the behavior of a flexible barrier impacted by a debris flow. Thanks to these investigations, the simplified calculation approach presented here has been defined and validated. The simplified analytical approach solves the non-linear problem of the load-displacement on the transversal ropes and allows quick reliable results without time-consuming numerical approaches (i.e. FEM). The implemented algorithm shows that a small error in evaluation of the behavior of the energy dissipater's devices leads to results very different from the reality. Thus, the design of the longitudinal ropes, and consequently of the lateral anchors, may be inappropriate. The calculation approach has been successfully used in several projects around the world.

It must be underlined that at present the main factor of uncertainty affecting the barrier design is due to the estimation of the debris flow pressure. However, further research has been undertaken on this matter.

REFERENCES:

- Conference Proceedings

1. Canelli, L., Ferrero, A.M., Migliazza, M., Segalini, A. 2012. Debris flow risk mitigation by the means of rigid and flexible barriers—experimental tests and impact analysis. *Nat. Hazards Earth Syst. Sci.* 12: 1–7 (www.nat-hazards-earth-syst-sci.net/12/1/2012/doi:10.5194/nhess-12-1-2012).
2. Cantarelli, G., Giani, G.P., Gottardi G., and Govoni L. 2008. Modeling rockfall fences. *The First World Landslide Forum*: 103-108. United Nations University. Tokyo.
3. Cruden, D.M., and Varnes, D. J. 1996. Landslide types and processes. *Turner A.K.; Shuster R.L. (eds) Landslides: Investigation and Mitigation*. Transp Res Board, Spec Rep 247, pp 36–75.
4. Ferrero, A.M., Giani, G.P., Segalini, A. (2010). Numerical and experimental analysis of debris flow protection fence efficiency. *Proc. European Rock Mechanics Symposium (Eurock 2010)*, Lausanne, CH. Balkema, Rotterdam: 578–578
5. GEO. 2011. Design Requirements for Flexible Debris-resisting Barriers. *Geotechnical Engineering Office, Civil Engineering and Development Department*. The Government of the Hong Kong Special Administrative Region (Draft as at 12.10.2011)
6. Grimod A. and Giacchetti G. 2013. High energy rockfall barriers: a design procedure for different applications. World Mining Congress, Montreal, August 2013
7. Huang, K., Yang, C., and S.W. Lai, S.W. 2007. Impact force of debris flow on filter dam, *Abstracts, Vol. 9, 03218, 2007 S Ref-ID: 1607-7962 /gra / EGU2007-A-03218 European Geosciences Union 2007*

- Journal

1. Hungr, O., Evans, S.G., Bovis, M., and Hutchinson, J.N. 2001 *Review of the classification of landslides of the flow type. Environmental and Engineering Geoscience*, VII, 221-238.
2. Hungr, O., McDougall S., and Bovis, M. 2005. Debris-Flow Hazards and Related Phenomena. *Jakob, M. and Hungr, O., Eds., Praxis-Springer, Berlin. Heidelberg, 2005. Chapter 7.*
3. Lo, D.O.K. 2000. Review of Natural Terrain Landslide Debris-resisting Barrier Design. *GEO Report No. 104*. Geotechnical Engineering Office, 91 p
4. Pierson, T.C., 1986, Flow behaviour of channelized debris flow, Mount. St. Helens, Washington. In: A.D. Abhrams (ed). *Hillslope process*(pp.269-296). Allen Unwin, Boston
5. Segalini, A., Brighenti, R., Ferrero, A.M., Umili, G. 2013. Comparison between the mechanical behavior of barriers against rock fall vs debris flows. *Rock Mechanics for Resources, Energy and Environment – Kwasniewski & Lydzba (eds) - 2013 Taylor & Francis Group, London, ISBN 978-1-138-00080-3*
6. Shun, O., Hiroshi, I., Yshiharum, I., Takaahi, Y., 1997. Development of new methods for countermeasures against debris flow. In: - *Recent developments on debris flows Armanini and Masanori (eds.)*

7. Sun, H.W. and Law, R.P.H. 2011. Design Requirements of Flexible Debris-resisting Barrier. A Note on the Key Design Requirements of Force Approach. *Geotechnical Engineering Office, Civil Engineering and Development Department*. The Government of the Hong Kong Special Administrative Region
8. Sun, H.W. and Law, R.P.H. 2012. A preliminary study on impact of landslide debris on flexible barriers. *Geotechnical Engineering Office. Standard and Testing Division. Technical Note 1/2012*. The Government of Hong Kong Special Administrative Region
9. Takahashi, T. 1991. Debris flow. *IAHR Monograph*, A.A. Balkema, Rotterdam, 165 pp

Estimation of Cambridge Argillite Strength Based on Drilling Parameters

Evan Lonstein¹, Jean Benoît², Stanley Sadkowski, P.E.³ and Kevin Stetson, P.E.³

¹*GZA Geoenvironmental, Inc., Portland, ME, USA (formerly graduate student at the University of New Hampshire)*

²*University of New Hampshire, Department of Civil Engineering, Durham, NH, USA*

³*Sanborn, Head & Associates, Inc., Westford, MA, USA*

ABSTRACT:

This paper presents the results from extensive laboratory strength testing of bedrock samples from the Boston, Massachusetts area, and provides correlations to drilling parameters recorded during the coring process. Results from unconfined compressive strength testing, splitting tensile strength testing (using the Brazilian test), and the point load test method were compared to the recorded drilling parameters and calculated compound parameters such as the Somerton Index and the Drilling Energy. The rocks tested were mostly Cambridge argillite with some diabase, basalt, and sandstone. The objective of this paper is to demonstrate that measurements while drilling (MWD) can provide designers of deep foundations with a better approximation of the strength of the bedrock matrix by correlating drilling parameters to more conventional laboratory test methods, and field measurements such as rock quality designation, with potential for more efficient, reliable, and cost-effective foundation designs.

1 INTRODUCTION

A subsurface exploration program for the design and construction of a 21-story building in Boston, Massachusetts included a series of eight boreholes drilled in rock down to depths of 47 m to 54 m. The foundation for this building consisted of drilled caissons 2.4 to 3 m in diameter, socketed into rock. Column design loads ranged from 17,800 to 42,260 kN. The 50-mm diameter cored boreholes were drilled using rotary techniques with 101.6 and 127-mm inside diameter flush-jointed casing and water as the drilling fluid. Rock coring was performed at each location using an NX-sized split core barrel. This provided approximately 14 to 21 m of bedrock cores consisting of Cambridge argillite, diabase, sandstone, and basalt.

Drilling parameters were recorded for each boring using a drill rig equipped with a measurements while drilling (MWD) system. These parameters were an integral part of the rock characterization and the design of the caisson rock sockets.

The MWD system consisted of in situ recordings for every 5 mm of drilling in terms of advance rate, thrust pressure, torque, rotation rate and, drilling fluid pressure and flow rate. Using these measurements, compound or combination expressions of drilling parameters were used to assist in the data interpretation. The MWD system can identify stratigraphy and weak or fractured zones within the bedrock and help support conventional descriptive methods such as core logging. These visual observations described the lithologic variability, degree of weathering, rock structure and the rock quality designation (RQD).

Using MWD measurements proved to be invaluable in the design of the caissons. Comparison of the MWD data with logging techniques and the RQD allowed differentiation between natural breaks and drilling breaks caused by either the action of drilling or core

extraction. Consequently, the lengths of the caissons were reduced by approximately 50% leading to a substantially more cost effective design (Sadkowski et al., 2008).

During the design phase for the caissons, a limited number of laboratory compressive strength tests were performed on some of the rock cores. Following design and construction of the building, an independent testing program, as part of a Masters Project at the University of New Hampshire (UNH), was undertaken using the rock cores to develop a relationship between compressive and tensile strengths and, drilling parameters. The cored rocks were cut, prepared and tested in accordance with ASTM standards. Samples were then tested by the Unconfined or Uniaxial Compression Test (UCT), the Splitting Tensile Test (STT) or Brazilian Test, and the Point Load Test (PLT). The strength was determined for each tested sample and correlated to the drilling parameters recorded in situ at the appropriate depths. Based on these results, relationships between strength and the drilling parameters were developed for each rock type. This paper presents the results of the laboratory tests and the ensuing correlations.

2 SITE GEOLOGY

The subsurface conditions at the site consist of 32 to 35 m of unconsolidated material overlying bedrock. Below a 2.1 to 4.6 m layer of fine to coarse miscellaneous debris (asphalt, ash, brick, glass, concrete, and wood) is 0.3 to 1.5 m of peat followed by a thick layer of marine clay with a thickness of 9 to 15 m. Overlying the bedrock is 10 to 19 m of glacial deposits. Groundwater table height ranged from 1.4 to 5 m below ground surface.

The bedrock found in the eight borings across the site consisted of an overlying layer of highly weathered rock ranging in thickness from 0.3 to 2 m. The bedrock is predominantly Cambridge argillite with diabase, sandstone and basalt intrusions at some of the boring locations. The argillite is soft to medium hard, slightly to severely weathered, sound to extremely fractured,

light gray, aphanitic rock with shallow to steeply dipped bedding, with very close partings along bedding planes. The rock quality designation (RQD) was calculated on-site and was typically 40 to 50 percent ranging from 0 to 90 percent. According to Barosh and Woodhouse (2011/2012) the Cambridge argillite is a slightly metamorphosed rock part of the Upper Proterozoic system with an age estimated to be between 457 and 1,600 million years. The argillite is also part of the Boston Bay Group and is the most widespread rock type in the Boston area especially in downtown Boston. Diabase was found in four of eight borings and is moderately hard, slightly to moderately weathered, slightly to moderately fractured, greenish gray, fine grained rock with closely spaced joints, moderately dipping to vertical. The RQD was typically 30 to 50 percent and ranged from 11 to 57 percent. Sandstone was encountered in three of eight borings and is moderately hard, slightly weathered, sound to moderately fractured, light gray, fine grained rock with joints that are closely spaced, moderately dipping to vertical. The RQD was typically 60 to 70 percent and ranged from 30 to 74 percent. Basalt was also encountered in two of eight boreholes and is moderately hard, slightly to moderately weathered, extremely fractured, greenish dark gray, and aphanitic. The RQD was 0 percent.

3 DRILLING PARAMETERS

Measurements while drilling are computerized systems which monitor sensors installed on standard drilling equipment. These sensors continuously collect data on drilling without interfering with the drilling process. The MWD system collected data such as depth, time, drilling (advance) rate, rotation rate, down force, torque, water pressure, and mud pressure. The MWD system used for this project was a Jean Lutz CL88n recorder installed on a Failing Stratastar 15 truck-mounted drill rig. The drilling data is digitally displayed in real time to help

the driller with the drilling progress and maximize the quality of the rock cores. The data is also stored electronically for further analysis.

The MWD system can be used to indicate changes in lithology and fractures in the bedrock. For example, under constant down force and rotation rate, a change in drilling (advance) rate and/or torque could suggest a joint, a fracture or a void/cavity in the rock.

Several methods of interpretation have been developed using compound parameters. These parameters combine individual parameters into expressions that reflect the resistance of rock to drilling. Table 1 presents two of the compound parameters that were used in this study: the Somerton Index (Somerton, 1959) and the Drilling Energy (Pfister, 1985).

Table 1: Compound Parameters used for MWD Analysis in this Study

Name	Equation	Units	Reference
Somerton Index	$S_d = P \sqrt{\frac{\omega}{V}}$	Unitless	Somerton, 1959
Drilling Energy	$W = \frac{T\omega}{V}$	KJ/m	Pfister, 1985

P= down force (KN), ω = rotation rate (rpm)

V = drilling (advance) rate (m/hr for Somerton or m/min for Drilling Energy)

T = torque (KJ).

The Somerton Index was developed through a series of laboratory drilling tests in concrete specimens. The Index gives an indication of rock resistance. It uses advance rate,

rotation rate, and down force. Drilling Energy is the amount of energy needed to penetrate or destruct a medium. It uses drilling (advance) rate, rotation rate, and torque. Both of these compound parameters are indicative of rock hardness and, therefore, strength.

4 ROCK TESTING

A series of tests were carried out at the University of New Hampshire in an effort to develop correlations between rock drilling parameters and laboratory strength tests. The tests performed were the Unconfined or Uniaxial Compression Test (UCT), the Splitting Tensile Test (STT) or Brazilian Test, and the Point Load Test (PLT). The UCT is designed to find the uniaxial or unconfined compressive strength (UCS or q_u) of intact rocks while the Splitting Tensile Test (STT) determines the tensile strength (σ_t). The PLT is an index test used to correlate its strength index to compressive and tensile strengths. Table 2 summarizes the number of laboratory tests performed at UNH for this study.

Intact specimens were identified for testing in the core boxes based on available lengths and core quality. According to ASTM D7012-10 “Uniaxial Compression Test”, a length to diameter ratio of 2.0 to 2.5 is required for the UCT. Only the cores that were greater than ten centimeters could be used for this test. Each specimen was prepared to pass parallel and shape conformance according to ASTM D4543-08 “Preparing Rock Cores”. Every intact rock core that met these requirements was tested for unconfined compressive strength. As shown in Table 2, a total of 53 samples were tested for compressive strength. An Instron compression testing machine was used to load the samples at a loading rate of 0.5 MPa/s until failure. The output data from the tests were used to identify the load at failure or the peak load to calculate the strength as well as the static elastic modulus.

Table 2: Summary of Laboratory Strength Tests

Rock Type	Avg. RQD	UC Test	Tensile Test	Point Load Test
		<i>Number of Tests</i>		
Argillite (UNH)	40-50	28	38	35
Diabase (UNH)	30-50	15	13	6
Sandstone (UNH)	60-70	10	5	2
Argillite (other sources)	-	49	-	38

The Splitting Tensile Test (STT), or the Brazilian Test, uses a thin disk loaded on its side allowing the sample to split in tension in a direction perpendicular to the loading. The required thickness to diameter ratio is 0.2 to 0.75 according to ASTM D3967-08 “Splitting Tensile Strength Test”. The cores that could be cut to 1.0 cm to 3.75 cm in thickness were used for this test. These also had to be prepared in accordance to ASTM D4543-08. A total of 56 samples were tested also using the Instron compression testing machine but loaded at a slower rate of 0.1 MPa/s until failure. The output data for this test yielded the peak load for the determination of the tensile strength.

The Point Load Test (PLT) uses steel cones above and below a test specimen to develop a tension crack parallel to the axis of loading. According to ASTM D5731-08 “Standard Test Method for Determination of the Point Load Strength Index of Rock and Application to Rock Strength Classifications”, the samples are required to have a length to diameter ratio greater than 1.4. Consequently, the samples considered had to be longer than 7.0 cm. The samples were aligned in accordance with ASTM D5731-08 for the isotropic conditions of the Cambridge argillite. From the PLT, an Index is obtained from which the compressive and tensile strengths

can be estimated empirically. Table 3 shows the formulations used to determine strengths for all tests.

Table 3: Unconfined and Tensile Strength Expressions

Name	Equation
Unconfined Compressive Strength	$q_u = \frac{P}{A}$
Splitting Tensile Strength	$\sigma_t = \frac{2P}{\pi dt}$
Point Load Strength Index	$(I_s)_{50} = \frac{P}{D^2}$

q_u = unconfined compressive strength

σ_t = tensile strength

P = peak load

D and d = core diameter

t = thickness

A = cross-sectional area of core

$(I_s)_{50}$ = point load strength index normalized to a 50 mm diameter core

5 RESULTS

Laboratory Strength Testing

A total of 53 tests were performed at UNH to determine the unconfined compressive strength (UCS) on the various rock types. Figure 1 shows the UCS results with respect to depth for the UNH results as well as the results from 49 other tests reported in the literature and conducted by GEI Consultants, Inc. and Haley & Aldrich, Inc. from the Central Artery/Tunnel Project in Boston, Massachusetts. All of the samples from those tests were referred to as gray argillite and were assumed to be from the same formation as the Cambridge argillite that was tested at UNH. As illustrated on Figure 1, there appears to be a trend indicating a slight increase in strength with depth for the sandstone, the diabase and the argillite. For the combined UNH Cambridge argillite and the argillite from other sources, the increase can be quantified as approximately 0.4 MPa/m. The compressive strength of the Cambridge argillite ranged from 12.5 to 42.5 MPa for those test depths.

Woodhouse and Barosh (2011/2012) report engineering properties as shown in Table 4 for the Cambridge argillite for the Boston area. The results are given in terms of unit weight, unconfined compressive strength and tangent modulus at 50%. Woodhouse and Barosh (1991) also characterize the argillite as having extremely variable engineering properties. They state a mean value of unconfined strength of 130.9 MPa with a range from 34.8 to 259.9 MPa. The depths for the results presented in Table 4 were not given.

A total of 56 specimens were tested using the Splitting Tensile or Brazilian test to determine the tensile strength. Figure 1 also compares the tensile strength with depth where an increasing trend is observed for the argillite and the diabase. However, from the limited number of tests on the sandstone, a reverse trend is shown with the deepest rock having lower strength.

More extensive testing is needed to support this observation. The tensile strength ranged from 1.73 to 8.20 MPa. The average values of tensile strength for the Cambridge argillite is 4.73 MPa, the diabase is 8.37 MPa, and the sandstone is 8.47 MPa.

Table 4: Engineering Properties of the Cambridge Argillite (from Woodhouse and Barosh, 2011/2012)

Location & Rock Type	Unit Weight (kg/m ³ ; pcf)§§				Unconfined Compression f_c (N/m ² ; psi)§§				Tangent Modulus E_{150} (N/m ² ; psi)§§			
	Low	Average	High	No. Tests	Low	Average	High	No. Tests	Low	Average	High	No. Tests
Dorchester Tunnel* Argillite	2,691 168.0	2,747 171.5	2,810 175.4	15	34,480 5,000	103,430 15,001	236,840 34,350	15	39,990 5,800	62,740 9,100	84,120 12,200	15
MBTA Red Line Extension** Argillite	2,538 158.4	2,747 171.5	2,844 177.5	52	41,990 6,090	131,420 19,060	255,120 37,000	50	20,690 3,000	47,580 6,900	63,430 9,200	18
MBTA Red Line Extension** Melaphyric Dike Rocks***	2,606 162.7	2,738 170.9	2,861 178.6	12	12,620 1,830	67,570 9,800	166,860 24,200	10	14,480 2,100	24,130 3,500	31,030 4,500	3
MBTA Red Line Extension** Tuff/Trachyte§	2,518 157.2	2,739 171.0	2,884 180.0	6	29,650 4,300	103,620 15,030	250,980 36,400	6	29,650 4,300	59,300 8,600	74,470 10,800	5

Notes: Table data from Hatheway & Paris (1979).

*Data taken from Haley & Aldrich (1977).

**Data taken from Bechtel (1978).

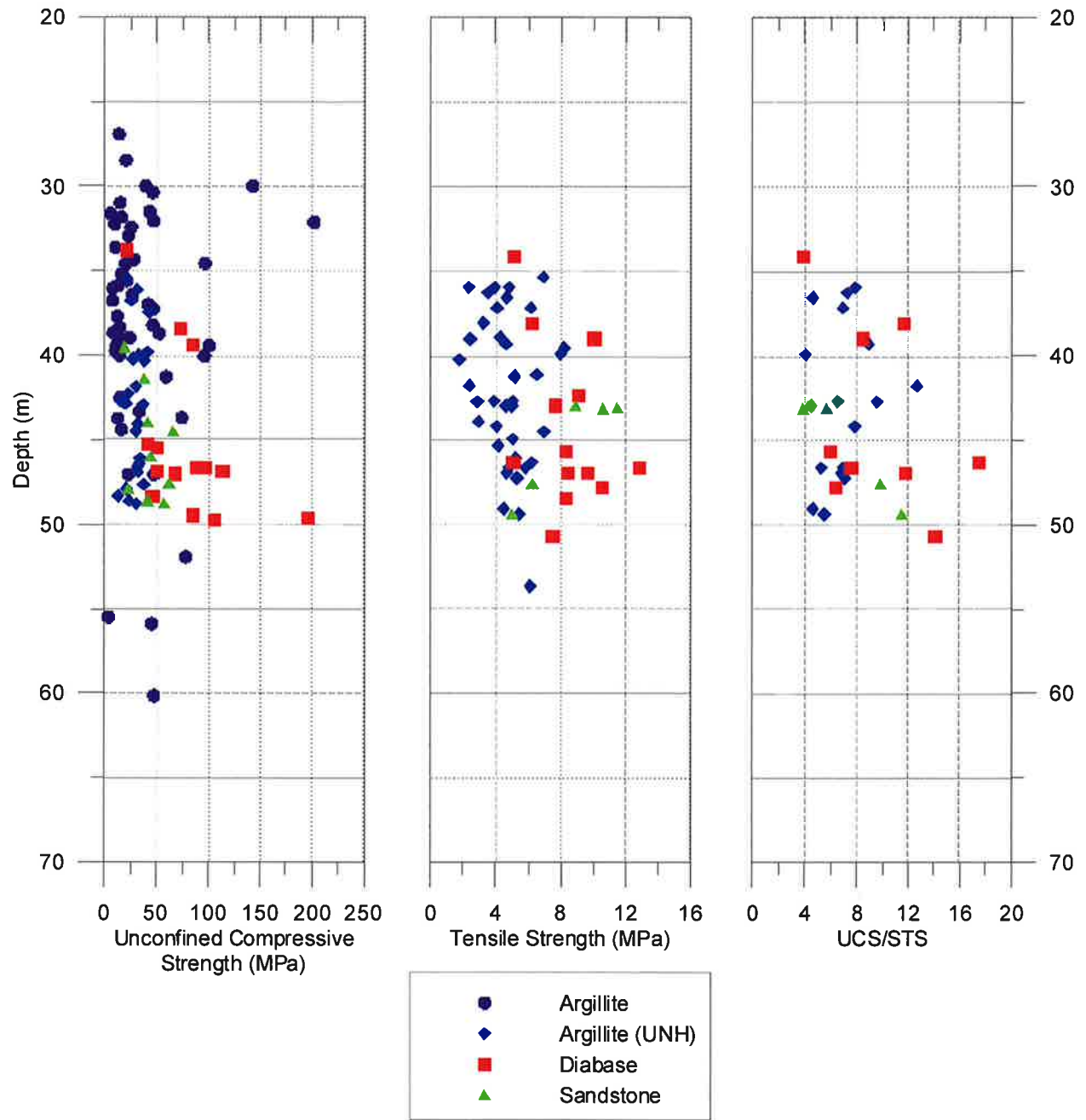
***Rock types include diabase, andesite, basalt & altered varieties of these rocks.

§ Rock previously identified as dark gray to black tuff; believed to be analogous to dark gray to black trachyte appearing as irregular sill-like intrusion in Porter Square exploration shaft.

§§ Metric units shown above English units in each data group.

Figure 1 presents the ratio of compressive to tensile strength with depth for the UNH tests. The compressive strength to tensile strength ratio ranged from 4.1 to 12.7. There seems to be an overall increasing trend even for the sandstone.

Figure 1: Unconfined Compressive Strengths (UCS), Splitting Tensile Strengths (STS), and UCS/STS Ratios for Cambridge Argillite, Diabase, and Sandstone for the Boston Area

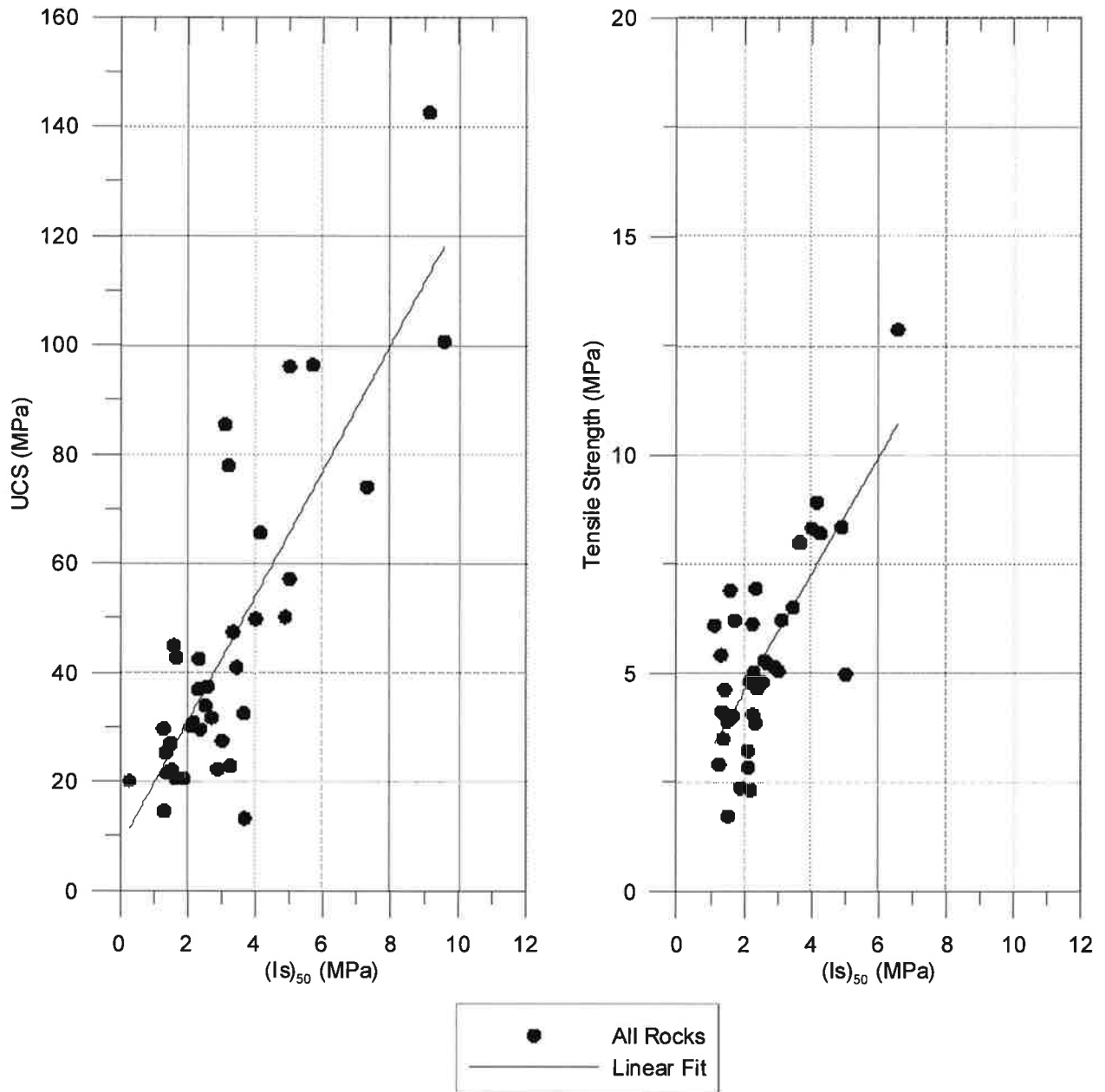


A total of 43 samples were also tested using the point load test apparatus. From this test a strength index is obtained which can be correlated to unconfined and tensile strengths. The subscript 50 refers to a sample of 50 mm used in normalizing the index. Munfakh et al. (1998) reports that the unconfined/uniaxial strength is typically 20 to 25 times that of the point load strength index with a typical value of 24 shown in most publications. The coefficient ranges from 15 to 50 for anisotropic rock conditions. Correlations to tensile strength have also been reported as $0.8 (I_s)_{50}$ (ISRM, 1985).

Figure 2 shows the unconfined laboratory strengths against the point load strength index values used to obtain the empirical correlations given in Table 5 for all rocks including the argillite tested at UNH and the argillite from the Central Artery/Tunnel Project. As expected, the linear fit for all rocks is similar to that of the argillite only since only eight other point load tests were carried out on the sandstone and diabase. The figure shows very good agreement between the UNH testing and that of the Central Artery/Tunnel Project. The figure also shows a similar correlation for the tensile strengths with the point load index for all rocks and for the argillite tested at UNH.

Using the results from this testing program, site specific point load test correlations for three of the rocks (argillite, diabase and sandstone) were developed for both UCS and tensile strength as shown in Table 5. The results from the tests done on the Central Artery/Tunnel Project are also included in the Table. These correlations were developed using unconfined and tensile strength values from the same borehole, the same rock type, and at similar depths for the point load tests and are shown as site specific. The coefficients found for the argillite on this project significantly differ from values in the literature, reinforcing the observation made by Woodhouse and Barosh (2011/2012) about the variability of this rock within the Boston area. It

Figure 2: Unconfined Compressive Strengths (UCS) and Splitting Tensile Strengths (STS) versus the Point Load Index for All Rocks Tested from the Boston Area



clearly highlights the need to develop more site-specific correlations for various rock types. In addition, in this case the accepted published coefficients significantly overestimate the strengths and thus are not conservative.

Table 5: Point Load Test Correlations Comparison

PLT Correlation	Equation
Typical q_u	$q_u = 24(I_s)_{50}$
Typical σ_t	$\sigma_t = 0.8(I_s)_{50}$
“site” specific – all rocks q_u	$q_u = 13.3(I_s)_{50}$
“site” specific – all rocks σ_t	$\sigma_t = 1.95(I_s)_{50}$
“site” specific - q_u for Argillite (UNH)	$q_u = 11.9(I_s)_{50}$
“site” specific - σ_t for Argillite (UNH)	$\sigma_t = 2.1(I_s)_{50}$
“site” specific - q_u for Argillite (Other Sources)	$q_u = 13.6(I_s)_{50}$

q_u = unconfined compressive strength

σ_t = tensile strength

$(I_s)_{50}$ = point load strength index normalized to a 50 mm diameter core

Drilling Parameters

The Somerton Index and Drilling Energy values were calculated for each of the UCT specimens at the appropriate depth intervals. Figure 3 shows the comparison between the UCS and the Somerton Index and the Drilling Energy, respectively. The rate of increase for all rocks with Somerton Index is 0.05 MPa/Index, and with drilling energy is 0.001 MPa/KJ/m. Table 6 shows average values along with the range and standard deviation for the Somerton Index, the Drilling Energy and the unconfined compressive strength for each rock type.

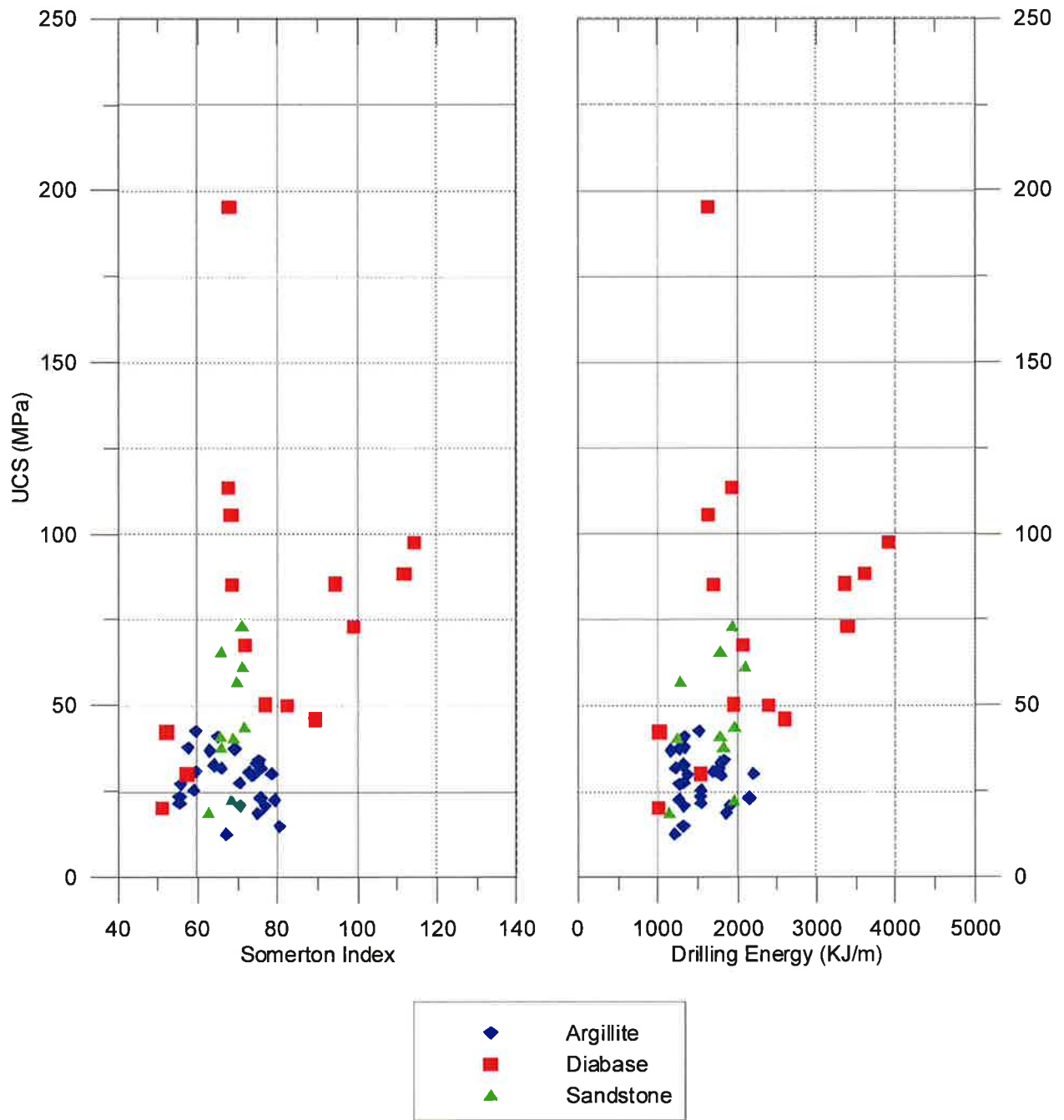
Table 6: Summary of Average Rock Data

Rock Type	Average Somerton Index	Average Drilling Energy (KJ/m)	Average UCS (MPa)
Argillite	69.0 ± 7.6	1540 ± 294	28.6 ± 7.6
Diabase	79.7 ± 19	2302 ± 909	79.7 ± 41
Sandstone	67.9 ± 2.8	1673 ± 335	43.2 ± 15
Basalt*	83.3	2426	184

*No standard deviation, since only one data point

In Figure 3, the diabase has a noticeably large range of Somerton Index values, varying from 51 to 112 with an average value of about 80. Diabase intrusions often have variable structures including vesicles, phenocrysts and segregation of grain sizes. The graph reflects the

Figure 3: Unconfined Compressive Strengths (UCS) as a function of Drilling Parameters in the Boston Area



variability of the composition of the diabase. For the sandstone the range is 63 to 72 with an average of 68. The argillite varies from 55 to 79 with an average value of 69. Overall, it can be seen that based on Somerton alone, it is not possible to identify the material type.

The figure also shows the Drilling Energy in relation to the UCS. For the argillite the range is from 1168 to 2200 kJ/m with an average of approximately 1540. For the diabase the values range from about 1015 to 3900 with an average of 2300 while the sandstone ranges from 1140 to 2100 with an average of 1675. The results show less scatter than with the Somerton Index, indicating that torque maybe a better indicator of strength than down pressure on the coring bit. Figure 4 shows the tensile strength test results with respect to the Somerton Index and the Drilling Energy. The results show an overall increasing trend but with significantly less scatter in tension than in compression, even for the diabase. Figure 5 shows graphs of unconfined compressive strengths using the point load test site specific correlations as a function of the Somerton Index and the Drilling Energy, respectively. As with the previous laboratory test results, the trends and values are similar but in this case with less scatter. Overall the results seem to suggest that tensile resistance may be a better indicator of energy required to core in these types of rocks.

Using the load-displacement curves from the unconfined compressive strength tests, static elastic modulus values were calculated and compared to the MWD compound parameters. Figure 6 shows the correlations between elastic modulus and the compound parameters. Although a significant amount of scatter is shown in the data, an increasing trend can be observed with the Somerton Index and the Drilling Energy values.

The rock quality designation (RQD) was determined on site for each core run using conventional logging techniques. Figure 7 shows the RQD with respect to depth depicting

Figure 4: Splitting Tensile Strengths (STS) as a function of Drilling Parameters in the Boston Area

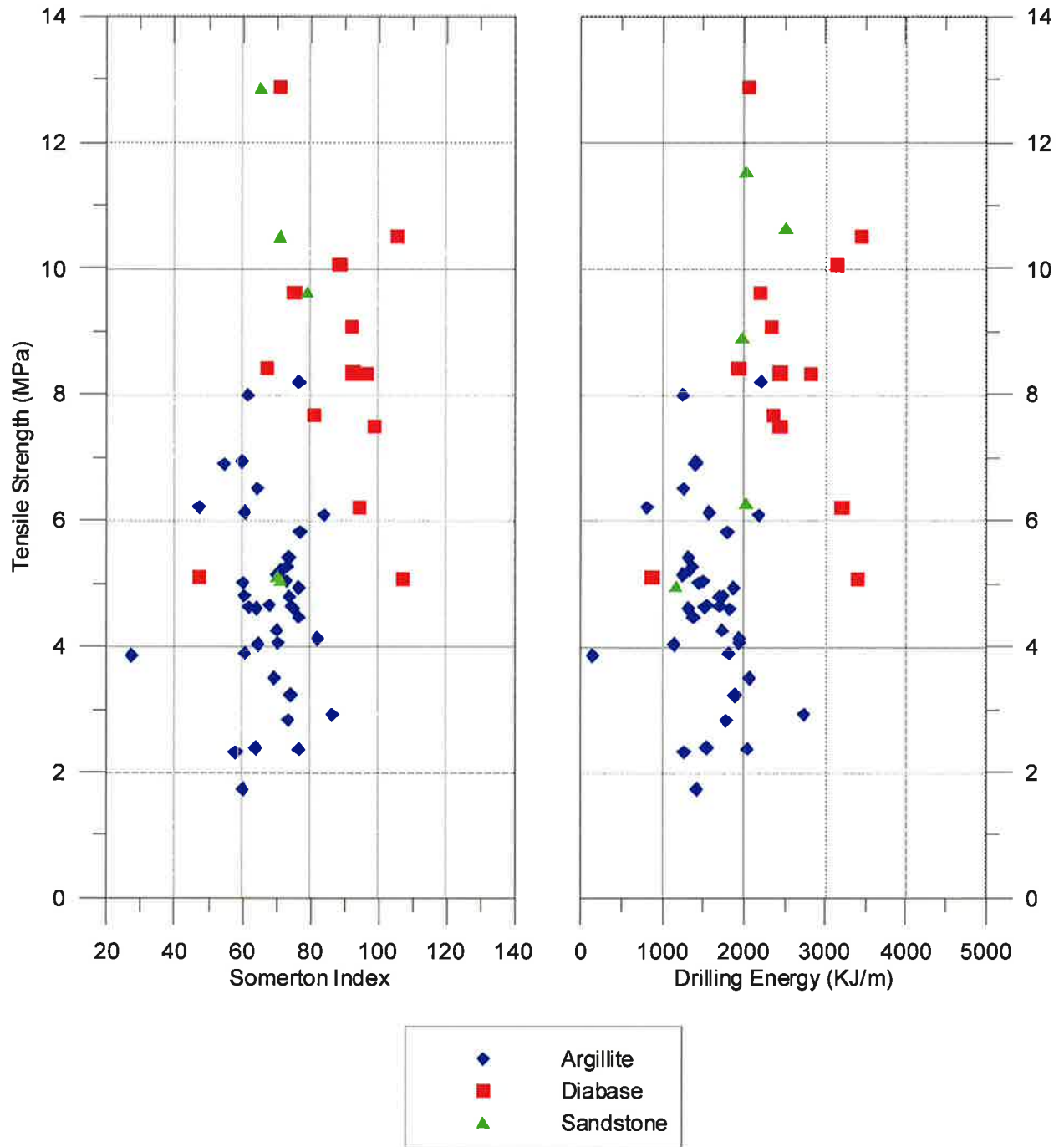


Figure 5: Corrected Point Load Strength Index as a function of Drilling Parameters in the Boston Area

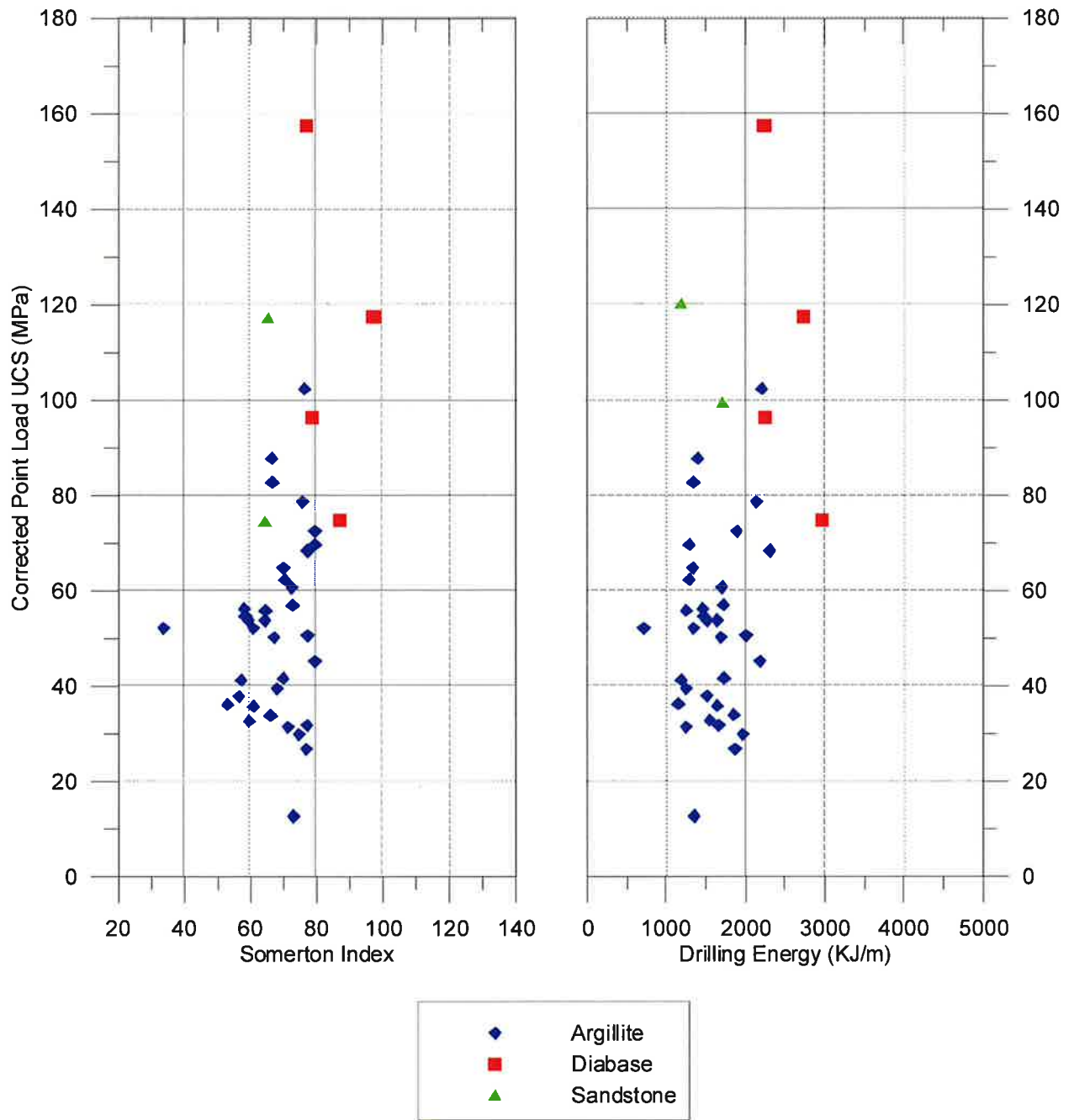


Figure 6: Elastic Modulus as a function of Drilling Parameters in the Boston Area

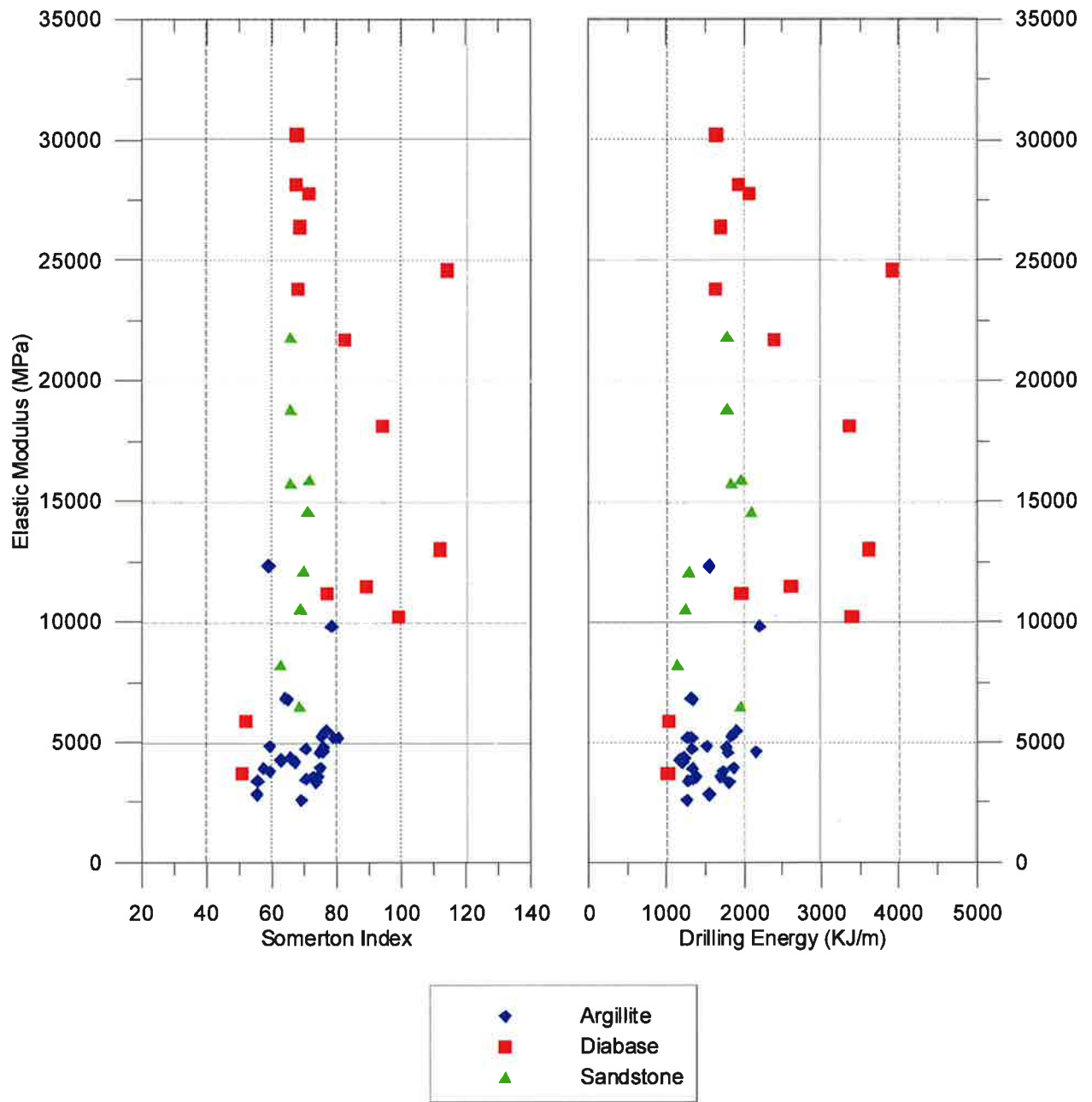
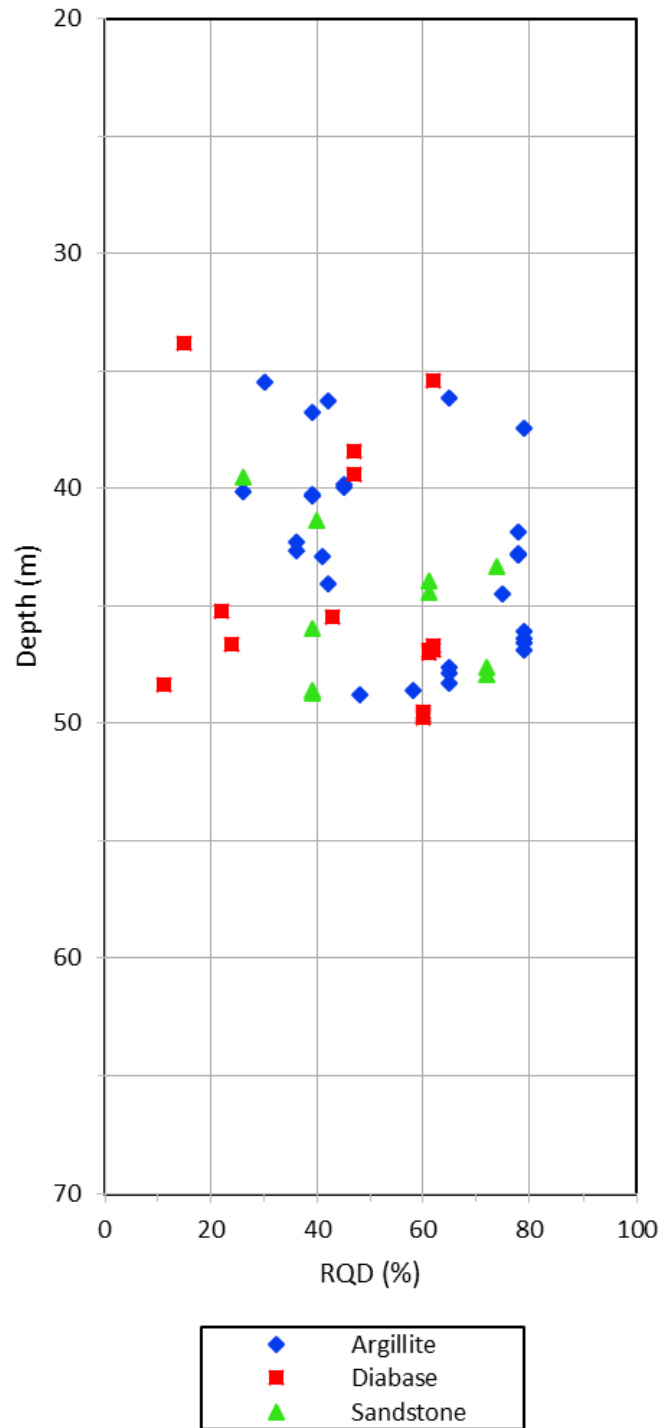


Figure 7: Rock Quality Designation (RQD) for Cambridge Argillite, Diabase, and Sandstone for the Boston Area



significant scatter without any clear trend. Because of the fragility of the argillite and its well defined bedding planes, samples obtained from the coring were thought to have numerous fractures from drilling breaks and possibly during core extraction as opposed to natural breaks. Consequently, relationships between the Somerton Index and the Drilling Energy as shown in Figure 8 provides better insight into the rock quality in situ. It can be seen that for the argillite and the sandstone there exists a linear relationship indicating a proportional increase in RQD with increases in the Somerton Index and the Drilling Energy. The results with the diabase do not show a clear trend. The sandstone also appears to be less influenced by the drilling action. It was clearly documented on this project (Sadkowski et al., 2008) that drilling parameters significantly enhanced the quality of the information which led to a more economical design based on shortened caissons. The parameters allowed differentiation between natural breaks and those induced by drilling. This is substantiated by the splitting tensile testing results and correlations with drilling parameters, which show less scatter than with the compression testing results thus suggesting rock coring in the argillite is predominantly a tensile process.

The Cambridge argillite had very distinct bedding planes that were noted before each test with respect to the horizontal axis. No significant correlation was evident and thus the orientation of the bedding planes did not seem to affect the strength in a consistent manner in this testing program. However, in cases where there was a weak zone along a bedding plane, the rock did fail along that surface, and consequently did affect the strength.

After the results were compiled, the values were then averaged for each rock type. Table 6 showed these values and Figure 9 graphs the relationships with strength against the Somerton Index and the Drilling Energy, respectively. The standard deviation is also shown in Table 6 along with the average values. The relationship between the Somerton Index and the Drilling

Energy with the UCS shows an increasing trend. A more robust relationship was found using a linear trend analysis. The R-squared values for the linear trend of the UCS vs. Somerton Index and the UCS vs. Drilling Energy on Figure 9 are 0.87 and 0.99, respectively.

All of the average strength data collected from UNH and from other projects in the Boston, MA area are shown in Table 7. Some of the values are very similar with the findings at UNH, while others are significantly different. Several factors may help to explain these differences: depth of specimens, variations in geological history and mineral composition of the rocks at various locations, and different coring or testing techniques. The Somerton Index or Drilling Energy values were not obtained for these other projects as a MWD system was not used while coring. Nevertheless, the correlations are very encouraging and accuracy of the relationships are likely to be substantially improved with additional field measurements for all rock types.

Figure 9: Average Unconfined Compressive Strength as a function of Average Drilling Parameters in the Boston Area

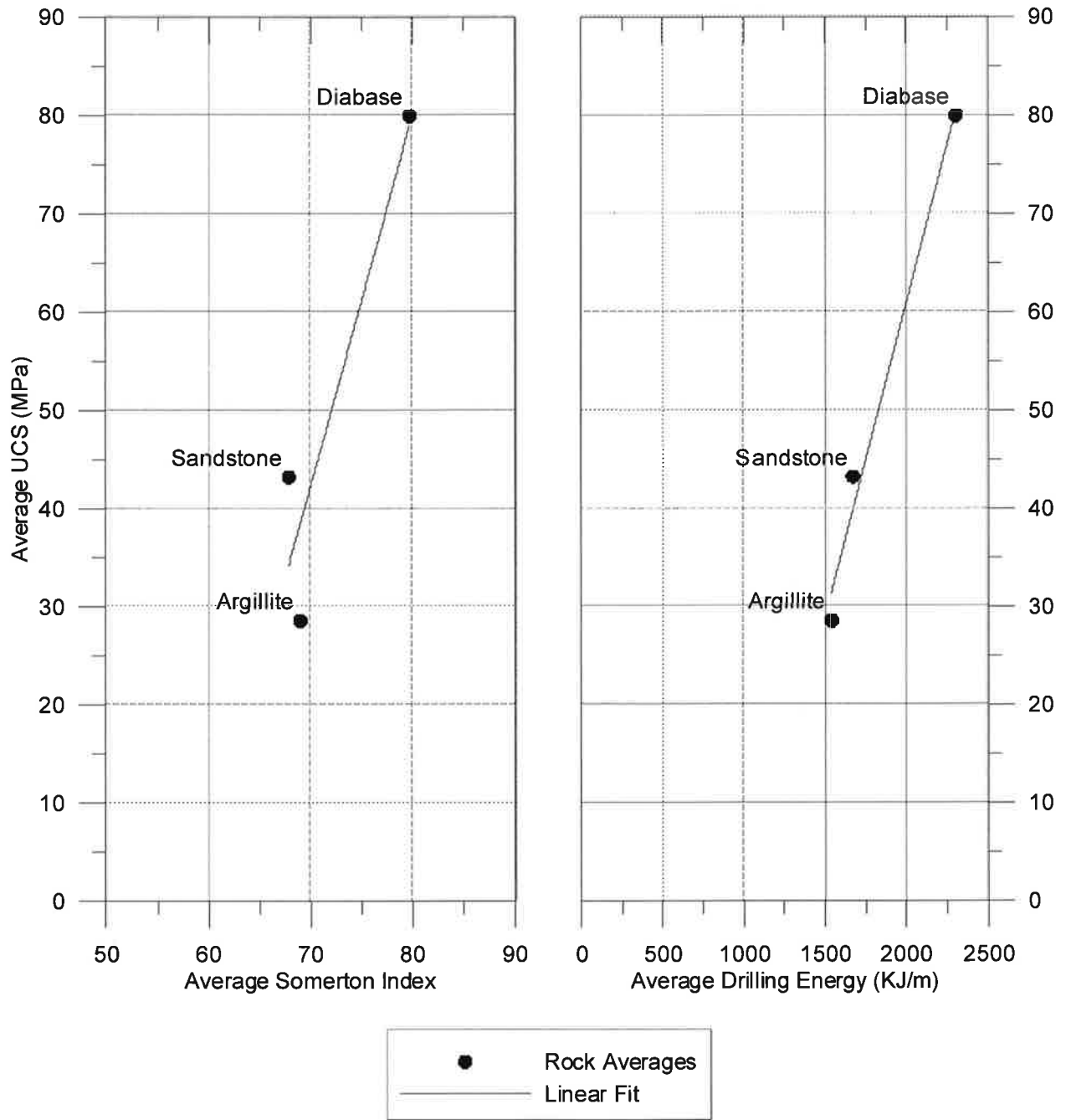


Table 7: Summary of Strength Data of Bedrocks in the Boston Area, MA

Source	Rock Type	Average UCS (MPa)	Average (Is) ₅₀ (MPa)
UNH (2012)	Cambridge Argillite	28.6	2.14
Metcalf & Eddy (1989)	Argillite	-	6.48
Sverdrup (1990)	Argillite	21.4	-
Parsons (1990)	Sandy Argillite	123.0	5.24
GEI D011A (1992)	Gray Argillite	18.6	-
GEI D015A (1992)	Gray Argillite	28.0	-
H&A D001A (1992)	Gray Argillite	33.7	3.57
H&A D004A (1992)	Gray Argillite	79.8	4.50
UNH (2012)	Diabase	79.9	5.09
Metcalf & Eddy (1989)	Diabase	-	13.7
Sverdrup (1990)	Diabase	79.3	-
Parsons (1990)	Diabase	97.9	5.62
UNH (2012)	Sandstone	43.2	3.16
Woodhouse and Barosh (2011/2012)	Cambridge Argillite	103.4 – 131.4	-

6 CONCLUSIONS

For deep foundations, the use of an MWD system could prove to be more efficient and cost effective. The MWD system used in this study provided information regarding the presence of fractures and weak zones within the bedrock. From the results of this study, it appears that reasonable estimates can be made for unconfined and tensile strength based on the MWD data.

The rock strength appears to correlate better with Drilling Energy based on torque than with the Somerton Index which is based on down force. This however could vary depending on rock type as well as drill bit type and wear condition. The Point Load Test historical empirical coefficient of 24 relating the point load strength index I_s to compressive strength was found to be too high for these rocks and thus unconservative. For this study, the values were found to be 13.3 for all rocks and 13.6 for the argillite only. Therefore, published values should be used with caution and site-specific correlations should be developed accordingly. Using the MWD system and appropriate strength correlations can reduce the need for extensive laboratory testing and avoid reliance on RQD values which are greatly affected by the drilling process. In situ rock strength can be estimated on-site for more efficient and less conservative designs.

7 ACKNOWLEDGMENTS

The authors are indebted to Mr. Michael Yako of GEI Consultants for providing additional data on argillite in Boston, Massachusetts from the Central Artery/Tunnel Project. Special thanks to Mr. Americo Santamaria for his help with the figures in this paper.

8 REFERENCES

- ASTM Standard D4543, 2008, "Standard Practices for Preparing Rock Core as Cylindrical Test Specimens and Verifying Conformance to Dimensional and Shape Tolerances," ASTM International, West Conshohocken, PA, 2008.
- ASTM Standard D7012, 2010, "Standard Test Method for Compressive Strength and Elastic Moduli of Intact Rock Core Specimens," ASTM International, West Conshohocken, PA, 2010.

ASTM Standard D3967, 2008, “Standard Test Method for Splitting Tensile Strength of Intact Rock Core Specimens,” ASTM International, West Conshohocken, PA, 2008.

ASTM Standard D5731, 2008, “Standard Test Method for Determination of the Point Load Strength Index of Rock and Application to Rock Strength Classifications,” ASTM International, West Conshohocken, PA, 2008.

Barosh, P.J. and Woodhouse, D., “Geology of the Boston Basin”, *Civil Engineering Practice, Journal of the Boston Society of Civil Engineers Section/ASCE*, Special Edition – A City Upon a Hill: The Geology of the City of Boston & Surrounding Region, Volumes 26 & 27, 2011/2012.

Broch, E. and Franklin, J.A. May 1972. *The Point-Load Strength Test*: 689-692.

GEI Consultants, Inc. October 1992. Final AGC Report.

Haley & Aldrich, Inc. February 1992. Geotechnical Laboratory Rock Test Results for the Central Artery (I-93)/Tunnel (I-90) Project.

Metcalf and Eddy. February 1990. Geotechnical Interpretive Report: Tunnels, Shafts, and Diffuser.

Munfakh, G., Wyllie, D., and Mah, C. W., 1998, *Rock Slopes Reference Manual*, Federal Highway Administration, FHWA HI-99-007.

Parsons Brinckerhoff Quade & Douglas, Inc. March 1990. Massachusetts Water Resources Authority Boston Harbor Cleanup Project 1989 Marine Boring Program Geotechnical Interpretive Report.

Pfister, P. 1985. Recording Drilling Parameters in Ground Engineering. *Journal of Ground Engineering*. Vol. 18 (No. 3): 16-21.

- Sadkowski, S.S., Stetson, K.P. and Benoît, J. “Investigating Rock Quality Using Drilling Parameters in Boston, MA, USA”, Proceedings of the Third Second International Conference on Site Characterization ISC-3, Taipei, Taiwan, April 1-4, 2008, pp. 1359-1364.
- Somerton, W.H. 1959. A Laboratory Study of Rock Breakage by Rotary Drilling. *Journal of Petroleum Technology*. Vol. 216: 92-97.
- Sverdrup Corporation. October 1990. Contract Documents for Inter-Island Tunnel Contract Package No. 151 for Massachusetts Water Resources Authority.
- Woodhouse, D. and Barosh, P.J., “Geotechnical Factors in Boston”, *Civil Engineering Practice, Journal of the Boston Society of Civil Engineers Section/ASCE*, Special Edition – A City Upon a Hill: The Geology of the City of Boston & Surrounding Region, Volumes 26 & 27, 2011/2012.

Geotechnical Solutions for Widening of Interstate 95

Sarah McInnes, P.E.

Pennsylvania Department of Transportation, Engineering District 6-0
7000 Geerdes Boulevard
King of Prussia, PA 19406
610-205-6544
smcinnnes@pa.gov

Michael Yang, Ph.D., P.E.

Michael Baker Jr., Inc.
300 American Metro Boulevard - Suite 154
Hamilton, NJ 08619
609-807-9534
myang@mbakercorp.com

Robert Crawford, P.E.

James J. Anderson Construction Company, Inc.
6958 Torresdale Avenue
Philadelphia, PA 19135
215-331-7150
bobc@jjaconstruction.com

Acknowledgements

The authors would like to thank The U.S. Federal Highway Administration; PennDOT Engineering District 6-0; James J. Anderson Construction Company, Inc.; Michael Baker International; URS Corporation's Fort Washington Office; Dawood Engineering; The Neel Company; Elastizell Corporation of America; GeoPier Foundation Company, Inc.; Archie Filshill, Ph.D.; Theresa Andrejack Loux, Ph.D.; and Earth Engineering, Inc. for their work on the various aspects of this project.

Disclaimer

Statements and views presented in this paper are strictly those of the author(s), and do not necessarily reflect positions held by their affiliations, the Highway Geology Symposium (HGS), or others acknowledged above. The mention of trade names for commercial products does not imply the approval or endorsement by HGS.

Copyright Notice

Copyright © 2015 Highway Geology Symposium (HGS)

All Rights Reserved. Printed in the United States of America. No part of this publication may be reproduced or copied in any form or by any means – graphic, electronic, or mechanical, including photocopying, taping, or information storage and retrieval systems – without prior written permission of the HGS. This excludes the original author(s).

ABSTRACT

PennDOT's multi-billion dollar I-95 corridor reconstruction effort includes replacement of the existing mainline viaducts and roadway in Northeast Philadelphia from Vine Street to the Cottman Avenue Interchange. A major aspect of the corridor reconstruction is the Girard Avenue Interchange Reconstruction (referred to as section GIR) in the Fishtown and Port Richmond neighborhoods of Philadelphia just north of I-95's connection to I-676, the Vine Street Expressway, and Center City. This interchange services 180,000 vehicles per day and is the connection point for major Philadelphia arterial routes including Delaware Avenue, Aramingo Avenue, Allegheny Avenue, Richmond Street and Girard Avenue.

The widening of I-95 through section GIR requires abutments, wing walls and modular retaining walls to be constructed on weak underlying soils with average N-values of less than 10 and maximum allowable settlement of less than one inch. As depth to rock in this area was frequently determined at or greater than 90 feet, shallow foundations combined with either improvement of the existing underlying soil or undercut replacement and backfill with lightweight material at the structures were determined to be the most effective options.

Ultimately, in the GR2 Section, a combination of undercut replacement and backfill with lightweight cellular concrete and selective areas of ground modification using impact stone columns were implemented to support the mainline widening. The project initial design and contractor proposed changes implemented during construction will be presented. In addition, settlement monitoring readings taken during and after construction will be included and discussed in an effort to compare the as-measured settlement and soil properties, such as elastic moduli, to the settlement predictions and soil properties used in the design, which were derived from in-situ testing.

INTRODUCTION

PennDOT's multi-billion dollar I-95 corridor reconstruction effort includes replacement of the existing mainline viaducts and roadway in Northeast Philadelphia from Vine Street to the Cottman Avenue Interchange. A major aspect of the corridor reconstruction is the Girard Avenue Interchange Reconstruction (referred to as section GIR) in the Fishtown and Port Richmond neighborhoods of Philadelphia just north of I-95's connection to I-676, the Vine Street Expressway, and Center City. This design section, which is part of the overall I-95 corridor rehabilitation project, includes the Girard Avenue interchange and its associated ramps and side roads. This interchange services 180,000 vehicles per day and is the connection point for major Philadelphia arterial routes including Delaware Avenue, Aramingo Avenue, Allegheny Avenue, Richmond Street and Girard Avenue. The GIR project comprises eight design sections, GR0 through GR7. Reconstruction of the bridges, retaining walls and sign structures of section GR2 is discussed in the paper.

The widening of I-95 through section GIR requires abutments, wing walls, retaining walls and sign structures to be constructed on areas of weak underlying soils and maximum allowable settlement of less than one inch. As depth to rock in section GR2 was found to be at or greater than 90 feet, shallow foundations combined with ground improvement of the existing underlying soil was found to be ideal during design. During construction, the contractor submitted a value engineering proposal recommending undercut replacement and backfill with lightweight material at the structures.

Ultimately, in the GR2 Section, a combination of undercut replacement and backfill with lightweight cellular concrete and selective areas of ground modification using impact stone columns were submitted as a value engineering proposal and subsequently approved and implemented to support the mainline widening.

PROJECT DESCRIPTION

Construction Section GR2 involves widening I-95 between Frankford Avenue to the south and Palmer Street to the north. Currently within this area, I-95 is constructed on an embankment fill. Three local streets pass beneath the interstate via three single-span main line bridges, Shackamaxon Street, Marlborough Street and Columbia Avenue. There are two existing retaining walls supporting I-95 within this area, one on the southbound side between Frankford Ave. and Shackamaxon St., and one on the northbound side between Marlborough St. and Columbia Ave. The existing bridge foundation types are spread footing founded on soil and were constructed in the 1960s.

This construction section involves the replacement and widening of the three mainline I-95 bridges and the two walls mentioned above, the construction of three new retaining walls supporting the I-95 roadway, and two sign structures. The majority of the widening (30 to 35 ft.) will occur on northbound I-95 and minor widening (4 to 6 ft.) will occur on the southbound side. Bridge construction will be accomplished primarily within three stages. In the first stage, traffic will be diverted to the center portion of the existing bridges while the outside portions are widened and reconstructed. The second and third stages of construction will shift traffic to the

newly constructed outside lanes while the central portion of the bridges are reconstructed. Figure 1 illustrates the proposed widening of 95 and the location of the three bridges. I-95 trends to the northeast in this area and the Delaware River is located east of the highway.



Figure 1: Bridge Locations

The retaining walls support 95 adjacent to Shackamaxon St. and Marlborough St. and the sign structures are adjacent to the walls.

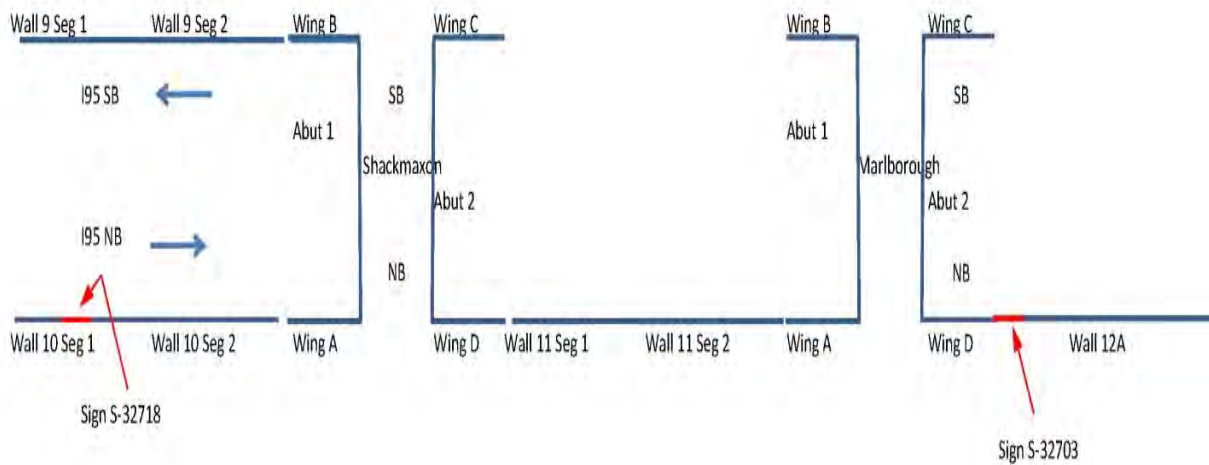


Figure 2: Structure Locations

SOILS AND GEOLOGY

The project is situated in the Lowland and Intermediate Upland Section of the Atlantic Coastal Plain Physiographic Province. It is located near the boundary of the Coastal Plain and the Piedmont Physiographic Province, which is known as the Fall Line. The dominant topographic landform consists of flat, upper terrace surfaces cut by shallow valleys and the Delaware River floodplain. The area is underlain by unconsolidated to poorly consolidated sand and gravel deposits over complexly folded and faulted metamorphosed sedimentary and igneous rocks, primarily schist and gneiss.

The Soil Survey Map of Bucks and Philadelphia Counties indicate Urban Land is the predominant soil series within the general project area. This designation represents highly variable and disturbed materials, generally including fill, resulting from previous construction and various land uses over time.

Figure 3 presents a portion of the Pennsylvania Geological Map (Philadelphia and Camden Quadrangles) with the project location indicated. As shown, the project site is mapped as being underlain by the Quaternary-aged Trenton Gravel (Qt). The Trenton Gravel formation consists of gray to pale reddish-brown, very gravelly sand with interbedded, cross-bedded sand and clay-silt layers. These interbedded layers form a wedge that begins at the Fall Line and thickens toward the southeast.

Oligoclase-mica schist (Xw) of the Wissahickon Formation underlies the unconsolidated formations described above. This metamorphic rock is composed of quartz, feldspar, muscovite, and chlorite mineral constituents. The oligoclase-mica schist variation of the Wissahickon Formation is coarsely crystalline, excessively micaceous, and has abundant feldspar. The estimated thickness of the Wissahickon Formation is 8,000 to 10,000 feet. A sometimes deep saprolitic zone often forms above this rock as the result of weathering.

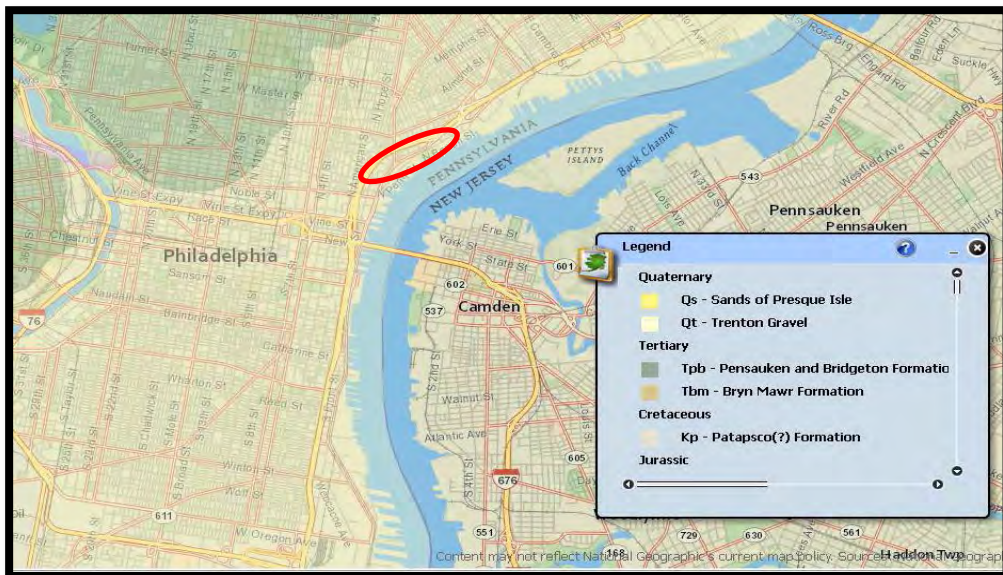


Figure 3: Geology Map

SUBSURFACE INVESTIGATION

The subsurface investigation program for the structures of GR2 began with 35 test borings. Due to many layers of loose and/or soft soils found in the borings, 16 cone penetrometer tests (CPTu with pore pressure readings) were performed to obtain a better understanding of the extent and nature of these soils. Additionally, since some of the loose soils encountered had a tendency to "heave" into the hollow stem augers when beneath the water table (i.e. running sands), some SPT N-values were thought to be artificially low. The CPTu probes were performed to verify the in-situ consistency or density of the soils, as well as perform pore pressure dissipation tests to better evaluate consolidation settlement.

Laboratory testing was performed on dozens of soil samples from the test borings. Particle-size analysis, Atterberg limits, natural moisture content, organic content, and AASHTO/USCS classification were performed. Additionally rock core samples were tested for unconfined compression strength. This new information, coupled with the 1960s test borings for original construction and the significant lab testing provided a thorough picture of the subsurface conditions. The subsurface investigation for this project verified the mapped soils and bedrock and confirmed the general soil stratigraphy and provided a higher level of confidence for the foundation design.

SUBSURFACE CONDITIONS

The subsurface conditions at the project site were generally similar with fill overlying alluvial deposits overlying a saprolite layer of varying thickness above bedrock. The Marlborough Street bridge evidenced the worst case conditions of very deep rock (>100 ft.) and layers of loose soil throughout the profile. The conditions at this bridge are typical of the subsurface conditions for the southern portion of GR2 and were used to develop the foundation recommendations. The subsurface profiles prepared during design showed the subsurface soil conditions are variable between and within the limits of each foundation element. In general, the test borings encountered three broad soil types consisting of fill, alluvial deposits, and residual (saprolite) soils. The general soil conditions across the site were similar and varied slightly, even when compared to the previous borings (1960s) and the CPTu tests. The profiles prepared foundation design included the test borings from the original design of 95 and the CPT test results in addition to the new test boring data.

Beneath the existing embankment the borings encountered a fill zone approximately 5' to 20' thick. Materials within this fill zone consisted of generally medium dense silty sand or sandy silt with gravel classified as SC-SM/A-4 and SM/A-1-b. It was known that existing foundations were also in the fill layer which posed a problem for some foundation types.

The fill materials are underlain by a varying thickness of alluvial and organic deposits, typical of a river environment. The thickness of this material is dependent on top of rock surface which dips from northwest to southeast varying from 15 ft. to more than 100 ft. The alluvial deposits vary widely in nature due to deposition from the Delaware River. Many layers of granular and fine-grained soils are indicated and soil types found include SM/A-2-4, SM/A-1-b, SP-SM/A-3, SC-SM/A-2-4, SC-SM/A-4, MUA-4, CUA-6, OUA-5, OH/A-7-6, and OUA-7-5. Organic content tests performed resulted in organic contents ranging from 3% to 21%. When preparing the models for settlement calculations, up to nine stratigraphic soil layers were necessary.

Beneath the alluvium a layer of residual soils and saprolite consisting of weathered-in-place rock ranges from 5 to more than 30 ft. in thickness. These soils contain a large amount of mica and generally show the fabric of the native rock. These soils are described as micaceous, silty, fine to medium sand with varying amounts of gravel. Samples within this layer were lab classified as SM/A-1-b.

Beneath these layers in all of the borings mica schist bedrock was encountered. The top of intact bedrock sharply drops off in elevation from northwest to southeast towards the Delaware River. The rock is generally described as soft to medium hard, slightly to highly weathered, and very closely to medium fractured. The schist was generally described as mica schist, however, biotite, chlorite and feldspathic schist were also used as a descriptor.

Based on data from the CPTu report, the CPTu probes generally show higher correlated N60 N-values compared to the SPT N-values from adjacent borings. It was determined that the loose material below the water table was running sands which artificially lowered the N-values during SPT testing.

DESIGN CONSTRAINTS AND JET GROUTING

The existing spread footings for the Marlborough and Shackamaxon bridges were embedded approximately 10 to 15 feet below street level. The existing footings may have been very deeply embedded as a conservative alternative to using driven piles, which may have been deemed impractical due to the great depth to bedrock (as well as the undefined nature of the top of rock surface based on the original borings). Alternatively, the deep embedment may have been deemed necessary in order to place the footings below any pre-existing building foundations.

Due to constructability concerns related to demolishing and removing the existing deep foundations and required staged construction it was determined during design that the existing bridge foundations would be left in place and the proposed foundations would be above the existing foundations. Due to the widening, there is a large amount of areal overlap between the existing and proposed foundations, especially on the northbound side where there is significant widening. Deep foundations, while typically more expensive than shallow foundations, were also considered for the replacement bridge but dismissed due to cost and impracticability. Spread footing on soil foundations for the replacement bridges would be highly practical and the most economical foundation alternative, especially considering that the existing spread footing on soil foundations have apparently performed acceptably. Based on the bearing capacity shown on the existing plans, it was understood the minimal additional load from the new bridges would not cause settlement at the existing foundation locations however there was concern for differential settlement and stress concentrations in the widened areas. Because the existing footings are embedded so deep, there is enough space to construct new spread footings above the existing bridge footings, thereby allowing the existing footings to be left in place. Although the existing foundations for the retaining walls were not to be left in place, the same concern of differential settlement existed for the retaining walls.

Due to settlement concerns at the Marlborough and Shackamaxon bridges, the maximum allowable settlement was limited to one half inch at the proposed abutments where the highway was widened and extends past original structure. Poor soil conditions generated large calculated settlements at these locations (as much as 4.5 inches). Based on the desire to construct shallow

foundations rather than require drilling of a deep foundation, a variety of ground improvement techniques were examined. Because settlement was the controlling factor for the majority of the structures within the GR2 section of the project, it was recognized by the design team that the need for a consistent and effective ground improvement method and evaluation methodology for foundation design was required. It was determined, based on a variety of factors including cost, predictable quantities, speed of installation, minimizing the impact to I-95 and previous successful use on section GR0, that jet grouting was required at locations where the proposed foundation does not overlie the existing foundation. Jet grouting had been performed successfully during the previously construction of Section GR0 where it was used to underpin an existing high voltage oil-filled electric line to limit settlement within a very soft, organic silt layer created by proposed roadway embankment.

Jet grouting was deemed to be the most practical option to stabilize the ground beneath the widened portion of the Marlborough Street and Shackamaxon Street Bridges and Retaining Walls 9 through 12A. The soil conditions at this structure are highly variable, but jet grouting has the ability to be performed within all types of soil and quantities can also be determined to an accurate degree. Additionally, since jet grouting involves drilling a small diameter hole in order to reach the treatment depth, penetrating through any pre-existing building foundations or rubble fill can be readily accomplished without any additional provisions. Jet grouting ground improvement was formally recommended to be used in conjunction with spread footing foundations to achieve a uniform foundation stiffness across the entire footprint of the new foundations to ensure a uniform structure response for the entire bridge and retaining wall system. The jet grouting was proposed to extend laterally a minimum of 5 feet beyond the proposed footing footprint.

Following is the list of design elements and general design recommendations outlined in the foundation reports that apply to the bridge structures:

1. The existing abutment foundations are to remain.
2. The proposed bearing pressure must be equal to or less than the existing allowable bearing pressure at the existing BFE.
3. Jet grouting is to be used as a ground improvement at locations where the proposed footing extends past the existing footing, with the exception of at the abutments where the embankment is at full height. Jet grouting must extend 5 feet laterally past the proposed footing footprint.
4. Settlement is to be limited to less than 0.5 inches.
5. A geogrid reinforced coarse aggregate mat will be utilized to help mitigate the differential settlement that would occur between the jet grouted areas and the overlap area.

All soils were to be removed to the top of the existing footing and backfilled with a geogrid reinforced coarse aggregate mat to the proposed BFE elevation. The geogrid reinforced coarse aggregate mat proposed between the two footings and above the jet grouted areas should help reduce the effects of the “hard edge” that will be created between the end of the existing footing and the extended abutment lengths.

The Marlborough Bridge and Shackamaxon Bridge (approximately 500 to 600 feet apart) and the four retaining walls adjacent to them (walls 9 to 12) have similar soil conditions so to provide a consistent subsurface evaluation across the GR2 section, the foundation analysis for the walls followed the same methodology and jet grouting procedure as was proposed for the bridges.

CONTRACTOR ALTERNATE: LIGHTWEIGHT CONCRETE AND STONE COLUMNS

Following advertisement and award of the GR2 contract, the successful low bidder, James J. Anderson Construction Co., Inc. of Philadelphia (JJA), met with several jet grouting specialty contractors to discuss cost, schedule and proposed means and methods. Of particular concern was the project build environment and the close proximity of commercial and residential properties to the treatment area. JJA's previous experiences with jet grouting produced large amounts of excess slurry during installation. This required effective onsite control measures be implemented to contain and manage the runoff for the spoils being produced. For the GR2 project, the small work zones and immediately adjacent homes and businesses eliminated the available space for berms, trenching or other conventional control methods. While different means of slurry control such as pumping, vacuum trucks and re-phasing the grouting sequence were investigated, the resulting additional cost and schedule impact necessitated JJA to investigate alternate settlement control designs for submission as a value engineering initiative.



Figure 4: Proximity Proposed Jet Grouting Treatment Limits To Buildings

The GR2 widening for I95 occurs on either side of the interstate with the proposed new structures replacing areas of existing embankment. Given the proposed structure locations were

already partially preloaded by these existing embankments, JJA first investigated load balancing with lightweight backfills as an alternative to jet grouting.

The preliminary load balancing design indicated that, as the proposed widened roadway elevation was several times higher than the existing sloped embankments, very low unit weight backfills of less than 10 p.c.f. would be required to completely balance the small existing preload and avoid undercutting. As such, JJA and their geotechnical engineer, Earth Engineering, Inc. of East Norriton, Pennsylvania, proposed a preliminary design using geofoam for the majority of structure backfill locations. While at the design roadway heights this material did offer a sufficient reduction in bearing stress to match the existing embankment preload and control settlement, concern over the long term creep behavior and hydrocarbon vulnerability of geofoam forced the design team to investigate other, albeit heavier, lightweight materials. Ultimately, lightweight cellular concrete was selected for the value engineering submission. Although several times heavier than the geofoam, this material exhibits very low long term creep behavior and was extremely resistant to hydrocarbon attack.

The lightweight cellular concrete value engineering submission was based on conventional LRF design and elastic settlement analysis utilizing the bearing soil properties and design parameters taken from the original PennDOT design. The physical properties for the lightweight cellular concrete were derived from an industry standard supplier, The Elastizell Corporation of Ann Arbor, Michigan, and incorporated. Those properties used were; 30 p.c.f in-place unit weight, 40 p.s.i. unconfined compressive strength, and a 35 degree angle of internal friction. Proceeding with the design supposition that settlement would control, the various structures were load balanced to meet the design criteria of 0.5 inches maximum settlement for abutments and 1.0 inches maximum settlement for the MSE walls and sign structure foundations. Typical sections of the load balanced structures and backfills were then analyzed for PennDOT/AASHTO mandated design loads to ensure the minimum performance ratios for overturning, sliding and global stability were met or exceeded. Concurrently, the load balanced preliminary design sections were sent to and reviewed by the MSE wall supplier, The Neel Company of Springfield, Virginia, for internal stability within their MSE T Wall components.

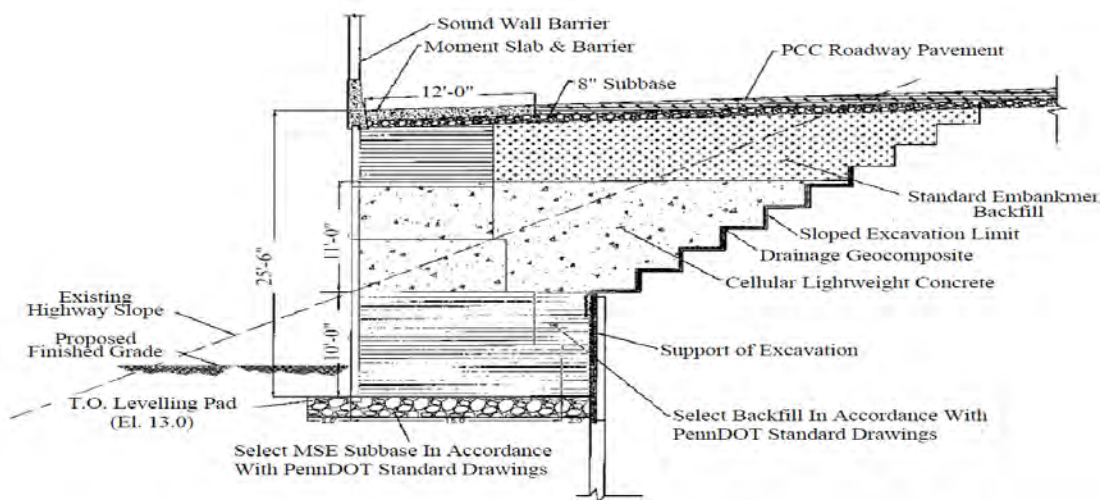


Figure 5: Typical Section of MSE Wall With Lightweight Cellular Concrete Backfill

The accepted design directed varying heights of lightweight cellular concrete backfill behind the MSE walls governed primarily by the subsurface conditions and their susceptibility for settlement. Throughout all wall locations, the lightweight cellular concrete backfill comprised 20 percent to 50 percent of the total structure backfill. At the abutments, lightweight cellular concrete comprised 70 percent to 90 percent of the total structure backfill height and, at all but one location, was supplemented by over-excavation of the foundation soil and replacement with lightweight cellular concrete to effectively load balance for settlement. This increase was due to the more restrictive ½” maximum settlement required for the abutments and across the “hard edge” zones. A summary of lightweight cellular concrete percentage by structure is presented in Table 1.

Table 1: Lightweight Cellular Concrete Backfill As Percentage Of Wall Height

Structure Type	Structure Location & Number	NB / SB	Structure Component	LW Cellular Concrete Backfill As Percent of Wall Height (%)	Additional Excavation & Replacement With LW Cellular Concrete (ft.)
BRIDGE ABUTMENT / WING	SR0095 Over Shackamaxon S-26064	NB	Abut 1	90	4.0
			Wing A	90	4.0
			Abut 2	90	6.0
			Wing D	90	6.0
		SB	Abut 1	90	1.0
			Wing B	90	2.0
			Abut 2	90	0.0
			Wing C	90	0.0
	SR0095 Over Marlborough S-26901	NB	Abut 1	70	6.0
			Wing A	70	6.0
			Abut 2	70	4.0
			Wing D	70	4.0
		SB	Abut 1	70	0.0
			Wing B	70	0.0
			Abut 2	0	0.0
			Wing C	0	0.0
SIGN STR.	Sign Structure S-32718	SB	Tower A	IMPACT STONE COLUMN IMPROVEMENT	
		NB	Tower B	50	0.0

Table 1 (Cont'd): Lightweight Cellular Concrete Backfill As Percentage Of Wall Height

Structure Type	Structure Location & Number	NB / SB	Structure Component	LW Cellular Concrete Backfill As Percent of Wall Height (%)	Additional Excavation & Replacement With LW Cellular Concrete (ft.)
WALLS	MSE Retaining Wall 9 S-32707	SB	Segment 1	25	0.0
			Segment 2	25	0.0
	MSE Retaining Wall 10 S-32599	NB	Segment 1	50	0.0
			Segment 2	50	0.0
	MSE Retaining Wall 11 S-32669	NB	Segment 1	25	0.0
			Segment 2	25	0.0
	C.I.P. Retaining Wall 12 S-32472	NB	Segment 1	20	0.0

At one location, on the SB side of GR2 at sign structure S-32718, the design determined load balancing with lightweight cellular concrete could not satisfy all the design requirements. Although backfilling with lightweight cellular concrete could achieve a design settlement of 1.0 inches, at this load reduction the structure could not meet the minimum performance ratio required for overturning. As such, ground improvement with impact stone columns was selected for that specific location. This method offered improvement of the elastic modulus within the existing foundation soil to meet settlement and allow sufficient structure backfill weight to resist overturning while minimizing concern over slurry control within the GR2 build environment.

Once all components of the design were completed and finalized by JJA and their geotechnical engineer, the value engineering initiative was submitted for Department and FHWA review in May 2013 offering a proposed \$300,000.00 savings if implemented. Conditional approval for construction was issued on August 1, 2013 with construction beginning one week later.

CONSTRUCTION AND SETTLEMENT MONITORING

Over-excavation at the abutments and wing walls was started in August 2013. Simultaneously with these excavations, the lightweight cellular concrete supplier mobilized on-site and calibrated their equipment in conformance with the approved QC and placement plans. The lightweight cellular concrete was produced by controlled introduction of a foaming agent to a grout mixture consisting of Type 1 cement and water just prior to pumping to the point of placement. The foaming agent expands the grout via air bubble creation within the material

matrix during pumping to produce a very high air entrained grout at the point of placement. Once abutment over-excavation was completed and the lightweight cellular concrete equipment was calibrated to the GR2 site specific requirements of 30 p.c.f. unit weight and 40 p.s.i unconfined compressive strength, placement was initiated.

Lightweight cellular concrete placements were held to a three feet maximum with a minimum 24 hours between subsequent lift applications. Replacement of the excavated areas with lightweight cellular concrete took 2 days with another three days required following final lift placement to the start of footing construction. During placement, QC measures were followed which included wet unit weight sampling every 100 cubic yards and unconfined compressive strength sampling every 300 cubic yards.

Simultaneously with the abutment and wing wall undercut and replacement, impact stone column ground improvement at the SB sign structure foundation also proceeded. The small treatment area was 20 feet-6 inches wide by 22 feet long and contained 56 stone columns of 20 inch diameter and 31 feet deep. JJA contracted a specialty contractor, Geopier Foundation Company, Inc. of Mooresville, North Carolina to perform the ground modification. The specialized equipment consisted of a 130,000 pound excavator fitted with a 12 inch diameter mandrel and hopper. To produce an impact stone column, the penetration end of the mandrel was closed, the mandrel inserted using vibration 31 feet to the limit of treatment and coarse aggregate was supplied via a conveyor to fill the mandrel and hopper. Then the penetration end of the mandrel was opened and the mandrel withdrawn 3 feet depositing a 12 inch diameter 3 feet long column of stone. Then the mandrel tip was closed and the mandrel re-driven 2 feet using vibration to compress the deposited stone column into a 20 inch diameter 1 foot tall stone "pillow". This process was repeated until a 31 feet high column of 1 foot height stone "pillows" is produced. Ground modification is effected not only by the stone column creation but also through densification of the subsurface resulting from the re-driving to increase the stone column's diameter and produce a "pillow". Installation of the 56 impact stone columns was completed by November 2013 and the sign structure foundation and stem proceeded.

Once the undercut/replacement with lightweight cellular concrete and simultaneously occurring impact stone column ground improvement were complete, the abutment, wing wall, and sign structure foundations, MSE leveling pad and first course of T Wall construction proceeded. This was followed by the construction of the abutment stems, wing wall stems, sign structure stems and installation of the second course of T Wall units. During this construction phase, settlement monitors in the form of settlement plates at the abutments and wing walls and wall mounted survey targets on the T Walls were installed. Monitoring was performed from this point forward to track actual structure settlements during construction (dead load application) and after returning these structures to beneficial use (live load application).

At this point, backfilling started within the T Wall sections using regular weight backfill consisting of coarse aggregate approved by the T Wall manufacturer and PennDOT. As backfill approached the adjacent un-backfilled wing wall areas, it was sloped on a one to one gradient to zero backfill at a point fifty feet from the wing wall footing. This was done to create a "transition" zone between the T Wall structure sections, which could undergo one inch of allowable settlement and required only fifty percent or less of their backfill height to be

lightweight cellular concrete, and the wing wall sections which were limited to 0.5 inches of allowable settlement and required nearly full height lightweight cellular concrete backfill.

Upon completion of the regular weight backfill at the T Walls, installation of lightweight cellular concrete proceeded again leaving the abutments and wing walls un-backfilled. Lifts for the T Wall were chosen at 2.5 feet, half of the height of a T Wall unit, and maintained the one to one gradient as the backfill approached the wing wall “transition” zones. In conjunction with the lightweight cellular concrete placement, a drainage geocomposite was placed against the excavated surface at the rear of the T Wall stems, between the virgin earth surface and the impervious lightweight cellular concrete, to alleviate any buildup of excess hydrostatic pressure. This drainage geocomposite layer extended the full height of lightweight cellular concrete placement, except the undercut areas.



Figure 6: Lightweight Cellular Concrete Sloped at Transition Zone

Once lightweight cellular concrete in the T Wall areas reached full backfill height, i.e. to the bottom of the original design roadway section elevation, backfilling of the abutments, wing walls and “transition” zones followed. Just prior to abutment and wing wall backfill, a drainage geocomposite was again installed between the lightweight cellular concrete and virgin earth interface. In the case at the abutments and wing walls, however, which had little or no coarse aggregate backfill, the drainage geocomposite was connected to the weep drain systems of these structures. Lightweight cellular concrete lifts again proceeded in 2.5 feet lifts. Cure time between lifts, unit weight and unconfined compressive strength sampling remained as previous and settlement monitoring was performed weekly. The final lightweight cellular concrete lift was placed in March 2014. Upon completion of the lightweight cellular concrete installation, the roadway, approach slabs, moment slabs, barrier, sound walls and sign structures were completed in accordance with the Contract plans. The southbound lanes of I-95 section GR2 were opened to traffic on June, 2014 and the northbound lanes in May 2015 in conjunction with the traffic

control staging for this and adjacent projects. Settlement monitoring during construction was performed on a weekly basis. As such, settlement with time, settlement with increases in bearing pressure during construction and total settlement to date were all captured. For the purposes of satisfying PennDOT’s maximum allowable settlement requirements, the total settlement through application of full construction dead load plus traffic were paramount.

Figure 7 presents the predicted settlements for the I95 GR2 structures without load balancing or treatment of the underlying soil.

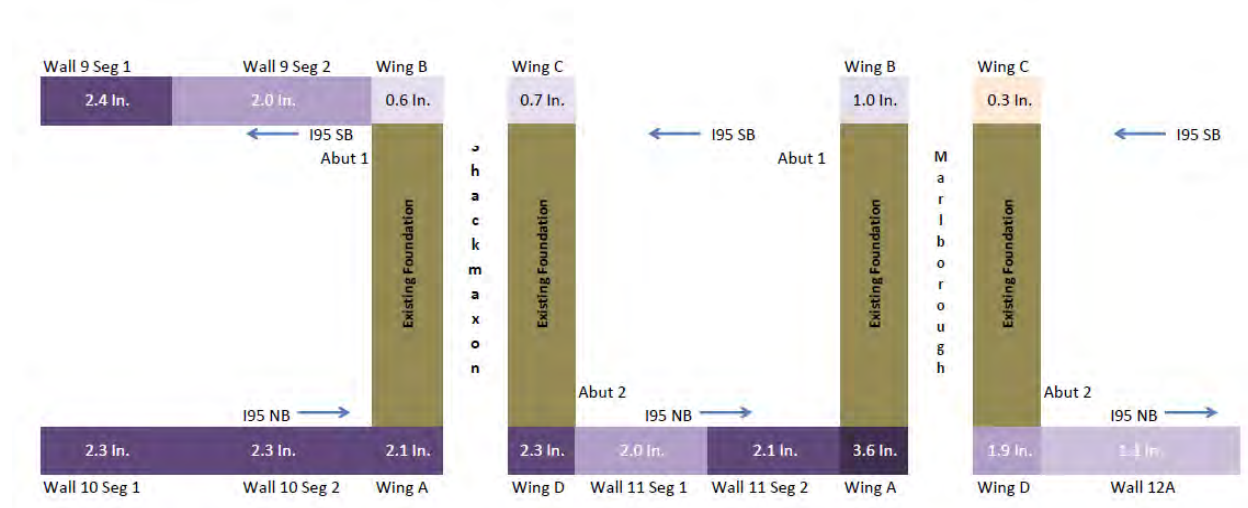


Figure 7: GR2 Predicted Settlements Without Load Balancing Or Ground Modification

Figure 8 shows the maximum allowable predicted settlement by structure as required by PennDOT. Also in Figure 8, the total measured settlement with load balancing from field monitoring is shown by structure in yellow outside the diagrammatical representation.

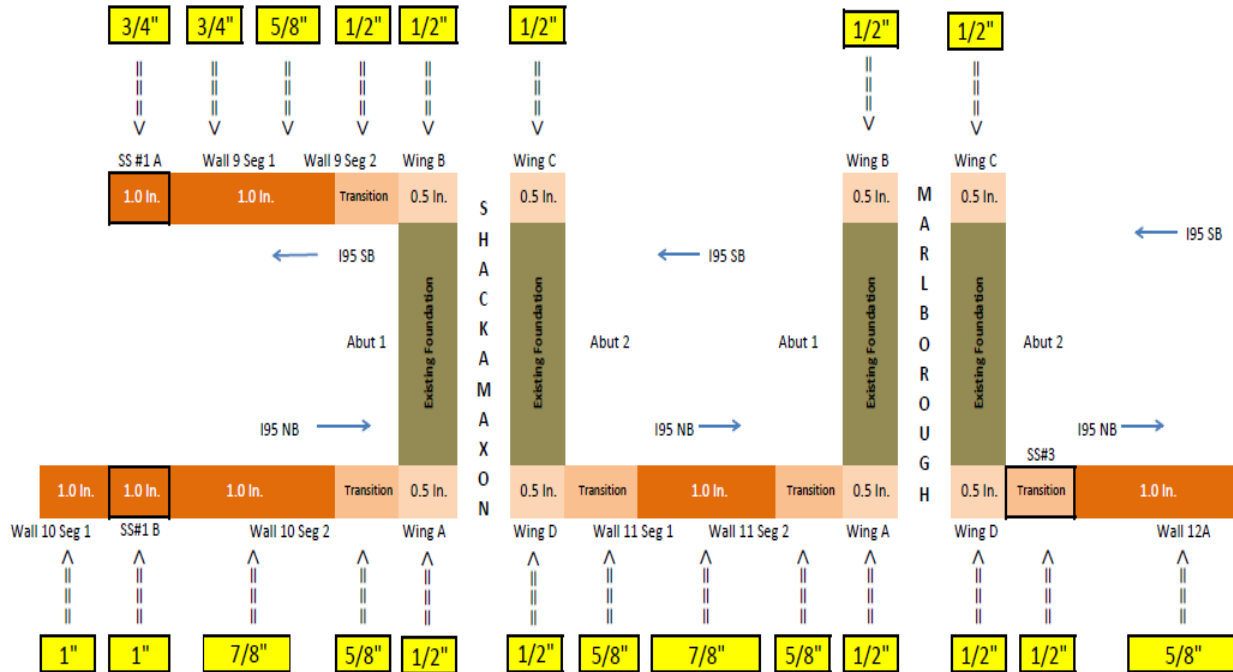


Figure 8: GR2 Allowable Settlements And Measured Settlements (Yellow) From Load Balancing Using Lightweight Cellular Concrete Backfill

As discussed, settlements at the abutments and wing walls, specifically across the “hard edge” regions where the new foundations extended past the existing foundations were the areas of greatest concern. Maximum allowable settlement for these regions was limited to ½”. In these areas, near full height lightweight cellular concrete backfill was supplemented by additional load compensation via undercutting and replacement with lightweight cellular concrete to meet the more stringent settlement limit. Measured settlements in these areas confirmed this additional load balancing was needed.

As for the overall settlement prediction at all the GR2 structures, the design as-constructed is performing at or better than predicted under full dead and traffic loading.

PREDICTED VERSUS ACTUAL SETTLEMENT AND SOIL ELASTIC MODULUS

In order to further investigate the soil properties used in design, the measured settlement at wing wall A for the Shackamaxon Street Bridge was compared to settlement predicted by Schmertmann, et al. (1978). Wing wall A is located in the widened section of I-95 northbound as shown in the Figure 2. The calculated results will be compared with the monitored settlement to verify the analytical method and the soil properties determined from preconstruction in-situ testing.

Schmertmann et al. (1978) proposed the following equation for settlement prediction:

$$\rho_i = C_1 \cdot C_t \Delta p \cdot \sum_{i=1}^n \frac{\Delta z_i}{E_{si}} \cdot I_{zi} \quad (\text{Eq. 1})$$

Therein, C_1 is the correction to account for strain relief from embedment; C_t is the correction of time dependent increase in settlement; Δp is net applied footing pressure; Δz_i is suggested depth increment, I_{z_i} is the influence factor at suggested depth; E_{s_i} is the elastic modulus at suggested depth.

Based on preconstruction standard penetration testing (SPT) and laboratory results performed at wing wall A, the soil beneath the shallow foundation can be classified into the 6 layers as summarized in Table 2.

Table 2: Shackamaxon Wing Wall A Soil Elastic Modulus By Layer

Depth (ft.)	Soil Type	SPT No.	Elastic Modulus (tsf)
0-9.0	Silt with Gravel	6-16	42-155
9.0-10.5	Silty Sand	27	296
10.5-14.0	Gravel with Sand	22-25	389-451
14.0-31.5	Sandy Silt	1-20	5-116
31.5-57.0	Silty Sand	8-40	38-303
57.0-64.5	Gravel with Sand	24-100	157-691

The Schmertmann equation derives E_{s_i} from an empirical correlation between the soil elastic modulus and the SPT number. This correlation is based on series of experiments used to determine the elastic moduli of granular soils. The above table also includes the derived elastic moduli values for the six soil layers classified at wing wall A. Based on these elastic moduli, the total settlement calculated by equation 1 is 0.48 inches, which is consistent with the settlement monitoring results measured. This similarity of calculated results and field measured results further indicates the soil properties used for design are accurate and reasonable.

CONCLUSIONS

This paper presents an alternate method for design, construction and settlement mitigation applied to shallow foundations on weak underlying soils for the widening of I-95 Section GR2 in Philadelphia. The original jet grouting ground improvement design and an alternate design using load balancing with lightweight cellular concrete and areas of impact stone column ground improvement are discussed. The actual measured settlements taken during and after construction were recorded and compared to those predicted by the value engineering design. For this application, the following conclusions were derived.

1. Load balancing (compensation) with lightweight cellular concrete had a significant effect on reducing the settlement from the underlying weak soil. The settlement was able to be controlled sufficiently to meet the 0.5 inch maximum settlement requirement in critical areas.

2. Load balancing (compensation) with lightweight cellular concrete and ground improvement with impact stone columns demonstrated the ability to control settlement while providing an economic advantage over jet grouting ground improvement.
3. Comparison between the measured settlements and those predicted by the design indicates the soil properties were properly derived from the in-situ testing data and applied reasonably using elastic settlement analyses.

REFERENCES

1. Berg and Dodge, "Atlas of Preliminary Geologic Quadrangle Maps of Pennsylvania", Pennsylvania Bureau of Topographic and Geologic Survey, 1981.
2. Geyer, McGlade and Wilshusen: "Engineering Characteristics of the Rocks of Pennsylvania", Pennsylvania Bureau of Topographic and Geologic Survey, 1982.
3. Pennsylvania DCNR, "The Geology of Pennsylvania", 1999.
4. URS Corporation, Foundation Recommendation Reports prepared for 0095 Section GR2, July 2011.
5. Dawood Engineering, Inc, Foundation Recommendation Reports prepared for 0095 Section GR2, July 2011.
6. Schmertmann, J. H., P. Brown and J. Hartman, "Improved Strain Influence Factor Diagram", Journal of the Geotechnical Engineering Div. ASCE, Vol. 104, No. 8, pp 1131-1135, 1978.

Title:

**Telegraph Hill Rock Slope Improvement Project:
Construction Issues and Value Engineering Proposals**

Martin J. Woodard, PhD PG PE
GeoStabilization International
PO Box 4709
Grand Junction, CO 81502
(540)-315-0279
marty@gsi.su

Prepared for the 66st Highway Geology Symposium, September, 2015

Disclaimer

Statements and views presented in this paper are strictly those of the author(s), and do not necessarily reflect positions held by their affiliations, the Highway Geology Symposium (HGS), or others acknowledged above. The mention of trade names for commercial products does not imply the approval or endorsement by HGS.

Copyright Notice

Copyright © 2010 Highway Geology Symposium (HGS)

All Rights Reserved. Printed in the United States of America. No part of this publication may be reproduced or copied in any form or by any means – graphic, electronic, or mechanical, including photocopying, taping, or information storage and retrieval systems – without prior written permission of the HGS. This excludes the original author(s).

ABSTRACT

Telegraph Hill is a well-known topographic high located in San Francisco, California and topped by the Coit Tower landmark. The bay side of Telegraph Hill was historically quarried for rock material between the 1800's through early 1900's and was famously used as ballast for ships leaving the Golden Gate after unloading cargo. Situated within these old quarries is the Telegraph Hill project, which is comprised generally of greywacke sandstone and minor shale interbeds of the Franciscan Assemblage. The project location includes the steep exposed rock faces of these old quarry operations and is approximately 150 feet in height with an condominium complex at the toe of the slope that has been impacted by significant rockfall as recently as 2012.

The rock slope improvement project follows numerous historic attempts to remediate the slope and includes rock scaling, installation of post-tensioned rock anchors, shotcrete, and a dual system pinned mesh system. This presentation discusses the construction issues related to the project as well as value engineering alternatives, including the use of passive dowel anchors and newly developed corrosion resistant elements, proposed for the project.

HISTORY OF THE SITE

Telegraph Hill owes its name to a windmill-like structure erected in 1849 for the purposes of signaling the city the nature of the ships engineering the Golden Gate area. The type of structure is referred to as a marine telegraph. From 1850's to just past the turn of the century ships would enter the bay with cargo, but ballast was needed when leaving the port. Telegraph Hill was the source of much of the ballast used in this process and the remaining high wall is clearly visible both in historic photographs as well as in its present condition. Around the turn of the century the last blasts of this quarry is reported to have occurred.

According to historic research quarrying operation has ceased since around 1930. Since that time this old highwall has had numerous failures including significant rock slides in 1949 and 1958. On January 23, 2012 a portion of the highwall rock slope gave way. The rock mass toppled through the existing catchment fence that was constructed in the early 1990's and impacted a vehicle parked on Winthrop street below.

Topography and Geologic Setting

This slope is characterized as very steep east-facing slopes located along the northeastern face of Telegraph Hill. The slope ranges from approximately 120 to 140 feet in height and is primarily nearly vertical in nature.

Telegraph Hill is located within the Coast Range Geomorphic Province and in the project area is characterized by rolling hills with moderate (up to 300 feet) elevation. The bedrock of the site is primarily comprised of Jurassic-Cretaceous-aged Franciscan Complex bedrock materials; mainly sandstones with very isolated interbeds of shale. The outcrops of sandstones exhibit moderately steep (20-30 degree dip) bedding.

The site can be affected by strong seismic ground shaking due to numerous active faults in the region, with the San Andreas Fault being the closest major active fault. The site is expected to experience peak ground accelerations in the order of 0.4g.

Site Conditions

In January 2012 a 60-foot tall near vertical section of the rock slope released as a rockslide. The day of the rockslide a "light" rainfall occurred, but was preceded by several days of moderate rainfall in the area. The rockslide debris fell from the steep slope and onto the adjacent Winthrop Street destroying a catchment fence and a car parked on Winthrop Street and rocks came to rest against the foundation of the nearby residential structure.

Geologic analysis of the site concluded that the primary lithology consisted of sandstone of the Franciscan Complex. In general the sandstone can be characterized as slightly to moderately weathered, closely to moderately fractured, thick to massive bedded, and interbedded with isolated shales. The sandstone is moderately strong with beds moderately dipping to the northwest.



Figure 1 – Historic Photograph of Coit Tower atop Telegraph Hill. Note the excavation on the forefront of the image. This is the project location.



Figure 2 – Rockslide event circa 1949.

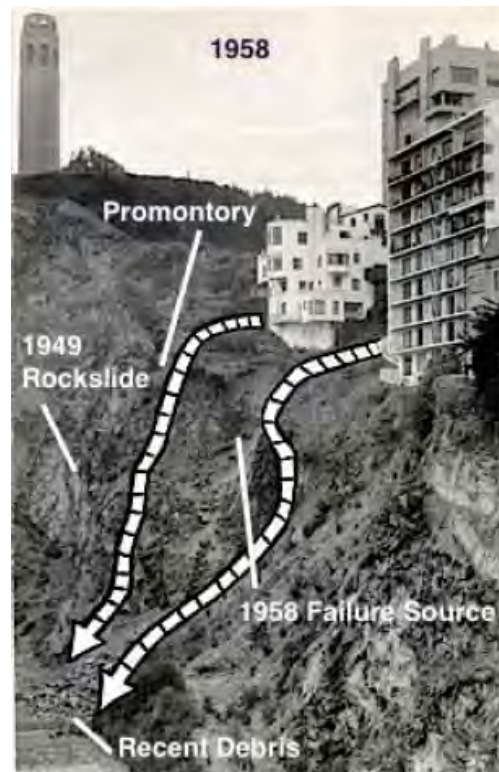


Figure 3 – Rock slide event circa 1958, also showing the location of the 1949 rock slide.

The rock mass contains three primary steeply dipping joints. The first joint (J_1) dips towards the southeast at generally a 70-degree inclination and is the sliding joint of the 2012 failure. This joint is sub-parallel to the rock face and is generally open in aperture and continuous up to 40 feet in length. The second joint (J_2) is a northwest-facing joint that dips also at approximately 70 degrees. J_2 is the release joint for the 2012 rockslide. A third joint (J_3) dips towards the southwest at nearly 70 degrees and appears to have a lesser control on the 2012 failure, but is more prominent in other areas of the slope. The bedding is continuous and dips to the northwest at approximately 30 degrees. There are also several shear zones within the rock face with a typical orientation towards the southeast at 80 degrees. The rock mass around the shear zone can be characterized as nearly a broken rock mass.

Overall the slope contains discontinuity sets that are adversely orientated and prone to slides and topples. Many of the joints near the surface are dilated and contain infilling of various sorts. Groundwater does have a control on stability on the face of this highwall. Seeps were visible during construction as well as were observed shortly after the failure in 2012.



Figure 4 – Results of the January 2012 Rock Slide onto Winthrop Street.

The consultants identified the failure mechanism as a progressive deformation along the high-angle joints resulting in the loading and consequent fracturing and buckling of the lower portion of the block. This results in a reduction in joint strength, including additional forces such as pore-water pressure, until catastrophic failure of the block occurs. To simplify and model this type of failure mode, and to develop remediation strategies, the consultants utilized a plane failure mode for the block analysis, which was appropriate. Geometries of specific rock blocks were identified and a number of scenarios were run that included a static both dry and water filled (25% fracture filled). This was initially done to develop back-calculated shear strength for the subject rock blocks. After back-calculated shear strength was determined an anchor capacity (required reinforcement) was determined using an adequate safety factor of 1.5. Subsequent analysis was performed that also included included a seismic coefficient.

CONSTRUCTION DOCUMENTS

The Telegraph Hill rock slope is owned by two different entities. The northern section of the slope is publically owned and the southern section is privately held. Two different consulting firms were hired for the public and private sides, respectfully. Even though two different firms were contracted for the different sides there were similarity in designs that allowed for a nearly indistinguishable sectioning of the rock slope for bidding processes.

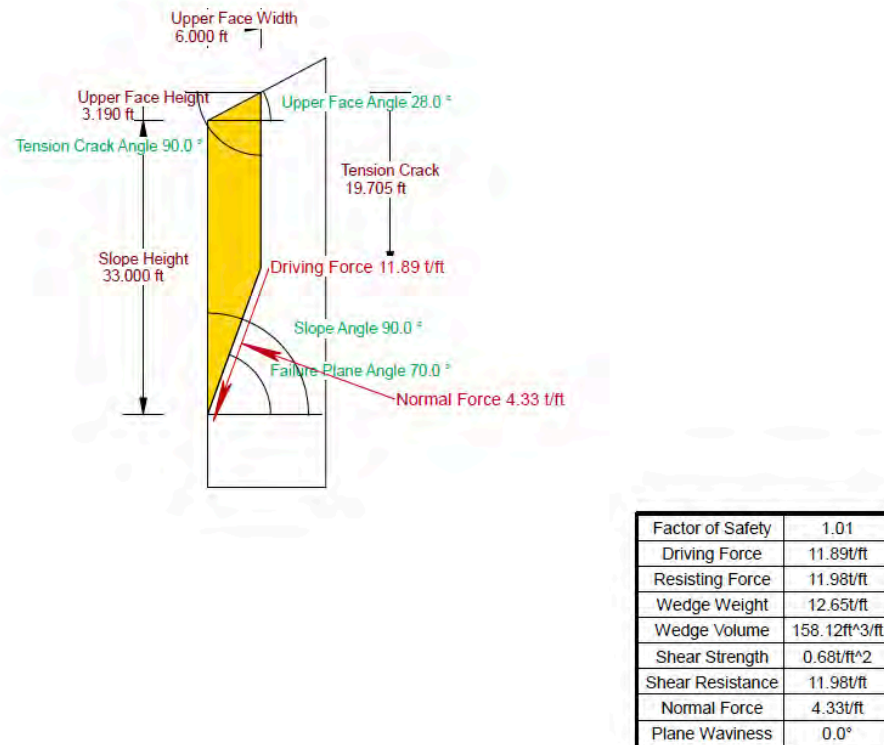


Figure 5 – Example of the back analysis method used on isolated blocks. This analysis was done by the author and matches the reported analysis of the contracting documents.

The general design was for post-tensioned anchors to be installed on an 8-foot center-to-center spacing for the majority of the rock face. These anchors were to provide two purposes that includes its function as an anchor to support rock blocks, but to also act as the pin in a pinned mesh system. Also included in the design were wire mesh support anchors and shotcreting of sections in the weathered zone near the brow of the slope. For proposal purposes the estimates were nearly 400 post-tensioned anchors (varying in length between 20 and 30 feet with the majority being 30 foot long). The mesh system was devised to account for containing the smaller sized potential blocks using a high-tensile strength mesh in conjunction with containing larger blocks with a stronger cable net. For bidding purposes it was assumed that approximately 35,000 square feet of both meshes would be installed.

During the bidding process it became apparent that the cost of construction far exceeded the necessary funds available. At this point in the process GeoStabilization offered an alternative design to be considered.

ALTERNATIVE DESIGNS

Our alternative design primarily concentrated on two attributes of the project to reduce costs while providing adequate performance and safety. The first attribute we provided an alternative on was to identify the areas where there was adequate catchment for contained rocks and replace the pinned mesh system with a draped mesh alternative. The second alternative was

to replace the majority of post-tensioned anchors with passive rock dowels with equal or greater capacities. The resulting savings of these alternatives would result an approximately 1.2 million dollars. The following are brief discussions on the alternatives.

Draped Mesh Alternative

A pinned mesh system acts in a manner to contain rocks on the slope. It utilizes an anchoring system placed in the hillside to actively place the mesh onto the slope, or pin the mesh to the slope, on a patterned basis to contain potential rocks from falling from the slope. The primary advantage of this system is that it contains rocks on the slope and prevents them from falling to the base of the slope. The primary disadvantage of this system is that pockets of falling blocks could build up in pockets in the system and potentially overstresses section of the system. If this occurs maintenance of the system may become necessary, and the maintenance can be difficult and expensive.

A draped system is placed over the slope in a similar manner, but without the mid-slope patterned pins. Consequently, rock blocks that become loose will fall in a controlled manner between the mesh and the slope and eventually fall to the base of the slope. The primary advantage of this system is that the installation is less expensive than a pinned mesh system due primarily to a quicker installation time. The primary disadvantage of this system in comparison to the pinned mesh system is that periodic maintenance will be required to clean up the base of the slope of rockfall debris.

Rock Dowel Alternative

According to the bidding documents design called for the use of post-tensioned grade 75 #10 bars. The bars are to be provided with double corrosion protection (DCP) as specified by the Post Tensioning Institute (PTI) and post-tensioned to (50 kips) with test loads of (67 kips). Based on the construction documents 395 anchors were to be installed in the project area with 5-inch diameter holes. Each anchor is to be provided at 30-foot lengths, but may be adjusted in the field based on field conditions. If longer lengths are required couplers are to be used to extend bar lengths.

Our alternative design proposed the replacement of this system with the use of the grade 150 #8 MMFX Steel All-thread bar by Williams Form installed within 4-inch holes as passive dowels. The capacity of the MMFX bar exceeded the performance requirements of the bidding document bars. In addition we proposed to add redundancy to the system by installing post-tensioned anchors in lieu of dowels for up to 60 dowels, if field conditions warrant.

To account for the draped mesh alternative we further proposed installing the #8 MMFX bars flush to the face without a plate and nut. Removing the plate and nut from a dowel system, which are redundant to the securing of the rock face, will allow the drape mesh to move without being caught by the dowels extended from the rock face (FHWA-CFL/TD-11-002).

Both active anchors and passive dowels are commonly used in the reinforcement of rock slopes (FHWA-CFL/TD-11-002). Dowels are fully grouted passive elements that are frequently

used, including in seismic retrofit projects such as the Golden Gate Bridge in California (Stewart et al., 2011). It is recommended that passive dowel systems be used in rock masses where significant movement has not previously occurred. This is because they are passive elements that require an infinitesimally small movement of the rock mass to occur prior to their strength being activated.

It is an interesting note to compare the active element (post-tensioned anchors) to passive elements (dowels) is how they function. The first comparison can be made examining the material properties of the bars themselves as they function. While tensioning and testing the post-tension element on this project there was a nominal 15-foot free-stressing length. This is the theoretical length of the bar that is stretched to place the load between the plate and nut of the system down to the bond length. In testing for this project the typical elongation during this testing was around 0.5 inches. If one examines the function of a dowel, it is commonly stated that it is initially a passive element and when movement occurs it becomes an active element. In typical rock masses most discontinuities in which movement occurs is sometimes up to several inches, perhaps feet, in width. Since the bar is completely encased in grout we can say that the length over which stretching occurs is generally less than 1-foot. Simple material property calculations show that to convert the passive element into an active element it takes approximately .05 inches of movement. Therefore, to transition a passive dowel into an active element the length of elongation in the steel, or the movement of the rock required is approximately a magnitude less.

Further issues complicate the use of post-tensioned systems. One of the most commonly reported issues is that for several reasons, such as erosion of the rock near the rock/plate interface, the tension on the anchor is lost (FHWA-CFL/TD-11-002). Functionally if this occurs for this element to actively secure the block a minimum movement equal to the tensioning elongation will need to occur to equal the functional capability of a rock dowel.

It is also cited in Context Sensitive Rock Slope Design Solutions (FHWA-CFL/TD-11-002) that dowels can be used in highly fractured and weak rocks that cannot hold a tensioned rock bolt.

CONSTRUCTION

Prior to the award of the project it became apparent that budgetary timing was critical. Due to the length of permitting processes it became impractical to utilize the alternative designs. To remediate the site and to fit into the budgetary constraints for the project the overall scope, or area of work, was reduced by about 35 percent and concentration of efforts were placed in the more critical areas.

During construction a major concern surfaced in the ability of the rock mass to support the 50 kip loads placed on it from the installation of anchors. In several locations the rock mass could be considered weathered and broken. During one specific anchor loading the force placed on the rock mass broke the rock mass rendering that anchor unsatisfactory. Figure 6 shows the rock mass around an anchor test in which the rock mass was broken by the application of the load.



Figure 6 – Image of a rock anchor and surrounding rock mass after testing. Application of the test load fractured the rock mass and caused the rock anchor incapable of carrying the designed load.

As a result of this test results and a clear view of the rock mass a decision was made to flash coat a significant portion of the slope to allow successful drilling, installation and testing of the anchors. A total of approximately 70 cubic yards of shotcrete was placed on the slope.

Figure 7 shows a significant portion of the slope that was flash coated with tinted shotcrete prior to drilling and installation of anchors.

Ultimately, approximately 256 anchors (predominantly post-tensioned anchors), 42,000 square feet of mesh, and just over 70 cubic yards of shotcrete were placed on the slope to successfully remediate the slope for rockfall and rock slide hazards.



Figure 6 – Image of a portion of the south side of the slope where a flash coat of shotcrete was applied before drilling and installation of the anchors. Flash coating was necessary due to the observed weak rock conditions.

REFERENCES:

1. Andrew, R., Brtingale, R., and Hume, H. *Context Sensitive Rock Slope Design Solutions*. Report No. FHWA-CFL/TD-11-002. FHWA, U.S. Department of Transportation, 2011.
2. Stewart, H.E., Fippin, R.L., Crouthamel, D.R., Walker, J., and DeWitt, K. Assessment and Implementation of Rock Slope Support Measures Beneath the Golden Gate Bridge. *American Rock Mechanics Association ARMA 11-404*.

**A Challenging Emergency Rockfall Project Along The North Cascades
Highway, Washington**

Marc Fish, L.E.G
Washington Department of Transportation
PO Box 7365
Olympia, WA 98512-7365
360-709-5498
fishm@wsdot.wa.gov

Michael Mulhern, Geotechnical Specialist
Washington Department of Transportation
PO Box 7365
Olympia, WA 98512
360-709-5583
mulhern@wsdot.wa.gov

Acknowledgements

The authors would like to thank the Northwest Region, Mount Vernon Project Office for their assistance in completing this project on time and as designed.

David Crisman and Staff, WSDOT, Mount Vernon, Project Engineer's Office

Disclaimer

Statements and views presented in this paper are strictly those of the author(s), and do not necessarily reflect positions held by their affiliations, the Highway Geology Symposium (HGS), or others acknowledged above. The mention of trade names for commercial products does not imply the approval or endorsement by HGS.

Copyright

Copyright © 2010 Highway Geology Symposium (HGS)

All Rights Reserved. Printed in the United States of America. No part of this publication may be reproduced or copied in any form or by any means – graphic, electronic, or mechanical, including photocopying, taping, or information storage and retrieval systems – without prior written permission of the HGS. This excludes the original author(s).

ABSTRACT

In December, 2014 the WSDOT Geotechnical Office was requested to inspect a rock slide that occurred at a previously known unstable slope location along State Route 20 near mile post 142.7, in the North Cascades, Washington. Fortunately, this slope was located along a section of the highway that was closed for the winter. Our initial on-highway review indicated that approximately 7500 yds³ of material failed from the slope and came to rest on the highway. Our on-slope inspection revealed that approximately 11,000 yds³ of highly distressed phyllitic rock remained on the slope, bound upslope by a +5-ft-wide tension crack. The tension crack was located approximately 100 feet above the highway and was about 70 feet long. The detached rock mass was perched on an irregular set of joints dipping adversely out of the slope at roughly 50°. There were indications that the rock mass had moved since the initial failure, or was still moving. Through repeated ground-based LiDAR scans over several months, several feet of additional movement was measured without the occurrence of a catastrophic failure. This emergency mitigation project had significant issues to overcome that included safety and environmental concerns, contracting issues, weather, and pressure to open the highway early due to a mild winter. The slope remediation included conventional surveying and routine ground-based LiDAR scanning to monitor for slope deformation, and the use of a long-reach excavator, slope scaling, surface and trim blasting, debris removal, and slope reinforcement to stabilize the slope.

INTRODUCTION

In mid-December 2014, a rock slide occurred at a previously known unstable cut slope along State Route 20 near mile post 142.7 in the North Cascades, Washington (Figure 1). With the exception of occasional rockfall, this slope had shown no observable signs of recent movement over the last 15 or more years. The slide was located along a section of the highway that was closed for the winter. Our initial estimates were that approximately 7,500 yds³ of material was on the highway with another 11,000 yds³ of highly distressed material still on the slope. Our measurements indicated that the distressed rock mass was perched on an irregular set of joints, dipping adversely out of the slope at roughly 50°. There were additional indications that the rock mass had moved since the initial failure, or was still moving. As part of our site reconnaissance, we traversed the slope above the failure and observed an approximate 70 foot long +5-ft-wide tension crack that was located nearly 100 feet above the highway. An emergency project was initiated to mitigate the slope that took 30 working-days to complete over a three and a half month time period. As the project progressed, there was increased pressure to open the highway early due to a mild winter.

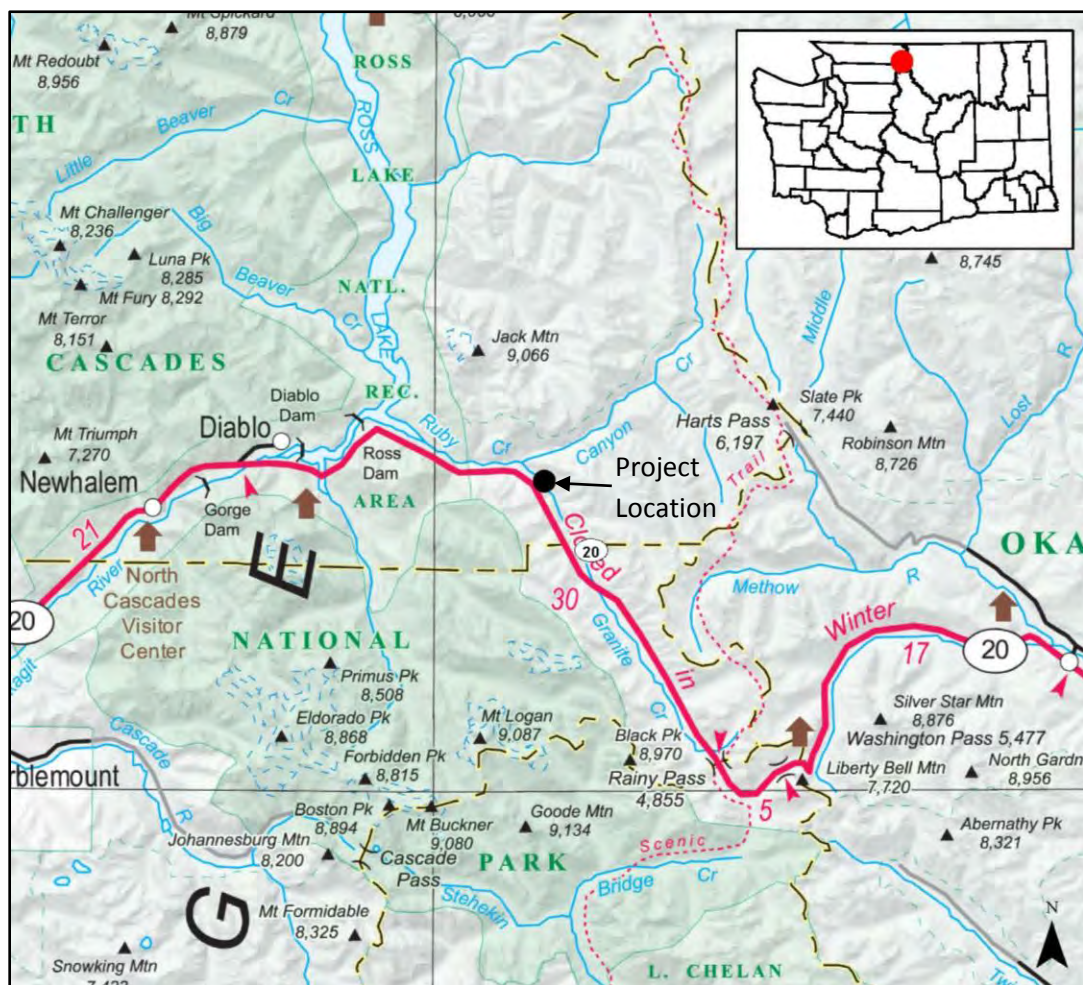


Figure 1: Site vicinity map.

SITE GEOLOGY

The project lies within the highly complex Ross Lake Fault Zone of the North Cascades Range. This fault zone separates highly metamorphosed rocks of the Chelan block from unmetamorphosed rocks of the Methow block. Structural evidence for an early period of strike slip and a strong discontinuity in metamorphic grade and metamorphic history exists across the fault zone. Rocks in the metamorphic core were uplifted 15–25 km relative to rocks on either side (Haugerud and Tabor, 2009).

This rock cut is approximately 105 feet high and 350 feet long. It is composed of moderately weathered, blocky, strong, low-to-high grade phyllite of Tertiary age (Figure 2). The slope was constructed utilizing uncontrolled blasting techniques nearly 50 years ago. Three major discontinuities exposed in the slope create the potential for large planar and toppling type failures. The natural slope above the cut is oriented around 45 degrees and is mantled with less than 5 feet of colluvium.

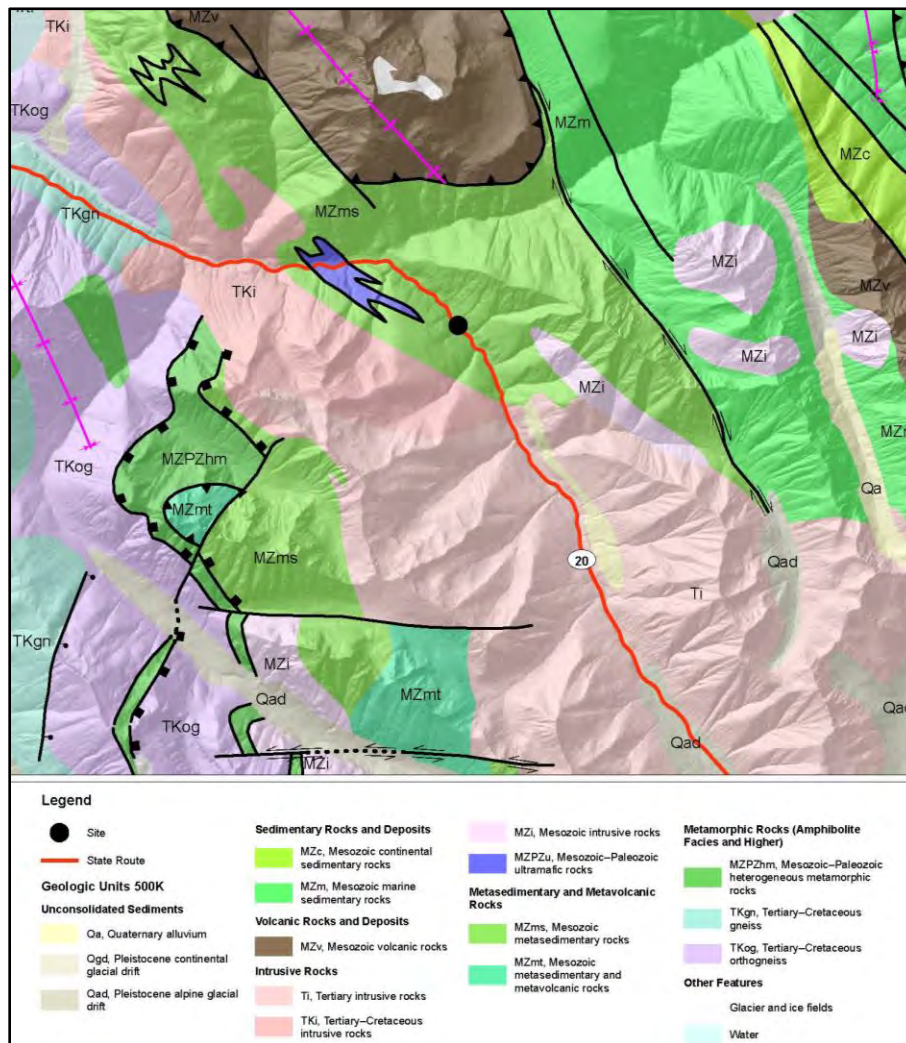


Figure 2: Geology map of the project area.

Immediately east of the rock cut, an intermittent stream drains surface water from the slope. The surface water is conveyed down to the valley bottom and Granite Creek through a cross-culvert located just beyond the eastern limits of the slope. Ground water was also observed seeping from some of the roadway-dipping joints within the limits of the rock cut.

GEOTECHNICAL INVESTIGATION

Our geotechnical investigation consisted of a review of pertinent geotechnical information, several highway-level slope inspections, several on-slope inspections from above the rockcut, an on-slope inspection while rappelling from ropes, and several ground-based LiDAR scans.

Our initial site visit revealed many large boulders, trees, and rock debris scattered beneath the slope covering both travel lanes of the highway (Figures 3 & 4). We estimated the debris to be up to 10 feet deep along the eastbound travel lane. We observed numerous large detached blocks and leaning trees remaining on the slope. While we were conducting our highway-level slope inspection, minor rockfall continued to originate from several different locations on the slope. Using a laser range finder we measured slope heights and distances, collected field developed cross sections, and determined the slope distance to the top-of-cut from highway level (~135 ft). We also traversed the area above the top-of-cut to look for ground fractures or other evidence that would suggest the failure is progressing further upslope (Figure 5).

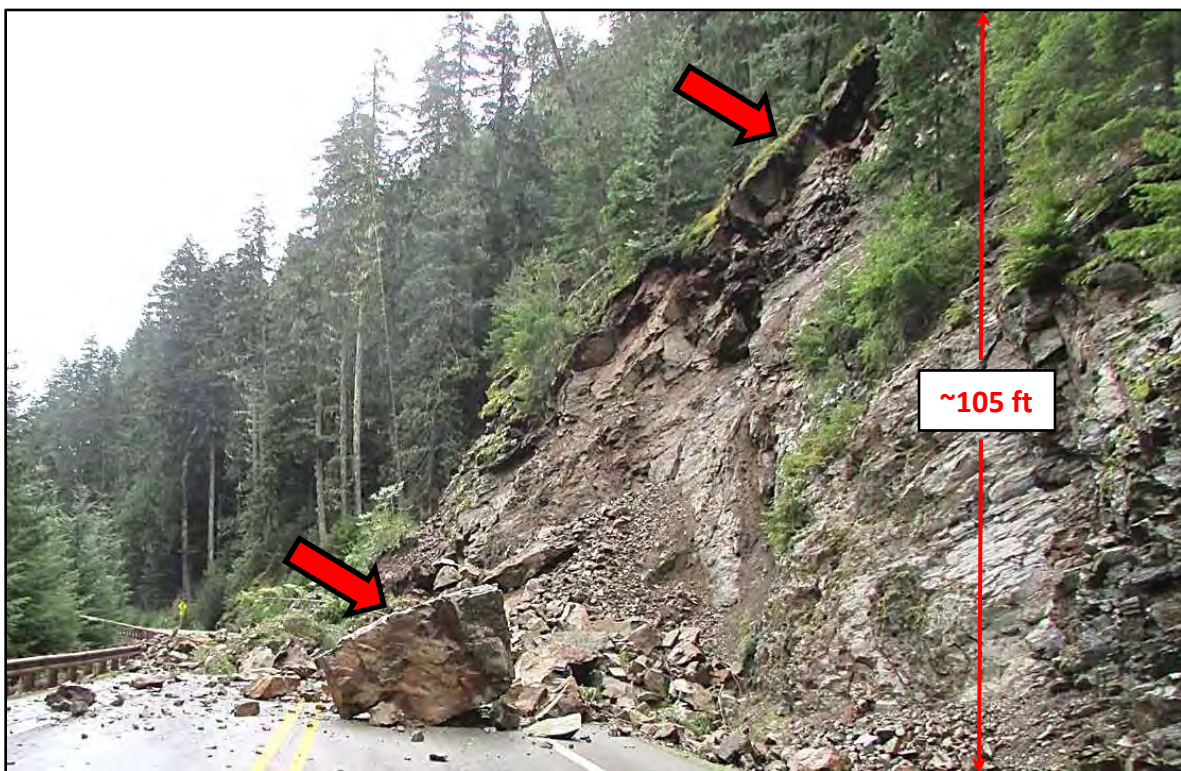


Figure 3: Western view of debris on the slope and scattered over both lanes of the highway.



Figure 4: Eastern view of debris on the slope and scattered over both lanes of the highway.



Figure 5: Looking down from the top-of-cut at a large tension crack, debris, and Granite Creek.

Shortly after our initial site visit, we requested a ground-based LiDAR (Light Detection and Ranging) scan of the slope. This approach allows for the accurate location of a precise and

very closely spaced network of points that can be used to measure slope heights and orientations, including block sizes and discontinuities. Several ground-based LiDAR scans were done over a 3 month period to measure different discontinuity orientations as they became uncovered, and to detect changes in the slope. These LiDAR scans allowed us to determine which portions of the slope were actively moving and by how much, and which areas of the slope were not moving (Figure 6). The digital terrain models (DTMs) developed from the LiDAR scans allowed us to extract a large quantity of block and discontinuity measurements in a very short period of time.

We also conducted an on-slope inspection while rappelling from ropes in order to get an up-close view of the numerous detached blocks, to acquire manual compass readings of discontinuities, and to evaluate other areas of weathered or potentially unstable sections of the slope (Figure 7). We observed large open fractures up to 10 feet in width, large detached blocks the size of a small car, and highly unstable sections of the slope (Figure 8). At the completion of our field inspections, we conducted a literature review and looked at recent geologic maps of the area, unstable slopes data, and digital photo logs of the state highway system. Our review revealed that this rock slope is located in an area of highly distressed bedrock of the Ross Lake Fault Zone, has occasional rockfall, and that a highly persistent roadway dipping discontinuity near the toe-of-slope existed prior to the slope failure (Figure 9).

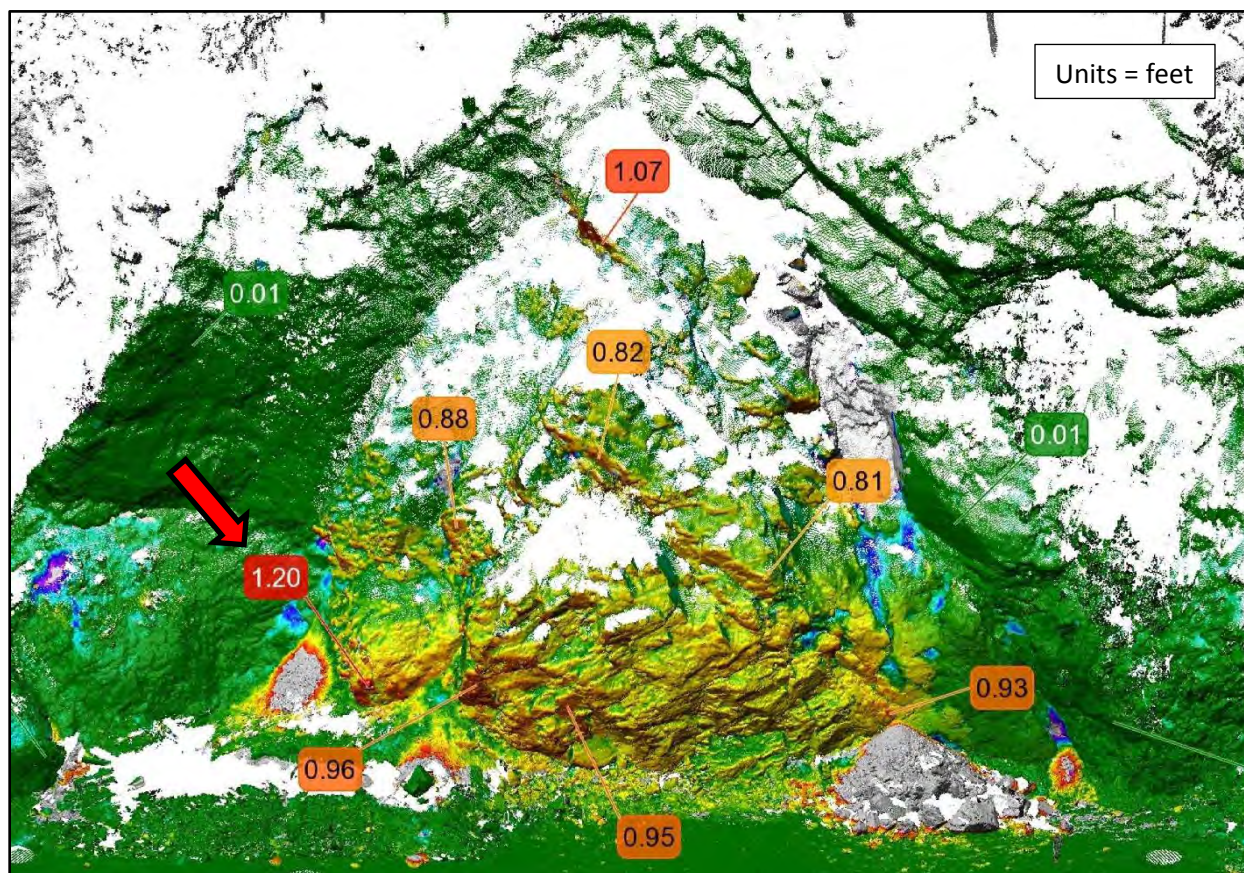


Figure 6: LiDAR change analysis showing slope movement in feet between days 22 and 41.



Figure 7: Collecting discontinuity measurements while rappelling on the slope.

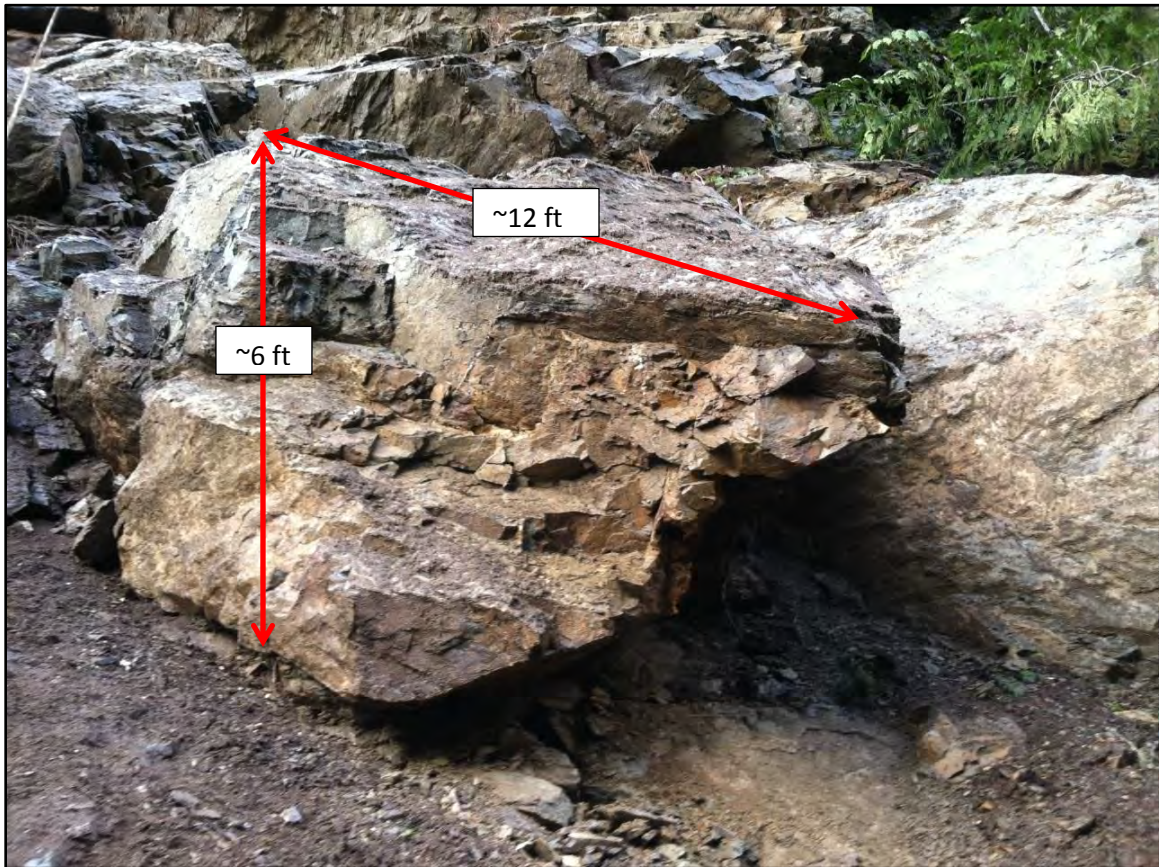


Figure 8: A large detached block on the slope.



Figure 9: The slope before the failure with a roadway-dipping discontinuity near the toe-of-slope.

GEOTECHNICAL ANALYSIS

Using the DTM developed from the first ground-based LiDAR scan, we calculated the slope height to be ~105 feet, the slope width to be ~350 feet, and the slope distance from the slope crest to the highway to be ~135 feet (Figure 10). We also used this data and the DTM to construct a subsurface model of the distressed rock mass remaining on the slope (~11,000 yds³) (Figure 11) and calculated the amount of debris that originally fell from the slope (~7,500 yds³).

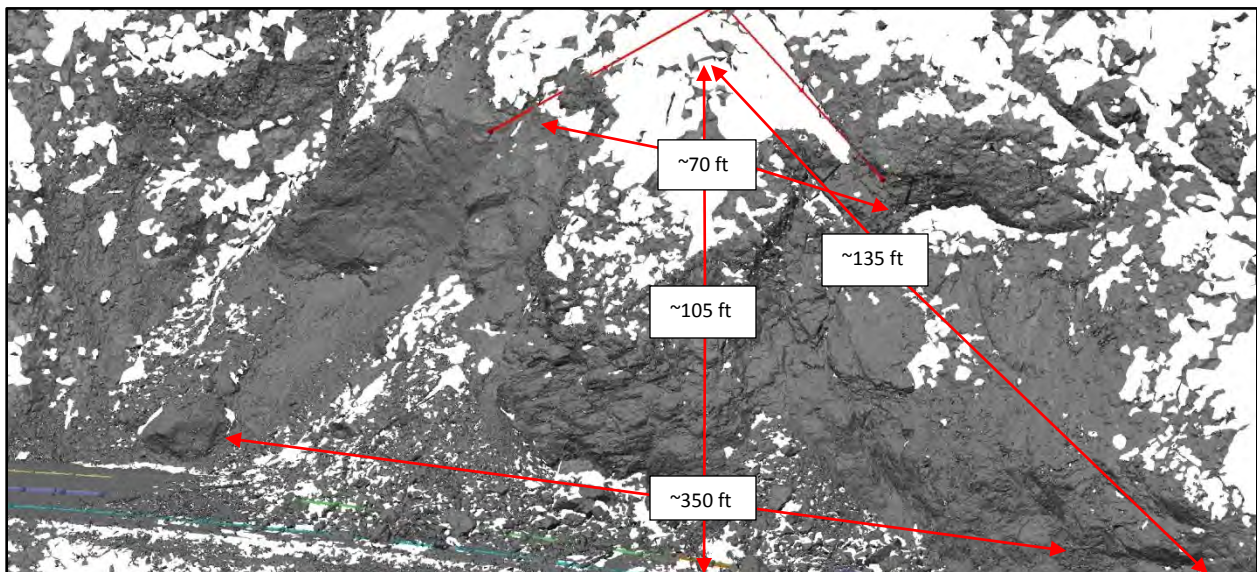


Figure 10: A DTM developed from the ground-based LiDAR scan after the initial slide.

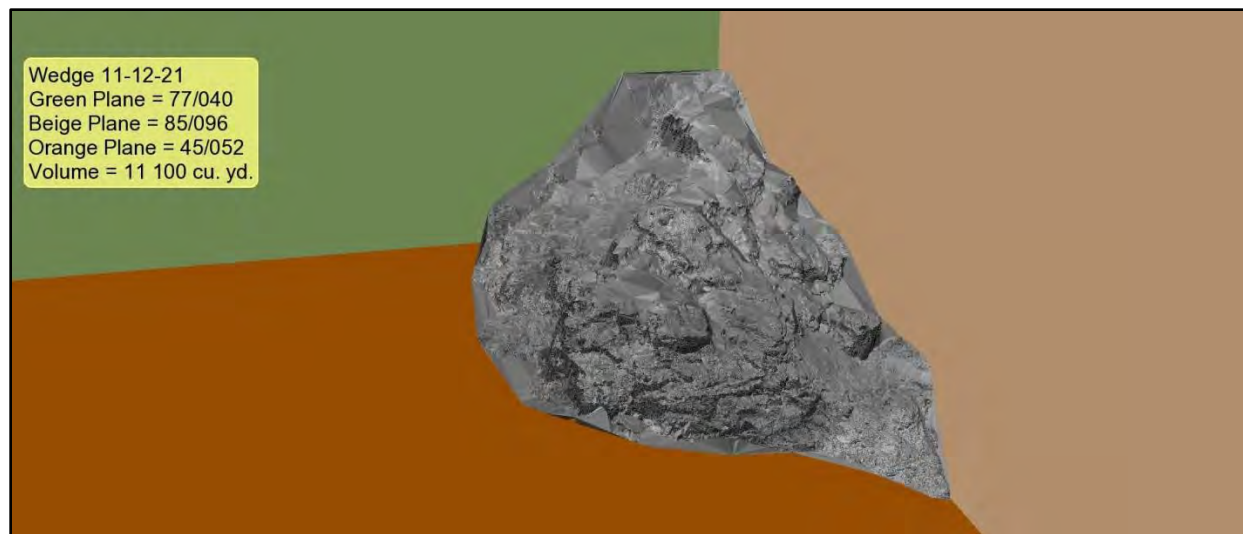


Figure 11: A subsurface model of the distressed rock mass (~11,000 yds³).

In conjunction with the discontinuity measurements that we manually collected while rappelling from ropes, discontinuity measurements acquired through the ground-based LiDAR scans were also used to measure the geologic structure within the slope for areas inaccessible to safely map. The major joint sets we identified were D_1 : $73^\circ/316^\circ$, D_2 : $77^\circ/040^\circ$, D_4 : $85^\circ/096^\circ$, and D_5 : $45^\circ/052^\circ$ and the slope (S_1) is oriented at about $67^\circ/055^\circ$. Using stereographic projection, these joint sets were analyzed for potential planar, wedge, and toppling-type failures (Figure 12). To evaluate the geometry and stability of surface wedges and sliding blocks, we conducted a deterministic analysis on intersecting ($D_1:D_5$ and $D_1:D_4$) and the near parallel (D_2 and D_5) joint sets to the slope. Using conservative friction angles and no cohesion, we conducted back-analyses on several rock blocks and wedges that were adjacent to the failing rock mass. These rock blocks and wedges were identified as being potentially unstable, or that would be left unsupported after the distressed rock mass was removed. We then calculated the amount of reinforcement that would be required for each rock block or wedge to achieve a factor-of-safety of at least 1.25. We assumed the presence of tension cracks partially filled (10%) with water behind the rock mass, although these were not observed for the majority of the blocks we analyzed. To reinforce these rock blocks and wedges we used a combination of 25 kip and 100 kip passive rock dowels. Our analyses also assumed that the existing rock joint patterns in conjunction with horizontal drains could effectively limit the buildup of water pressures in the slope.

Our change-based LiDAR analyses (Figure 6) indicated that several feet of differential slope movement has occurred over a period of a couple of months and that the rate of movement is accelerating (Figure 13). Consideration was given to constructing a buttress in front of the distressed rock mass. Our limit-equilibrium analyses indicated that a buttress would be marginally effective at mitigating the slope movement, but it would not provide adequate protection from falling rocks above (Figure 14). Also, a buttress could only be considered a temporary solution, because its width would take the entire eastbound lane of the highway.

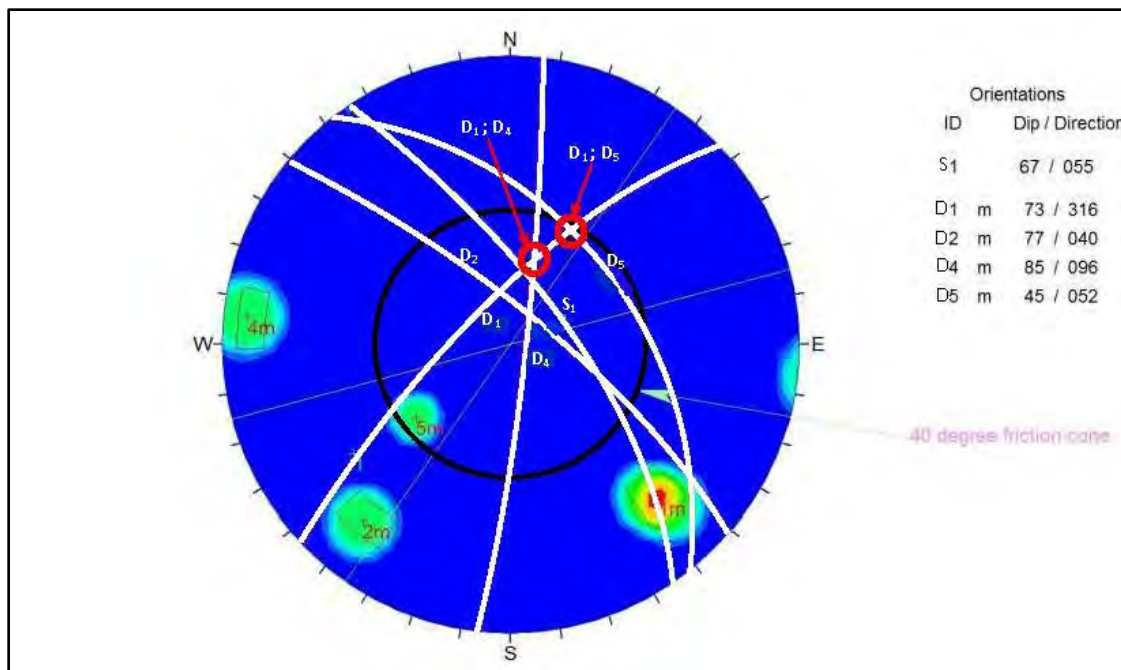


Figure 12: Stereographic projection of the discontinuity data.

Since the highway was already closed, additional consideration was given to just letting the slope fail, followed by slope scaling, analysis, and then slope reinforcement. This was not considered an acceptable approach, because of the uncertainties as to when the slope would actually fail and if there would be enough time to mitigate the slope prior to the highway reopening. There was also concern for the safety of recreational vehicle users and cross country skiers that would be accessing the high country through the project site. After these options were no longer considered viable, our efforts turned towards additional slope monitoring/changed-based analyses and developing additional geotechnical recommendations to remove the distressed rock mass and to stabilize the slope. We needed to overcome a couple of significant challenges in developing our recommendations. These challenges included: 1.) Possibly stranding construction equipment at the project site until spring due to a large snow storm and an avalanche, which are common for this area, and 2.) how to safely place workers and equipment on or below a slope that is exhibiting accelerated movement.

GEOTECHNICAL RECOMMENDATIONS

Based upon our initial site reconnaissance and our data collection and analysis, we developed recommendations that included tree cutting near the brow of the slope, brow rounding, mechanical excavation of the detached rock mass with a long-reach excavator, limited on-slope safety scaling, and at the completion of the excavation, the installation of horizontal drains and rock dowels along the back wall of the slope and within several potentially unstable blocks that remained on the slope (Figure 15). We recommended for the excavation to proceed from the top-of-slope downward and for a ramp to be constructed to maximize the 154-foot

reach of the excavator. The ramp would also serve as a protective berm to stop falling rock from impacting the excavator (Figure 16).

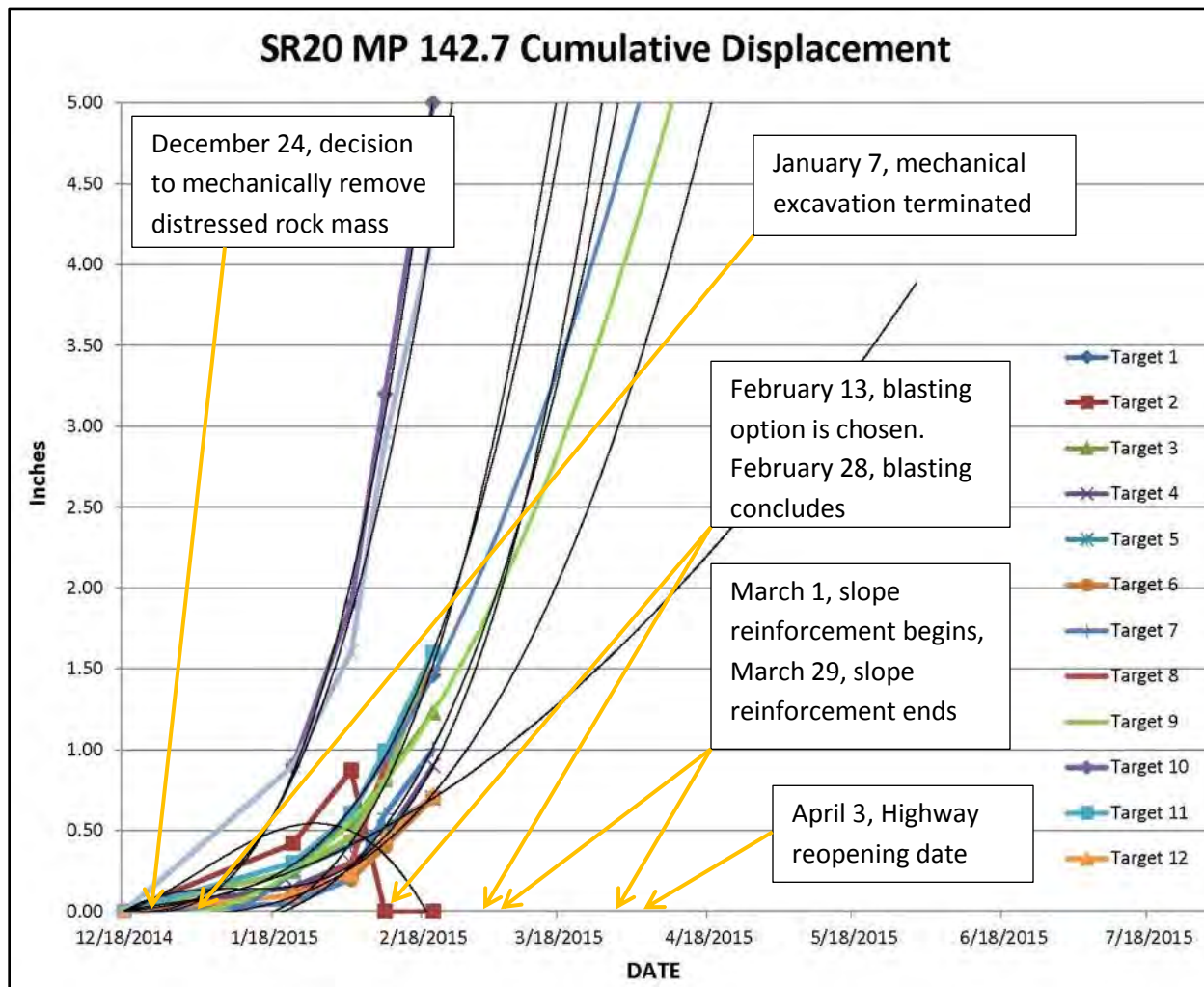


Figure 13: Graphed cumulative displacement of slope targets showing accelerated movement and the steepening of the curves towards failure.

After the first week of construction, we needed to amend our recommendations due to the ineffectiveness of the mechanical excavation and an approaching winter storm. After additional slope monitoring, analyses, and consultation with a specialty contractor and a geotechnical consultant, our amended recommendations included replacing the mechanical scaling with trim blasting, followed by limited on-slope safety scaling and slope reinforcement. We envisioned the trim blasting as utilizing carefully positioned drill holes that could be drilled from either a wagon drill, spider drill, or by hand. The workers and the equipment would be tied-off to stable trees or bars placed into stable bedrock outcrops further upslope. We recommended for the work to progress from the top-of-slope downward through small shots until the detached material was safely removed from the slope.

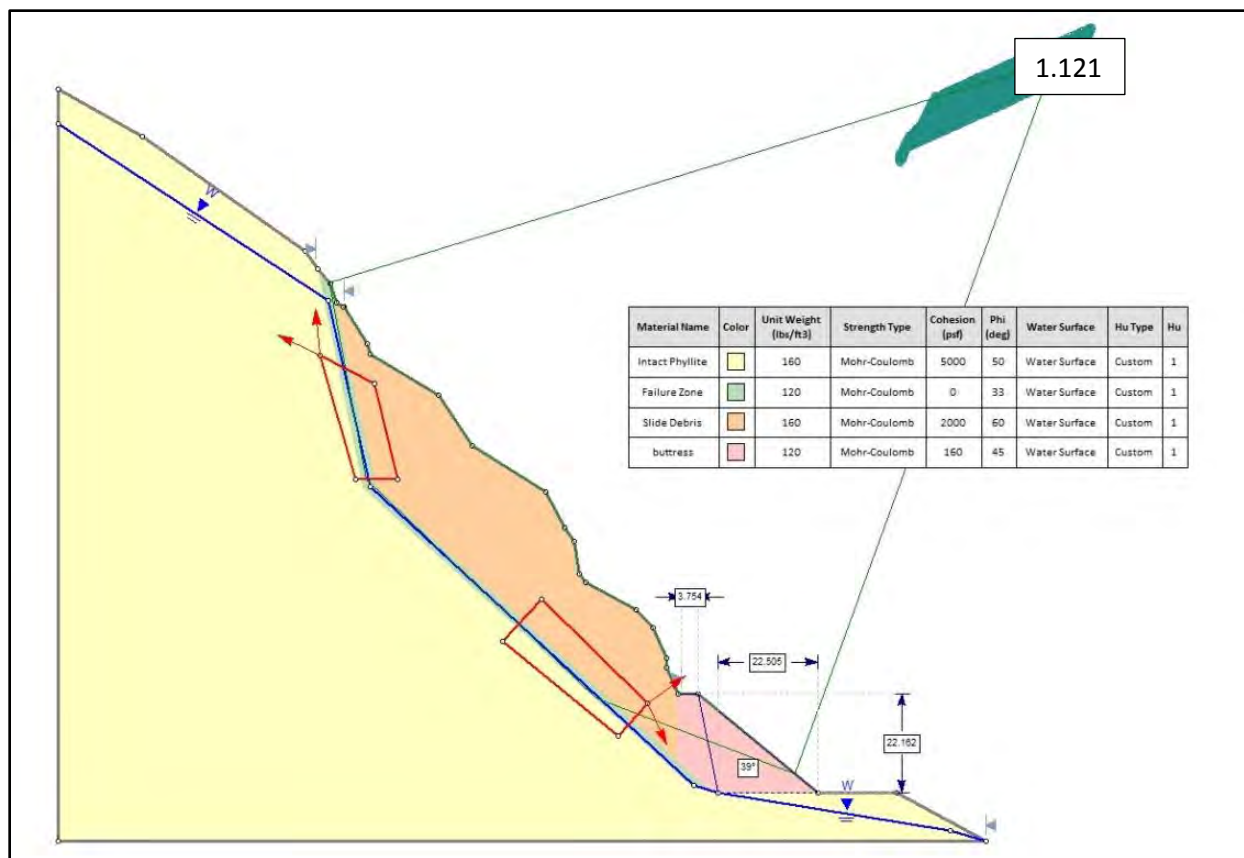


Figure 14: Limit-equilibrium analysis for a potential buttress constructed in front of the detached rock mass.

CONSTRUCTION

Due to heavy snow fall and avalanche danger, the North Cascades Highway is closed to highway traffic every winter until late spring or early summer. With no highway traffic, the contractor was able to utilize the entire width and a long length of the highway to construct this project. Even with a closed highway, there were many construction constraints this project had to overcome:

1. The federal emergency funding limited the project to a total of 30-working days.
2. The project was located just beyond a couple of large avalanche chutes that routinely deposit deep snow and debris on the highway.
3. The project was within the Mount Baker National Forest.
4. The pristine Granite Creek was situated just below the highway and the project site.
5. The project was in a designated owl habitat area that prohibited blasting after March 1.
6. The closest cell phone service was nearly 20 minutes away from the project site.
7. Because of a mild winter and lack of snowfall, there was pressure to open the highway early.

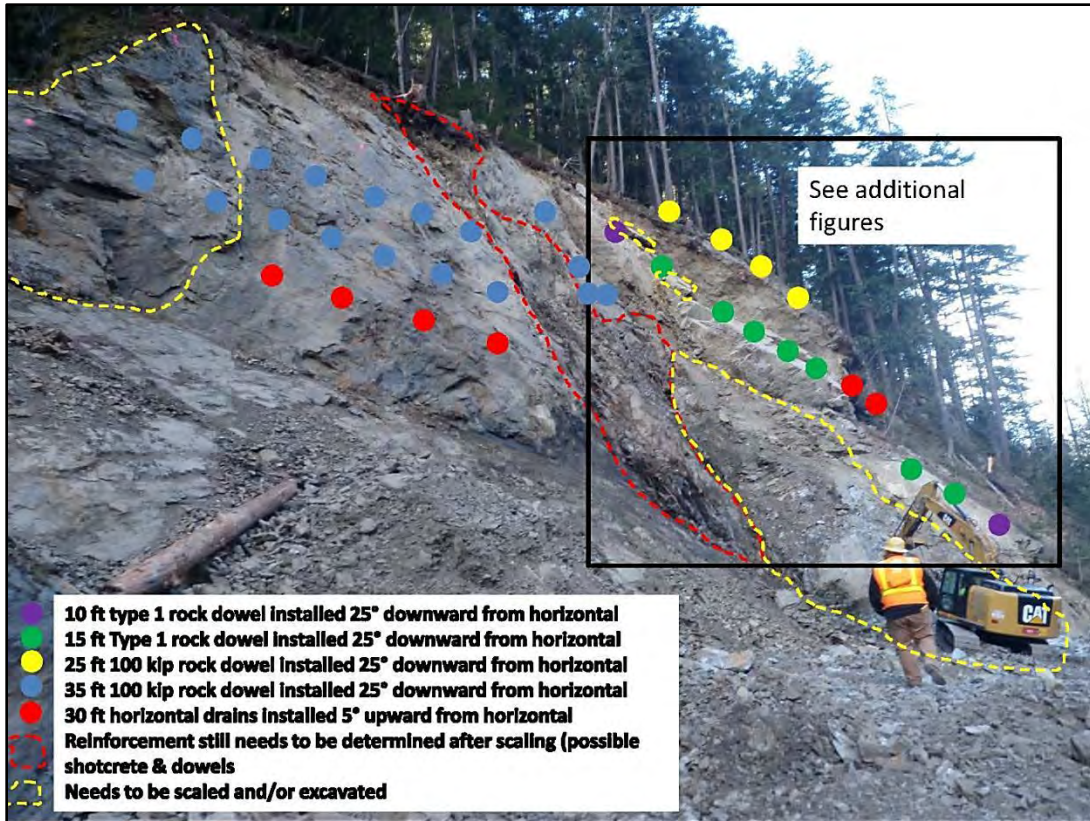


Figure 15: Recommended slope reinforcement in the eastern, middle, and western sections.



Figure 16: A long-reach excavator removing debris from the slope while on a ramp.

8. Although the highway was closed to traffic, it was accessible to recreational vehicles and cross country skiers. The Department tried to discourage public access through the site due to safety concerns.
9. The project was also located approximately 4 hours away from our geotechnical office and 1.5 hours from services.

Because the slope was actively moving, debris was left near the base of the slope to buttress the main area of active movement and to help prevent a catastrophic slope failure. WSDOT survey also monitored specific points on the slope for movement every 15 minutes with a total station and conducted ground-based LiDAR scans on an every other week basis to help ensure worker safety on the project (Figure 17).



Figure 17: The red dots were monitored for movement every 15 minutes with a total station.

After considerable slope monitoring, analysis, and planning, our initial recommendation was amended from mechanical excavation to trim blasting because the long-reach excavator was top heavy and could only excavate the upper portion of the slope that was within its reach. Also, the location of the ramp that provided both safety and additional reach for the excavator took a long time to construct and was too far away from the slope, thus limiting the reach of the excavator. Finally, a winter storm that was fast approaching threatened to trap the excavator on the opposite side of the avalanche chutes for the remainder of the winter.

WSDOT had an “on-call” agreement with a local contractor to remove the debris from the highway and to stabilize the slope. Although the Department was paying “force account” to construct this project, they had limited ability in requiring the contractor use a specific subcontractor or use specific construction methods. This limited contracting ability led to some less than desirable construction techniques that included the use of surface charges and horizontal drill holes for blasting. Fortunately, the horizontal drill holes were kept far enough away from the back wall of the excavated slope to minimize any slope damage. Unfortunately, the contractor had difficulty keeping the horizontal drill holes open and the few holes that they

were able to drill were ≤ 10 feet in length. Because the horizontal drilling was less effective, the contractor had to rely on the surface charges to remove most of the dangerous blocks on the upper portion of the slope (Figure 18). Also, the surface charges were loud, removed only limited amounts of debris from the slope, and contributed to some minor damage to the back wall of the slope (Figure 19). After several horizontal drill-hole blasts and multiple surface charge blasts, most of the middle-to-upper portions of the detached rock mass had been removed. The remainder of the rock mass in the middle-to-lower portion of the slope was then removed utilizing a combination of a hoe-ram and an excavator (Figure 20).



Figure 18: Surface charges placed on the slope.



Figure 19: Minor blast damage to the back slope from the surface charges.



Figure 20: A hoe-ram and an excavator removing material from the lower portion of the slope.

After the completion of blasting, another subcontractor conducted slope scaling to remove the remainder of the loose material on the slope. Based upon further analyses, additional recommendations were then developed that included more rock dowels and horizontal drains (Figures 21 & 22). Once the slope was safe to install the reinforcement, the subcontractor mobilized a crane-supported drill rig and a bencher drill to the project site. These drills were then used to drill the recommended rock dowel and horizontal drain holes (Figure 23).

CONCLUSION

This mid-December 2014 rock slide that completely covered State Highway 20 was fully mitigated within the 30-working day project window, for a total cost of about 1.2 million dollars. The project was completed prior to April 3, 2015, which was the earliest highway reopening date on record. Debris was kept out of Granite Creek, blasting was completed prior to March 1, and approximately 7,500 yds³ of displaced material was removed from the highway and another 11,000 yds³ of highly distressed material was safely removed from the slope, while it was still moving. To stabilize the freshly exposed back wall of the slope, the contractor installed 870 linear feet of 100 kip rock dowels, 350 linear feet of 25 kip rock dowels, and drilled another 162 linear feet of horizontal drains to help keep water pressures from building-up within the slope. Damaged guardrail was also replaced and barrier was sited beneath the slope to control minor rockfall from reaching the travel lanes (Figure 24).

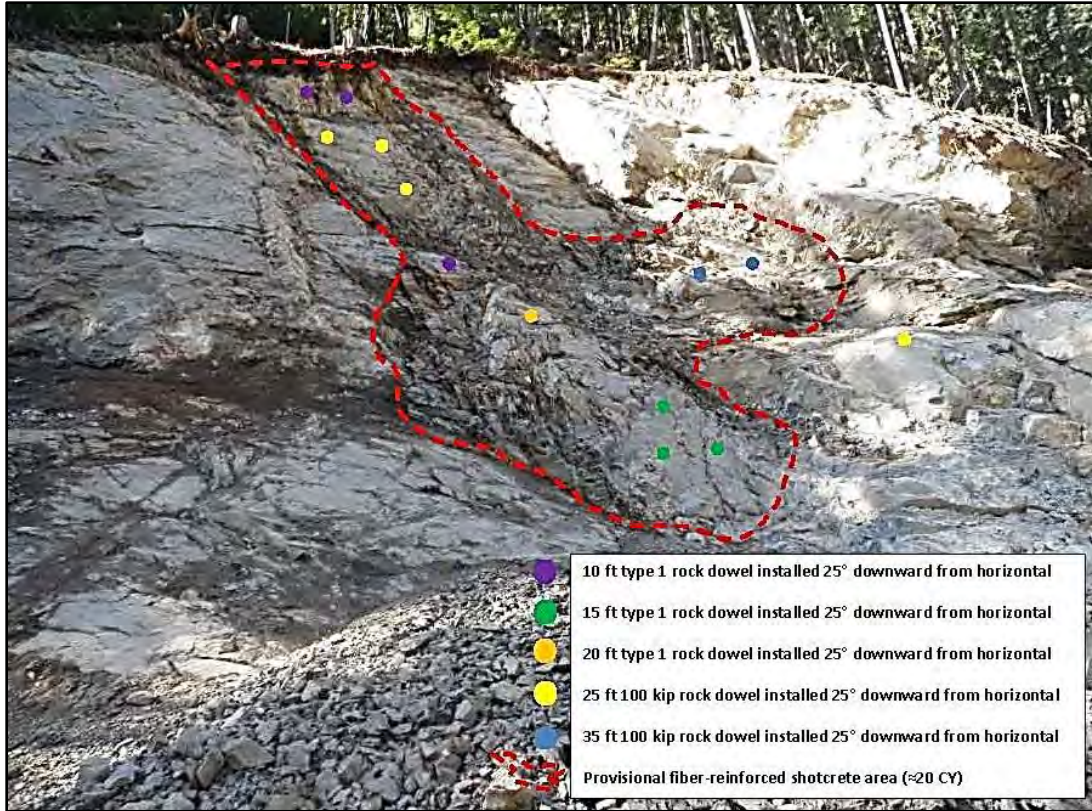


Figure 21: Additional recommended slope reinforcement in the middle section.



Figure 22: Additional recommended slope reinforcement in the eastern & western sections.



Figure 23: Drilling the dowel locations from a crane and a man-lift.



Figure 24: View of the completed project from the east.

REFERENCES

Haugerud, Ralph A. and Tabor, Rowland W; “Geologic Map of the North Cascades Range, Washington”, U.S. Department of The Interior, U.S. Geological Survey, 2009

Proactive Interferometry and Point Data Integration

Budge Slide Monitoring

John S. Metzger

IDSNA, 15000 W. 6th Avenue, Suite 104,
Golden, Colorado, 80401, 303-232-3047
j.metzger@idscorporation.com

Enrico Boi

IDSNA, 15000 W. 6th Avenue, Suite 104,
Golden, Colorado, 80401, 303-232-3047
e.boi@idscorporation.com

Cliff Preston

IDSNA, 15000 W. 6th Avenue, Suite 104,
Golden, Colorado, 80401, 303-232-3047
c.preston@idscorporation.com

Jason Rolfe

Tributary Environmental, P.O. Box 6854,
Jackson, Wyoming, 83002, 307-690-7258
jason@tributaryenvironmental.com

Acknowledgements

We would like to thank the Budge and Karns families for their support over several months. The Budge family for allowing access several times to their property during a period of stress and instability. A special thanks to the Karns family, for allowing us to site the radar on their property, and for the security and freedom of access.

Mr. Wallace Ulrich was invaluable in his professional sharing and consideration. His passion for Jackson and its citizens is unwavering, and his technical and geological knowledge is an ongoing inspiration.

Professor Roger Bilham – University of Colorado

IDS Corporation provided the availability of the radar instrument for an extended period, as well as the Technical team for site deployment, support, and data analysis.

The Town of Jackson, Wyoming

Bob McLaurin – Town Manager, Larry Pardee – Director of Public Works

Mr. Robert Swintz, Andy Bergen

Tributary Environmental – GPS data points, aerial images, and ground control truthing. Timely collegial support for instrument interventions and security.

The Geologists of Jackson Hole

Phil Gyr – Nelson Engineering

George Machan – Landslide Technology

Disclaimer

Statements and views presented in this paper are strictly those of the authors, and do not necessarily reflect positions held by their affiliations, the Highway Geology Symposium (HGS), or others acknowledged above. The mention of trade name for commercial products does not imply the approval or endorsement by HGS.

Copyright Notice

Copyright © 2015 Highway Geology Symposium (HGS)

All Rights Reserved. Printed in the United States of America. No part of this publication may be reproduced or copied in any form or by any means – graphic, electronic, mechanical, including photocopying, taping, or information storage and retrieval systems – without prior written permission of the HGS. This includes the original authors.

ABSTRACT

JACKSON, WY. , April 2014 – An area just off West Broadway at the intersection of Budge Drive, in the town of Jackson, Wyoming, exhibited cracking and significant displacement between April 15th and 19th, 2014. A home cut in half, families displaced, property values in question, evacuated commercial real-estate, a broken water main, city utility corridor impacted, potential for greater losses, all were facets of the event faced by citizens of the town of Jackson, Wyoming.

As a contribution to the science of monitoring the slide, respecting the geological context and potential community impact as well as an opportunity to align with traditional geotechnical instrumentation and engineering planning, we placed an IBIS radar on location and began a period of regular scanning in January, 2015. Our period of interest included the winter months and the change of seasons that could create anomalies during the transition from frozen, to a thawing and precipitation laden spring terrain.

Would we see regular, consistent movement? Movement across the Andesite feature at mid-slide that had exhibited activity in different vectors? Would velocities increase during periods of precipitation and temperature fluctuation? Would the point and extensometer data support similar results, or differences? This investigation outlines the opportunity for fulltime monitoring and presents radar data and information from an extensometer. Efforts to access point data acquired during 2014 were unsuccessful. Our own initiative to integrate corner reflector references stalled due to insufficient funding. Figures 1 and 2 present the Interferometer (IBIS) and a time series of selected data-points (Area 1).



Figure 1: IBIS Radar Interferometer - Scanning Through Raydel Window at Jackson, WY.

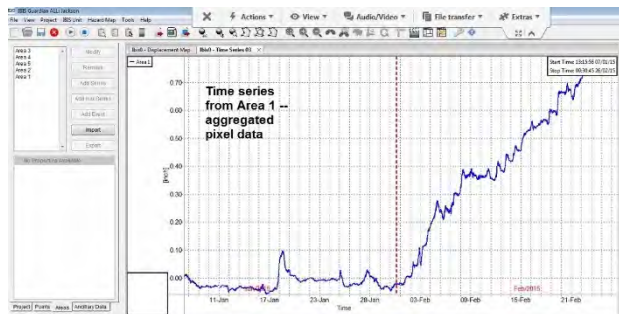


Figure 2: Time Series Data 1/11 to 2/26, 2015 – Area 1.

The monitoring term was completed in early May, 2015. Throughout the period on site we were in communication with local experts, Town of Jackson staff, and local transportation and geotechnical practitioners. Our efforts to complete ground point integration as well as broader data exchanges with official and professional entities proved only marginally successful. There remain legal, contractual, procedural, and sectoral challenges to a more open and community supportive integration of efforts. The dataset proved valuable, exhibited seasonal effects, and informal reporting was shared with citizens and local professionals. The hardware exhibited reliability of 99.7 percent and was suitable to task.

INTRODUCTION

Landslide and at-risk areas of rock-fall continue to challenge local communities, state agencies, scientific, and emergency response agencies. Recent events around the globe continue to highlight the results of the confluence of need for residences, businesses, and transport corridors and the natural and man-influenced terrain from which roads, rail, and habitation environments are built near, on, or through.

Geotechnical professionals and civil engineers have at their hand any number of tools to mark, detail, monitor, and assess natural materials and their strength, interpret natural terrain and man-made sites for construction or development, and manage or monitor preparation, builds, and environmental effects of these actions.

The ground based, or terrestrial radar interferometer is one such tool. Born of the integration of basic radar concepts and the application thereof for monitoring surficial displacements in support of slope monitoring and the management of operational, natural, and urgent events caused by the elements or man-influenced actions. The product of early cooperation between government and university research and applied science, the instrument's commercialization process commenced with real effect in 2003. For more than twelve years terrestrial radar for mining and civil works has been available and in use across the globe.(1)

We acknowledge that the rapid pace of inception, development, and application of interferometric tools has led to ongoing challenges across academic and professional practice sectors as well as the practitioners' fields of experience and work. There is often a tension between familiar tools and predictable results, and new tools and applications plus the learned tasks, analysis, and qualified experience of use. We also suggest that a decade on, and with the current sectoral leading tools, there is no better time to afford, value, and institute the direct application of GB-InSAR together with instruments tried and true in the practitioners' toolkit.

Why Jackson, and the Budge Slide?(2) In our review of the initial reports, coming just following the dire incident in Washington (Oso), on March 22nd, 2014(3)...surely, why not? If there was an opportunity to acquire a wide-field view, with real-time data, at sub-millimeter detail, where there were fortunately no fatalities or injuries, but that potential remained...could we not better support community and regional decision makers, affected citizens, emergency response personnel, and workers active in mitigation or remediation efforts?

We thought someone would be interested, if only for a trial and to know perhaps what was "not" active, or what may lie abreast of the immediate headscarp and visually active area. Actually, no one called or e-mailed, in response to our initial contacts.

While reviewing accounts in the press and on the Town of Jackson website, we identified citizens with specific or potential interest in the issue of public safety, transport corridor management, geology, and geotechnical support. During our search we made contact with a local geo-professional who suggested we reach-out to a respected former state geologist (Wyoming). In early May 2014, we visited Jackson, the site of the slide, and in coordination with local citizens decided to deploy the radar interferometer.



Figure 1: IBIS Interferometric Radar at the Karns Residence Facing the Budge Slide, May, 2014.

The cost was relative, as we had offered deployment first, costs after – data would be shared, analyzed, and evaluated as a priority. The instrument scanned for about three weeks. We reviewed the data and continued to share with area contacts in an effort to develop local sustainability for a longer deployment, one that could lay the foundation for additional sharing of the dataset and its usefulness in decision making and substantive discussions about the slide and its wider impacts.

Transport Corridor Considerations

As a part of our consideration for acting further on the data from the exploratory scanning in May of 2014, we looked at the potential impacts on infrastructure near the slide area, principally the issues likely to be faced if the slide continued to develop as indicated, or became a more active event, though one without detailed information of the larger impact area should the slope fail across Budge Drive and into the right of way of US highways 26, 89, 189,191 as some comments and event modeling brought to light.(4)

“**Jackson** [1] is in [Northwest Wyoming](#), close to the south end of [Grand Teton National Park](#). It is the gateway to two of the United States' best-known national parks, Grand Teton itself and nearby [Yellowstone](#). Many famous people maintain vacation homes in and around this area. The combined elements of beautiful mountain scenery, Old West heritage, tourist traps and celebrity residents give this small town a unique atmosphere both cosmopolitan and frontier.”(5)

US Highway corridors in the region of Jackson, WY

- US 89 - “In Wyoming, U.S. 89 passes through many scenic sites including [Grand Teton National Park](#), the [Jackson Hole](#) valley, the Snake, and the [Star Valley](#).

Passing northward along the western border of Wyoming with Idaho, U.S. 89 enters the [Grand Teton National Park](#). Here, U.S. 89 is the backbone visitor highway for two [U.S. National Parks](#). ...”(6)

- US 189 - “US 189 enters [Wyoming](#) from the west co-routed with [Interstate 80](#). The routes separate east of [Evanston](#), where US 189 proceeds north to the [Jackson Hole](#) area. At Hoback Junction, south of [Jackson](#), US 189 rejoins its parent route, [US 89](#).”(7)
- US 191 – “...Continuing north, the road traverses increasingly mountainous terrain, entering the [Bridger-Teton National Forest](#) and passing through the small community of [Bondurant](#) before descending through the narrow Hoback River Canyon to an intersection with [US 26](#) and [US 89](#) at Hoback Junction. The route then follows the [Snake River](#) valley northward to [Jackson](#). US 191 is concurrent with US 189 between Daniel Junction and Jackson, and with US 26 and US 89 between Hoback Junction and Jackson. ...”(8)
- US 26 – “From Alpine, US 26 is co-signed with [U.S. Route 89](#) east and north to Hoback Junction, then co-signed with US 89, [U.S. Route 189](#), and [U.S. Route 191](#) to [Jackson](#). US 189 ends in Jackson, and the other three highways continue their concurrency through [Grand Teton National Park](#) up to Moran. ...”(9)
- WYOMING 22 – “WYO 22 passes through Teton,^[11] and later the community of [Wilson](#), a [census-designated place](#) (CDP). On the eastern border of Wilson, at 13.51 miles (21.74 km), WYO 22 intersects the southern terminus of [Wyoming Highway 390](#) (Moose-Wilson Road) before crossing the [Snake River](#).^[12] WYO 22 continues east to the town of [Jackson](#) where it ends at [U.S. Highway 26/89/189/191](#) (Broadway).”(10)

General Idea of Area Traffic Counts

We read and reviewed some information on corridor traffic counts to have an idea of the potential issues that could be faced by an active event and the site’s potential broader impact on the above mentioned highways. In the context of a current proposal, (2015 Jackson/Teton Integrated Transportation Plan): APPENDIX H: NORTH BRIDGE TRAFFIC IMPACT ANALYSIS – there is information on recent (summer 2014) daily traffic levels on West

Broadway (US89/191/26/189) and a forecast of additional traffic under the North Bridge (project) consideration.(11).

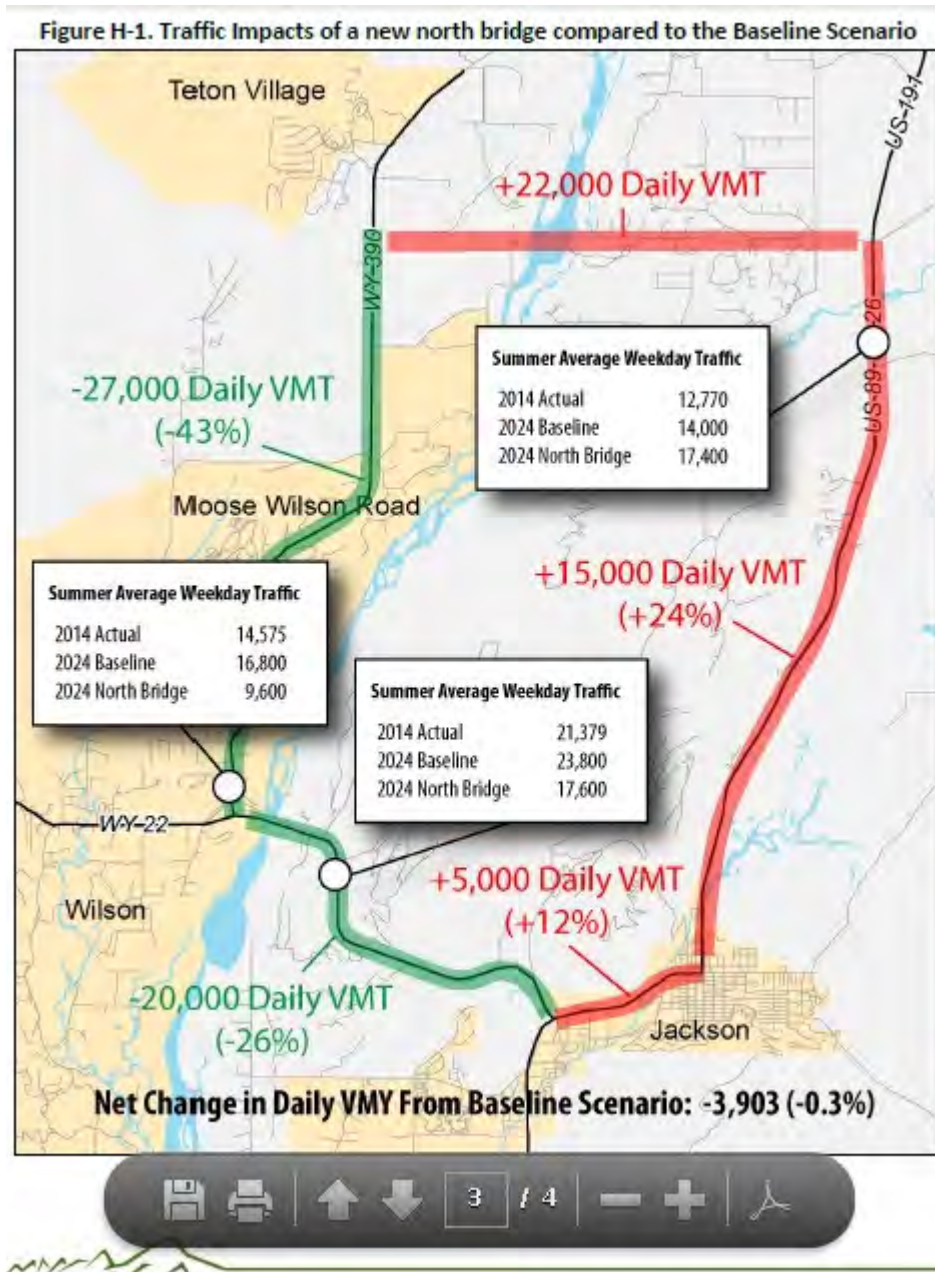


Figure 2: Figure H1 from the APPENDIX H: NORTH BRIDGE TRAFFIC IMPACT ANALYSIS Document.

Other Infrastructure Impacts

Aside from the Town of Jackson's infrastructure (utility) at-risk across the visible and potential slide area, we noted a recent project – the Wyoming Centennial Scenic Byway was nearing completion. The byway path lays across the breadth of the visible and potential at-risk areas of the slide.

The community had received significant grant amounts as a part of the ongoing development in this corridor, for example "...In 2011, the Town of Jackson submitted an application for \$1,253,575 to the National Scenic Byways Program which provides grants to States and Indian tribes to implement projects on highways designated as National Scenic Byways or All-American Roads, or as State or Indian tribe scenic byways. The Town was awarded the full amount of the grant request, which also included a \$1,292,191 project overmatch. ..."(12)

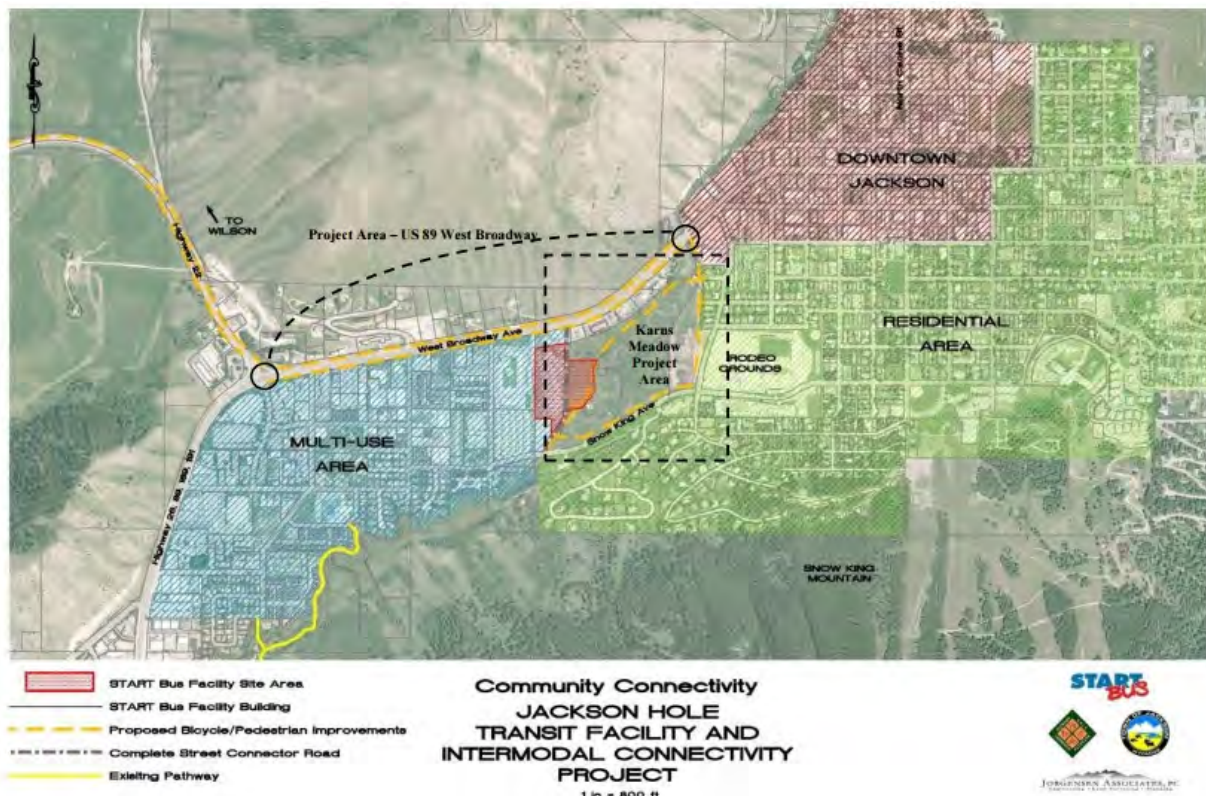


Figure 3: Scenic Byway Project Area - Budge Drive is at Center-left, North of West Broadway Ave.

This type of information and the ongoing interest among our community links formed an additional basis for considerations to re-establish monitoring and acquire a representative and longer-term dataset. Suggestions for additional monitoring, site review, and cognizance of potential broader structural and impact issues were being raised by area professionals and government agencies. We thought that a longer term dataset might be used for the benefit of the community, and as an effort to engage local administration, state agency professionals, and civil

works monitoring interests in a broader and ongoing effort. In any case, we were prepared to share our findings with interested practitioners and professionals.



Figure 1. Map showing approximate extent of deposits from potential secondary landslide. (Orthophoto image of active landslide area courtesy of Jason Rolfe, of Tributary Environmental, Jackson, Wyoming)

Figure 4: USGS Overlay image of Runout – Potential.

THE RE-DEPLOYMENT

Considering a redeployment in the winter season of 2014/15, a trailered enclosure was chosen to better protect the IBIS unit. IDSNA staff deployed the unit, and started the Guardian (data processing and analysis software) Project. The dataset for this presentation is comprised of scans that began on January 11th, 2015.



Figure 5: IBIS Unit Scanning Through Raydel Window.

DATA ACQUISITION

IBIS System Specifications

IBIS System Specifications	
Accuracy*	+/-0.004 inch (0.1mm)
Range Resolution	Up to 29.5 inch (.75m)
Cross-Range Resolution	Up to 4.4mrad - (4.4m @ 1Km, 8.8m @2Km)
Operating Range	32.8 to 13, 123 feet (10m to 4000m)
Operating Temperature	-4°F to 131°F (-20°C to 55°C)
Acquisition Time interval	3-5 min
Operating Frequency	Ku band Model: 17,05GHz-17,35GHz
EIRP power	Ku band Model: 26dBm
Power Consumption	120W @ 110/230Vac
Certification	CE (Europe), FCC (USA), IC (Canada)
Environment	IP 66
Software specifications	
IBIS Controller	Acquisition configuration and management, Power Supply Control Status information, Preliminary data processing, Data Transfer
IBIS Guardian	Real time data, interferometric processing, Automatic atmospheric correction, User defined alarm, Email and sms alarm forwarding, export to external software (GIS), External DTM importation

* The displacement measurement accuracy of +/-0.004 inch (0.1mm) can be obtained for quality measurement points under stable weather conditions.

The Guardian Project

The Project folder contains the acquisition area information, acquired data, system details, georeferenced data, user defined scan area, scenario analysis information, and alerts.

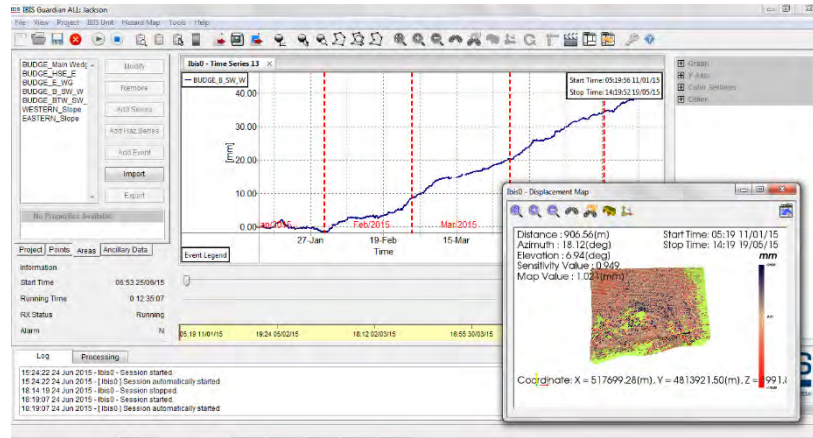


Figure 6: IDS Guardian Software Interface.

Data Views



Figure 7: Visual Image of Budge Slide from the Karns site, February, 20th, 2015.

The radar data were georeferenced to the DTM below. A GPS (with RTK differential correction) was used to collect points across the scenario as well as from each side of the IBIS linear scanner.** The project mask was selected to include areas to the north, west, and east of the “main” area of visible instability at the intersection of Budge Drive and West Broadway.

** Note: This effort was contributed by Tributary Environmental staff as support for the general data set and likely interest in ground-point associations.

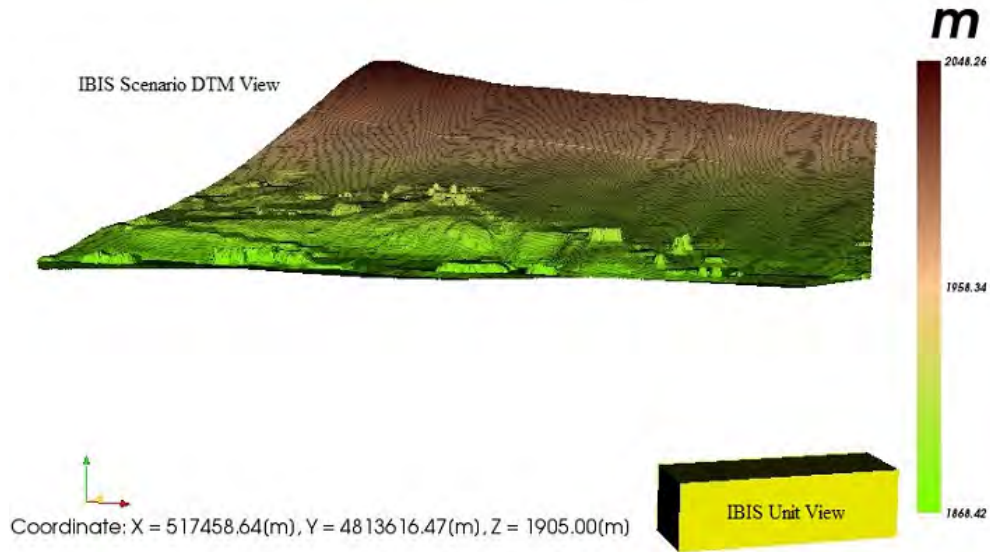


Figure 8: DTM Imported into the Guardian Analysis Software - Note Range Values in Meters (user configurable).

Interferometry and the Data View

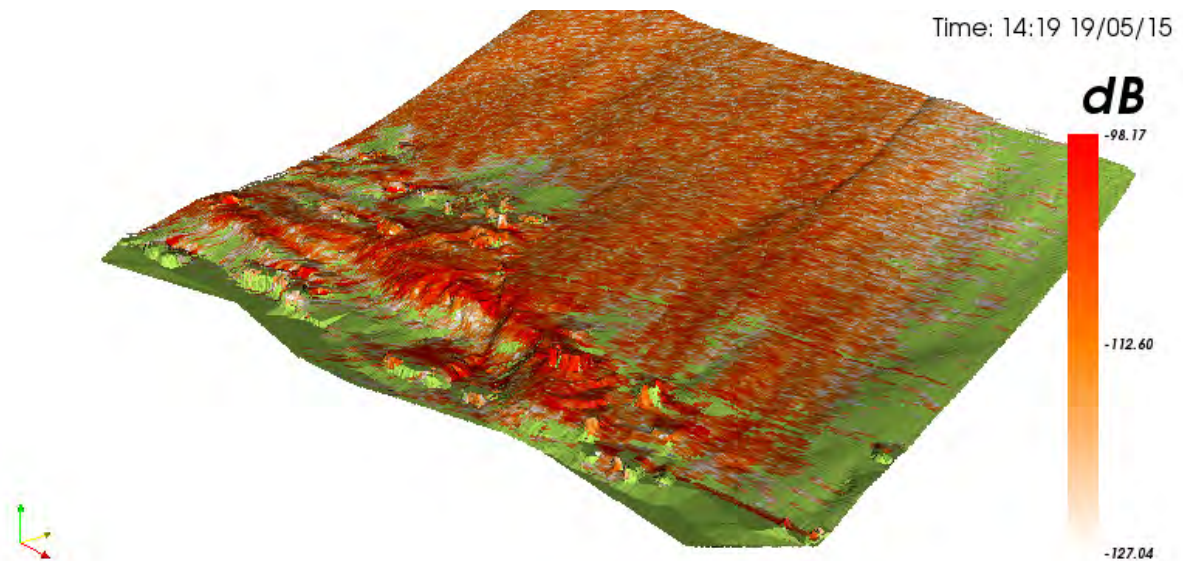


Figure 9: Project Scenario Amplitude Map and DTM.

Data are acquired through a series of scans along a 6.56 foot (2 meter) linear rail. This process – of moving the sensor array along the rail, results in the synthetic aperture technique. This creates the equivalent of a 6.56 foot (2 meter) array, with a very high cross range resolution. The SAR images are used to compare differences in phase and to generate maps of deformation. Displacements are measured in a line-of-sight vector toward the radar. During every acquisition, a radar “echo” is collected from each pixel. This echo brings back to the instrument, information

of signal amplitude $|A(n)|$ and a phase ϕ . The amplitude is related to the pixel backscattered power (high amplitude = strong reflector). Phase is an angle that ranges in the interval. An interferogram, is a map of the phase difference between any two acquisitions ($\Delta \phi$).

Atmospherics

As a component of every acquisition, the atmosphere the energy travels through has some effect on the signals' path. Within the system processing there are advanced algorithms derived from satellite interferometry that act as “filters” for data returns that are seen as highly variable, widespread, and uncorrelated in time.

This type of automatic processing does not require a user to select a “known” area of “stability” and in fact supports a firmer data quality for areas that exhibit regular correlation and high frequency, e.g. displacement.

Snowfall and Precipitation

We share this detail as it is a common question where terrain includes snowpack, or where there is seasonal snowfall and frequent accumulation. We anticipated snow events and the possibility of a snow pack covering areas of the Budge slide scenario (terrain). We have interpreted data for several years at sites where there is significant snowfall and have regularly noted that radar waves travel at a slower speed within the snow pack resulting in a shorter wavelength. Our consideration of data influenced by snowfall accumulations is illustrated here:

IBIS displacement, Δd , is calculated from the change in phase, $\Delta \phi$:

$$\Delta d = -\frac{\lambda_{air}}{4\pi} \Delta \phi$$

$$\Delta \phi = \Delta \phi_{atm} + \Delta \phi_{noise} + \Delta \phi_{movement} + \Delta \phi_{snow}$$

$\Delta \phi_{snow}$ can be calculated as a function of snow thickness, Δh_{snow} :

$$\Delta \phi_{snow} = \frac{4\pi c \Delta h_{snow}}{\lambda_{air}} \left(\frac{1}{v_{snow}} - \frac{1}{c} \right)$$

Therefore measured displacement as a result of changing snow thickness is:

$$\Delta d_{snow} = \Delta h_{snow} \left(1 - \frac{c}{v_{snow}} \right)$$

Assuming: $c > v_{snow}$

Positive movement is towards radar, positive Δh_{snow} represents an increase in snow depth where h_{snow} is snow thickness

The changing thickness of the snowpack results in a phase change in IBIS data. The data period (winter/spring) included several snow and precipitation events, though the overall snow

cover was much less than anticipated, allowing for generally good acquisition conditions throughout the period.

Colleagues' Extensometer Data

Extensometer, prism, inclinometer, and piezometer data had been collected from various installations across the site in 2014.(13) In the fall of 2014, a remotely accessible extensometer was placed in the fractured and heavily dilated graben area to the east of the Budge home. The eastern side of the affected area was generally more active and posed concern as being closest to the Walgreens property and installation – where little information was available in reference to ongoing activity or direction of any ongoing mitigation and or remediation efforts.

We had access to and were monitoring the extensometer data (Ulrich/Bilham), while also observing returns from the areas where it was sited within the radar data. Also, we looked at precipitation events – snow and later rain, and how the data indicated activity that aligned with the specific events, and the aftermath.(14)

On several occasions we had informal and associative communications surrounding various events(15). We endeavored to share our data with local citizens and professionals who made requests or were providing their own information. Relative to monitoring and the nature of such, there generally includes the consideration of risk, of risk level and processes, and open dialog and discussion of applied actions and communications.

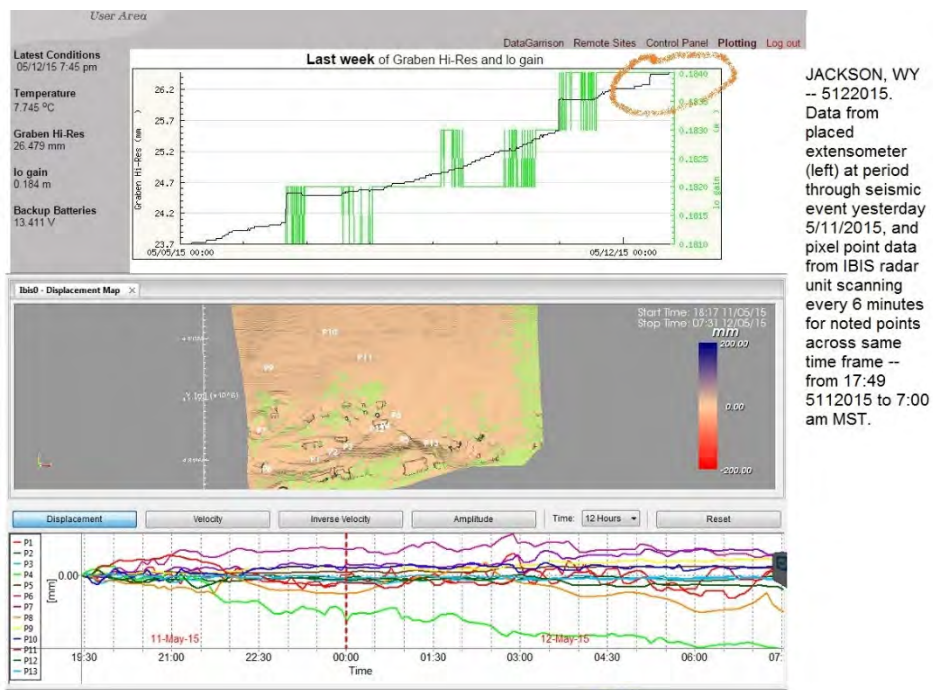


Figure 10: Local (Teton, Cty.) Seismic event of 5/11/2015 extensometer and selected points (radar) data time series.

Acquisition of Ground Points

Questions were raised about relative positions of data returns (IBIS) and ground interpretations. There are means and protocol to verify controversial information originating at a specific "point" in the scenario. Size specific objects (corner reflectors) can be applied in the field which create a known and distinct return. The highly reflective radar signal can be absolutely discerned and linked to a ground point. We note that this type of truthing had been done as a part of the early research and development of the instrument (IBIS). There exists a case study of a comparison between targets acquired and monitored by a "Total Station", and a microwave (radar) instrument. Corner reflectors have a usefulness where there may need to be a definitive indicator and or where a physical structure (tower, stack, building) exists in the acquisition area and is of interest.

Considering the Budge Slide area contained both natural structures, and items (trees) as well as poles, buildings, and power cables there was an awareness to address the mix of reflectors in the scenario with corner reflectors at known points. We prepared for a campaign of selected points by including these in our GPS data acquisition. Ground-truthing is an ageless part of geological mapping, and our colleagues were keen to complete a related and specific review of data from the selected points. Investigators supported the questions that were raised, however clarification remains incomplete at this time.

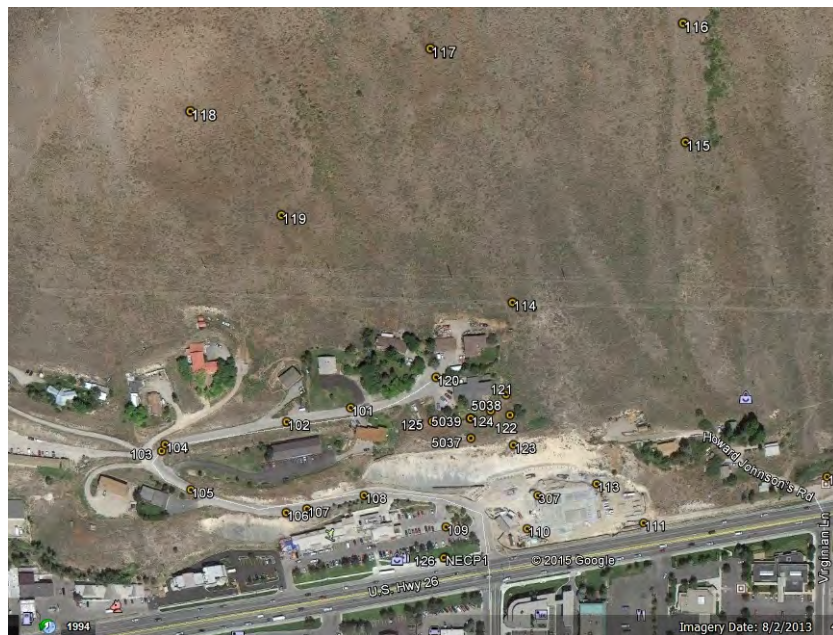


Figure 11: 30+ Points Available for Corner Reflector Placement.

REVIEW OF DATA

The dataset consists of scans on 5 minute intervals from 5:19 on 1/11/2015 to 14:19 on 5/15/2015. From the Karns property site to the Budge home is approximately 6,237 feet. There was no specific downtime as a result of any system event. Power supply issues occurred on the

AC line and with the Verizon Hot-Spot for data transfer. Radar scanning continued throughout the deployment. The unit was accessible remotely through a wireless link and was monitored from Golden, CO, on a regular basis.

The data exhibits a range of displacements across the scan scenario. Snowfall, and melt, as well as heavy precipitation events were noted, confirmed by communication with local support, and provide evidence of the environmental considerations when doing analysis and referencing weather instruments. There was a weather station on-board the trailer and this data were considered in looking after the system health and considering any needs for off-site support.

The goal in the course of the exercise was to include specific ground points as references for analysis, as well as to complete an overall data product for sharing and decision making. Budgetary limits and limited resources (staff) were specific obstacles in bringing the inclusive corner reflector (points) references to complete that consideration in the effort. Data presented below is offered as exhibited and illustrative interferometric results indicating displacements in a line-of-site direction toward (negative values) and away (positive values) from the position of the IBIS (Karns property site). The cell resolution was 2.06 feet (0.63 meter). Data time series graphs exhibit results for named areas or for specific “points” noted.

General Observations

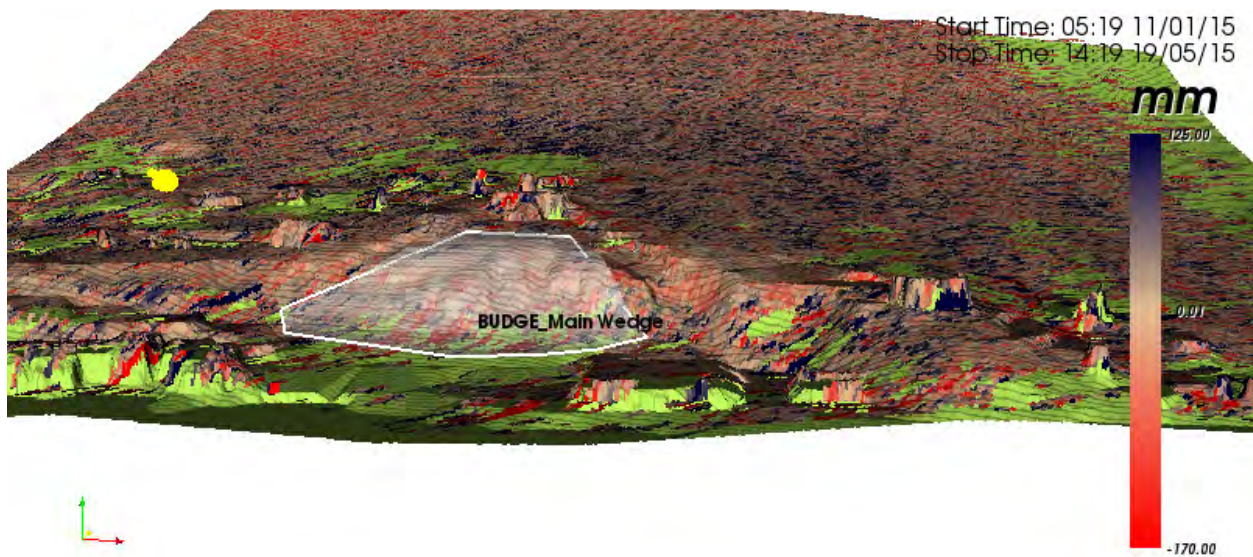


Figure 12: Budge Slide Data (all) and DTM. Yellow Arrow Is Line of Site To IBIS. Area Shown Is BUDGE_Main Wedge.

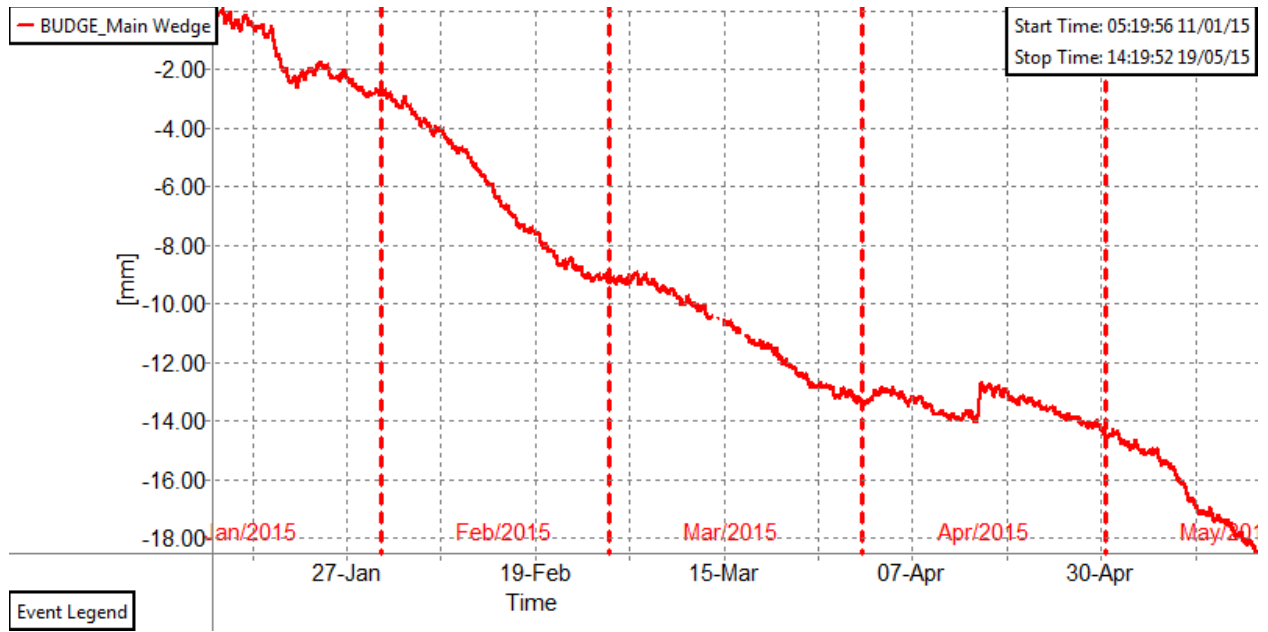


Figure 13: BUDGE_Main Wedge Time Series Data.

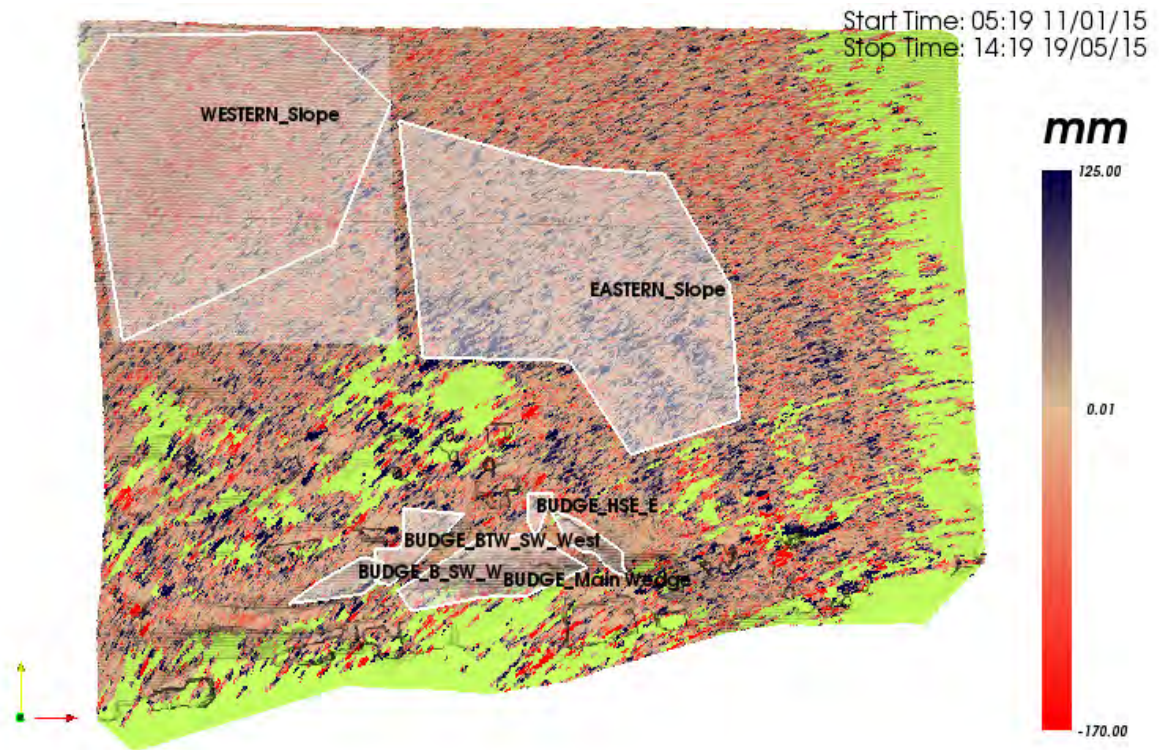


Figure 14: BUDGE_Areas – Top View - Time Series = Aggregated Displacement of Each Scan for All Cells.



Figure 15: BUDGE_HSE_E -- Area on East Side of House. See Figure 14.

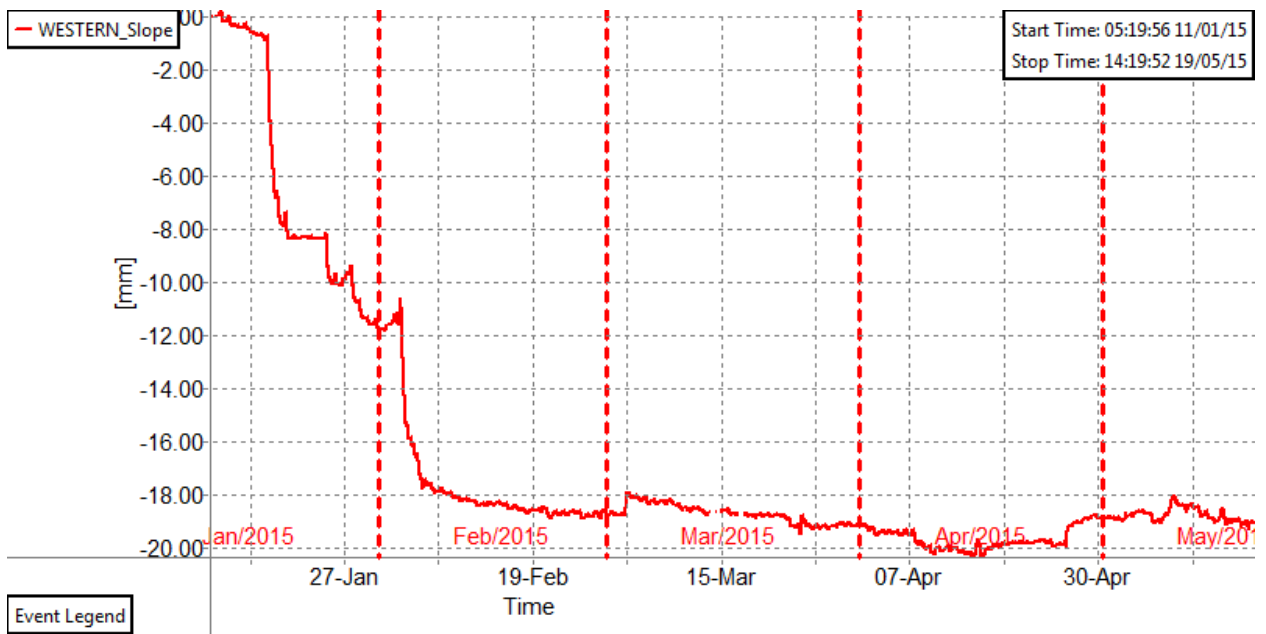


Figure 16: BUDGE_Areas -- Western Slope. See Figure 14.

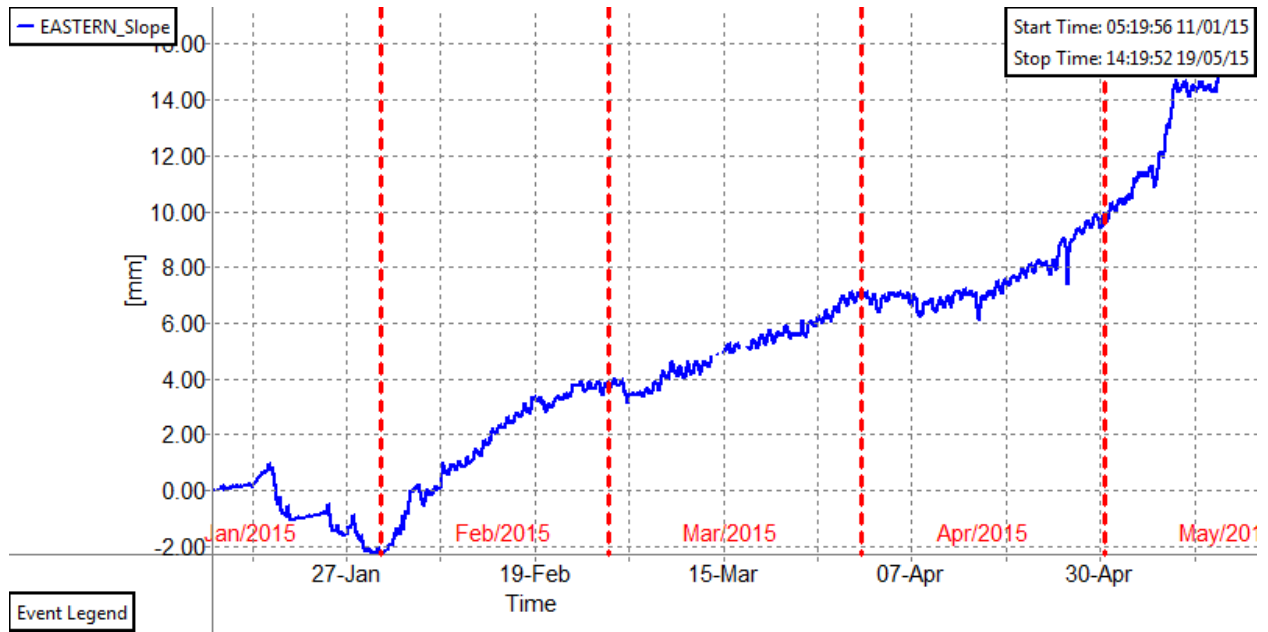


Figure 17: BUDGE_Areas - Eastern Slope - See Figure 14.

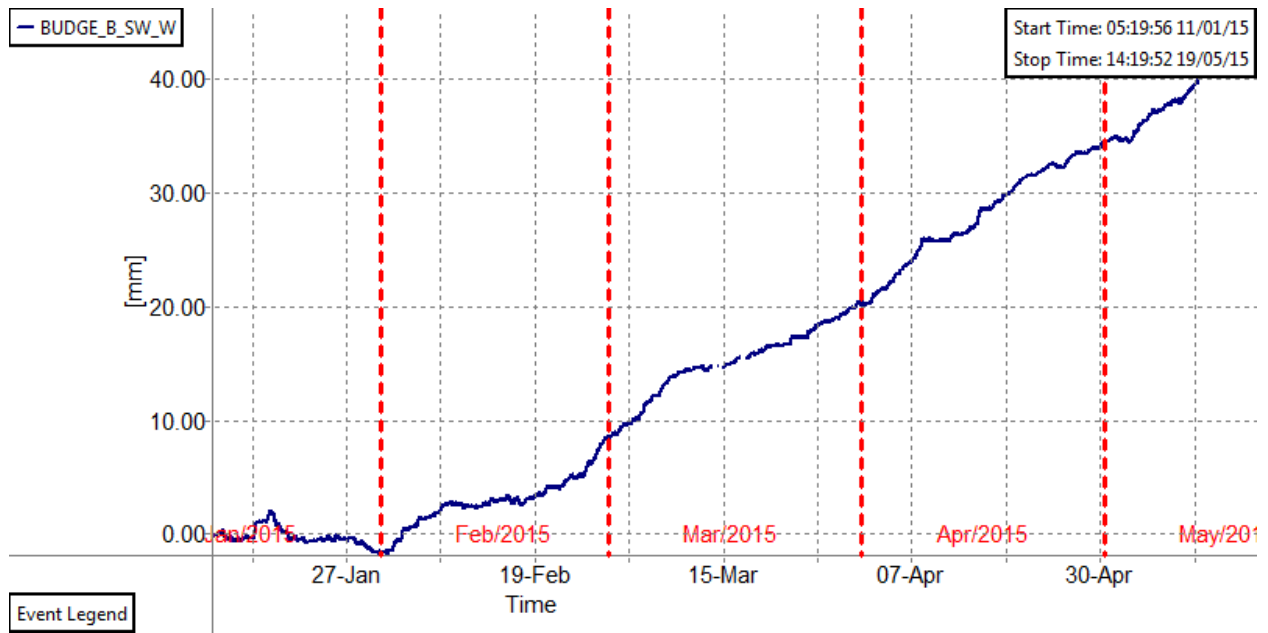


Figure 18: BUDGE_Areas - Behind Sidewinders - See Figure 14.

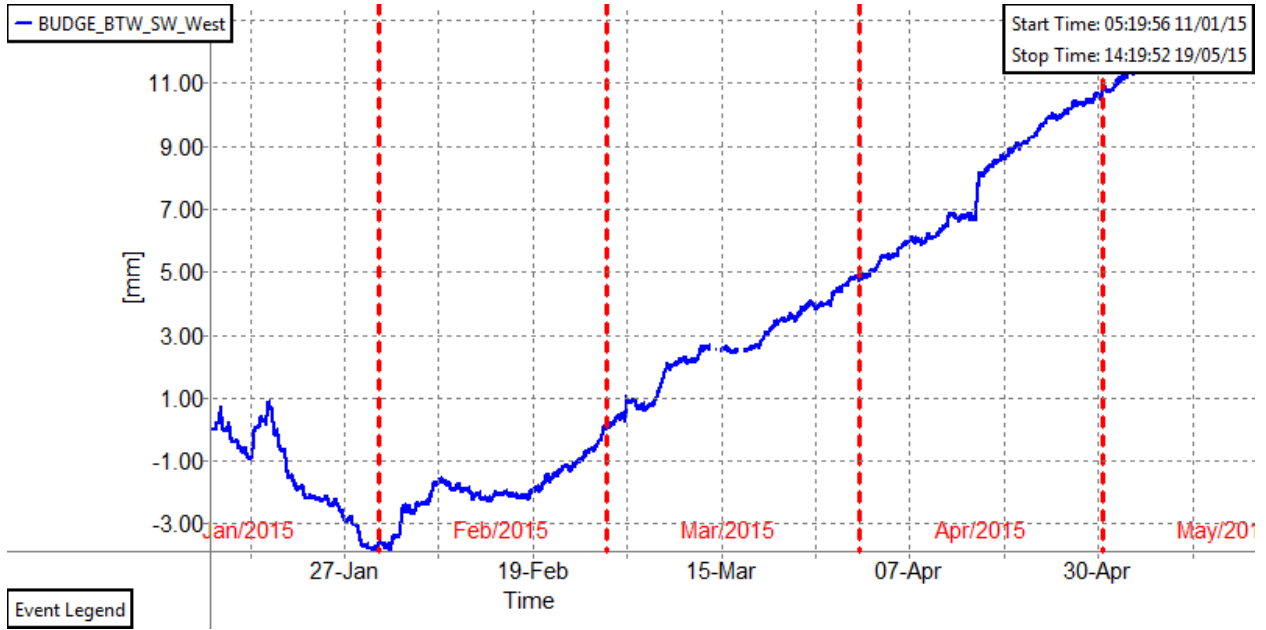


Figure 19: BUDGE_Areas - Between Main Wedge and Behind Sidewinders (area). See Figure 14.

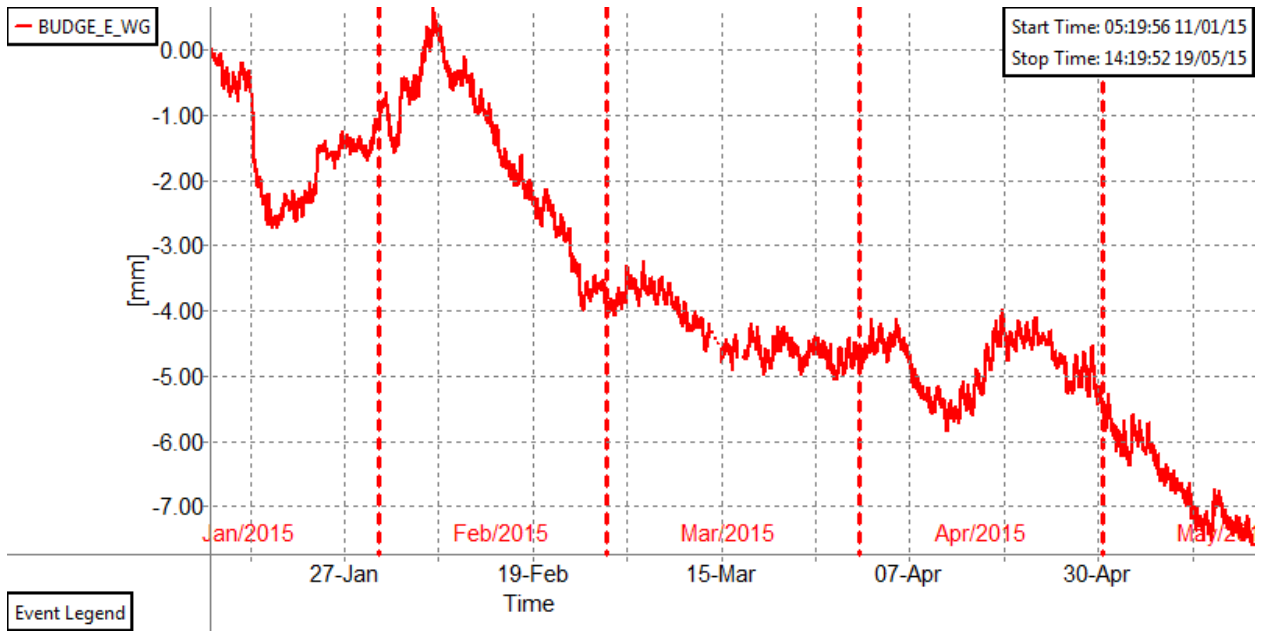


Figure 20: BUDGE_Areas - Behind Walgreens East. See Figure 14.

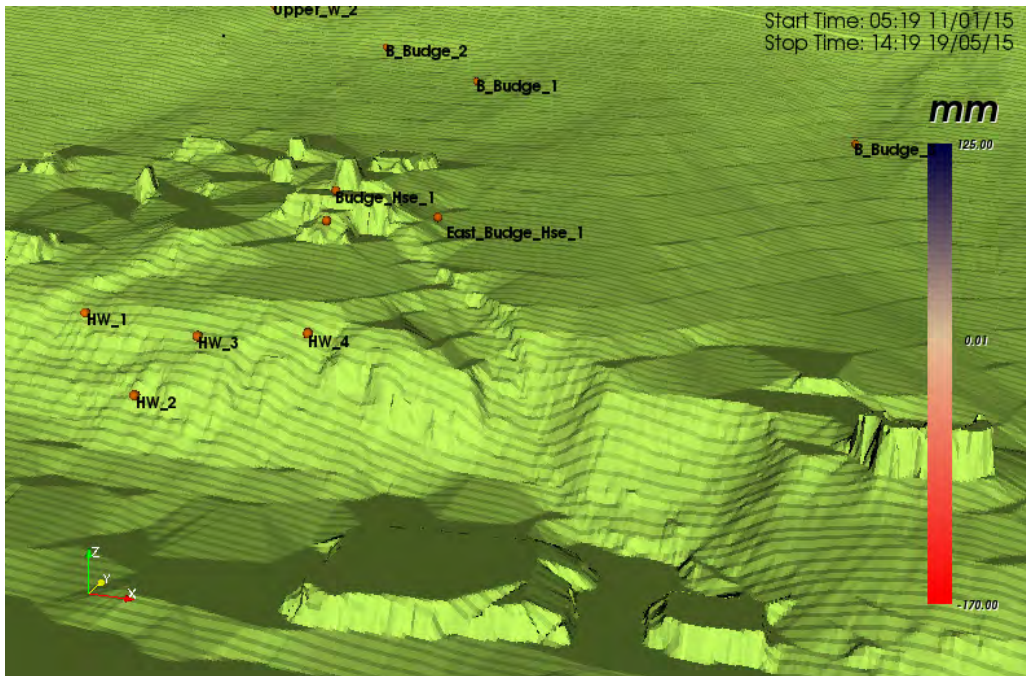


Figure 21: BUDGE_DTM - With Points at Budge House, behind Budge House and Across Slide Headwall.

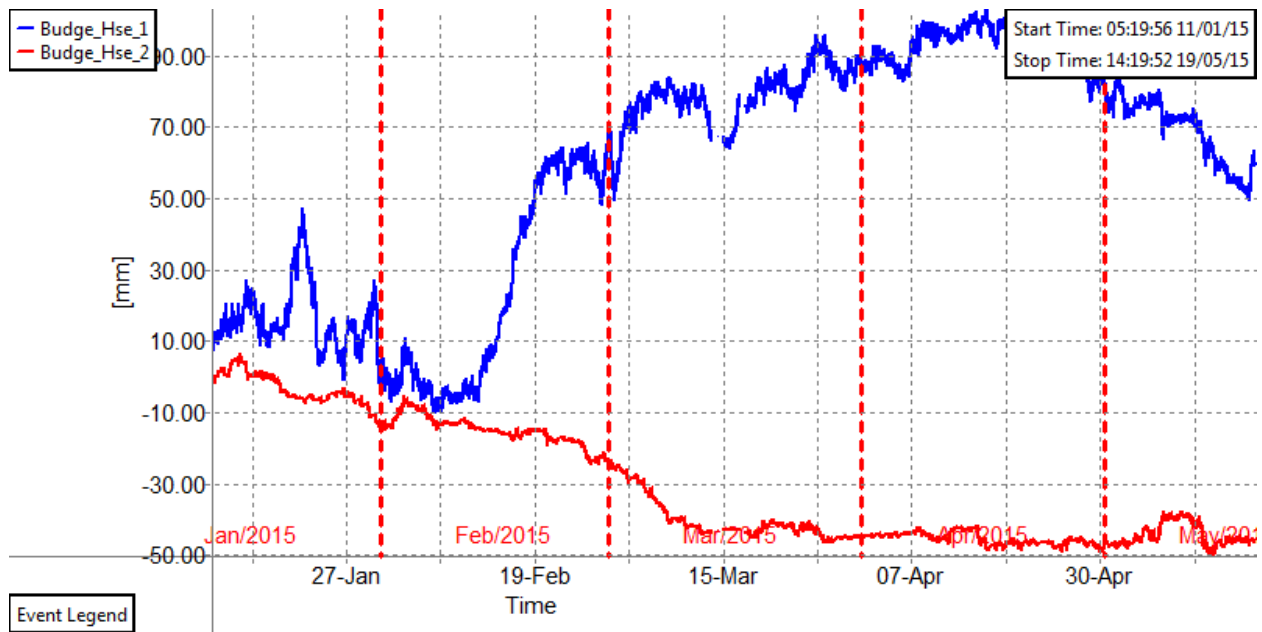


Figure 22: BUDGE_Points - Budge House Points - Upper (1) and Sheared (2) sections. See Figure 21.



Figure 23: BUDGE_Points - Behind the Budge Home - See Figure 21.

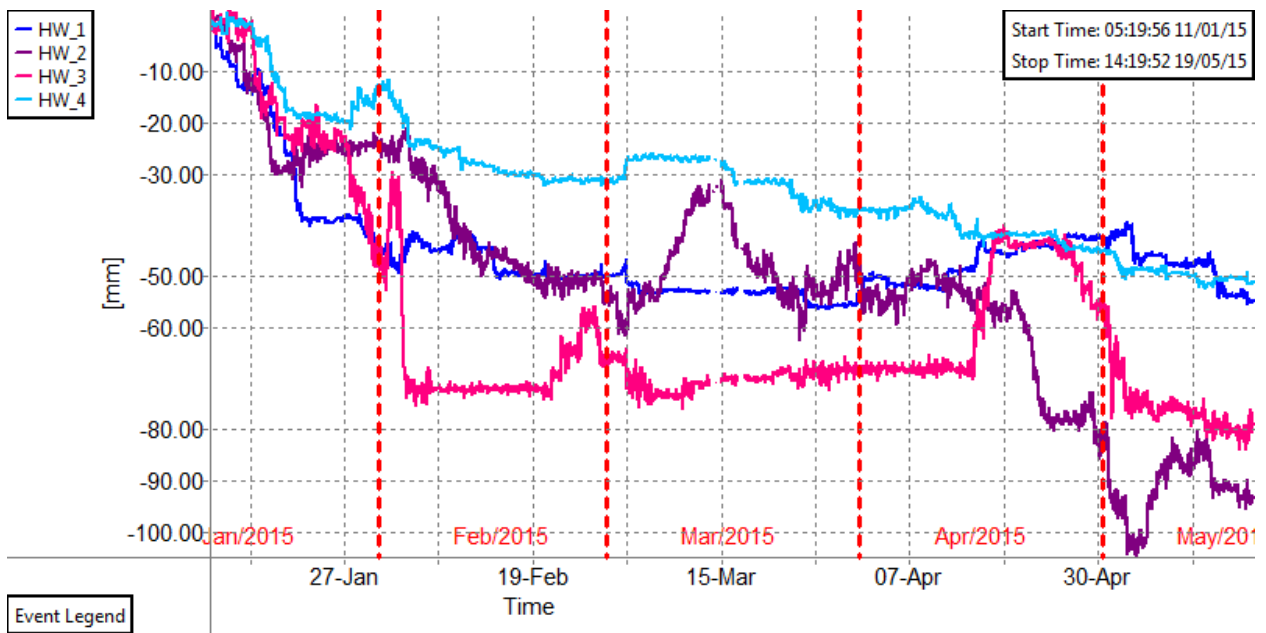


Figure 24: BUDGE_Points - Four Points Selected Across Slide Headwall.

CONCLUSION

The variety of displacements noted across the scan area support other investigators considerations that the slide at the Budge site remains an active and at-risk event that would benefit from an on-going and integrated data monitoring exercise.

There is a clear opportunity to support a community, contribute to event and site safety, and produce a valuable and open data source through real-time monitoring of this type of at-risk events that may impact public safety. The sharing and integration of data resources contributes additional value to officials, responders, and contracted engineering and technical staff. At commercial rates of less than \$40.00 an hour, a highly accurate and alerts-capable system can add significantly to the overall mitigation and remediation effort. Further specific ground-truthing across the scenario is a worthwhile component of additional monitoring activities.

There remains an opportunity to support decision making officials and professionals as the scenario at the site ages and is further influenced by the environment and any large scale mitigation or remediation efforts. The IBIS system offers the ability to scan a large area with high accuracy and in real-time, while calculating progressive displacements, managed within an interface that supports alerts (SMS, e-mail), georeferenced results, full-time or itinerant placements, and fully reviewable and interactive data sets.

REFERENCES

University Report

1. C. Atzeni¹, M. Barla², M. Pieraccini¹, F. Antolini², *Safety-critical monitoring of natural and engineered slopes with ground-based Synthetic Aperture Radar: a review of the state of the art.* ¹Department of Information Engineering, Università degli Studi di Firenze, ²Department of Structural, Building and Geotechnical Engineering, Politecnico di Torino, 2013, 19 p.

Website

2. “time-lapse video of Walgreens landslide”. By Jim Stanford on April 18, 2014 <http://www.jhunderground.com/2014/04/18/time-lapse-video-of-walgreens-landslide/>. Accessed April, 2014.
3. GEER Oso Landslide Report, http://www.geerassociation.org/GEER_Post%20EQ%20Reports/Oso_WA_2014/GEER_Oso_Landslide_Report.pdf. Accessed September, 2014.

Letter from Federal Agency

4. Godt Ph.D, Jonathan W. and Baum Ph.D., Rex L. *Letter to Bob McLaurin, Town of Jackson, PO Box 1687, 150 East Pearl Avenue, Jackson, WY, 83001.* United States Department of the Interior, U.S. Geological Survey, Geologic Hazards Science Center, December, 12th, 2014.

Website

5. Jackson (Wyoming). [http://wikitravel.org/en/Jackson_\(Wyoming\)](http://wikitravel.org/en/Jackson_(Wyoming)). Accessed August, 2014.
6. U.S. Route 89. https://en.wikipedia.org/wiki/U.S._Route_89#Wyoming. Accessed December, 2014.
7. U.S. Route 189. https://en.wikipedia.org/wiki/U.S._Route_189#Wyoming. Accessed December, 2014.
8. U. S. Route 191. https://en.wikipedia.org/wiki/U.S._Route_191#Wyoming. Accessed December, 2014.
9. U. S. Route 26. https://en.wikipedia.org/wiki/U.S._Route_26#Wyoming. Accessed December, 2014.

10. Wyoming Highway 22. https://en.wikipedia.org/wiki/Wyoming_Highway_22. Accessed December, 2014.
11. Jackson/Teton Integrated Transportation Plan 2015: North Bridge Traffic Impact Analysis (large). [http://www.tetonwyo.org/compplan/LDRUpdate/ITP/AppendixH_NorthBridgeTrafficImpactAnalysis\(large\).pdf](http://www.tetonwyo.org/compplan/LDRUpdate/ITP/AppendixH_NorthBridgeTrafficImpactAnalysis(large).pdf). Accessed June, 2015
12. Joint Information Meeting – Agenda Documentation: September 26th, 2012. <http://www.tetonwyo.org/cc/docs/StaffReports/2012-JIM/10-01-III-D-ALL.pdf>. Accessed August, 2014.

Unpublished Consulting Reports

13. Landslide Technology, Conceptual mitigation options report Budge Drive landslide, West Broadway Avenue, Jackson, Wyoming: to Town of Jackson, Wyoming, June 19th, 2014. 73p, 1 appendix.
14. Bilham, Roger, *Budge Landslide extensometer report April-November – to Wallace Ulrich*, November 14, 2014, University of Colorado, Boulder.

Website

15. M1.8 – Wyoming: Tuesday, May 12, 2015 at 03:37:08/UTC Monday, May 11, 2015 at 21:37:08 Local. <http://earthquake.usgs.gov/earthquakes/dyfi/events/us/20002eiu/us/index.html>.

Evaluation of D-cracking Durability of Indiana Carbonate Aggregates for use in Pavement Concrete

Belayneh Desta

Purdue University
Lyles School of Civil Engineering
550 Stadium Mall Drive, West Lafayette, IN. 47907-2051
Tel:765-494-5015 Fax:765-494-0395; Email: desta@purdue.edu

Terry West*

Purdue University
Department of Earth Atmospheric and Planetary Sciences
550 Stadium Mall Drive, West Lafayette, IN. 47907-2051
Tel: 765-494-5015 Fax: 765-494-3296; Email: trwest@purdue.edu

Jan Olek

Purdue University
Lyles School of Civil Engineering
550 Stadium Mall Drive, West Lafayette, IN. 47907-2051
Tel:765-494-5015 Fax:765-494-0395; Email: olek@ecn.purdue.edu

Nancy Whiting

Purdue University
Applied Concrete Research Initiative
1205 Montgomery Street
West Lafayette, IN 47996-2382
Tel: 651-785-6585; Email: whiting@ecn.purdue.edu

*presenter and contact

ABSTRACT

Concrete pavements are susceptible to damages from freezing and thawing in cold climates if not properly designed or built with durable materials. Certain types of sedimentary rocks, mainly limestone and dolomite are prone to freeze-thaw (FT) durability problems. As a result, concrete pavements containing such aggregate and exposed to a FT environment may develop a series of closely spaced cracks located near (and nominally parallel to) the longitudinal and transverse joints. This kind of deterioration is traditionally known as D-cracking. The D-cracking resistance of these aggregates depends on characteristics of their internal pore system, mineralogy (crystallinity), and the amount of clay in the microstructure. The importance of these factors with respect to D-cracking resistance of the aggregate is still not fully understood.

In the state of Indiana, limestone and dolomite deposits are the main sources of aggregates for pavement concrete. This study involved evaluation of eighteen carbonate aggregate samples collected from fourteen quarries in Indiana. These samples included materials from different geological formations and represented variable freeze-thaw resistance. In order to evaluate the FT performance of these aggregates in concrete pavements, they were used to fabricate prismatic concrete test specimens (3 x 4 x 15 in.). These concrete prisms were subjected to over 350 FT cycles following the ASTM C666 (ASHTO T161) Procedure B test parameters. In addition to determining the values of durability factor (DF) for concrete, the researchers also measured the percent of dilation of the concrete beams (as per Indiana Department of Transportation (INDOT) ITM 210 test method) and evaluated performance of aggregates using recently modified Indiana Department of Transportation Hydraulic Fracture Test (HFT) equipment and procedures. To investigate the influence of mineralogy on freeze-thaw performance of aggregates, they were subjected to additional tests which included: thin section petrographic analysis, determination of aggregate chemical composition using inductively coupled plasma optical emission spectroscopy (ICP-OES), and evaluation of the percentages of insoluble residue following the ASTM D3042.

The study identified a quicker method to assess freeze-thaw performance of concrete aggregates and the influence of aggregate pore properties on concrete durability. The study determined that the INDOT modified HFT equipment and process can successfully (with 95% accuracy) predict the D-cracking resistance of a given aggregate assuming 0.05% dilation as the failure criterion. The amount of iron and sulfur determined using the ICP-AES test related to the freeze-thaw performance of the carbonate aggregates tested, however, additional testing should be performed using aggregate from additional sources to verify this finding before it is considered for use as a quick indication of expected FT performance.

1. INTRODUCTION

Cracking of concrete pavements from freezing and thawing is common in cold climates if D-crack susceptible aggregates are used. D-cracking involves creation of closely spaced, nominally parallel cracks mainly near longitudinal and transvers joints in concrete pavement. This type of cracking within concrete is caused by freeze-thaw deterioration of coarse aggregates of carbonate origin such as limestone and dolomite.

D-cracking resistance of carbonate aggregates within concrete depends on aggregate's physical properties, such as pore structure (pore size distribution, total pore volume, and continuity of pores), and mineralogy (composition, type and strength of the crystals and the amount of argillaceous material). However, it is still not fully understood as to how critical each of these factors is with respect to D-cracking durability of the aggregate. Hence, a better understanding of the influence of these aggregate properties is extremely important to avoid incorporation of non-durable aggregate into concrete pavements.

A large number of carbonate aggregate sources are available in Indiana for use in concrete pavement. Over the years the Indiana Department of Transportation's (INDOT) has developed the Certified Aggregate Producer (CAP) Program for identifying FT durable aggregate. The main feature of this program is testing all concrete aggregate sources every one to three years (Using the ITM 210 procedure), depending on variability of sources and historical test results. However, the testing can take several months. In addition, the natural variability within aggregate sources may require frequent testing to ensure FT durability. Hence there is a desire to develop and implement rapid evaluation techniques to assess the susceptibility of carbonate aggregates as the rock is quarried or prior to use in construction. More information about the test method and acceptance criteria is presented in section 3.1 and in ITM 210 (available online at www.in.gov/indot/div/mt/itm/pubs/210_testing.pdf).

The main objective of this study was to evaluate carbonate rock properties from a variety of geologic formation in Indiana and relate them to aggregate freeze-thaw performance in concrete pavements. The study also evaluates the potential applicability of the Hydraulic Fracture Test (HFT) as a quick test method for determining the D-cracking resistance of carbonate aggregates quarried in Indiana.

2. AGGREGATE SELECTION

A total of eighteen carbonate aggregate samples were selected from fourteen Indiana quarries to represent statewide variation in geology and D-cracking performance. The aggregate samples were grouped into three D-cracking performance groups: Group A -aggregates known to be durable, Group B – aggregates known to be non-durable aggregates, and Group C - aggregates with variable or unknown performance. Each group consisted of six aggregate sources. Table 1 provides a list of the rock formations and geologic age of the eight aggregate sources. Table 2 gives the megascopic description of the aggregates. Figure 1 shows bedrock geology of Indiana and location of aggregate quarries sampled for testing in the course of this study.

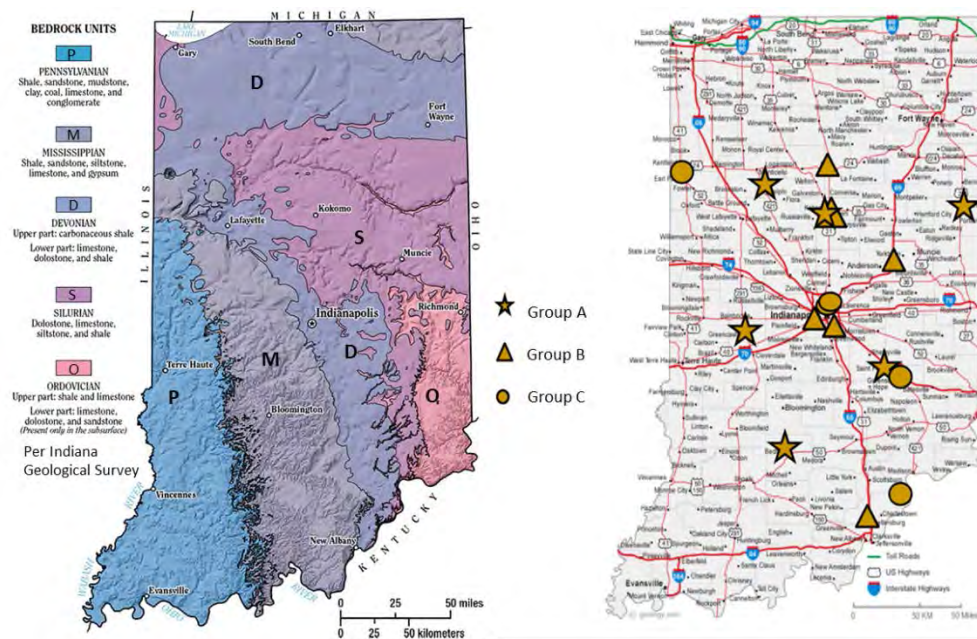


Figure 1: Bedrock map of Indiana and location of aggregate quarries selected for testing [1].

Bedrock map taken from IGS website, <http://igs.indiana.edu/Bedrock/>

Table 1: Carbonate aggregate sources selected for testing.

Group	Aggregate Source	Formation	Geologic Period
Group A	A1	Salamonie Dolomite	Silurian
	A2	St. Genevieve Formation	Mississippian
	A3	Reefal Formation	Silurian
	A4	St. Genevieve Formation	Mississippian
	A5	Wabash Formation	Silurian
	A6	Salamonie Formation, Laurel Member	Silurian
Group B	B1	Mississinewa	Silurian
	B2	Mississinewa	Silurian
	B3	N.Vernon, Jeffersonville	Devonian
	B4	Mississinewa, Louisville Formation	Silurian
	B5	Wabash-Liston Creek	Silurian
	B6	N.Vernon, Jeffersonville	Devonian
Group C	C1	Louisville Formation; Salamonie Formation	Silurian /Ordovician
	C3	Louisville Formation	Silurian
	C4	Louisville Formation	Silurian
	C5	Jeffersonville Geneva Dolomite	Silurian
	C6	Mississinewa, Louisville, Salamonie Formation	Silurian
	C7	N.Vernon, Jeffersonville	Devonian

Table 2: Megascopic description of carbonate aggregate samples

Aggregate Source	Aggregate Description
A1	Gray & pink, fine grained, angular dolomite w/ 1.7 % unweathered chert
A2	Gray & dark gray, fine grained, angular limestone
A3	Gray, fine grained, angular dolomite
A4	Gray, coarse and fine grained, angular limestone
A5	Gray, fine grained, angular to rounded, dolomite
A6	Gray, fine grained, angular, limestone w/ 1.8 % unweathered chert
B1	Gray, fine grained, angular, dolomite w/ 1.3% calcareous
B2	Gray, mostly angular, fine grained limestone w/ 2.3 % unweathered chert
B3	Dark gray to white, mostly angular, fine grained, limestone w/ 1.8 % unweathered chert
B4	Gray, mostly angular, fine grained limestone
B5	Light gray, angular & rounded, fine grained limestone w/ 1.4 % unweathered chert
B6	Gray to dark gray, angular & rounded fine grained limestone
C1	White to gray, angular to rounded, fine grained dolomite
C3	Gray, greenish gray & dark gray, angular, fine grained limestone
C4	Gray, angular, fine grained limestone
C5	Gray to light gray, angular, coarse grained limestone
C6	Gray to pinkish and greenish gray, angular, coarse & fine grained limestone
C7	Gray to dark gray, angular, fine grained limestone w/ 1.8 % unweathered chert

3. DISCUSSION OF TEST RESULTS

Aggregate from each of the sources was separated into 1", 3/4", 5/8", 1/2", 3/8", and #4 size fractions. The size fractions from each source were then proportioned to produce the specific gradations required for each test. Samples of aggregate from each source were subjected to characterization tests such as specific gravity and absorption, insoluble residue, inductively coupled plasma optical emission spectroscopy (ICP-OES), and hydraulic fracture test (HFT). In addition, concrete prisms were prepared from these aggregate samples and subjected to freeze-thaw testing. The experimental findings are presented below.

3.1 Concrete Freeze-Thaw Test

Concrete mixtures were produced from all aggregate sources in accordance with the Indiana test method ITM 210 which is based on ASTM C666 Procedure B (freeze in air, thaw in water). The target air content of the fresh concrete was 6.5 (± 1.5) percent to ensure that any FT

durability problems of concrete can be attributed to the coarse aggregate and not to the cement mortar matrix. Three 3 in. x 4 in. x 15 in. concrete prisms were fabricated from each concrete mixture and tested for freeze-thaw durability following ITM 210.

The average dilation (percent expansion) and durability factors of freeze-thaw specimens were determined. The average dilation of the freeze-thaw specimens reported here is the average expansion of at least 2 of the three test beams after 350 cycles of freezing and thawing. The durability factor (DF) numbers were calculated using standard procedures described in ASTM C666 using measured values of the relative dynamic modulus of elasticity (RDME) of each specimen. INDOT's aggregate acceptance criterion with respect to its D-cracking (FT) resistance stipulates that the average dilation of at least two of the three test beams be less than 0.060% after 350 cycles of freezing and thawing [3]. The freeze-thaw test results are presented in Table 3 and in Figure 2.

Table 3: Freeze-thaw test results

Aggregate Source	A1	A2	A3	A4	A5	A6
Dilation, %	0.004	0.003	0.007	0.012	0.005	0.020
DF	97	98	99	99	96	94
N/ND	D	D	D	D	D	D
Aggregate Source	B1	B2	B3	B4	B5	B6
Dilation, %	0.163	0.270	0.085	0.179	0.244	0.084
DF	69	36	76	62	36	75
D/ND	ND	ND	ND	ND	ND	ND
Aggregate Source	C1	C3	C4	C5	C6	C7
Dilation, %	0.144	0.146	0.092	0.004	0.023	0.081
DF	86	61	77	96	94	78
D/ND	ND	ND	ND	D	D	ND

Note: D=durable, ND=non-durable

Based on INDOT's 0.060% expansion acceptance criteria, all aggregate sources in Group A and two sources in Group C (C5 and C6) passed the freeze-thaw test while all sources in Group B and four sources in Group C tested as non-durable with dilation exceeding 0.060% expansion (as shown in Figure 2 and in Table 3). All the durable aggregates had dilations equal to or less than 0.023% and DF equal to or greater than 94, and all the non-durable aggregates had dilations equal to or greater than 0.081% and DF equal to or less than 86. The range of both the dilations and the DF for the non-durable sources are ten times wider than those of the durable sources. There was excellent correlation between percent dilation and durability factor which yielded an R-squared value of 0.91 [1].

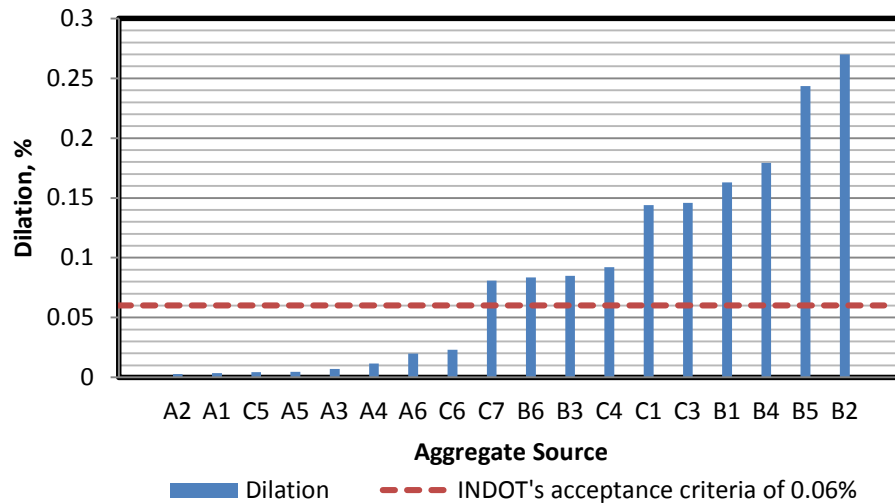


Figure 2: Percent dilation compared against INDOT's acceptance criteria.

3.2 Specific Gravity and Absorption

The absorption and the specific gravity values for all aggregate sources were determined according to AASHTO T85, *Specific Gravity and Absorption of Coarse Aggregate*. The testing was performed on aggregates with the same gradation as that used to produce the freeze-thaw test specimens. Table 4 summarizes the results of these tests. For the durable aggregates, the specific gravities ranged from 2.48 to 2.75 and the absorption values ranged from 0.87% to 5.20%. On the other hand, for the non-durable aggregates, the specific gravities ranged from 2.57 to 2.69 and the absorption values ranged from 1.08% to 4.81%. It is interesting to note that both, the specific gravity values and the absorption values for the non-durable sources are falling in the narrower ranges than those of the durable sources.

Carbonate aggregates having high absorption are often associated with durability problems. Most agencies do not allow the use of such sources in concrete paving applications. For example, the INDOT limits the maximum percentage of absorption of aggregates to 5.0% [3]. According to INDOT's specifications, two freeze-thaw durable aggregate sources (A5 and C5) would be considered unsuitable for use in paving applications.

Table 4: Bulk specific gravity (BSG) and percent absorption (%ABS) results

Aggregate Source	A1	A2	A3	A4	A5	A6
BSG (SSD)	2.63	2.62	2.75	2.68	2.49	2.69
%ABS	2.39	1.69	0.87	0.88	5.20	1.10
D/ND	D	D	D	D	D	D
Aggregate Source	B1	B2	B3	B4	B5	B6
BSG (SSD)	2.57	2.66	2.64	2.67	2.65	2.62
%ABS	4.81	2.33	1.36	2.66	1.47	1.08
D/ND	ND	ND	ND	ND	ND	ND
Aggregate Source	C1	C3	C4	C5	C6	C7
BSG (SSD)	2.69	2.67	2.68	2.48	2.66	2.65
%ABS	2.66	1.47	1.08	5.13	1.79	1.36
D/ND	ND	ND	ND	D	D	ND

Note: D=durable, ND=non-durable

Some transportation agencies are more conservative in specifying the maximum allowable absorption. As an example, the Minnesota Department of Transportation (Mn/DOT) considers quarried carbonate aggregates (Class B) with absorption capacity values greater than 1.75% not suitable for pavement concrete [4]. Based on this specification, four of the durable sources (A5, A6, C5, and C6) would be rejected and six non-durable sources (B3, B5, B6, C3, C4, and C7) would have passed this specification while they are failing. These cases suggest that screening aggregates for freeze-thaw durability based solely on the absorption capacity potentially leads to incorrect acceptance criteria. It should be noted, however, that this reasoning is only applicable for cases that use the same criteria (i.e. the dilation not greater than 0.060%) as Indiana when establishing the FT (D-cracking) durability of the coarse aggregates.

3.3 Hydraulic Fracture Test (HFT)

The HFT was performed on all aggregate sources using the newly developed INDOT's HFT equipment. In this test, oven-dry aggregates are placed in the HFT chamber; the chamber filled with water and pressurized using a compressed nitrogen gas to force water into the aggregate pores. When the pressure is released rapidly, compressed air trapped within the aggregate pores expands and tries to escape, expelling water from the pores and creating internal stresses in the aggregate particles. This is believed to be similar to the pressure developing in aggregate particles exposed to freezing and thawing environment [2].

If the pore structure of the aggregate does not allow rapid expulsion of water upon pressure release internal hydraulic pressure will develop in the aggregate particles. When the pressure exceeds the strength of individual aggregate particles the particles will fracture.

The amount of fracturing is believed to be an indication of potential freeze-thaw durability of the aggregate and it is designated as PCMR. The PCMR is defined as the percent change in mass retained on each sieve from before any HFT testing (0 cycles) to that measured after 50 cycles of HFT testing, divided by an initial mass. For the coarser sieves ($\frac{3}{4}$ -in, $\frac{5}{8}$ -in, and $\frac{1}{2}$ -in), the change in mass on each respective sieve is divided by the initial mass retained on that sieve, for the smaller sieves ($\frac{3}{8}$, $\frac{5}{16}$, $\frac{1}{4}$, #4 than $\frac{1}{2}$ -in), which had no initial mass, the mass on each respective sieve after 50 cycles is divided by the total sample initial mass. Eight PCMR variables were computed from the HFT test data for each aggregate source, and were designated as P34, P58, P12, P38, P516, P14, P4 and P0.

Statistical analysis was performed on the experimental data, and a linear regression model shown in Equation 1 was developed to predict the average percent dilation using parameters obtained from HFT results (PCMR). In the regression model, the percent dilation was used as the dependent (or response) variable whereas the PCMR values was used as independent variables.

The dilation model that provided the best fit between the percent dilation and HFT results (PCMR) is shown in Equation 1. The model statistics is as follows: $R^2 = 0.892$, R^2 (adj.) = 0.853, SEE = 0.029, n=16, Model P-value < 0.0001.

$$\% \text{ Dilation} = 8.25E-2 + 6.33E-3 * P34 + 9.64E-2 * P38 - 3.12 * P14 + 4.3 * P4$$

(Eq.1)

Where:

P34 is PCMR the percent change in mass retained on $\frac{3}{4}$ in. sieve

P38 is PCMR the percent change in mass retained on $\frac{3}{8}$ in. sieve

P14 is PCMR the percent change in mass retained on $\frac{1}{4}$ in. sieve

P4 is PCMR the percent change in mass retained on #4 sieve

The dilation model correctly predicts the freeze-thaw durability for 14 of the 18 sources tested. One of the four sources incorrectly identified by this model as non-durable source was, in fact, freeze-thaw-durable. This source was source A3 (a fine-grained dolomite of reefal formation). The remaining three sources incorrectly identified as durable were in fact nondurable sources B3, B6 and C7 (Devonian period limestone sources), with dilations ranging from 0.081% to 0.085%. The model-predicted dilation values ranged from 0.055% to 0.0597%, barely within the INDOT 0.060% acceptance criterion.

The model appears to lose some sensitivity in predicting the FT performance of sources in the mid-range dilation values (at or below 0.085%). Considering this fact, if a dilation of 0.050% were used as the acceptance criteria for HFT results, the model predicted the durability with 95% accuracy, with only one source (A3) being identified as non-durable. More detailed descriptions of the model development can be found in [1, 5].

3.4 Inductively Coupled Plasma Optical Emission Spectroscopy (ICP-OES) Test

The ICP-OES test was used to determine the elemental composition of the aggregates. The ICP-OES technique uses inductively coupled plasma to produce excited atoms that emit electromagnetic radiation at wavelengths unique to a particular element. The intensities of these emissions indicate the concentration of the element in the sample being analyzed.

The purpose of the analysis was to investigate the role of elemental composition on the freeze-thaw performance of the aggregates. Five aggregate sources, two durable (A2 and A3) and three non-durable (B2, B6, and C1), were selected for the analysis.

As one would expect when testing carbonate aggregates, calcium and magnesium were the major elements. Aluminum, iron, manganese, potassium, sodium, and sulfur were the primary minor elements (impurities). The elemental composition of aggregate from these five sources is shown in Table 5.

Table 5: Elemental constituents of the aggregates (weight percentage)

Aggregate Source	D/ND	Calcium (%)	Magnesium (%)	Other (Impurities) (%)
A2	D	91	6	2
A3	D	64	35	1
B2	ND	82	15	3
B6	ND	97	1	2
C1	ND	64	35	1

Note: D=durable, ND=non-durable

The percentage of calcium ranged from 64% to 97%, whereas magnesium ranged between 1 and 35%. The composition of the minor elements (impurities) ranged between 1 to 3%. Sources A3 and C1 had the lowest (1%) percentage of minor elements (impurities). The least durable aggregate, Source B2, had the highest percentage of impurities (3%). The sources A3 and C1 had identical amount of calcium, magnesium, and minor elements (impurities). Even though these two sources have identical elemental composition, their freeze-thaw durability is different; source A3 is freeze-thaw durable, but C1 is not.

Table 6 summarizes the content and composition of the minor elements in the aggregates. Of the minor elements, iron ranged from 0.22% to 1.39% and sulfur ranged from 0.52% to 1.20%.

Table 6: Content and Composition of minor elements

Aggregate Source	D/ND	Aluminum %	Iron %	Manganese %	Potassium %	Sodium %	Sulfur %
A2	D	0.32	0.70	0.03	0.13	0.07	0.87
A3	D	0.08	0.45	0.08	0.03	0.11	0.55
B2	ND	0.19	1.39	0.08	0.17	0.04	1.20
B6	ND	0.07	0.50	0.11	0.06	0.04	1.15
C1	ND	0.05	0.22	0.04	0.03	0.07	0.52

Note: D=durable, ND=non-durable

As shown in Table 7, it appears that there is a better correlation between the total amounts of minor elements (impurities) with DF than with dilation. There is no significant correlation between aluminum content and dilation or DF. Sodium, potassium, and manganese showed a very low correlation with dilation and DF. The lack of correlation between the impurities and the percent dilation indicates that the type of impurities does not relate to the FT expansion.

Table 7: Correlations between minor elements and DF and Dilation

Element	DF		Dilation, %	
	R-squared	Relationship	R-squared	Relationship
Aluminum	0.0004	Neither	0.0158	Negative
Iron	0.6477	Negative	0.3860	Positive
Manganese	0.1490	Negative	0.0268	Positive
Potassium	0.3796	Negative	0.1964	Positive
Sodium	0.4619	Positive	0.3494	Negative
Sulfur	0.5267	Negative	0.2119	Positive
Total Impurity	0.5708	Negative	0.2646	Positive

Sulfur and iron contents combined correlated with DF yielded an R-squared value of 0.685. As shown in Figure 3, as the combined content of sulfur and iron increased, the durability factor (DF) decreased.

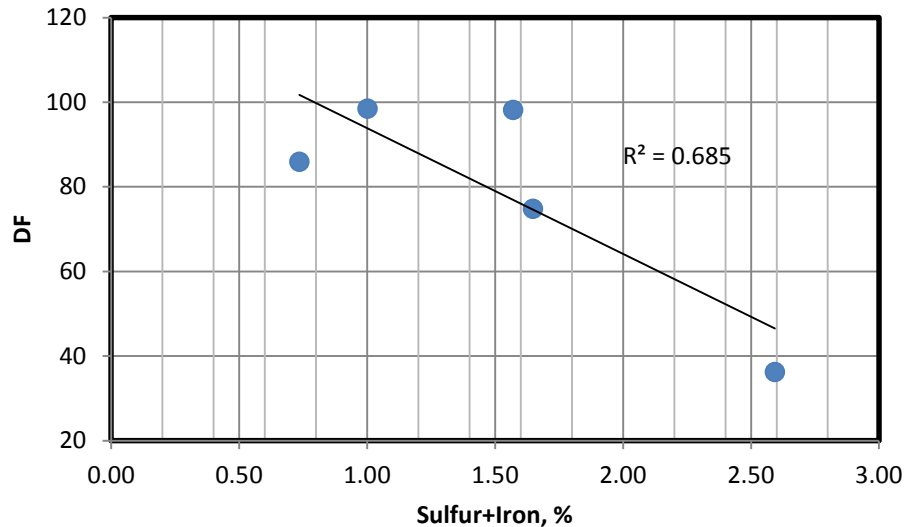


Figure 3: Relationship between DF and Sulfur+ Iron content

The significant effect of iron content on the aggregate durability properties is seen in aggregate source B2 that had twice as much iron as any other sample tested. This might be the reason that this aggregate source is the least durable. This perhaps should not be surprising as some DOTs consider pyrite (FeS_2) a spalling material susceptible to pop-outs from freezing and thawing and restrict the amount allowed in concrete gravel sources [4]. If the correlation shown in Figure 3 holds true for other aggregate sources, it would imply that identifying the amount of iron and sulfur may provide a quick indication of the freeze-thaw performance.

3.5 Acid Insoluble Residue Test

The acid insoluble residue test was performed on all aggregate sources according to ASTM D3042, *Insoluble Residue in Carbonate Aggregate*, to determine the amount of sand, clay and other non-carbonate materials present in the microstructure of aggregates. Sample size used was 200 grams instead of 500 grams as specified in ASTM D3042. Percent insoluble residue, -75 μm (#200) fraction and +75 μm (#200) fraction were determined (as shown in Table 8).

Linear regression analysis performed on the data revealed that there is no linear relationship between the content of the insoluble residue and freeze-thaw results. Also, no correlation was found between the amount of -75 μm (#200) and +75 μm (#200). However, the range of the amount of -75 μm (#200) for the non-durable sources is 2.6% to 28.1%, a 80% wider range than that of the durable sources that ranged from 2.0% to 19.7%. Both the durable and non-durable sources had similar ranges of the amount of +75 μm (#200). Among the non-durable sources, B1 had the highest amount of -75 μm (#200) at 28.1%. This particular source exhibited the highest percentage of fractures in the HFT. As it is presented in section 3.6, this source is described as argillaceous dolomite.

Table 8: Acid insoluble residue result

Aggregate Source	A1	A2	A3	A4	A5	A6
-75 μ m (#200),%	6.0	13.3	2.1	13.7	7.9	11.0
+75 μ m (#200),%	19.7	9.2	12.5	8.3	10.0	3.6
D/ND	D	D	D	D	D	D
Aggregate Source	B1	B2	B3	B4	B5	B6
-75 μ m (#200),%	28.1	13.3	5.4	5.3	17.8	9.7
+75 μ m (#200),%	16.6	8.0	10.8	7.0	8.3	5.1
D/ND	ND	ND	ND	ND	ND	ND
Aggregate Source	C1	C3	C4	C5	C6	C7
-75 μ m (#200),%	3.2	7.4	11.6	2.0	16.2	2.6
+75 μ m (#200),%	19.4	15.5	7.2	15.2	11.2	2.3
D/ND	ND	ND	ND	D	D	ND

Note: D=durable, ND=non-durable

3.6 Petrographic Analysis of thin Sections

Thin sections for all aggregate sources were prepared and analyzed using polarized, petrographic microscope. Information about texture, type of porosity, presence of ferruginous materials, and size of crystals were obtained. Also, the samples of aggregates are classified based on Folk's classification system [6]. Table 9 summarizes the result of these analyses.

Table 9: Microscopic description of aggregate samples under plain and polarized light

Source	Petrographic Description, Average Grain Size, and Composition
A1	Crystalline dolomite, 0.08 mm, with trace iron oxide
A2	Broken fossil limestone, 0.025 mm, with trace iron oxide
A3	Fine grained dolomite, 0.075 mm
A4	Coarse fossil limestone, 2.25 to 0.275 mm
A5	Fine grained dolomite, 0.075 mm, with trace iron oxide
A6	Coarse fossil, dolomitic limestone, 0.375 mm
B1	Crystalline, argillaceous, calcareous, cherty dolomite, 0.05 mm
B2	Crystalline, dolomitic, fossiliferous, limestone, 1 mm fossils, 0.05 mm matrix, with iron oxide and quartz
B3	Coarse, broken fossil limestone, 0.9 to 0.09 mm
B4	Calcareous fossils in dolomite matrix, 0.75 mm with 0.075 mm ground mass
B5	Calcareous fossils in dolomite matrix, 0.45 mm with 0.05 mm ground mass
B6	Coarse, whole fossil limestone, 0.45 mm, with iron oxide and quartz
C1	Crystalline dolomite, 0.125 mm, with quartz
C3	Coarse broken fossil limestone, 0.75 to 0.45 mm, with trace iron oxide
C4	Fossiliferous dolomitic limestone, 0.55 mm, 0.075 mm dolomitic ground mass
C5	Crystalline, angular grained, limestone, 0.075 mm, with iron oxide
C6	Coarse fossil, dolomitic limestone, 0.375 mm with 0.15 mm dolomitic ground mass
C7	Crystalline, angular grained, limestone, 0.095 mm. with trace iron oxide

The thin section analyses revealed that both samples from St. Genevieve Formation, A2 and A4, were fossiliferous limestone from Mississippian period. Almost half of the aggregate sources sampled from the Silurian period are durable and the remaining being non-durable. Of the dolomitic limestone sources, 70% of them were non-durable; the durable ones being A6, C5, and C6. Fine-grained dolomite sources (A3 and A5) appeared to be durable. All pure dolomite sources (A1, A3, and A5) were durable with the exception of C1. Aggregate sources containing large pores (ie: vuggy = pores larger than grains or crystals) (A1, A3, A5, and C5) were found to be durable. Figure 4 shows micrograph of aggregate from source A1 showing large pores (some of them highlighted by the presence of yellow epoxy in the voids).

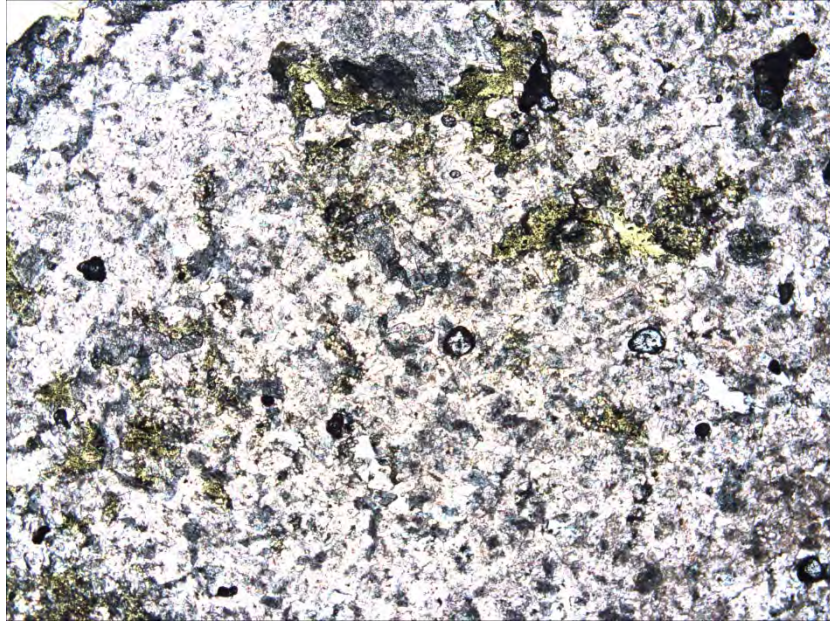


Figure 4: Photomicrograph of aggregate source A1 (field width 4mm)

4. SUMMARY

Various laboratory tests were performed on eighteen carbonate aggregate samples collected from fourteen quarries in Indiana (representing several different geological formations) and with a history of freeze-thaw performance varying from excellent to poor. The objective of this investigation was to develop a better understanding of the influence of the pore characteristics and mineralogy of aggregates on their freeze-thaw (D-cracking) resistance.

Based on the experimental results the following points are highlighted:

- Of the eighteen aggregates tested, eight were found to be freeze-thaw durable whereas the remaining ten sources were non-durable based on the INDOT's threshold dilation value of 0.060% in freeze-thaw test.
- Absorption values of aggregates did not directly correlate with freeze-thaw dilation results. Hence, screening aggregates for freeze-thaw durability based only on their absorption may lead to misdiagnosis.
- The linear statistical model developed correlating the average percent of dilation in the freeze-thaw test using parameters obtained from HFT results can predict the expected dilation with 95% accuracy if 0.050% value is used as pass/fail criterion.
- Combined amounts of iron and sulfur elements correlated, to some degree, with the durability factor. As the combined content of sulfur and iron increased, the durability factor decreased.
- The least durable source contained the highest amount of elemental iron.

- There was a modest ($R^2=0.5708$) correlation between total amounts of minor elements (impurities) with DF
- Identifying the amount of iron and sulfur using the ICP-AES test may provide a quick indication of the expected freeze-thaw performance of carbonate aggregate. However, additional testing should be performed using aggregate from other sources to verify this finding.

5. ACKNOWLEDGMENTS

Many thanks to: Bob Rees, INDOT Chief Geologist for all his help in obtaining aggregates and identifying the geologic formations of each source, Kelly Cook for running the ICP test, and Dr. Chris Andronicos for use of petrographic equipment.

6. REFERENCES

1. Desta, B., Whiting, N., Snyder, M., "Hydraulic Fracture Test to Determine Aggregate Freeze-Thaw Durability," Joint Transportation Research Program Publication No. FHWA/IN/JTRP-2014/15), <http://docs.lib.purdue.edu/jtrp/1565/>
2. Janssen, D. J., and Snyder, M. B. Resistance of Concrete to Freezing and Thawing. Report, SHRP-C-391. Strategic Highway Research Program, National Research Council, 1994.
3. INDOT Standard Specification, Aggregate Specification and Requirements, 2014
4. Mn/DOT Standard Specification for Construction, Coarse Aggregate for Portland Cement Construction, 2014
5. Desta, B., Whiting, N., Olek, J. Snyder, M., and Nantung, T., "Quick determination of freeze-thaw durability of concrete aggregates using the Indiana DOT Hydraulic Fracture Test equipment," TRR Journal, January 2015
6. Folk, R.L., 1959, Practical petrographic classification of limestones: American Association of Petroleum Geologists Bulletin, v. 43, p. 1-38.

Sources of Nitrate in Groundwater Near Roadway Rock Blasting Sites

Krystle Pelham

New Hampshire Dept. of Transportation
Bureau of Materials and Research
Concord, NH 03301
Kpelham@dot.state.nh.us

David M. Langlais,

Hoyle, Tanner & Associates, Inc.
I-93 Exit 3 Project Field Office
Windham, NH

Prepared for the 66st Highway Geology Symposium, September, 2015

Acknowledgements

The author(s) would like to thank the individuals/entities for their contributions in the work described:

Megan Murphy – HTE Northeast, Inc.
Patrick Massicotte - HTE Northeast, Inc.
Roger Keilig - HTE Northeast, Inc.
USGS stable isotope laboratory
NHDOT Research Advisory Council

Disclaimer

Statements and views presented in this paper are strictly those of the author(s), and do not necessarily reflect positions held by their affiliations, the Highway Geology Symposium (HGS), or others acknowledged above. The mention of trade names for commercial products does not imply the approval or endorsement by HGS.

Copyright Notice

Copyright © 2015 Highway Geology Symposium (HGS)

All Rights Reserved. Printed in the United States of America. No part of this publication may be reproduced or copied in any form or by any means – graphic, electronic, or mechanical, including photocopying, taping, or information storage and retrieval systems – without prior written permission of the HGS. This excludes the original author(s).

ABSTRACT

Explosives used in blasting operations, natural and anthropogenic sources of nitrate such as septic systems, fertilizers, and decomposing vegetation can potentially contaminate groundwater with nitrate in the vicinity of construction sites and make identification of blasting impacts difficult. Blasting operations for a private construction project in Windham, NH were indicated as the source of water quality impacts to private drinking water wells prompting the New Hampshire Department of Transportation (NHDOT) to implementing a proactive approach to limit the potential for impacts from blasting for ongoing NHDOT projects. NHDOT has developed a baseline drinking water monitoring program designed to detect potential impacts and to ensure alternative drinking water is provided throughout the construction phase of projects. In 2013, the U.S. Geological Survey and the New Hampshire Department of Transportation (NHDOT) began a study to determine the source and fate of nitrogen compounds near blasting sites using a combination of time series, isotopic, geochemical, hydrologic, and geologic data. Approximately 1.75 million cubic yards of rock were removed by blasting in several locations for roadway construction at a major highway construction site in southern NH.

Isotope ratios of nitrogen and oxygen in nitrate were used to identify sources of nitrate concentrations in groundwater from wells near the blasting sites. Wells near a rock excavation site where blasting was used shortly after the start of this study and wells with existing persistent nitrate contamination suspected to be the result of septic and past blasting were targeted for temporal sampling and analysis in an attempt to characterize nitrate sources. In general results show a low $\delta^{15}\text{N}$ signature from synthetic nitrate sources (including explosives) and a high ^{15}N signature from septic waste sources. Results also indicate that nitrate pulses in wells following blasting events can be distinguished isotopically from other local sources, and that reducing conditions in this geologic setting locally cause denitrification, resulting in lower nitrate concentrations. Transport and persistence of nitrate due to blasting operations and other nitrogen sources in fractured rock environments will be presented.

Introduction

Blasting operations and fragmentation of bedrock with explosives have been implicated as a source of nitrate contamination in groundwater but direct forensic evidence is limited. Nitrate is a component of ammonium nitrate, which is approximately 90 percent of commonly used explosives by weight¹. High nitrate concentrations in groundwater affected by explosives could be related to several processes including (1) leaching of nitrate from unexploded nitrate bearing compounds, (2) oxidation (nitrification) of reduced nitrogen components of explosives, and (3) injection of soluble gasses into the subsurface by blasting.

In New Hampshire and elsewhere, rock excavation for highway construction commonly requires blasting with ammonium nitrate based explosive emulsions. Elevated concentrations of nitrate in groundwater have been attributed to blasting in New Hampshire (reference) but direct forensic evidence of nitrate sources is lacking. Nitrate concentrations regionally are typically low whereas the concentration of the 5-170 mg/L have been observed in wells and springs near blasting sites. Potential non-blasting related nitrate sources have been identified as but are not limited to wastewater disposal (e.g. septic systems), fertilizers used in landscaping and agriculture, atmospheric deposition, and weathering of soils and rocks.

As part of the I-93 widening project in New Hampshire the New Hampshire Department of Transportation (NHDOT) anticipated that approximately 1.75 million cubic yards of rock will be removed for the roadway and detention basin construction. The blasting portions of the work are scheduled to be completed over a seven year period. The work would be completed in the Town of Windham where recent blasting projects for a commercial development and school allegedly caused impacts to groundwater. In light of these allegations and the anticipated significant quantity of rock required to be removed for the widening project, the NHDOT developed a proactive approach to limit the potential for impacts from construction projects and associated blasting. This approach included an initial baseline monitoring program of the area surrounding the contracts prior to any construction. Subsequently, a construction phase monitoring program was developed specific for each contract. Best Management Practices for use on all NHDOT blasting projects were developed for implementation. During the construction phase, analytical results of groundwater samples exhibited trends of increasing nitrate concentrations that were suggesting blasting activities as a cause. As a result additional investigation and sampling methodologies were required to evaluate sources of nitrate within the project limits to understand and mitigate the issue.

As a result of the need to further investigate the sources, the NHDOT and the U.S. Geological Survey commenced a study to utilize nitrogen and oxygen isotope ratios to evaluate sources of groundwater nitrate contamination in fractured-bedrock aquifer settings in 2013. This technique had been used in agricultural, urban and other settings but had not been thoroughly tested for identification of sources of nitrate near blasting sites. Distinguishing these potential nitrate sources is important in understand mitigation. The objective of this study was to demonstrate differentiation between blasting-related nitrogen and nitrogen from other potential sources and the impact of blasting operations on groundwater quality. Nitrate concentration and isotopic composition of many of the samples were affected by blasting. Isotope data indicated distinctive nitrate sources (synthetic and biogenic) but the reducing conditions in the aquifer caused changes in the nitrate concentrations and isotopic characteristics in many cases.

Study Area

The study area includes two highway contracts where bedrock was excavated using blasting in Windham New Hampshire (figure 1). The contracts include the construction of detention basins, realignment of the northbound and southbound barrels, new on- and off-ramps, relocation of a portion of NH Route 111, and construction of a park-n-ride facility. The new roadway areas that required blasting were dominantly forest covered and was located on wooded site slopes with outcrops of bedrock scattered through the area. Local surface water bodies include Canobie Lake utilized for a public water supply to the east and Cobbett's Pond developed with several residential homes and used for recreation to the west.

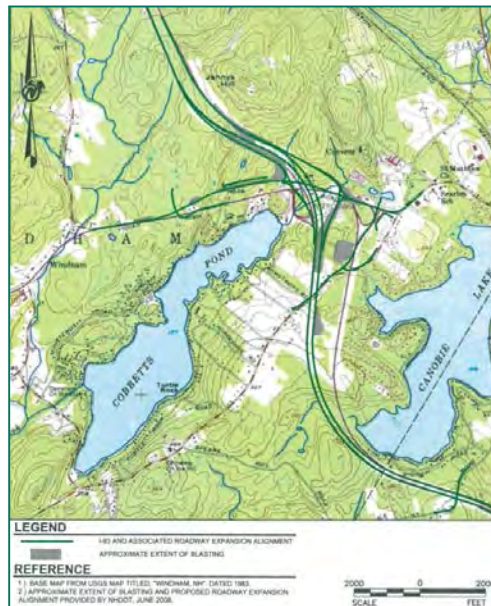


Figure 1. Site Location

The study area is covered by thin (<3m) layer of glacial till overlain by metamorphic bedrock. A potentiometric surface map from existing water level data was generated with available information (figure 2). In general groundwater flow was southward toward Cobbetts Pond with local various relative to topography. Developed areas have bedrock aquifer water-supply wells and septic systems for residential and commercial wastewater disposal.

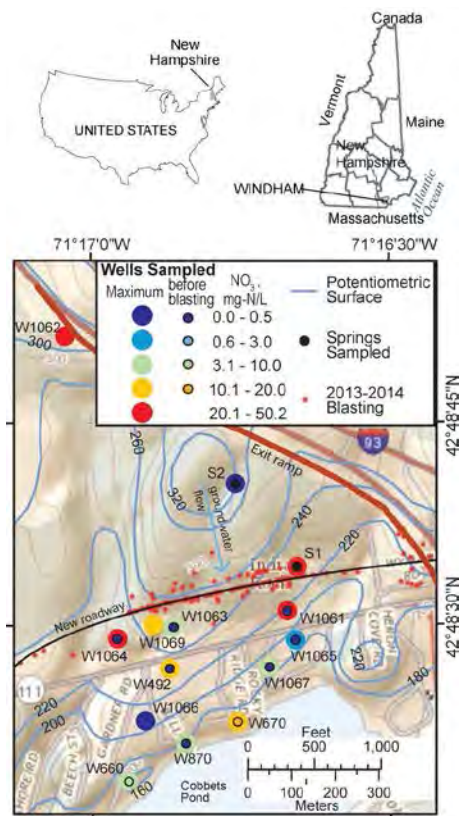


Figure 2. Potentiometric surface map, sample locations, blasting locations

Baseline Monitoring Program

Prior to the commencement of blasting in 2009 under the first construction contract let to develop a new southbound off ramp for exit 3 of interstate highway 93 the NHDOT and Golder Associates completed a baseline monitoring program recognizing the sensitivity of the area due to allegations from the private development. Utilizing a site conceptual hydrologic model water supplies were identified downgradient of the proposed blast areas that could be impacted by blasting effects and upgradient to establish baseline (preconstruction) water quality conditions. Permission was received from homeowners to collect samples from 41 water supply wells, two surface water points, within an approximate one mile radius of the project area. Samples were divided in two suites of parameters: a baseline list (table 1) and an extended list (table 2). The lists were compiled as parameters commonly associated with blasting impacts, either directly or due to byproducts of the explosives, or indirectly due to the blasting vibrations.

The analytical results indicated that arsenic, iron, manganese, nitrite, pH, radon, total dissolved solids, and/or turbidity exists above either USEPA or NHDES standards. A subset of the samples (fifteen) were analyzed for the extended list of hydrocarbon parameters (PAHs, DRO, MTBE) where MTBE was detected in two of the wells below regulatory limits.

Table 1. Baseline Analysis List

Baseline Analysis List
Nitrate
Nitrite
Ammonia

Table 2. Extended Analysis List

Extended Analysis List	
pH	Turbidity
Total Alkalinity	Polyaromatic Hydrocarbons
Iron (total and dissolved)	Total petroleum Hydrocarbons
Manganese (total and dissolved)	Methyl Tertiary Butyl Ether (MtBE)
Arsenic (total and dissolved)	Perchlorate
Hardness (total)	Radon
Total dissolved solids (TDS)	

Also utilizing the hydrologic model, estimated bedrock linear flow velocities were developed to determine the appropriate sampling frequency to implement in the construction phase for the various contracts for the ongoing groundwater monitoring to ensure protection of downgradient receptors.

Construction Phase monitoring and results

Based on information collected in the preconstruction investigations the construction phase monitoring Specification for a Hydrogeologist was developed for inclusion in the contract documents. The sampling during the ongoing construction projects consisted of Groundwater samples collected prior to the commencement of blasting activities, monthly throughout the blasting activities and while blasted rock is stockpiled and/or crushed, and once upon completion of the construction project. Groundwater samples collected prior to blasting activities and upon completion of construction were to be analyzed for the parameters in the Extended Analysis List (Table 2). Groundwater samples collected throughout blasting activities and while rock is stockpiled and/or crushed shall be analyzed for the Baseline Analysis List (Table 1). The Hydrogeologist was to employ the services of a laboratory accredited through the New Hampshire Environmental Laboratory Accreditation Program to analyze the samples. Laboratory results were provided to the homeowner.

Groundwater analytical data from the construction phases indicated the consistent trend of increasing nitrate detections as the blasting progressed followed by a decrease as time passed after the rock removal had ceased. The primary constituents from the analytical list that were detected were nitrite and benzene in the downgradient receptors. Groundwater remediation actions taken evolved over time from installation of long term anion exchange systems for whole house treatment to simply the provision of bottled water as the increasing trend of nitrate

contamination above regulatory limits was observed until data indicated the quality was back substantially below the regulatory limits.

As additional locations of blasting became more scattered as the work progressed based on construction scheduling and operations trends became less predictable. Overlap of impacts between contracts became a consideration. Figure 3 shows the trends in nitrate concentration alone which exhibited substantial variability with nitrate over time. In addition due to the densely populated nature of the study area and the numerous septic systems and other potential sources of nitrate the need to be evaluated. As a result the study was developed to evaluate the use of nitrogen and oxygen isotope ratios to assess if the attributing factors could be determined.

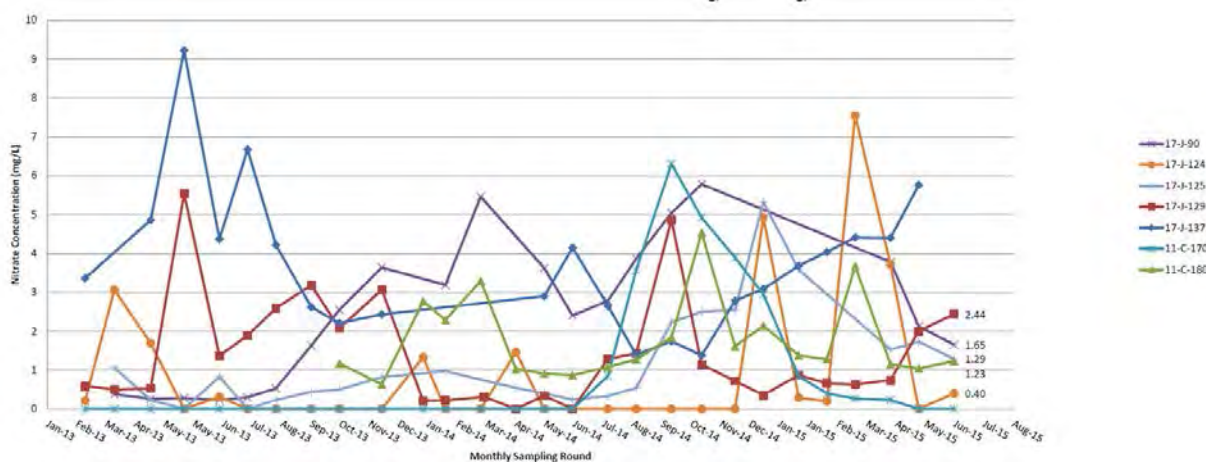


Figure 3. Nitrate contamination over time

Isotope Study design and analysis

In 2013 nineteen samples that were collected monthly in accordance with the NHDOT specification and requirements for the Hydrogeologist. Utilizing analytical data from the ongoing construction monitoring sample locations were chosen for the isotopic investigation. Twelve of the wells and two springs were selected. Eleven of the wells were drinking water supplies and one was a monitoring well where impacts were detected under earlier construction. Of the wells to be sampled, seven were located in the densely populated lakeside neighborhood where elevated nitrate concentrations had been detected in some locations prior to construction. For the study, USGS selected five of the wells for analysis before blasting activities to characterize background conditions. Following the first round, the remainder of the twelve wells and two springs; one from the toe of the proposed rock slope and one upgradient in a forested area; were selected to be analyzed at 2-month intervals for stable isotopes and additional analytes (Figure 2). In addition, rock fragments collected subsequent blasting operations were collected to provide isotopic characteristics of the blasting agent leachate.

During the sampling conducted for the isotopic study, temperature, specific conductance (SC), pH, and dissolved oxygen (O₂) concentrations were measured in the field. Water samples were analyzed in the laboratory for selected major elements and ions (B, Ca, Fe, K, Mg, Mn, Na, Br⁻, Cl⁻, NH₄⁺, NO₃⁻, NO₂⁻, PO₄³⁻, SO₄²⁻), dissolved gases (O₂, Ar, N₂, CH₄), VOCs, and stable isotope ratios ($\delta^{2}\text{H}$ and $\delta^{18}\text{O}$ of H₂O, $\delta^{15}\text{N}$ 123 and $\delta^{18}\text{O}$ of NO₃⁻, $\delta^{15}\text{N}$ of NH₄⁺ and N₂).

Samples from drinking-water wells were collected and analyzed by the NHDOT contractor for major elements and ions and VOCs. Major elements and ions in samples from the monitoring well, springs, and leachates were analyzed by USGS laboratories. Dissolved-gas concentrations were measured by the USGS Reston Groundwater Dating Laboratory. Stable isotope ratios were measured by the USGS Reston Stable Isotope Laboratory.

Results and Discussion

Isotopic data indicated distinctive nitrate sources (synthetic and biogenic), but reducing conditions in the aquifer caused changes in nitrate concentrations and isotopic characteristics in many cases. Temporal variations in blasting activities and groundwater responses also supported source identification.

Blasting compounds were a major potential source to groundwater impacts. The total mass of nitrogen in blasting compounds used on the site between 2013-2014 was 60,000 kg of total. Explosives used were largely in the form of bulk emulsions and ANFO. The amount of nitrogen remaining in the ground after blasting is unknown.

Blasting related nitrate peaks were characterized by low d15N and high d18O which is indicative of synthetic nitrate used in explosives. Additionally, the nitrate concentrations were unusually high in select wells near the blasting activities for short periods of time. Groundwater with blasting-related nitrate moved rapidly from the construction site to downgradient wells in the time frame of months and decreased to below regulatory standard over the time of year(s). In wells located in developed land use settings such as adjacent to Cobbetts pond with septic systems, located the furthest downgradient of the site, had relatively stable nitrate concentrations. Septic effects were identified with moderately high nitrate levels with elevated Mn, CL, and Ca. These locations also had higher d15N and lower d18O falling in the range of biogenic nitrate (Figure 3).

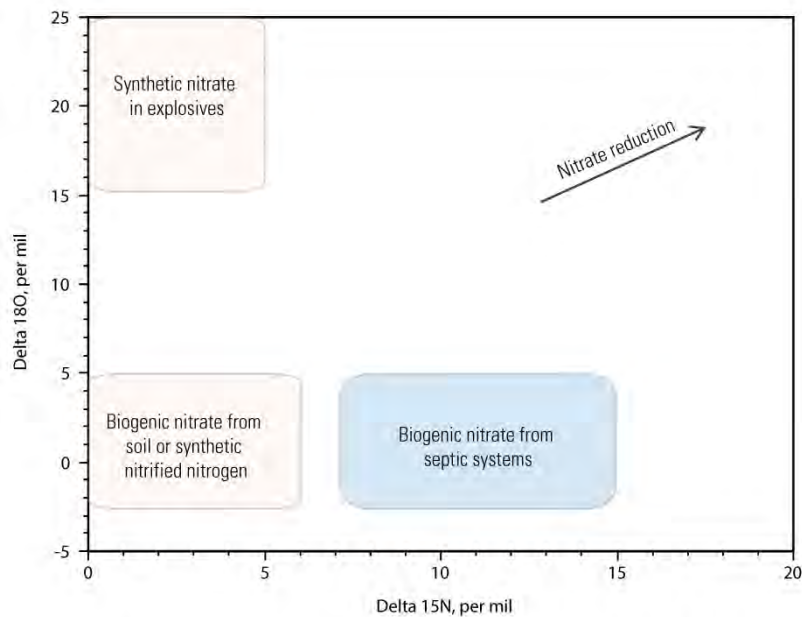


Figure 3. Graphs showing relation between delta15N and delta18O of nitrate.

Figure 3: Graph showing D15N and D18O of nitrate sources

Nitrogen from hydroseeding was also evaluated as a source of the groundwater impacts. The hydroseeding fertilizer did not contain nitrate and was urea based. The total documented mass of nitrogen applied-in hydroseeding fertilizer was less than 0.5 percent of the total nitrogen used for blasting in the study area.

Conclusion

The results of the investigation highlighted the transient, heterogeneous, and complex nature of groundwater contamination associated with blasting-related construction in crystalline rock terrains. With careful study design and appropriate choices in monitoring of isotopes, gasses, in parallel with general chemistry it is possible to determine the nitrate sources to groundwater near blasting operations. With a better understanding of the sources the NHDOT was able to select the appropriate response with regard to the nature of the impacts.

REFERENCES:

1. Institute of Makers of Explosives, Fixing the Ammonium Nitrate Security Program. In 475 News, Institute of makers of explosives: 2014.
2. Kern, B., Rock Blasting and Water Quality Measures That Can Be Taken To Protect 492 Water Quality and Mitigate Impacts. Program, D. D. W. S. P., Ed. 2010; p 8.
3. New Hampshire Department of Transportation, Exit 3 ~ southbound off-ramp & 541 northbound bridges Windham. New Hampshire Department of Transportation, Ed. 2010; p 2.
4. New Hampshire Department of Transportation, Exit 3 sb mainline, sb on-ramp and nh 543 route 111– Windham. New Hampshire Department of Transportation, Ed. 2014; p 2
5. HTE Northeast, Inc. *I-93 Exit 3 Construction – Contract I Bedrock Drinking Water Well 566 Monthly Sampling August 2013 Analysis Round NHDOT Project 13933-I Salem to Manchester 567 Towns of Windham & Salem, New Hampshire*; 2013; p 104. 568
6. HTE Northeast, Inc., I-93 exit 3 construction – contract I bedrock drinking water well 569 monthly sampling March 2014 analysis round NHDOT Project 13933-I Salem to Manchester 570 Towns of Windham & Salem, New Hampshire. 2014; p 62. 571 27
7. Golder Associates, Inc., *2012 annual summary report interstate 93, exit 3 – contract K 572 site area Windham, New Hampshire NHDES site no.: 200906017 groundwater management 573 permit no.: GWP-200906017-W-001 PROJECT RSN NO.: 21785*; Golder Associates Inc: 2013; 574 p 143.

**Soil and Rock Slope Stabilization for Bridge and Highway Reconstruction,
State Routes 9 and 125
Lisbon-Durham, Maine**

Andrew R. Blaisdell, P.E.
GZA GeoEnvironmental, Inc.
477 Congress Street
Suite 700
Portland, Maine 04101
(207) 358-5117
Andrew.Blaisdell@gza.com

Christopher L. Snow, P.E.
GZA GeoEnvironmental, Inc.
477 Congress Street
Suite 700
Portland, Maine 04101
(207) 358-5118
Christopher.Snow@gza.com

Prepared for the 66th Highway Geology Symposium, September, 2015

Acknowledgements

The authors would like to thank the following individuals/entities for their contributions to this project:

Leanne Timberlake – Maine Department of Transportation
Glenn Philbrook – Maine Department of Transportation
Kitty Breskin – Maine Department of Transportation
Kate Maguire – Maine Department of Transportation
Tim Merritt – Stantec Consultants
Gary Santy – Stantec Consultants
Russell Morgan – GZA GeoEnvironmental, Inc.

Disclaimer

Statements and views presented in this paper are strictly those of the authors(s), and do not necessarily reflect positions held by their affiliations, the Highway Geology Symposium, or others acknowledged above. The mention of trade names for commercial products does not imply the approval or endorsement by HGS.

Copyright Notice

Copyright © 2015 Highway Geology Symposium (HGS)

All Rights Reserved. Printed in the United States of America. No part of this publication may be reproduced or copied in any form or by any means – graphic, electronic, or mechanical, including photocopying, taping, or information storage and retrieval systems – without prior written permission of the HGS. This excludes the original author(s).

ABSTRACT

The project site has been eroded by the rapidly flowing waters of the Androscoggin River for thousands of years. Over the last 200-plus years, an upstream dam and its tailrace have contributed to the heavy scour along the riverbank and at the bridge. What remains of the riverbank is a 30-plus foot high scoured rock slope with a thin mantle of glacial till soil supporting the approach roadway at the top of the riverbank slope. Stability of the approach roadway is in jeopardy due to the progressive failure of the soil veneer supporting the embankment.

At the bridge site, the riverbed consists of irregular, exposed bedrock with eroded seams and unfavorable discontinuities beneath proposed structures.

The paper describes subsurface investigations including test borings, angled air-rotary probes, seismic refraction, optical and acoustic televiewer surveys and bedrock exposure mapping completed on foot and using ropes-access; engineering analyses including soil slope stability analyses, soil slope retention alternative evaluations, stereographic projection of bedrock discontinuities, kinematic analysis of the bedrock bearing surface, buttress design for the abutment foundation, and doweling and grouting assessment for pier foundation stabilization.

The objective of the exploration program was to provide sufficient, yet still cost-effective investigations and limit the risk associated with uninvestigated subsurface conditions, i.e. surprises. The design solutions were developed in close conjunction with the bridge and highway designers and the owner (Maine DOT) whose input allowed the geotechnical designs to achieve their desired balance between cost and risk.

INTRODUCTION

A bridge replacement project is being undertaken by the Maine Department of Transportation (MaineDOT) on Maine State Route 125 over the Androscoggin River between Lisbon and Durham, Maine. The riverbed is comprised entirely of exposed bedrock within the vicinity of the bridge, with prevalent outcrops with irregular dimensions and variable degrees of weathering and fracturing.

Maine State Route 9 travels west from the Durham side of the bridge, travelling up a large hill along the riverbank. Approximately 500 to 700 feet west of the existing Durham abutment; There are active, progressive, failure scarps up to 30 feet in height downhill from Route 9. MaineDOT has been monitoring and evaluating these scarps for several years. Due to the slope stability concerns and the proximity to the bridge project, approximately a half mile of Route 9 will be reconstructed to mitigate the potential impact on the road from the progressive failure.

GZA was retained by Stantec Consulting, the bridge and highway designer for the project, to serve as the geotechnical consultant for the project. Our scope of services included conducting initial field investigations, developing preliminary recommendations, designing and executing a supplemental investigation program, and developing engineering solutions and recommendations to reconstruct the riverbank soil slope to a stable configuration for the reconstructed portion of Route 9 and to mitigate potential instability of the bedrock that would support the Route 125 bridge foundations.

PROJECT AREA

Bridge Project

The existing bridge carries Route 9/125 (Canal Street) over the Androscoggin River in Durham and Lisbon as shown on the annotated aerial photograph, **Figure 1**.



Figure 1 – Project Site

The project consists of replacing an existing, 280-foot-long, two-span steel through-truss bridge constructed in 1936. Full-height cantilever abutments and piers support the bridge with spread footings bearing on exposed bedrock outcrops.

The replacement bridge is planned to consist of a 340-foot-long, two-span bridge with a steel plate girder and cast-in-place concrete deck, the approximate location of which is shown on **Figure 1**. The bridge will be supported on full-height cantilever abutments with wingwalls and a concrete pier, each supported by a spread footing bearing on bedrock. A single pier (Pier 1) is proposed to be located on the northern portion of the same bedrock pinnacle that provides footing support for existing South Pier.

The riverbed at the existing and proposed Route 125 bridge alignments is dominated by large, irregular bedrock outcrops. Locally, the Durham shoreline consists primarily of exposed bedrock extending up as high as about El. 95¹. The rock slope along the shore in front of proposed Abutment 1 (Durham abutment) was severely undermined at the time of our field exploration program. Between the proposed Durham abutment and the river, the height of the undermined cavity ranged from about 5 to 10 feet, and the depth extended between approximately 2 and 10 feet behind the face of the slope.

The most significant undermining occurred between the existing and proposed Durham abutments, where the height of the undermined area was approximately 20 feet and the depth extended approximately 10 feet behind the face of the slope. Large rock blocks were present at the base of the largest undermined area (approximately 40 feet Rt. of proposed baseline), assumed to have fallen out from the undermined area. The rock slope above and upstream of the undermined area is near vertical. The base of the near vertical/undermined portion of the rock slope was between El. 67 and El. 75. The approximate plan limits of the undermined area are shown on **Figure 1** and representative photographs are shown on **Figure 2**.



Figure 2 – Undermined Area, Durham Abutment

¹ Elevations discussed in this paper are in feet and reference the North American Vertical Datum of 1988 (NAVD 88).

The bedrock pinnacle that supports the existing South Pier and is proposed to support Pier 1 is oriented nearly parallel to the run of the river. The top of the pinnacle varies between approximately El. 75 and El. 85. The pinnacle extends down to the river bed in the south channel between about El. 60 and El. 65 and in the lower tailrace at approximately El. 50 to El. 54. Representative photographs are shown on **Figure 3**.

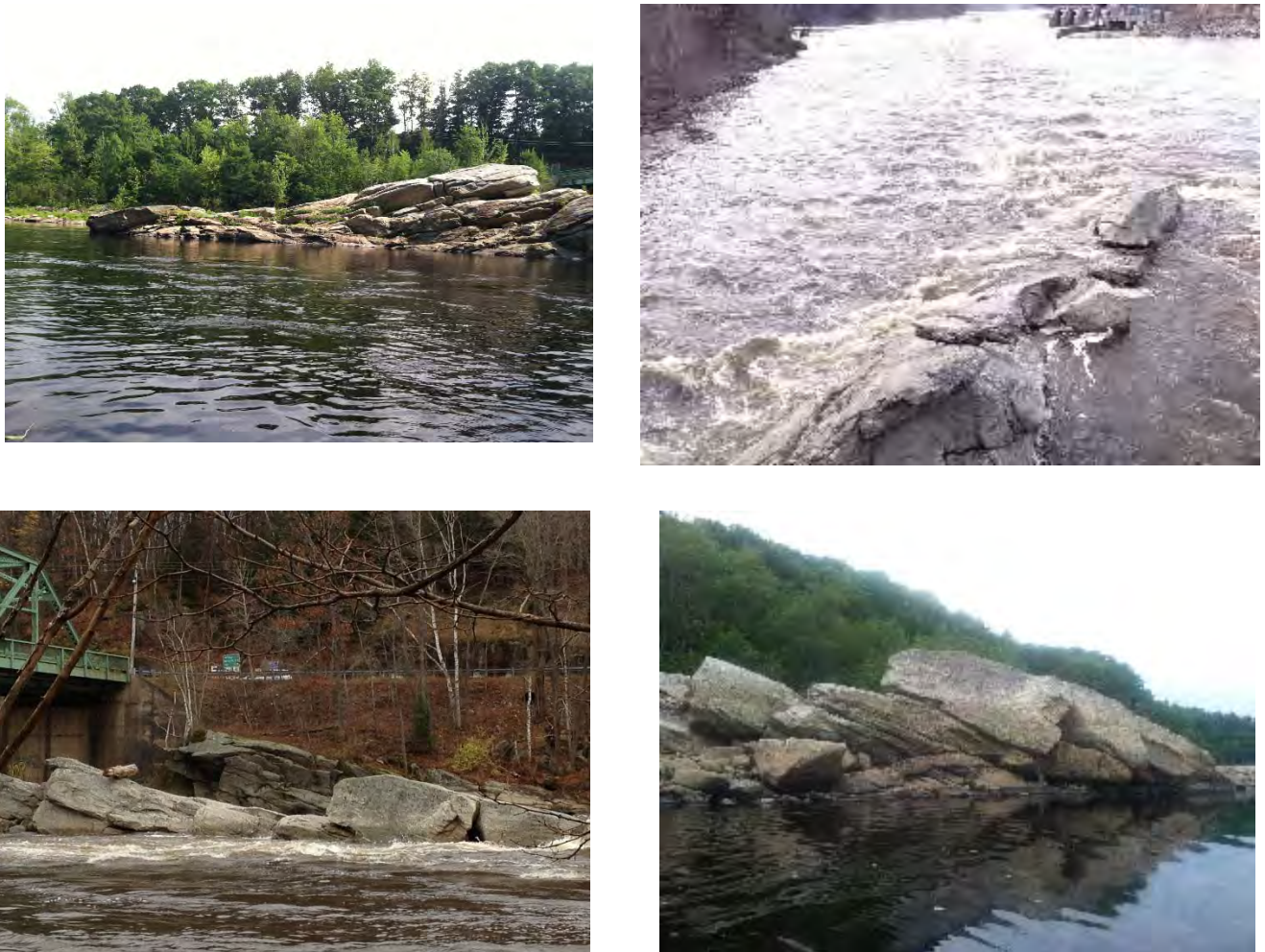


Figure 3 – Bedrock Pinnacle, Center Pier

The existing and proposed bridge alignments cross the Androscoggin River between 1,000 and 1,500 feet downstream from the Worumbo Dam. Worumbo Dam is a run-of-river dam and supports hydroelectric power generation. Because of the run-of-river status, water levels in the vicinity of the existing and proposed bridge vary by several feet seasonally and on a storm by storm basis. The 10-year return period flood (Q10) is at El. 80.2, the 100-year return period flood (Q100) is at El. 83.8, and the flood of record is at El. 90.8. Over the span of several site visits by GZA in late summer 2012 through mid-summer 2013, water levels have been observed between roughly El. 65 and El. 75. The typical observed water level during GZA's site visits in 2012 and 2013 has been roughly El. 70 near the proposed bridge alignment.

Excavation was made in the lower tailrace area of the dam in 1987. Based on our review of plans prepared for the work, bedrock excavation was completed to provide uniform depth at El. 51± in the primary tailrace (north channel) all the way from the dam structure to a point below the bridge, as well as limited rock excavation down to El. 60± in the south channel. The primary tailrace and south channel are shown on **Figure 1**.

Highway Project

The highway reconstruction project extends approximately one-half mile along Route 9 westward from the Route 125 bridge, as shown in **Figure 1**. The roadway is perched toward the top of a steep slope that extends down to the south bank of the Androscoggin River. Progressive failures have occurred along the riverbank slope below the roadway 500 to 700 feet west of the existing bridge. Bedrock outcrops are present at the bottom of the scarps. Representative photographs of the scarps taken during our work at the site are shown on **Figure 4**.



Figure 4 – Progressive Failure Scarps

OBJECTIVES AND PROJECT APPROACH

The primary objective of our work was to provide geotechnical engineering recommendations for design of the Route 125 bridge foundations and the reconstruction of the Route 9 roadway. Based on our initial site reconnaissance, it was apparent that three primary existing geotechnical/geological conditions required the most attention during design to develop recommendations and design details that would promote the future performance of the overall project:

1. Stability of oversteepened soil slopes and active failures downhill from Route 9;
2. Potential for bedrock structure/discontinuities to influence stability of new foundations bearing above the blasted, underwater tailrace rock slope beneath the proposed pier; and
3. Undermined rock beneath the proposed Durham abutment.

GZA proceeded with a multi-phased approach that included preliminary surface and subsurface explorations to provide a basis for development of preliminary design, followed by supplemental explorations to better define the conditions to allow detailing of the proposed solutions for the project documents.

Following the design phase, GZA was retained to provide geotechnical observations and recommendations during construction of the project, which is still underway at the time of this paper.

GEOLOGIC SETTING

Based on the Maine Geological Survey surficial geologic map of the Lisbon Falls South Quadrangle, the soil deposits at the site consist of thin drift. Thin drift is a glacial till deposit typically less than 10 feet thick that overlies bedrock, commonly with bedrock outcrops. At some locations, the unit has low areas or depressions filled with Marine Nearshore (silt / sand) and Marine Silty Clay of the Presumpscot formation.

The predominant bedrock at the site consists of the Hutchins Corner Formation (Berry and Hussey 1998); previously referred to as the Vassalboro Formation (Hussey 1983). The Hutchins Corner Formation consists of tectonically deformed, high-grade metamorphic rocks, primarily biotite-quartz-plagioclase granofels with interbeds of calc-silicate granofels and minor interbeds of pelitic schist. The area also contains intrusions of pegmatite granite.

FIELD INVESTIGATIONS

Initial Bridge Explorations

Between July and December 2012, GZA completed an initial phase of subsurface explorations for the bridge project to develop preliminary engineering recommendations suitable

for Stantec, the designer, to proceed with design development. The initial subsurface investigations for the bridge project are summarized in **Table 1**.

Table 1 – Initial Explorations, Bridge Project		
Type	Quantity	Depths
Test Borings	6	16 to 65.3 feet (10 to 55 feet into bedrock)
Borehole Geophysical Tests	3	Full core depth
Geologic Mapping	53 readings	--

At the bridge location, the team judged that the pier footprint and the Durham abutment footprint would not be readily accessible with typical truck- or track-mounted drilling equipment. Therefore, preliminary test borings were drilled outside of the proposed foundation limits at both locations; from the Route 9 roadway for the Durham abutment, and through the existing bridge for the pier. A minimum of 10 feet of bedrock was cored in each boring, with additional coring at locations adjacent to bedrock slopes (riverbank and tailrace/channel) to extend at least 5 feet below the lowest exposed rock slope elevation. GZA engaged Northeast Geophysical Survey (NGS) of Bangor, Maine to conduct borehole televiwer surveys (Acoustic Televiwer (ATV) and Optical Televiwer (OTV)) in selected bore holes to provide engineering data for discontinuities in the bedrock.

Geologic field mapping was undertaken on the exposed outcrops within, along and adjacent to the river to provide data for evaluating the stability of the rock mass in the area of proposed foundations. A GZA engineer made direct measurements of bedrock joints and features on existing exposures. A Brunton compass was used to collect strike and dip measurements on 53 features. Outcrops within and along the riverbank were accessed using kayaks, as shown on **Figure 5**.



Figure 5 – Bedrock Field Mapping by Kayak

GZA and Stantec emphasized the importance of high resolution survey data for this project to MaineDOT, particularly for the undermined rock slopes near the Durham abutment. To meet this objective, MaineDOT conducted a unique field survey program and data

interpretation, with the intent of approximating a LiDAR-type data set. Ledge data was collected for a tight grid of points through a “scanning” mode from a total station. Collection and processing of the data was conducted by MaineDOT and provided to GZA.

Initial Highway Explorations

From May through July 2011, prior to GZA’s work, MaineDOT had conducted test borings, auger probes and surface geophysical testing to provide data for assessment of the active slope movement between Route 9 and the riverbank. From August through November 2012, GZA conducted additional test borings to further characterize the existing conditions in the roadway and slope area. The initial subsurface investigations conducted by MaineDOT and GZA for the highway project are summarized in **Table 2**.

Type	Quantity	Depths/Lengths
Test Borings (MaineDOT)	2	8.2 to 11 feet
Auger Probes (MaineDOT)	5	1.9 to 10.4 feet
Seismic Refraction Line (DOT)	1	250 feet long
Ground Penetrating Radar (DOT)	2	710 to 720 feet long
Test Borings (GZA)	12	4.7 to 21.5 feet

The MaineDOT borings and probes were each drilled with augers and advanced to auger refusal. All of the MaineDOT borings and probes were drilled through the existing roadway. The seismic line was located on a lightly wooded narrow shelf between the roadway and the scarp portion of the slope, generally parallel to and approximately 40 to 60 feet north (down-slope) of the original roadway centerline. The GPR lines were laid out on the left and right paved shoulders of the existing roadway.

GZA’s borings included four through the road shoulders, four borings up-slope, and four borings down-slope. The four test borings on the down-slope were completed using a portable tripod rig to safely access the area above the scarp, and the remaining eight were completed using a trailer-mounted drill rig. The borings were generally oriented to allow creation of subsurface profiles for subsequent use in stability analyses. Six of the borings were drilled to auger refusal, and two borings were cored approximately 5 feet into bedrock.

Supplemental Bridge Explorations

Following identification of the primary geotechnical concerns, GZA designed a supplemental subsurface exploration program for the project. The overall intent was to provide a data set that would allow for reliable development of foundation design parameters and bearing levels for the bridge foundations, and to create representative cross sections to develop details for the new highway.

Considering the presence of poor-quality bedrock in the vicinity of the pier and Durham abutment, we judged that it was important to conduct additional test borings within the limits of the proposed foundations, to evaluate the continuity of potentially problematic layers, and if they

were present, to determine whether the exposure or orientation of these layers would be adverse to foundation design or performance. The supplemental subsurface investigations for the bridge project were conducted between May and July 2013 and are summarized in **Table 3**.

Table 3 – Supplemental Explorations, Bridge Project		
Type	Quantity	Depths
Test Borings	3	28.5 to 48.7 feet (25 to 40 feet into bedrock)
Borehole Geophysical Tests	3	Full core depth

Each boring was cored to an elevation corresponding roughly to the bottom of the adjacent riverbank or tailrace/channel. ATV and OTV borehole viewer surveys were conducted in each boring. The test borings were completed using a skid-mounted drill rig, which was placed over the Route 9 guardrail using a crane for the Durham abutment borings and transported up river on a pontoon barge and skidded partially off of the barge for drilling the pier boring. The skid drill rig configuration for the pier boring is shown in **Figure 6**.



Figure 6 – Test Boring at Bedrock Pinnacle

Supplemental Highway Explorations

The depth to bedrock was found to vary significantly over short distances during the preliminary slope/highway excavation phase. For the conceptual design alternatives considered for the slope, the bedrock elevation was a significant consideration impacting constructability and cost. Therefore, a supplemental exploration program was conducted for the highway project in August 2013 that included eighteen (18) rock probes, eight (8) test pits, three (3) seismic lines (seismic lines), and additional field mapping of accessible outcrop features. The supplemental subsurface investigations for the highway project are summarized in **Table 4**.

Type	Quantity	Depths/Lengths
Vertical air track rock probes	13	10 to 57 feet (5 feet into apparent rock)
Battered air track rock probes	5	31 to 65 feet (7 to 14 feet into apparent rock)
Test Pits	8	5 to 9 feet
Seismic Refraction Lines	3	150 to 750 feet long
Geologic Mapping	16 readings	--

Rock probes were completed along the southern and northern sides of the roadway, in the roadway shoulders, north and south of the roadway, and along the top of the slope north of the existing guardrail. The air track drill rig extended the boom out over the north guardrail to reach locations distant from the road. The rock probes lengths ranged from approximately 10 to 65 feet. Two of the probes met practical refusal in sand due to apparent binding of sand against the drill rods. The battered probes were drilled at inclinations ranging between 55 and 59 degrees from horizontal, with batter angles selected by GZA in an attempt to encounter rock at a desirable location to supplement top of rock elevation data. The conversion of battered probe data to top of rock coordinates, depth and elevation was based on the recorded bearing and azimuth of each probe.

GZA engaged NGS to conduct seismic refraction surveys adjacent to the proposed roadway alignment to evaluate depth to bedrock.

Additional geologic field mapping was undertaken along the Route 9 realignment project to provide supplemental data for evaluating the stability of the rock mass in proposed rock cut locations. A GZA engineer made 16 direct measurements of bedrock joints and features on existing exposures along the existing rock cut face along the south side of Route 9 that were accessible without climbing gear.

ENGINEERING CHALLENGES AND SOLUTIONS

GZA identified three primary elements of the combined bridge and highway project that would require the most attention to develop recommendations and design details that would promote the future performance of the overall project. These project elements and the associated engineering challenges are summarized in **Table 5**.

Project Element	Primary Engineering Challenge
Progressive Failures between Route 9 and River	Either stabilize existing slope OR prevent on-going movement from affecting road
Undermined Rock at Durham Abutment	Stabilize the undermined rock and prevent additional rockfall that could jeopardize support of the new abutment
Rock Slopes below Pier	Reinforce the bedrock pinnacle as necessary to mitigate potential adverse bedrock structure to affect pier foundation stability

GZA's evaluations and recommendations to address these conditions are described in the following sections.

HIGHWAY SLOPE MITIGATION AND DESIGN

Following the preliminary subsurface exploration program, GZA developed design-basis subsurface profiles and conducted global stability analyses to assess the potential cause(s) of the ongoing instability. Five soil units were identified above granite bedrock in the explorations, in order of descending depth below ground surface: less than 1 foot of Forest Mat, 2 to 5 feet of Fill (loose to dense Sand, some Gravel), 2 to 5 feet of Nearshore Deposit (very loose to very dense Sand and Silt), 2 to 7 feet of Marine Deposit (medium stiff to hard Clay and Silt), and 3 to 21 feet of Glacial Till (medium dense to very dense Sand with Gravel, cobbles and boulders). Groundwater was not observed in the test borings during drilling. Temporary observation wells were installed in two completed boreholes, and both were dry between October and December 2012.

Subsurface stratification was evaluated at three cross sections based primarily on straight-line interpolation of the strata between adjacent borings located on the same section. The idealized subsurface profile developed to analyze one of the progressive failure areas is shown in **Figure 7**.

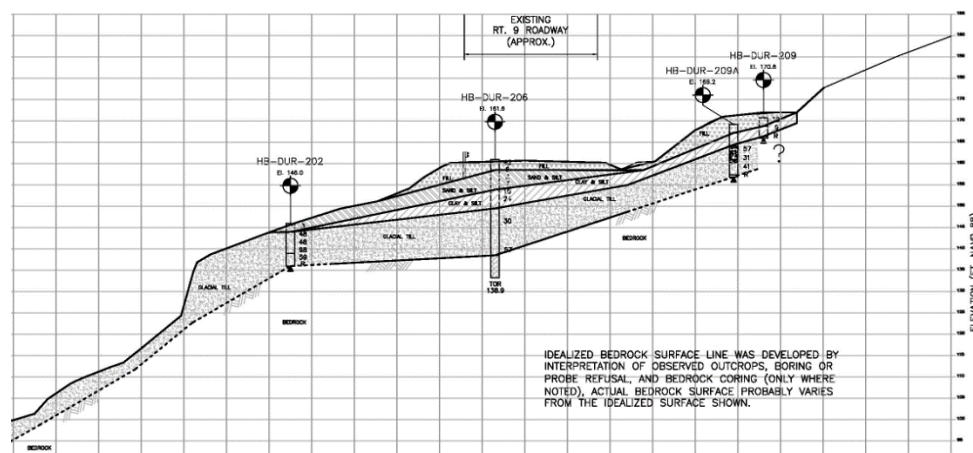


Figure 7 – Idealized Subsurface Profile through Failure Scarp

GZA conducted evaluations to assess the stability of the existing slopes. The stability analyses focused on the area around the two significant scarps that exist at the top of the riverbank slope, approximately 50 to 60 feet down-slope from the edge of pavement on Route 9.

The exposed failure scarps show that the overburden soil is sliding at the soil/rock interface. The soil exposed in the scarps consists of dense silty sand and gravel appears to be glacial till. The failures appear to be triggered by groundwater flow and made more tenuous by the steep slopes of both the rock and the ground surface. Therefore, although groundwater was not observed in the borings, the visual evidence was used as a basis of our model relative to groundwater conditions. Evaluations considered what GZA judged to be the probable range of groundwater conditions: from “deep” groundwater following the top of bedrock, to “shallow” groundwater following the top of glacial till and daylighting at the failure scarp. The low

groundwater condition was encountered during the field exploration program. The higher groundwater level was developed to approximate conditions that may occur following long periods of precipitation, or during spring melt.

GZA performed a series of analyses to assess rotational stability of the slope using the computer analytical software, “Slope/W,” developed by Geo-Slope International, based on the Modified Bishop method. The evaluation for potential failure surfaces was limited in two scenarios:

- Scenario 1: Arcs that initiate just above, and exit out through the existing failure scarp or steepest downhill face (representative of a progressive failure similar to those that are believed to have caused the failure scarps); and
- Scenario 2: Arcs that could initiate in the road and exit out through the existing failure scarp or steepest downhill face.

The analysis results for the Scenario 1 indicate that the factor of safety is at or below 1.0 for progressive failure at the existing scarps. We attribute this to the very steep angle of the scarp faces combined with fluctuating groundwater levels. Based on conversations with Kitty Breskin, P.E., MaineDOT Geotechnical Engineer, the scarps have migrated up slope, toward the roadway over the last several years. We hypothesized that the rate of migration would have been even faster, were it not for the reinforcing effects of vegetation (tree roots). If no mitigating measures are undertaken, we concluded that the scarps would eventually progress to the point where they could undermine the roadway. The rate of scarp progression is unpredictable, but it is linked to the frequency of heavy rainfall and/or melt conditions that tend to raise the groundwater level.

The analysis results for Scenario 2 show that the minimum factors of safety for failure arcs that extend into the roadway range from approximately 1.25 to 1.5 for dry slope conditions. If saturated conditions are assumed with groundwater at the top of glacial till level, the minimum factors of safety for failure arcs that extend into the roadway drop to approximately 1.0. However, since lower safety factor arcs exist at the scarp face under high groundwater conditions, we expect that the failure would be progressive (at the scarp face), rather than a single large arc extending all the way up into the roadway.

The results for Scenario 2 also show the importance of drainage on the uphill side of Route 9. Based on these results a proper drainage system was included as part of the roadway reconstruction to lower the maximum groundwater level and help stabilize the slope. The drainage system included a continuous underdrain extending along the uphill shoulder, 4.5 feet below pavement elevation, with additional lateral underdrains in proposed rock cut areas that daylight to riprap downspouts beneath the downhill shoulder.

Figure 8 shows representative results of GZA’s Slope/W analyses for Scenario 2. These results indicate that the calculated minimum factor of safety against rotational failure is less than 1 and is therefore unacceptable. AASHTO LRFD guidelines consider a minimum factor of safety of 1.3 acceptable for a slope that does not support or contain structural elements. Although a failure of the existing slope that extends into the roadway is considered unlikely in

the short-term, it was considered necessary to stop the migration of the progressive failures to protect the road over the longer term.

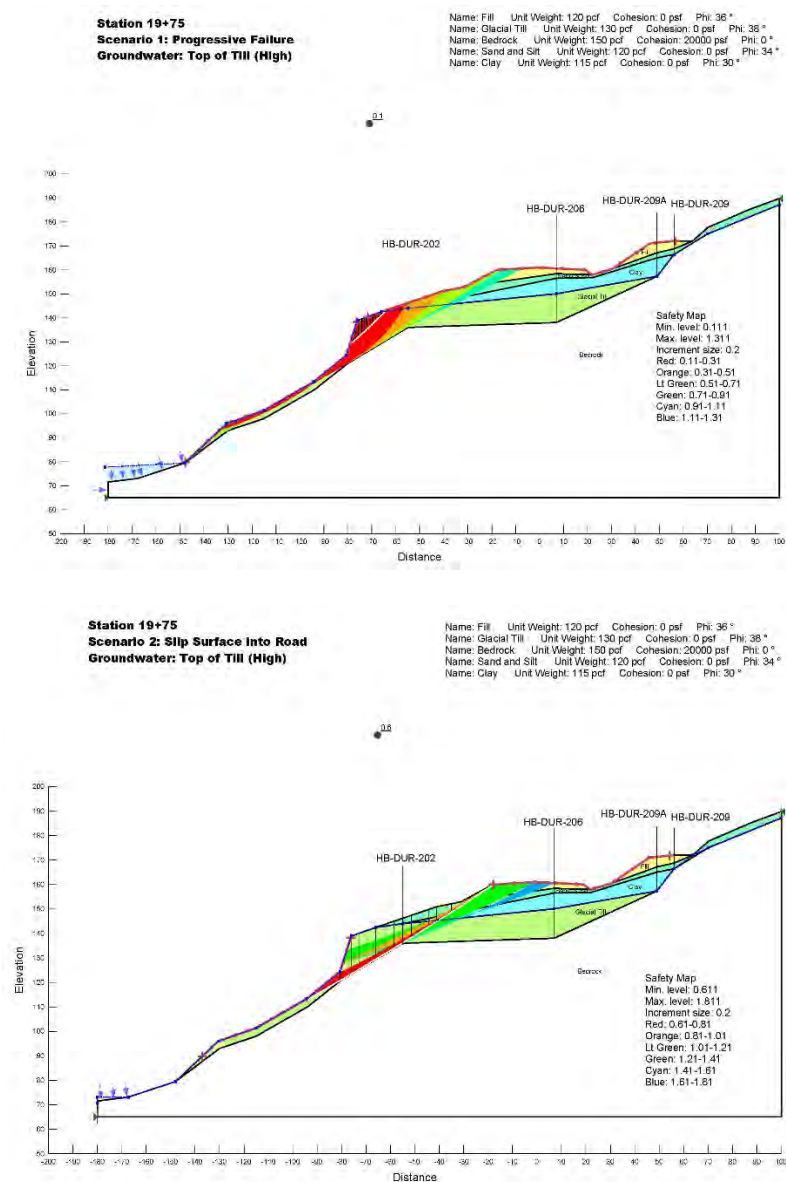


Figure 8 – Representative Slope Stability Output

Relocation of the roadway away from the failure scarps without exposing bedrock at the toe of the excavated slopes would delay, but not prevent, the progressive failures from reaching the roadway. Therefore, GZA provided conceptual alternatives for construction of a slope stabilization structure above the progressive failures to provide a means of protecting the reconstructed roadway. Options considered included precast concrete slabs with ground anchors; rock-socketed soldier beams and lagging, and T-wall. Each of these alternatives would include relocation of the road approximately one lane away (uphill) from the scarps.

Each of the stabilization alternatives would limit the earthwork during construction, and they would be designed to rely on support from bedrock such that all soil downhill of the structure could move towards the river, without impacting the reconstructed roadway. An alternative, non-structural solution was also considered. Relocation of the roadway away from the scarps could provide the desired performance if new cut slopes were constructed so that bedrock is exposed at the toe of the cut slope. Similarly to the structural solution, the progressive slope failures could occur without impacting the roadway. This alternative would involve significantly more earthwork than the structural solutions, as the roadway would be shifted much further into the uphill slope to allow the toe of the new cut slope to fall on bedrock and meet the design intent of this alternative.

GZA and Stantec developed preliminary pricing for review by MaineDOT for each alternative, and the cost estimates for all solutions were comparable. All of the structural solutions and the earthwork solution were estimated to cost between \$1.03 million and \$1.13 million. The earthwork solution had the highest estimated cost, but it was selected as the preferred alternative by MaineDOT due to simplicity of construction, and to avoid adding a structure to the State's inventory to maintain.

After the slope excavation alternative was selected, top of bedrock elevations became the critical data for final design development. Bedrock elevation was essential on the north (river) side of the proposed road to ensure that the cut slope would touch down on bedrock, meeting the design intent. On the south (uphill) side of the proposed road, bedrock elevation data would form the basis of ledge lines on the design sections and form the basis for rock excavation quantities and slope design.

GZA plotted the observed and interpreted bedrock elevation data from all available subsurface investigations, surface geophysical data and bedrock exposures in the Route 9 slope area. Initially, a top of rock elevation contour plan was developed that linearly interpolated between all of the points with no manual adjustments. Detailed review was required to assess locations where bedrock was shown to daylight above the existing ground surface and where it didn't match well with the bedrock exposures. Through this process, additional "dummy" bedrock elevation points were added to the model using engineering judgment in an effort to provide more realistic output. GZA developed a bedrock elevation contour plan and provided it to Stantec as an electronic document, which was then used to create ledge lines by cutting sections through the contours. An excerpt from the plan is shown in **Figure 9**.

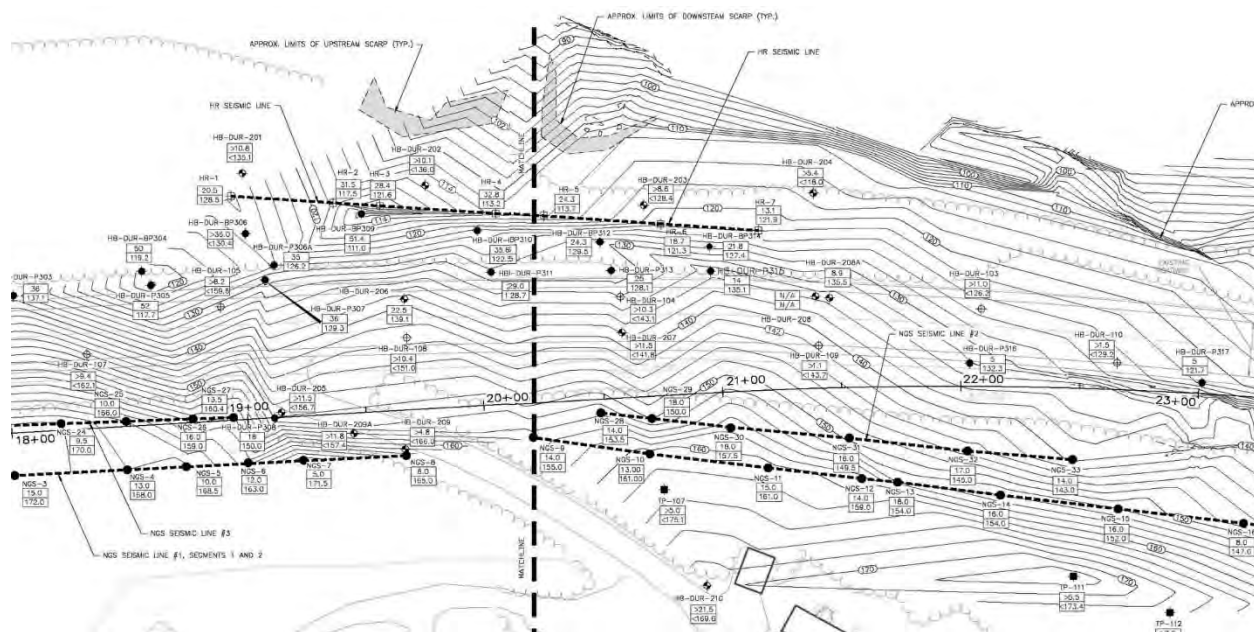


Figure 9 – Bedrock Elevation Contour Plan

The design team identified a potential stability concern for the cut slope toe terminating on rock. Seepage along the bedrock surface that daylighted at the toe of the soil slope could destabilize the toe of the slope, especially if it occurred before the slope was well vegetated. GZA and Stantec considered several options to promote stability at the toe of slope, including a bedrock key, and gabions and precast concrete blocks to act as a toe buttress. The preferred solution was a precast concrete slope buttress detail, which included regularly spaced rock dowels extending through the blocks, to allow them to be constructed on a sloping bedrock surface. The final slope buttress design detail is shown on **Figure 10**.

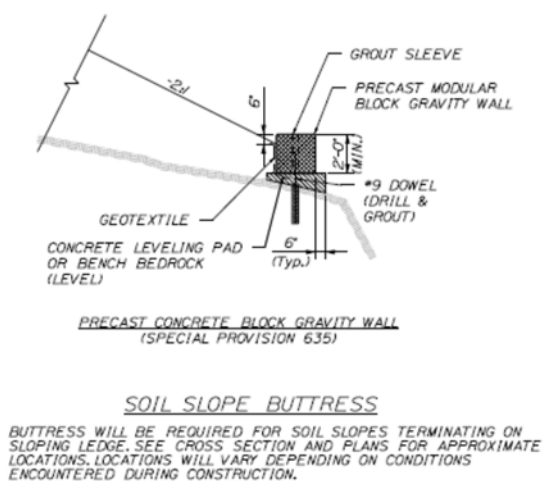


Figure 10 – Slope Buttress Detail

UNDERMINED ROCK SUPPORT AT DURHAM ABUTMENT

GZA developed a three-dimensional surface of the rock slope in AutoCAD using the MaineDOT Microstation files from their scanning survey and tied that data to known survey points at the boundaries of the MaineDOT survey. GZA interpreted the survey data provided by MaineDOT to develop two-dimensional cross sections of the undermined areas at the selected locations (28 feet Lt., Baseline, 20 feet Rt., and 40 feet Rt.) near the proposed Abutment 1, which are presented on **Figure 11**.

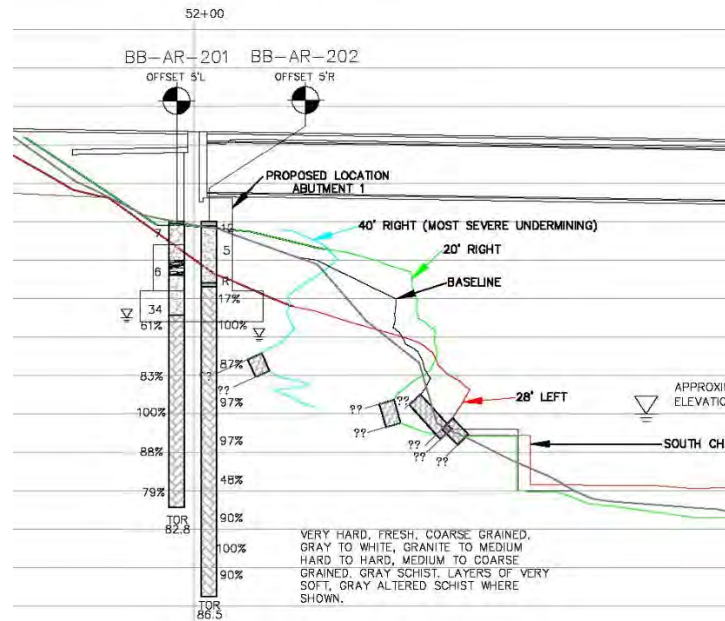


Figure 11 – Cross Sections through Undermined Rock

Based on the sections through the undermined cavity, it was found to be outside of the zone of influence of the proposed Durham abutment footing. However, the configuration did not appear stable, and additional loss of rock from the top of the undermined cavity could eventually threaten the rock supporting the footing.

It was necessary to geologically map the undermined cavity to characterize the exposed rock, but accessibility to the area was very difficult during the exploration phase. It was not feasible to access the area by foot, and when we were attempting to identify the presence of potentially erodible rock, it was too cold to safely use kayaks for access. Therefore, GZA rappelled on ropes to observe and evaluate the undermined area. GZA's access to the area is shown on **Figure 12**.



Figure 12 – Ropes Access to Undermined Area

Our engineer measured and documented discontinuities and assessed exposed bedrock materials. A band of soft to very soft Altered Schist was present at or near the bottom of the most significant undermined area. It was concluded that the undermining was caused by erosion of the Altered Schist under high water level conditions, resulting in loss of support and failure of large portions of the granite above.

To protect the new Durham abutment from undermining, a concrete buttress was designed to fill the undermined cavity, thereby retaining and protecting the exposed weak rock at the back of the undermined zone and supporting the overhanging rock mass to prevent additional loss of the rock face. The buttress was recommended to be supported on a clean, sound bedrock surface and to consist of structural concrete. Vertical dowels were recommended for lateral base resistance, and a French drain with weep holes through the buttress was recommended to prevent buildup of hydrostatic pressure. The buttress length was estimated to be 50 feet, but the limits couldn't be accurately determined on paper because of the highly variable conditions, so it was recommended that GZA assess the limits during construction. The design detail for the buttress is shown below in **Figure 13**.

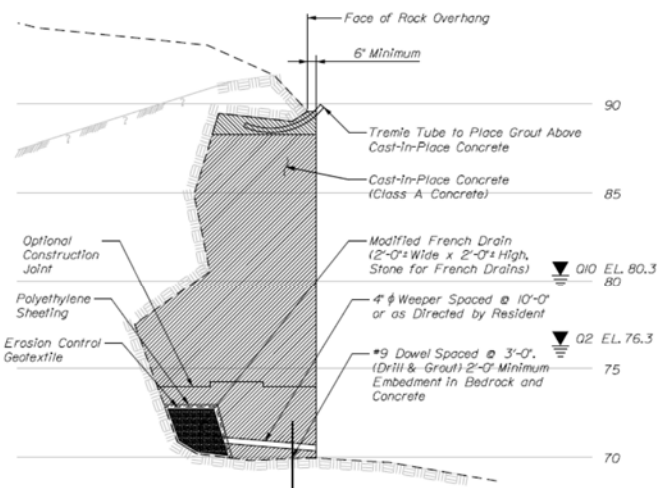
ROCK OVERHANG STABILIZATION NOTES

1. Dowels shall meet the requirements of ASTM A 615/A 615M, Grade 60 and shall be galvanized to ASTM A 153 or ASTM B695, Class 50, Type I. Payment for galvanizing will be considered incidental to the Structural Concrete Abutments and Retaining Walls - Class A Overhang Stabilization pay item. See Dowel Notes for installation details.

2. The Modified French Drain shall consist of Stone for French Drains meeting the requirements of Standard Specification 703.24 and shall be wrapped in Erosion Control Geotextile meeting the requirements of Standard Specification 722.03 (Class II).

3. Following Modified French Drain construction and prior to placing concrete the exposed portion of the Modified French Drain shall be covered with two layers of polyethylene sheeting or other material approved by the Resident to prevent the wet concrete from penetrating into the geotextile and stone.

4. Payment for rock overhang stabilization will be made under Item No. 502.211, Structural Concrete Abutments and Retaining Walls - Class A Overhang Stabilization. See Special Provision 502.



SECTION - ROCK OVERHANG STABILIZATION
(SECTION TAKEN DOWNSTREAM OF PROPOSED DURHAM ABUTMENT)

Figure 13 – Stabilization Buttress Design Detail

Construction of the concrete buttress began in December 2014. It was an unusually cold and snowy winter in Maine, resulting in difficult work conditions for all construction projects. The contractor mobilized a large crane, set it up above the undermined area, and retrieved the large rock fragments that had fallen to the bottom of the area. The entire buttress area was subsequently tented and heated throughout subgrade preparation and concrete placement.

The contractor worked to prepare a clean, sound bedrock surface to support the buttress in accordance with the plans. As the Altered Schist was removed in very close proximity to the frozen river, it became evident that the buttress would need to be dowelled in and supported on the more competent bedrock toward the back of the cave. Further removal of the altered material would have extended below the river water level, so it was left in-place.

Due to the unusual geometry of the work area and as anticipated during design, the actual configuration of the buttress was field-fit to provide protection of the problematic seam. The design and construction team worked together on site to fit the solution to the conditions encountered. Field customization included adjusting the French drain location toward the back of the cave, hand-selecting location of supporting rock dowels to ensure embedment in competent rock, and addition of additional socketed rebar into the back of the cave to reinforce the concrete section. The concrete was installed in three placements, including a levelling slab, and two more to achieve the full height of the buttress. Photographs taken during construction of the buttress are presented on **Figure 14**.

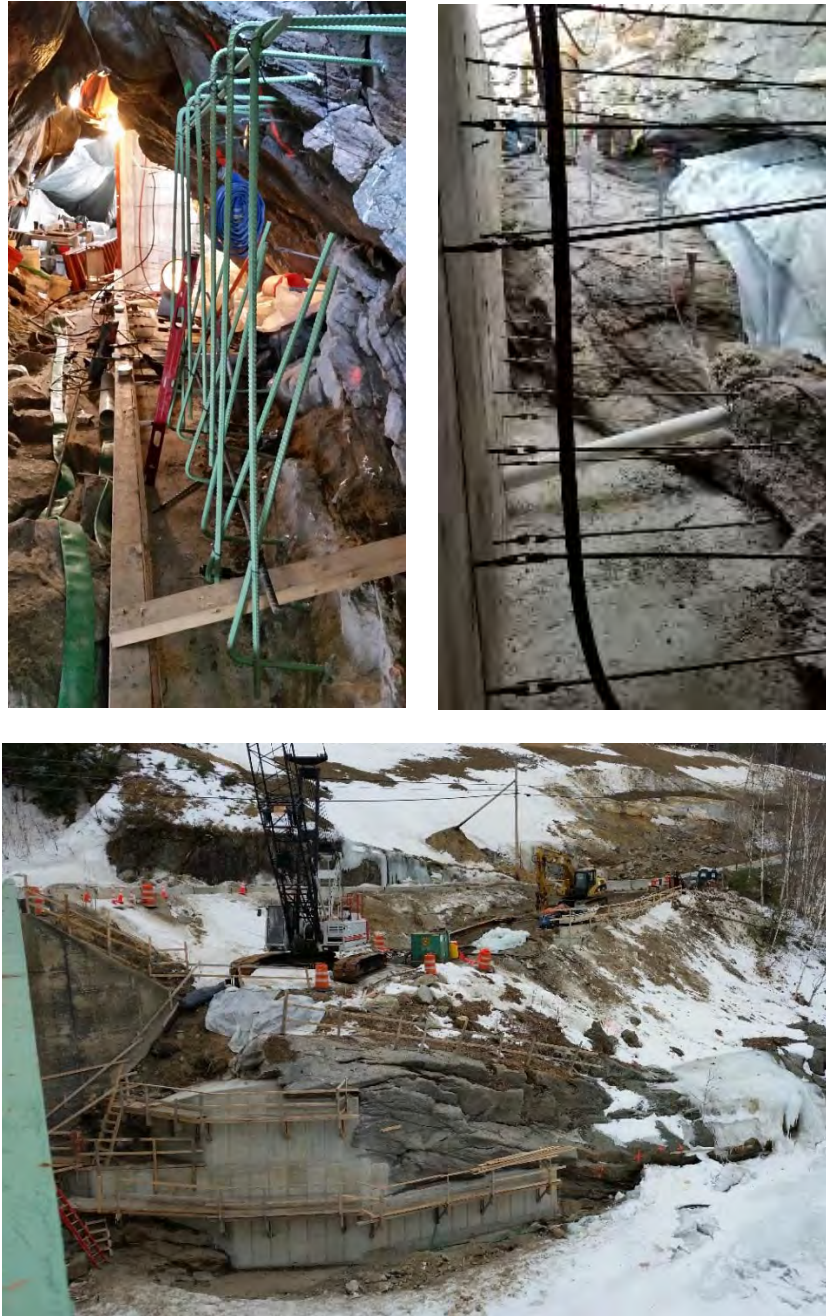


Figure 14 – Construction of the Stabilization Buttress

ROCK PINNACLE REINFORCEMENT AT PIER

The pier was planned to gain support on a bedrock pinnacle adjacent to excavated bedrock slopes to the south (south channel; approximately 10- to 15-foot-tall underwater slope) and to the north (main tailrace; approximately 18- to 25-foot-tall underwater slope). Representative top of rock (and surface) profiles were developed at three locations through the rock pinnacle that would support the proposed pier, as shown in **Figure 15** below.

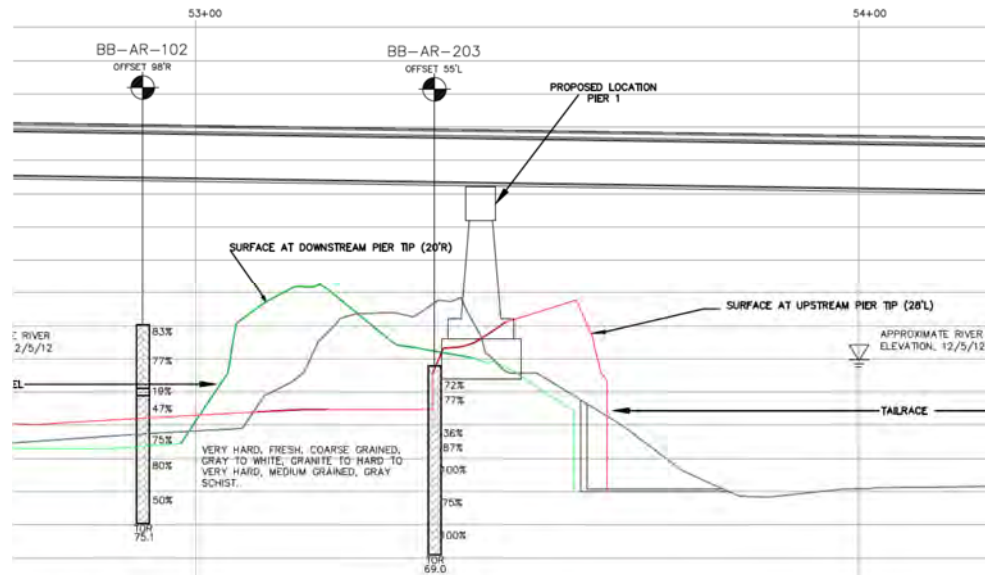


Figure 15 – Rock Profiles through Center Pier Rock Pinnacle

Due to current conditions, it was not practical to observe the condition of the rock slope below the river level. A combination of rock coring, borehole geophysics and hand measurements were used to develop data for our engineering evaluation of the pier foundation.

Given the steep side slopes and narrow width of the rock pinnacle, it was necessary to evaluate potential kinematic instabilities below the proposed footing level. Great circles, representing the central tendencies of the joint sets and the orientations of the underwater rock slopes were plotted for use in graphical evaluation of rock slope stability. A total of 108 joint observations were used in our engineering evaluations, including 31 field joint observations and 77 features from the televiewer data. **Figure 16** shows the great circles of the representative joint sets and the underwater rock slopes at the pier, along with 30-degree friction circles for possible sliding. The slope designated as P1N is the underwater rock slope north of the pier (along the main tailrace), and P1S is the underwater rock slope south of the pier (along the south channel). This figure was the basis of GZA's rock stability evaluations for Pier 1.

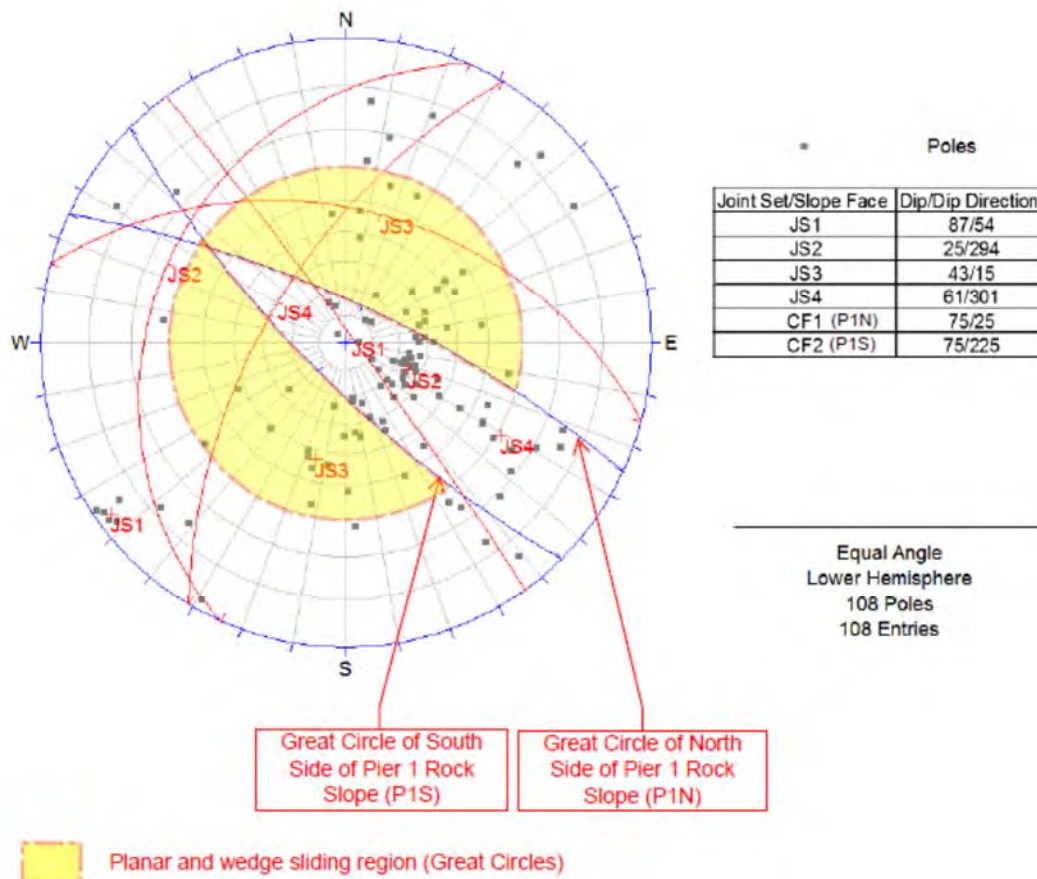


Figure 16 – Pier Rock Slope Stereonet

For P1N along the north side of Pier 1, there is a kinematically possible plane failure along JS3 (dip of approximately 43 degrees), and there are three combinations of joint sets that create kinematically possible wedges that could daylight in the rock slope. Joint set combinations JS1-JS3 and JS3-JS4 form wedges with lines of intersection having dips of approximately 32 degrees and 42 degrees, and joint set combination JS1-JS4 forms a wedge with a line of intersection having a dip of approximately 58 degrees. Considering the potential planar failure mode on JS3, and the three kinematically possible wedge failure modes, we recommended implementation of measures to preserve stability of the rock pinnacle beneath the pier footing.

We evaluated shear dowels drilled through potentially daylighting planes to support the rock mass. The design methodology was based on the potential planar failure along JS3. The height of the plane was assumed to be the maximum exposed underwater slope height along the main tailrace, and in addition to the self-weight of the sliding rock mass, the factored bearing pressure from the structural calculations was applied as a vertical surcharge. The required number and size of dowels was determined that would support the shear forces induced by the factored bearing pressure. Properties of the steel dowels were reduced by appropriate resistance factors consistent with LRFD methods.

Based on our evaluations, we recommended the installation of 24, Grade 60, No. 11 reinforcing bars, extending from at least 1 foot below the bottom of the tailrace to the top of the tremie seal. A special provision was prepared with water pressure testing (i.e., Packer testing) in the drilled dowel holes to assess each hole's ability to hold grout until it sets, and adjust the initial grout mix/consistency to limit erosion if significant water take was evident. The special provision also established criteria for consolidation grouting where necessary. The design details are presented in **Figure 17**.

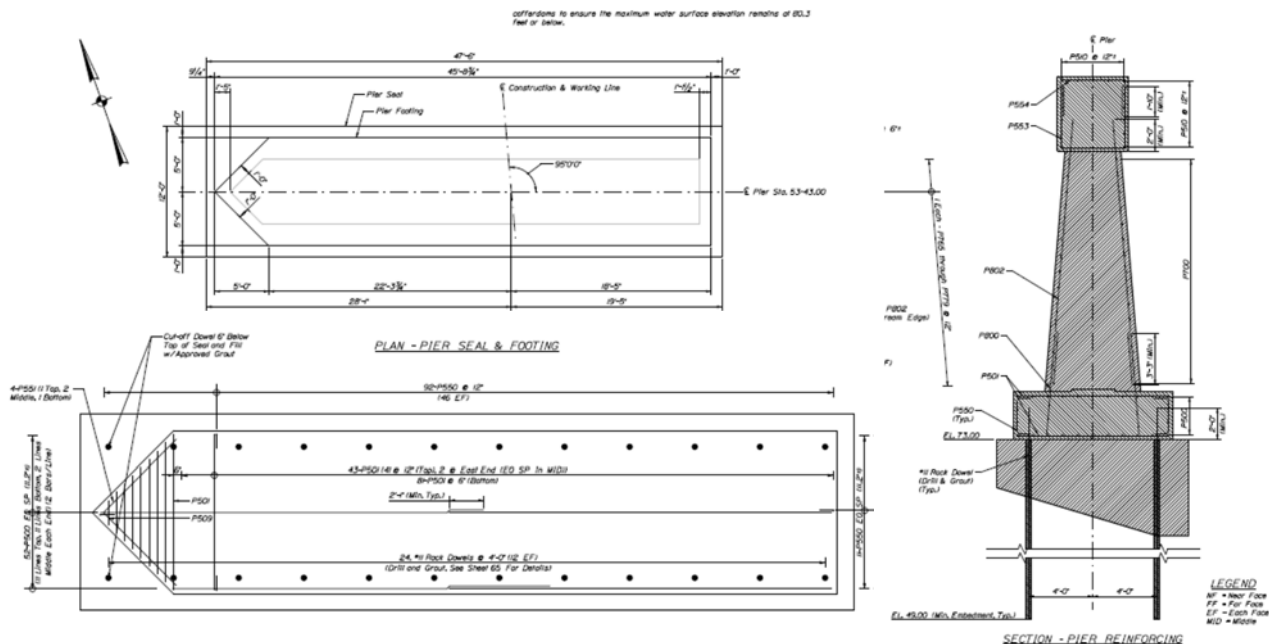


Figure 17 – Rock Pinnacle Reinforcement Details

EXPOSED BEDROCK CONDITIONS DURING ROCK EXCAVATION

The sequence of granite and schist that is present across the project area, which resulted in the undermining along the riverbank beneath the Durham abutment foundation, was observed prominently during foundation excavation for the Durham abutment.

During the initial exploration program, one test boring was drilled near the proposed Durham abutment, but it was through the adjacent roadway, over 30 feet away from the footing. It was this boring that encountered the altered schist most prominently, with variably altered schist extending from El. 86 to El. 71. Two additional borings were drilled within the abutment footprint during final design, and both encountered high-quality granite throughout the core depths, with top of rock between El. 83 and El. 87. The foundation design therefore was based on (but slightly lower than) the encountered granite elevations within the footing footprint, while bearing design considered the possible presence of schist, with a lower recommended bearing resistance than might be justified for the granite. The interpretive subsurface profile created through the three borings drilled near the Durham abutment showed distinctly different conditions between borings, suggesting that the granite intrusion reached the ground surface through a sequence of altered schist just above the river, as shown in **Figure 18**.

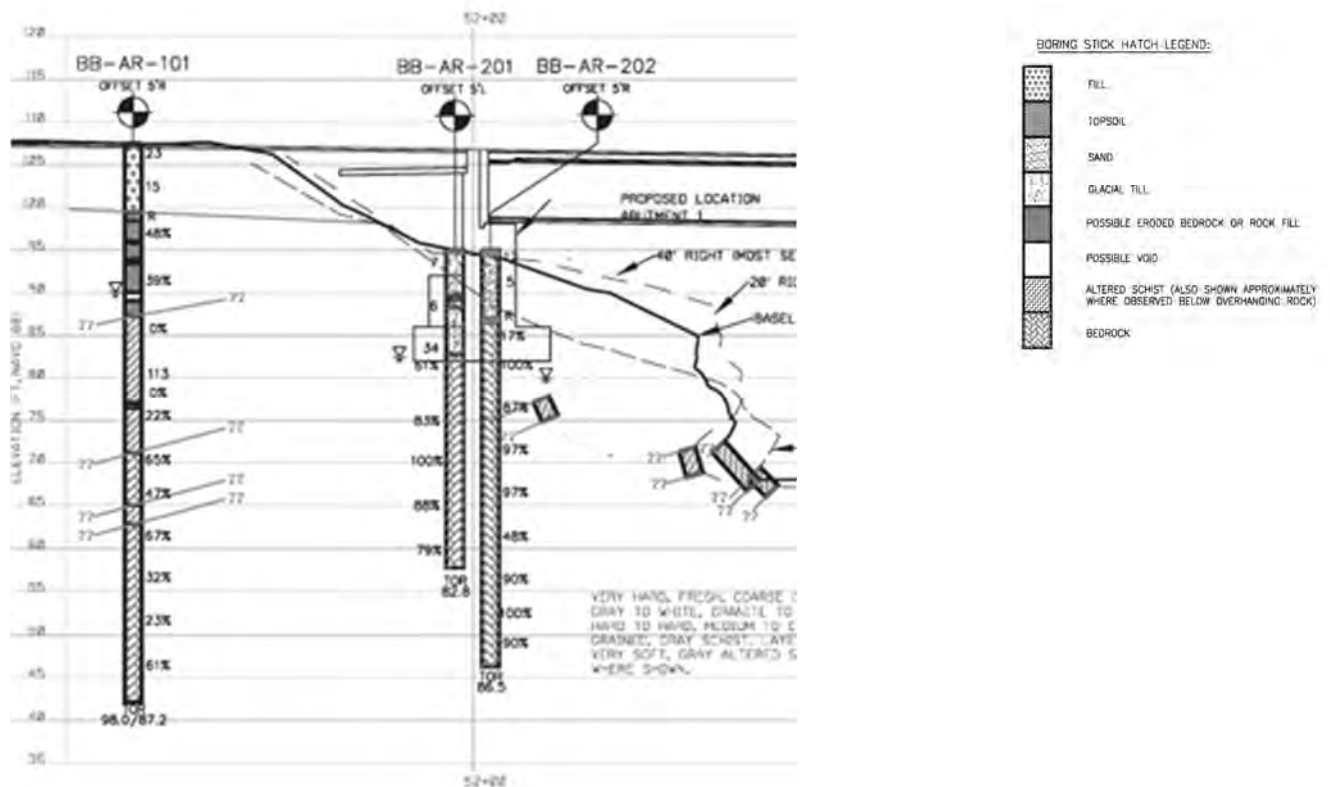


Figure 18 – Durham Abutment Interpretive Subsurface Profile

Foundation excavation activities at the Durham abutment exposed bedrock geology that was remarkably similar to the profile shown above in **Figure 18**, and also highly unusual in Maine. The very hard granite was encountered at the river side of the abutment footing, as high as approximately El. 89, or 7 feet above design bearing level. Due to blasting restrictions near the river, the contractor line drilled the excavation perimeter and hoe rammed to remove the granite, as shown below on **Figure 19**. The top of the granite dipped down at an angle of roughly 30 degrees towards the south, across the width of the footing and away from the river. Within the width of the abutment and wingwall footings, the granite surface dipped down below the design bearing level (El. 82), where variably altered schist was exposed at the contact. The contact zone between the schist and the underlying granite intrusion is shown in **Figure 19**, which is looking east at the east end of the wing wall foundation. Significant portions of the wingwalls and the back of the abutment footings were supported on moderately hard schist, but GZA observed the conditions to ensure that the softer altered schist was completely removed where exposed below the foundation bearing level to provide bearing support consistent with the design recommendations.



Figure 19 – Line Drilling to Excavate Granite Intrusion (top) and Contact Zone between Granite and Altered Schist (bottom)

Fortunately, the test borings provided a good representation of the exposed conditions, and the excavation of the altered schist was not extensive. The geometry of the cofferdam and adjacent roadway may have prevented significantly deeper excavation. In the absence of the supplemental test borings, it would have been very difficult to develop an appropriate foundation bearing elevation.

The orientation of the contact between granite and altered schist exposed in the foundation excavation is consistent with contacts exposed along the riverbank, and with the contact that forms the roof (granite) and base (moderately hard schist) of the cave where the buttress was constructed.

The roadway construction required blasting to the south of the realigned Route 9, south of the river. The completed rock slope also shows a contact between schist below, and granite above, and again, a variably altered schist layer is present near the contact, as shown in **Figure 20**. We observed seepage of water from the altered schist during a site visit in August 2015, despite a fairly dry period before. The sequence shown in **Figure 20** is indicative of another granite intrusion above the schist well above the Durham abutment area.



Figure 20 – Granite Intrusion over Altered Schist in Roadway Cut

CONCLUSIONS

The scope of the Route 125 bridge and Route 9 highway projects appears to be conventional: spread footings bearing on rock and roadway realignment. However, existing geologic conditions had significant, localized impacts on the design and construction considerations for both elements of the project.

An initial phase of subsurface explorations was conducted that would have been suitable for complete design of many similar projects, including several test borings with rock coring, borehole and surficial geophysical testing, and field bedrock mapping. However, through initial investigation of exposed and subsurface conditions and preliminary development of design parameters and details, it became evident that more thorough investigation was needed to reduce the risk and potential surprises associated with variable subsurface conditions and to provide a safe and constructible design. MaineDOT and the design team could see the importance of completing additional test borings, rock probes, borehole and surface geophysical testing, field bedrock mapping and test pits to improve our understanding of the conditions that influenced the design. The time and cost to provide a more thorough understanding of the subsurface conditions was judged by the design team to provide value to the project.

The specific sequence of metamorphism and igneous intrusion locally impacted a fairly competent schist deposit and created seams of uncharacteristically soft rock which in turn impacted bridge foundation designs. Design solutions were evaluated and detailed to mitigate these difficult geologic conditions for both portions of the project, while providing a combination of simplicity, cost effectiveness, and constructability.

FUTURE WORK

The pier foundation stabilization/construction and highway slope excavation and reconstruction remain to be completed in late 2015 through mid-2016. GZA will provide on-site observation during both phases of the work to evaluate the existing conditions and construction with respect to the design and to provide construction recommendations to address challenges that arise.

REFERENCES

1. Berry, Henry N., IV and Hussey, Arthur M, II , 1998, *Bedrock geology of the Portland 1:100,000 quadrangle, Maine and New Hampshire (PDF 19.5Mb)*: Maine Geological Survey, Open-File Map 98-1, color map, scale 1:100,000.
2. Hoek, E., Bray, J., *Rock Slope Engineering, Revised Third Edition*, Spon Press, New York, NY, 1981.
3. Weddle, T. K., *Surficial Geology, Lisbon Falls South Quadrangle*, Maine Geological Survey, Open File No. 97-49, 1997.

**Slope Stabilization and Scour Protection Using Small Diameter Reticulated
Micropiles Along Minisceongo Creek**

Nathan Beard, P.E.
GeoStabilization International
P.O. Box 4709
Grand Junction, CO 81502
(855) 579-0536
Nate@gsi.us

Prepared for the 66th Highway Geology Symposium, September, 2015

Acknowledgements

The author would like to thank the individuals/entities for their contributions in the work described:

Michael DiValentino – OCS Industries
Dr. Albert Molinas, P.E. – Hydrau-Tech, Inc.
William Metzger – NRG Bowline, LLC
County of Rockland Drainage Agency

Disclaimer

Statements and views presented in this paper are strictly those of the author(s), and do not necessarily reflect positions held by their affiliations, the Highway Geology Symposium (HGS), or others acknowledged above. The mention of trade names for commercial products does not imply the approval or endorsement by HGS.

Copyright Notice

Copyright © 2010 Highway Geology Symposium (HGS)

All Rights Reserved. Printed in the United States of America. No part of this publication may be reproduced or copied in any form or by any means – graphic, electronic, or mechanical, including photocopying, taping, or information storage and retrieval systems – without prior written permission of the HGS. This excludes the original author(s).

ABSTRACT

Minisceongo Creek is a tributary to the Hudson River and located in Rockland County, New York. In recent years a significant amount of scour has occurred along a nearly 1,000 linear foot stretch of the stream situated in glacial till; coincidentally this project is located in the area where subsurface utilities cross the creek. In 2011 and 2012 Tropical Storm Irene and Hurricane Sandy made landfall in New York and New Jersey, dropping massive amounts of rainfall in Rockland County. The Minisceongo Creek experienced record flows, causing severe embankment erosion.

The 85 foot tall embankments located along the south banks were primarily sandy gravel overlying large gravel boulder till of the riverbed. The storm events resulted in approximately 60 feet of horizontal erosion into the hillside, leaving unstable embankment slopes with grades around 2V:1H and exposed the underground utilities below and crossing the creek bed. Private property and residential dwelling units located along the top of the embankment were encroached upon and the electrical conduits and natural gas pipelines were exposed and unsupported for distances up to 140 feet.

To address the protection of the subsurface utilities, a large concrete buttress in combination with grouted riprap was installed. That buttress did not address the long-term stability of the adjacent embankments, future scour, or stability of associated areas above the river. A second system was later installed that included a combination of soil nail walls, reticulated scour-resistant micropiles, and a Shored Geosynthetically Confined Soil (SGCS) wall.

INTRODUCTION

Minisceongo Creek is a small stream with a drainage basin of approximately 17 square miles. It runs through West Haverstraw, New York, to its union with the Hudson River, located just south of the 1,200 MW Bowline Generating Station (Bowline). On the morning of August 28, 2011, Tropical Storm Irene made landfall in New York, dropping considerable amounts of rainfall within the Minisceongo Creek drainage basin and producing record flows. These flows caused significant amounts of scour along a nearly 1,000 linear foot stretch of the stream situated in glacial till. Coincidentally, this scour also occurred in the area where subsurface utilities cross the creek. This utility crossing consists of a 16-inch diameter gas line; a 24-inch diameter gas line; two 10-inch diameter, oil cooled, 345kV power conduits; and, two 5-inch diameter dielectric fluid recirculation conduits. The utility crossing is also located in a residential area and surrounded by houses, businesses, and several local roads.



Figure 1 – Vicinity Map (Google Earth 2010)

The south embankment was as tall as 85 feet and consisted primarily sandy gravel overlying the large gravel boulder till of the riverbed. The storm events resulted in significant erosion into the hillside, leaving unstable embankment slopes with grades around 2V:1H and exposed the underground utilities crossing the creek. Private property and residential dwelling

units located along the top of the embankment were encroached upon and the electrical conduits and natural gas pipelines were exposed and unsupported for distances up to 140 feet.

A subsurface investigation was completed to determine the engineering properties of the soil to complete stability analysis to design the stabilization system to protect the utilities. The investigation included borings, inclinometers, and piezometers. The first phase of design and construction was to stabilize the stream crossing within the limits of the Orange & Rockland Utilities Right of Way. This phase included a concrete buttress founded on micropiles along the south embankment and grouted riprap on both sides of the creek for a length of approximately 300 feet.



Figure 2 – Phase 1 Utility Crossing Stabilization



Figure 3 – Phase 1 Concrete Buttress at South Embankment

At about 8 p.m. on Monday, October 29, 2012, approximately 14 months after Tropical Storm Irene and just months after the completion of Phase 1, Hurricane Sandy made landfall along the New Jersey shore. Storm surge, heavy rain, and high winds began causing significant damage to the entire region many hours before Sandy made landfall. Sandy left Rockland County with more than two times the power outages of Irene and a similar increase in the amount of damage caused. Damage included severe scour along Minisceongo Creek on both ends of the work completed during Phase 1. The south embankment downstream of the concrete buttress scoured 60 feet into the slope for a length of 337 feet, coming within feet of undermining the private property above. The south embankment upstream of the concrete buttress scoured for a length of 140 feet with near vertical slopes heights greater than 40 feet.

The near vertical slopes were temporarily protected by vegetation at the crest of the slope. The root masses temporarily confined the soil, allowing the slope to stand at a near-vertical angle in many locations. As the material eroded, the vegetation and roots became exposed and the trees and shrubs inevitably fell causing more of the slope to slough.



Figure 4 – South Embankment Downstream



Figure 5 – South Embankment Upstream

Phase II

Phase II was competitively bid as a design-build project and awarded to Team Olori Construction Services Industries Inc. and GeoStabilization International (GSI). The solution selected was a best-value design-build-warranty solution that included the use of multiple rows of horizontal soil nails and reinforced shotcrete to stabilize the failing slopes and prevent further sloughing of the embankment. Due to the significant distance between the stream and the slope caused by the scour, GSI incorporated a Geosynthetically Confined Soil (GCS®) wall to fill this area to realign the embankment, provide a hydraulically improved typical section to minimize head losses or backwater impacts, prevent additional cutting of the embankment, and buttress the slope to provide the desired global stability. Backfill for the GCS wall was specified as a 0.5”-1.5” angular crushed stone with no fines. This allowed for high water flows to infiltrate and exit (free-draining) the system without disturbing the backfill or integrity of the system. Additionally, federally funded research shows that GCS structures, also referred to as Geosynthetically Reinforced Soil (GRS), are internally stable and can have bearing capacities and safety factors more than 10 times those of Mechanically Stabilized Earth walls. NCHRP-funded full scale shake table testing also demonstrated that GCS walls and abutments can also withstand extreme seismic loading.

GSI worked directly with Dr. Albert Molinas from Hydrau-Tech, Inc. to evaluate the scour potential to provide adequate countermeasures. Using topographic information, geotechnical information for sediment size, hydrology, and design layout, the hydraulic parameters and resulting contraction and abutment scour were computed for the 100-year design discharge along the design. The peak discharges for Minisceongo Creek are provided in Table 1. The 25-year flood peak discharge is 3,750 cfs and the 100-year peak flood discharge is 5,530 cfs.

Flooding Source	2-Year (cfs)	25-Year (cfs)	100-Year (cfs)
Minisceongo Creek above Route 9W	1,905	3,750	5,530

The installation of the concrete buttress during Phase 1 created an isolated section of stream with a narrower channel. This resulted in contraction scour due to the velocity, depth, and area for flow obstructed by the concrete buttress. The results of the scour analysis noted the following:

- Along the existing grouted riprap upstream and downstream from the existing concrete buttress, the scour protection consisted of 4-foot deep toe walls. These toe walls are subject to head-cutting resulting from the contracted segment of the channel immediately downstream and projected scour resulting from the contracted segment of the channel immediately upstream. The scour computations indicate that each type of scour would be limited to approximately 3 feet, meaning that the toe walls are therefore safe from potential scour.
- Along the GCS wall at the upstream entrance region, scour at the nose segment may be analyzed using abutment scour analogy. At this entrance location to the GCS wall, the flow depth is approximately 5 ft. According to Federal Highway Administration's HEC-23 Manual, an accepted scour countermeasure for abutment scour is a riprap layer and the width of the riprap protection should be 2 times the flow depth. The riprap protection alone at this location is sufficient to protect the GCS wall. The presence of 19-ft long micropiles provides additional scour protection, well beyond the FHWA suggested scour countermeasure.
- Along the GCS wall at the downstream end of the GCS wall segment, the channel is contracted. At this point, the maximum computed potential scour is 3 feet. According to Federal Highway Administration's HEC-23 Manual, an accepted scour countermeasure for contraction scour is a riprap layer. The width of the riprap protection should be 2 times the flow depth. The riprap protection alone at this location is sufficient to protect the GCS wall since it is thicker than the computed contraction scour. The presence of 19-ft long micropiles provides additional scour protection, well beyond the FHWA suggested scour countermeasure and ensures additional protection in the transition from the abutment scour region to contracted flow region.

To protect the system against long-term undercutting, 20-foot long scour-resistant micropiles and grouted riprap were included along the base of the soil nail and GCS walls to prevent scour and provide lateral resistance, improving the overall global factor of safety (FS). Furthermore, the bank stabilization design provided additional scour protection along its entire length due to the fact that all elements would be inter-connected to form a continuous embankment with minimal disturbance to oncoming flows.

In-situ soil properties were determined using a back analysis using limit equilibrium software program (Rocscience Slide v6.0). In a back analysis process, parameters are determined by conservatively assuming that the existing ratios between resisting and driving forces are at equilibrium. This is estimated by having the modeled FS calculated to be at or below a 1.0. From

this analysis the slope material, which is comprised mainly of silty sand with gravel with a unit weight of 120 lbs/ft³, were specified Mohr-Coulomb strength parameters with cohesion of 280 psf and internal angle of friction (ϕ) of 37 degrees.

The permanent soil nail stabilization system for the project was determined based on remediation methods applied to the back analysis models previously discussed. This system was designed to meet or exceed the following factors of safety:

- Global Stability (long-term): 1.5 static, 1.1 rapid drawdown
- Soil Nail Pullout Resistance: 2.0 static, 1.5 rapid drawdown
- Nail Bar Tensile Strength: 1.8 static, 1.35 rapid drawdown
- Facing Flexure: 1.5 static
- Facing Punching Shear: 1.5 static

Soil nails specified for the stabilization system were number 8, Grade 75, epoxy coated, all-thread rebar with a minimum yield strength of 59.3 kips and 38 mm B7X Geo-Drill Injection Anchor with a minimum yield strength of 90.7 kips. Micropiles consisted of 51 mm B7X Geo-Drill Injection Anchor with a minimum yield strength of 152 kips.

Number 8, Grade 75 bar was used for the modeling due to its lower yield strength. The tensile capacity of the soil nails used within the model was 32,944 lbs. The soil nail pullout design strength was 6 psi (ultimate strength of 12 psi). This was verified in the field during soil nail verification testing. The pullout input used within the model was 904 lbs/ft (based on a 4 inch diameter drill hole). The maximum nail loading experienced in any of the modes was 2,862 lbs/LF of repair system. The nails were spaced at 6-feet on center and therefore the design facing load (T_{\max_s}) of 17,172 lbs.

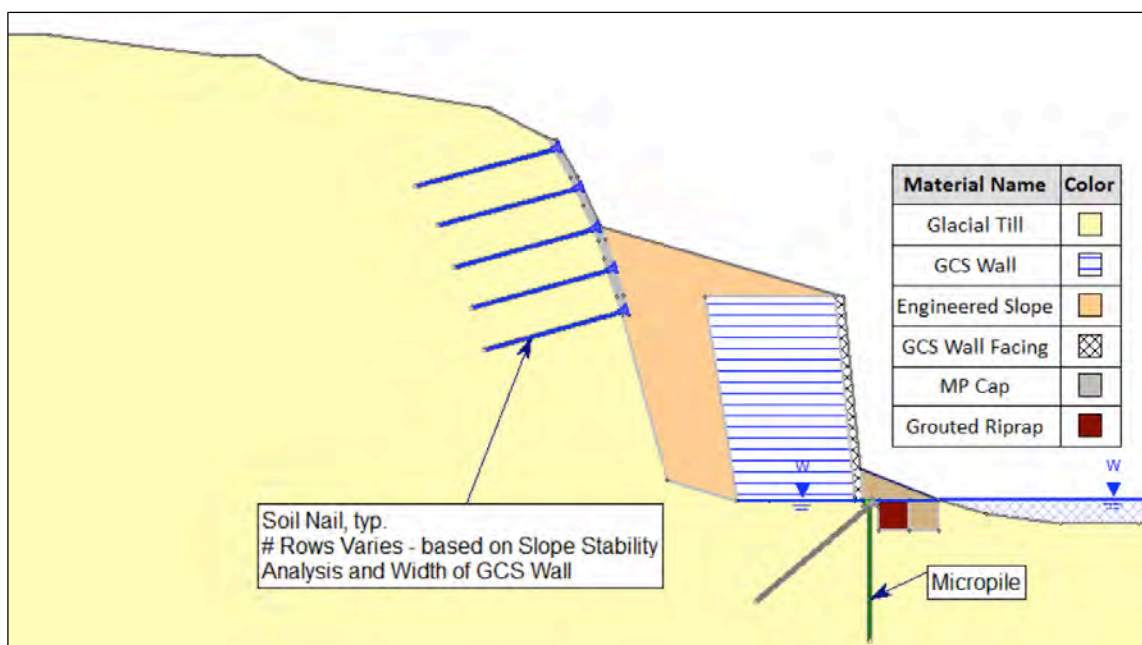


Figure 6 – Typical Downstream Cross-Section



Figure 7 – Downstream Stabilization

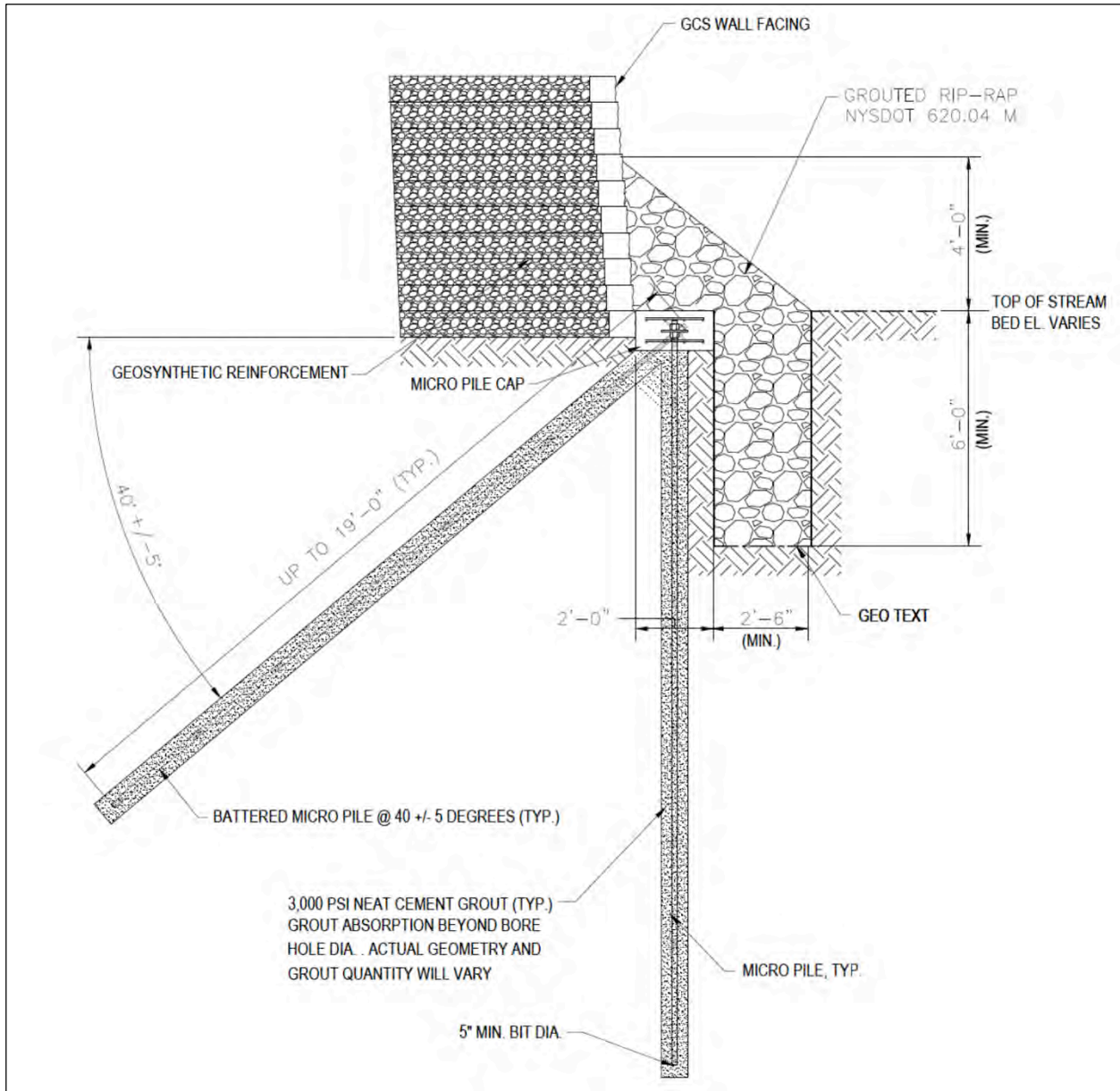


Figure 8 – Scour Resistant Micropile Cross-Section

Micropiles were installed within the system to resist scour and increase lateral capacity of the system. The micropiles were spaced every 18 inches along the base of the system for the entire length. Every third micropile was battered as shown in Figure 8 to resist buckling that may result from the GCS surcharge load in the event that scour occurs at a depth greater than four feet. The micropiles were pinned at the top and the tight spacing provided a subsurface “grout curtain” at depths of up to 19 feet.

All limit-equilibrium modeling included a storm event water elevation increase of 15 feet followed by a rapid drawdown event. Due to the permeability of the GCS wall and the weight of the system there was only minimal decrease in overall FS (>0.01).

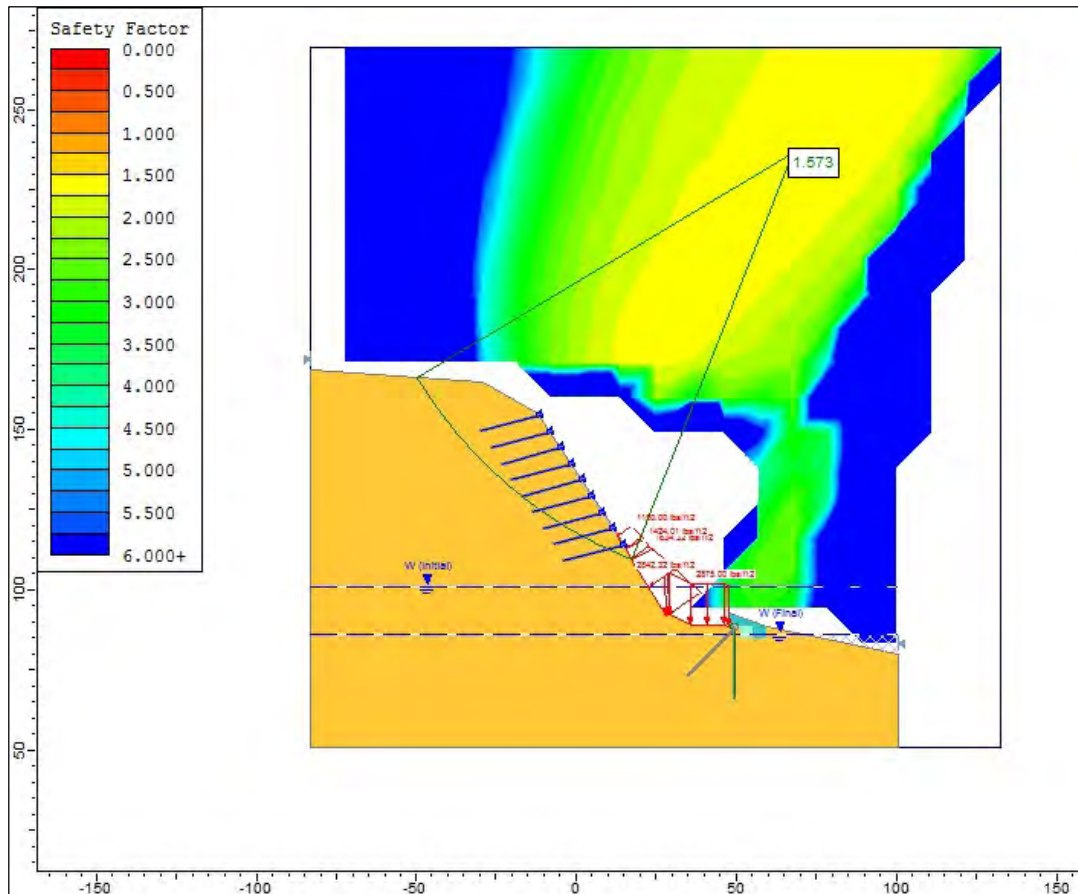


Figure 9 – Rapid Drawdown Modeling

In addition to scour and rapid drawdown, there was a concern that flood debris such as boulders and trees would impact the GCS wall system at high velocities. However, GCS walls have been built around the world as rockfall barriers. GCS rockfall barriers employed by the Colorado Department of Transportation in Debeque Canyon, Colorado have withstood impacts as large as 10,000,000 ft-lbs with only minor damage. Although the chance of minor block damage could not be discounted, that damage would not compromise the system performance and could be easily replaced with new blocks and/or reinforced shotcrete, as was demonstrated in the Debeque Canyon event.

The final project included over 18,000 linear feet of soil nailing which was completed with both track mounted and crane basket mounted drills, 17,800 SF of shotcrete, and over 5,000 SF of GCS wall. The project was completed in less than four months and on budget.



Figure 10 – Completed Project Upstream Section



Figure 11 – Completed Project GCS Wall

REFERENCES:

- Federal Government Reports
 1. Wu, J. and Ooi, P. *Synthesis of Geosynthetic Reinforced Soil (GRS) Design Topics*. Report FHWA-HRT-14-094. FHWA, U.S. Department of Transportation, 2015
 2. Lazarte, C., Elias, V., Espinoza, D., Sabatini, P. *Geotechnical Engineering Circular No. 7*. FHWA0-IF-03-017. FHWA, U.S. Department of Transportation, 2003
 3. Samtani, N. and Nowatzki, E. *Hollow-Core Soil Nails State-of-the-Practice. Report Unassigned*. FHWA, U.S. Department of Transportation, 2006

US-12, Greer to Kamiah, Idaho, Rock Slope Assessment and Design

William C. B. Gates, PhD, PE, PG
McMillen Jacobs Associates
1109 1st Ave., Suite 501
Seattle, WA 98101-2988
206-496-4829
gates@mcmjac.com

Brian Bannan, PG
Idaho Transportation Department, District 2
P.O. Box 837
Lewiston, ID 83501
208-799-5090
brian.bannan@itd.idaho.gov

Prepared for the 66th Annual Highway Geology Symposium, September 14-17, 2015

Disclaimer

Statements and views presented in this paper are strictly those of the author(s), and do not necessarily reflect positions held by their affiliations, the Highway Geology Symposium (HGS), or others acknowledged above. The mention of trade names for commercial products does not imply the approval or endorsement by HGS.

Copyright Notice

Copyright © 2015 Highway Geology Symposium (HGS)

All Rights Reserved. Printed in the United States of America. No part of this publication may be reproduced or copied in any form or by any means – graphic, electronic, or mechanical, including photocopying, taping, or information storage and retrieval systems – without prior written permission of the HGS. This excludes the original author(s).

ABSTRACT

US-12 enters Idaho at Lewiston, Idaho crossing the Snake River from Clarkston, Washington; and climbs along the original Lewis and Clark trail next to the Clearwater River past Orofino and upwards to Lolo Pass at the Montana border, approximately 170 miles in length. From Greer to Kamiah, US-12 snakes between high granitic cliffs and the river creating dangerous blind corners and obscuring potential rockfall debris in the highway. Between approximate MP-52 and MP-58, Idaho Transportation Department (ITD), District 2 has been reviewing concepts to widen the road, reduce the blind corners around the major rock slopes with the highest potential for rockfall, and avoid soil slopes which would require retaining walls. The project was divided into two Phases. Phase 1 includes four slopes with the highest kinematic potential for rockfall between MP-52 and MP-54 which range in length from about 100 to 1900 feet and are upwards to 200 feet high. During the fall of 2014, the authors using limited rope access rock climbing techniques mapped and characterized the geology of the rock slopes; and followed up with analysis of the kinematic stability and provided recommendations for design cuts. Recommendations included regrading and flattening of the rock slopes to eliminate rockfall problems and or installation of rock bolts on unstable blocks where grading was not practical or there was right of way (ROW) problem. Challenges affecting the constructability of the project include: pioneering access roads to the top of the proposed cutslopes, presplit drilling of thin sliver cuts on the steep rock faces, control of fly rock, blast vibrations and over pressure at the river's edge because of the prime fish habitat. In Phase I, the four rock slopes are presently in design review. Phase II includes at least 13 slopes exhibiting similar rock slope problems.

INTRODUCTION

Idaho Transportation Department (ITD) divides the State of Idaho into six districts to service the State's transportation system. US-12 transits District 2 diagonally from the west where the highway enters Idaho at Lewiston, crossing the Snake River from Clarkston, Washington climbing next to the Clearwater River past Orofino and upwards east to Lolo Pass at the Montana border, approximately 170 miles in length (Figure 1 and 2). The highway follows the original Lewis and Clark trail (Figure 3) from Lolo Pass to the junction of the Snake and Clearwater Rivers. From Greer to Kamiah, US-12 snakes between high granitic cliffs and the river creating dangerous blind corners (Figure 4). Most slopes have been stable and produced little rockfall since construction except for the rockslides that have occurred at MP-54 (Figure 5). Because of the limited space, rock catchment ditches are typically inadequate to arrest rockfall (Figure 6).

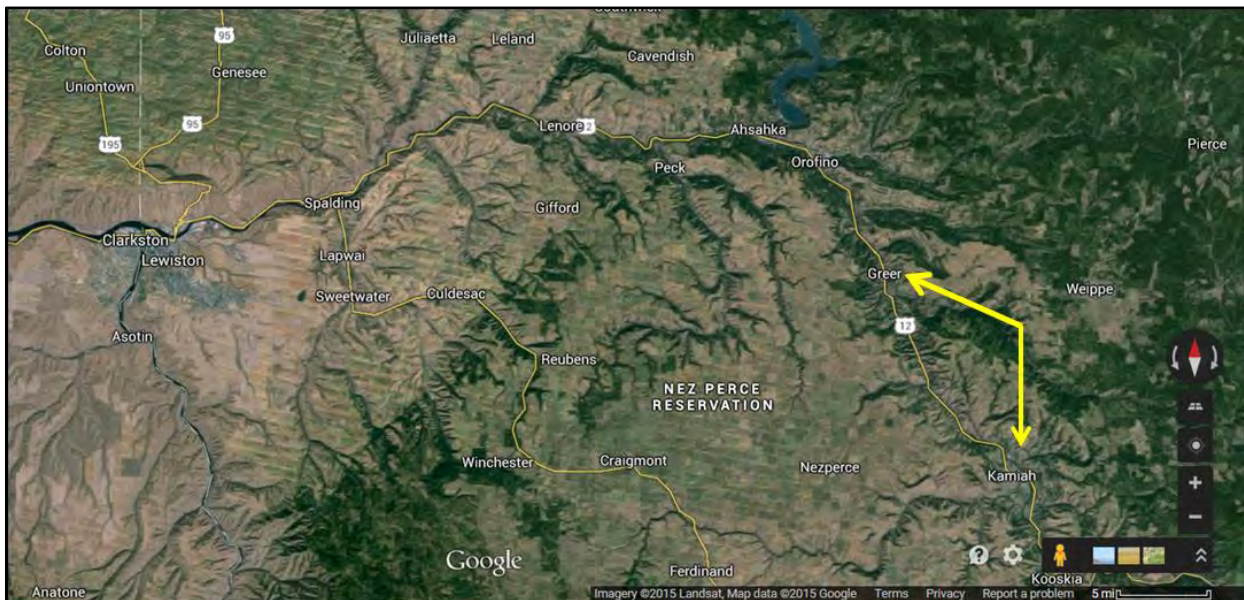


Figure 1: Project site map. The project is between Greer and Kamiah on US-12.

Between approximate MP-52 and MP-58, ITD, District 2 has been reviewing concepts to widen the road and reduce the blind corners around the major rock slopes with the highest kinematic potential for rockfall. The goal is to widen the road and reduce the blind corners. In addition as part of the design, ITD is avoiding the soil slopes and the need for retaining walls. The project was divided into two Phases. Phase 1 includes four rock slopes between MP-52 and MP-54 that exhibit higher kinematic potential for rockfall including a large rockslide scarp at MP-54.1. Figure 2 is a map of the project site showing the locations of the rock cut slopes. Phase II was broken down into 13 rock slope windows which appear to have the highest

kinematic potential for rockfall. The rock slopes range from about 75 feet long to several thousand feet in length and over 200 feet high. The work is ongoing. Phase I is in design review awaiting final design construction. Phase II: the authors are preparing to conduct a geologic reconnaissance and mapping July 2015.

ENGINEERING GEOLOGY

Regional Geology

The regional geology was mapped by Lewis and others (Lewis, et al, 2006). The Clearwater River has cut a deep canyon exposing granitic rocks that are characterized as Cretaceous medium grained biotite-muscovite Trondhjemite. Rocks are typically strong to very strong and massive.

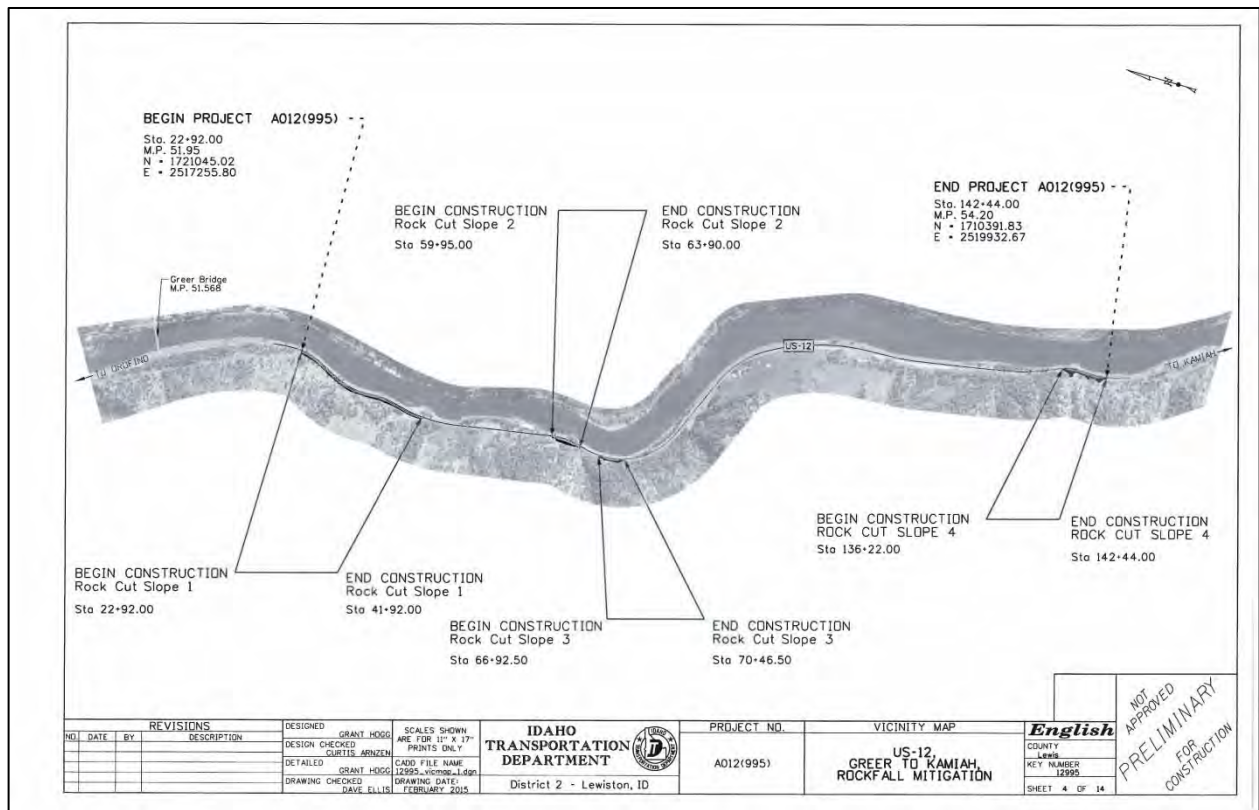


Figure 2: Preliminary construction map displaying locations of rock cut slopes 1 through 4.



Figure 3: US-12 follows the original Lewis and Clark Trail along the Clearwater River in Idaho.



Figure 4: Left photo; typical blind corners with inadequate site distance near MP-56. Right photo; displays inadequate rockfall catchment ditch problems near MP-54.

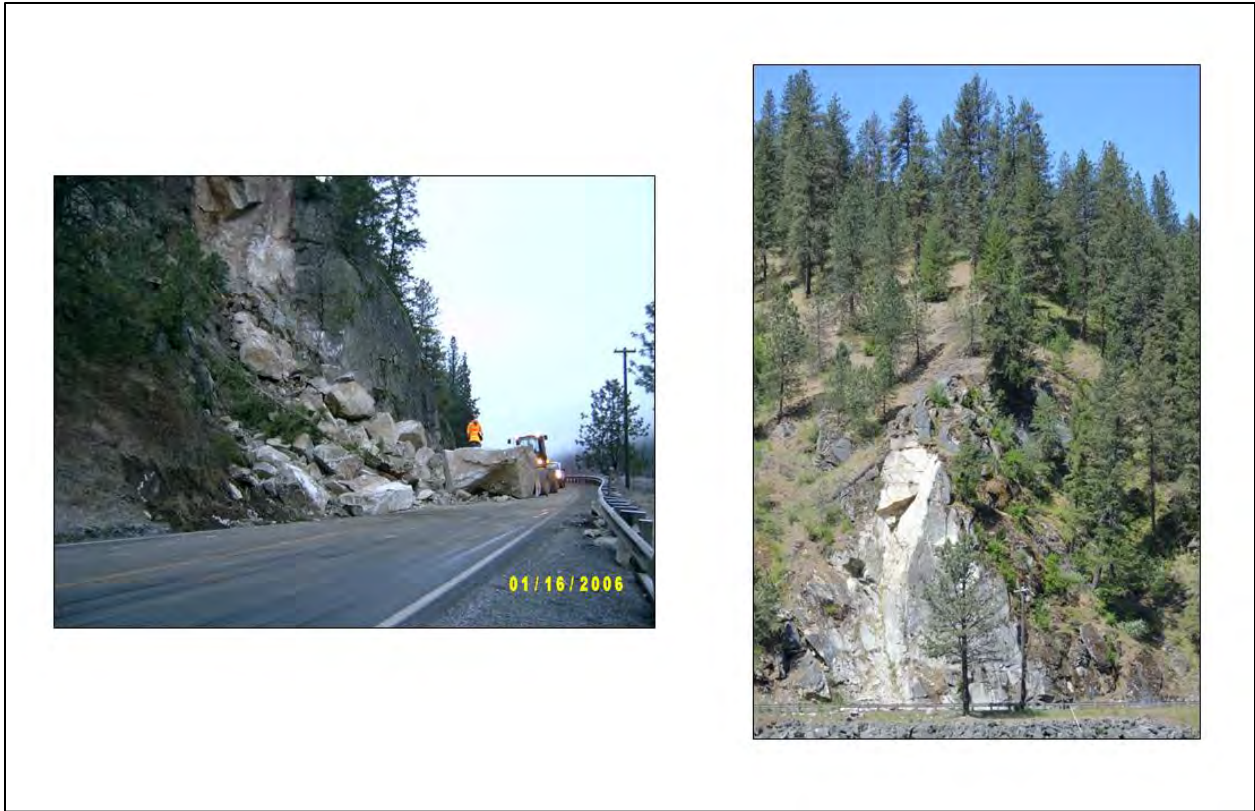


Figure 5: Rockfall problem area near MP-54, rock cut 4. Rock slope failed by wedge sliding on January 16, 2006.

Field Mapping Phase I Rock Cut Slopes 1-4

The rock cut slopes were subdivided into four manageable windows for geologic characterization. A window was typically length of the slope or 50 feet wide by the height of the rock cut. To characterize the geology, the teams conducted horizontal scan lines along the toe of the slope (Figure 7). In addition, vertical scanlines were completed using rappelling limited rope access techniques (Figure 7). Rock mass characteristics (RMRs, Bieniawski, 1989), geologic strength index (GSI) by Hoek and Brown (1997) and attitudes of the discontinuities were collected at each rock window sufficient to characterize the rock mass, assess the rock cut stability and develop reinforcement contingencies, including:

- Intact rock strength by geologic hammer method (ISRM, 1989);
- RQD (Palmström method, 1982);
- Spacing and characteristics of the discontinuities;
- Dip and dip direction of the discontinuities ;
- Rock mass characteristics, and;
- Friction angle estimated by tilt tests in the field.



Figure 6: Rockfall catchment zones typically are inadequate (less 90% catchment) to arrest the rockfall. Note blind corners.

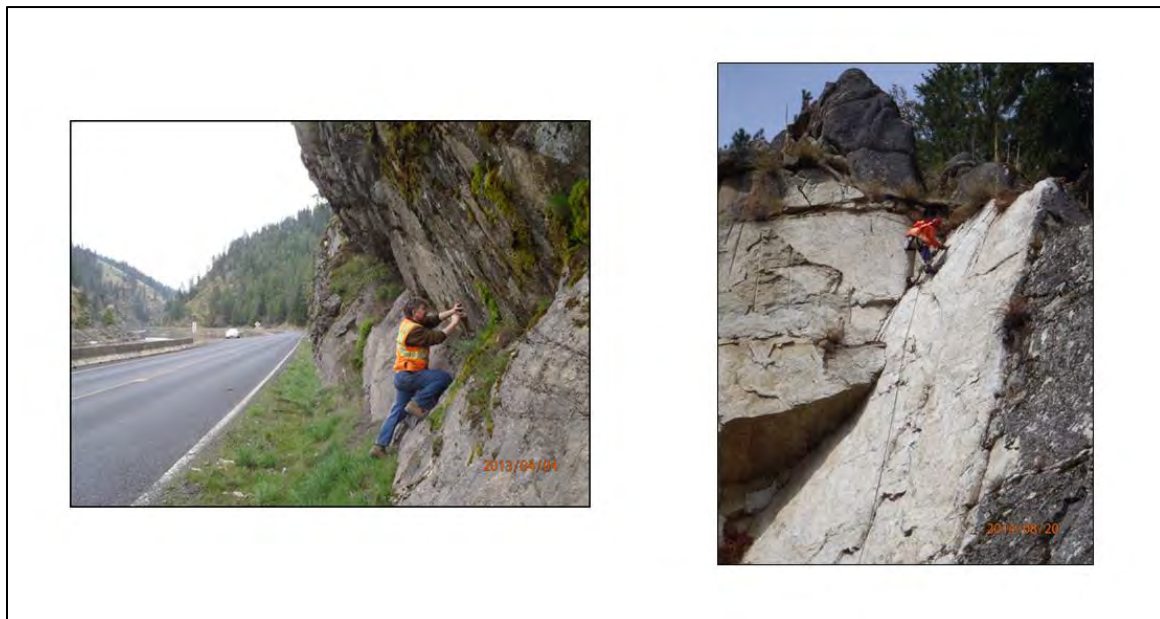


Figure 7: Horizontal and vertical scan line mapping.

Rock Slope History

Typically the structure of the granites cropping out along the highway are massive to blocky with spacing ranging from 1.5 to 5 feet between discontinuities. Based on hammer blows, the rocks are typically strong (R4) to very strong (R5) (3,600 psi to 14,500 psi). Between rock outcrops, the granite observed just beneath the soil has in some areas weathered to loose and/or weak, poorly cemented sandy decomposed granite (DG) forming unstable colluvium.

As built records of the highway show the cut slopes were constructed in 1935. The rock cut slopes appear to have been excavated using production blasting methods. The cuts were generally stable with little rockfall reported with the exception of Slope 4 at MP 54.1 (Figures 4 and 5). Wedge failures produced rock slides in 2006 and 2008. In 2008, a portion of an unsupported upper wedge block was removed by trim blasting.

Rock Slope Analysis

Once station limits were established for the four sections (Figure 2), the rock mass was characterized along horizontal and vertical scan lines and discontinuities (fractures, joints, beds, etc.) were measured. Over 300 discontinuity measurements were used in the kinematic analysis to identify potential planar, wedge and toppling failures. Measurements were limited to existing cut slopes within the four areas.

For each rock slope, we analyzed the kinematic stability facilitated with the Dips V.6 by RocScience. Where potential kinematic failures were identified, deterministic stability analysis using RocPlane, Swedge and RocTopple by RocScience was used to estimate factors of safety. Input parameters used in stability analysis were based on the rock mass properties observed in the field. We selected a cohesive strength of 1000 psf along the joint planes. The cohesive strength coincides with the friction strength of 36 degrees (Wyllie and Mah, 2004) that we observed in the field.

Based on the discussion above, for the analysis of each Rock Cut Slopes 1, 2, 3 and 4, we assumed the following:

- Unit weight of granitic rock is about 165 pcf;
- Friction on the planes was about 36 degrees, based on tilt tests and field observation;
- Cohesion (c);
 - Stable conditions, $FS > 1.3$, $c \approx 1000$ psf
 - Marginally stable to unstable conditions, $FS < 1.3$, $c \approx 0$ psf

Even though some of the slopes did not require reinforcement, during the assessment we evaluated key blocks on the slopes as marginally stable using RocPlane and Swedge assuming a cohesive strength on the failure planes of near or at zero. Based on the results, we developed reinforcement contingencies for planning purposes during construction and we assumed they may change based on field conditions.

Findings and Discussion

General

Between areas of strong competent granitic rock we observed areas where the rock has weathered to weak DG with its relict structure. The DG has further weathered into coarse gravelly sandy soil and colluvial deposits. These are areas of potential instability and sliding. One of ITD's goals is to avoid these areas and thus avoid the need of designing and constructing costly retaining walls.

There is little to no rockfall from most of the rock slopes and most the slopes have stabilized since the original construction of the highway (Figure 8). In all areas, we noted some mode of potential kinematic instability to include minor rockfall and raveling, planar sliding, wedge sliding and toppling (flexural and direct). Interestingly, each rock cut slope area exhibited a unique primary mode of potential instability or failure mechanism based on our field observation and the results of our kinematic analysis. The following is a summary for each rock cut slope.



Figure 8: Most of the cut slopes have been stable with some raveling and minor rockfall since the slopes were constructed in 1935.

Rock Cut Slope 1

Rock Cut Slope 1 (Figure 9) starts at MP-52.0 and stretches for about 2200 feet. Height of the rock cut face ranges upward to about 55 feet. At the top of the rock cut, the back slope rises for several hundred feet at about 36 degrees and mirrors the primary discontinuities dipping out of slope. Ditch width is about 11 feet and theoretically will retain 75% or more of the rockfall based on a 55 foot high, 0.25H: 1V slope (Pierson, et al, 2001). This is not an active rockfall area. Based on our field observation and kinematic analysis, the blocks may potentially fail by planar sliding into the highway, however, the rock slope appeared stable kinematically and key blocks exhibited a factor of safety around 2.57. Even though the faces of the slopes overhang in places, toppling was not an issue, because the bases of the blocks are wider than their height. Based on our analysis and observation, regrading to a flatter slope would not improve the factor of safety and patterned bolts would not be required. Recommendations to ITD included: trim blast the face of the slope to 0.25H: 1V, plan for a contingency of 200 LF of 25 kip rock bolts during construction should conditions change.

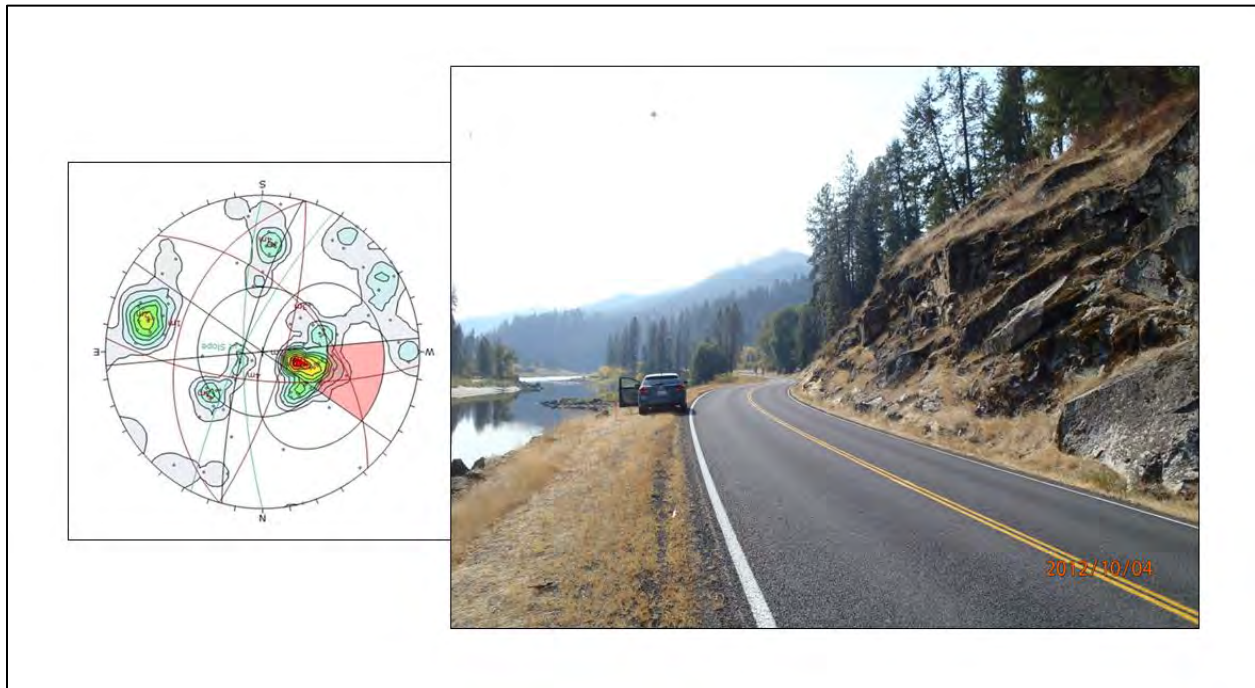


Figure 9: Rock cut slope 1, potential mode of failure is planar, sliding east into the road. Stereonet is oriented parallel to the cut slope face. North is to the bottom of the photo. Note toppling is kinematically possible but the geometry of the blocks did not support toppling.

Rock Cut Slope 2

Rock Cut Slope 2 (Figure 10) forms a blind corner near MP-52.7. The slope is about 400 feet long and over 200 feet high. Ditch width is about 11 feet and theoretically will retain 50% of the rockfall based on an 80 foot high, 0.25H: 1V slope (Pierson, et al, 2001). The back of the slope is bounded by a county road. Planar and wedge sliding are primary modes of failure in this area as displayed in the stereonet. However the wedges appear to have steep subvertical limbs and the blocks will probably fail primarily by planar sliding. Toppling was not a kinematic issue. Grading the slope to 0.75H: 1V will remove the critical failure planes. However, regrading would require additional right-of-way to include possible modification of the county road above the brow of the slope. Whereas steeping the slope to 0.25H: 1V requires rock bolts and there are no right-of-way issues. Recommendations to ITD included: stabilize slope by regrading and trim blasting to 0.25H: 1V and install 720 LF of 25 kip patterned rock bolts.

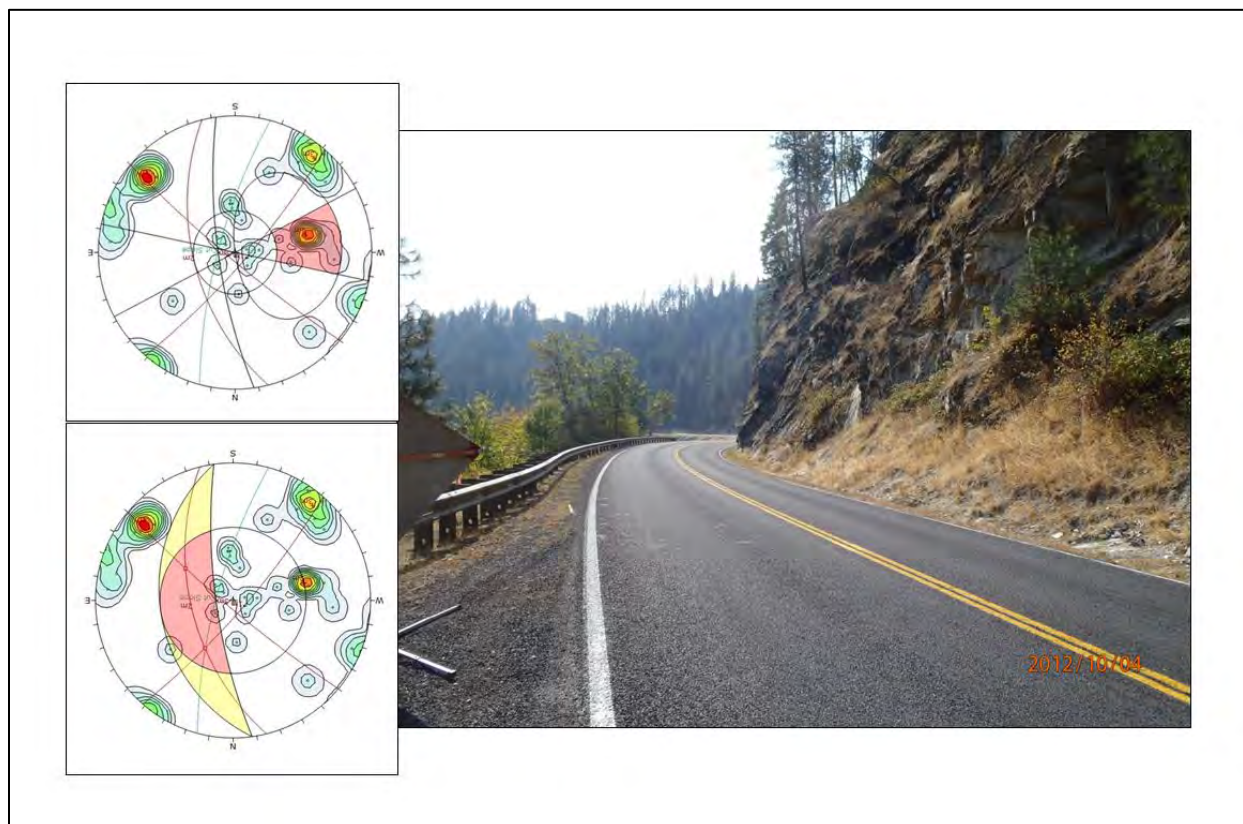


Figure 10: Rock cut slope 2, primary modes of failure may include planar and wedge sliding to the east into the road. Note the blind corner. The stereonet are oriented parallel to the cut slope face. North is to the bottom of the photo. Note potential for planar sliding in top stereonet. In the lower stereonet, two major wedges daylight the critical zone and are potentially kinematically unstable.

Rock Cut Slope 3

Rock Cut Slope 3 (Figure 11) is near MP-52.8 and is about 125 feet long and the rock face is over 30 feet high. Ditch width is about 11 feet and theoretically will retain 95% of the rockfall based on a 30 foot high, 0.25H: 1V slope (Pierson, et al, 2001). At this location, kinematic analysis indicates that toppling is the potential mode of failure. The probability for planar and wedge sliding appeared low based on the kinematic analysis. Regrading to a flatter slope will not improve the stability for this slope. Recommendations to ITD included: trim blast slope to 0.25H: 1V, plan for a contingency of 150 LF of 25 kip rock bolts during construction should conditions change or merit it.

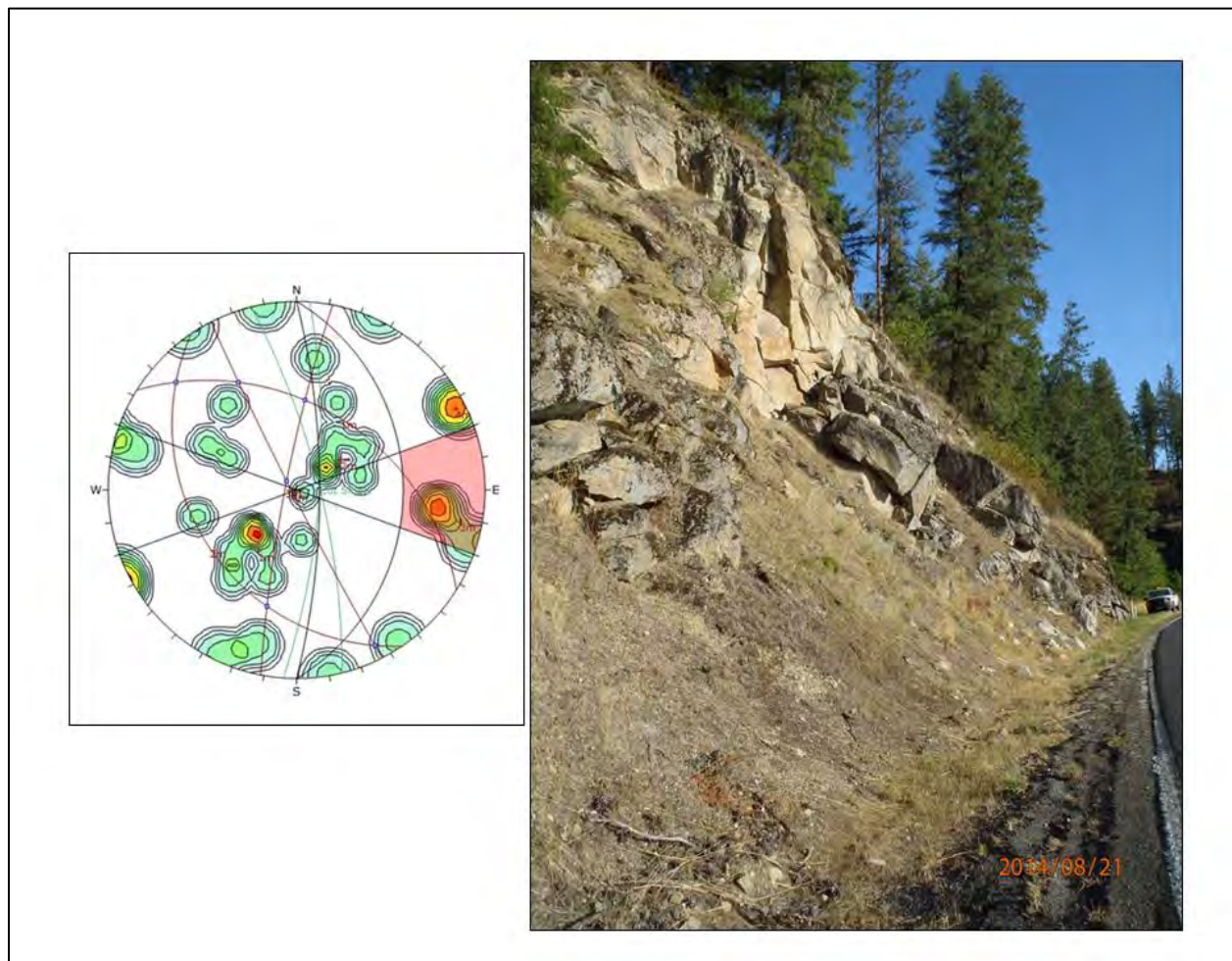


Figure 11: Rock cut slope 3, potential mode of failure is toppling to the east into the road. Stereonet is oriented parallel to the cut slope face. North is to the top of the photo. Note blocks at toe of slope that have failed by apparent toppling.

Rock Cut Slope 4

Rock Cut Slope 4 (Figure 12) is around MP-54.1. The slope is about 1125 feet long and about 75 feet high. Ditch width is about 11 feet and theoretically will retain 55% of the rockfall based on a 75 foot high, 0.5H: 1V slope (Pierson, et al, 2001). This area has a history of rockfall and rockslides as wedge failures (Figures 4 and 5). The kinematic analysis demonstrated that wedge sliding will occur for slopes steeper than 0.5H: 1V when the cohesive strength on both joint planes dropped to zero. Based on the kinematic analysis, the probability for planar sliding and toppling is low. Grading the slope to 0.5H: 1V will remove the wedge shaped blocks and improve the stability of the slope. Recommendations to ITD included: stabilize slope by regrading and trim blasting to lay slope back to 0.5H: 1V. Install 225 LF of patterned 25 kip rock bolts on selected blocks.

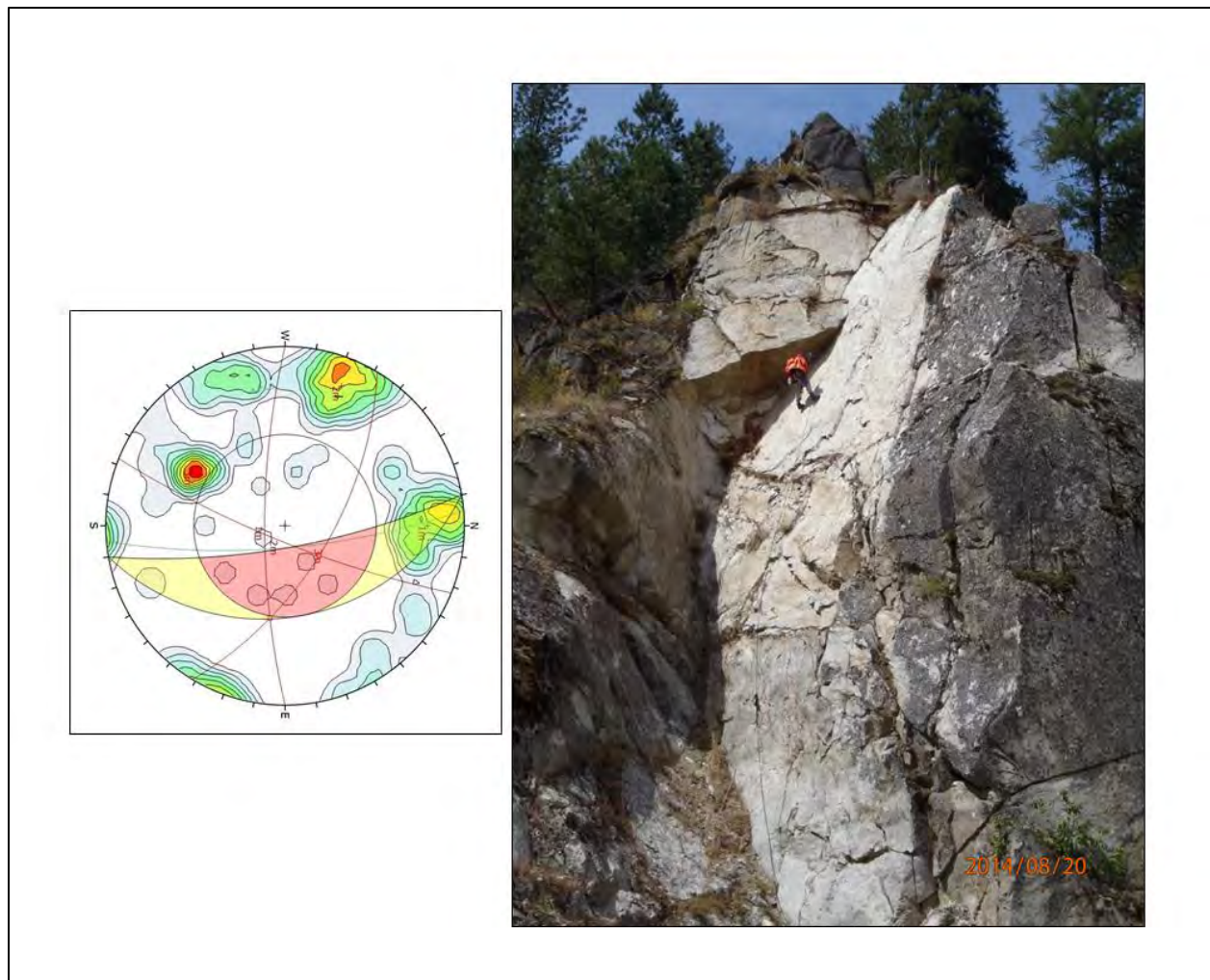


Figure 12: Rock cut slope 4, primary mode of failure is wedge sliding east into the road. Stereonet is oriented parallel to the cut slope face. North is to the right of the photo. Block above the geologist on rappel is kinematically unstable and should be removed.

FINAL DESIGN AND CONSTRUCTION

Phase I for Rock Cut Slopes 1 through 4 is still under design review. The authors provided recommendations to the ITD design group which included regrading and flattening of the rock slopes to eliminate rockfall problems and or installation of rock bolts on unstable blocks where grading was not practical or there was right of way (ROW) problem.

Challenges affecting the constructability of the project include:

- Pioneering access roads to the top of the proposed cutslopes;
- Presplit drilling of thin sliver cuts on the steep rock faces;
- Blasting thin sliver cuts with minimal burden; and,
- Control of fly rock, blast vibrations and over pressure at the river's edge because of the prime fish habitat.

As of this writing, the authors have been preparing to conduct the next geologic field reconnaissance of the Phase II portion of the project.

REFERENCES:

1. Bieniawski, Z.T. *Engineering Rock Mass Classifications*. John Wiley & Sons, 1989, pp. 51-91.
2. Hoek, E. and E.T. Brown. Practical Estimates of Rock Mass Strength; *International Journal of Rock Mechanics and Mining Science*, Vol 34, No. 8, 1987, pp 1165-1198.
3. International Society of Rock Mechanics (ISRM), *Rock Characterization, Testing and Monitoring, ISRM Suggested Methods*. Pergamon Press, Oxford, UK, 1981.
4. Palmström, A. The Volumetric Joint Count - A Useful And Simple Measure of the Degree of Rock Mass Jointing. In *Proceedings, IV Congress International Association of Engineering Geology*, vol. 2, New Delhi, India, 1982.
5. Pierson, L. A., and C. F. Gullixson, R. G. Chassie. Rockfall Catchment Design Guide, Final Report. Oregon Department of Transportation and Federal Highway Administration. 2001, 94p.
6. Reed, S. Lewis, Kauffman, J.D., Schmidt, K.L., Burmester, R.F. *Geologic Map of the Sixmile Creek Quadrangle, Clearwater, Idaho and Lewis Counties, Idaho*. Idaho Geologic Survey & University of Idaho, Moscow, Idaho, 2006.
7. Wyllie, Duncan and C. Mah. *Rock Slope Engineering: Civil and Mining*, 4th Edition. Spon Press, 2004, 431 p.

**Remediation of Slope Instability in Presumpscot Marine Clay
using Steel H-Piles**

Mile Brook Bridge over Outlet Stream, Winslow, Maine

Erin A. Force, P.E.

Haley & Aldrich, Inc.

75 Washington Avenue, Suite 1A

Portland, Maine 04101

(207)-482-4626

EForce@haleyaldrich.com

Wayne A. Chadbourne, P.E.

Haley & Aldrich, Inc.

75 Washington Avenue, Suite 1A

Portland, Maine 04101

(207)-482-4609

WChadbourne@haleyaldrich.com

Prepared for the 66th Highway Geology Symposium, August, 2015

Acknowledgements

The authors would like to thank the following individuals/entities for their contributions in the work described:

Peter A. Krakoff, P.E. – CPM Constructors
Laura Krusinski – Maine Department of Transportation

Disclaimer

Statements and views presented in this paper are strictly those of the author(s), and do not necessarily reflect positions held by their affiliations, the Highway Geology Symposium (HGS), or others acknowledged above. The mention of trade names for commercial products does not imply the approval or endorsement by HGS.

Copyright Notice

Copyright © 2015 Highway Geology Symposium (HGS)

All Rights Reserved. Printed in the United States of America. No part of this publication may be reproduced or copied in any form or by any means – graphic, electronic, or mechanical, including photocopying, taping, or information storage and retrieval systems – without prior written permission of the HGS. This excludes the original author(s).

ABSTRACT

The new, two-lane, 325-ft long replacement bridge required the approach embankments to be raised by 2 to 4 ft to improve the vertical profile of the roadway. As a result, engineering evaluations were conducted to assess the potential for global stability issues associated with a 40-ft thick layer of soft, marine clay located below the west embankment. The results of these evaluations showed that an approximately 100-ft long portion of the slope had a lower factor of safety than the minimum required by AASHTO LRFD.

Several remedial alternatives were considered, including use of lightweight fill to raise embankment grades, construction of embankment retaining walls, installation of slope reinforcing elements, conducting ground improvement and constructing a stabilization berm at the toe of the slope. Alternatives were evaluated based on technical feasibility, cost, environmental impacts and schedule impacts. Slope stabilization piles were determined to be the most cost-effective alternative, in part since pile driving equipment would already be on site to install the west abutment foundation piles. Equally as important, this alternative had the shortest installation time, which was another critical factor as the design-build project schedule developed by Maine Department of Transportation (MaineDOT) was aggressive.

Slope stabilization using reinforcement piles had not previously been used by MaineDOT, but the technique has been successfully used on projects outside the State. A total of 32, HP12x53 piles were installed using a vibratory hammer in four days to stabilize the west approach. This cost-effective and innovative approach played a part in the successful award of this \$5.4 million project to the design-build team.

INTRODUCTION

The original Mile Brook Bridge, constructed in 1947, was a 350-ft long, three-span structure that carried Garland Road across the Outlet Stream in Winslow, Maine (see Figure 1). As part of their annual bridge rating program, the Maine Department of Transportation (MaineDOT) determined that the bridge was structurally deficient and required replacement. The scope of the replacement project included a 325-ft long, two-span replacement bridge along with modifications to the approach embankments, including changes in vertical roadway profile necessitating raises-in-grade of 2 to 4 ft.



Figure 1 - Original Mile Brook Bridge during demolition. East approach embankment in the background and Outlet Stream in the foreground. (courtesy of Bryan Steinert)

Due to the relatively small size of the project, MaineDOT decided to deliver the project using a low-cost, design-build approach. Four teams were shortlisted based on qualifications and the contract was awarded to the shortlisted team that had the lowest responsive lump sum price proposal. The selected design-build team was led by CPM Constructors of Freeport, Maine. The bridge designer was Vanasse Hangen Brustlin, Inc. of Bedford, New Hampshire and the geotechnical engineer was Haley & Aldrich, Inc. of Portland, Maine.

SUBSURFACE CONDITIONS

An exploration program consisting of test borings and laboratory testing was conducted by MaineDOT and provided to the prospective bidders as part of the RFP for the project. Supplemental test borings and lab testing were conducted after project award to further define the subsurface conditions and engineering properties of the soils at the site. The subsurface conditions were highly variable along the bridge alignment. Along the approaches, up to 20 ft of previously-placed, granular embankment fill was encountered. Compressible Presumpscot

Formation marine clay was encountered beneath the west approach embankment, west abutment and center pier. Shallow bedrock (within 5 ft of ground surface) was encountered beneath the east approach embankment and east abutment. The marine clay deposit was determined to be 40 ft thick and typically consisted of a 10 to 15-ft thick stiff crust, underlain by soft, normally-consolidated, highly compressible clay. A thin layer of glacial till was present below the clay and above the bedrock. The depth to bedrock relative to pre-construction site grades varied considerably, from 2 ft at the east approach to 70 ft at the west abutment.

Characteristics of the Presumpscot Formation

The Presumpscot Formation consists of silt, clay and fine sand that washed out of the melting Late Wisconsinan glacier. Meltwater streams carried silt, clay and fine sand sediment in suspension to the ocean where it settled to the bottom and accumulated on the ocean floor. The subsequent coastal rebound of the land surface has exposed these sediments at the surface in areas of southern Maine. The formation may be well stratified with interbedded fine sand layers within the silt and clay or it can be massive. Marine shells are commonly found in the Presumpscot Formation and are well preserved in the unoxidized, bluish gray zone of softer sediment. In the upper, weathered portion of the formation, the typical color is brown and the shell material has dissolved leaving only an imprint. This sediment is typically stiff to hard with a blocky fracture pattern. The Presumpscot Formation varies in thickness, has a relatively flat to gently sloping surface and extends from coastal areas of southern Maine inland up to approximately elevation 200 (Marine Limit). (*1*)

The undrained shear strength of the marine clay stratum at this site was estimated using in-situ vane shear tests conducted during drilling of the test borings in conjunction with consolidated undrained triaxial shear tests on thin wall tube samples collected from the west approach slopes. Measured peak undrained shear strengths varied from 715 to 1,875 pounds per square foot (psf) in the vane shear tests and 980 to 1,000 psf in the consolidated undrained triaxial shear tests.

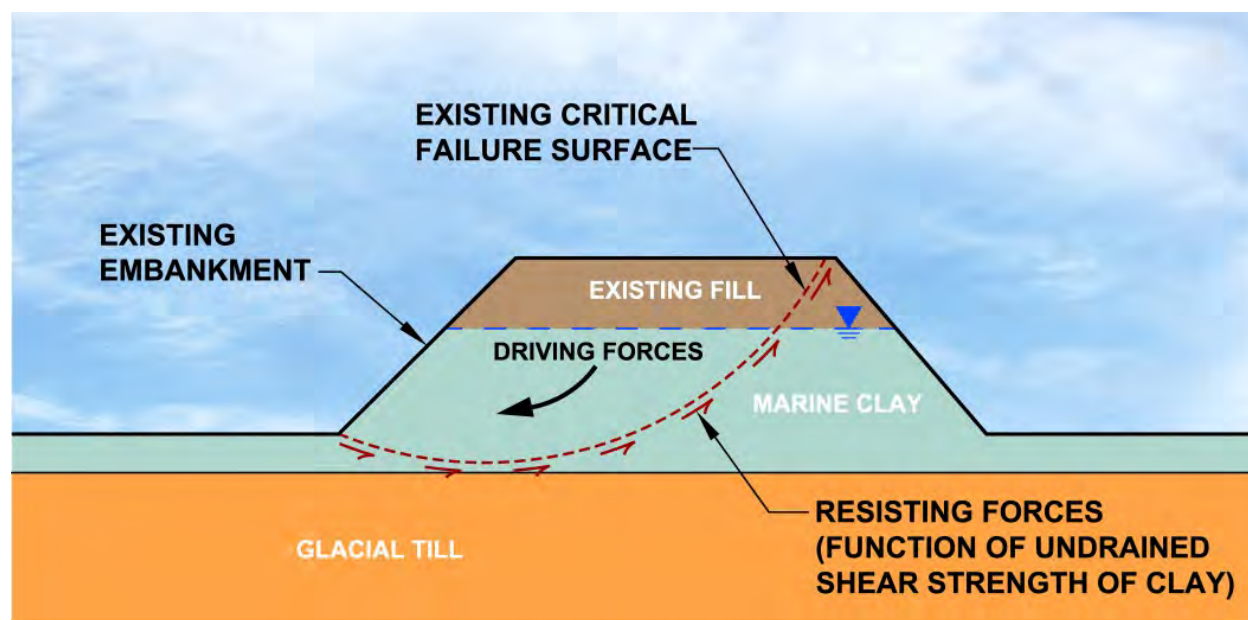
BRIDGE FOUNDATION SYSTEM AND EMBANKMENT STABILITY

Due to the highly variable nature of the subsurface conditions at the site, the replacement bridge was supported on a combination of shallow foundations bearing on rock at the east abutment and pier, and deep foundations at the west abutment. The pile foundation at the west abutment consisted of Grade 50 steel, HP12x53 section H-piles driven through the man-placed fill, compressible marine clay soils and glacial till, to bedrock. Pile lengths ranged from 55 to 60 ft due to the variability of the bedrock surface within the abutment footprint.

The real challenge for the project did not involve the design and construction of the bridge foundation systems, but rather involved achieving the required global stability factors of safety for the bridge approach embankments. The western approach embankment for the existing bridge was up to 55-ft high. As part of the replacement project, portions of the west approach roadway were proposed to be raised by approximately 2 to 4 ft to improve the vertical profile of the roadway. As a result of the raise-in-grade, geotechnical engineering evaluations

were needed to assess the potential for stability, settlement and downdrag issues associated with the marine clay underlying the west approach embankment.

A series of computer-assisted, two-dimensional global stability evaluations were performed to evaluate the west embankment. Both static and pseudo-static (seismic) evaluations were conducted through the abutment, wingwalls and at 50-ft intervals along the approach embankment, transverse to the roadway alignment. The results of global stability evaluations showed that an approximately 100-ft long portion of the northern side of the west approach embankment (see Figure 6) had a lower factor of safety than was required by the AASHTO LRFD Bridge Design Specifications (see Figure 2 and 3).

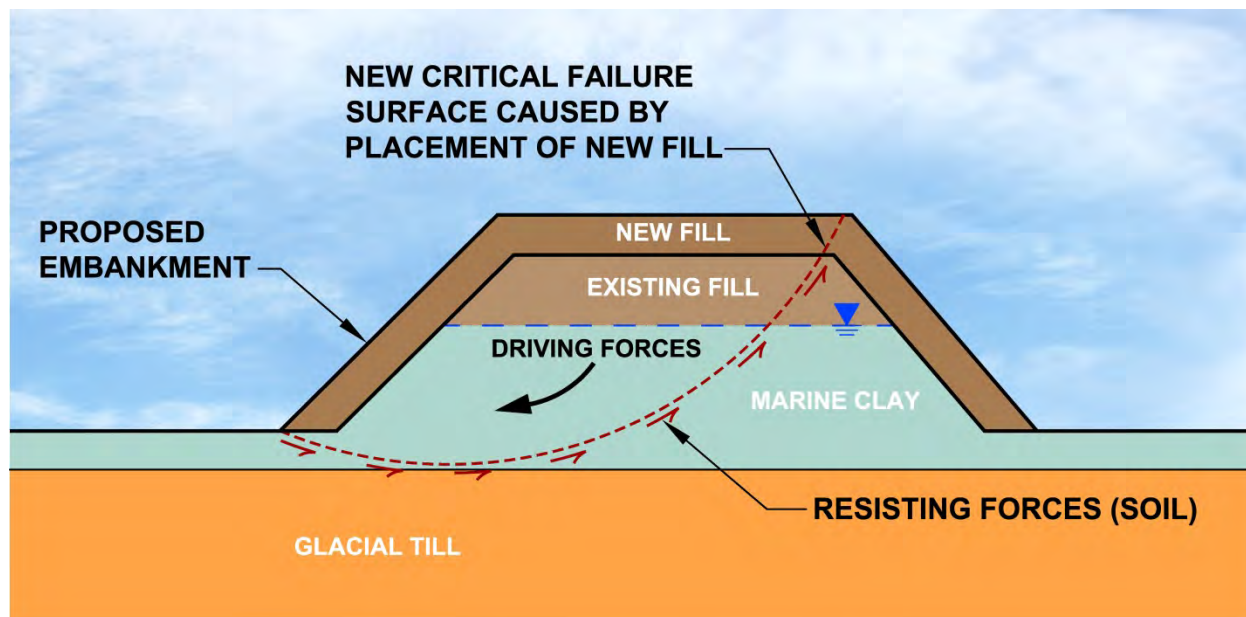


$$\text{Factor of safety} = \frac{\text{sum of resisting forces}}{\text{sum of driving forces}}$$

$$\text{Factor of safety for existing conditions} \approx \text{Minimum required factor of safety (FS min. required)}$$

$$\text{FS min. required} = 1.3 \text{ (slopes) to } 1.5 \text{ (slopes supporting structural elements)}$$

Figure 2 – Existing west approach embankment was marginally stable prior to construction.



Factor of safety for proposed conditions < FS min. required

Therefore the resisting forces need to be increased
to achieve FS min. requirements

Figure 3 – Fill placement needed for new vertical road profile would have caused an unstable condition. (courtesy of Terri McEleney)

Increasing the global stability factor of safety to acceptable levels can be accomplished by either decreasing the driving forces by using lightweight fill to raise embankment grades or by removing soil and constructing retaining walls, or by increasing resisting forces by conducting ground improvement, installing soil reinforcement elements, or constructing a stabilizing berm at the toe of the embankment slope. The technical feasibility and cost impact of each of these options was considered during design development. Although construction of a stabilizing toe berm was determined to be technically feasible and the most cost effective alternative, it was dismissed as it would have caused both right-of-way and environmental impacts. Therefore, slope stabilization piles (Figure 4) were selected by the team as the most cost-effective alternative to alleviate the stability concerns, particularly since pile driving equipment and pile materials were already going to be used to support the bridge construction. The alternative had the shortest installation time of all the alternatives, which was another critical factor as the project schedule developed by MaineDOT was aggressive.

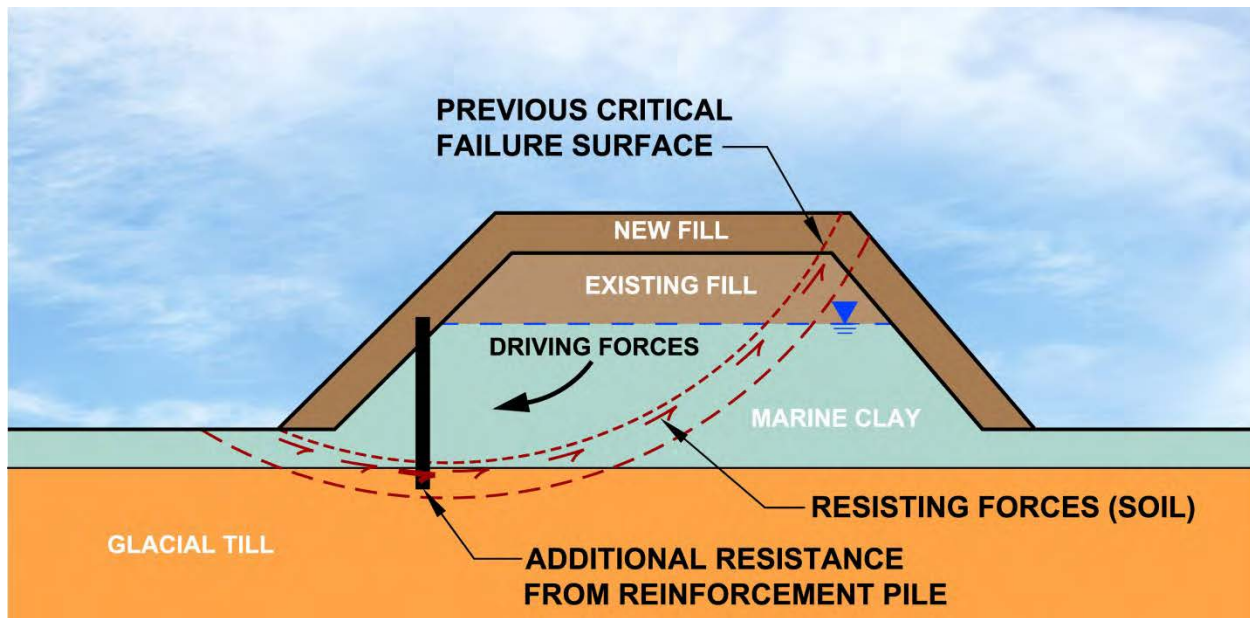


Figure 4 – Stabilization piles advanced to depth so that failure surface shifts down below the bottom of the piles, into dense glacial till. New deeper critical failure surface has acceptable factor of safety. (courtesy of Terri McEleney)

Slope Stabilization Pile Design

Slope stabilization using reinforcement piles had not previously been used by MaineDOT, but Haley & Aldrich had used the technique successfully on projects outside the State of Maine. The following design methodology was used to develop the design criteria for the slope stabilization piles (2,3):

1. Perform slope stability analysis of the condition without stabilizing elements. This was completed using the computer program Slide 5.0 by Rocscience Inc.
2. Determine the unbalanced forces from the analysis performed in Step 1 (i.e., the amount by which the resisting forces must be increased through the use of stabilizing elements, to achieve the minimum required factor of safety). The minimum required factor of safety used on this project was 1.3/1.5 static (embankment only/embankment supporting structural elements) and 1.0 seismic. This step was completed using output exported from Slide.
3. Conduct lateral pile evaluations to determine the loads and moments in the stabilization piles when the minimum stabilizing force calculated in Step 2 is applied to the piles (see Figure 5). This was completed using the computer software LPILE Plus Version 5.0 by Ensoft, Inc (4). Sheetpiles were also considered and analyzed using WALLAP Version 5.04 by Geosolv.
4. Determine the minimum section modulus, pile size and pile spacing needed to resist the minimum stabilizing force using the results of the lateral pile evaluations in Step 3.

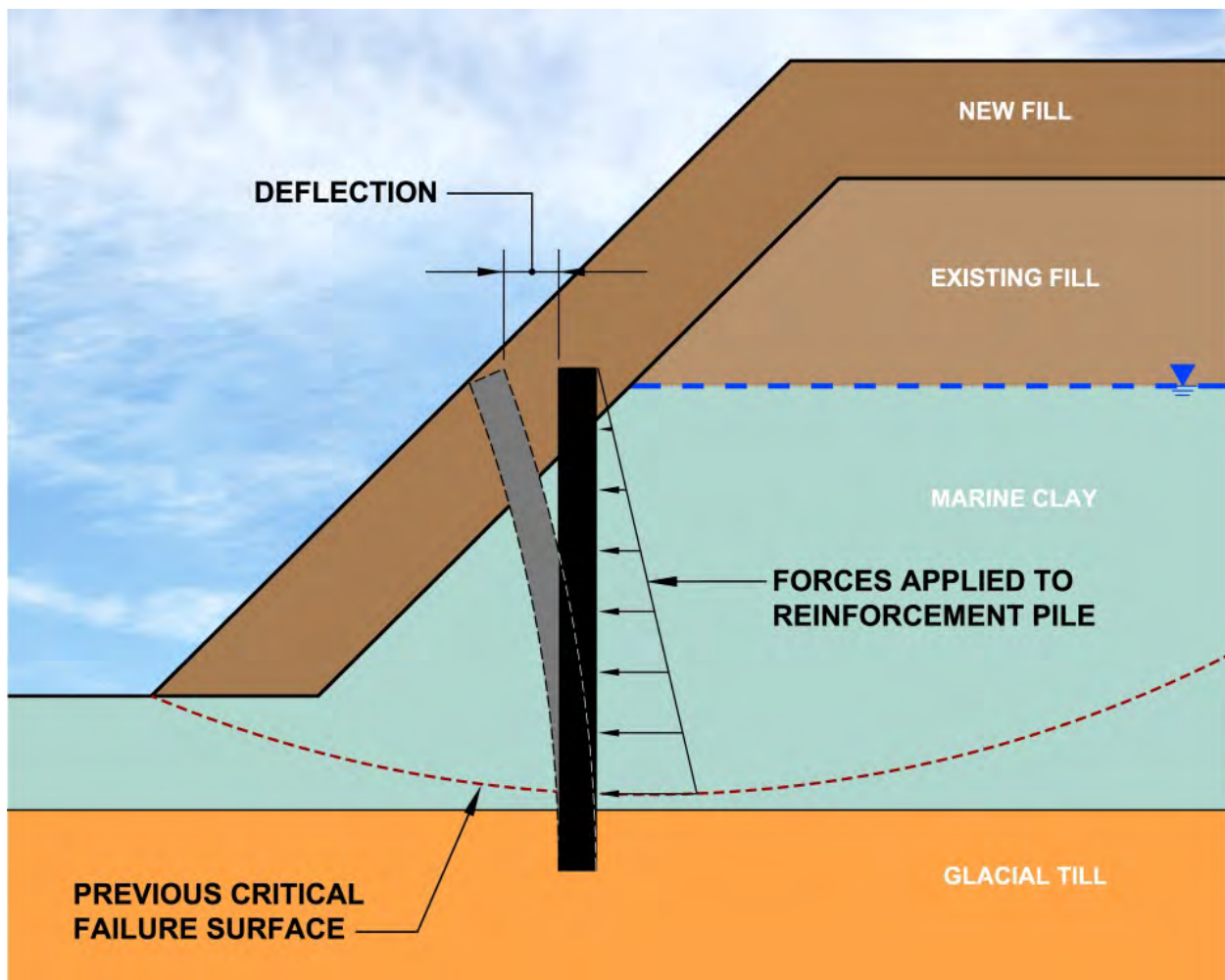


Figure 5 – Lateral pile evaluations were used to determine spacing and sizing requirements of stabilization piles such that deflections are limited to maintain pile stability (i.e., fixity at bottom of pile). (courtesy of Terri McEleney)

Slope Stabilization Pile Results

Based on the results of the evaluations, the following general design requirements were established for the slope stabilization piles:

- H-piles need to be manufactured from minimum grade 36 steel.
- Slope stabilization piles need to be installed approximately 50 ft north of the roadway centerline, near the mid-point of the slope. Reinforcing elements also need to be installed immediately behind the west abutment to provide stabilization of failure surfaces through the abutments and wingwalls (see Figure 6).
- The reinforcing elements need to be advanced to the top of the glacial till deposit.

approach, 26 piles along the north side of the west embankment and 6 piles behind the west abutment and wingwalls. The piles were spaced 4 ft center-to-center, driven through the Presumpscot marine clay and into glacial till. The reinforcing elements were installed near the mid-point of the slope (see Figure 7) and behind the proposed west abutment.



Figure 7 – Installed HP12x53 stabilization piles along the north side of the west approach embankment. (courtesy of Bryan Steinert)

Prior to installation, CPM Constructor's earthwork crew constructed a bench along the embankment slope to provide a level work area to install the piles. The piles were installed using an H&M 1700 vibratory hammer supported by a Link Belt LS-318 Crawler Crane (see Figure 8). Minimum installation depths of reinforcing piles were determined prior to installation based on the supplemental test boring obtained after project award and prior to final design. Determination of whether piles had achieved the required installation depth was based on observations made by Haley & Aldrich during construction. The piles were cut off at least 2 ft below finished embankment grades.



Figure 8 – Installation of HP12x53 stabilization pile by CPM Constructors using an H&M 1700 vibratory hammer supported by a Link Belt LS-318 Crawler Crane. (courtesy of Bryan Steinert)

CONCLUSIONS

The design-build team was faced with the difficult task of designing a cost-effective method for providing slope stabilization of a reconstructed roadway embankment bearing on soft marine clay. With all members of the team working together closely, a slope stabilization pile system was selected, designed and detailed. This stabilization alternative was determined to be the most cost-effective solution, in part since it used readily available materials and equipment that would already be on site to install the bridge foundation piles. Equally as important, this alternative had the shortest installation time (only four days) and therefore minimal schedule impacts. This was the first time this slope stabilization method had been used on a MaineDOT project. The bridge has been in service for more than 2.5 years, and no signs of slope movement have been observed.

REFERENCES:

1. Thompson, W.B. *Surficial Geology Handbook for Coastal Maine*. Maine Geological Survey, Department of Conservation, Augusta, Maine, 1979.
2. Duncan, J.M. and Wright, S.G. *Soil Strength and Slope Stability*. John Wiley & Sons, New Jersey, 2005.
3. Poulos, H.G. Design of reinforcing piles to increase slope stability. *Canadian Geotechnical Journal*, Vol. 32, 1995, pp. 808-818.
4. Ensoft, Inc. Section 2.1.4.5 – Use of Piles to Stabilize Slopes. *LPILE Plus 5.0 for Windows – Technical Manual*, 2004, pp. 2-30.

INSTALLATION OF FLEXIBLE SNOW NET STRUCTURES ALONG I-90 SNOQUALMIE PASS WASHINGTON

Chris Ingram, President
HI-TECH Rockfall Construction, Forest Grove, OR, U.S.A.



ABSTRACT: HI-TECH Rockfall Construction is currently constructing the largest avalanche barrier project ever undertaken in the U.S. These nets range from 3 meters in height up to 4 meters in order to control avalanches along I-90 in Washington State. In all HI-TECH will install 1229 meters of snow nets. The project consists of 322 meters 4.0/3.5 nets, 278 meters of 3.5/3.2 nets and 651 meters of 3.0/3.2 nets. These nets are installed at 4 different locations along the highway corridor. The major requirement for the contract provided explicitly for the snow nets designed in full accordance with the Swiss Guidelines for snow supporting structures and approved by the WSL. The design team included Kane Geo-Tech, Maccaferri, HI-TECH Rockfall and Dr. Ing. Roberto Castalidini, consultant from Italy.

The major challenges for construction of the flexible snow nets were the very rough and uneven terrain and the lack of access to where the nets were to be constructed and adverse drilling conditions. The snow nets required very high anchor loads due to the abnormal snow pressures and heavy snow density of 400 kg/m² that we see at this location. With the use of specialized drill rigs and a helicopter HI-TECH's highly skilled employees were able to overcome the challenges and construct the flexible snow nets on budget and on time.

INTRODUCTION

The installation of flexible snow supporting structures along a major transportation corridor at Snoqualmie Pass, Washington U.S.A. was undertaken by HI-TECH Rockfall Construction Inc. The project consisted of several different heights and capacities of the snow supporting structures in an area of very uneven terrain with difficult access in four different locations. The specifications called out for the contractor to submit an approved layout and design and all snow supporting structures were required to be snow nets approved by WSL. Maccaferri Inc.-USA was contracted to supply the required snow supporting structure materials and Dr. Ing. Roberto Castaldini was contracted to oversee the design and layout of the systems.

BACKGROUND

Interstate 90 in Washington State is the east to west lifeline and continues across the U.S. from coast to coast. The average daily traffic through this corridor is 30,000 vehicles per day with an increase to 58,000 on the week-ends. The highway has been closed off and on many times in past years due to avalanches covering the highway. The Washington State Department of Transportation has provided avalanche control in this corridor over the years using explosives. During times when active avalanche control was ongoing it required that the highway be closed for hours at a time. In 2007 WSDOT began a study to determine if the use of snow supporting structures could be used to control the avalanches and allow for the highway to remain open continuously during the winter months without interruption to traffic flows. The low altitude at the pass of 3022 feet allows for winter rains which when combined with the normal snowfalls provides for extremely heavy snow densities at the site. Average snowfalls at this site in the last five years have been 419 inches annually. A second study and final report was completed in 2010 and it was determined that the use of flexible snow nets was a viable option for this site. The project was put to bid in 2011 by WSDOT and consisted of 1229 meters of 2.5m, 3m, and 3.5m flexible snow nets. Final design and layout was to be submitted for approval to WSDOT by the contractor.

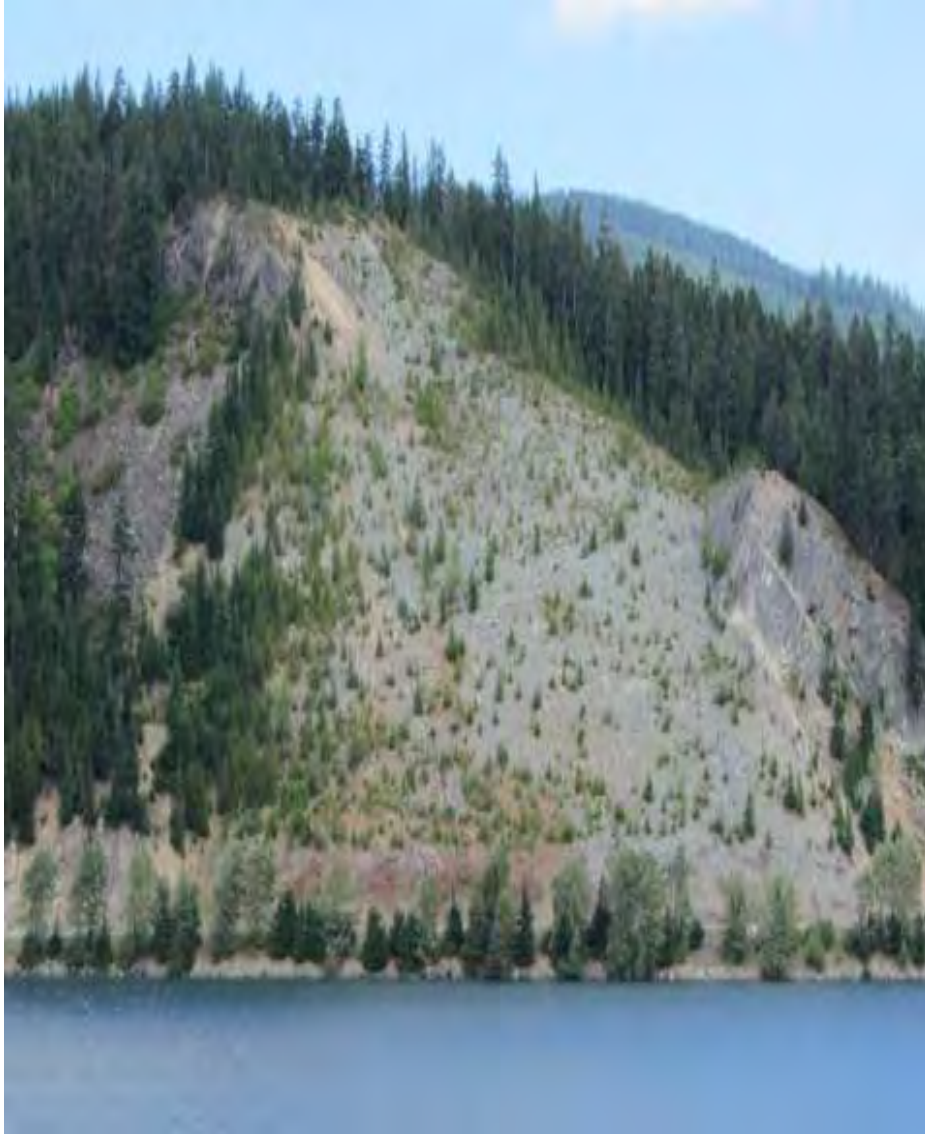


Figure 1. View of area called slide curve

SNOW STRUCTURE DESIGN

Dr. Ing. Roberto Castaldini was forwarded all the preliminary design information completed by WSDOT for his review. During this process it was discovered that due to the heavy density value of 600 kg/mc listed in the 2010 WSDOT final design specifications. No WSL certified systems could be provided. For this reason, at first, Dr. Ing. Castaldini proposed to proceed to a calculation of the structures for the specific case. This would have taken time and maybe a higher cost and meant not using standard snow nets. WSDOT reviewed the data gathered and determined the snow density listed in the 2010 report was in error and amended the density to 400kg for design purposes. The project was full of challenges to provide an adequate and

66th HGS 2015 Ingram

accurate design, these challenges included very steep and smooth slope surfaces, very high glide and creep velocities, intense and heavy snowfalls, difficult subsurface conditions and the fact that this was the first project of its type in the U.S. and was to protect a major transportation corridor. The snow nets approved by the WSL were calculated in full accordance with the Swiss Guidelines assuming a typical snow density of the Alps that is 270 -300 kg/mc. With a snow density of 400 kg/mc the loads on the structure are higher. For this reason it was necessary to upsize all of the original snow nets listed in the contract by WSDOT Providing for structures characterized by larger Dk value from 2.5m to 3m, 3m to 3.5m and 3.5m to 4m and in glide factor or N value from 2.5 to 3.2 which allowed for the snow nets to have a higher Sn value and therefore meet the criteria required for snow retention and using WSL certified structures. Other adjustments necessary due to the heavy snow density, depth and very steep terrain were to shorten the distance between the lines or L value and add artificial slope roughening at many of the locations to reduce the glide factor. After many meetings, site visits and months of correspondence HI-TECH was finally able to submit a design that met all the criteria listed in the bidding documents. This design was subsequently approved by WSDOT allowing for the materials to be ordered so the construction phase could be scheduled.



Figure 2. Dr. Castaldini laying out steep smooth surface

To use stronger (i.e. models with higher Dk and higher N) standard snow supporting structures in a context different from that of the Alps the designer has to be very careful!

To check Dk, N and S'N, S'Q was necessary but not sufficient

The acting loads on snow nets change not only in modulus but also in the direction, due to the fact that the snow net will be partially filled in back.

It is always necessary to calculate the acting loads on the partially back filled structure and to compare them with those which the standard structure can do

FLEXIBLE SNOW NET MATERIALS

Maccaferri USA was chosen to supply all of the materials for the flexible snow nets. As there are no manufacturing facilities in the U.S.A. for these structures they had to be manufactured in Italy and then shipped to the U.S. The coordination of this portion of the project was very critical. The order consisted of 4.0/3.2, 3.5/3.2 and 3.0/3.2 flexible snow supporting structures. All of these systems use different sizes of anchors cables, foundation bars, posts, bracing ropes and associated hardware. In order to assure construction activities could begin quickly, all of the anchors and foundation bars were shipped first followed by the remaining snow net materials. It was critical to tag and label all of these materials separately in order to keep track of the many different sizes being shipped. Also the packaging of the materials was important so as to not mix different materials from different sized structures in the same shipping container for ease of sorting.

ANCHOR DESIGN AND CONSTRUCTION

The anchors for the project required HI-TECH to contract with a U.S. based geotech engineer to determine drilling depths and hole diameters to achieve the required pull-out strength. The project specifications called out sacrificial anchors to be installed in all the different ground conditions that would be encountered to prove the bond strength of the anchor design. Kane Geo-Tech of Stockton, CA, U.S.A. was selected based on their vast experience in designing and testing of ground anchors for rockfall mitigation and debris flow practices. With the different capacities and sizes of the flexible structures on the project there were 18 different anchor capacities overall. Some of the challenges of the design were the fact that WSDOT was requiring all the anchors to be tested to 2 times the design load to assure that the anchors would not fail. It was determined that the materials supplied for the flexible structures could not withstand that type of testing and failure of the wire rope cables would occur as the loads needed to be pulled during the testing far exceeded the breaking strength of the material. After many meetings and discussions it was determined that HI-TECH could upsize the material for the sacrificial tests to prove the bond strength between the grout and ground conditions, however the testing criteria would remain at 2 times the design load. More meetings and discussions were required for the production anchors and the testing criteria got reduced from 2 times to 1.6 times and then finally to 1.35 times design load. The Owner required 100% of all the anchors installed to be tested. This included every production anchor. Having to deal with the very steep and uneven terrain required specialized drilling equipment. The hole diameters ranged from 50mm to 100mm and the depths from 1.7 meters to 4.5 meters into solid rock. HI-TECH brought in wagon drills and Spyder backhoes with specialized drills mounted on the arm to drill all of the holes. These machines have the capability to be winched and crawl around in steep and uneven terrain while still having the ability to level themselves and productively drill in those conditions.



Figure 3. Wagon Drill



Figure 4. Spyder Drill

A portion of the shorter depth 2” holes were hand drilled by HI-TECH employees with the use of 30k hand held rock drills. To date 70% of the anchors are installed and grouted and we have had no test failures.

CONSTRUCTION OF THE FLEXIBLE STRUCTURES

The uneven ground conditions required that many of the foundations were above ground piers. These foundations required engineering by a structural engineer to assure that they would allow for the snow nets to function properly. These piers ranged from 30cm to 120cm above existing ground. The use of a helicopter was required to fly all the required materials for the foundations to specific points on the slope.

The concrete was mixed on the slope and poured into the forms. Water for mixing had to be pumped up the slope from as far away as 200 meters to temporary storage containers that were placed on the slope. Once the foundations were constructed, the installation of the post and nets was the next step.

The snow net lines were laid in a level area approximately 11Km from the slope as this was the only area large enough to accommodate our needs. The lines were laid out in 2 and 3 post setups to be prepared to be lifted by the helicopter and placed up on the slope.



Figure 6. Completed pier footing



Figure 7. Materials ready for fly

Alberto Grimaldi from Maccaferri was onsite during this time to ensure that the system was being properly installed. HI-TECH had previously used helicopters to install rockfall draperies on over 100 projects in the past but had never installed flexible snow nets before. The installation went very smooth as we averaged 110 meters per day in place. This operation required 4 men at the yard area and 10 men up on the slope.

To date approximately 20% of the flexible structures are in place and complete and the remaining 80% will be complete by October 2015. HI-TECH is continuing construction of anchors and foundations at upper slide curve and should be complete with that portion this year. Lower slide curve is still awaiting final approval from the changes recommended by Dr. Castaldini in his site visit this year. This area had the most uneven terrain and loose rock on the slope and required grading to be done prior to lay-out. The initial grading is complete and we are beginning final grading for the lay-out this year.

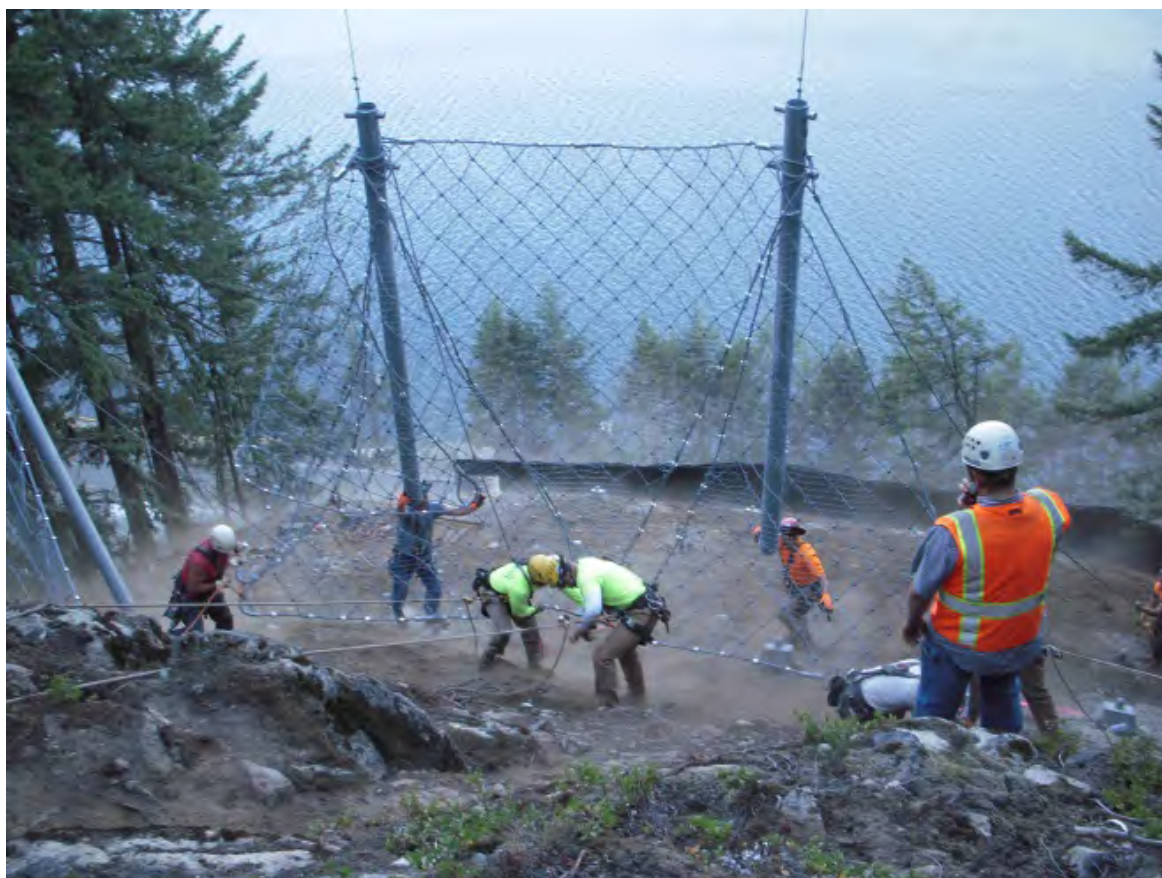


Figure 8 Helicopter installing post & nets



Figure 9. Helicopter installing post & nets



Figure 10. Initial grading of lower slide curve

CONCLUSION

The design and construction of flexible snow supporting structures is a very precise, detailed and complicated undertaking. The construction of flexible snow supporting structures is typically done in areas with little or no access with normal equipment. While HI-TECH has over 20 years of experience in constructing rockfall barriers and working in areas with little or no access we found that constructing the flexible snow supporting structures was very challenging. They are quite different from rockfall barriers as the tolerance levels for the anchors and foundations are much more stringent. The project during the construction phase has gone smoothly. Most of the challenges have been in the design and layout of the systems. It is very important that when designing these structures that the design team reach out to the experts in this field. This project being the first of its kind in the U.S.A. could have benefited from having more accurate data in the preliminary stages of the design and involving more experienced experts in the field to come up with a more accurate and precise design in the bidding stages. The project budget from original bid date has increased by over 125% as all of the systems had to be upsized, all of the lines had to be spaced closer together increasing the linear footage of structures to be built and artificial slope roughening was added. These changes have cost the owner approximately \$4,000,000.00 USD above the original bid price.

Acknowledgements

Dr. Ing. Roberto Castaldini for his knowledge and expertise in flexible snow supporting structures. Alberto Grimald for his experience and help in installation of the snow supporting structures.

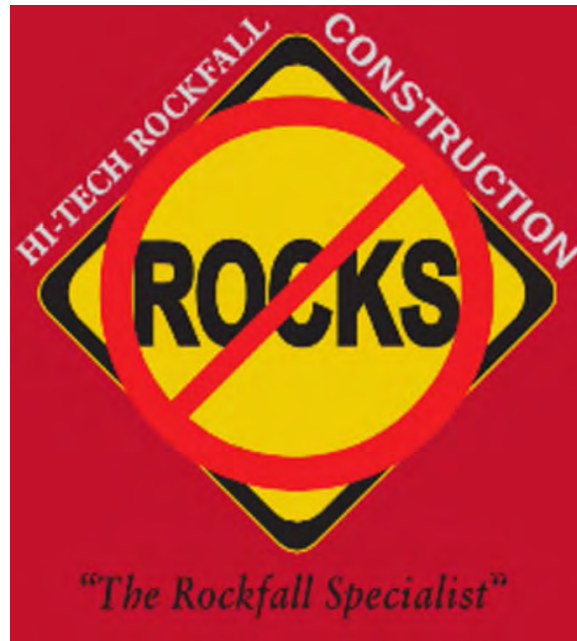
Disclaimer

Statements and views presented in this paper are strictly those of the author(s), and do not necessarily reflect positions held by their affiliations, the Highway Geology Symposium (HGS), or others acknowledged above. The mention of trade names for commercial products does not imply the approval or endorsement by HGS.

Copyright Notice

Copyright © 2015 Highway Geology Symposium (HGS)

All Rights Reserved. Printed in the United States of America. No part of this publication may be reproduced or copied in any form or by any means – graphic, electronic, or mechanical, including photocopying, taping, or information storage and retrieval systems – without prior written permission of the HGS. This excludes the original author(s).



Stabilizing A Slope Using A High Strength Wicking Geotextile

John C. Folts, PE
TenCate Geosynthetics
365 South Holland Drive
Pendergrass, GA 30567
(706)-693-2226
j.folts@tencate.com

Prepared for the 66th Highway Geology Symposium, September, 2015

Acknowledgements

The author would like to thank the individuals/entities for their contributions in the work described:

Marc Burke – Edge Environmental, Inc.
Andy Gerberich – GetsCo, Inc.
John Parrish – GetsCo, Inc.

Disclaimer

Statements and views presented in this paper are strictly those of the author, and do not necessarily reflect positions held by their affiliations, the Highway Geology Symposium (HGS), or others acknowledged above. The mention of trade names for commercial products does not imply the approval or endorsement by HGS.

Copyright Notice

Copyright © 2015 Highway Geology Symposium (HGS)

All Rights Reserved. Printed in the United States of America. No part of this publication may be reproduced or copied in any form or by any means – graphic, electronic, or mechanical, including photocopying, taping, or information storage and retrieval systems – without prior written permission of the HGS. This excludes the original author(s).

ABSTRACT

This project utilized the draining and reinforcing properties of a High Strength Wicking Geotextile used to stabilize a failed detention pond. The existing pond had multiple surficial failures within its 2:1 (Horizontal: Vertical) highly plastic clay and silt side slopes. Upon reaching saturation, the slopes became unstable and sloughed into the floor of the detention pond.

The original design called for the soils within the failed zones to be removed and replaced with a conventional stone filled wire basket retaining structure. The plans called for the placement of stone filled wire baskets to a height that would reduce the side slopes to a stable angle of repose. During construction, it was apparent that access to the site was limited, making the project more expensive than originally proposed.

A value engineered option using a high strength wicking geotextile was evaluated and determined to be an economical alternative. The geotextile was placed in multiple lifts horizontally along the previously failed sections of the pond and backfilled with the onsite soils. The geotextile provided strength and drainage allowing for the reconstruction of the slopes at the pre-existing slope angles. The cost savings achieved by using the on-site soils as backfill along with the high strength wicking geotextile was significant enough to keep the project moving forward.

BACKGROUND

The failure of the side slopes (figure 1) along a detention pond in the Weldon Ridge Subdivision, located in Cary, NC, required a significant amount of repair in 2014. The original design plans included removing the spoils that had sloughed into the detention pond and installing a typical gravity gabion basket retaining wall (figure 2). During construction it was determined that access into the site was restricted which made getting stone to fill the baskets an extremely expensive option, therefore alternative solutions were investigated.



Figure 1. Observed slope failure (2014)



Figure 2. Proposed wall and slope area to be reconstructed

DESIGN

The local geosynthetic distributor contacted the geosynthetic manufacturer's Engineers to help with the product selection. The revised design incorporated the use of multiple layers of the high strength wicking geotextile for both its reinforcing strength and drainage ability. The design called for the high strength wicking geotextile to be placed horizontally in layers spaced 2 feet apart and extending into the embankment approximately 13 feet, longer with an overlap, if water was encountered (figure 3).

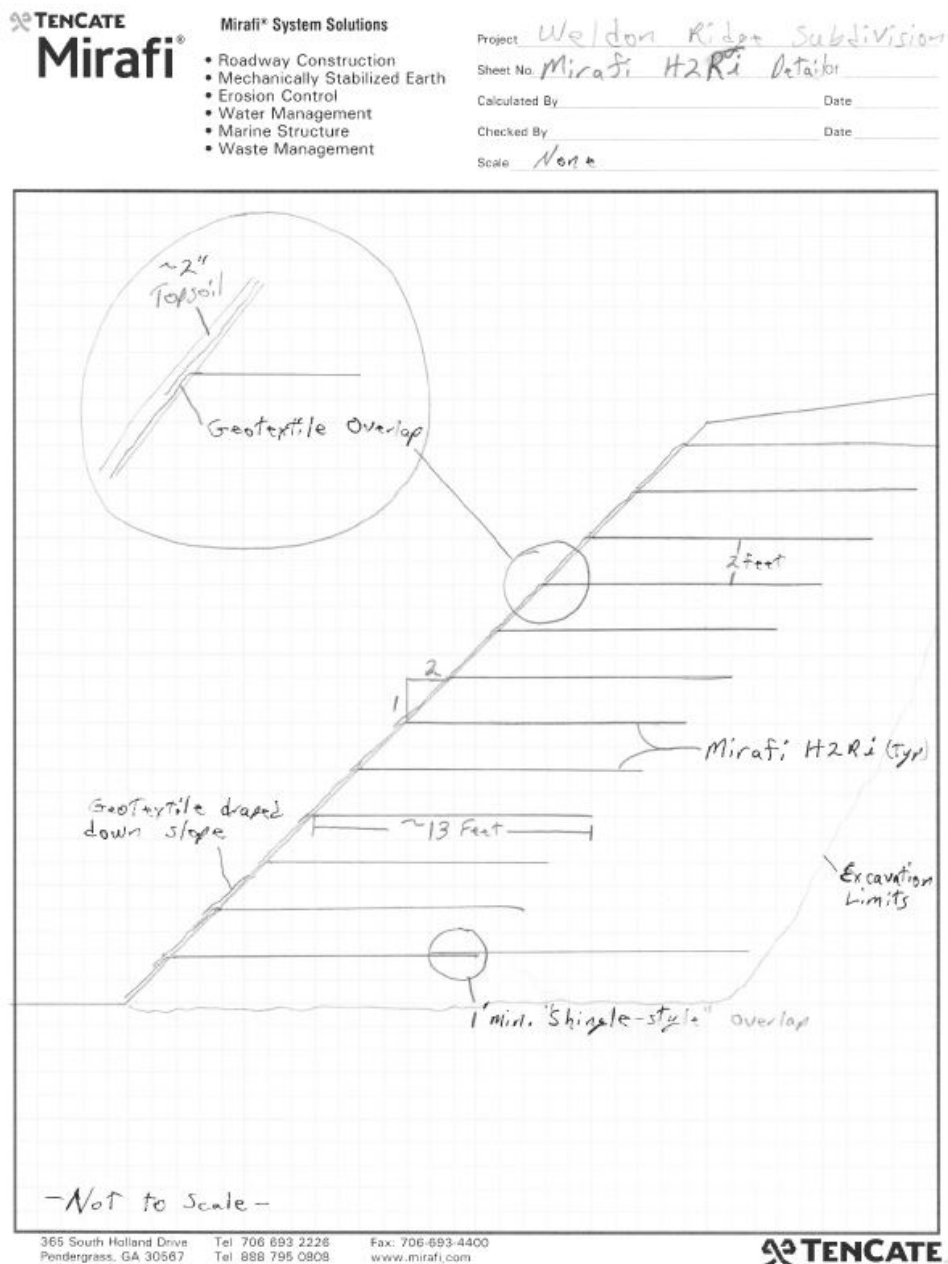


Figure 3. Final grading of the high strength wicking geotextile reinforced slope.

CONSTRUCTION

Construction was performed in relatively short sections (less than 50 feet along the slope) to allow for the reuse of the on-site soils. The high strength wicking geotextile was placed so it would drain in the direction of the detention pond. The geotextile was installed “shingle style” (figure 4) when it needed to be extended beyond the 15 foot roll size so it would optimize the water flow.

The geotextile was placed into the embankment and extended down the slope approximately 2 feet to protect the slope’s face from surficial movement and erosion.



Figure 4. Horizontal installation of high strength wicking geotextile.

The on-site highly plastic clay soils (classified as CH) were allowed to be used for backfill and were placed in lifts of 12 inches or less and compacted using a walk behind vibratory sheepsfoot roller (figure 5).



Figure 5. On-site soil placement in compacted lifts.

The geotextile extended to the face of the slope and then down the slope approximately 2 feet and was covered with a few inches of soil. The idea was to allow for the vegetation to grow into the end of the geotextile and help remove the water. The final grade along the slope face was smoothed over with the excavator (figure 6).



Figure 6. Final grading of the high strength wicking geotextile reinforced slope.

During construction, bedrock was encountered in one area and water was observed seeping into the excavation. The geotextile was extended approximately 22 feet into the slope to capture the water. The next day water was observed coming out of the slope face in that area (figure 7). This was proof that the wicking of the water was already occurring.



Figure 7. Water observed at face of slope during construction.

CONCLUSION

The detention pond construction was completed in August of 2014 with a total project savings of approximately 25%. The original cost estimate was ~\$200,000.00, but with the implementation of the innovative high strength wicking geotextile, the final project cost was ~\$150,000.00. The timeline for construction was also sped up by not having to import material via the difficult access trails.

The utilization of the high strength wicking geotextile allowed for the slopes to be constructed at the original design heights of up to 25 feet with a 2:1 (H:V) slope. This approach helped to reinforce the unstable slopes as well as provide drainage and surface protection.

A site visit was made in August 2015 to observe the vegetative growth and to visually inspect the slopes. Vegetation had been established and no visible signs of slope movement within the reinforced areas could be seen (figure 8).



Figure 8. Completed detention pond after 1 year (2015).

REFERENCES

- Conference Proceedings
 1. Xiong Zhang A.M. ASCE, and Nicholas Belmont. Use of Wicking Fabric to Help Prevent Differential Settlements in Expansive Soil Embankments. *Department of Civil and Environmental Engineering, University of Alaska, Fairbanks, 2011. Geo-Frontiers 2011*© ASCE 2011, pp 3923.

**ICEFALL HAZARDS ALONG U.S. TRANSPORTATION CORRIDORS –
ARE ROCKFALL CATCHMENT DITCHES SUFFICIENT?**

David J. Scarpato, P.E.
President
Scarptec, Inc.
Monument Beach, Massachusetts, USA
dave@scarptec.com

Prepared for the 66th Highway Geology Symposium, September 2015

Acknowledgements

The author(s) would like to thank the individuals/entities for their contributions in the work described:

Alaska Department of Transportation

Disclaimer

Statements and views presented in this paper are strictly those of the author(s), and do not necessarily reflect positions held by their affiliations, the Highway Geology Symposium (HGS), or others acknowledged above. The mention of trade names for commercial products does not imply the approval or endorsement by HGS.

Copyright Notice

Copyright © 2015 Highway Geology Symposium (HGS)

All Rights Reserved. Printed in the United States of America. No part of this publication may be reproduced or copied in any form or by any means – graphic, electronic, or mechanical, including photocopying, taping, or information storage and retrieval systems – without prior written permission of the HGS. This excludes the original author(s).

ABSTRACT

Ice accumulation can unknowingly wreak havoc on surface rock excavations and lead to an increase in the frequency of rock and icefall events along highways subject to significant precipitation and cold temperatures. Although icefall may logically be treated as a variation of a classic rockfall problem, there are some significant differences between rockfall and icefall hazard evaluation. These differences are primarily related to the transient nature of ice accumulation thickness and distribution. Ice slabs can fall from high above, or can slide or topple depending upon underlying slope geometry. High-energy icefall impacts can also generate shatter, which can result in the release of ice projectiles. Based on a preliminary poll of DOT's in various northern tier states subject to ice development, icefall hazards are not routinely considered as part of the rock slope design process. Ditches designed to accommodate rockfall capture may not be sufficient to mitigate icefall events, and in such cases, other treatments and engineering controls may be warranted. Engineered netting systems can maintain rockfall events; however, ice can accrete to the outside of the netting and present itself as an icefall hazard. Ice build-up mitigation techniques can consist of drainage elements, periodic cold-weather maintenance efforts, or topographic enhancements. In cases where source zone treatment is not permissible, engineered barriers may be incorporated for mitigating the risk of icefall impact to the traveling public. This paper will cite project examples and describe some of the challenges associated with icefall evaluation, prediction of ice distribution, ditch effectiveness, the importance of long-term monitoring and maintenance programs, and mitigation strategies for dealing with the under-represented problem of icefall.

INTRODUCTION

The incidence of icefall could be considered an underrepresented and underappreciated natural hazard. Following the Varnes (1978) landslide classification system, the term “*icefall*” can be used as a general term to describe the travel of a mass of ice under the influence of gravity by falling, bouncing or rolling. Ice loading and icefall from roof structures are well-documented in the literature and public domain, but cases of icefall emanating from rock excavations, at least until recently, are relatively rare. Recent increases in documented cases of icefall may be attributed to regionally increased precipitation due to climate change and anthropogenic construction in remote terrain. It may also be that we are actually looking for this ghost-like hazard, after only just a few publicized events. An initial paper on icefall hazards was published and presented at the International Snow Science Workshop (Scarpato & Woodard, 2012), in order to help chart a path toward defining icefall hazard, risk to public safety, and to initiate a discussion on mitigation measures to reduce the potential impacts from falling ice. This paper builds upon the previous one, and on additional recent studies by the author, with a specific focus on catchment ditch design adequacy.

ICE ACCRETION ON EXCAVATIONS

Significant ice accumulation affects many excavations subject to cold weather conditions, including rock slopes as well as some tunnels. The prolonged and cyclical nature of ice accretion on rock excavations results in more significant detrimental effects for the following reasons:

1. Rock mass behavior is frequently controlled by “discontinuities” in the rock mass such as joints, faults, bedding planes, or fractures. Discontinuities control the size and modes of failure in a rock mass and serve as the primary conduits for water flow. In climates subject to cold-weather conditions, water within discontinuities can result in:
 - i. Ice formation along discontinuities where water flow is present, resulting in ice over-hangs or classic “icicle” formations;
 - ii. Ice-jacking of rock blocks, whereby expansion mechanics results in prying action within discontinuities resulting in increased rockfall;
 - iii. Elevated water-pressures on discontinuity planes, due to ice-dammed conditions can result in increased rock slope instability as described by Hoek (1981).
2. Bedrock generally consists of geomaterials that are lithified and/or mineralized, resulting in higher intact material strength than that of soil. Where slope behavior is controlled by discontinuity orientation and strength, this results in:
 - i. Rock slopes that are designed and constructed at steeper face angles than that for soil slopes;
 - ii. Steeper slope angles can result in slope faces and “back-slopes” (i.e. flatter areas beyond the slope crest) that are closer to engineered features below, such as roadways. This geometry can result in increased ice and rockfall impacts.

ROCK SLOPE ICEFALL HAZARDS

Icefall hazards can consist of *direct ice particle impact*, *impact shatter*, or *secondary debris splattering*. Direct impact can result in serious injuries and roadway closures.

Direct Impact

Direct icefall impact hazards can be most significant, and result from point-to-point contact with pavement, pipelines, utilities, or vehicles (Figure 1). Direct impact hazards for icefall can be similar to direct impact from rockfall with respect to energy and collision damage.



Figure 1 – Direct icefall impact damage to small pick-up truck along Seward Highway near Anchorage, Alaska. Photo courtesy of Anchorage Daily News, 6 April, 2012.

Impact Shatter

Impact shatter results when an ice particle breaks-up upon initial contact with a substrate, like pavement, walls, rock outcrops, or a roadside ditch. Similar to “flyrock”, an unintended consequence from rock blasting, smaller ice projectiles can be liberated even if direct impact is within a dedicated rockfall area. Such near-horizontal projectiles could enter, for example, a roadway and cause a hazard to the traveling public.

Secondary Impact Splatter

Impact splatter hazards could be considered a subset of shatter and results upon initial ice particle contact, where the substrate material yields and is sent travelling away from the point of impact. An example of this could entail an ice block impact in a wet, soil-filled rockfall ditch, where soil, water, and small fragments of rock are cast horizontally, resulting in debris entering the roadway.

ICEFALL CASE HISTORIES

Documented cases of icefall events impacting roadways, until recently, are hard to come by. There are numerous cases of icefall impact injuries in city environments, with the ice falling from bridges or tall buildings in cities like Chicago, Illinois (Willis Tower) and Dallas, Texas (Cowboy Stadium). There are also documented cases where ice climbers have been killed or injured by falling ice in alpine environments. However, there are only a handful of specific cases where icefall emanating from a slope has directly impacted a roadway resulting in injuries or damage. Cases of known icefall impacts to roadways include:

Seward Highway in Alaska, April of 2012

During spring melting, a very large slab (approx. 60 ft. in height) of ice fell and struck a small pick-up truck just south of the Anchorage city limits on 6 April 2012, seriously injuring the driver. It is the author's opinion that the slab became partially detached from the rock slope surface due to loss of adhesion, and that the bottom of the slab became fractured due to progressive increases in loading. Upon loss of strength at the base of the ice slab, failure likely commenced as a combination of near-vertical slab fall and subsequent crushing. This resulted in the generation of a large ice debris pile that developed outward and into the roadway. There was likely a minor rotational component of the failure as internal slabs fell, rotated, shattered, and entered the roadway. Note that the author was retained as an expert consultant relative to the event.



Figure 2 – Direct icefall impact damage to small pick-up truck along Seward Highway near Anchorage, Alaska. Photo courtesy of Anchorage Daily News, 6 April, 2012.

Terrace, British Columbia, 4 February 2011

A falling piece of ice near Terrace, British Columbia hit a Greyhound bus on February 4, 2011, resulting in an injury to the bus driver and the local highway and railway being temporarily shut-down (Figure 3 below).



Figure 3 – Icefall impact to tour bus outside Terrace, British Columbia. Photo from Terrace Standard, 15 February 2011.

U.S. Route 2, Gilead/Bethel, Maine

While employed with a previous employer (Haley and Aldrich, Inc.), the author was involved with projects that considered the effects of ice accumulation on rock slopes throughout New England. One such example was the U.S. Route 2 project in Bethel, Maine, where two ice shedding events resulted in icefall both during and after construction. The first event was in 2008 during construction, when an ice block measuring approximately 10 ft. in maximum dimension landed on a temporary bench. The second event(s) occurred in 2010, just after construction, when two to three smaller ice fragments, measuring between approximately 0.5 ft. and 2.25 ft. landed in the roadside ditch, with one block resting on the pavement at the white paint striping. Further down the project alignment, there was an additional icefall event in April of 2011, although the 2011 event was completely contained within the locally widened roadside ditch and snow mobile trail area. Although there were no safety incidents as a result of these icefall events, the Maine Department of Transportation (Maine DOT) took an aggressive approach after evidence of icefall, and the author completed an extensive icefall evaluation and developed feasibility-level icefall mitigation recommendations for the project.

Other Cases

It is likely that there are many other instances where icefall has impacted roadways which are as of yet unreported. The author has informally been told that a handful of DOT's in the Rocky Mountains and New England have observed evidence of icefall within catchment ditches during the time of the spring melt. Internationally, the Swiss and Norwegian Ministries of Transportation have dealt with icefall and have designed netting systems and/or barriers to mitigate the effects of icefall along specific transportation corridors. Finally, as reported by personal communication (Gauthier, 2013), there have been localized impacts to roadways in the Canadian Province of Quebec. Note that the author has also witnessed specific instances where ice has accreted to the outside of rock slope drapery and anchored netting type systems. In addition to loading the netting, at one such site the ice was found to shed from the outside of the system and impact the traveled way below.

ICEFALL MECHANICS

Large or global ice block failures are subject to the same mechanics as rock block failures (e.g. sliding, toppling, and falling). Ice block sliding for example can be assessed, at least preliminarily, with limit equilibrium slope stability analyses. Ice adhesion can be considered as an equivalent cohesion component of the stabilizing force, until melting commences at which point adhesion to the host rock surface is significantly reduced. These types of failure mechanisms in the source zone can be assumed at the moment of incipient failure; however, a block of ice observed at the side of a road may be perceived as an “icefall” event. Management controls dictate how such a failure is perceived and recognized. Source zone controls make use of design elements that are intended to manage the block in the source zone. Conversely, impact area controls are intended to allow for block failure and subsequent fall, but limit the horizontal distance that the block can travel. Understanding how large slabs of ice may fail can be helpful in estimating the impact area and risk to the traveling public (Figure 4).



Based on previous project-specific icefall analyses, the author has generally found the following to be true for preliminary icefall hazard evaluations:

- i. Conventional rockfall models can be used to complete sensitivity analyses and develop preliminary design evaluations;
- ii. Normal and tangential coefficients of restitution and block unit weight variations did not result in significant changes in block bounce height or horizontal travel;
- iii. As is the case with modeling rockfall on rock slopes, variations in slope surface roughness resulted in the most significant variations in bounce height and horizontal rollout distances.

Disadvantages to using a conventional rockfall analysis approach for icefall evaluations include:

- i. Reduced confidence and reliability of material substrate conditions based on climatic variations. Ice falling on loose dry-pack snow will produce different results than ice falling on rock;
- ii. Reduced reliability of slope substrate geometric properties, including surface roughness. An undulating ice surface will produce different results than a flat planar ice surface;
- iii. Difficult to quantify spatial and temporal variability of icefall source areas and substrate conditions, both of which are tied to climatic variability;
- iv. Difficulty in quantifying ice block material properties in the source zone, including thickness, density, and gradation.
- v. Mass reduction due to break-up, deformation, and shatter mechanics are not accounted for.

INDUSTRY STATE-OF-KNOWLEDGE & DESIGN CRITERIA

The engineering community in the United States (and Canada), particularly the civil and geotechnical engineering community, has historically been remarkably quiet regarding icefall hazards. During the author's evaluations of project-specific work, we wanted to define the nationwide level of industry knowledge regarding icefall hazards. We reached-out to federal transportation authorities and various state DOT's in U.S. northern tier states. The consensus was that icefall hazards were either not considered or not acknowledged, due to the following factors:

- i. Documented icefall events are relatively rare;
- ii. Evidence of injury resulting from icefall events is very rare;
- iii. No reliable industry-wide engineering design criteria that considers icefall;
- iv. Icefall is difficult to record and monitor due to potential for rapid phase change (i.e. melting);
- v. The location and development of ice is not consistent from year-to-year.

Furthermore, the definition of icefall is also open to interpretation, by those in the civil engineering community and by public officials and the media. True icefall events may be initially described as "avalanches", "falling ice", "falling snow", or "ice slides". With such

variation in how an event is initially defined and characterized, the quantity of true icefall events is likely under-reported.

Rockfall Hazard Rating Systems (RHRS) have been adapted for use by select DOT's nationwide, and provide a method for slope "ranking" based on roadway geometric characteristics and slope geotechnical properties. Many RHRS are state-specific due to regional geologic or climatologic features, with the first state-side RHRS being pioneered by Oregon DOT in 1989 (Pierson, 1991). The value of such a system is that it allows agencies to relatively rank slopes given state-specific geologic and climatic considerations as part of a broader rock slope inventory program, and provide for long-term monitoring and maintenance treatments and budgetary demands. Such a system does include a "Climate and Presence of Water" ranking category (or similar), and may consider the general effects of ice accretion on rock slope; however, currently icefall is not explicitly considered in RHRS's. Such a system could be adapted to include icefall explicitly, or a similar icefall hazard rating system could be created, using RHRS as an analog.

The Rockfall Catchment Area Design Guide (Pierson et al., 2001) put forth by Oregon DOT is another pioneering piece of industry available design criteria for the design of rockfall catchment ditches. The Design Guide provides much of criteria needed for ditch design; however, seeing that (as the name implies) it is intended for use associated with rockfall, icefall retention is not considered as part of the recommended ditch design procedure.

Given the facts presented above, rockfall catchment ditches in the United States and Canada are not specifically designed for icefall retention. Icefall may be retained de facto by relatively wide catchment ditches that were designed for high hazard slopes with significant rockfall problems. But for slopes in Northern Tier States with narrow catchment ditches and even for those with relatively low rockfall hazards, significant climate-dictated icefall hazards may present themselves and should be considered as part of the catchment ditch design process.

ICEFALL HAZARD ASSESSMENT FOR ROCK SLOPES

In regions subject to extended winter conditions, specifically the Northern Tier States, Alaska, and Canada, icefall hazard assessment should generally consist of the following steps:

- i. Hazard acknowledgement;
- ii. Observation and monitoring of ice build-up conditions during winter and early spring months (in the northern hemisphere);
- iii. Observation of rock slope conditions in spring and summer months, to look for signs of bedrock scour (e.g. polished surfaces), absence of overburden soil, rock slope surface irregularities where ice can accumulate, and evidence of vegetation damage (e.g. trees with sharp bends, loss of vegetation);
- iv. Identification of upslope water sources, including annual snowpack, persistent surface runoff, streams, and groundwater discharge;
- v. Where potential source areas for icefall have been identified, a monitoring program should be established, whereby a trained geotechnical engineering professional will periodically inspect the slope. It is entirely reasonable to assume that such a program

could be incorporated within the framework of a state-specific Rockfall Hazard Rating System (RHRS) and rock slope inventory program (RSIP). In states where no such programs exist, such programs can be initiated or a state-specific Icefall Hazard Rating System can be established. Icefall hazard studies can be initially focused on areas where ice development is documented or where icefalls have historically occurred;

Depending upon site-specific observations, site history of producing icefall events, level of risk to asset holders or public safety, and the climate in a specific region, specific slopes can be ranked, monitored, and if warranted, maintained. Defined icefall hazard areas can be tracked and updated using GIS-based asset management tools.

ICEFALL MITIGATION STRATEGIES

Icefall mitigation strategies, much like rockfall mitigation, can entail source zone or impact zone remedial treatments. Source zone treatments are implemented with the aim of either removing the hazard or securing material such that it does not exit the source area. Impact zone treatments allow for failure of the material at the source zone, but limit the horizontal movement of the falling material.

Source Zone Treatments

Given the technology currently available, source zone icefall mitigation treatments can include:

- i. Removal – Ice removal via mechanical means including machine or manual scaling, trim blasting, or possibly by use of impact cannon if the block is free-hanging on at least one side. If not completed by experienced contractors/operators, this can be dangerous;
- ii. Topographic Alterations – Includes slope re-design and/or re-grade, taking into consideration up-slope source area(s), with the intent of either limiting the accumulation volume of snow and ice or adding geometric features that allow for capture and retention. This also can include synthetic or natural vegetative topographic enhancements, like strategically-placed woody vegetation. Costs associated with re-design/re-grade can be significant, although results would be highly effective;
- iii. Enhanced Surface and Subsurface Drainage – As part of any re-grading efforts, alternative surface water drainage paths/areas can be designed and re-trained, to minimize presence of water on the slope. Internal (subsurface) rock slope drains can also be installed in specific cases, if warranted.

Impact Zone Treatments

Given the technology currently available, impact zone icefall mitigation measures can include:

- i. Dedicated Catchment Area – A designed catchment area, one which considers both ice and rockfall, is highly effective at capturing falling slope debris. Difficulties with

- such a remedial approach for existing slopes may include road shifting or controlled blasting in order to create horizontal width needed for such a ditch. Catchment areas designed only for rockfall may not be sufficient for icefall retention, given that ice blocks may be large and ditches may fill with ice or snow and be sloping toward the highway in the winter months;
- ii. Impact Barriers – High-energy impact barriers and fences, similar to those used for rockfall, can be fashioned to accommodate falling ice debris. Geobruigg has presented a case history in Switzerland where such a barrier was used for defense against ice slides. This is especially true if material is falling from beyond the back-slope and possesses a significant horizontal trajectory or if the roadside catchment area decreases in depth due to accumulation of snow and ice. Such barriers can be installed directly within the impact zone or anywhere between the source zone and impact zone, to capture falling up-slope material. Engineered wall or berms could also be considered. Barriers can be expensive and design must consider aesthetic impacts, maintenance requirements, and need to be designed with various snow and ice loading considerations. Secondary ice throw from primary impact also needs to be considered for roadside barriers;
 - iii. Rockfall Netting – Conventional and high-strength rockfall drapery can be fashioned for use to limit small to moderate volume ice accretions on rock slopes, although the mechanics of the application would be markedly different than for most typical slope drapes. Drapery has the propensity to actually attract ice due to its large surface area, opening width, and intrinsic permeability, so such drapes will require periodic maintenance. This treatment would not be applicable for large volume ice flows, as the material would simply adhere to the face and adhesive forces would be too significant to overcome and loading may over-stress the system. Such a treatment could be considered for both rock and icefall, and could be applied in both the source and impact zone. The Norwegian Ministry of Transportation has implemented combined rockfall and icefall netting systems, which make use of “stand-offs” or solid bar (e.g. rock bolt) type elements which keep the netting off of the face some defined distance. The intent of the stand-offs is to keep the ice within the limit of the netting, based on annually persistent ice development.

CONCLUSIONS

Icefall hazards embody “ghost” like attributes, and present significant difficulties for the civil (and even mining) engineering community and for hazard mitigation planners alike. Evidence of icefall can be observed one day, and gone the next due to changing climatic conditions. Documented icefall occurrence is somewhat rare in relation to rockfall. Given increased anthropogenic construction in remote areas and long-term forecasts for increased precipitation due to climate change, the increasing risk of icefall impacts to highway corridors and the traveling public is very real. Given limited case histories of documented impacts, constrained public budgets, and the absence of icefall mitigation design criteria from the engineering community, government regulators and civil engineers alike have had very little to work with.

Based on the author's experience evaluating icefall hazards, we recommend that state and federal authorities (e.g. FHWA, DOT's) consider including the effects of ice development on rock slopes, as part of state-specific RHRS's. For states where such a program exists, capital investment costs will be minimal. For states where no such mechanism currently exists, such a program should be initiated. The capital investment required for such a venture could be relatively significant if starting new. In order to minimize up-front financial impact, an initial risk-based evaluation (preliminary ranking program) could be completed for rock slopes with observed ice build-up and/or documented evidence of icefall, and short to intermediate term solutions can be adapted. Given the relationship between ice accumulation and rockfall, the most efficient monitoring mechanism would be to consider both ice and rock in any long-term monitoring program.

Ice accumulation abatement and icefall mitigation technologies are still in their infancy, particularly for geotechnical features like rock slopes. Source zone treatments, as described herein, can require significant expense, construction time, and aesthetic impacts. Impact area treatments, for example adjacent to a roadway, can also be expensive and unsightly, and can require significant long-term maintenance. All designed mitigation strategies need to take into consideration reduced reliability due to snow and ice loading and snow/ice thickness variability. For the case of excavations, the slope design process needs to take icefall into consideration in order to avoid costly "after-the-fact" remedial treatments like re-excavation/redesign, scaling, mesh drapery, or high-energy impact barriers.

Current rockfall catchment ditch design criteria does not explicitly incorporate ice development and its impacts on rock slope stability, including rockfall and icefall. Icefall impacts to the roadway generally occur with slopes that have limited rockfall catchment ditch widths. Slopes that present limited rockfall hazards may still pose significant icefall hazards because ice can develop on a relatively clean and stable slope face. For proposed new rock slopes and those existing slopes that will be trim blasted for remedial purposes, the roadside ditch must be designed with both rockfall and icefall in mind.

As a final remark, the assessment of ice accumulation on slopes requires an interdisciplinary approach, with input from experts in geotechnical engineering, avalanche hazards, glacial geomorphologists, and cold-regions engineering practitioners. Hazards directly adjacent to the slope would be considered by geotechnical engineers; however, if frozen accumulation is large-scale (e.g. regional) and not just localized, avalanche hazard specialists may provide useful insight into when snow will undergo thermodynamic changes into ice, or alternatively, where up-slope frozen deposits have slope profiles that are conducive to large run-out icefall or ice slide events.

REFERENCES:

Gauthier, F., Personal Communication, Center for Natural Hazards Research at Simon Fraser University, 16 August 2013.

Hoek, E., and Bray, J.W., 1981: *Rock Slope Engineering*, London Institute of Mining and Metallurgy, E & FN Spon, 358 pp.

Pierson, L.A., Gullixson, C.F., Chassie, R.G., 2001: *Rockfall Catchment Area Design Guide*, Oregon Department of Transportation and Federal Highway Administration, 78 pp.

Pierson, L.A., 1991: *The Rockfall Hazard Rating System*, Oregon Department of Transportation, 11 pp.

Scarpato, D. & Woodard, M., 2012, *Evaluation & Mitigation of Icefall Hazards for Civil Engineering Works*, International Snow Science Workshop (ISSW), Anchorage, Alaska.

Varnes D. J., 1978: *Slope movement types and processes*, Landslides, Analysis and Control. Transportation Research Board, Sp. Rep. No. 176, pp. 11–33.

<http://www.thenorthernview.com/news/115565779.html>, *Greyhound bus is hit by falling ice on highway*, February 8, 2011 edition.

http://www.terracedaily.ca/show7605a0x300y1z/GREYHOUND_STRIKES_FALLING_BLOCK_OF_ICE_ON_HIGHWAY_16, February 5, 2011.

<http://www.adn.com/article/20120412/transportation-department-investigating-ice-fall-trapped-woman>, April 12, 2012.

<http://www.adn.com/article/20120406/falling-ice-traps-driver-closes-highway>, April 6, 2012.

Stabilization of Paleo Stream Deposits Using High Tensile Steel Mesh

Scott D. Neely, P.E.

Terracon Consultants, Inc.
4685 S. Ash Avenue; Suite H-4
Tempe, AZ 85282
(480)-897-8200
sdneely@terracon.com

Prepared for the 66th Highway Geology Symposium, September, 2015

Acknowledgements

The authors would like to thank the individuals/entities for their contributions in the work described:

ADOT Geotechnical Section
Jackie Noblitt – Stanley Consultants, Inc.

Disclaimer

Statements and views presented in this paper are strictly those of the authors, and do not necessarily reflect positions held by their affiliations, the Highway Geology Symposium (HGS), or others acknowledged above. The mention of trade names for commercial products does not imply the approval or endorsement by HGS.

Copyright Notice

Copyright © 2013 Highway Geology Symposium (HGS)

All Rights Reserved. Printed in the United States of America. No part of this publication may be reproduced or copied in any form or by any means – graphic, electronic, or mechanical, including photocopying, taping, or information storage and retrieval systems – without prior written permission of the HGS. This excludes the original author(s).

ABSTRACT

The SR 87 Curve Realignment project is located north of the Phoenix metropolitan area approximately 40 miles and was partially required due to safety issues related with accidents, some of which were fatalities because of how tight the curve was and that it is located at the bottom of a 6% grade that is 4½ miles in length. To flatten the curve, the existing hillside must be excavated and the resulting slope stabilized. Though the existing paleo-stream deposits on the slope did not appear to be unstable, they could not meet the minimum factor of safety (FOS) of 1.5 in accordance with Arizona Department of Transportation (ADOT) requirements. The new slope cut into the paleo-stream deposits would have to be designed to meet the minimum FOS requirement. Existing slope geometry inhibited laying the slope back sufficiently to meet the minimum required FOS, therefore, a slope stabilization system using high tensile steel mesh and grouted bar anchors was chosen from a list of five options to stabilize the slope. This paper will present the other alternatives and their shortcomings, and will provide the advantages and disadvantages, costs and logistics of the high tensile strength steel mesh and grouted bar anchor stabilization alternative.

INTRODUCTION

The project site is located along State Route 87 (SR 87) about 40 miles north of the Phoenix metropolitan area. The highway is bifurcated for most of its length from Mesa to Payson, Arizona. At the project location, the highway was not bifurcated and is adjacent to Slate Creek. The project site is at the bottom of approximately 4½ miles of 6% grade roadway. A truck escape ramp was part of the project and was located about 1-mile uphill of the project site (See Figure 1)

In Figure 2, the photograph shows the highway previous to this project had both directions of traffic at the same elevation and the super was below current standards. This project flattened the curve (increased the radius of curvature), created grade separation between the north and south bound lanes, increased the ditch width to 15 feet, and required the stabilization of the slope south of the roadway.

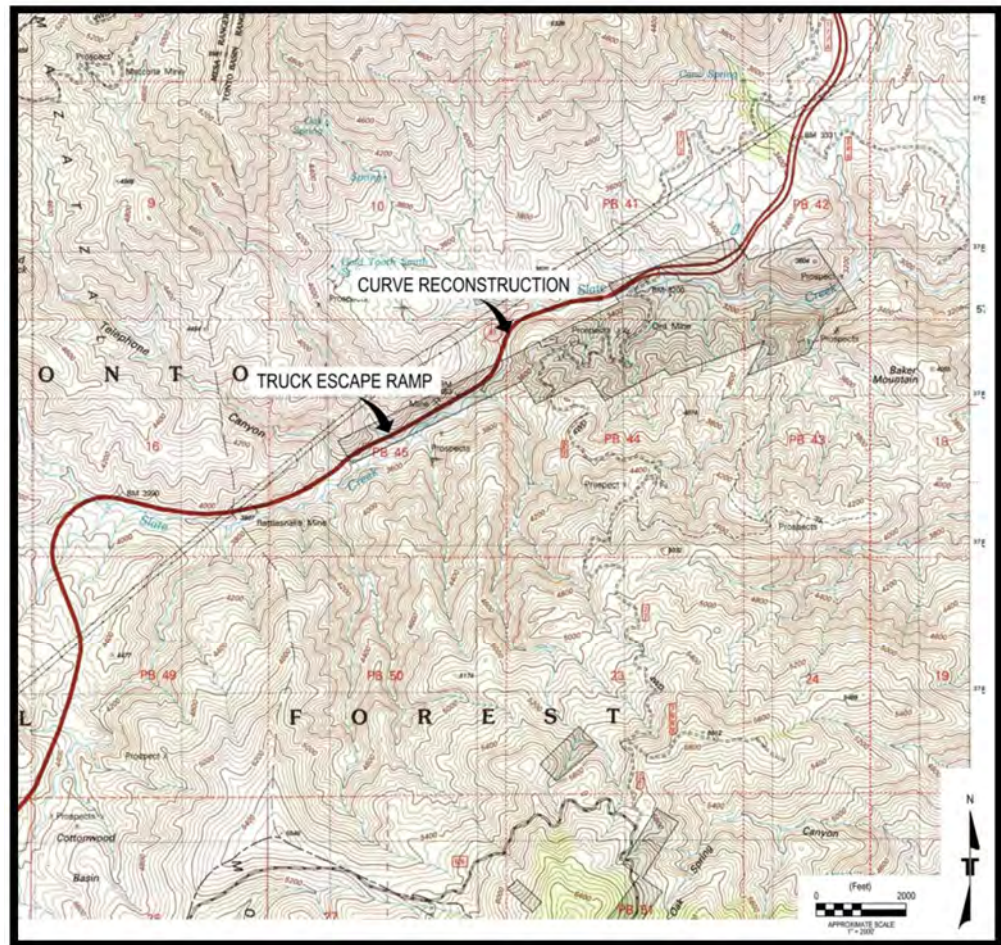


Figure 1 - Topographic Map of the Project Site.

The cut slope area to be stabilized is about 50,000 square feet and existed at a slope of about 1.3H:1V (horizontal:vertical) prior to construction. The factor of safety of the existing slope was below the minimum requirement of 1.5. Due to the 1.3H:1V slope of the ground above the cut slope area it could not be laid back at a slope ratio that would increase the factor of safety to 1.5 and therefore, the ground needed to be stabilized to meet the minimum factor of safety requirement.



Figure 2 – Photograph of the Curve Realignment looking north.

GEOLOGIC SETTING

The geology at the project site curve realignment site is characterized by paloe-stream deposits overlying primarily phyllite, a transitional unit between the slate/ schist and the quartzite. The paleo-stream deposits were presumably deposited by Slate Creek sometime in the past. The phyllite is a relatively soft rock with moderate to low strength which mechanically degrades over time. The quartzite is a very hard rock present on the higher portions of the existing slopes.

Foliations within the phyllite and quartzite generally dip at between 60 and 85 degrees to the north-northwest as mapped by (¹Spencer, et al, 2004). We measured the foliations within the phyllite and quartzite to be dipping at between 64 and 89 degrees at azimuths between 294 and 348 degrees (west-northwest to the north-northwest). Our measurements agreed well with the orientation of the foliation as mapped by Spencer. Three joint sets were measured within the quartzite. Two of the joint sets are nearly vertical while the third joint set is dipping at 54 degrees at an azimuth of 042 degrees (northeast).

EXPLORATION TECHNIQUES

Terracon's field exploration program was performed in two phases, with the first phase comprised of five borings advanced by coring methods and three hollow stem auger (HSA) borings. To increase our coverage of the site at a relatively low cost, 13 geophysical surveys were performed to better assess the subsurface conditions across a larger portion of the site. The borings located on the side of the hill were advanced using helicopter mobilized drill rigs using HQ3 coring methods. The hollow stem augers were advanced in the existing roadway with a truck-mounted CME-75 drill rig utilizing 4¼-inch inside diameter hollow-stem augers.

Terracon completed seven seismic refraction traverses (SL-1 thru SL-7) and three multi-electrode resistivity (MER) lines (RL-1 thru RL-3) within the proposed slope cut area of the project. The seismic refraction lines used a DAQLink III seismograph with 24 geophones to derive the subsurface seismic velocity information. The MER lines used an Advanced Geosciences Inc. (AGI) SuperSting and 112 electrodes. The dipole-dipole method of collection was used, to derive subsurface resistivity information.

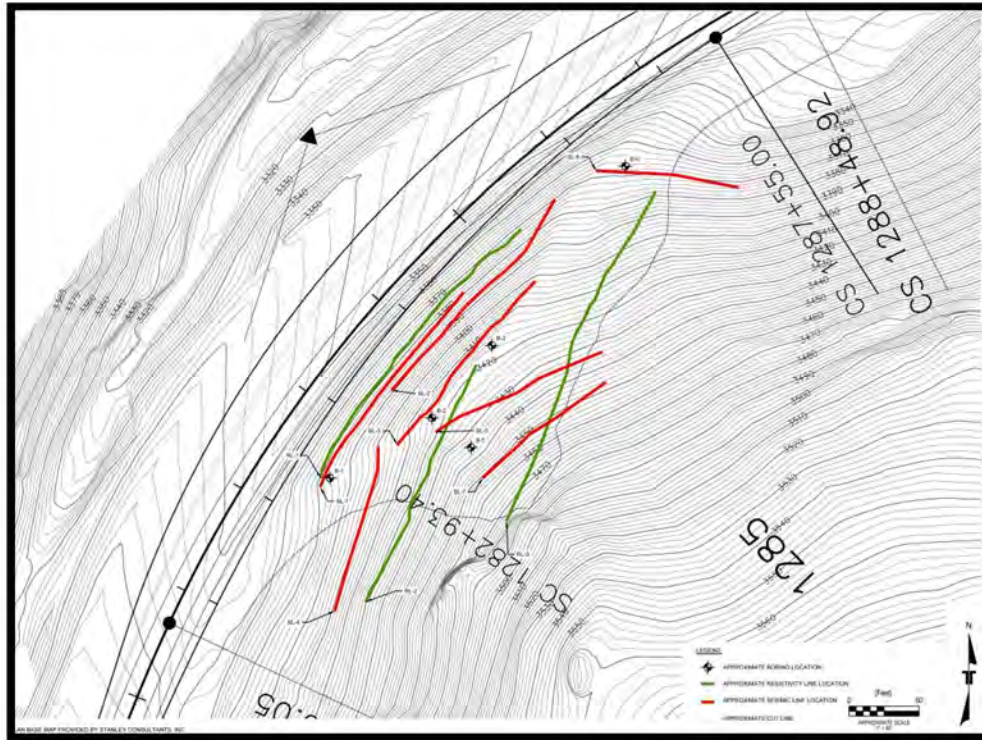


Figure 3 – Site Plan of Boring and Geophysical Locations

CUT SLOPE SUBSURFACE PROFILE

Results of the field exploration indicated there were paleo-stream deposits consisting of poorly graded gravel with clay and sand overlying early Proterozoic phyllite or quartzite. The borings indicated the stream deposits varied in vertical thickness from about nine feet to 40 feet and contained cobbles and boulders within the deposition. The stream deposits are uncemented to slightly cemented. The underlying phyllite and quartzite bedrock materials were completely

weathered to slightly weathered. The degree of weathering varied with no specific correspondence between depth and degree of weathering.

The percent recovery of the core samples obtained within the stream deposits varied from 12 to 95, with a Rock Quality Designation (RQD) of 0%. The percent recovery of the core samples obtained within the phyllite varied from 57 to 100, with RQD values in the range of 0 to 34, with an average RQD of about 8. The percent recovery of the core samples within the quartzite varied from 10 to 85, with an average RQD of about 23.

The purpose of the seismic refraction and MER surveys was to determine the boundary between the paleo-stream deposits and the underlying phyllite bedrock materials. The presumption in the seismic refraction analyses, was that the paleo-stream deposits would have a slower p-wave velocity than the underlying phyllite bedrock materials. The presumption in the MER analyses, was that the paleo-stream deposits would have lower resistivity due to the infiltration of surface water. The analysis for either method therefore involved determining the location of the bottom of the paleo-stream deposits and the top of the undisturbed phyllite bedrock by interpreting the change in p-wave velocity or resistivity with depth.

Typically, materials having a p-wave velocity less than 5,000 feet per second are considered to be soil and those materials with a p-wave velocity above 5,000 feet per second are considered intact bedrock. The results of the seismic refraction surveys indicated p-wave velocities typical of soil extending to depths of 30 to more than 60 feet at the location of the surveys. However, using the depth to bedrock as determined in the borings and plotting this depth on the corresponding seismic survey, the upper bedrock materials fall within the soil like p-wave velocity range. Based on the p-wave velocity of the bedrock materials encountered throughout the entire project site, the completely weathered phyllite and quartzite have engineering characteristics more characteristic of dense soil rather than weak bedrock. As observed on the site, the quartzite has highly variable weathering, with some of the quartzite characteristic of a dense soil and other portions of the bedrock standing vertical above surrounding grades for approximately 20 feet (See Figure 2).

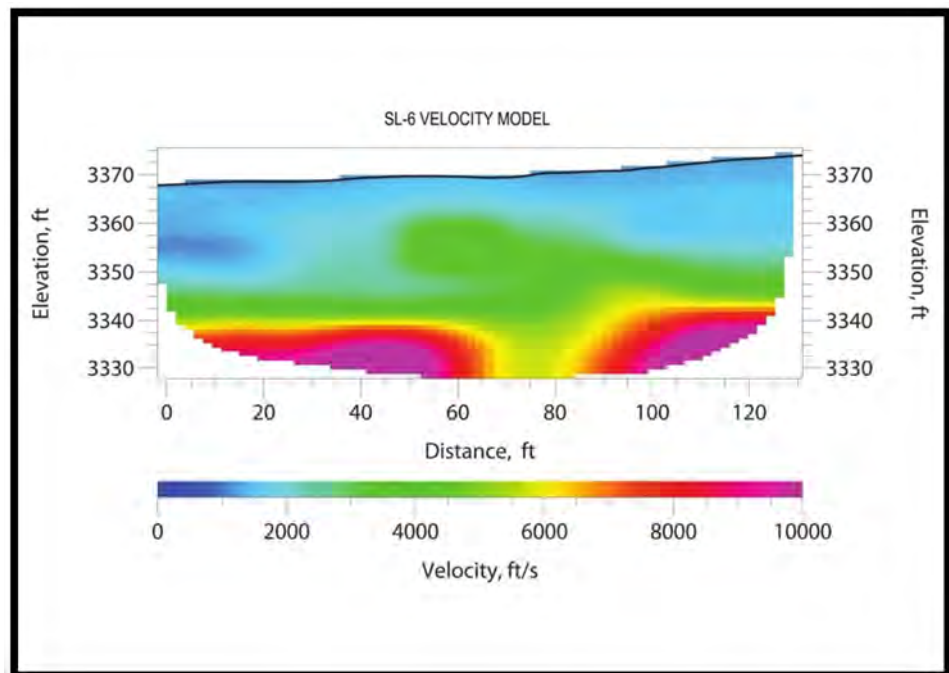


Figure 4 – Typical Plot of Seismic Refraction Line Survey

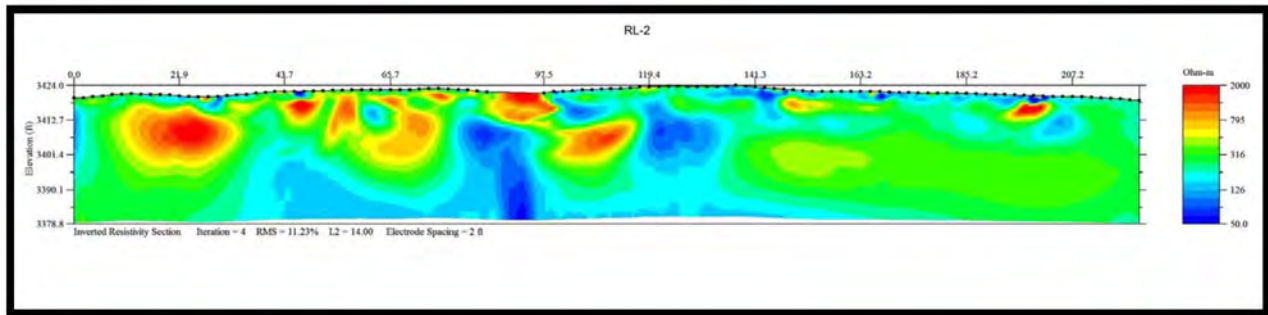


Figure 5 – Typical Plot of MER Line Survey

The actual field conditions as encountered during the drilling of the anchors generally supported the exploration results though the stream deposits were 0% to 20% thicker than indicated by our exploration. The MER survey results were too ambiguous to be of any use, and therefore were not considered in the final analyses of the subsurface conditions.

CUT SLOPE STABILIZATION ALTERNATIVES

The long term stability of the slope was entirely tied to and dependent upon the stability of the stream deposits. The previously existing paleo-stream deposits on the 1.3H:1V slope cut were determined to be at an approximate factor of safety of 1.0 against slope instability. Flattening of the slope cut angle without other retaining structures was not physically possible, as a flatter slope would not have daylighted at the top of the slope cut. Therefore, any slope configuration to be considered for this project would need to be 1.3H:1V or steeper and would need to be able to stabilize the paleo-stream deposits since it had the lower shear strength of the two materials encountered on the project.

Based on the foregoing information and analyses, and a desire to reduce the visual impact of any reinforcement, various alternatives were considered and their relative risk and costs were estimated. The alternatives are presented below and are generally in the order of expected increasing cost of construction and decreasing risk of slope instability and required maintenance.

- **Alternative 1** - Cut the slope at 1.3H:1V and expect debris to erode and slough to the bottom of the slope. This alternative would require a constant maintenance effort to clear the area and roadway. A flatter slope angle without other retaining structures is not physically possible as it will not daylight at the top of the slope cut. Total cost for approximately 41,000 cubic yards of excavation was about \$450,000.
- **Alternative 2** – Considering the relatively small amount of stream deposits remaining after the slope has been excavated to a 1.3H:1V configuration, a slight variation on Alternative 1 was considered and included the removal of all the stream deposits down to the phyllite bedrock surface. This would have increased the amount of materials removed from the project but would have also reduced the risk of slope instability and the future maintenance associated with leaving this relatively thin layer

of stream deposits in place. This alternative would have also exposed a large amount of the quartzite outcrop at the top of the hill and put at risk a toppling failure of the outcrop. Total cost for approximately 50,000 cubic yards of excavation was about \$550,000.

- **Alternative 3** - Cut the slope at 1.3H:1V and add reinforcement consisting of steel wire mesh anchored by rock bolts to increase stability of the excavated face to a minimum factor of safety of 1.5. Some wire mesh products can be colored to match the color of the weathered rock. Total cost for approximately 30,000 cubic yards of excavation and 50,000 square feet of mesh and 12,600 feet of anchor length was about \$1,000,000.
- **Alternative 4** – This alternative would have been similar to Alternative 3 in that the slope would have been cut at the proposed 1.3H:1V configuration angle, and then concrete plates would have been anchored with rock bolts to stabilize the stream deposits. The concrete plates could have been suppressed into the ground a couple of feet and then buried after the anchors had been loaded and tied off. Thus the reinforcement would be less visible than the wire mesh alternative. This alternative was not priced as it was aesthetically not acceptable.
- **Alternative 5** – Multi-tiered soil nail walls. Preliminary analyses indicated a three tiered wall system would have been required to stabilize the slope at the maximum section. This alternative was not priced due to poor performance of soil nail walls in the vicinity and it was not aesthetically acceptable.

At the completion of a design team meeting it was decided that Alternative 2 was the preferred alternative. However, after further exploration and analyses, Alternative 2 was not considered feasible and the recommended alternative for slope reconstruction became Alternative 3. Due to the amount of “sliver” cuts that would have been created near the top of the cut slope with a 1.3H:1V slope ratio, it was decided to increase the slope to 1.2H:1V and thus reduce

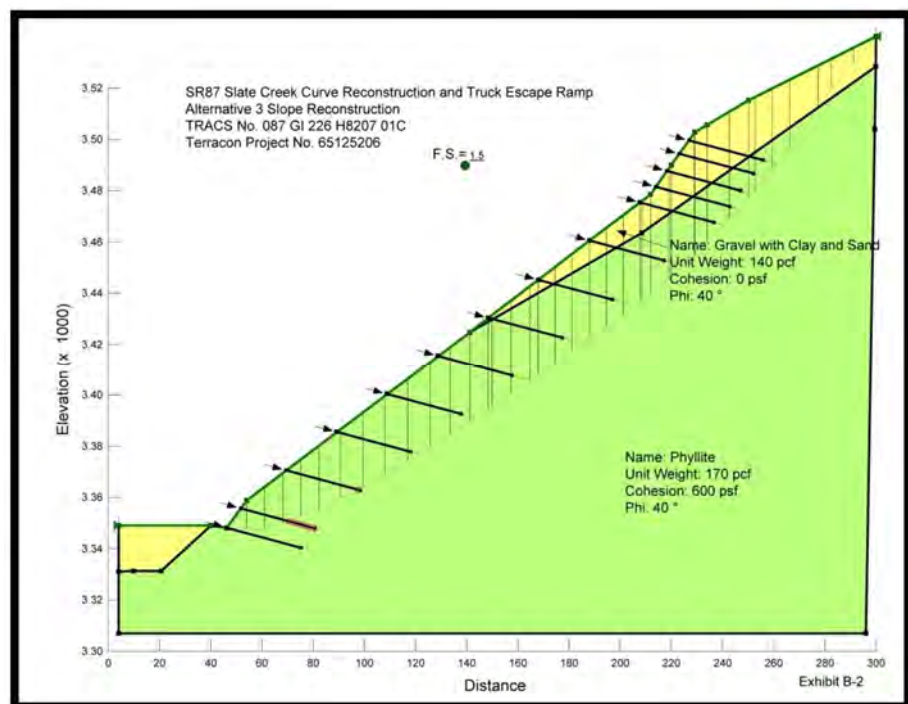


Figure 6 – Cross Section of Alternative 3 showing the potential failure plane.

the “sliver” cuts that would have been required. A gabion basket slope ditch was added at the top of the cut slope to reduce the erosion potential of surface water from above the slope causing significant soil movement. A cross section of this alternative without the gabion basket slope ditch is shown as Figure 6.

DESIGN PARAMETERS

Shear strength parameters used for the stability analyses of existing and conceptual slope configurations were based upon laboratory data developed during our exploration, laboratory test data, correlations to field and laboratory test data, experience with similar soils/bedrock and end use conditions. The shear strength data used in the engineering analyses is summarized in Table 1.

TABLE 1			
Material Type	Drained Shear Strength Parameters		Ultimate Grout to Ground Bond Stress (psi)
	c' (psf)	φ'	
Paleo-Stream Deposits	200	40	30
Phyllite Bedrock	600	40	30

Since we did not know definitively how much of any single anchor would be founded in the paleo-stream deposits vs. the phyllite bedrock, one single grout to ground bond stress value was used for the entire project. The factor of safety applied to the ultimate grout to ground bond stress was 2.0, and thus the allowable bond stress was 15 psi.

Two verification tests were performed, one in the phyllite bedrock and one in the paleo-stream deposits. The verification test drilled within the phyllite was drilled to a depth of 25 feet and 4 inches in diameter. The bonded length was 15 feet. The verification test within the paleo-stream deposits was drilled to a depth of 15 feet, was 4 inches in diameter and had a bonded length of 12 feet. The verification test was loaded to 200% of the design grout to ground bond stress at the phyllite test location and to 300% at the paleo-stream location. After subtracting the elastic elongation of the bar from the total deflection, the deflection within the phyllite bedrock was 0.068 inches, while the deflection within the paleo-stream deposits was 0.29 inches.

Both verification test anchors showed nearly linear displacement vs. load graphs and did not have any creep during the 10 minute hold interval. For the paleo-stream deposits where the test was increased to 300% of the design stress, indicates the bond stress is much higher than 45 psi, which is triple the design stress.

STABILITY ANALYSES AND SLOPE MESH STABILIZATION DESIGN

The design of the slope mesh stabilization system was performed considering internal system performance and global stability.

The design of the mesh slope stabilization system was based on the computer program RUVOLUM developed by GEOBRUGG of Romanshorn, Switzerland. In general, this program models shallow infinite and localized slope type failures. Stability is increased when the mesh slope stabilization system and intermediate nails/anchors are applied in the model. This approach of stabilizing near surface soils was exactly our scenario on this project, and therefore, the use of this program and the mesh slope stabilization system was chosen to stabilize the slope.

The program RUVOLUM performs analyses of the entire system including the grouted bar anchors, high tensile steel mesh, steel plates, subsurface conditions, and geometry of the slope. The program considers sliding of the entire soil mass parallel to the slope at a specified depth, soil wedges moving out from between rows of grouted bar anchors, shear of the grouted bar anchors, and punching shear of the high tensile strength mesh. Schematic cross sections of these potential failure modes are shown in Figure 7.

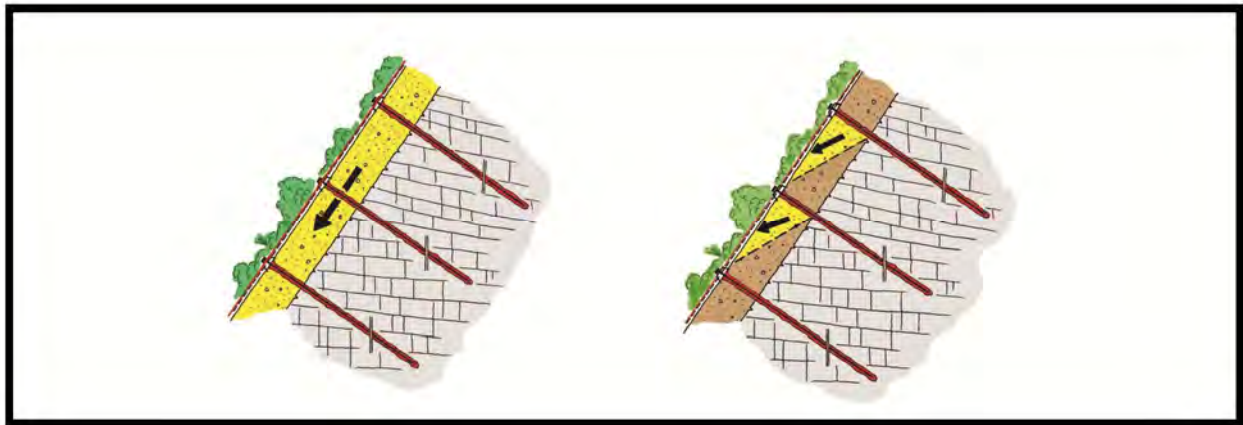


Figure 7 – Cross Section of Slopes with Potential Failure Parallel to the Slope Face and Potential Failure Between Rows of Anchors

The global slope stability analyses were performed using Slope/W slope stability software and the general limit equilibrium method (GLE) of analyses. Multiple cross-sections were modeled at varying slope heights in order to determine the required number and length of anchors. The final outcome of the global stability analyses is shown in Figure 6 above. It should be noted that the length of the anchors varied from 15 to 40 feet depending on overall slope height. This is not due to the load on the anchor from the mesh system, but rather the requirement to increase the global factor of safety to the minimum 1.5. Much shorter anchors could have been used if their only purpose was to hold the mesh slope stabilization system in place.

CONCLUSIONS

- The use of geophysical surveys was instrumental in increasing our coverage of the site at a relatively low cost, however, the results are harder to interpret.
- The use of the high tensile steel mesh was key to stabilizing the near surface paleo-stream deposits encountered on the site.
- The grouted bar anchors add significantly to the global stability of the project, and were the determining factor on increasing the global stability to the minimum factor of safety of 1.5.



Figure 8 – Photograph of the finished cut slope with the mesh fully installed and the seeding effort half completed.

REFERENCES:

1. Spencer, J.E., et al, 2004, *Compilation Geologic Map of the Reno Pass Area, Central Mazatzal Mountains, Maricopa and Gila Counties, Arizona*, Arizona Geological Survey, Open File Report 04-03, Tucson, Arizona.
2. Neely, S.D. and Clark, D.R.; *Geotechnical Engineering Report; Slate Creek Curve Reconstruction and Truck Escape Ramp; SR87, MP 226 and MP 229, Gila County, Arizona*, Terracon Consultants, Inc., Project No. 65125206, dated August 13, 2013.

3. RUVOLUM; *Manual for the software to dimension the TECCO slope stabilization system*, Geobruigg AG Protection Systems, dated July, 2008 – E03/DF.
4. Neely, S.D., *Slate Creek Curve and Truck Escape Ramp Design Plan Set, Sheet Nos. 42 through 48 of 109*, Terracon Consultants, Inc., Project No. 65125206, dated June 6, 2014.

Rockslope Stability in Karst Terrain

Vanessa C. Bateman
Chief, Geology Section
Nashville District, US Army Corps of Engineers
vanessa.c.bateman@usace.army.mil
615-736-7906

Abstract

While the risks associated with sinkholes in karst terrain are well documented, the risks to both the public and infrastructure that are presented by both natural and man-made rock slopes in karst terrain are often misunderstood. Rock cut design, even where a rockfall catchment ditch is included, seldom accounts for the unstable epikarst zone and for the secondary toppling failure mode in more competent rock evident in many karst areas. Vertical karst chimneys and weathering along joints can produce substantial stability problems in the remaining rock face. The secondary toppling failure mode often develops from the combination of solution widened joints in the rock face and from differential weathering of the rocks in the stratigraphic sequence. This failure mode is most often forgotten where the geology is relatively flat lying leading practitioners to discount the possibility for a structurally controlled rock failure in an area that is not considered to be structurally complex. Where the epikarst zone is deep, this can leave large unstable rock boulders and columns surrounded by soil that are relatively stable in-situ, but present rockslope stability risks where they are exposed. The geology of middle Tennessee, particularly in the outer Central Basin, Highland Rim and at the margins of the Cumberland Plateau is such that many of these problems can be expected and these issues should be accounted for in design. Illustrations of these problems are given from multiple sites including the Cordell Hull Dam access road, Center Hill Dam Left Rim Grouting platform and along several Tennessee highways.

Introduction

Karst terrain presents many challenges to the practitioner and while the risks associated with sinkholes are well documented, the risks to the public and infrastructure by natural and man-made rock slopes are often misunderstood. Practitioners with insufficient knowledge, or who do not engage geologists in the design process can often mistake these areas as presenting little risk for overall rock slope design. Much energy is expended on looking for sinkholes, while overlooking the problems on rock cuts or natural rock slopes. The problem is compounded in areas where the rock is not considered to be structurally complex and the bedding is relatively flat-lying. This can lead a practitioner to a false sense of security that there will be no structural problems with a rock cut in these areas. However, there are few sedimentary rock formations without any structural features (joints, faults, valley stress relief features, etc.). Differential weathering of exposed formations can interact with these structural features to cause problems such as secondary toppling, particularly where there are vertical karst chimneys present in the rock or where there are joints/faults that are parallel or sub-parallel to the existing rock face. Additionally, the “mudcutters,” as they are often called in Tennessee, in the epikarst zone can extend much farther into the rock than is often initially supposed. This can leave large boulders or columns that are surrounded only by soil. These may be perfectly stable in-situ, but when exposed are unstable and can lead to substantial increases in construction costs.

Two mini case studies are included in this paper to illustrate the potential problems: Cordell Hull Dam access road and the Center Hill Dam Left Rim Grouting Platform. The Center Hill project is used as an example of constructed rock slopes that encountered more extreme epikarst. The Cordell Hull Dam Access Road project is used to discuss the problems presented by an already existing slope. Three illustrations from rock cuts along Middle Tennessee highways are also included in order to demonstrate that these are not isolated problems.

Geology of Central Tennessee

The geology of the Middle Tennessee Region provides a good setting to explore the rock slope stability problems in karst terrain. Figure 1 below shows the Physiographic Provinces of Tennessee. Projects in this paper are located at the margins of the Central Basin and the Highland Rim and are shown on the figure.

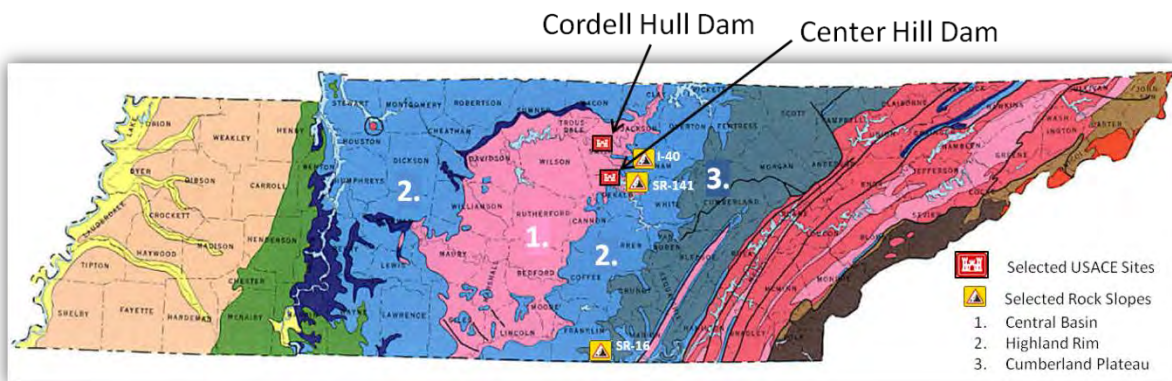


Figure 1. Physiographic Provinces of Tennessee with selected sites shown¹

The pink area in the central part of the state is the Central Basin. It contains gently dipping, near horizontal Ordovician limestone formations that with some shale members [Lebanon Limestone, Carters, Hermitage, Bigby-Cannon and Leipers-Catheys Limestone]. The Highland Rim, shown in light blue surrounding the Central basin is generally underlain by Mississippian age limestone and chert [Fort Payne Formation] as well as Devonian shale [Chattanooga Shale]. The central part of Tennessee is a topographic basin, but a structural dome, with numerous joints cutting the formations.

Cordell Hill Dam Access Road

Moore's bluff, which rises above the Cumberland River on the right bank of the River along and below Cordell Hull Dam consists of relatively flat lying limestones of the Hermitage Formation at the base, followed by the Cannon member of the Bigby-Cannon formation. The Hermitage Formation at this

¹ After Tennessee Division of Geology, *Generalized Geologic Map of Tennessee*; accessed February 2012: http://www.tn.gov/environment/tdg/images/geolog_1.jpg and Miller, R.A., 1974, *The Geologic History of Tennessee, Bulletin 74, State of Tennessee, Department of Environment and Conservation, Division of Geology.*

location is relatively shaley and thin bedded. It weathers far more readily than the massively bedded, Cannon formation. Bedding is flat lying with an overall regional dip of two degrees ESE. Regional vertical joints, some of which are solution widened and valley stress relief joints are present and nearly parallel to the bluff face. These well developed joints interact with the bedding planes and differential weathering of the Hermitage formation to cause numerous large rockfalls. The more massive bedding of the Cannon Formation means that these blocks can reach a considerable size.²

The access road to Cordell Hull Dam in Carthage, TN illustrates the problems that can develop over time in a natural rock cut in karst terrain. This access road had experienced numerous small rockfalls over the years, but the number and size started accelerating in 2011. This rock cut, was made by the river with some small scale blasting used to widen the cut at the base to widen the road and provide parking for fishing access. Differential weathering of some of the Hermitage shaley layers at the base was mitigated by a shotcrete finish, but overall most of the cut was left in its original condition. A scaling contract was let in 2012 to address these problems and remove the large unstable columns and boulders on the face.



A: Photo taken 16 January, 2010



B: Photo taken 30 November, 2011

Figure 2. Photos of Rockfall along Cordell Hull Dam Access Road from 2010 and 2011

Numerous vertical joints daylighted on the face of the cut, leaving large columns and boulders in place on the slope. These columns reached considerable size, some extended more than halfway up the more than 100 ft bluff. Over time as these joints weathered the face became increasingly unstable with larger boulders falling. Photo A in Figure 3 shows a widened joint exiting the face for most of the bluff height in 2010. Photo B in Figure 3 shows the joint taken in 2012 after the vegetation was cleared from the face. Workers and man-lift shown in the photograph give an idea of scale. Over time, these joints widen and the column becomes increasingly unstable and can rotate outwards onto the road. Figure 4 shows a massive column of rock that has separated from the face with an open joint on either side of the block shown. The center of gravity of this large boulder was slowly moving outwards as the small wedge below weathered faster than the overlying rock and root and ice jacking continued to open the joint. It was still being supported by a small wedge of rock, but the block itself was very unstable and was removed during the 2012 scaling contract³.

² Elson, M. et. al. USACE Cordell Hull Bluff and Bank Stabilization and Rip Rap Repair, Cordell Hull Dam, Carthage, TN Section 31 23 05.01, Contract: W912P5-09-D-0010-0005, 2012.

³ Contract to GCCS, Inc. Louisville, KY with rock scaling subcontractor Ameritech Slope Constructors, Asheville, NC



A: Column Above Comfort Station



B: Close up taken in 2012

Figure 3. Two Photos of a Typical Rock Joint Exiting the face at Moore's Bluff causing stability problems at the site. Note shotcrete at the bottom of the slope placed to protect the lower shaley layers from differential weathering.

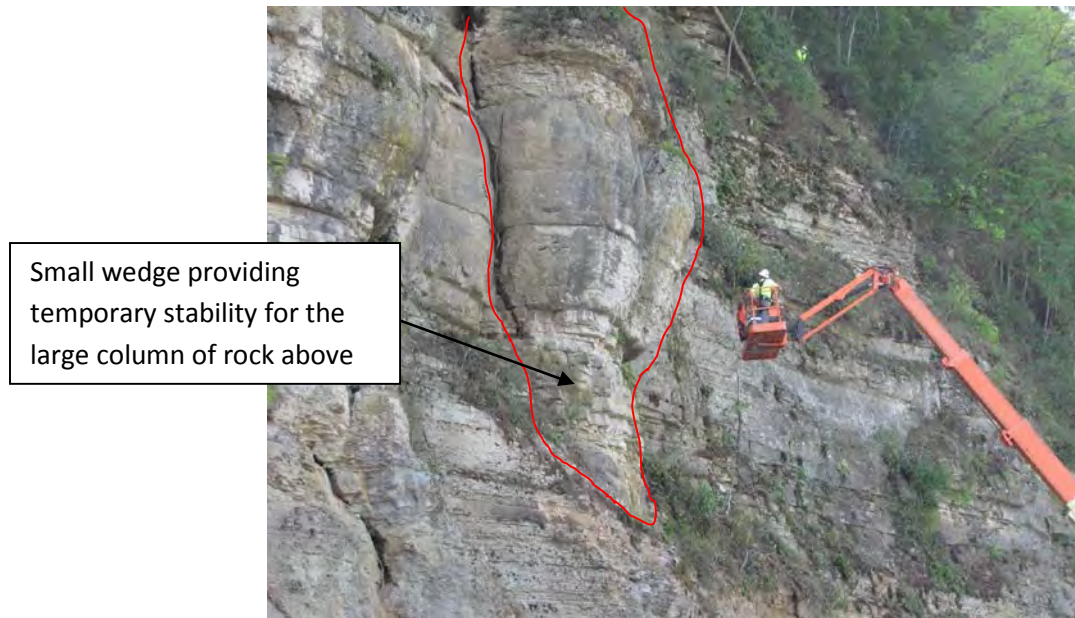


Figure 4. Large Column at Station 20+50

Many of these large columns on-site were removed by using air-bags placed in the opened joints behind them. These large boulders were actually already completely detached from the surrounding rock fabric, and were being held in place by a center of gravity located just behind their existing footing which was continuing to weather. Figure 5 shows the removal of one of these large columns by use of an airbag.

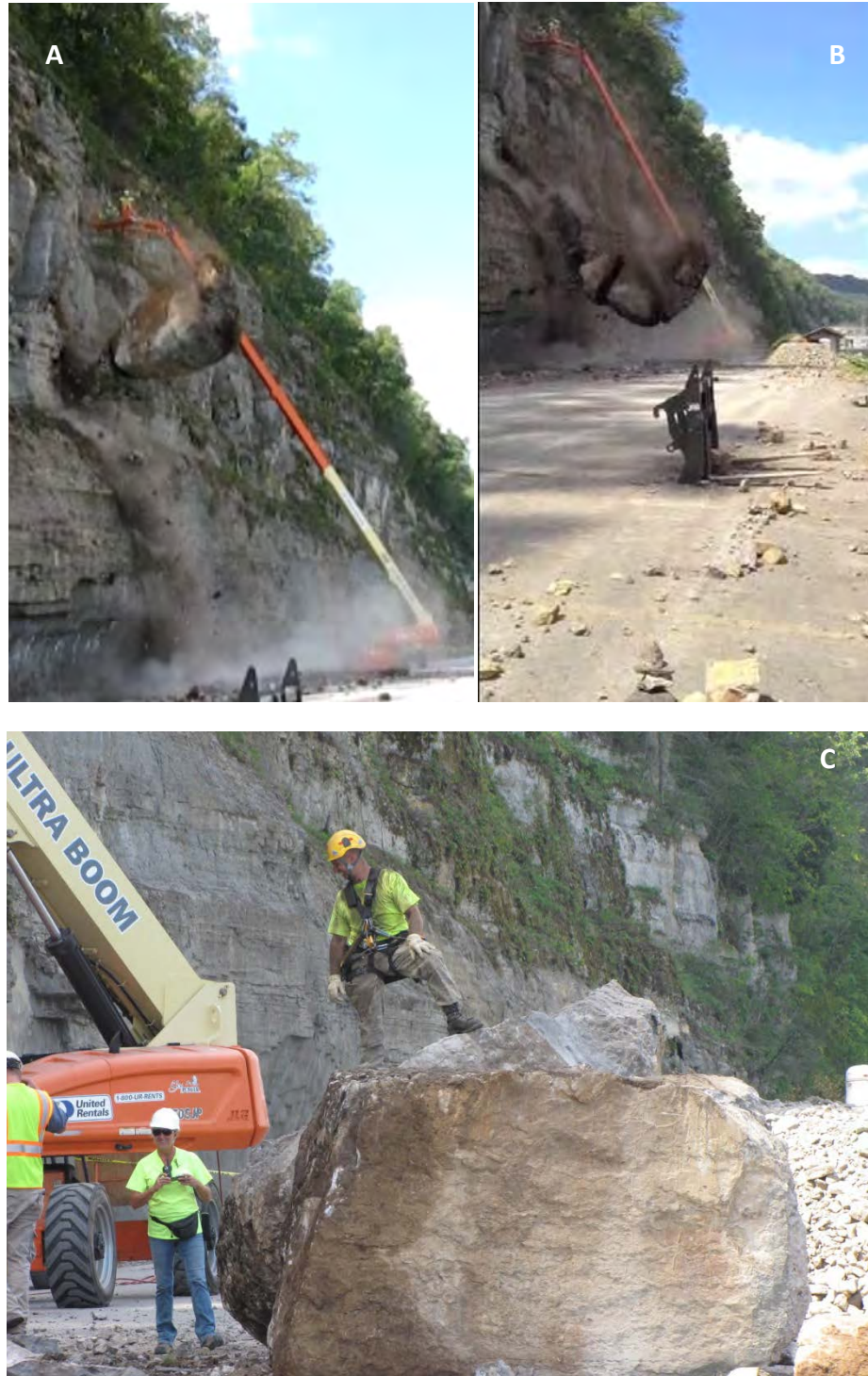


Figure 5. Removal of Large Boulder on Slope by Air-bagging in Joint (2012)

Much of the instability of the rock cut at Cordell Hull was due to existing joints that were solution widened, but also due to valley stress relief joints, which in some cases were also solution widened. Valley stress relief joints are not unique to karst terrain, but given that horizontally bedded limestone is often not considered structurally complex, these joints are often unanticipated in the rock slope design. Several examples from highways in Tennessee shown below illustrate this problem.

Highway Rock-Cuts in Tennessee with Similar Stability Problems

Figure 6 below contains two photographs of similar geological problems on two existing Tennessee Highway rock slopes that are natural cuts. SR 141 located less than 50 miles from Cordell Hull along the Caney Fork River in Dekalb County shows a similar pattern to what is seen at the Cordell Hull Dam Access Road Site. Again, there is more massive rock located on top of limestone that is more weathered, producing large overhangs and columns of rock. As with the Access Road, this bluff on SR 141 at LM 0.6 is located along a river, this time the Caney Fork. Numerous rockfalls have occurred at the site, but with its very low ADT and high expense, this segment has not yet been repaired. Figure 6 Photo A shows rock columns that look almost identical to what was removed at Cordell Hull. Small karst features can be seen in some of the rock columns. Figure 6 Photo B shows a large open vertical joint that extends behind the rock face.

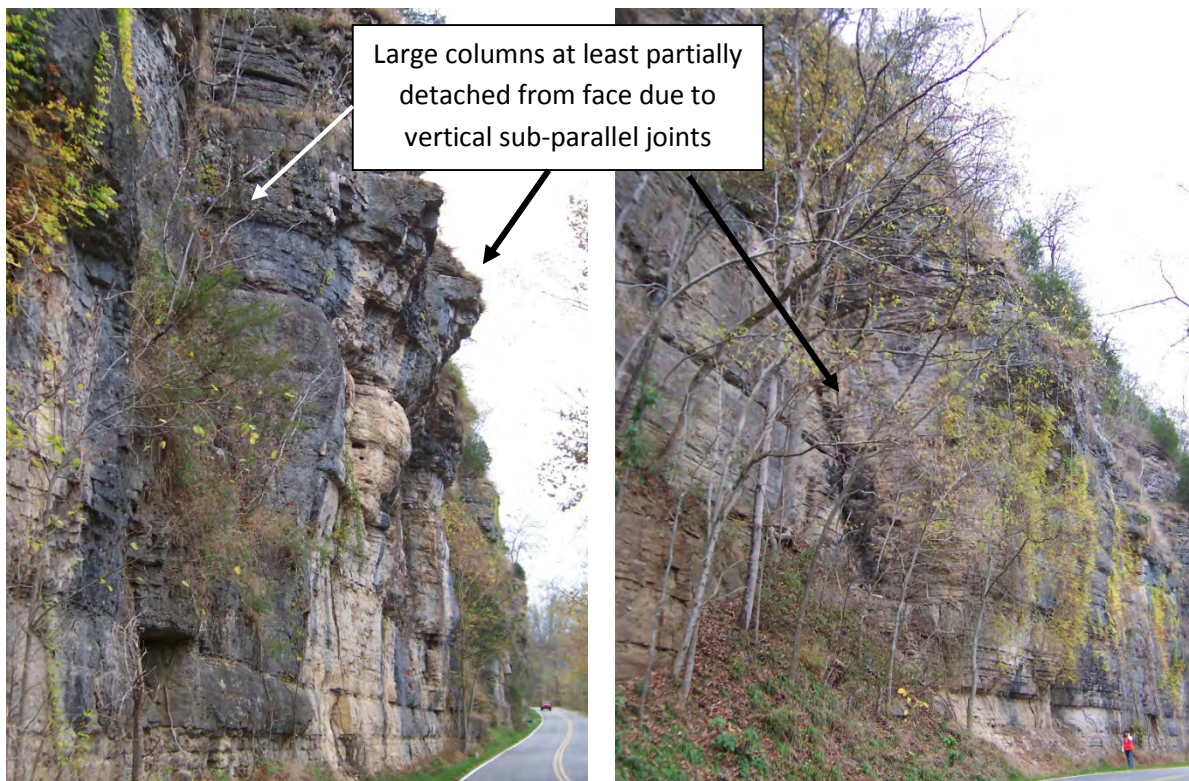


Photo A: Multiple Columns in Slope

Photo B: Large Open Joint behind Rock Face

Figure 6. Natural Rock Slope on SR-141 in Trousdale County, TN

A slightly different situation exists in the photograph in Figure 7 below, which shows solutioning directly leaving unstable columns and boulders on a natural rock cut face along I-40 in Putnam County in the Highland Rim. There are also solution widened joints here, but no valley stress relief jointing is present.



Figure 7. Solutioning in Limestone along Natural Rock Slope Face on I-40 in Putnam County, TN located at margin of Highland Rim and Cumberland Plateau

Many of these same issues can also be seen in constructed slopes across the state. A good example of this is SR-16 in Franklin County, TN located at the edge of the Highland Rim and Cumberland Plateau. This rock cut contained numerous problems which led to several large scale rockfalls. Shale layers, located at the base and in the middle of this rock cut, were weathering quickly and undermining the limestone blocks above. These blocks were cut by solution widened joints and also by sub-parallel valley stress relief features. Figure 8 photo A shows the secondary toppling failure mode with rock at the base of the cut successively failing. The underlying shale formation at this cut is undermining the overlying rock which is releasing along the vertical joints in the face. Figure 8 Photo B shows a large open vertical joint. Figure 8, Photo C is another view of the same section of the cut as shown in Photo A.

This cut, as can be seen in Figure 9, also contains a large cavity which is interacting with the vertical joints in the face to undermine stability of the cut. Here we can see the brown weathered face of the remaining rock where a boulder has already fallen from the slope and existing vertical joints and tension cracks developing in the limestone beds just above the cave. Half-casts can be seen in the face from original construction. Several large rockfalls prompted the Tennessee Department of Transportation to recommend a repair in 2010.⁴ A project was let to contract to repair this section of rock cut in 2012.⁵

⁴ Bateman, V., 2009. Preliminary Geotechnical Report, Rockfall Mitigation Assessment SR 16, LM 17.7 Right, Franklin County Tennessee.

⁵TDOT Letting CNL-251 The rockfall mitigation on S.R. 16 between log miles 17.5 and 17.8., 2012.



Figure 8. SR-16, Franklin County, TN – Shale layers undermine overlying larger limestone boulders with vertical joints leading to secondary toppling failure of the rock



Figure 9. Cavity Located in base of rock cut undermining rock above along vertical joint face

Center Hill Dam Left Rim Grouting Platform Construction

The left rim grouting platform construction at Center Hill Dam in Lancaster, Tennessee further illustrates the problems that can be encountered when constructing rock cuts in karst terrain. Here a somewhat more

extreme epikarst than is usual in Tennessee was encountered on the flanks of the large hill to the left of the main dam embankment where a rock cut was used to construct a grouting platform. Figure 10 below shows the locations of the grout lines installed at the site to deal with a karst driven potential failure mode at the dam.



Figure 10. Aerial Photograph of Center Hill Site illustrating Grout Curtain Installation from 2009-2010.

Center Hill Dam, as shown in Figures 1 and 10 above, is located on the dissected outer edges of the Central Basin and the Highland Rim. Figure 11 below shows the general geology map of the site with the Ordovician Aged limestones typical of the Central Basin and Devonian Chattanooga Shale and overlying Mississippian Fort Payne formation of the Highland Rim. The geology of this area interacted to produce a highly developed vertical karst system that solutioned along existing structural joints and valley stress relief joints that developed due to the uplift of the Nashville Dome and along the flanks of an anticline located very near Center Hill Dam.⁶

⁶ USACE, 2012 Major Rehabilitation Engineering Report Supplement, Center Hill Dam, Appendix G. and Stearns, RG and Reesman, AL, "Cambrian to Holocene Structural and Burial History of the Nashville Dome," *The American Association of Petroleum Geologists Bulletin*, v. 70, No. 2, February 1986, pp. 143-154

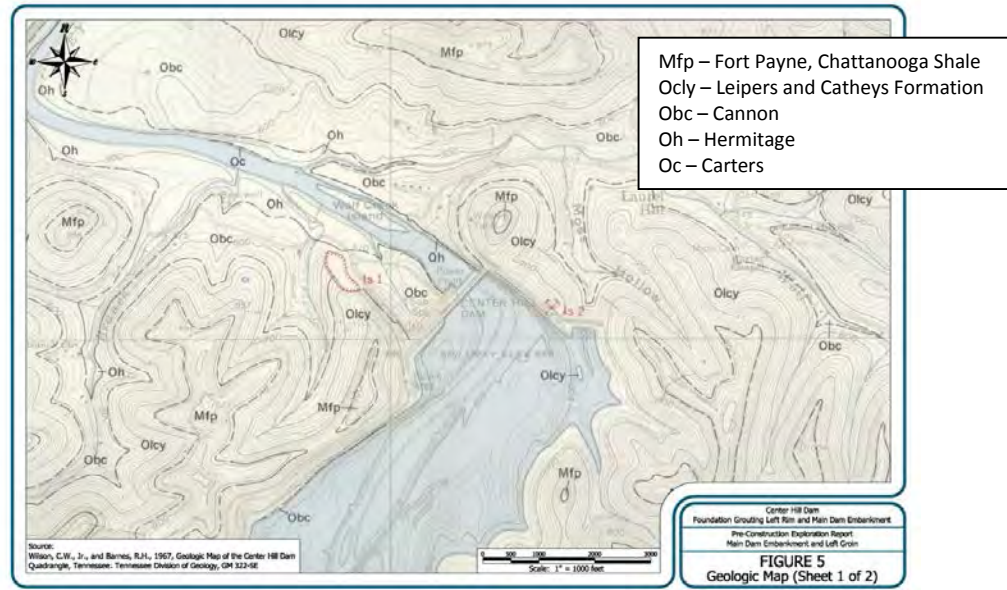


Figure 11. General Geology Map in the Vicinity of Center Hill Dam⁷

The extent of the karst development in the vicinity of Center Hill Dam has been controlled by a confluence of factors⁸:

1. *Multiple periods of uplift of the Nashville Dome resulting in extensive jointing with variations in the joint orientations between formations;*
2. *The unconformity between the Catheys and Cannon formations; and*
3. *Deep incision of the Caney Fork River at the dissected margin of two of Tennessee's physiographic provinces.*

Center Hill Dam is located in a portion of the dome that has experienced the maximum amount of uplift, 450 feet, over the last 2 million years.⁹ A regional jointing pattern that is generally both parallel and perpendicular to the Nashville Dome has been widely reported in the geological literature.¹⁰

This has resulted in the development of a karst system that is somewhat structurally controlled, with large karst shafts developing along intersecting vertical joints, and solution widened joints found across the site. Karst development can be opportunistic, forming where water has the easiest access. Stearns and Reesman, 1986, note that the current depth of the river cannot be fully explained by uplift.¹¹ Karst development along these structural joints is necessary to explain the current depth of the river which takes a 90 degree turn both upstream and downstream of the existing dam. Further complicating the geological

⁷ Wilson, C.W., Jr. and Barnes, R.H., "Geologic Map of the Center Hill Dam Quadrangle, Tennessee." Tennessee Division of Geology 1967.

⁸ USACE, 2012 Major Rehabilitation Engineering Report Supplement, Center Hill Dam, Appendix G.

⁹ Stearns, R.G. and Reesman, A.L., 1986, Ibid Footnote 6.

¹⁰ This regional joint pattern has been noted by Wilson along the eastern edge of the Nashville Dome, further discussion also see Stearns and Reesman, 1986.

¹¹ IBID, Footnote 6

situation and likely contributing to the more extreme epikarst at the site is the presence of pyrite in the overlying Chattanooga Shale.¹² Waltham and Fooks note that karst development tends to concentrate close to boundaries “...where allogenic drainage is supplied from impermeable rock outcrops.”¹³ The acidic drainage at this allogenic margin may have further accelerated the development at the site. Figure 12 below shows a karst shaft with strong iron staining from the water seeping out of the Chattanooga shale bedding interface with the underlying limestone, an indicator of acidic drainage.

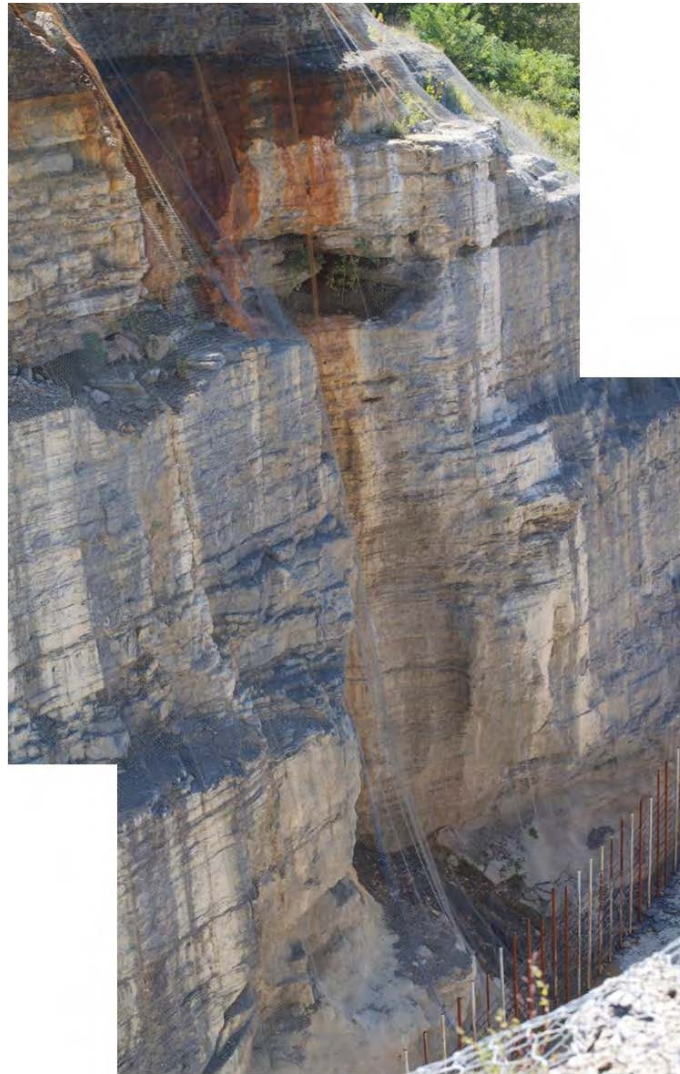


Figure 12. Acid Drainage Staining vertical karst feature in left Rim cut – Center Hill Dam ¹⁴

¹² TDOT. 2007. Guideline for Acid Producing Rock Investigation, Testing, Monitoring and Mitigation. Prepared by Golder Associates, Inc., Lakewood, CO. October, 2007. See Appendix and Maps

¹³ Waltham, A.C. and Fooks, P.G. “Engineering classification of karst ground conditions” published in *Speleogenesis and Evolution of Karst Aquifers*, republished from *Quarterly Journal of Engineering Geology and Hydrogeology*, 2003, vol 36, pp 101-118. pp. 44 and 104.

¹⁴ Site photographs taken at Center Hill Left Rim Cut. October 3, 2011.

Numerous karst features are present in the two rock cuts that were constructed in order to build the left rim grouting platform. However, what appeared to be the most unexpected problem was the significant epikarst zone located on the flanks of the left rim cuts. This weathered limestone, was excavated after a slide began in the overlying soil. This area, featuring deep vertical mudcutters and isolated boulders was named “Adobe Village” by the local USACE personnel. Figures 13 and 14 show views of this area.



Figure 13. View of “Adobe Village” on the flanks of the left rim cut. Figure 14 below shows a wider angle view

Even where the surrounding rock mass was more competent, towards the center of the hill, there were still numerous large vertical mudcutters, karst features filled with soil that “cut” the rock. These were covered by shotcrete as the excavation proceeded. Unfortunately, the depth of these features was poorly understood prior to their excavation. Figure 15 shows the excavation of one of these mudcutters when the excavation was still near the top of the constructed slope. Figures 16 and 17 show the entire cut as constructed, with several unstable blocks left near the top of the slope. Soil nails with a shotcrete face were installed in order to stabilize the face as the excavation proceeded. Figure 18 shows the excavation of one of the mudcutters and installation of the soil nails.

Unstable blocks on the slope caused problems during construction as numerous smaller rocks fell onto the work platform. Concern grew that the larger boulders could also displace, potentially killing or injuring workers below. As a result of these problems, and a re-assessment of the risks presented to the dam from features located this far from the dam, grouting of the left rim was abandoned in 2010. Closure had been achieved on the majority of the line, but the area underneath the tallest segment of the rock cut, the grouting was never finished. These problems during construction led to considerable cost over-runs.



Figure 14. View of Adobe Village from Left Rim Grouting Platform



Figure 15. Excavation of mudcutter at the top of the left rim excavation - 2008

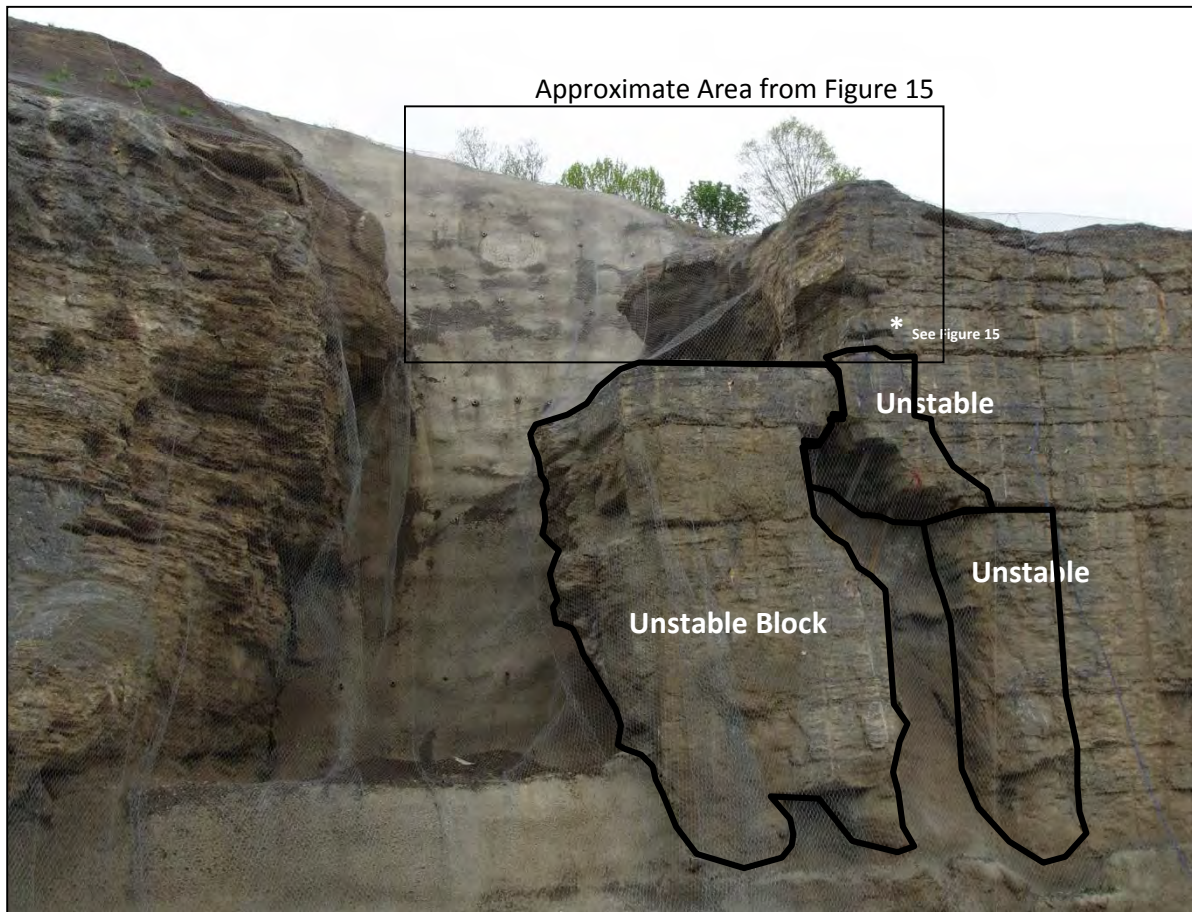


Figure 16. Unstable Blocks incorporated into Left Rim Cut. Largest block appears to be nearly fully detached from the surrounding rock by the vertical features. Photo 2010.

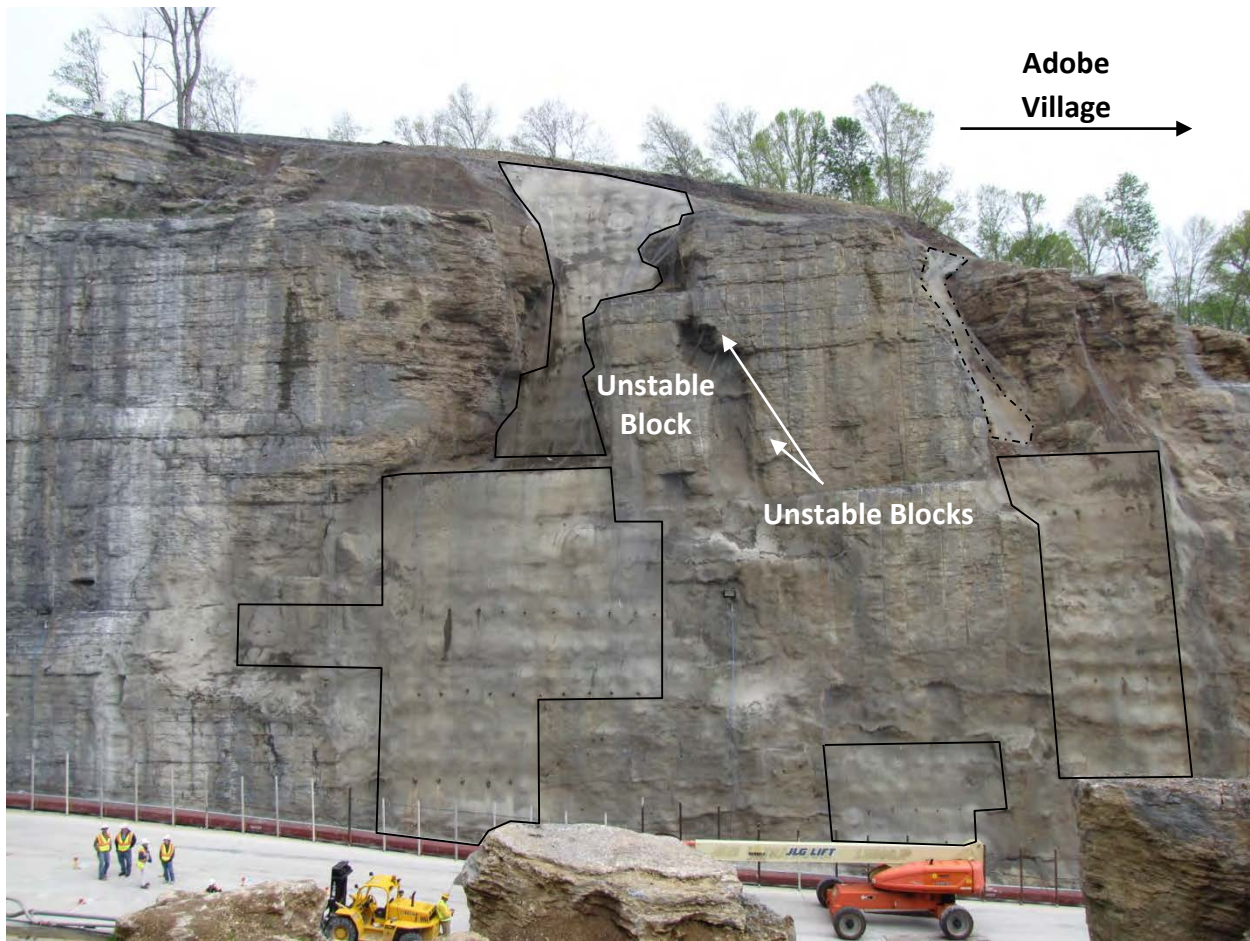


Figure 17 Unstable Blocks incorporated into Left Rim Cut view from the work platform, Jan 2014. Soil nails and shotcrete face areas are outlined in black.



Figure 18. View of Vertical Clay Seams and Soil Nail Installation, September 2008

Even where the mudcutters were less extreme, rockfall developed along the open karst shafts exposed in the face. Figure 19 shows the development of rockfall down a karst shaft in the face from 2008-2012.

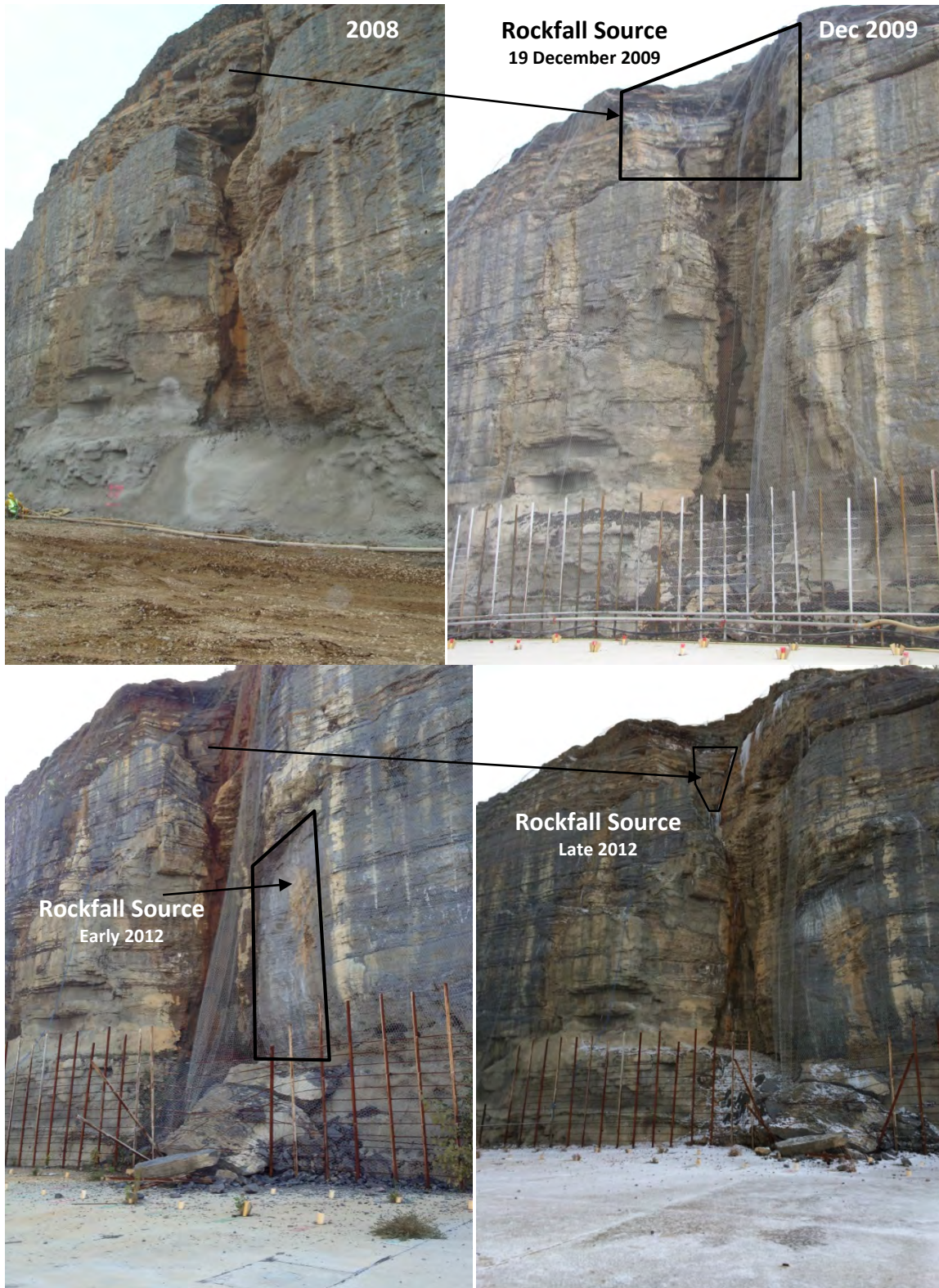
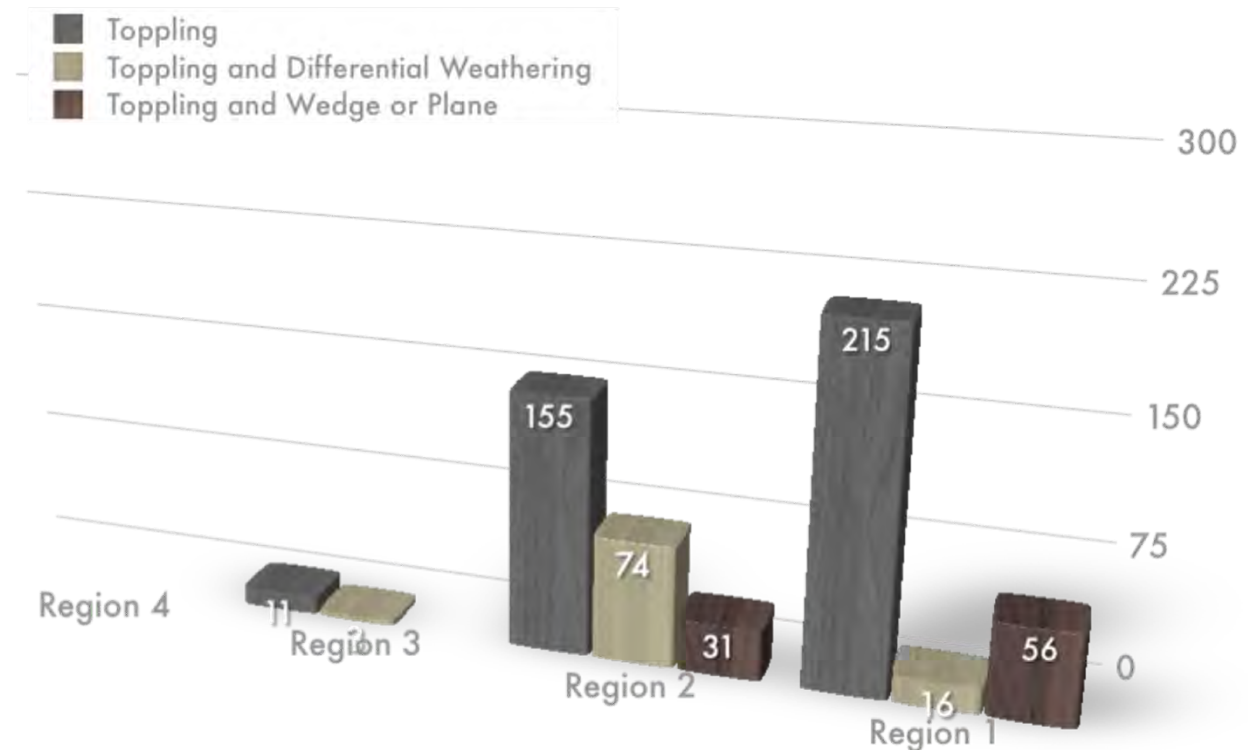


Figure 19. South Side Left Rim Cut Vertical Feature illustrating rockfall since excavation.

These pictures, taken of the same karst shaft shown in Figure 12, illustrate the stability concerns from a rock slope that was not designed to incorporate these features. The Center Hill Left Rim Grouting Platform was not designed with any of the standard rockfall catchment guidance that would typically be used on projects today.¹⁵ However, even if a design guidance document had been used, the catchment guideline may only have been sufficient for the type of rockfall seen in Figure 19. Such design tables were not meant to be used for large scale structural failure of rock. Where additional problems exist in the rock face, further design time is needed to ensure that the rock cut is stable and the rockfall catchment zone is sufficiently wide.

Secondary Toppling along Tennessee Roadways

TDOT’s Rockfall Hazard Rating Program identified 166 sites along Interstates and State Routes in the two regions (2 and 3) that are located in Central Basin, Highland Rim and margin of the Cumberland Plateau discussed in this paper that had a toppling failure mode¹⁶. This toppling failure mode is most often secondary toppling, and as can be seen from the graph below, often occurs with differential weathering.



¹⁵ See TDOT STANDARD DESIGN DRAWING LIBRARY - DRAWING NO. RD01-S-11B; accessed in 2015 at <http://tn.gov/assets/entities/tdot/attachments/DetailRockCutSlopeandCatchment.pdf> and Pierson, L.A., Gullixson, C.A. and Chassie, R.G, Oregon Rockfall Catchment Area Design Guide, FINAL REPORT SPR-3(032), December 2001 accessed in 2015 at http://www.oregon.gov/odot/td/tp_res/docs/reports/rokfallcatchareadesmetric.pdf

¹⁶ TDOT Rockfall Hazard Rating Program data as of 2011; Bateman, V.C. “Secondary Toppling: Failures of Sedimentary Rock in Tennessee,” presented at the 9th Annual Technical Forum on Geohazards in Transportation, Lexington, KY, 2009.

A view of the rockfall data from TDOT's rockfall program shows that far from being an unlikely failure mode, secondary toppling is significant rock failure mode present across the state.

Conclusions

As always, good site reconnaissance, site exploration and experience with the local geology will lead to better results where the results of these investigations are understood and incorporated into the design. Far too often practitioners have ignored the potential structural complexity and problems of horizontally bedded limestone and karst terrain, focusing only on the issue of sinkholes. However, solution openings in limestone and other karst rocks can present some unique challenges to the designer of rock cuts.

Drilling programs must be designed to capture potential problems and spacing that might be assumed for non-complex horizontally bedded rock may not be sufficient for good rock cut design. The epikarst shown at the flanks of the Center Hill Left Rim cuts may be more extreme than generally encountered in Tennessee, but the conditions that produced these features exist all along the dissected margins of the Central Basin and the Highland Rim. Floating boulders and disconnected blocks are well documented in the literature and the possibilities of these problems should be accounted for during exploration. Where a potential failure mode is not recognized during exploration, it is unlikely to be properly identified and designed against. The potential for cave openings in the rock wall must also be accounted for in the design.

Particular attention also needs to be paid to the structural geologic situation even were we have horizontally bedded limestone and few area faults. This can lead to a false sense of security where the practitioner assumes the situation out in the field is less complex than is actually the case. Joints that may be parallel or sub-parallel to the face are particularly significant and may be unlikely to be revealed from an exploration program using only vertical drilling. Inclined drilling and small scale area geologic mapping can be of significant benefit in identifying these problems.

Additionally, secondary toppling failures of the type discussed in this paper and structural issues resulting from the interaction of vertical joints, differential weathering and mudcutters may be beyond the scope of standard rockfall design tables and should be accounted for separately in the design. Where block sizes are large, and more horizontal momentum of rock toppling from the face can be expected, different design methodologies should be used.

Only a handful of examples were used in this paper to illustrate the issues, but as was shown by TDOT's Rockfall Hazard inventory, these problems can be widespread. Practitioners must not assume that horizontally bedded means that the problems out in the field are simple. Likewise, karst terrain may present more challenges to the designer than just sinkholes. Complacency in an exploration program can lead to substantially increased costs during construction, to potential safety issues and to designs that do not meet project goals.

**Geotechnical Designs to Build on
Liquefiable and Compressible Soil in Salem, Massachusetts**

Tulin Fuselier, P.E.

Kleinfelder
215 1st Street, Suite 320
Cambridge, MA 02142
(617)-497-7800
TFuselier@Kleinfelder.com

Zia Zafir, PhD, P.E.

Kleinfelder
3077 Fite Circle
Sacramento, CA 95827
(916)-366-1701
ZZafir@Kleinfelder.com

Jennifer MacGregor, P.E.

Kleinfelder
215 1st Street, Suite 320
Cambridge, MA 02142
(617)-497-7800
JMacGregor@Kleinfelder.com

Stefanie Bridges

Kleinfelder
215 1st Street, Suite 320
Cambridge, MA 02142
(617)-497-7800
SBridges@Kleinfelder.com

Acknowledgements

The authors would like to thank The Massachusetts Bay Transportation Authority (MBTA) for this work opportunity, as well as our project team:

Fennick McCredie Architecture
Desman Associates
Consigli Construction
DGI-Menard
GEI Consultants

Disclaimer

Statements and views presented in this paper are strictly those of the author(s), and do not necessarily reflect positions held by their affiliations, the Highway Geology Symposium (HGS), or others acknowledged above. The mention of trade names for commercial products does not imply the approval or endorsement by HGS.

Copyright Notice

Copyright © 2015 Highway Geology Symposium (HGS)

All Rights Reserved. Printed in the United States of America. No part of this publication may be reproduced or copied in any form or by any means – graphic, electronic, or mechanical, including photocopying, taping, or information storage and retrieval systems – without prior written permission of the HGS. This excludes the original author(s).

ABSTRACT

The Massachusetts Bay Transportation Authority (MBTA) is addressing accessibility throughout their facilities. Improvements at the Commuter Rail Station in Salem, Massachusetts include a five-level parking garage replacing the existing parking lot, a pedestrian bridge replacing the existing stairway connecting track level with downtown Salem, two accessible elevators, and a full-length accessible high-level platform.

Subsurface explorations at the site encountered fill overlying loose, potentially liquefiable saturated sands, overlying soft marine clay deposits extending to till and rock at about 60 to 80 feet depth. Deep foundations bearing on rock were recommended for structural support of the garage, bridge, and platform. Ground improvement using vibratory stone columns (VSCs) was also recommended to address the liquefaction and lateral spreading potential, and to improve the seismic site classification from Class F to Site Class E.

The project team evaluated value-engineering options. The final design included the installation of over 470 Controlled Modulus Columns™ below the garage and bridge footings. Over 825 VSCs up to 30 feet in depth were installed below the parking garage and platform. Post-VSC treatment testing was conducted during construction to review compliance with the specified performance criteria.

The cooperative design and installation required coordination between the design and construction teams to maximize cost and schedule efficiency for the project. These methods allowed the project to move forward, ultimately saving the client millions of dollars in construction costs.

INTRODUCTION

The Massachusetts Bay Transportation Authority (MBTA) is addressing accessibility throughout their system and facilities. One of these facilities is the Commuter Rail Station in Salem, Massachusetts (hereinafter the “site”), which serves more than 2,000 passengers daily and hosts regular MBTA bus service.



Figure 1- New Parking Garage and Pedestrian Bridge at the MBTA Commuter Rail Station in Salem, Massachusetts (Looking North from Bridge Street)

The improvements at the Salem station consist of a new five-level parking garage (shown in Figure 1) to provide additional parking capacity at the station, two accessible elevators, a full-length high-level (“full-high”) commuter rail platform, and a pedestrian bridge that enhances accessibility from downtown Salem to the station (see Figure 2). Site improvements also include a passenger drop-off/pick-up area, secure bicycle parking, and improved traffic flow patterns for buses and taxis. The new garage increases parking capacity from the previous 340 parking spaces to about 700 spaces. An enclosed waiting area in the garage and platform canopies offer shelter for passengers accessing the train along the new platform.

BACKGROUND

A site description and history, as well as discussions of initial design for the site improvements were presented at the 64th Highway Geology Symposium in 2013⁽¹⁾. A summary is provided herein.

The site is a triangular shaped parcel located at 252 Bridge Street in Salem, Massachusetts. It is bound to the north by a seawall with the North River beyond, by the elevated Bridge Street to the south, and by the MBTA commuter rail platform and railroad tracks to the east. The commuter rail tracks pass under Bridge Street through a tunnel. A separate freight railroad track runs parallel to the seawall along the northern edge of the site.



Figure 2 - New Pedestrian Bridge and Stairs Connecting Bridge Street to the New Train Platform (Looking South towards Bridge Street)

Prior to the start of construction the site served as a surface parking lot and was mostly covered with bituminous pavement. Site grades ranged from about El. 9 to El. 10.5 feet. A retaining wall and stairs separated the surface parking lot from the railroad tracks, which range from about El. 10 feet at the northern end of the site to about El. 4 feet at the southern end near Bridge Street. Pedestrian access from Bridge Street (at about El. 27 feet) was previously by way of a staircase near the tunnel under Bridge Street.

The new parking garage was constructed along the eastern side of the site. Figure 3 shows the pre-construction and construction conditions at the site. The new garage building is a pre-cast concrete building with no below grade space except for the elevator pits. The building column loads are up to 2200 kips, and the fundamental period in one direction is 0.56 seconds. The ground floor of the building is 3 to 6 feet above pre-construction grades and set above the newly established flood level for the area.

The new “full-high” commuter rail platform extends about 900 feet along the eastern side of the site. An average of 3.5 feet of fill was placed for construction of the new platform. The concentrated platform and canopy loads at the top of footing are up to 26 kips including the raise in grade.



(a) Pre-Construction (June 18, 2010)

(b) During-Construction (September 27, 2014)

Source: "252 Bridge Street, Salem, MA" $42^{\circ} 31' 28'' N$ and $71^{\circ} 53' 47'' W$. Map data: ©2015 Google, ©2015 Europa Technologies, June 2015.

Figure 3 - Pre-Construction and Construction Conditions at the Site

Prior to use as a commuter rail station, the site served as the Salem Train Depot with locomotive maintenance facilities. Kleinfelder acquired site history, old photos, and fire insurance (Sanborn) maps dating back to 1890 that showed locomotive turntable and roundhouse structures amidst a number of tracks leading to and from the maintenance facilities. The foundations of these facilities were suspected to have remained buried in place. Kleinfelder recommended that a geophysical exploration be performed using the ground penetrating radar (GPR) and electromagnetic (EM) conductivity survey methods to explore the presence and locations of buried structures with respect to proposed foundation locations, as well as for construction methods and sequencing considerations.

A 1940's photograph of the site showing a locomotive turntable, tracks, and roundhouse is shown in Figure 4. Figure 4(a) shows the results of the EM survey. The survey results strongly suggest the presence of subsurface structures resembling the historical turntable and roundhouse structures as indicated on the Sanborn maps and old site photographs.

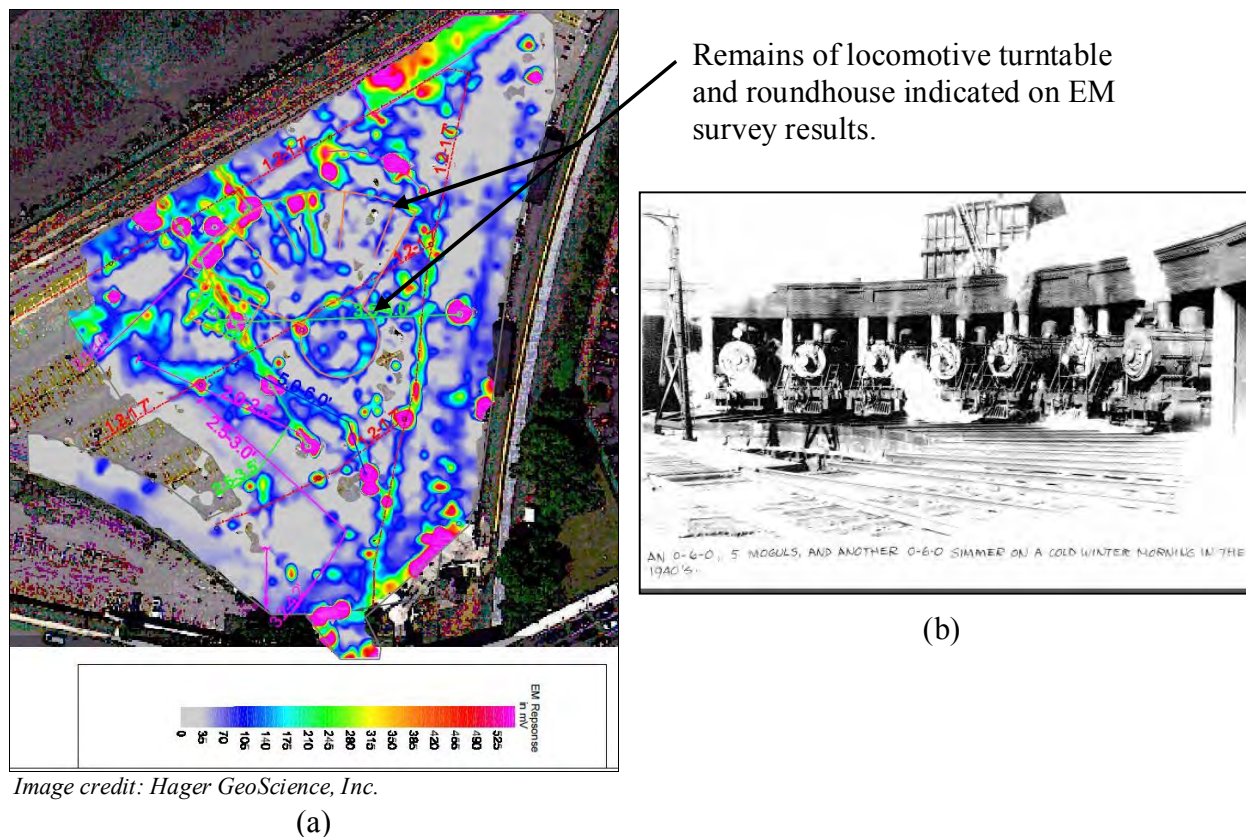


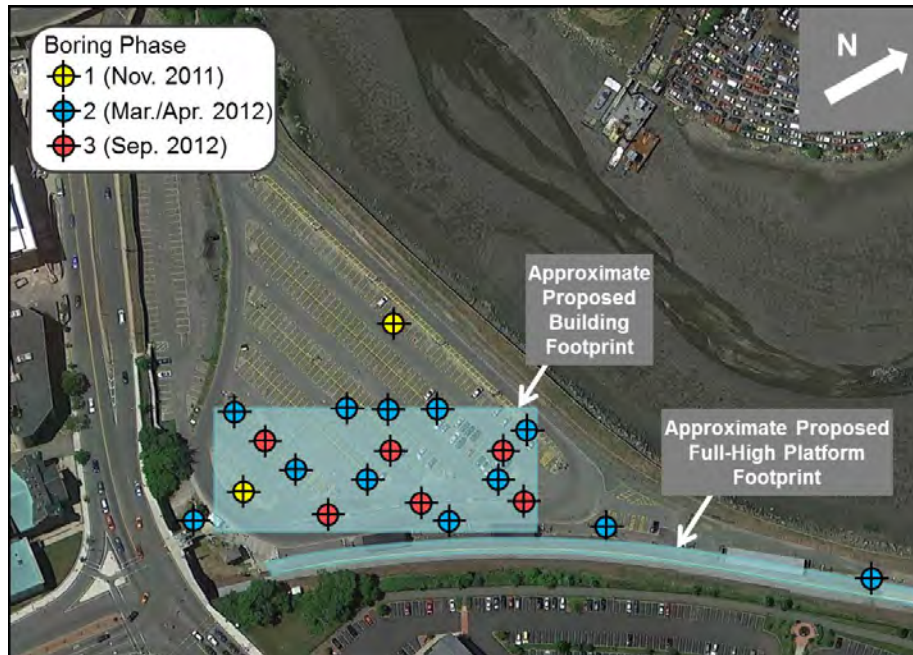
**Figure 4 - (a) EM Survey Results Indicating Remains of Turntable and Roundhouse
(b) A 1940's Photograph of Locomotive Turntable and Roundhouse.**

Based on the historical significance of the site and geophysical survey findings, an archaeological exploration was conducted at the site by Public Archaeology Laboratory Inc. (PAL) under State Archaeological Permit number 3356. PAL subsequently issued a findings clearance memorandum which included locations, descriptions and photographs of the structural remains uncovered, including the foundations of the locomotive roundhouse, turntable, and related structures. Following this work, the Contractor was able to remove the archeological remnants as part of the construction project.

SUBSURFACE CONDITIONS

Geotechnical Explorations

Kleinfelder performed a total of 21 test borings in three phases. The test borings extended to depths up to 100 feet below ground surface. Some of the boring locations were selected specifically at building column locations intersecting the buried structures identified in the geophysical exploration to get an indication of the thickness and depth of the buried structures. The buried structures were not encountered in any of the 21 borings drilled at the site. The approximate test boring locations are shown in Figure 5. The third phase of borings was performed specifically to assess the extent of potentially liquefiable soils on site.



Source: "252 Bridge Street, Salem, MA", June 18, 2010, $42^{\circ} 31' 28''$ N and $71^{\circ} 53' 47''$ W.
Map data ©2015 Google, ©2015 Europa Technologies, January 2013.

Figure 5 - Subsurface Exploration Location Plan

The geotechnical explorations generally indicated subsurface conditions consisting of about 5 to 15 feet of fill underlain by a layer of loose sand and silt deposits up to about 20 feet thick. A discontinuous layer of organics was encountered across the site beneath the upper sand layer, overlying a thin discontinuous layer of sand, underlain by soft marine clay deposits. The soft marine clay deposits ranged from about 30 to 60 feet thick and extended to a relatively thin layer of glacial till (2 to 10 feet thick). Rock or weathered rock was encountered between 60 and 80 feet below ground surface and generally increased in depth from south to north across the site. The rock was described as moderately strong to very strong syenite.

Groundwater was recorded at approximately 5 feet below ground surface. Based on the shallow groundwater level and the presence of loose, saturated sands and silts, the site was classified as potentially liquefiable when subjected to earthquake ground shaking.

Soil Liquefaction Assessment

Soil liquefaction describes a phenomenon in which saturated soil loses shear strength and deforms as a result of increased pore water pressure induced by ground shaking during an earthquake. Dissipation of the excess pore pressures will produce volume changes within the liquefied soil layer, which causes settlement of foundations and slabs on grade. Shear strength reduction combined with inertial forces from the ground motion may result in lateral migration (lateral spreading), extensional ground cracking of liquefied material, and slope failure. Factors known to influence liquefaction include soil type, structure, grain size, relative density, confining pressure, depth to groundwater, and the intensity and duration of ground shaking. Soils most susceptible to liquefaction are saturated, loose sandy soils and low plasticity clays and silts.

In the past decade, several concentrated efforts have been done to come up with a uniform guideline for field-based simplified liquefaction analyses. Youd et al. (2001)⁽²⁾ published general guidelines for liquefaction analyses, which presented the consensus of a task committee comprising more than 20 members from all over the country. However, subsequent earthquakes in Turkey and Taiwan provided additional data to researchers, especially for low plasticity clays and silts which resulted in significant modifications to liquefaction evaluation methods, especially for soils with higher fines contents. Two of the most widely used new methods have been presented by Seed et al. (2003)⁽³⁾ and Idriss and Boulanger (2008)⁽⁴⁾. Liquefaction potential analyses for the site were performed following these two methods using the field standard penetration test (SPT) data from the 21 borings and laboratory test data.

The evaluation of liquefaction in response to an earthquake was based on a comparison of a soil's resistance to liquefaction and the cyclic load or demand placed on the soil by the design earthquake. A safety factor against liquefaction triggering is commonly defined as the ratio of the cyclic shear stress required to cause liquefaction (cyclic resistance ratio, or CRR) to the equivalent cyclic shear stress induced by the earthquake (cyclic stress ratio, or CSR). As mentioned earlier, dissipation of excess pore water pressures causes settlements. A layer may not experience liquefaction but it can still experience some settlements due to dissipation of excess pore water pressure. Therefore, a factor of safety criteria (FOS) of 1.1 was used for settlement calculations per Martin and Lew (1999)⁽⁵⁾. This means that liquefaction induced settlements were calculated for those layers where FOS against liquefaction triggering was less than 1.1. Kleinfelder estimated liquefaction induced settlements using procedures by Idriss and Boulanger (2008)⁽⁴⁾ and Cetin et al. (2009)⁽⁶⁾.

Two important input parameters for the liquefaction analysis are the peak ground acceleration (PGA) and the earthquake magnitude. According to the Massachusetts State Building Code (which is based upon the 2009 International Building Code), in absence of a site-specific ground motion hazard analysis, the PGA can be assumed as $S_{DS}/2.5$. Based on the S_{DS} of 0.477g, a PGA of 0.19g was calculated and used in the liquefaction analysis. In order to estimate controlling magnitude at the site, Kleinfelder used the 2008 USGS interactive deaggregation tool, which resulted in controlling earthquake magnitude of 5.8. Based on the results of the liquefaction potential evaluation, subsurface soils at the site included potentially liquefiable soils, indicating liquefaction induced settlements at the site, especially at the northern portion of the site which is closest to the river.

Lateral Spreading Potential

Lateral spreading is a post-liquefaction phenomenon consisting of blocks of soil “laterally spreading” due to either a gently sloping ground or an open face such as an open creek or river channel. During lateral spreading, blocks of non-liquefied soil “float” on top of liquefied soils below. Lateral spreading has been observed in previous large earthquakes, even for gently sloping sites, at distances of over 500 feet from a free face. Lateral spread movements are typically greatest near a free face (such as the river channel) and diminish with distance from the free face.

Due to the proximity of the North River, potential for lateral spreading is high at this site especially at the northern portion of the site. Laterally spreading soils can induce significant lateral deformations and increased lateral loads on the deep foundations. In many cases, the deformations and increased loads exceed the allowable limits.

FOUNDATION DESIGN RECOMMENDATIONS

Liquefaction Mitigation

Liquefaction, earthquake-induced settlement, and lateral spreading hazards would result in severe damage and potential collapse of structures if left unmitigated. As a result, ground improvement was recommended for mitigation of this potential and to improve the seismic site classification for the garage building from Site Class F to Site Class E in accordance with the Building Code.

Ground improvement techniques can be used to replace, densify, or solidify in-situ soils to increase liquefaction resistance, reduce static compressibility, and increase strength (USACE 1999)⁽⁷⁾. Kleinfelder considered several ground improvement techniques, and vibro-replacement stone column (VSC) methods were selected as the preferred ground improvement technique.

VCSs are a densification and reinforcement technique wherein a vibratory probe (“vibroflot”) is advanced vertically into the ground. As the probe advances, it displaces and densifies the soil laterally. After the probe has reached its intended depth, gravel is introduced from the probe tip or from the ground surface as the probe is withdrawn. The probe is reinserted in 1- or 2-foot increments as it is withdrawn to further compact the gravel and surrounding soil. Vibro-replacement methods are most commonly used for liquefaction mitigation in sandy to silty material. In addition to the densification of the native soil, the stone columns can act as drains to assist in relieving pore water pressure buildup during and following earthquake shaking.

The VSCs recommended for the site varied in depth from 15 to 30 feet, depending on the depth and thickness of the liquefiable layer. The stone columns were installed within the building footprint and at the northern end of the platform.

Foundation Design

The contract documents included two alternatives for support of the garage and pedestrian bridge columns: deep foundations or ground improvement with drilled displacement columns (DDC). The deep foundation alternative included drilled shafts extending to bedrock. Deep foundations transmit the structural load to below the potentially liquefiable soils to the underlying bedrock.

The project team identified DDCs as a possible cost effective solution for support of the proposed garage during a value engineering study. In DDC systems, soils displace radially around a displacement tool (a purpose-built auger head), densifying the soils around the displacement tool point. Grout is injected under pressure as the displacement tool is withdrawn. With the densification and injected grout, the soil strength and stiffness increases. DDCs are not

structurally connected to a building and therefore are a type of ground improvement system such that the building can be supported on shallow footings founded on top of the DDC elements.

The general Contractor (Consigli) and their specialty subcontractor (DGI-Menard, Inc.) used Controlled Modulus Columns™ (CMCs™) as DDC elements below the garage columns. The project documents specified the removal of the buried turntable and roundhouse structures prior to the start of the VSC and DDC installations to limit obstructions during installations.

CONSTRUCTION PHASE

Salem Station remained an active railroad station and bus terminal during construction of the new parking garage and platform. Therefore, the construction was undertaken in two phases: Phase 1 included construction of the garage, pedestrian bridge, and the adjacent portion of the platform; Phase 2 included construction of the northern half of the platform.

Vibratory Stone Columns

Kleinfelder prepared performance specifications for installation of the VSCs, specifying minimum soil density that was to be obtained in post-installation confirmatory test borings. The acceptance criteria for the ground improvement program was based on minimum Standard Penetration Test (SPT) $(N_1)_{60-cs}$ values with a moving average of at least 15 over an interval of 6 feet with no value less than 12 for soils with fines content equal to or less than 15 percent. For soils with equal to and greater than 15 percent fines, the acceptance criteria was based on a factor of safety against liquefaction greater than 1.1 with a reduction factor applied to cyclic stress ratio due to replacement of the soils with crushed stone.

Kleinfelder based the required depth of ground improvement on the pre-construction boring data. Three improvement zones were defined as shown in Figure 6. The 15 and 20-foot in length VSCs were installed using an excavator-mounted VSC rig, while the 30-foot in length VSCs needed to be installed using a crane assembly (Figure 7).

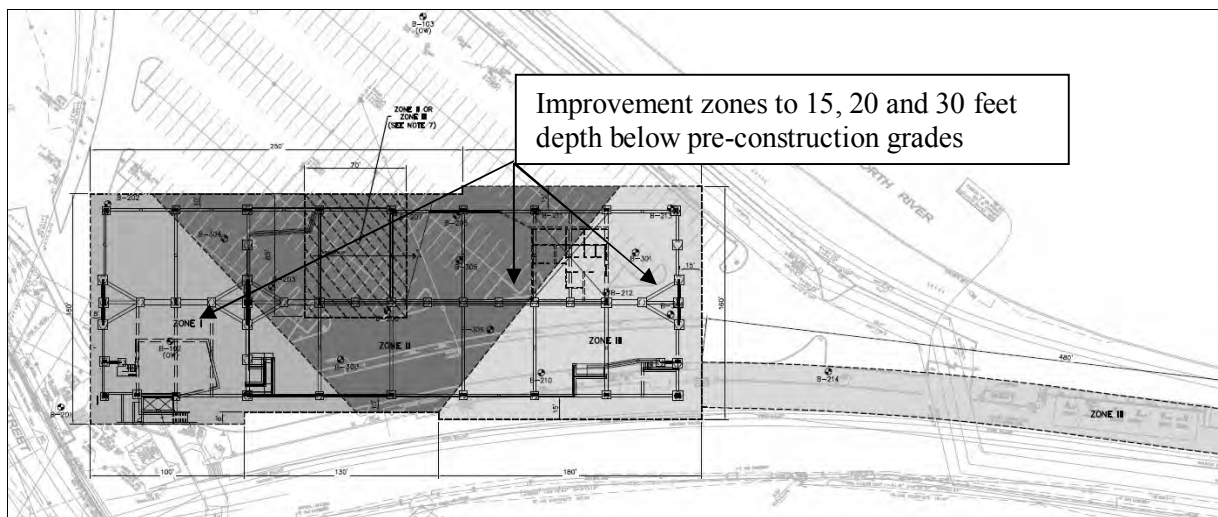


Figure 6 - Ground Improvement Zones Defined in Contract Drawings

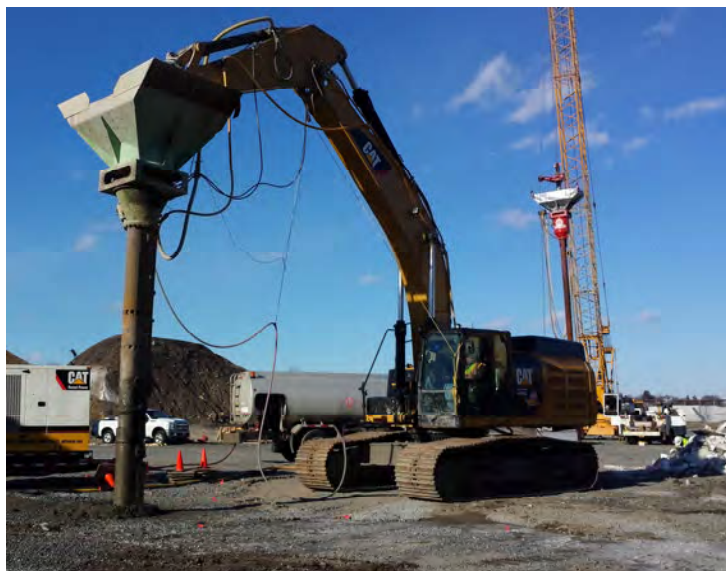


Figure 7 - VSC Attachments

VSC attachment on an excavator in the foreground and hanging from a crane in the background.

Post-soil improvement SPT borings, one for every 2,200 square feet of improved area, were conducted by Kleinfelder throughout the installation area of the VSCs. Based on the ground improvement acceptance criteria, fines percentage and Atterberg limits testing had to be conducted on many samples from the post-VSC installation confirmatory borings. Depending on the confirmatory boring N-values and field classification, samples for fines content testing were selected and sent to the geotechnical testing laboratory directly from the field within a day of drilling to provide information to the Contractor in a timely manner to prevent schedule delays. The factor of safety against liquefaction triggering was calculated using the Idriss and Boulanger (2008)⁽⁴⁾ method based upon the STP data and laboratory test results within a day of receiving the laboratory data. This process required continuous coordination between the field and office personnel, as well as the Contractor.

The majority of VSCs within the parking garage were installed during normal working hours. Due to the proximity of the Phase 2 VSCs below the northern portion of the platform, the Phase 2 VSCs were completed at night when the commuter rail trains were not operating.

The VSC installations along the northern platform were complicated by the presence of numerous subsurface obstructions, likely buried rip-rap, encountered at depths ranging from 2 to 22 feet below grade near the commuter rail tracks. Due to the proximity to the existing commuter rail tracks to the east and freight tracks to the west, excavation to remove the obstructions encountered during Phase 2 was not feasible. Two additional borings were advanced at the northern platform to further assess the liquefaction potential specifically in the localized area where the buried obstructions were encountered. The additional SPT and laboratory data from these two borings demonstrated that the factor of safety against liquefaction was greater than 1.1. Therefore sections of the Phase 2 VSCs were not installed.

Overall, nearly 825 VSCs, 30-inch in diameter were installed, and 27 post-installation test borings were completed. The post-installation boring data indicated that the ground had been

successfully improved to meet Kleinfelder's acceptance criteria given in the project specifications.

Drilled Displacement Columns (CMCs™)

Kleinfelder also prepared performance specifications for the installation of drilled displacement columns. In this project, DGI-Menards's Controlled Modulus Columns™ were used as drilled displacement columns. The DDC specification included requirements for a static load test to confirm that the load carrying and settlement characteristics of the installed columns were consistent with the design assumptions. The specification also included maximum settlement allowance. The Contractor performed numerical modeling using the computer program Plaxis to assess the viability of CMCs™ under the building loads.

The CMC™ elements were designed as ground improvement to reduce settlement below the garage column footings. Therefore, a load test to 150% of the design load was performed to confirm that the load transferred to the CMC™ tip was consistent with the load transfer predicted by the Plaxis model. The load test CMC™ was instrumented with three dial gauges at the top of the element to measure deflection; a load cell to measure the applied load, and six strain gauges to measure the load at different elevations within the CMC™ element. At the design load of 150 kips, there was no measured movement of the CMC™ tip. At an applied load of 225 kips (150% of the design load), approximately 92 kips were measured at the CMC™ tip which was less than the tip load of 98 kips estimated by the Plaxis model likely due to the greater frictional capacity in the fill material than assumed in the model. To further assess the CMC™ capacity, the applied load was increased to about 300 kips at which point the CMC™ showed movement indicative of failure.



Figure 8 – CMC™ Installation

Nearly 470, 15.5-inch diameter, 150-kip capacity CMCs™ were installed extending to bedrock or into the thin till layer. The installation of the CMCs™ resulted in minimal spoils from the site as part of the foundation construction, resulting in savings for the project as compared to traditional deep foundations.

Transfer of the column loads from the spread footing into the CMC™ elements requires placement of at least 6-inches of structural fill between the top of the CMC™ elements and the bottom of the footings. Placement of the structural fill required careful excavation to expose the top of the CMC™ element below each footing. Figure 9 shows the in-place CMCs™ below a footing.



Figure 9 - Garage Footing Subgrade with Exposed CMCs™

CONCLUSION

The Salem Commuter Rail Station was in need of site improvements to improve accessibility of the station, relieve congestion with additional parking, and improve access from the historic downtown to serve its residents and visitors. Some of the proposed site improvements included a parking garage, pedestrian bridge, and new train platform.

With the potential for liquefaction and lateral spreading at the site, and the project's budgetary limits, the project team was challenged to look at alternative foundation systems. Ground improvement measures were recommended to mitigate a lateral spreading potential and to improve the seismic site classification for the garage building from Site Class F to Site Class E. The project team worked together to provide an alternative foundation system consisting of drilled displacement columns instead of the deep foundation options. Nearly 470 Controlled Modulus Columns™ and 825 vibro-replacement stone columns were installed. Partly due to the use of CMCs™ in place of deep foundations and the generation of minimal amounts of spoils, the project saved millions.

REFERENCES

1. Fuselier, T. H. and Woodward, N. *Cooperative Geotechnical Data Designs to Build on Liquefiable Sands and Compressible Clays in Salem, Massachusetts*. Proceedings of the 64th Highway Geology Symposium, 2013. pp. 332-347.
2. Youd, T. L., Idriss, I. M., Andrus, R. D., Arango, I., Castro, G., Christian, J. T., Dobry, R., Liam Finn, W. D., Harder, L. F., Jr., Hynes, M. E., Ishihara, K., Koester, J. P., Laio, S. S. C., Marcuson, III, W. F., Martin, G. R., Mitchell, J. K., Moriwaki, Y., Power, M. S., Robertson, P. K., Seed, R. B., Stokoe, II, K. H. (2001). *Liquefaction resistance of soils: Summary report from the 1996 NCEER and 1998 NCEER/NSF workshops on evaluation of liquefaction resistance of soils*. Journal of Geotechnical and Geoenvironmental Engineering, 127(10): pp. 817–833.
3. Seed, R.B., Cetin, K.O., Moss, R.E.S., Kammerer, A., Wu, J., Pestana, J. and Riemer, M., Sancio, R.B., Bray, J.D., Kayen, R.E., Faris, A. (2003) *Recent Advances in Soil Liquefaction Engineering: A Unified and Consistent Framework*, 26th Annual ASCE Los Angeles Geotechnical Spring Seminar, Keynote Presentation, H.M.S. Queen Mary, Long Beach, California, April 30, 2003.
4. Idriss, I. M., and Boulanger, R.W. (2008). *Soil Liquefaction During Earthquakes*, EERI Engineering Monograph MNO-12.
5. Martin, G.R. and Lew, M. eds. (1999). *Recommended Procedures for Implementation of DMG Special Publication 117 — Guidelines for Analyzing and Mitigating Liquefaction Hazards in California*, Southern California Earthquake Center, Los Angeles, pp. 63.
6. Cetin, K.O, Bilge, H.T., Wu, J., Kammerer, A.M., Seed, R.B. (2009). *Probabilistic Model for the Assessment of Cyclically Induced Reconsolidation (Volumetric) Settlements*, Journal of Geotechnical and Geoenvironmental Engineering, Vol. 135, No. 3, pp. 387-398.
7. US Army Corps of Engineers (1999). *Guidelines on Ground Improvement for Structures and Facilities*, US Army Corps of Engineers, Technical Letter, No: 1110-1-185, Washington.

Rock slope monitoring using oblique aerial photogrammetry along Interstate 70 in DeBeque Canyon, Colorado: A CDOT Geotechnical Asset Management pilot project

Ty Ortiz

Colorado Department of Transportation

ty.ortiz@state.co.us

(303) 398-6601

Dave Gauthier

BGC Engineering Inc.

dgauthier@bgcengineering.ca

(613) 893-4920

Nicole Oester

Colorado Department of Transportation

Nicole.oester@state.co.us

(303) 398-6603

Robert Group

Colorado Department of Transportation

Robert.group@state.co.us

(303) 398-6600

Abstract: The Colorado Department of Transportation has been working to integrate geohazards into a Geotechnical Asset Management (GAM) program. The program measures the risk that geohazards present to the transportation system, which is the product of the likelihood of a particular geohazard to affect the system and the consequence of the geohazard event on the system. Rockfall and rockslides are major geohazards affecting Colorado highways, and developing a site-specific approach to measure and evaluate the risk associated with these hazards has proven difficult. In this paper we report on a pilot study, the objective of which is to test the efficacy of oblique aerial photogrammetry (OAP) for rock slope monitoring along Colorado highways, and to evaluate the utility of the results for measuring the site-specific likelihood of rockfall for integration into the risk calculation. In the fall of 2014 we collected over 2500 oblique aerial photographs of rock slopes along Interstate 70 in DeBeque Canyon. These were collected manually from a moving helicopter in 10 sections totaling approximately 13 miles. The survey was repeated in the spring of 2015. We used the ‘structure from motion’ photogrammetry approach to develop detailed 3d models of the slopes at different times, directly from the photos. The models were aligned using a best-fit algorithm, and were then compared quantitatively for change. In the paper we discuss: the field and desktop methods, and describe the level of effort required to achieve high-quality results; examples of detected changes for different geological settings; the efficacy and utility of this approach for rock slope monitoring; and, the potential for integration into a GAM risk calculation. We also explore the general and site-specific limitations of OAP for monitoring rock slope hazards.

Old Problem Requires Innovative Investigation

Geotechnical Investigations of the Chippawa Power Canal Culvert Foundation

Gabriele Mellies

Golder Associates Ltd.
6925 Century Avenue, Suite 100
Mississauga ON L5N 7K2
(905)-567-4444
gabriele_mellies@golder.com

Mark Telesnicki

Golder Associates Ltd.
6925 Century Avenue, Suite 100
Mississauga ON L5N 7K2
(905)-567-4444
mark_telesnicki@golder.com

Tony Sangiuliano

Ontario Ministry of Transportation
1201 Wilson Avenue
Downsview ON M3M 1J8
(416)-235-5267
Tony.J.Sangiuliano@ontario.ca

Acknowledgements

The authors would like to acknowledge the Ontario Ministry of Transportation for its support of this work.

Disclaimer

Statements and views presented in this paper are strictly those of the author(s), and do not necessarily reflect positions held by their affiliations, the Highway Geology Symposium (HGS), or others acknowledged above. The mention of trade names for commercial products does not imply the approval or endorsement by HGS.

Copyright Notice

Copyright © 2015 Highway Geology Symposium (HGS)

All Rights Reserved. Printed in the United States of America. No part of this publication may be reproduced or copied in any form or by any means – graphic, electronic, or mechanical, including photocopying, taping, or information storage and retrieval systems – without prior written permission of the HGS. This excludes the original author(s).

ABSTRACT

Highway 420 crosses over the Chippawa Power Canal in Niagara Falls, Ontario supported by a large 22m span concrete culvert structure. The culvert, founded on dolostone bedrock and covered with 16 m of backfill, has experienced some displacements along some of the culvert sections. Significant deterioration of the canal walls above the water level has also been observed. The walls below water could not be visually assessed. The observations raised questions regarding the stability of the culvert and a geotechnical investigation was initiated to determine the causes of the culvert displacements and the rock wall deterioration and to assess the risk to the highway.

A major challenge in undertaking the geotechnical investigation was that the power canal had to be kept in service during the investigation. The rapid flow rate and the fact that the canal walls were partly under water did not allow direct access and necessitated a variety of investigation methods. Three state-of-the-art investigation methods were applied: 1) an extensive borehole investigation, 2) a LiDAR survey to investigate the canal walls above water level, and 3) an underwater Sonar survey focused on the walls below water. The methods had to be compatible to combine the three data sets into one single model. The resulting integrated model will allow for a comprehensive stability analysis and assessment of the wall conditions and will consequently enable the determination of appropriate remedial measures.

INTRODUCTION

Highway 420 in Niagara Falls, Ontario crosses over the Chippawa Power Canal on a large cast-in-place concrete arch culvert structure which is founded on bedrock along the canal walls. **Figure 1** shows Highway 420 and the Dorchester Road underpass at the location of the canal crossing. Over the years, displacements of some of the culvert's concrete segments were observed together with significant deterioration of the canal walls above the water level in the canal. No information was available for the underwater wall sections but deteriorations were expected as well. The Ontario Ministry of Transportation (MTO), owners of the bridge and culvert, awarded a Consultant Assignment to Morrison Hershfield (MH) to investigate the cause of the culvert movement, evaluate the stability of the rock canal face, assess the risk of culvert failure and provide remedial measures. MH retained Golder Associates Ltd. (Golder) to undertake a geotechnical investigation to determine the causes of the displacements and the canal wall deterioration and to assist in the risk assessment.



Figure 1: Highway 420 and Dorchester Road underpass (left) crossing over the Chippawa Power Canal on a large concrete arch culvert (right)

Problem Statement

The specific challenge of this project was to collect the required data from the canal walls above and below water level and the bedrock foundations in order to adequately characterize the rock mass. Several constraints had to be considered in finding suitable data collection methods and these did not allow for traditional mapping and direct observation methods. Site access restrictions imposed by Ontario Power Generation (OPG) and the fact that the canal had to be kept in operation during the investigation without the possibility of lowering the water level posed challenges for the investigation. Furthermore, due to the rapid water flow in the canal of about 3.5 metres per second floating vessels or divers were not permitted in the canal.

As a result, direct access to the walls to perform traditional mapping was not possible and access from above, using for example rope access techniques, was also rejected due to safety

concerns. Although the upper wall areas above the water level could be inspected visually, the obscured canal wall areas below the water level did not allow for any visual inspection. Furthermore, since large sections of the canal walls were covered by shotcrete or concrete a comprehensive visual assessment of the bedrock was further hindered.

The project site conditions dictated a requirement for different investigation methods for the rock faces above and below the water. Additional information on the bedrock was required for the analysis of the culvert stability. The integration of survey results stemming from different methods into one data set was seen as a major objective.

BACKGROUND

The approximately 13 km long Chippawa Power Canal in Niagara Falls, Ontario was built to divert water from the Welland River to the Sir Adam Beck power station located at the bank of the Niagara River. The canal was constructed between 1917 and 1921 and the walls and bottom of the canal were lined with shotcrete and concrete respectively (**Figure 2**).

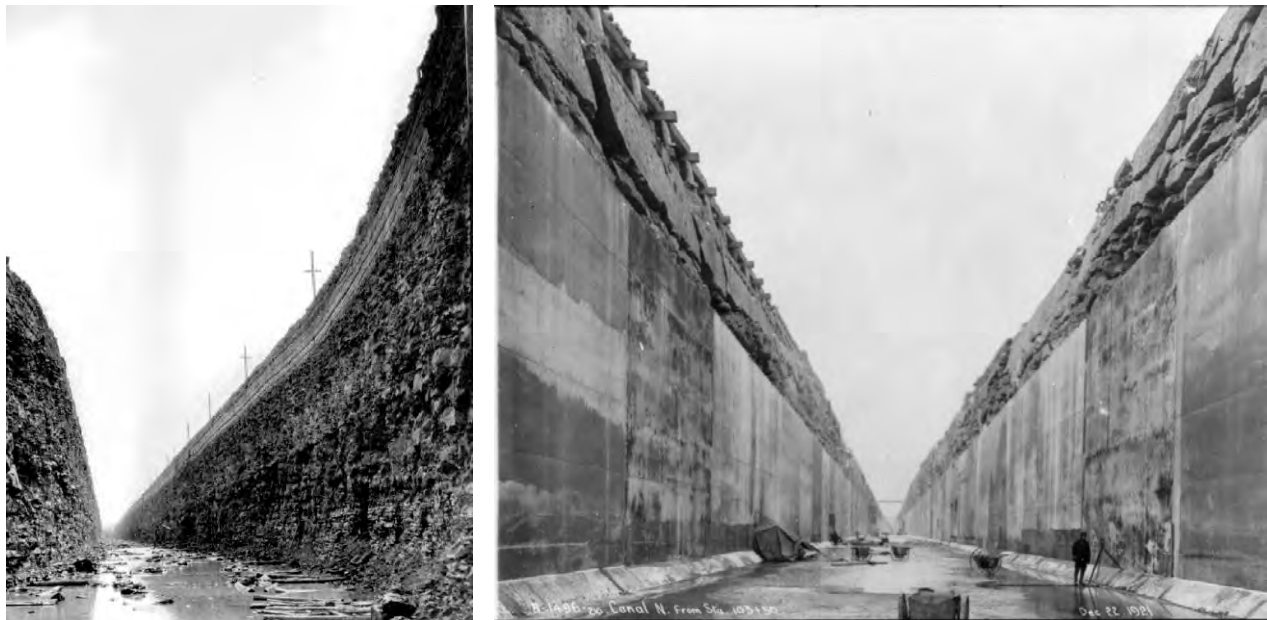


Figure 2: Chippawa Power Canal during construction (left: canal excavation in rock, 1920 (photo: www.nflibrary.ca); right: concrete lining on canal walls and bottom, 1921 (photo: www.collectionscanada.gc.ca))

In 1964/65 the canal was rehabilitated, at which time it was deepened and locally widened. The width and depth of the canal varies over its length; at the investigated site, the canal has a width of approximately 15 to 17 metres and a depth of approximately 20 metres. The water level in the canal varies; at the time of the investigation the water level was approximately at elevation 168.7 metres (depth of water in the canal approximately 12 metres).

In the early 1970s the Chippawa Power Canal Arch Culvert was built to allow the construction of the mainline and the ramp lanes of Highway 420 as well as the Dorchester Road underpass above the power canal. The arch culvert has a total length of 207 metres and consists

of eight cast-in-place concrete arches (segments), each of which is 25.9 metres long. The east entrance of the culvert is shown in **Figure 3**. The culvert has a span of 22.7 metres, a rise of about 7.6 metres, and is supported on strip footings parallel to the canal walls that are founded on dolostone bedrock. Highway 420 and the Dorchester Road underpass were constructed above the culvert in 1972.



Figure 3: Concrete arch culvert (left) spanning over the Chippawa Power Canal (right)

Over the years, differential displacements of approximately 100 mm have been noted at the joint between two culvert segments (**Figure 4**), in particular in the haunches of the concrete arches.



Figure 4: Displacements of culvert segments (right: detail of displacements)

In addition to the culvert distortion, the shotcrete and concrete liner on the canal walls exhibit severe deterioration and spalling. The exposed rock face itself has undergone major degradation, slaking and undermining underneath the concrete sidewalks, adjacent to the culvert foundations. **Figure 5** shows the south side wall of the canal with areas of failed shotcrete and a section of undermined sidewalk.



Figure 5: Deterioration of shotcrete lining and rock faces along canal walls

MATERIAL AND METHODS

The goal of the data collection was to gather suitable data that would allow an assessment of the canal wall conditions above and below water and provide information regarding the rock mass as well as the bedrock conditions underneath the culvert footings. Since direct access to the canal walls was not possible, various remote sensing techniques were evaluated.

A combination of standard investigation methods and innovative surface mapping technologies was finally chosen to allow an assessment of the canal wall conditions and the culvert foundations. **Figure 6** illustrates the applied methodology to collect and integrate the required data.

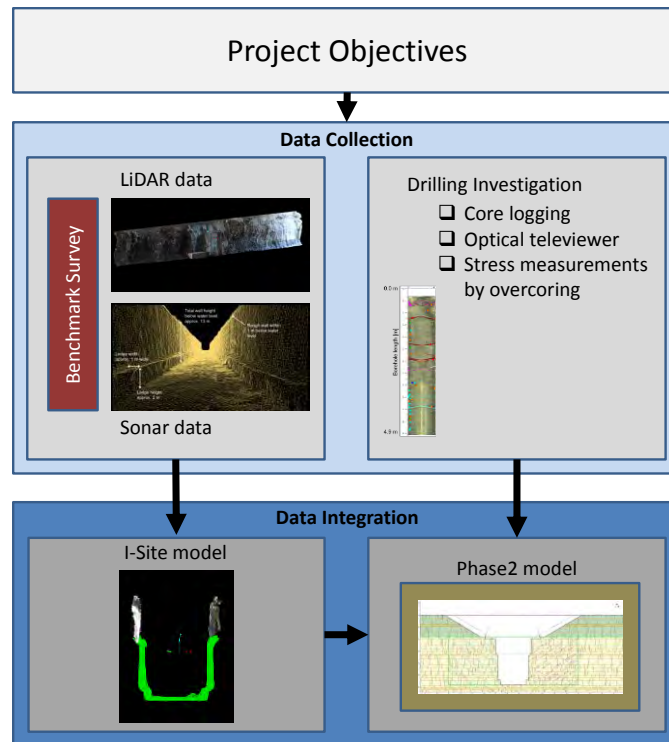


Figure 6: Applied Methodology

Project Objectives

The proposed methodology starts with a detailed definition of the project objectives. When choosing survey technologies to collect data, special attention should be given to the optimum data resolution required for the subsequent analyses as the data volume can cause significant limitations with respect to usability.

Data Collection

Surface Investigation

A *terrestrial LiDAR survey*, also referred to as 3D laser scanning, uses laser light pulses to image objects. LiDAR systems commonly available today can collect data points at a rate of more than 1,000,000 points per second. The data points (point cloud data) can be used to create a 3D triangulated surface onto which high resolution photographs can be draped. The 3D surface can be used to determine the orientation of major features such as joint sets in the rock mass or the magnitude of rock overhangs. This method was chosen to investigate the conditions of the vertical surfaces above water due to the resolution and accuracy of the data and the ability to map the canal walls including any features of interest without directly approaching the walls.

The LiDAR survey was carried out by Tulloch Engineering of Huntsville, Ontario as a sub-contractor to Golder. The survey was carried out from the sidewalks inside the culvert using a HDS7000 Laser Scanner from Leica. Spatial data of the canal wall faces above the water level was collected and used to generate detailed point cloud data (x, y, and z coordinates) of the entire

walls. The result is a detailed high-resolution surface model of the canal walls that allows the identification of deteriorated wall areas as well as structural mapping of the exposed rock faces.

Another investigation technique for surface data collection that was reviewed during the planning stage was digital photogrammetry. However, the accuracy of LiDAR was considered higher than the one of photogrammetry. Since it is planned to repeat the surface survey regularly, the higher accuracy was the decisive factor for the use of LiDAR. In addition, LiDAR was considered less sensitive to the difficult light conditions in the culvert.

An *underwater Sonar survey* uses underwater sound propagation to image objects and can be used to investigate vertical and horizontal surfaces below water. This remote survey technique provides 3D scans as well as 2D images of the surveyed surfaces without the need of entering the water body (i.e. using underwater vessels or divers). This method was selected to investigate the underwater portion of the canal walls.

The underwater Sonar survey was carried out by ASI Group Ltd. of St. Catharines, Ontario as a sub-contractor to Golder. The survey was carried out from the sidewalks within the culvert using a pole mounted scanning Sonar unit that was suspended from the sidewalks into the canal. Two different Sonar technologies were used:

1. Acoustic Sonar profiling was used to collect three-dimensional point cloud data (x, y, and z coordinates) of the submerged structures using a Blueview BV5000-1350 Multi-beam Profiling Sonar. This survey provides a detailed 3D surface of the underwater walls and bottom of the canal which enables the identification and measurements of deteriorated wall areas and accumulations of debris on the canal bottom.
2. Sonar imaging was used to generate two-dimensional image scans of the vertical canal walls using a Kongsberg MS1071 Series 675 kHz Scanning Sonar. This survey results in a two-dimensional image of a surveyed surface and provides information regarding the texture of the wall surfaces (for example joints or cracks, scour, protruding anomalies like overhangs etc.).

Other underwater investigation methods that were reviewed during the project planning stage included diving, side scan Sonar and the use of a remote-operated vehicle (ROV) to survey the rock faces from the bottom of the canal. However, these methods were considered not feasible. The use of divers and/or manned vessels was considered too dangerous due to the high flow rates in the canal; the latter method would be required for towing side-scan Sonar equipment through the canal. The high flow rate also prevents the use of an ROV to survey the rock faces from the bottom of the canal. In addition, side-scan Sonar is more suitable to survey horizontal areas (for example, the base of the canal) rather than vertical faces (the sides of the canal).

If not already available, surveyed control points have to be established to allow for referencing of the LiDAR and Sonar survey data to a *global geodetic coordinates system*.

Subsurface Investigation

An extensive drilling program was developed to investigate the subsurface conditions. The investigation comprised of (i) **logging of rock core** retrieved from several drillholes; (ii) **downhole geophysical survey** of the drillholes to obtain image scans of the borehole walls as well as oriented structural data of the rock mass; (iii) **in-situ stress measurements** using the overcoring method to provide an assessment of the site specific horizontal stresses in the bedrock and (iv) **packer testing** to gather information on the hydraulic conductivity of the rock.

The borehole investigation carried out from inside the culvert focused on the bedrock foundations below the arch culvert footings and consisted of six boreholes that were drilled from the sidewalks inside the culvert using a small portable electric HILTI coring drill. The inclined boreholes were drilled 5 metres each into the bedrock foundation underneath the arch culvert footings. The locations of the holes were chosen close to the area where the displacements of the culvert were observed. The retrieved rock core was logged for characteristics of rock mass and discontinuities (including RQD, core recovery, fracture frequency, etc.). Rock core samples were used for laboratory testing (including unconfined compressive strength, elastic modulus, freeze-thaw and slake durability, etc.).

In addition to the core logging, an optical televiewer survey using an ALT Optical Borehole Imager (ALT-OBI40) was performed in all six boreholes in order to collect optical images of the borehole walls including structural and directional information about the discontinuities encountered in the holes. The optical televiewer generates a high resolution digital image of the inside of the borehole wall and is capable of capturing structural features as narrow as 0.1 mm at a radial resolution of 1 degree. The data is recorded together with data from an internal magnetometer and a tiltmeter allowing the determination of the orientation (dip and dip direction) of the structural features recorded. The survey data was then processed using WellCAD software (Advanced Logic Technology Ltd.) and oriented to magnetic north prior to image interpretation.

A further borehole was drilled from ground surface at a location approximately 30 m away from the culvert. The hole was advanced into bedrock and used to carry out in-situ stress measurements using overcoring in order to define the stresses in the rock that might impact the stability of the canal walls. Reportedly, pop-up failures occurred during the construction of the canal and the stress measurements were intended to determine the actual stresses in the vicinity of the canal. In addition, packer testing was carried out in the borehole to define the hydraulic conductivity of the rock.

An additional six boreholes were drilled vertically from Highway 420 grade and these focused on the backfill material above the culvert. The locations of these holes were chosen close to the area where the displacements of the culvert were observed. Soil samples were used for laboratory testing (including moisture content, grain size distribution, Atterberg limits, etc.).

Data Integration

In a *first data integration step*, the LiDAR and Sonar surface data was used to create a combined surface model in I-Site Studio 5.0 (*I*). This model was used to generate cross sections of the canal and to perform a visual analysis of the canal walls. In a *second data integration step*, the surface model was combined with the subsurface data gathered during the drilling investigation to create a holistic model that incorporates both surface information as well as subsurface information regarding the overburden and rock mass.

RESULTS

Surveying of Culvert Layout and Reference Points

The culvert alignment was surveyed and the surveyed layout transferred to highway grade to accurately determine the borehole locations above the culvert. The culvert layout below Highway 420 is shown in **Figure 7**. In order to reference both the LiDAR and the Sonar data to a global coordinates system, common reference points had to be established in the field that could be used for both surveys. This was important as the goal was to combine both data sets and allow a comprehensive assessment of the condition of the wall surfaces.

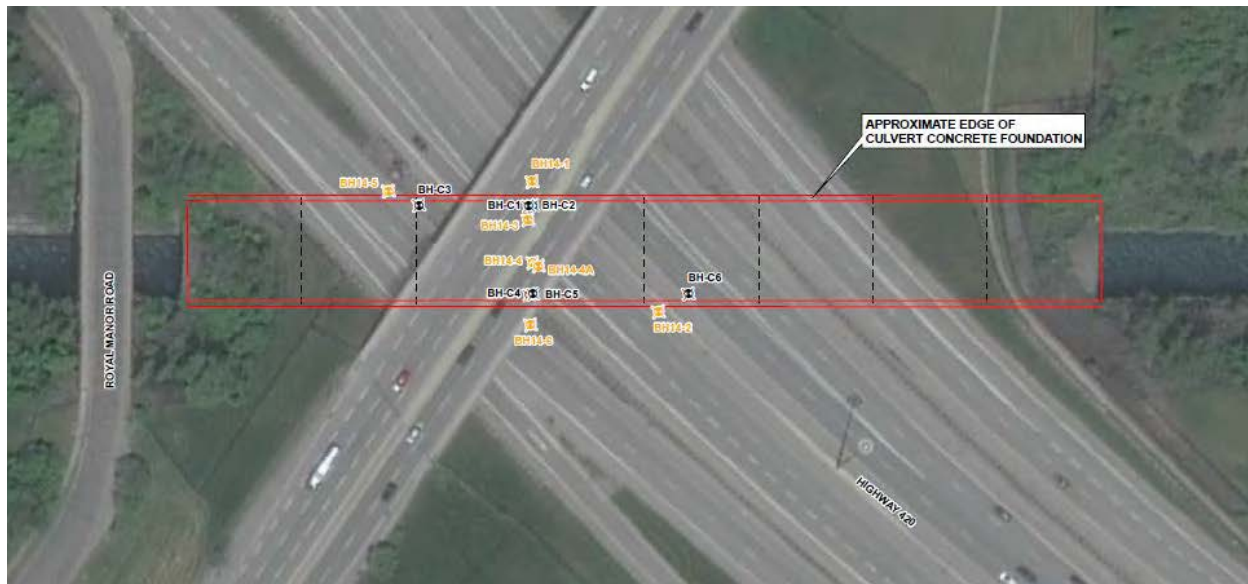


Figure 7: Location of power canal below Highway 420 and Dorchester Road underpass

LiDAR Survey of Canal Walls above Water Level

The LiDAR survey provided a detailed 3D point cloud of the canal walls above the water level which was processed with the I-Site Studio software (*I*). The data was used to assess the condition of the wall and to identify areas of deteriorated shotcrete, undermined and eroded areas as well as structural features along the walls. In addition, the data allowed for structural mapping of the rock in areas where the rock face is exposed. However, since most of the canal walls are covered with shotcrete or concrete, the mapping results were very limited. The example of the

LiDAR survey results provided in **Figure 8** shows the rough wall surface that is largely covered with shotcrete or concrete structures.

It was evident that many areas of the canal walls have undergone significant deterioration and the dimensions of these areas were measured from the LiDAR data in order to determine the extent of remediation required. The data also showed that large areas of the canal walls are still covered with shotcrete or concrete and have, therefore, not changed significantly since the rehabilitation of the canal in 1965.

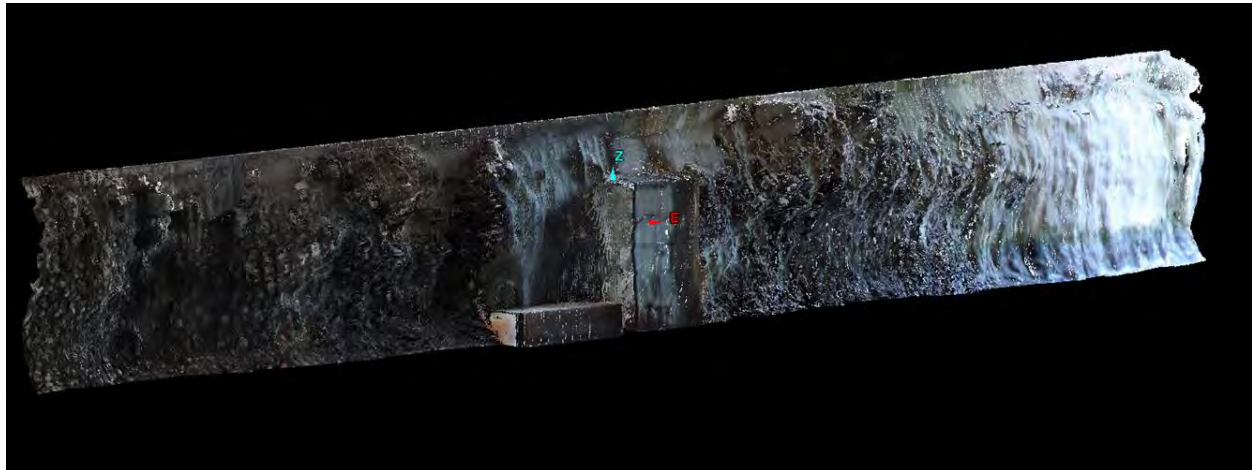


Figure 8: Example of LiDAR survey results showing the canal walls above water level

Sonar Survey of Canal Walls below Water Level

The 3D point cloud data resulting from the acoustic Sonar profiling was processed with I-Site Studio 5.0 software (*I*) and the surface model was used to assess the condition of the canal walls below water level and identify areas where the walls have deteriorated. It was noted that the walls are generally intact and no areas of significant deterioration were identified except from the upper approximately 1 m of wall below the water level. The data also gave information about the dimensions of the canal and revealed small ledges at the toe of the walls. Some accumulations of debris were noted on the bottom of the canal as well as on the ledges. **Figure 9** shows an example of the collected acoustic Sonar data.

Due to the water flow in the canal, movements of the scanning equipment could not be entirely avoided and affected the data quality. The accuracy of the data was estimated to be +/- 150 mm.

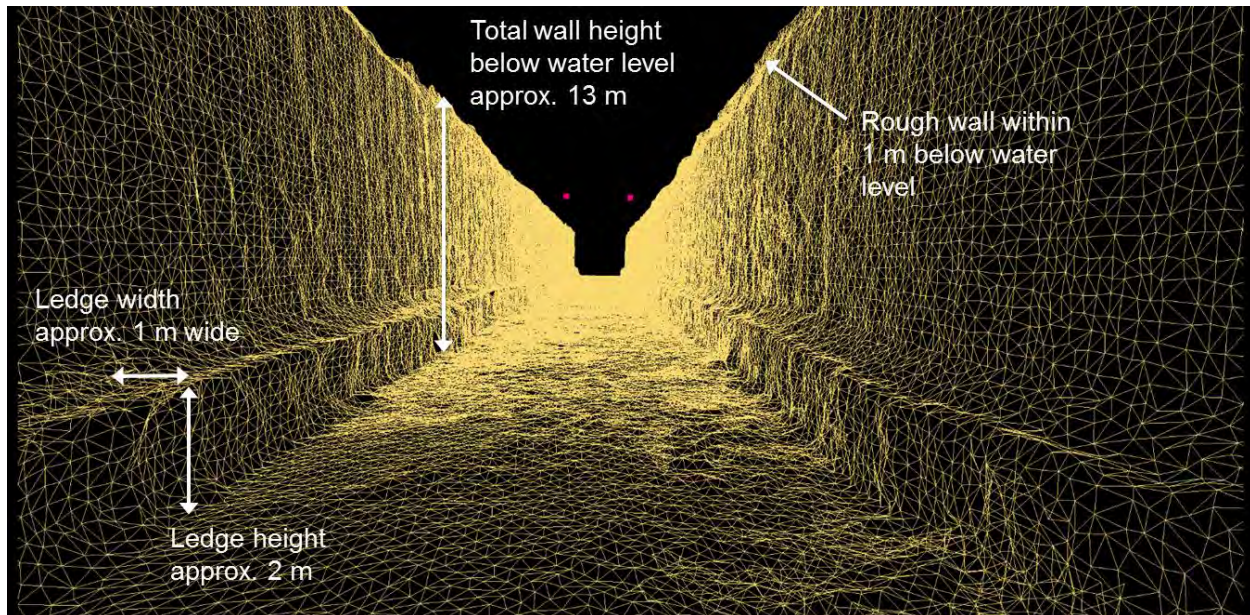


Figure 9: Example of 3D acoustic Sonar profiling results showing the canal walls and bottom below water level

The two-dimensional image scans of the vertical canal walls resulting from the Sonar imaging results in a two-dimensional image of a three-dimensional surface and provides information about the texture of the wall surfaces (like joints, scour, overhangs, ledges etc.). **Figure 10** provides an example of the collected imaging Sonar results. The image shows the canal walls and the bottom of the canal as well as the ledges along the wall toe. Some debris was identified on the canal floor; however, no significant accumulations of debris were observed. Vertical and horizontal joints were observed on the walls, indicating that the walls are covered with concrete.

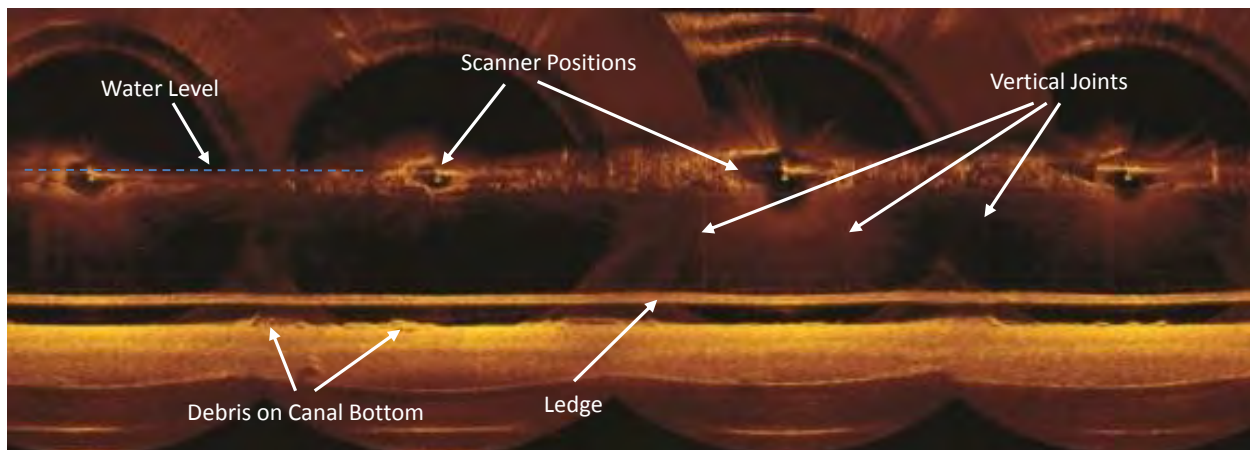


Figure 10: Example of 2D Sonar imaging results showing the canal walls below water level

Drilling Investigation

The approximate locations of the boreholes inside and above the culvert are shown in **Figure 11**. The borehole investigation carried out from inside the culvert focused on the bedrock foundation below the arch culvert footings. The information gathered from the rock core indicates a fresh to slightly weathered, strong to medium strong dolostone with thin shale interbeds belonging to the Lockport Formation.

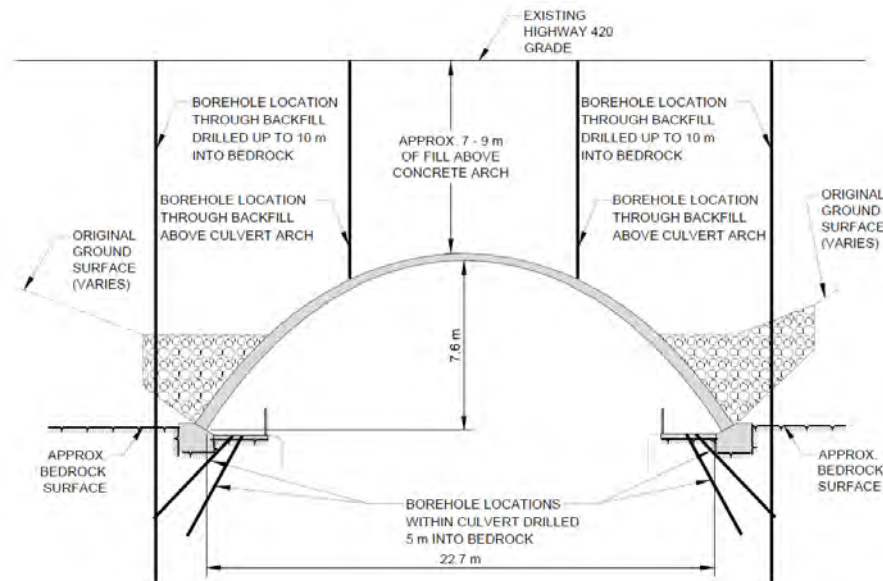


Figure 11: Cross section through Chippawa Power Canal Culvert with drilling locations inside the culvert

The borehole images and structural data gathered with the televiewer survey indicated horizontal bedding planes and several open discontinuities on both sides of the canal that were dipping towards the canal walls. **Figure 12** (left side) provides an example of the borehole images showing several open and inclined structural features. This observation was consistent with observations that were made by Golder at the time of the culvert construction (2). The oriented structural data was used to prepare stereoplots using the DIPS 6.0 software from Rocscience (3) and to perform a kinematic analysis of potential failure modes along the canal walls. The results indicate slight chances of planar and toppling failures.

The stress measurements in the vicinity of the culvert were carried out to investigate the potential impact of the stresses in the rock mass on the canal walls. The results indicate that in the investigated area the major principal stress is oriented approximately parallel to the canal and that the major stress is significantly higher than the minor principal stress. This result is in accordance with historical measurements in the general project area (4). It is expected that the minor principal stress has relaxed since the excavation of the canal. This is supported by the Sonar investigation results that show no significant movements along the walls or the bottom of

the canal. A typical stress measurement result is shown in **Figure 12** (right side). A piezometer installed in this borehole indicated a water level approximately 3.5 m below the bedrock surface.

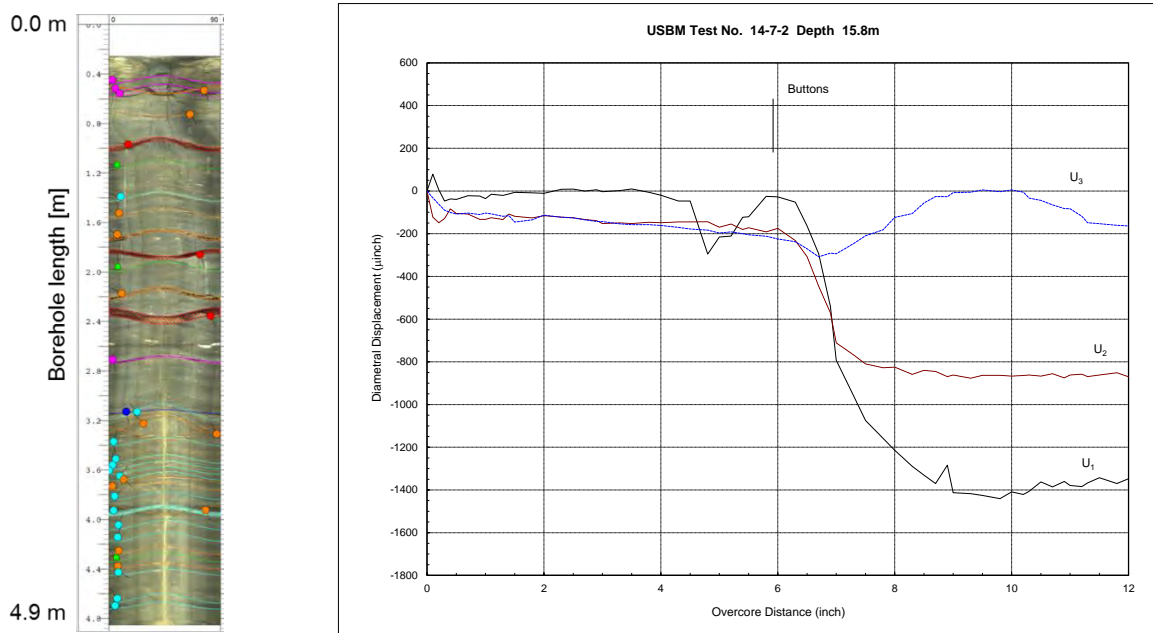


Figure 12: Results of optical televiewer survey (left) and overcoring (right)

The drilling investigation from Highway grade focused on the backfill material above the arch culvert. The backfill material consisted mostly of firm to hard clayey silt with layers of silt and some sand, gravel, cobbles and boulders. No indication was found of uneven loading due to the compaction of the backfill. A piezometer installed in one of the boreholes is dry to date.

Data Integration

In a first data integration step, both the LiDAR and the Sonar data sets were processed using the I-Site Studio 5.0 software (*I*) to develop a three-dimensional surface model of the canal walls. This model allowed an assessment of the wall conditions and determination and measurements of wall features of interest including size and depth of deteriorated and eroded wall sections. In addition, the LiDAR data allowed structural mapping of the rock along the wall areas where the shotcrete lining had fallen off the walls. **Figure 13** shows the integrated 3D surface model of the canal walls.

The two data sets matched up well when combined; however, some small data gaps occurred along the water level elevation. The reason for these gaps could be that some areas at the transition zone between upper and lower walls were not reached by the laser or sonar beams. Some gaps were probably caused by fluctuating water levels occurring between the execution of the LiDAR survey and the Sonar survey. The overall assessment of the walls was not affected by the data gaps.

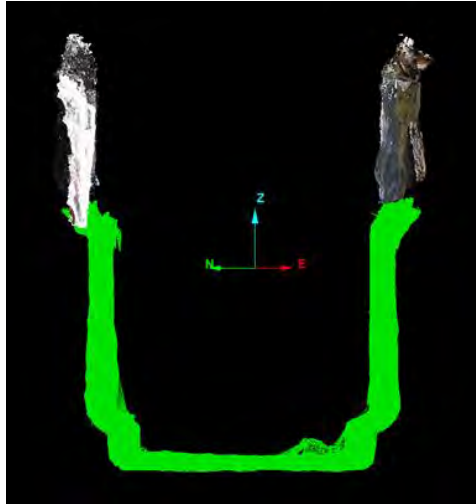


Figure 13: 3D surface model of the canal walls

In a second data integration step, the information from the surface model was combined with the data collected during the subsurface investigation and integrated in a 2D model of the canal and the bedrock using RS2 (Phase2 9.0) (5), a 2D elasto-plastic finite element stress analysis program, in order to perform a stability analysis of the canal walls and culvert foundation. Bedrock information including unconfined compressive strength, elastic modulus, rock mass characterization and in-situ stress was included in the model as was information regarding the discontinuities in the rock, including orientation of joints and bedding. **Figure 14** shows the 2D model of bedrock and canal walls. The bedrock was modelled with a discrete joint network and several stages were used to model the excavation of the canal.

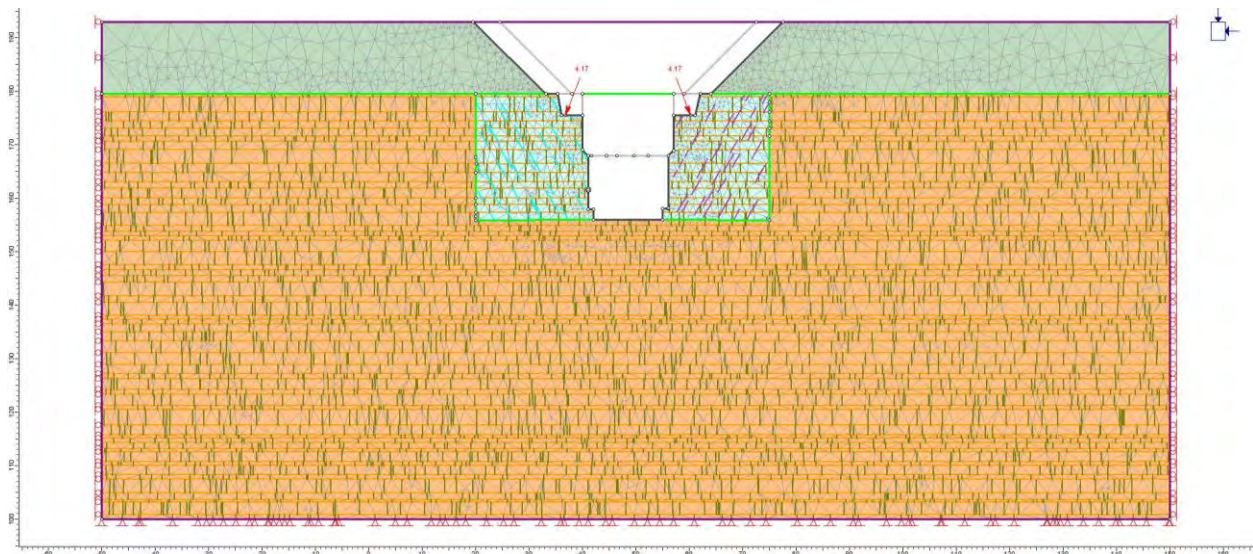


Figure 14: 2D model of canal and surrounding bedrock (RS2 (Phase2 9.0))

This model is to be used for a stability analysis of the canal and the bedrock foundation below the culvert footings.

DISCUSSION

The different investigation components allowed for the collection of various data of the canal wall surfaces and the bedrock. Both remote survey methods used provided surface data of the walls above and below the water level in the canal that enabled an accurate assessment of the wall conditions and form the basis for recommendations for remedial measures. The drilling investigation provided subsurface data that enabled the determination of meaningful input parameter for the RS2 model and allow for an analysis that is based on consolidated findings.

Some challenges had to be overcome during the data collection that was carried out from inside the culvert:

- The culvert is accessible only from a small steep path that leads to the north sidewalk inside the culvert. All equipment that was used in the various investigations had to be lightweight in order to be carried on this path. For the investigation from the south side of the canal, a pulley system was installed inside the culvert that was used to transport the equipment across the canal. The pulley system worked well and allowed transporting all material and equipment safely across the canal, including survey equipment, drill rig and rock core boxes.
- Due to the rapid water flow in the canal, it was difficult to stabilize the Sonar equipment that was lowered into the water. ASI used a pole mounted to the sidewalk guardrail to lower the equipment into the water. The pole was stabilized with ropes fixed to the pole and pulled downstream and upstream.
- The drilling from the sidewalks had to be carried out with a portable drill that was small enough to be carried down the access path and drill inside the culvert with very limited headroom but was able to retrieve rock core of NQ size diameter. The small electric Hilti drill that was used proved to be suitable to fulfill these requirements.

A further problem arose during the first data integration step. The high resolution LiDAR survey results provided a very detailed ‘image’ of the canal walls. However, the high resolution of the point cloud data resulted in a very large data set of more than 23 GB that caused problems during the subsequent data processing with standard computer hardware. In an attempt to make the data more manageable, the point cloud data sets were broken up into several sets prior to processing and were then filtered significantly during the data integration process with I-Site Studio (*I*). The remaining density of the point cloud data still provided sufficient detail to assess the wall conditions. However, these difficulties showed the importance of thoroughly defining the project objectives prior to the data collection.

The 2D model is to be used to perform stability analyses of the canal walls and the bedrock foundation underneath the culvert foundation. The model will be used to investigate the required bedrock thickness between the culvert footings and the face of the canal walls. The analysis will also focus on the potential for wedge failures along the canal walls that might impact the culvert foundations.

SUMMARY AND CONCLUSIONS

The presented project had to deal with several constraints and safety concerns, prohibiting the use of standard techniques. Remote sensing methods were selected including LiDAR for the areas above the water level and two Sonar survey methods for an evaluation of the underwater sections. An extensive drilling program complemented the investigations by adding subsurface information. All investigations inside the culvert were carried out from the sidewalks in the culvert without the need of approaching the walls directly. The drilling, using special portable equipment from the sidewalks in the canal, allowed the data collection in the area of concern underneath the culvert foundations.

The chosen methodology proved to be suitable to reach the project goal of collecting and integrating surface data of the canal walls and subsurface data of the bedrock. The investigation methods for the canal wall surfaces consisting of LiDAR and Sonar surveys provided reliable data that was required to assess the wall condition above and below the water level. The data was subsequently used as input to the surface model of the canal. The investigation method for the subsurface conditions included an extensive drilling investigation comprising traditional core logging, geophysical surveying, and overcoring and delivered the data for a realistic model of the bedrock. Surface and subsurface data were integrated into a 2D elasto-plastic finite element stress analysis program.

The results of the various investigations resulted in a holistic model of the canal and the bedrock. The next project step will be to use this model for a comprehensive stability assessment of the site.

REFERENCES

1. MaptekTM. *I-Site Studio 5.0 software online help*. MaptekTM Pty Ltd. Accessed May 2015.
2. Golder, H.Q. *Foundations for Bridge No. 10 over the Chippawa Canal, Niagara Falls, Ontario*. H.Q. Golder & Associates Ltd., Mississauga, Ontario. November 1970.
3. Rocscience Inc. *DIPS 6.0 software online help*. Rocscience Inc., Toronto, Canada. Accessed May 2015.
4. Lo, K.Y. et al. *Report on Stress Relief and Time-dependent deformation of Rock*. NRC Special Project No. 7307, Faculty of Engineering Science, The University of Western Ontario, London, Ontario, 1975, pp. 59-71.
5. Rocscience Inc. *RS2 (Phase2 9.0) software online help*. Rocscience Inc., Toronto, Canada. Accessed May 2015.

**Debris Flood Assessment and Mitigation Design:
Trans-Canada Highway, Alberta**

Alex Strouth, Joe Gartner
BGC Engineering Inc.
710 10th Street – Suite 170
Golden CO 80401
(303)-727-0996
astrouth@bgcengineering.com
jgartner@bgcengineering.com

Kris Holm, Matthias Jakob
BGC Engineering Inc.
980 Howe Street – Suite 500
Vancouver BC Canada V6Z 0C8
(604)-684-5900
kholm@bgcengineering.com
mjakob@bgcengineering.com

Prepared for the 66th Highway Geology Symposium, September, 2015

Acknowledgements

The authors would like to thank the following individuals and entities for their contributions in the work described:

Martin Buckley, Dale Mather – Municipal District of Bighorn No. 8
Roger Skirrow – Alberta Transportation
Andy Esarte – Town of Canmore

Disclaimer

Statements and views presented in this paper are strictly those of the author(s), and do not necessarily reflect positions held by their affiliations, the Highway Geology Symposium (HGS), or others acknowledged above. The mention of trade names for commercial products does not imply the approval or endorsement by HGS.

Copyright Notice

Copyright © 2015 Highway Geology Symposium (HGS)

All Rights Reserved. Printed in the United States of America. No part of this publication may be reproduced or copied in any form or by any means – graphic, electronic, or mechanical, including photocopying, taping, or information storage and retrieval systems – without prior written permission of the HGS. This excludes the original author(s).

ABSTRACT

This paper provides an overview of the 2013 debris flooding near Canmore, Alberta and the subsequent debris-flood risk assessments and flood protection designs, with special attention given to mitigation design elements along the Trans-Canada Highway.

Three-days of heavy rainfall in Alberta, Canada in June 2013 caused extensive flooding in the southwestern portion of the province. Debris floods were prevalent on alluvial fans and caused extensive and long-lasting highway closures, almost completely severing Bow Valley from access from either side. Sediment and debris blocked numerous culverts and bridge underpasses, and choked channels, which led to flow avulsions, bank erosion, and flooded communities and roadways. The province of Alberta, including Alberta Transportation and individual municipalities, responded to the event by initiating studies to systematically identify, prioritize, and assess flood and debris-flood hazards and risks, and to design and implement risk reduction measures that improve resiliency and reduce consequences of future floods.

The flood event and subsequent assessments and designs have highlighted three important themes that should be considered when designing culverts, bridges, and flood protection works for highways in mountainous terrain. Each theme is illustrated in the paper with case study examples.

- Importance of accurately recognizing the hydro-geomorphic process type
- Benefits of using a risk-based approach to design
- Importance of recognizing interaction of highways with other elements on fans

Each theme is illustrated in the paper with case study examples.

INTRODUCTION

Heavy rainfall in Alberta, Canada in June 2013 caused extensive flooding in the southwestern portion of the province that led to Alberta's worst natural disaster and estimated damage costs on the order of \$6 Billion (1). Major rivers flooded and inundated downtown Calgary, and smaller tributary creeks caused extensive damages in unexpected locations. Debris floods were prevalent on developed alluvial fans and caused extensive highway closures, with particularly high consequences near the Town of Canmore.

When three days of record-breaking rainfall began, many of the tributary creeks to the Bow River were dry. As rainfall intensified in the evening, water began flowing in the creeks and continued to rise through the night. Bulldozers and excavators were deployed in an effort to maintain the function of the culverts along the TransCanada Highway, however these efforts were soon overwhelmed due to the rising flood waters and high rates of sediment transportation.

Sediment and debris blocked numerous culverts and bridge underpasses, and choked channels, which led to flow avulsions, bank erosion, and flooded communities and roadways. The Trans-Canada Highway was closed for seven days (Figure 1). Highways, roads, communities, railways and critical infrastructure were all severely affected. In some locations highway and roadway embankments caused ponded floodwaters and, in other locations, fast flowing water undermined house foundations. Following the initial emergency response and recovery efforts, the province of Alberta, including Alberta Transportation and individual municipalities, commissioned studies to quantify damages and design measures to reduce the likelihood and severity of such damages in future events (2-26). Along the Trans-Canada Highway, these studies included work by BGC Engineering Inc. (BGC) to systematically identify, prioritize, and assess flood and debris-flood hazards and risks, and to design and implement risk reduction measures that improve resiliency and reduce consequences of future floods.

This paper summarizes important considerations for debris-flood risk reduction design based on lessons learned at alluvial fans in Bow River Valley, near Canmore, Alberta. The paper focuses on the following three themes:

- Importance of accurately recognizing the hydrogeomorphic process type
- Benefits of using a risk-based approach to design
- Importance of recognizing interaction of highways with other elements on fans

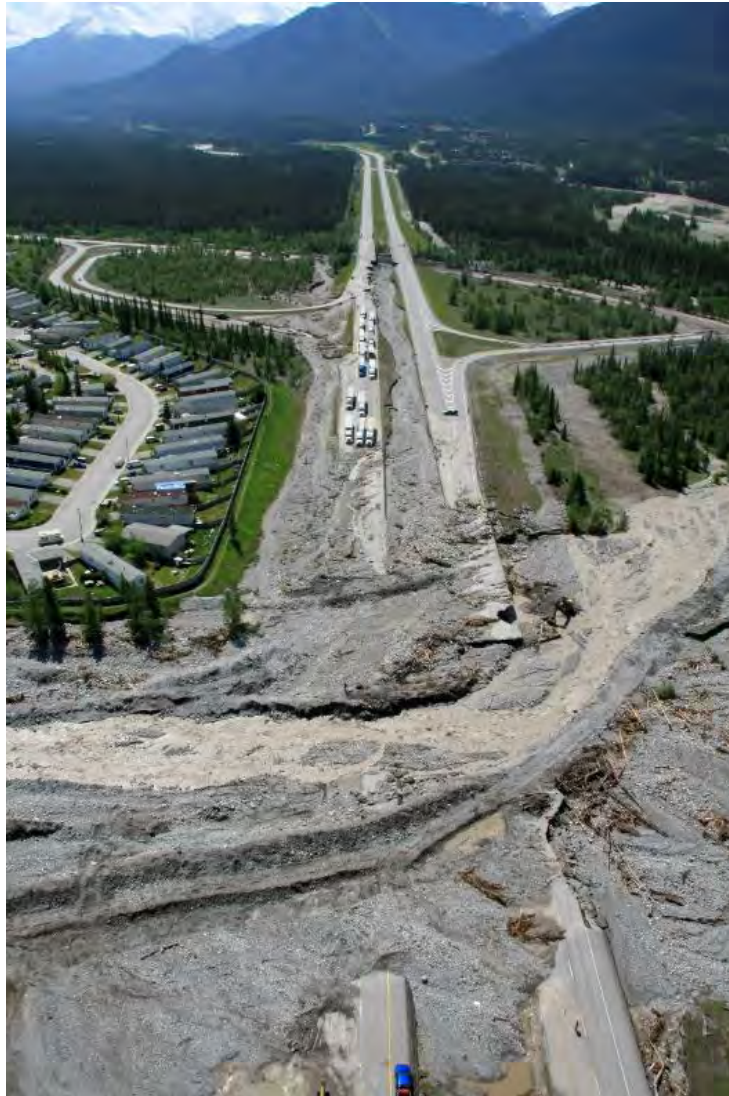


Figure 1. Trans-Canada Highway overwhelmed by the June 2013 debris flood at Cougar Creek in Canmore, Alberta. Town of Canmore.

HYDRO-GEOMORPHIC PROCESS TYPE

Floods, Debris Floods, and Debris Flows

Steep mountain creeks are typically subject to a spectrum of hydro-geomorphic processes that range from clear water floods to debris floods to debris flows in order of increasing sediment concentration. There is a continuum between these processes in space and time with floods transitioning into debris floods and eventually debris flows through progressive sediment entrainment. Conversely, dilution of a debris flow through partial sediment deposition and tributary injection of water can lead to a transition towards debris floods and eventually floods. The distinction between floods, debris floods and debris flows is important, as they differ in flow mechanics and potential consequences. Misinterpretation of the process can lead to under-

designed mitigation measures, the failure of which can result in damage or loss of life. Alternatively, it can also lead to over-designed measures that are unnecessarily expensive to build and maintain.

Debris flows typically require a channel gradient in excess of some 30% for transport over long distances and have volumetric sediment concentrations typically in excess of 50-60%. They can achieve velocities up to 10 m/s (36 km/hr) and carry garage-size boulders in partial suspension and through saltation. Their peak discharge may be up to 50 times higher than those of 200-year flood peak discharge calculated for the same stream through regional analysis (27). Depending on flow velocities and flow depth, their impact forces can destroy normal wood frame structures as well as concrete foundations.

Debris floods (also known as hyperconcentrated flows) are very rapid surging flow of water, sediment, and debris that typically occurs where channel gradient is between 3% and 30%. Debris floods have a lower proportion of sediment and debris (typically in the range of 4% to 20% by volume) compared to debris flows, but they mobilize more sediment than clear water floods. The peak discharge of a debris flood can be up to three times the design peak discharge estimated for the clear water flood (27). Debris floods can be highly erosive along steep portions of the channel, and also cause extreme riverbed aggradation in places where channel gradients decrease and channels widen, such as on fans, where development tends to be located. Aggradation results in burial of low-lying areas and structures and reduction of the channel's flood conveyance capacity, which can lead to high rates of bank erosion and flow avulsions.

Debris flows, debris floods, and "normal" clear water floods need to be treated differently analytically to avoid erroneous design input estimates that can stem from the inappropriate use of specific methods (28). For example, standard regional streamflow analyses strongly under-predicts observed peak discharges in steep creeks prone to debris floods or debris flows (e.g.27). As such, debris flow or debris flood channel crossings that were designed based solely on standard streamflow analyses may not withstand heavy sediment loads or intense bank erosion, leading to failure of abutments or blockage and channel avulsion. The principal differences in analysis of the different processes are summarized in Table 1.

Analytical Method	Floods	Debris Floods	Debris Flows
Standard frequency analysis using data from hydrometric stations at the creek in question	appropriate	not appropriate	not appropriate
Regional analysis	appropriate	appropriate, only if calibrated by observed debris floods	not appropriate
Flood routing models to determine peak flow at specific locations	appropriate	appropriate, only if calibrated by observed debris floods	not appropriate
Reconstruction of event frequency from paleoenvironmental proxies (e.g. dendrochronology, radiocarbon dating, air photo interpretation)	Rarely used but can be helpful in some instances to extend gauged record	appropriate and necessary	appropriate and necessary

Cougar Creek Example

The active channel of Cougar Creek flows through an alluvial fan in Canmore, Alberta that contains over 4000 persons and \$450 million in buildings development (9-10). Historical air photographs indicate that several avulsion channels were present until extensive development on the fan in the late 1970's and early 1980's restricted the creek to one main channel. The debris-flood event during 2013 resulted in sediment mobilization, channel aggradation and lateral bank erosion that damaged homes located along the channel banks (Figure 2) and closed the Trans-Canada Highway (Figure 1). Avulsion at one channel crossing upstream of the highway, Elk Run Boulevard, was averted only by continually excavating channel sediment throughout the event. Avulsion at this location could have resulted in flows into the central portion of the fan, which would have increased the severity of damage and potential for loss of life.



Figure 2 - Flooding on Cougar Creek threatened many residences (left) and channel aggradation lead to a braided river that caused significant bank erosion near Elk Run Boulevard (right). Town of Canmore.

Following a disaster response phase, design of short-term and long-term debris-flood risk reduction measures commenced with the understanding that debris flooding is the dominant hydro-geomorphic process at Cougar Creek. The risk reduction measures focus on capturing sediment mobilized in the water shed before it reached the developed fan, and providing an erosion protected channel that could convey the flood waters through the community and beneath the Trans-Canada Highway without bank erosion, re-mobilization of fan sediment, or flow avulsions.

The short-term risk reduction elements were constructed in 2014 and consisted of a flexible ring net barrier to capture sediment near the fan apex (Figure 3), an excavated channel, and articulated concrete mats lining the channel to prevent re-mobilization of sediment (Figure 4). Long-term risk reduction elements are currently being designed and include a barrier at the fan apex to retain sediment and, and attenuate peak discharge; and downstream grade control structures to reduce fan sediment re-mobilization, improve conveyance of flows, and protect the banks. The long-term design may also include increasing the conveyance capacity of local roads, railroad, and the Trans-Canada Highway crossing of Cougar Creek.

Design of the long-term risk reduction elements was based on quantitative hazard and risk assessments. The hazard assessment focused on estimating the frequency and magnitude (e.g. discharge, sediment volume) of debris-flood events and modelling the intensity of flows (e.g. depth, velocity) for representative debris-flood scenarios considered in the risk assessment. (Figure 5). The risk assessment focused on safety risks (i.e. loss of life) for persons occupying buildings on the fan, and economic risks (i.e. annualized direct damage costs). Risk reduction designs were optimized by identifying the minimum debris barrier height that would reduce both individual and group safety risks to tolerable levels. The cost of mitigation was justified based on comparison to the economic risk associated with leaving the hazard unmitigated. Further risk reduction will be achieved according to the ALARP (“as low as reasonably practicable”) principle, for example through improved emergency response measures. The ALARP principle recognizes that it is impracticable to completely eliminate risk, but risks should be reduced when it reasonable to do so.



Figure 3 - Flexible debris net located at the head of the Cougar Creek fan is 40 m wide by 6 m tall and is designed to trap coarse sediment, while allowing fine grained sediment and water to pass. BGC Engineering.



Figure 4 - Excavated channel with articulated concrete mats to prevent mobilization of sediment along the active channel of the Cougar Creek alluvial fan. Photographed during construction. BGC Engineering.

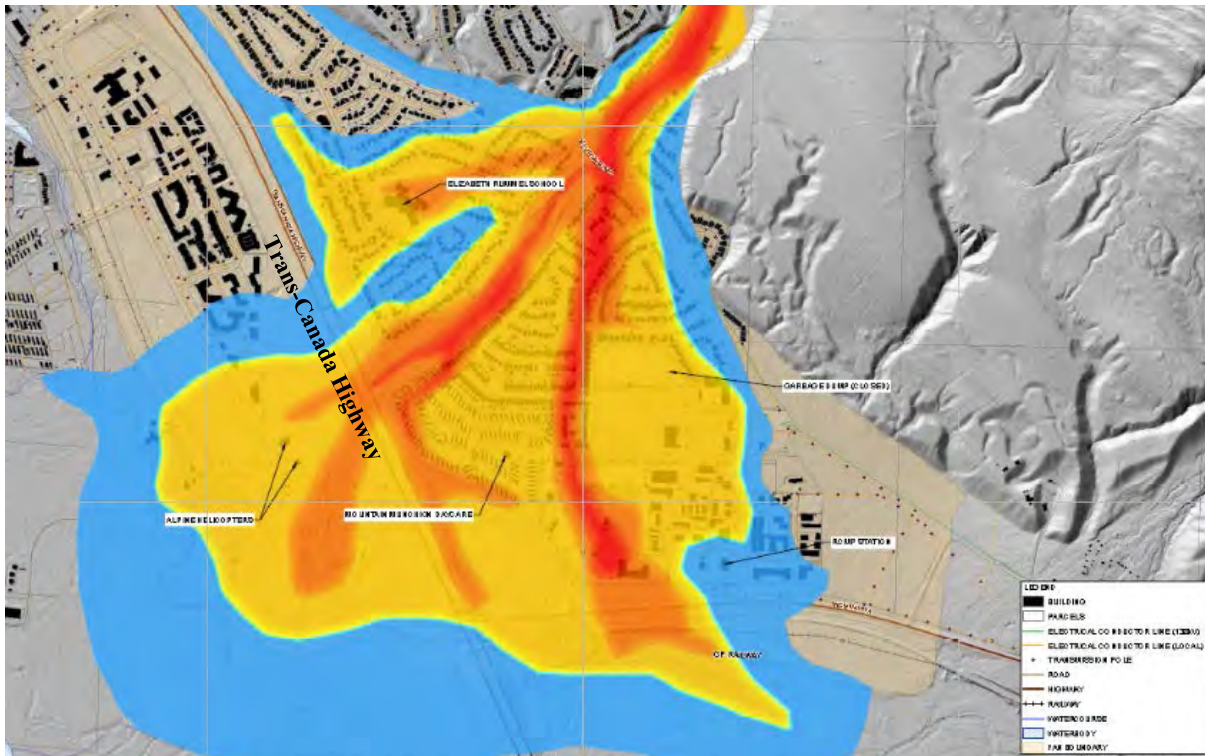


Figure 5 - Composite debris-flood hazard intensity map at Cougar Creek, considering multiple flood magnitudes. Hazard intensity ranges from very fast flowing and deep water (red) to slow flowing shallow and deep water with little or no debris (blue).

RISK-BASED DEBRIS-FLOOD MANAGEMENT

Hazard-Based versus Risk-Based Methods

Alberta's current flood management approach focuses on the flood hazard without explicit consideration of flood consequences. Flood hazard mapping has been produced by the Government of Alberta since the 1970s. Floods only relate to inundation by rivers or creeks of their surrounding terrain, and they do not explicitly include debris floods or debris flows, although these processes have not been purposely excluded. For flood hazards, standard practice has been to estimate the discharge and flood stage of a 100-year return period flood using hydrological methods, and use this as the basis for design of flood protection measures. This hazard-based method, while based on sound assumptions, does not specifically address debris-flow and debris-flood hazards, and does not account for consequences to elements at risk. This method is less useful for prioritizing funds, and can lead to unacceptable damages to critical infrastructure or communities when the flood protection works are overwhelmed. A hazard-based design method for highways would lead to similar culvert or bridge conveyance capacity designs at each fan shown in Figure 6, despite the extremely high consequences of flow avulsion at the highly developed fan.



Figure 6. Comparison of roads crossing an undeveloped fan (left) and the highly-developed Cougar Creek fan (right) in Bow River Valley. Current practice would call for the same conveyance capacity design at each fan. BGC Engineering.

Risk-based approaches to design that explicitly and systematically evaluate the consequences of flooding are favored over the current hazard-based approach, and were recommended in the 2015 report of the Auditor General of Alberta (29). Risk-based approaches are ideal for site prioritization and resource allocation, as well as detailed design of risk reduction measures. They transparently justify costs associated with risk management, and facilitate communication of design decisions with stakeholders and the public. Additionally, risk-based approaches provide a framework for incrementally funding and upgrading risk management works in response to increases in highway usage or changes in adjacent development.

Risk assessments do not consider all possible risks that could be associated with a flood, debris flood or debris flow. Rather, the risk assessment considers ‘key’ risks that can be systematically estimated, compared to risk tolerance standards, and then used for decision making and optimization of mitigation strategies. ‘Key’ risks for highways often include traffic disruption, capital damage costs, or loss of life.

Figure 7 illustrates a risk management framework that has been used for design of measures to reduce debris flood risks at communities and highways on developed debris flood fans in Bow River Valley.

<u>Risk Communication and Consultation</u> By way of maps, reports, signage, warning systems, public meetings, and educational materials	1. Project Initiation a. Recognize the potential hazard b. Define the consultation zone (study area) and level of effort c. Define roles of the client, regulator, stakeholders, and QRP d. Determine ‘key’ risks to be considered in the assessment	<u>Land Management Planning and Regulation</u> Ongoing review of the risk management process for land use and development permitting
	2. Hazard Assessment a. Identify and characterize the hazard b. Develop a hazard frequency-magnitude relationship c. Identify hazard scenarios to be considered in risk estimation d. Estimate hazard extent and intensity parameters for each scenario	
	3. Risk Assessment a. Characterize elements at risk and determine vulnerability criteria b. Estimate risk: the probability that hazard scenarios will occur, impact elements at risk, and cause particular consequences.	
	4. Risk Evaluation a. Compare estimated risk against tolerance criteria b. Prioritize risks for risk control and monitoring	
	5. Risk Control a. Identify options to reduce risks to levels considered tolerable. b. Select option(s) providing the greatest risk reduction at least cost c. Estimate residual risk for preferred option(s)	
	6. Action a. Implement chosen risk control options b. Define ongoing monitoring and maintenance requirements	

Figure 7 - Risk management framework (adapted from CSA 1997 (30)).

Alberta Transportation Example

Alberta Transportation is using risk-based methods as part of a two phase project to prioritize flood, debris-flood, and debris-flow hazard sites along about 3,400 km of highways in southwest Alberta, and design risk reduction measures at specific sites. The objectives and scope of work for each phase differ, but each focus on the concept of risk, and a systematic evaluation of consequences associated with the hazards. Table 2 compares the two project phases.

	PHASE 1 – PRIORITIZATION	PHASE 2 – RISK REDUCTION DESIGN
Project Type	Regional (multiple sites)	Site Specific (single site)
Objective	Identify & prioritize hazard & risk sites	Risk reduction design & implementation
Scope of Work	Screening-level assessments focused on comparing sites	Detailed assessments focused on design of risk reduction measures
	Qualitative risk assessment	Quantitative or qualitative risk assessment
	Assessments based primarily on remotely-collected digital data sets	Assessments based primarily on site-specific field data
	Field work to ground truth results	Field work to characterize hazards & elements at risk
	Conceptual risk reduction designs	Detailed risk reduction designs

The prioritization studies identified locations where floods, debris floods, and debris flows are likely to cause the greatest disruption to transportation along southwest Alberta's highways, and where risk management efforts and expenses are most warranted. The study began by identifying and delineating the hazard sites based on aerial imagery and digital elevation models. Hydro-geomorphic process type and magnitude at each hazard site were interpreted based on characteristics of the watershed, such as area, gradient, and relief, with reference to fans where the process type was known based on previous more detailed study. Statistical analysis was also completed to predict hydro-geomorphic process types based on Melton Ratio (watershed relief divided by the square root of the watershed area), watershed length, and fan gradient.

Due to the abundance of information collected and analyzed, an online interactive map was created to provide an effective tool for displaying the results of the fan inventory and risk-based prioritization of the hazard sites. The tool enables the user to search and navigate to specific hazard locations, where the location name, process type, and priority rating are listed, along with a database of all supporting information and related reports.

The risk-based approach to prioritizing the hazard sites considered the relative likelihood that an event will occur, result in flow outside the normal stream course (e.g. unmanaged flows), and result in some level of traffic disruption. The assessment was qualitative, and aimed at comparing the different sites. The calculation of priority scores and weightings used in the calculation was developed specifically for the project, and was tailored to the information that could be efficiently collected. Priority scores considered factors that describe the hazard: relative flood and debris-flood frequency, susceptibility to channel avulsion, susceptibility to bank erosion, potential for landslide dams to form in the watershed; and factors that describe the potential consequences: traffic frequency, location of roadside facilities and potential road closure duration.

Design of risk reduction measures at high priority hazard sites is planned to be based on site-specific hazard and risk assessments, generally following the risk management framework shown in Figure 7.

INTERACTION OF HIGHWAYS AND COMMUNITIES

Debris-Flood Risk Transfer

Highways can increase or decrease debris-flood risk to buildings and adjacent infrastructure that occupy the same alluvial fan. For example, a highway embankment can either contribute to flooding on the upstream side of the road, or protect elements from flooding that are located on the downstream side of the road. Also, flow avulsion from channels often occurs where roads cross channels, and flows that escape a channel are often re-directed along roads.

Risk reduction design at any single element, especially roads and highways, should not be done in isolation without assessment of risk to adjacent elements. Designs should consider how the highway affects the debris-flood risk to buildings and other infrastructure located on the alluvial fan. Comprehensive risk reduction design that considers all elements at risk from a specific hazard is a best practice. This comprehensive design approach requires clear communication and involvement of all stakeholders on the fan, which can include highway agencies, private residences and businesses, local governments, state and federal government, First Nations, as well as pipeline and utility operators. Risk reduction designs that are completed for a single element on the fan without input from other stakeholders can lead to inefficient designs, disgruntled neighbors, and transfer of risk.

The following sections provide two examples of debris-flood risk interaction between the Trans-Canada Highway and communities on alluvial fans in Bow River Valley:

- Heart Creek – Highway embankment reduces debris-flood risk to downstream homes
- Harvie Heights Creek – Highway embankment contributes to flood risk of infrastructure

Heart Creek

The Trans-Canada Highway crosses Heart Creek near the apex of its alluvial fan (Figure 8). A residential neighborhood is located on the alluvial fan downstream of the highway. Heart Creek crosses beneath the Trans-Canada Highway through a 7 m wide by 2.5 m high box culvert. During the June 2013 debris-flood event, the box culvert blocked with sediment, causing the flow to overtop the highway. Downstream of the highway, within the residential area, Heart Creek aggraded rapidly, which led to overtopping of the channel and significant channel widening. This flow flooded several residences and incised the fan, which undermined houses, before discharging to the Bow River. Bow River bank erosion added to the losses on Heart Creek fan.

Debris-flood hazard and risk were assessed for the community following the June 2013 event, and it was determined that the channel capacity within the community, downstream of the highway, was too small to convey the design peak debris-flood flow of 50 m³/s (18,19). A

conceptual mitigation design study concluded that it was not feasible, or desirable, to increase the channel to the needed size because it would impinge on residential properties along the channel (15). Instead, the conceptual design proposed to use the highway embankment to reduce risks to residential development. The design called for covering the existing box culvert with a grizzly rack that encourages the culvert to become blocked when the downstream channel capacity is reached. A flood diversion berm constructed along the highway embankment would then direct flood flow to an adjacent undeveloped area and on to the Bow River (Figure 8).

If the highway debris-flood mitigation design had been completed without consideration of risks to adjacent homes and had simply involved increasing the highway culvert capacity, it would have increased flood risk to the residential community downstream. The comprehensive risk reduction design process, which considered all elements at risk on the fan, instead chose to reduce the culvert capacity and protect both the highway and community with a flood diversion berm. This option minimized channel disturbance within the community and used the existing highway embankment as a primary component of debris-flood protection. It also provided a basis to justify mitigation costs in provincial funding applications by the community.



Figure 8 - Proposed Heart Creek debris-flood mitigation design. Google Earth.

Harvie Heights Creek

The Trans-Canada Highway crosses Harvie Heights Creek fan near the toe of the fan, adjacent to Bow River (Figure 9). During the June 2013 debris floods, sediment from Harvie Heights Creek clogged a culvert under the Trans-Canada Highway. Water was trapped by the highway embankment, and a water treatment plant located adjacent to the highway was flooded to its eaves with standing water, along with flooding of roads, businesses, and other infrastructure (Figure 10). Flood water eventually overtopped the highway, which blocked the single access point to the community and closed all west-bound traffic on the highway (16, 17).

A conceptual debris-flood mitigation design study (14) concluded that the most effective method to reduce risks to the highway, community, and other infrastructure was to increase the capacity of culverts beneath the highway and to protect the culverts from sedimentation. If the highway risk assessment had been completed in isolation, it may have concluded that the infrequent flooding of the highway, leading to temporary closure, was acceptable. This would have resulted in no upgrades to the culvert system. However the design approach showed that this would result in unacceptable risk to the adjacent community, and that risks to both the community and highway could be efficiently reduced with the proposed culvert upgrade designs.



**Figure 9 - Harvie Heights creek fan, during typical summer season (without flooding).
BGC Engineering.**



Figure 10 - Flooding of water treatment plant at Harvie Heights Creek fan. Jackie Latvala.

CONCLUSIONS

After being affected by a devastating flood and debris-flood event in June 2013, the province of Alberta, Alberta Transportation, and individual municipalities, are rebuilding and improving defenses against similar future events. The flood event and subsequent assessments and designs have highlighted three important themes that should be considered when designing culverts, bridges, and flood protection works for highways in mountainous terrain:

- The hydrogeomorphic process types (e.g. clear water flood, debris flood, debris flow) that can occur in a waterway must be accurately recognized, characterized, and incorporated into the design.
- Risk-based assessment and designs, which consider the consequences associated with flood and debris-flood events, are more powerful tools than the current hazard-based design approach. Risk-based approaches can be adapted for screening level studies to prioritize sites or site-specific risk reduction studies and allow consideration of risks that go beyond the highway system.
- Highways can increase or decrease flood and debris-flood risks to adjacent infrastructure and buildings, and the interaction between the highway and other elements on the fan must be considered when assessing risks and designing risk reduction measures for the highway.

REFERENCES:

1. Wood, J. 2013. *Province boosts cost of Alberta floods to \$6 billion*. Calgary Herald 23 Sept 2013. Web 27 May 2015.
2. Golder Associates, 2013. *Flood Inspection Summary Reports (Highways 66 and 68)*. Multiple inspection summary reports prepared by Golder (Project No. 13-1376-0052) for Alberta Transportation.
3. Thurber Engineering Ltd. 2013. *Highway and Geotechnical Assessments of Flood Damage – Highways 40:10 / 40:12 (Kananaskis Country) Consulting Services Contract CON0014934*.
4. AMEC Earth and Environmental (AMEC), 2013. *Highway and Geohazard Assessments of June 2013 Flood Damage- Highways 940 (Forestry Trunk Road) and 532 (Kananaskis Country) Consulting Services Contract CON0014932. Revision 1 – Updated to Non-DRP Site Cost Estimates and Assessments*.
5. BGC Engineering Inc. (BGC), 2013. *Cougar Creek 2013 Forensic Analysis and Short-term Debris-Flood Mitigation*. Final Report prepared for the Town of Canmore dated December 11, 2013.
6. BGC Engineering Inc. (BGC), 2014. *Three Sisters Creek Debris-Flood Hazard Assessment*. Final Report prepared for the Town of Canmore dated October 31, 2014.
7. BGC Engineering Inc. (BGC), 2014. *Exshaw Hazard Debris-Flood Hazard Assessment*. Draft Report prepared for the MD of Bighorn No. 8 dated September 29, 2014.
8. BGC Engineering Inc. (BGC), 2014. *Jura Hazard Debris-Flood Hazard Assessment*. Draft Report prepared for the MD of Bighorn No.8 dated September 29, 2014.
9. BGC Engineering Inc. (BGC), 2014. *Cougar Creek Debris-Flood Risk Assessment*. Final Report prepared for the Town of Canmore dated June 11, 2014.
10. BGC Engineering Inc. (BGC), 2014. *Cougar Creek Debris-Flood Hazard Assessment*. Final Report prepared for the Town of Canmore dated March 7, 2014.
11. BGC Engineering Inc. (BGC), 2015. *Steep Creek Fan Hazard Inventory and Prioritization*. Report prepared for Alberta Ministry of Environment and Sustainable Resource Development dated August 31, 2015, 91 pp.
12. BGC Engineering Inc. (BGC), 2015. *Steve's Creek Debris-Flow Hazard Assessment*. Final Draft Report prepared for the Municipal District of Bighorn in preparation.
13. BGC Engineering Inc. (BGC), 2015. *Grotto Creek Debris-Flood Hazard Assessment*. Final Draft Report prepared for the Municipal District of Bighorn, in preparation.
14. BGC Engineering Inc. (BGC), 2015. *Harvie Heights Creek Preliminary Debris-Flood and Debris-Flow Mitigation Design*. Final report prepared for the Municipal District of Bighorn dated May 25, 2015.
15. BGC Engineering Inc. (BGC), 2015. *Heart Creek Preliminary Debris-Flood Mitigation Design*. Final report prepared for the Municipal District of Bighorn dated April 24, 2015.
16. BGC Engineering Inc. (BGC), 2015. *Harvie Heights Creek Debris-Flood Risk Assessment*. Draft Report prepared for the Municipal District of Bighorn dated February 24, 2015.

17. BGC Engineering Inc. (BGC), 2015. *Harvie Heights Creek Debris-Flood and Debris-Flow Hazard Assessment*. Draft Report prepared for the Municipal District of Bighorn dated February 24, 2015.
18. BGC Engineering Inc. (BGC), 2015. *Heart Creek Debris-Flood Risk Assessment*. Final Report prepared for the Municipal District of Bighorn dated May 25, 2015.
19. BGC Engineering Inc. (BGC), 2015. *Heart Creek Debris-Flood Hazard Assessment*. Draft Report prepared for the Municipal District of Bighorn dated February 24, 2015.
20. BGC Engineering Inc. (BGC), 2015. *Cougar Creek Debris Floods: Risk Reduction Optimization*. Final Report prepared for the Town of Canmore dated February 2, 2015.
21. BGC Engineering Inc. (BGC), 2015. *Stoneworks Creek Debris-Flow Hazard Assessment*. First Draft Report prepared for the Town of Canmore dated January 29, 2015.
22. BGC Engineering Inc. (BGC), 2015. *Exshaw Creek and Jura Creek Debris-Flood Risk Assessment*. Final Report prepared for the MD of Bighorn No. 8 dated January 22, 2015.
23. BGC Engineering Inc. (BGC), 2015. *Three Sisters Creek Debris-Flood Risk Assessment*. Final Report prepared for the Town of Canmore dated January 20, 2015.
24. BGC Engineering Inc. (BGC), 2015. *Stone Creek Debris-Flow Hazard Assessment*. Final Draft Report prepared for the Town of Canmore dated January 16, 2015.
25. BGC Engineering Inc. (BGC), 2015. *Stone Creek Debris-Flow Risk Assessment*. Final Draft Report prepared for the Town of Canmore dated May 21, 2015.
26. BGC Engineering Inc. (BGC), 2015. *Cougar Creek Debris-Flood Risk Update*. Draft Report prepared for the Town of Canmore dated May 21, 2015.
27. Jakob, M. and Jordan, P., 2001. Design flood estimates in mountain streams – the need for a geomorphic approach. *Canadian Journal of Civil Engineering* 28: 425-439.
28. Jakob, M., Clague, J.J. Church, M., 2015. Rare and dangerous; Recognizing extra-ordinary floods in stream channels. *Canadian Water Resources Journal*.
<http://dx.doi.org/10.1080/07011784.2015.1028451>.
29. Auditor General, 2015. *Report of the Auditor General of Alberta* dated March 6, 2015.
30. Canadian Standards Association (CSA), 1997. CAN/CSA – Q859-97 Risk Management: Guideline for Decision Makers. 55 p.

Bridges in Appalachian-Type Karst Geotechnical and Foundation Design Concerns

Joseph A. Fischer, P.E. President
Geoscience Services
1741 Route 31, Clinton, NJ 08809
geoserv@hotmail.com

Mr. William Kochanov, P.G.
Department of Conservation and Natural Resources
Pennsylvania Geological Survey
3240 Schoolhouse Road, Harrisburg, PA;
wkochanov@pa.gov

Joseph J. Fischer
Geoscience Services
1741 Route 31, Clinton, NJ 08809
geoserv@hotmail.com

Disclaimer

Statements and views presented in this paper are strictly those of the author(s), and do not necessarily reflect positions held by their affiliations, the Highway Geology Symposium (HGS), or others acknowledged above. The mention of trade names for commercial products does not imply the approval or endorsement by HGS.

Copyright

Copyright © 2015 Highway Geology Symposium (HGS)

All rights reserved. Printed in the United States of America. No part of this publication may be reproduced or copied in any form or by any means – graphic, electronic, or mechanical, including photocopying, taping, or information storage and retrieval systems – without prior written permission of the HGS. This excludes the original author.

ABSTRACT

The subsurface peculiarities of karst are seldom recognized by project planners. This becomes readily apparent when the bottom falls out, the sinkhole is elevated to disaster status, and the event makes spectacular news headlines.

Areas of karst terrane have long been recognized through historical accounts and data compiled by state and federal agencies, professional organizations, and municipalities. Obtaining background data is simple. LIDAR imagery is another tool that can strip away the veneer of urban development and identify topographic features indicative of karst. A site reconnaissance should complement the aerial review.

Indirect methods, such as geophysics, may be of use if carefully planned and performed with an understanding of the “vagaries” of karst., and the results integrated with the data.

Bridge foundation types must reach competent material, which in a karst environment generally means unweathered bedrock. Competent rock should be expected to be at variable depths and must be considered in any investigation program. Likewise, any deep foundation design must be flexible enough to include provisions for field changes in foundation element lengths. Grouting, both high- and low-mobility, is often used in karst terrane for foundation improvements.

The paper examples two sites located less than 10 miles apart in a known karst area. One of the bridges has performed satisfactorily, the other, newer bridge (replacing one that was a victim of karst-related problems) is showing evidence of continuing settlement and is being actively monitored.

INTRODUCTION

Karst underlies a significant portion of the United States (see Figure 1, National Karst Map [Ref. 1]) and many bridges and highways are founded atop carbonate bedrock. The blue line(s) trending north/south from Alabama to New York State on Figure 1 represents regions underlain by Appalachian karst; hard, ancient (some 300 million years old) carbonate rocks that have been subjected to several orogenic events resulting in twisted, folded and fractured rocks that exhibit remarkably sudden changes in subsurface material quality and character over short horizontal and vertical distances.

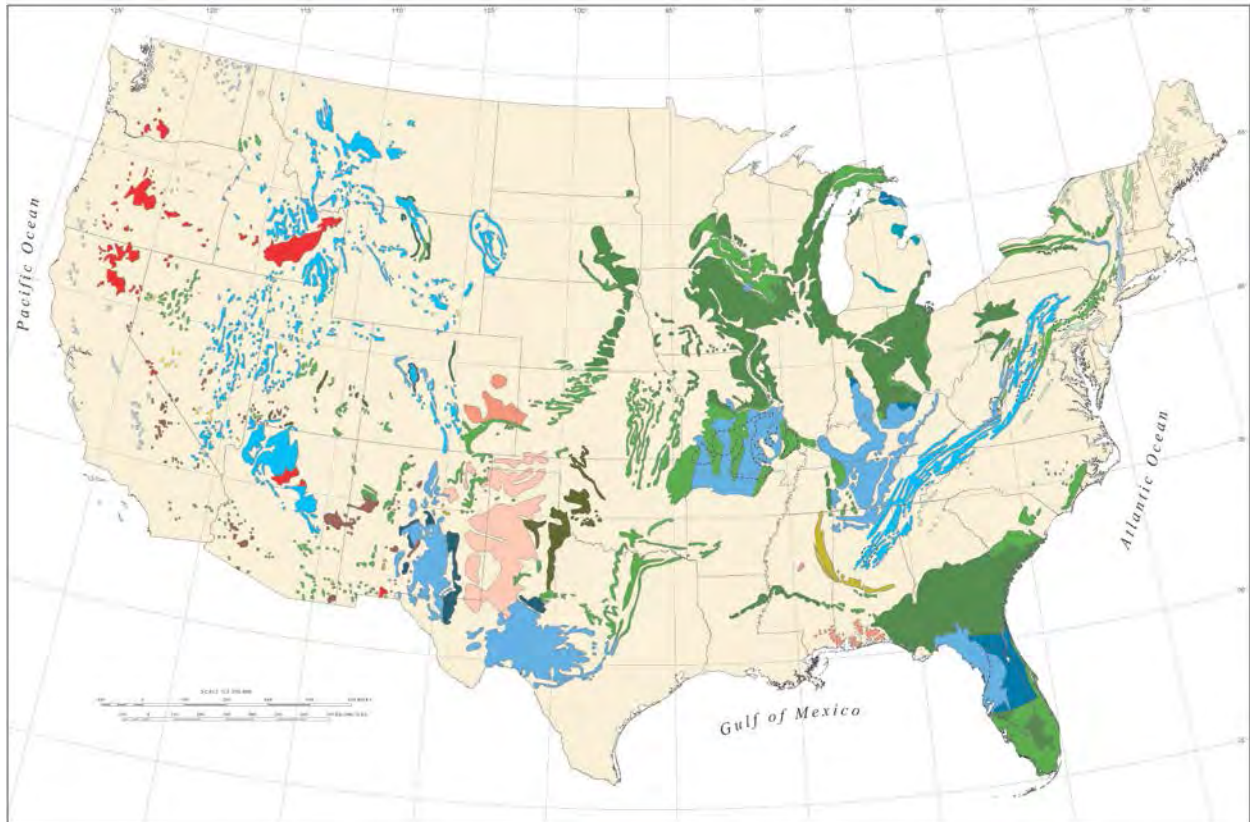


Figure 1: National Karst Map (1)

Besides the national Karst Map, the United States Geologic Survey and most individual State geological surveys provide much more detailed mapping that can be used to ascertain if a project area is underlain or otherwise affected (stormwater runoff or environmental and engineering concerns) by soluble carbonates. For example the Pennsylvania Geological Survey also provides maps and overlays of possible and known karst features such as sinkholes and closed depressions in solution-prone carbonate rocks (e.g., Kochanov, 1987 [Ref. 2]). Additional detail can be gained by acquiring drilling logs and contacting State Geological Survey personnel for unpublished information. The authors have even interviewed local farmers about past sinkhole occurrence and cavers in an effort discern the extent and direction of the solutioning below or near a site.

PRELIMINARY GEOTECHNICAL ENGINEERING

Sinkhole occurrence has been a major source of journalistic and internet fervor for the last few years, but the rocks causing the problems are much older. The ancient carbonate rocks of the Appalachian Valleys and in the mid-continent of the U.S. can be quite strong ($\geq 10,000$ pounds per square inch in compression tests) when unweathered (e.g., the Natural Bridge in Natural Bridge, Virginia). However, the geotechnical engineer or engineering geologist must understand the potential for highly variable nature of the subsurface along a section of highway or below bridge abutments. There very well may be cavities and soil voids hidden below the surface in these areas.

After evaluating the information developed from readily available sources, one should view past and present aerial photographs, LIDAR or satellite imagery of the site or route. These images are relatively easy to obtain and may provide clues to geologic structure, sinkhole occurrence and remediation, and portions of fields avoided by farmers because of sinkholes or shallow bedrock. Comparing aerial photographs taken over time and under a variety of soil moisture conditions can often provide a great deal of useful information.

SITE/ROUTE INVESTIGATIONS

Obviously, hard data is required along a route or at a bridge site. The preliminary evaluation using the information developed to that date should be used to plan a scope of geotechnical investigation that better defines the site conditions and to identify the problems possible and likely to occur as a result of the subsurface conditions. The investigation can be phased so as to decrease up-front costs and allow for a steady increase in knowledge of the conditions that will affect construction. Performing much of this work during the contract or site acquisition negotiations can be quite useful in deciding to redirect a route or move a bridge location. One must respect the variations that can exist and realize that a single foundation type may not be economical for use at each bridge pier location.

The investigation should include a geologic reconnaissance using the data developed early in the process including aerial imagery. Other techniques could include geophysics (Ref. 3), but geophysical studies are suspect, particularly in Appalachian karst, as a stand-alone tool. Apparently, the best results in karst terrane is the combined use of geophysics and test borings (Ref. 4), however, the geophysicist must be prepared to use the most advanced techniques and analytical tools. For example, a recent major project atop Appalachian karst incorporated a two-phase resistivity survey, two separate test boring programs, test pits, air-track probes and grouting in an effort to characterize a large site. After more than a million dollars in investigation costs, the project geotechnical engineer quietly put aside the geophysical data and performed the final analysis upon the basis of the test pits, borings and probes (Ref. 5).

The aforementioned investigation was performed in accordance with local "Limestone Ordinance" procedures by experienced personnel. The data most valuable to this project were provided by rotary-wash test borings while monitoring water loss quantities and depths, and sampling the rock using a double- or triple-tube core barrels. Also of great use was the monitoring of "grout takes" and depths in the test borings and air-track probe holes drilled.

FOUNDATION SUPPORT SOLUTIONS

A number of foundation support solutions are available to carry highway structure loads over karst terrane across a bedrock “trough”. Sometimes a firm base can be achieved by excavation and backfill with appropriate supporting materials. Bridging a void with a strong, reinforced concrete pad is another alternate, if there is available means to support the slab. However, a pile or caisson foundation may be needed to economically reach adequate supporting materials. Being able to drill through and below a large diameter pile or caisson can be quite informative and can be achieved with present-day instrumentation and equipment. Filling voids with either low- or high-mobility grout with additives to reduce or eliminate shrinkage, reduce the weight of the grout and/or increase fluidity has been successfully used. However, grout shrinkage is an important consideration when the purpose is to fill voids.

Deep dynamic compaction (DDC) has been used on a number of highway projects (Ref. 6) with reasonable success. However, its success is dependant upon the subsurface conditions and even with large weights dropped from a great height, the depth of effectiveness can be limited. Also, noise and flying soils and rock can be a hazard. Vibrations exist, but are generally not as bad as might be expected, and can be a clue to the foundation conditions near the location of the weight drop. Recording or feeling differences in the amplitude and frequency of these vibrations in the vicinity of the work (at a safe distance of course) can help identify suspect areas with an experienced investigation team.

A TALE OF TWO BRIDGES

The capriciousness of Appalachian karst is evident in two case histories for bridges on a four-lane state highway less than 10 miles apart in Pennsylvania (Ref. 7 and 8).

The earlier (southerly) bridge construction was a new, almost 1,800-foot long, double-span highway bridge over the Lehigh River, Lehigh Canal and two sets of railroad tracks (one in use, one abandoned) for a section of State Route 33 that is a connector for two major east/west interstate highways. The newer case is a replacement bridge crossing the Bushkill Creek on a portion of the same highway that continues north to the Pocono Mountains.

Case 1

The southerly bridge crosses over Cambrian-aged, folded and faulted carbonates of the Leithsville (limestone) and Allentown Formations (dolomite), both well-recognized as being solutioned.

The design and construction teams were composed of an experienced national design firm, a local geotechnical firm and another international firm experienced in rock mechanics. Drilling and testing took place over a three year period.

The geologic information and interpretation provided in the geotechnical report was based upon boring data, laboratory testing of NQ-sized core from vertical and angled borings, and bedrock permeability measurements. The boring data was interpreted to indicate a section of overturned rock with high secondary porosity resulting from water flow through fractures and solutioned zones (Ref. 7).

As a result of the length of the southerly bridge and the variability of the soil and bedrock conditions, three foundation types were employed for the five support locations. At three locations, rock sockets were drilled into the bedrock. Driven piles were used to support the mid-section of the bridge and southerly abutment was founded upon a “spread foundation”.

Because of a large scale foundation investigation and the engineering/geologic know-how that guided the foundation investigation and an experienced design team, the bridge has performed satisfactorily for some 15 years. There is no evidence of distress noted by the authors of this paper in their many passages across this bridge.

Case 2

The more northerly set of bridges in this discussion is atop Epler Formation (dolomite) close to its contact with the Jacksonburg Limestone. A more complete discussion of geological and cultural surroundings for this case is discussed in References 8 and 9. In 1999, sinkholes were first noted along the Bushkill Creek, a stream that passes alongside an active quarry roughly a mile upstream from the area of interest (See Figure 2).

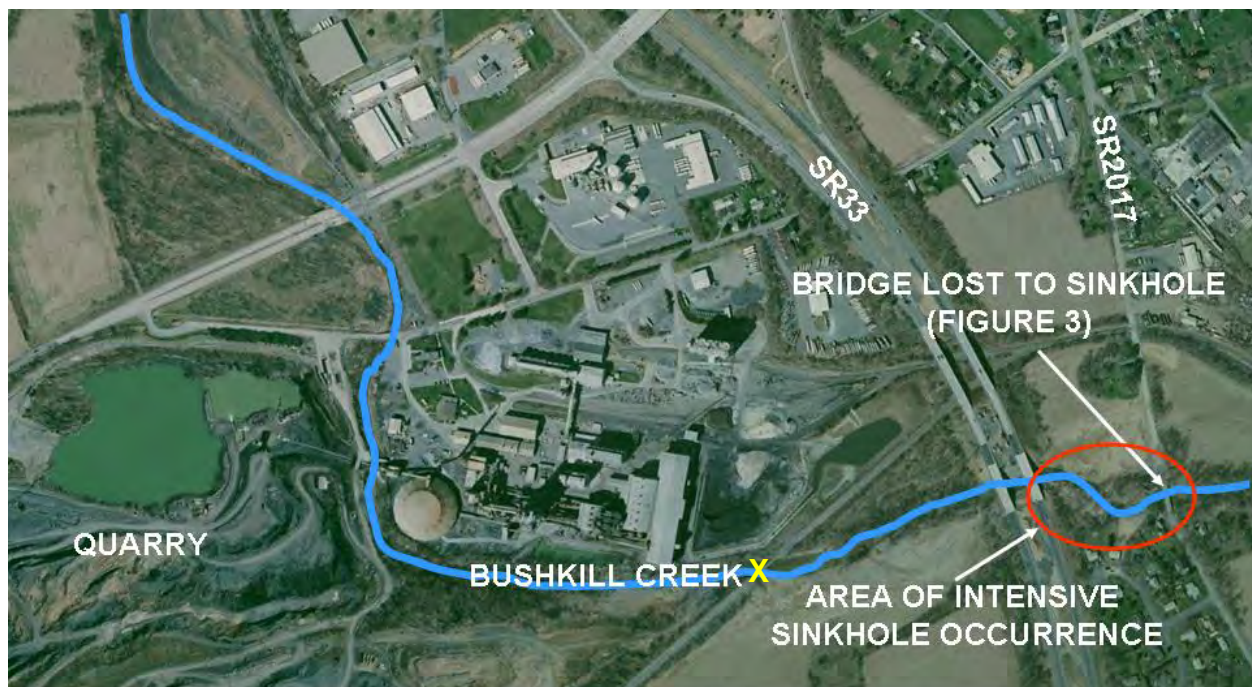


Figure 2 – Area of interest.

In October of 2000, the SR 2017 bridge was damaged and closed. In 2001, a railroad bridge crossing the creek (see yellow X on Figure 2) about a half mile downstream from the quarry was damaged by a sinkhole. The northbound SR33 span was lost in January 2004. Figure 2 shows the SR33 and SR 2017 bridge locations and the quarry to the west. The missing section of the SR 2017 bridge after the formation of sinkhole along the edge of the Bushkill Creek, adjacent to the north abutment is shown as Figure 3.



Figure 3 – North Abutment of SR 2017 Bridge over the Bushkill Creek after October 2000 sinkhole.

Much of Pennsylvania and eastern New Jersey were in the grips of a drought from September 1995 through November 2002. The drought years were followed by a period of above-normal precipitation. High precipitation events due to Tropical Storm Dennis (5.5 cm/2.2 inches) and Floyd (16 cm/3 inches) in 1999 were also coincident with the onset of sinkhole activity. And then there was Tropical Storm Ivan in the summer of 2004.

Water pumped from the nearby quarry was discharged into the Bushkill Creek. The pumping rate increased from 25 million gallons per day (MGD) 1999 to 55 MGD in 2001. The combination of the karstic landscape, the impact of the drought and subsequent rain events, the zone of influence established by the quarry's pumping of ground water, and the modifications to the Bushkill Creek as a result of the construction of SR33, all may have contributed towards sinkhole development in the locale (Ref. 9).

The quarry mines Jacksonburg Limestone and the SR33 and SR2017 bridges are founded upon both the Jacksonburg Limestone and the underlying Epler Formation (depending upon which abutment) with the contact following the Bushkill Creek in that locale. As pumping increased in the quarry, flow increased in the Bushkill Creek and sinkhole formation along both sides of the creek increased. It is not hard to draw a relationship, though that relationship is probably quite complex in that there is some question as to whether the quarry is mining water from further downstream in the Bushkill Creek.

We are not privy to the results of any geotechnical information for the original highway bridge, other than some piles reached a depth as great as 360 feet. Although the vagaries of karst have been well-documented for many years (e.g., Ref. 10), little has been disseminated in regard to the initial subsurface investigations for the first bridge. Because of settlement, the subsequent investigation for the replacement of the affected major highway bridge was undertaken by the

PA Dept. of Transportation and Dept. of Environmental Protection. A site geologic reconnaissance was performed by State geological survey personnel and one result of that reconnaissance is provided as Figure 4.

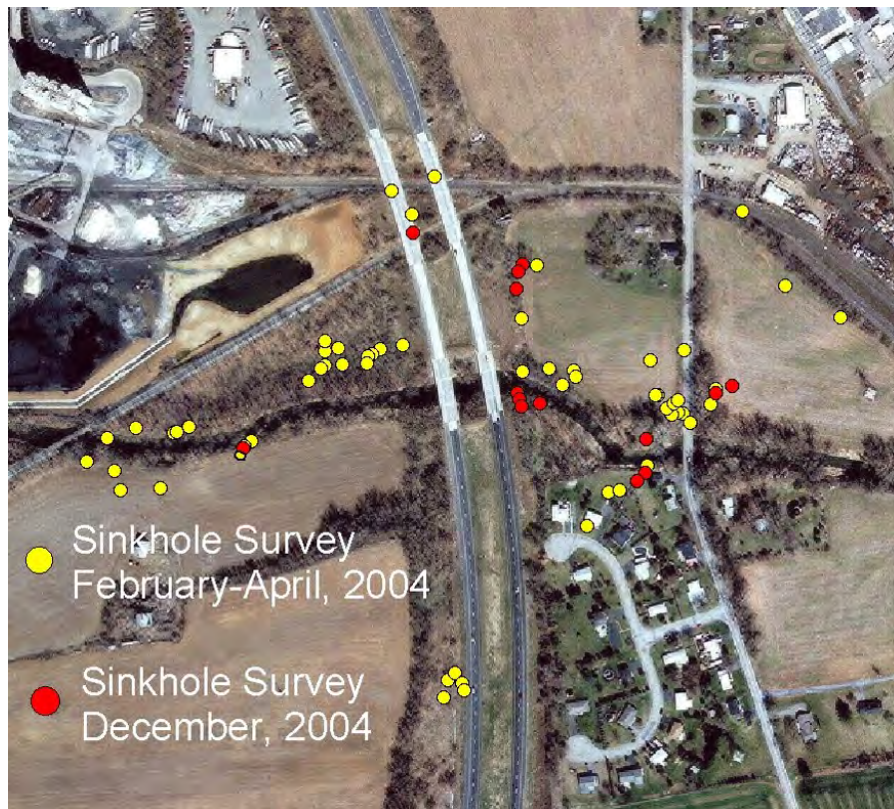


Figure 4 – Area showing sinkholes identified in 2004. New sinkholes occurring in December are in the general area as those inventoried earlier that year.

To stabilize the area for the new SR33 bridge that showed signs of settlement, several options were evaluated. One solution was to place an impermeable liner in the creek bed through the area. Several studies were performed to evaluate the possible impacts of a liner and that alternative was eliminated and additional subsurface exploration was planned. The quarry volunteered the use of their hydro-tracks and drillers to the PADOT for their investigation. Although the quarry hydro-track drillers undoubtedly had experience in drilling in karst, their lack of exposure to geotechnical techniques and demands for information likely made them ill-suited for such a large and complicated geotechnical investigation. Inexperienced drilling or field geotechnical personnel will likely not be able to interpret and understand the conditions that are being revealed by the large, quarry-type drilling equipment.

A series of test borings, six in each of the four lanes of travel, were drilled in addition to 16 hydro-track probes. The most useful information from the borings was apparently the ground water temperature, but conductivity and pH were also measured. That data showed 170-foot deep area of elevated ground water temperatures, with zones of flow at about 165 feet below the ground water level, likely indicating a highly weathered zone in the bedrock located some 75 feet away from the central portion of the creek bed. The top of the presumably sound bedrock in this

central zone of weathering was some 100 feet below ground surface. The overall results of the water quality and seepage data showed a high volume of the flow within the creek is recycled back into the quarry. At the end of that study, two new bridges were constructed to support all lanes of the highway.

Evaluation for possible foundation solutions were made and pin piles were chosen even though six of the test borings indicated the presence of soil-filled bedrock cavities, weathered zones within the bedrock, voids and fractures not observed in the hydro-track probes.

Pin piles were installed to support the new spans. We understand that some pin pile lengths exceeded 100 feet during installation and that variations in the rock surface (initial refusal) were encountered. We wonder if pin piles have enough rigidity to withstand being drilled through variably soft, deep soils and carbonate rocks with voids and cavities, even if drill holes were continued into sound rock. .

Despite the best efforts for investigation and design, the new spans have started to move. Sinkhole occurrence continues (Figure 5). The erosion and enlargement of the sinkholes has not stopped with one exposing the pile foundation of the south abutment of the northbound lanes of the replacement SR33 bridge.



Figure 5 – Recurring sinkhole adjacent to SR33 bridging crossing the Bushkill Creek. Taken in April of 2015.

CONCLUSIONS

As these two cases show, the quality and extent of the geotechnical investigation used to provide input for remediation and design can make a huge difference in the performance of any structure built atop karst.

An extensive geotechnical investigation is usually economically daunting to the administrators of a project to be constructed in karst terrane. The money is most often spent at the very beginning of the project and offers no other tangible product than a report, which may inform the powers that the project is going to be more expensive to construct because of poor subsurface conditions or the need for remediation. Perhaps this is the reason for the large disparity between the two similar projects discussed herein.

However, these two cases also show that project economies go well beyond the construction phase. Thus, the extra money spent on a substantive geotechnical investigation can pay significant, future economic dividends when working in karst.

REFERENCES

- (1) Weary, D.J., D.H. Doctor, J.B Epstein and R.C. Orndorff, Characterizing Regional Karst Types under the Framework of the New National Karst Map [Internet]. 2008. [Place of publication unknown]: U.S. Dept. of Interior, USGS; [Thursday, 10-Jan-2013 15:23:25 EST]. Available from: URL: <http://pubs.usgs.gov/sir/2008/5023/07weary.htm>.
- (2) Kochanov, W.E.. Sinkholes and Karst-Related Features of Northampton County, Pennsylvania. Pennsylvania Dept. of Natural Resources, Bur. of Topographic and Geologic Survey, Open File Report 8702, 1987,.
- (3) Fischer, J.A., D.L. Jagel, J.J. Fischer and R.S. Ottoson, 2004. The Expectations and Realities of Geophysical Investigations in Karst. In Proc. of 55th Highway Geology Symp., Sept. 7-10, Kansas City, MO, pp 94-103.
- (4) Benson, R.C., R.D. Kaufmann, L. Yuhr, and D. Martin, 1998. Assessment, Prediction and Remediation of Karst Conditions on I-70, Frederick, MD. In Proc. of 49th Highway Geology Symp., Sept. 10-14, Prescott, AZ, pp 303-312.
- (5) Connor, J.M., M.J. McMillan, R.W. Greene, J.A. Fischer, J.G. McWhorter and D.L. Jagel, 2008. Electrical Resistivity in Northeastern U.S. Karst – A Case history, in Sinkholes and the Engineering and Environmental Impacts of Karst, ASCE Geotech. Special Publ. No. 183.
- (6) Federal Highway Administration, 1995. Dynamic Compaction, Publ. No. Geotechnical Engineering Circular No. 1. FHWA-SA-95-037. October, pp 108.
- (7) Meyers, J., W. Peterson, R. King and D. Wyllie, 2001. Rock Foundations for Route 33 Bridge Over the Lehigh River, ASCE Geotech. Special Publ. No. 113.

(8) Petrasic, K.W., 2006. Extreme Karst: Investigation at PA State Route 33, NJDOT. In Proc. of 58th Highway Geology Symp., Oct. 16-18, 2007, Pocono Manor, PA.

(9) Kochanov, W.E., 2007. The Competing Needs of Development and Resources in the Karst Terrain of the Lehigh Valley, Eastern Pennsylvania. In Proc. of 58th Highway Geology Symp., Oct. 16-18, 2007, Pocono Manor, PA.

(10) Fischer, J.A. and R. Canace, 1989. Foundation Engineering Constraints in Karst Terrane. Proc. of Foundation Engineering: Current Principles and Practices, v. 1, ASCE, p. 29-42.

Attenuators for controlling rock fall:

Do we know how they work? Can we specify what they should do?

Duncan Wyllie, P.Eng.

Wyllie & Norrish Rock Engineers
850 – 789 West Pender Street
Vancouver, BC V6H 1C2
604-418-4617
dwyllie@wnrockeng.com

Tim Shevlin, PG

Geobrugg North America, LLC
4676 Commercial Street SE
Salem, OR 97302
503-423-7258
tim.shevlin@geobrugg.com

Prepared for the 66th Highway Geology Symposium, September, 2015

Acknowledgements

The author(s) would like to thank the individuals/entities for their contributions in the work described:

Tina Chen, Alastair Grogan - Wyllie & Norrish Rock Engineers
Andrew Mitchell – University of British Columbia
Emil Anderson Construction

Disclaimer

Statements and views presented in this paper are strictly those of the author(s), and do not necessarily reflect positions held by their affiliations, the Highway Geology Symposium (HGS), or others acknowledged above. The mention of trade names for commercial products does not imply the approval or endorsement by HGS.

Copyright Notice

Copyright © 2010 Highway Geology Symposium (HGS)

All Rights Reserved. Printed in the United States of America. No part of this publication may be reproduced or copied in any form or by any means – graphic, electronic, or mechanical, including photocopying, taping, or information storage and retrieval systems – without prior written permission of the HGS. This excludes the original author(s).

ABSTRACT

Rock fall attenuator systems, also known as hybrid rock fall barriers or hanging nets....do we know how they work, do we know what should be specified to have the intended rock fall mitigation? What is the mitigation strategy? Is the expectation to slow the rock down or stop the rock?

A joint testing program is being carried out by Wyllie & Norrish Rock Engineers Ltd. and Geobrugg North America, LLC to measure and validate the performance of rock fall attenuator systems. The preliminary stages of full-scale testing have been conducted at the Nicolum Quarry in Hope, BC. Tests were conducted using natural rocks and steel reinforced concrete cubes with dimensions of 0.75 m and 1 m dropped from heights of 60 m.

The preliminary tests were documented with a high speed camera and load cells on the support ropes. The videos have been analyzed to determine the change in the rock fall velocity and energy, and the deflection of the attenuator net. The objective of the tests is to find how to optimize system designs to minimize the impact energy that is absorbed by the net and the support structure.

INTRODUCTION

Protection against rock fall hazards is not a new endeavor. Very broadly there are two common types of rock fall protection which include barriers for catching and stopping rock fall or meshes which are commonly draped across the ground surface allowing controlled movement the rock down a slope. A cross between these two end members is a protection system called an Attenuator System, also known as a hybrid rock fall barrier, and sometimes referred to as a hanging net

Attenuator Systems are a common rock fall mitigation system employed in North America. They have been used successfully a number of years, but they are not standardized like rock fall barriers, and until recently have not been tested under full-scale conditions. In recent years testing of attenuator systems has been performed by a numbers of researchers to better understand how these systems work. This paper summarizes the preliminary findings of a joint testing program is being carried out by Wyllie & Norrish Rock Engineers Ltd. and Geobruigg North America LLC to measure and validate the performance of rock fall attenuator systems.

ROCKFALL BARRIERS AND TESTING

Flexible rock fall barrier systems are a protection measure that intercept falling rocks and catches the rock, dissipating the rock fall impact energy through total system deflection. In general rock fall barriers consist of a structural net supported by steel posts and wire ropes often containing energy absorbing brakes (Figure 1; Badger and Duffy, 2012; Andrew, et al., 2011).

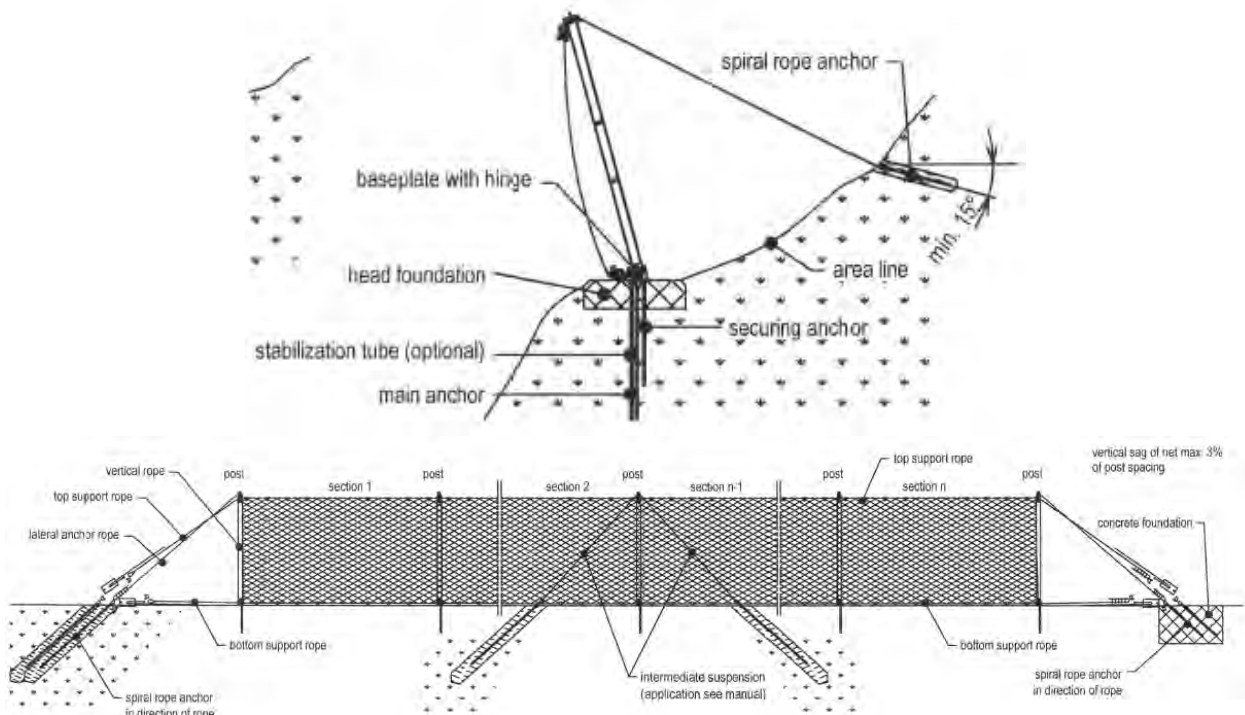


Figure 1 Schematic of a Rock fall Barrier GBE-1000A System

DRAPED MESHES

Another very common rock fall mitigation measure is a rock fall drapery system that has been employed since at least the 1950s in North America (Badger and Duffy, 2012). Rock fall draperies are passive mesh systems placed over the entire area where rock fall is anticipated to control the descent of falling rocks directing them to a planned catchment area at the base of the slope or mesh terminus (Figure 2; Badger and Duffy, 2012; Muhunthan et al., 2006; Wyllie and Norrish, 1996; Bertolo et al., 2007; Andrew, et al., 2011). A detailed analysis of draped mesh design, title *Design Guidelines for Wire Mesh/Cable Net Slope Protection*, was completed in 2005 by Washington State University (Muhunthan, et al., 2005).

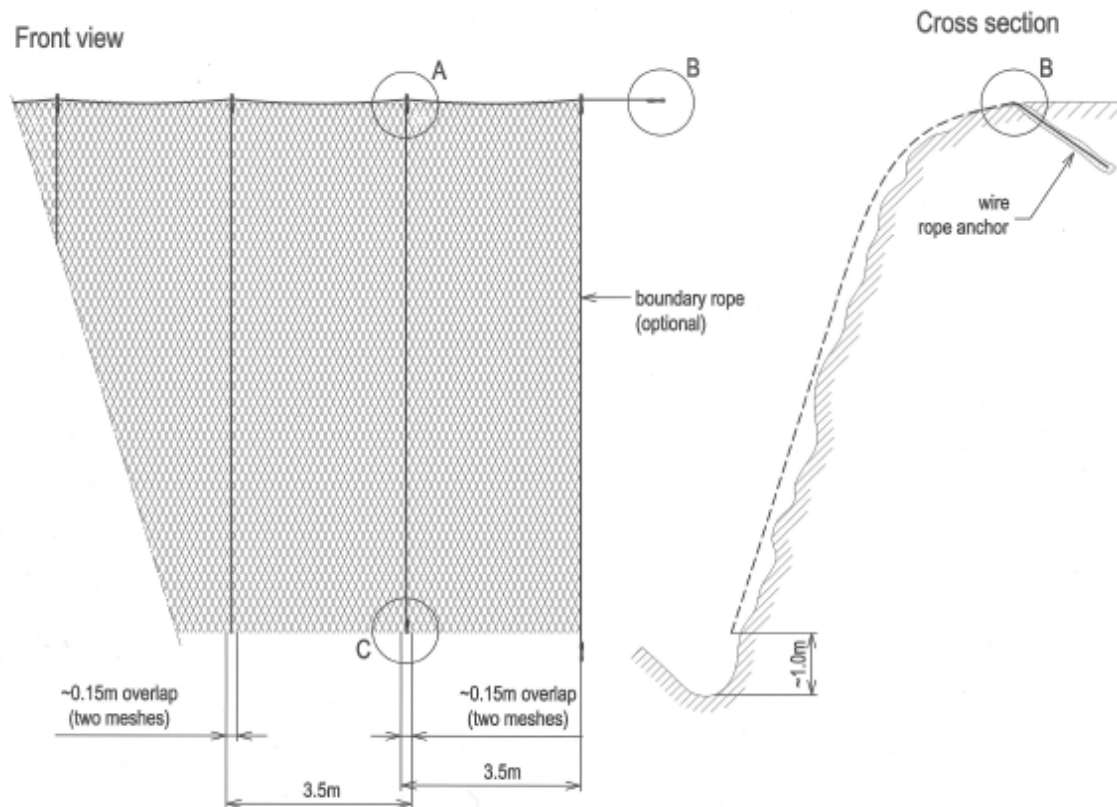


Figure 2: Schematic of a standard rock fall drapery system.

The Muhunthan study looked at both extrinsic and intrinsic factors that affect drapery design and performance. Extrinsic factors including system anchoring, slope conformance, and installation dimensions, which control fabric tautness; and in turn affects deformability and energy dissipation. Intrinsic factors include stiffness, weight, puncture strength, and corrosion resistance (Badger and Duffy, 2012; Muhunthan et al., 2005).

This study was comprehensive, but draped mesh design continues to be somewhat qualitative based on designer's experience and rules of thumb due to the complex interactions between the moving rock, the slope, and the mesh. This is illustrated by the very common application of a rule of thumb that associates block size to only two types of rock fall fabric. Often system performance is further tied to fabric unit weight and total system weight is not considered, but clearly is a controlling factor relative to rock fall mitigation. These generalities neglect many of the intrinsic and extrinsic factors of rock-mesh-slope interaction that are difficult to estimate or too complex for everyday design.

ATTENUATOR SYSTEMS

Attenuators are a combination of traditional rock fall barriers and drapery systems. These systems hybridize the best features of both a rock fall barrier and a slope drapery (Figures 3 and 4). Hybrid drapery addresses rock fall source areas, both underneath and upslope of the installation, and controls the rock's descent under the mesh, combining the performance of standard unsecured draperies and flexible rock fall fences. (Fish et al., 2012; Eliassen, 2011; Badger et al., 2008). No internal, side or bottom anchoring of the fabric is generally included, allowing for controlled deformation of the fabric and attenuation of the rock fall trajectory to the base of the installation (Fish et al., 2012). Similar to drapes, the tail of the netting is open, allowing the rocks to pass through the system while reducing their velocity and controlling their trajectory (Mumma, 2012). They are intended as low maintenance passive barrier systems (Glover et al., 2010; Badger et al., 2008).

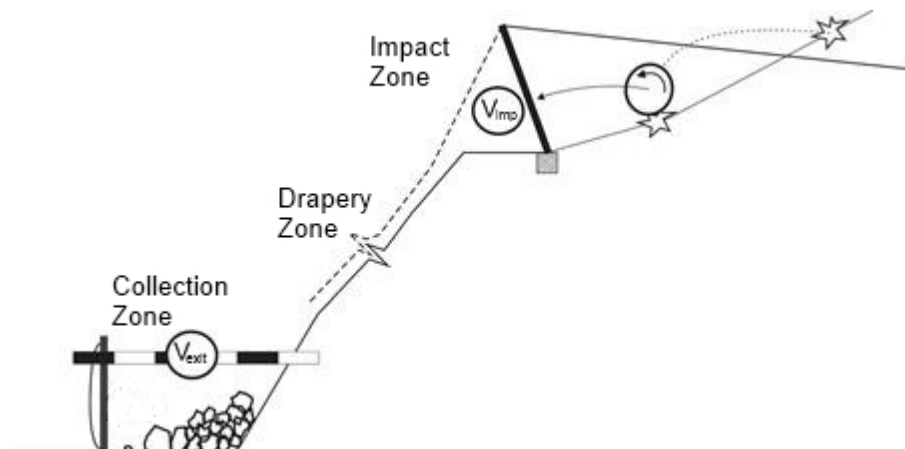


Figure 3: Sketch of typical post supported attenuator system
 V_{imp} = impact velocity; V_{exit} = exit velocity from Mumma, 2012.



Figure 4: Catchment area of attenuating structure (left) and guided boulder along rock face (right) from Glover et al., 2012.

Rock fall attenuator systems don't completely halt falling rocks, but intercept rock fall trajectory and guide it under a tail drape. In this way, the kinetic energy is only partially dissipated through barrier impacts deforming the netting and interaction with the slope during its passage to the base of slope (Glover et al., 2011). This design is superior to other types of rock fall protection in several ways (Andrew et al., 2012):

- The system is able to withstand much greater energies because it is designed to attenuate the energy of the rock fall, not arrest the rock.
- The system slows and redirects the rock so that it can be captured in a catchment area.
- In areas of snow avalanches or debris flows, the flow can travel under the system without causing damage.
- Rocks do not accumulate in the system but are allowed to pass through, resulting in less maintenance.

Existing Attenuator System Testing

Due to the dynamic nature of rock fall, similar to rock fall barriers, attenuator systems need to be tested to validate system performance as well as analyze system function. This new series of full-scale attenuator testing being jointly carried out by Wyllie & Norrish Rock Engineers, Ltd. and Geobrugg North America, LLC address the need to measure and evaluate the performance of rock fall attenuator systems. However, by no means is this testing series the first full-scale testing of attenuator systems.

The use of attenuators has been in practice for decades by private and public agencies in North America (Badger et al., 2011). In recent years, as the attenuator system has become more popular, a number of full-scale tests have been completed (Badger et al., 2008; Sassudelli et al., 2007; Glover et al., 2010; Glover et al., 2012; Arndt et al., 2009). Finite element testing has also been completed on attenuator systems (Muhunthan and Radhakrishnan, 2007; Boettichler, 2011). It is beyond the scope of this paper to compare the results of these research projects with our test results, but it is clear that additional work needs to be completed.

Future Attenuator Test Work

This series of testing attempts to address some of the needed additional work cited in the above mentioned studies:

- Attenuator design needs to consider how these systems work in conjunction with the terrain in which they are installed (Boetticher, 2011; Arndt et al., 2009; Glover et al., 2011).
- Choice of netting properties (weight, length and mesh size) that are tailored to terrain properties (slope angle, surface roughness, and material), and expected rock fall hazard (shape, size, and velocity), are the challenging decisions the rock fall engineer must face.
- Tests that focus on natural rock fall trajectories with both translational and rotational energy components are necessary over testing performed on inclined ropeway with no rotational energy to the block (Arndt et al., 2009; Glover et al., 2010).
- Attaining natural rock fall impacts into attenuators systems at energies higher than 100 ft.-tons (270 kJ) to 184 ft.-tons (500 kJ). (Badger et al., 2012)
- Further testing is needed before definitive attenuator design guidelines can be developed (Arndt et al., 2009; Glover et al., 2012). Additional tests may address some of the limitations attributed to previous testing where higher than 90 foot (36 m) drop height, varied slope and net angles, slope induced rotational impacts, higher total kinetic energies.
- Evaluation of (a) how the attenuator absorbs the initial impact in the “fence” portion of the system, and (b) how the “tail” portion of the system contributes to the further attenuation of the kinetic energy of the rock fall blocks as they pass through the system (Glover et al., 2010; Eliassen, 2011).

NICOLUM ATTENUATOR TESTING

This paper summarizes the preliminary results of the rock fall attenuator testing program carried out during January and February of 2015 at Nicolum Quarry near Hope, British Columbia, Canada (Figure 5a and 5b). The tests were documented with instrumentation and camera systems. A total of 26 tests, comprising both blocks of rock and reinforced concrete cubes, were carried out. These preliminary tests of the attenuator system were “proof of concept” tests to evaluate all components of the system and test site to determine how future tests may be conducted.

Nicolum Quarry was first identified as a suitable test site in February 2013, partly based on previous tests carried by the quarry owner, the British Columbia Ministry of Transportation and Infrastructure (MoTI) in the 1990’s. The next 18 months were spent on access negotiations and planning, design and rock fall testing feasibility activities. The site preparation and attenuator net construction was carried out between September 3 and October 18, 2014 but testing was delayed until early 2015 due to availability of work crews and ice storm damage to the site. The rock fall testing was carried out in two phases – first on January 26 and 27, 2015, and second on February 17, 2015.

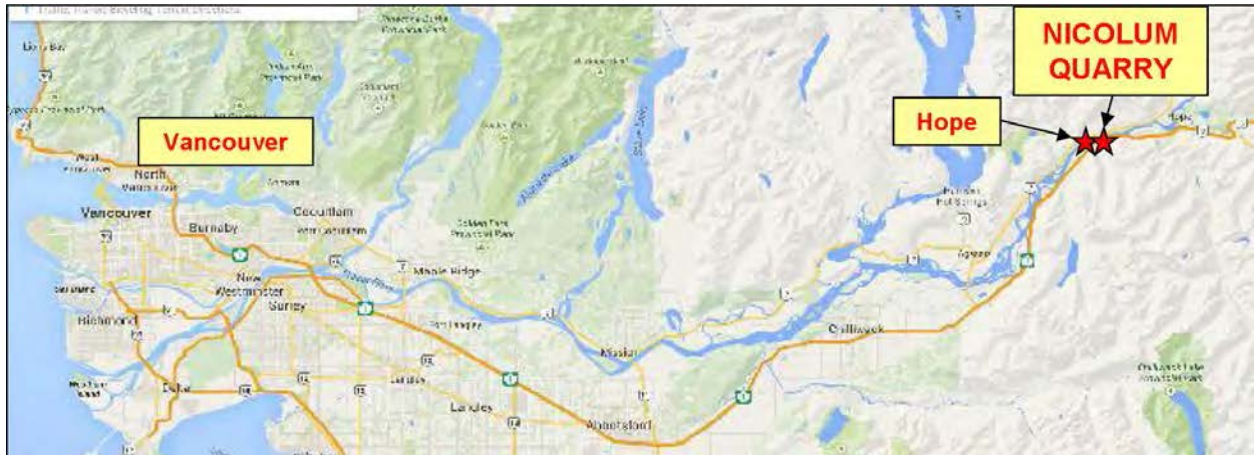


Figure 5a: Nicolum Quarry Location Hope, BC



Figure 5b: Nicolum Quarry Test Site

Nicolium Test Site Profile

The total fall height from the crest of the rock face to ground level was 180 ft. (55 m), although an additional fall height of about 16.5 ft. (5 m) could be achieved by extending the boom of the excavator to drop the blocks. The overall angle of the rock face was 60 degrees comprising two benches and near vertical rock faces (Figure 6).

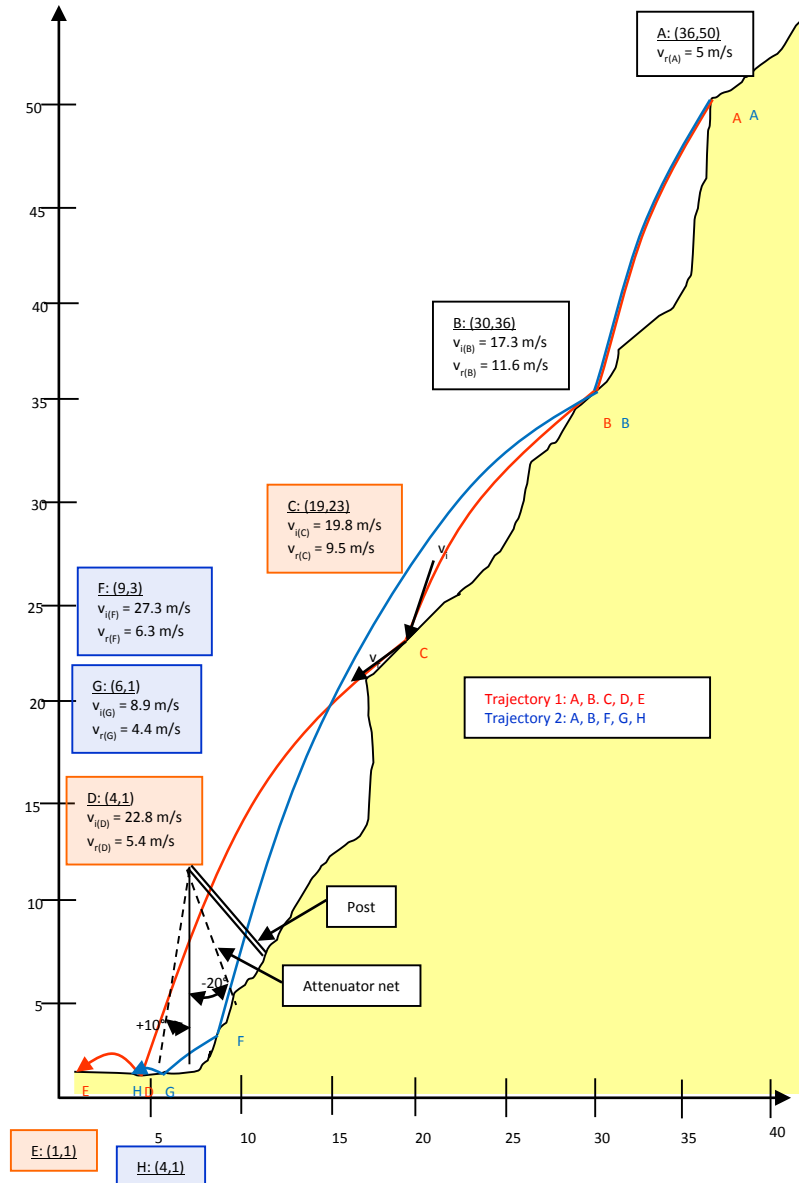


Figure 6:

Quarry Test Site Profile.

Nicolium

Attenuator system design and construction

The attenuator system was a Geobrugg's RXE-1000A Attenuator System consisting of a ROCCO ring net (7/3/300) approximately 30 ft. (9 m) wide by 36 ft. (11 m) tall, supported by 26.25 ft. (8 m) long steel posts attached to a hinged base plate, and support cables running from the top of the posts to anchors in the rock face (Figure 7). The steel posts supporting the ROCCO ring nets were spaced at 34.5 foot (10.5 m) and installed at an angle of 45 degrees. The support ropes were attached to the granite rock face with 6.5 ft. (2 m) long wire rope cable anchors. Additionally, vertical cables were attached to the sides of the ring nets and secured to concrete blocks at the toe of the slope.

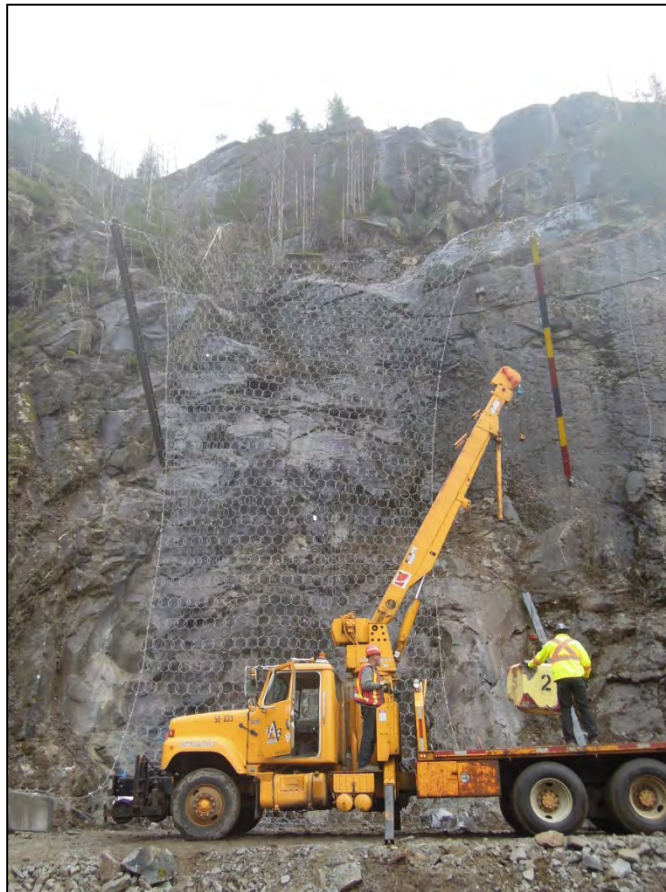


Figure 7: RXE-1000 Attenuator Net System from Geobrugg Protection Systems

After the initial round of testing the layout of upslope support ropes originally sharing an anchor centered between the posts were modified to go directly above each post to individual anchors. The original layout resulted in the cables (and load cell) being vulnerable to impact from rock falls.

Test blocks

Natural granitic blocks approximately 1.5 foot ft. (0.45 m) in diameter and cubic reinforced concrete blocks were used for testing. The dimensions of the two concrete blocks were 14.88 ft³ (0.42 m³) and 35.28 ft³ (1 m³) cubes. The concrete blocks incorporated lifting eyes on two faces and were painted yellow with emphasis on the corners, and each face numbered to maximize their visibility in the videos (Figure 8).

Figure 8: Concrete Test Blocks before testing.



Consideration was given to installing a 3-D accelerometer/data acquisition system in the concrete blocks. It was decided not to use accelerometers for the proof of concept testing because of the cost and the uncertainty in interpreting the results based on other researcher's experience.

Instrumentation and photography

The equipment described below was used to record the loads in the support ropes, the post base plate anchors, and the velocity and location of the rock falls.

Load cells:

A total of four, S-type tension load cells were installed on the western half of the system including the upslope, top, and lateral support ropes. Each support rope incorporated a turnbuckle so that the tension in each cable could be adjusted to approximately an equal tension.

A center hole compression load cell was installed on each of the two rock anchors holding the base plate of the western post. Wedge washers were used to ensure that the load was uniformly applied to the surfaces of the cells.

Data acquisition system

A high speed data acquisition system was built to record the loads generated in the six load cells. A trigger was built that simultaneously started the data acquisition system and the high speed camera, allowing frames on the videos to be exactly matched with the load cell readings.

Photography

Three cameras were used running at a variety of frame rates in both side and profile view to record the rock fall impacts

RESULTS

A total of 26 tests were conducted. This involved use of the excavator to drop the test rocks/concrete cubes from a location at the crest of the slope where it was found that the rocks were most likely to impact the net. The fall height from the drop point to the ground was 180 ft. (55 m). It was found that the blocks of rock tended to break into fragments when they impacted the rock face, and that unreinforced corners of the concrete blocks shattered. Despite care being taken to drop the blocks from the same location, the trajectories followed unpredictable paths with blocks falling close to the base of the slope not reaching the net, and others passing over or past the sides of the net.

Analysis of high speed videos

The high speed videos were analyzed with ProAnalyst software that has the ability to measure both translational and rotational velocities frame-by-frame. The accuracy of these analyses is highly dependent on being able to clearly identify markers on the blocks that can be tracked as the block moves. This was achieved by painting the concrete blocks yellow with contrasting corners, and numbering each face to assist in measuring rotational velocity.

Impact velocities – translational and rotational

The translational impact velocities varied between 26 ft./sec (8.23 m s⁻¹) and 75.45 ft./sec (23 m s⁻¹), with an average of 53 ft./sec (16.2 m s⁻¹). The velocities of the blocks of rock and the concrete cubes were similar.

The rotational impact velocities were more difficult to measure on the high speed camera images than translational velocity because of the need to identify unique markers on the rotating blocks, and particularly on the blocks of rock. In Test #12, the block of rock was rotating at 39 rad/sec, while the average rotational velocity of three of the concrete cubes was 7 rad s⁻¹. The blocks also undergo a significant change in rotational velocity during contact with the net as impact energy is partially transferred from the moving block into the net.

Rock fall masses

The masses for the reinforced concrete blocks were determined by weighing each block, and making an allowance for chipped corners after they had been used for several tests. For the blocks of rock, the weight was estimated by measuring the approximate diameter of the blocks, and calculating the weight assuming that the blocks were spherical shape and the rock unit mass is 2650 kg m^{-3} (165 lb. ft^{-3}). This theoretical mass was then multiplied by 0.6 to account for the actual irregular shape of the block; this is a standard technique used to calculate the weight of rip rap, for example.

Impact energy

The impact kinetic energies were calculated from the following standard equations:

$$KE_{\text{translational}} = \frac{1}{2} m v^2 \text{ and } KE_{\text{rotational}} = \frac{1}{2} I \omega^2$$

Analysis of the test videos showed that the blocks of rock, with dimensions up to about 0.7 m, had impact energies in the range of about 5 to 55 kJ. The attenuator was able to stop these rocks with no damage to any net component. The 0.42 cu. m concrete blocks had significantly greater impact energies, and again, the attenuator was able to stop these blocks with no significant damage. The 0.42 cu. m concrete blocks had impact energies of about 300 to 400 kJ.

Overall, the attenuator functioned as intended by redirecting the trajectory of the falling block into the ground so that the attenuator system is shown to be self-cleaning as intended. A significant portion of the impact energy was absorbed when the block landed on the ground.

Load cell results

The load cells recorded details of the magnitude and duration of the portion of the impact load that was transferred through the net into the support ropes. Integration of the load wave forms provided information of the impulse induced in each support rope, as well as the total impulse in all the guy wires. It was then possible to assess how the initial energy at the point of contact with the net was partitioned between the net, the support ropes and the rock fall impact in the planned catchment area. It would appear that the variation in the load cell readings is related to the impact position on the net.

Attenuator Energy Efficiency

The energy efficiency of an attenuator system is defined as follows:

$$\text{Efficiency} = \frac{\text{Energy after impact}}{\text{Energy at point of impact}}$$

That is, a high efficiency net is one for which little reduction in velocity (or energy) occurs during contact with the net, so that most of the impact energy is retained in the moving block and redirected to a safe fallout zone. This is in contrast to protection structures that completely stop rock falls such that the efficiency is zero.

Analyses of the high-speed videos clearly show two aspects of the velocity changes during contact with the ring net:

- **Translational velocity** - blocks move at high speed during contact with the net which shows that redirection of the blocks by the net occurs with little reduction of velocity, and little absorption of energy.
- **Rotational velocity** – blocks rotate counter-clockwise prior to impact, but the friction between the net and the irregular rotating block applies a torque to the block that reverses the direction of rotation to clockwise.

Analysis of the test results is in progress to determine the energy efficiency. Preliminary results indicate that the efficiency of attenuators is at least 40 per cent.

CONCLUSIONS

The proof of concept testing showed:

- The attenuator functioned as predicted – the test blocks were redirected by the net with no significant loss of energy, with most of the initial energy being absorbed by impact in the ditch. Attenuators are efficient rock fall mitigation systems.
- The loads in the support ropes and rock anchors holding the base of the posts were low, which is consistent with the observation that little impact energy is absorbed by the system.
- The cells recorded the portion of the impact energy transferred through the net to the guy wires.
- The instrumentation and the trigger to coordinate the camera and data acquisition system worked well.

The preliminary test results are positive and encouraging and additional testing is planned. The additional tests are expected to add to the body of knowledge on the complex performance of attenuator systems that will hopefully lead to guidelines or standard parameters for specifying attenuator systems.

REFERENCES:

Badger and Duffy. 2007. Drapery Systems. *In Landslides: Investigation and mitigation*. Transportation Research Board

Andrew, R.D., R. Barttingale, and H. Hume. 2011. Context Sensitive Rock Slope Design Solutions. Publication FHWA-CFL/TD-11-002. Federal Highway Administration, Central Federal Lands Highway Division, Lakewood, Colo.

BADGER, T.C., J.D. DUFFY, F. SASSUDELLI, P.C. INGRAHAM, P. PERREAULT, B. MUHUNTHAN, H. RADHAKRISHNAN, O.S. BURSI, M. MOLINARI, and E. CASTELLI (2008) Hybrid Barrier Systems for Rockfall Protection, in A. Volkwein et al. (eds) Proceedings from the Interdisciplinary Workshop on Rockfall Protection, Morschach, Switzerland, pp. 10-12.

MUHUNTHAN, B., S. SHU, N. SASIHARAN, O.A. HATTAMLEH, T.C. BADGER, S.L. LOWELL, J.D. DUFFY (2005) Analysis and Design of Wire Mesh/Cable Net Slope Protection, Washington State Transportation Center, Seattle, Washington, WA-RD 612.1, 267p.

MUHUNTHAN, B., H. RADHAKRISHNAN (2007) Finite Element Analysis of Hybrid Barrier for Rock Fall Slope Protection, Final Report, Washington State University Dept. of Civil & Environ. Engineering,

Geobrugg Jubilee Conference Bad Ragaz, Switzerland, 20th June 2001 From the timber fence to the high-energy net. Developments in rockfall protection from the origins to the present. Extract from a presentation by Dr. Raymund M. Spang* and Eng. grad. Reinhold Bolliger** / *Dr. Spang Geotechnical Consultants Ltd., Witten, Germany / **Formerly of Brugg Drahtseil AG, Brugg/Switzerland

Gerber, W. *Guideline for the Approval of Rockfall Protection Kits*. Swiss Agency for the Environment, Forests and Landscapes (SAEFL), and the Swiss Federal Institute (WSL), Berne, Switzerland, 2001. www.environment-switzerland.ch/publications.

ETAG27. *Guideline for European Technical Approval of Falling Rock Kits*, (February, 2008), European Organisation for Technical Approvals, Brussels, Belgium, 2008.

Arndt, B., Ortiz, T., Turner, K., “*Colorado’s Full-Scale Field Testing of Rockfall Attenuator Systems*”, Transportation Research Circular E-C141, Transportation Research Board, October 2009.

Badger, T.C., B. Dobrev, M. Anderson, H. Radhakrishnan, and B. Mununthan, 2011, Structural design of a hybrid drapery system, in Moelk, M et al., eds., Proceedings for the Interdisciplinary Workshop on Rockfall Protection, Innsbruck, Austria, pp. 3-5.

Sasiharan, N., B. Muhunthan, T.C. Badger, S Shu, D.M., D.M. Carradine (2006), Numerical analysis of the performance of wire mesh and cable net rockfall protection systems, Engineering Geology pp121-132.

Richard D. Andrew, Ryan Bartingale and Howard Hume, (2011) FHWA-CFL/TD-11-002, *Context Sensitive Rock Slope Design Solutions*

Bertolo, P., C. Oggeri, D. Peila, 2011. *Full-scale testing of draped nets for Rock fall protection* NRC Research Press website cgj.nrc.ca.

Glover, J.; Volkwein, A.; Gerber, W.; Denk, M., 2011: Design criteria for rock fall attenuating systems. [Abstract] Geophys. Res. Abstr. 13: EGU2011-13273.

Von Boetticher, A.; Glover, J.; Volkwein, A.; Denk, M., 2011: Modelling flexible wire netting applied to rock fall attenuating systems. [Abstract] In: Mölk, M.; Melzner, S.; Sausgruber, T.; Tartarotti, T.(eds.) Book of abstracts: Interdisciplinary Workshop on Rockfall Protection 2011, 17.-19.05. Congresspark Igls, Innsbruck. Innsbruck, RocExs. 71-72.

Glover, J.; Volkwein, A.; Dufour, F.; Denk, M.; Roth, A., 2010: Rockfall attenuator and hybrid drape systems - design and testing considerations. In: Darve, F.; Doghri, I.; El Fatmi, R.; Hassis, H.; Zenzri, H. (eds) Third Euro-Mediterranean Symposium on Advances in Geomaterials and Structures. Third Edition, Djerba, 2010. 379-384.

Wyllie, D.C. and Norrish, N.I. 1996. Stabilization of rock slopes. In *Landslides: Investigation and mitigation* Transportation Research Board, National Academy Press, Washington, D.C. pp 474-504. TRB Special Report 247.

Badger T.C. and J.D. Duffy. 2012. Drapery Systems In *Rockfall: Characterization and Control* Transportation Research Board, National Academy Press, Washington, D.C. pp 554-576.

Badger T.C. and J.D. Duffy. 2012. Flexible Rockfall Fences In *Rockfall: Characterization and Control* Transportation Research Board, National Academy Press, Washington, D.C. pp 526-553.

Louisville Bridges: Then and Now from a Geotechnical Perspective

Louisville, Kentucky

Mark A. Litkenhus, PE

Stantec

1409 North Forbes Rd.

Lexington, KY 40511

(859)-422-3000

Mark.litkenhus@stantec.com

Acknowledgements

The author would like to thank the individuals/entities for their contributions in the work described:

Walsh Construction
Jacobs
Hayward Baker

Disclaimer

Statements and views presented in this paper are strictly those of the author(s), and do not necessarily reflect positions held by their affiliations, the Highway Geology Symposium (HGS), or others acknowledged above. The mention of trade names for commercial products does not imply the approval or endorsement by HGS.

Copyright Notice

Copyright © 2010 Highway Geology Symposium (HGS)

All Rights Reserved. Printed in the United States of America. No part of this publication may be reproduced or copied in any form or by any means – graphic, electronic, or mechanical, including photocopying, taping, or information storage and retrieval systems – without prior written permission of the HGS. This excludes the original author(s).

ABSTRACT

The Kentucky Transportation Cabinet (KYTC) has been evaluating improvements to the interchange junctures of I-65, I-64 and I-71 in downtown Louisville, Kentucky and a second bridge over the Ohio River to the east for many years. As early as 2000, Stantec began preliminary geotechnical explorations in support of initial designs, later to be known as Two Bridges, One Project.

Redesign and major construction of three interstates through a major city has its challenges. You take that and include deep outwash deposits as thick as 130 feet, create conditions that can be difficult for foundations and embankments.

This paper presents Stantec's history with the project as it went from a traditional design – bid – build, to a design-build. The paper will primarily focus on the downtown section. A review of previous explorations combined with new explorations, foundation recommendations, along with what is being seen during construction will be highlighted. It will also include a few issues and how they were overcome.

INTRODUCTION

The Kentucky Transportation Cabinet (KYTC) has been evaluating improvements to the interchange junctures of I-65, I-64 and I-71 in downtown Louisville, Kentucky and a second bridge over the Ohio River to the east for many years. Stantec, (formerly Fuller, Mossbarger, Scott and May Engineers, Inc.) initially became involved in 2000 to provide preliminary geotechnical information for a possible tunnel on the East End portion of the project. By 2003, KYTC had completed environmental hurdles that allowed the movement of final design for the Downtown River Crossing and Interchange as well as the East End Crossing.

The Ohio River Bridges Project addresses cross-river transportation needs in Louisville and Southern Indiana for the long term with two new bridges and rebuilding of a major interstate highway interchange. It will provide safer trips, less congestion, improved access to destinations in the region, and serve as a major hub in the nation's highway transportation system. Figure 1 is a regional map showing the location of the project.



Figure 1. Regional Location Map

STANTEC'S HISTORY

As mentioned above, Stantec provided preliminary geotechnical information in 2000. In 2005, Stantec took a larger geotechnical role when the Louisville Bridges gained approval to start on the "Two Bridges, One Project" campaign. This phase divided the project into six sections, three for Downtown and three for the East End, as depicted in Figure 1. Stantec lead the geotechnical efforts for Sections 1, 2, 4 and 5 which included both roadway portions with Kentucky and both Ohio River Bridges.

For the sake of this paper, the focus will be on Sections 1 and 2 of the Downtown portion, the Kennedy Interchange and the I-65 Bridge over the Ohio River. Geotechnical explorations were performed between 2005 and 2008 on approximately 80 bridges and 20 retaining walls. The roadway alignment at that time was a completely new alignment south of the current interstate. Over 363 borings were advanced to encompass over 24,000 feet of drilling. A large portion of this drilling was performed in areas considered to be environmentally sensitive. Keep in mind that we are in an old community with years of industrial growth and change. Figure 2 is an example of the industrial setting.



Figure 2. Drilling along an existing side street.

For KYTC, this project became one of the first to use LRFD methods. As such, close coordination was provided between KYTC and FHWA. Commercially developed computer software was just being developed for evaluating retaining walls. Stantec played a key role in evaluating new programs and troubleshooting issues.

REGIONAL PYSIOGRAPHIC AND GEOLOGIC SETTING

The project is located in the northwestern portion of Central Kentucky within the Outer Bluegrass Physiographic Region. The topography within the Outer Bluegrass varies from rolling hills to relatively flat, low-lying areas adjacent to major drainage features. The project is located east of downtown Louisville, and south of the Ohio River. The Ohio River will influence groundwater levels within the project site. Topography within the vicinity is relatively flat, with local relief generally less than five feet. However, highway embankments dissect the area and can rise as much as 35 feet above the surrounding terrain.

Available geologic mapping (Geologic Map of Parts of the Jeffersonville, New Albany, and Charlestown Quadrangles, Kentucky-Indiana, USGS, 1974) (*I*) shows the project alignment to be underlain by Outwash deposits of the Pleistocene geologic period. The mapping describes the Outwash as varying in thickness up to approximately 130 feet and consisting of sand, gravel, silt and clay deposited as alluvium by low-gradient rivers formed by glacial melt waters. Situated in an older city, the site also contains a layer of brick, rubble and debris 10 to 20 feet below the surface.

Structure contours are not depicted within the immediate vicinity of the site because of insufficient data. However, structural contours drawn on top of the Waldron Shale in the Jeffersonville Quadrangle and the base of the New Albany Shale in the New Albany Quadrangle indicate the bedrock is relatively flat. The mapping shows the Springdale Anticline to be located approximately 3.8 miles southeast of the project, but does not note any faults or other detrimental geologic features to be present within the immediate vicinity of the project site.

MOVE TO DESIGN BUILD

As the engineering cost estimates began coming in, it became obvious to KYTC that a different form of funding and procurement was needed if this project was going to move forward. Therefore, the decision was made around 2009-2010 to move the alignment back to within the existing interstate corridor as a cost reduction measure and convert to a Design-Build procurement method.

Stantec joined the Walsh team as a subconsultant to Jacobs to pursue the Kennedy Interchange. Proposal work began in May 2012 and involved the normal Design-Build flurry of weekly meetings, redesign of previous work, exploring new areas, re-evaluating all the foundations and looking for ways to economize pricing where ever possible.

Walsh was awarded the project in January 2013. With the alignment being moved back within the existing interstate corridor, new geotechnical explorations were required for the new bridges and walls. This effort could not be performed during the proposal pursuit, therefore when the contract was awarded; the geotechnical work was already behind. An additional 175 borings and over 50 CPT holes were performed for the 40 new bridges and 21 retaining walls planned. We also performed 9 additional borings and PS suspension logging for the new bridge over the Ohio River. Figure 3 shows drilling for the Ohio River Bridge within the Great Lawn area.



Figure 3. Drilling within the Great Lawn area.

With drilling being on the critical path, we mobilized 4 to 6 drill crews. The item that was different for us under this Design-Build scenario was being treated more like a contractor versus an engineering consultant. The submittals required for contractors are lengthy and being the high profile nature of the project, went through considerably more scrutiny.

FOUNDATION RECOMMENDATIONS

The Downtown portion of this project mainly focused on bridge foundations and retaining wall footings. For the bridges, the typical foundation type included friction H-piles, end-bearing H-piles, drilled shafts and micropiles. The initial bridges along I-65 that would be constructed first were designed with friction H-piles. Because of the high N-values seen during SPT sampling, the team had concerns about drivability. Therefore, Walsh performed field tests using a variety of hammers in order to evaluate what size hammer would be required.

The field tests proved to be critical as the pile driving was much easier than expected. However, with the easier driving came the lack of friction capacity needed for the friction piles. PDAs were used to monitor driving, capacity and setup. Based upon the data, capacity was only about 25% of what was expected and there was essentially no setup. Multiple pile types were

tested and all had similar results. This created a design change from friction piles to all end bearing H-piles. Walsh ultimately utilized a Delmag D30-32 hammer which provides 75 ft.-kips of energy for all pile driving.

With the field testing complete, we were able to change most of the larger pile sections to smaller sections. Many of the deeper/longer piles had been increased in size to handle the predicted difficult driving. This decrease in pile size helped offset the change to longer piles for bridges originally designed with friction piles. Figure 4 shows a H-pile foundation.

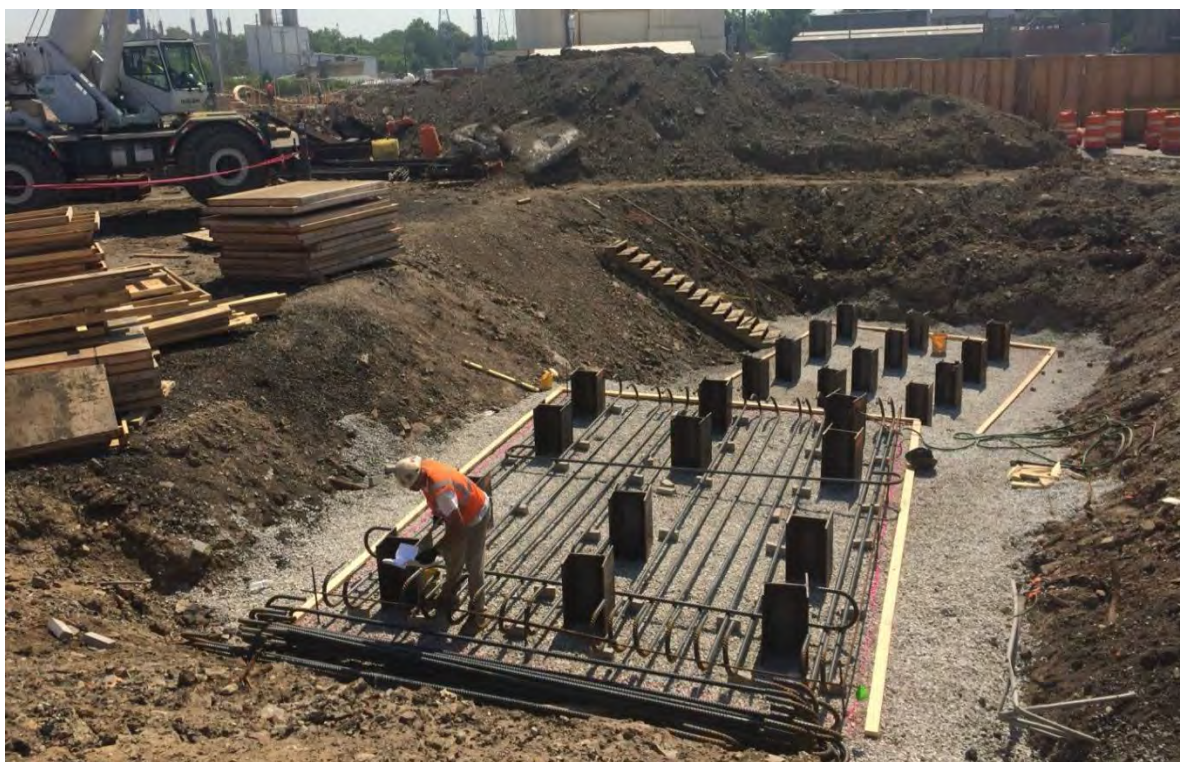


Figure 4. Typical H-pile foundation.

Jacobs provided the geotechnical engineering related to the retaining walls. The main concerns the project team and KYTC had with the retaining walls were settlement and poor bearing conditions. With the assistance of Hayward Baker, many wall foundations included stone columns. Test embankments were constructed early, that included instrumentation, to confirm designs and predicted settlements. Stantec assisted with the installation of the instrumentation. Figure 5 includes some of the equipment used for stone column installation.



Figure 5. Stone column installation.

The Ohio River Bridge foundations were primarily constructed on drilled shafts varying from 8 feet to 12 feet in diameter. A technique shaft was constructed that included four Osterberg cells to verify parameters used for end bearing and side friction. The shaft included a nominal 90 inch diameter rock socket approximately 30 feet into rock. In addition, the team performed static testing to evaluate lateral loading. The testing resulted in values that were similar to predicted values used for preliminary sizing of the shafts. Figure 6 shows initial wiring and preparation for the O-cells.



Figure 6. Rebar cage and initial O-cell installation.

CONSTRUCTION

Micropile foundations were used on a few select footings because of utility restraints and the need for a small footing footprint. The micropile size that was used was 9-5/8". A load/verification test was performed at each foundation as well as proof testing one micropile per foundation. Micropiles were typically extended into bedrock 10 to 15 feet. Figure 7 depicts a micropile test setup.



Figure 7. Micropile proof testing.

The team was allowed to reuse a foundation that is currently a part of the existing Kennedy Bridge. However, in order to reuse the footing, the Team needed to understand what the footing consisted of and its current condition. The original design drawings identified multiple options, but no one knew which option was chosen. Walsh exposed the footing for the Team to visually inspect. The foundation consisted of spiral welded pipe piles filled with concrete and appeared to be in very good condition. Figure 8 demonstrates the efforts utilized to expose the footing for inspection.



Figure 8. Inspection of existing foundation.

CONSTRUCTION ISSUES

During the driving of H-piles, the contractor dealt with a lot of cavitation around the piles. The amount of cavitation varied at different bridge sites and at times made worse due to wet weather conditions. These depressions were backfilled with flowable fill prior to pouring the footing.



Figure 9. Cavitation after pile driving.

The I-65 Bridge over the Ohio River experienced problems during a concrete pour of a drilled shaft. The shaft was 12-foot in diameter and had basically lost its tremmie seal under 130 feet of water. The issue was not realized until after about the initial 60 feet had been poured. Cross hole sonic logging was performed with little to no reading between tubes. Stantec was called out to perform coring of the shaft from top to bottom around the perimeter, and perform unconfined rock testing. Figures 10 and 11 show some of this work.



Figure 10. Cross hole sonic logging of drilled shaft.



Figure 11. Concrete coring around perimeter of drilled shaft.

The results indicated that the bottom 60 feet of the 120 foot long shaft contained concrete of varying strength and quality that did not meet the design criteria. Therefore, the design team redesigned a new shaft that basically incorporated a smaller shaft (7.5 foot diameter) within the original shaft and extended it deeper into the bedrock. Walsh drilled out the center of the 12-foot shaft with great care so that the hole was maintained straight. Figure 12 is one of the drills utilized by Walsh to construct the drilled shafts.



Figure 12. Drilled shaft drill.

The current construction is progressing on time. There has been discussions about an early bridge opening over the Ohio River. Late winter snows and early Spring floods have made those opportunities tough.



Figure 13. Progress as of May 29, 2015.

REFERENCES:

1. United States Geological Survey, Geologic Map of parts of the Jeffersonville, New Albany, and Charlestown Quadrangles, Kentucky-Indiana, USGS, 1974.

The Importance of Residual Shear Testing in Evaluation of Landslides in Glaciolacustrine Deposits

Andrew J. Smithmyer, P.G.

Gannett Fleming, Inc.
207 Senate Avenue
Camp Hill, PA 17011
(717)-763-7212
asmithmyer@gfnet.com

Frank P. Namatka, P.E.

Gannett Fleming, Inc.
207 Senate Avenue
Camp Hill, PA 17011
(717)-763-7212
fnamatka@gfnet.com

Richard D. Bohr, P.E.

Penn DOT Engineering District 4-0
55 Keystone Industrial Park
Dunmore, PA 18512
(570)-963-4110
rbohr@pa.gov

Prepared for the 66th Highway Geology Symposium, September, 2015

Acknowledgements

The author(s) would like to thank the individuals/entities for their contributions in the work described:

We would like to thank PENNDOT District 4-0 for allowing us to prepare and present this paper.

Disclaimer

Statements and views presented in this paper are strictly those of the author(s), and do not necessarily reflect positions held by their affiliations, the Highway Geology Symposium (HGS), or others acknowledged above. The mention of trade names for commercial products does not imply the approval or endorsement by HGS.

Copyright Notice

Copyright © 2015 Highway Geology Symposium (HGS)

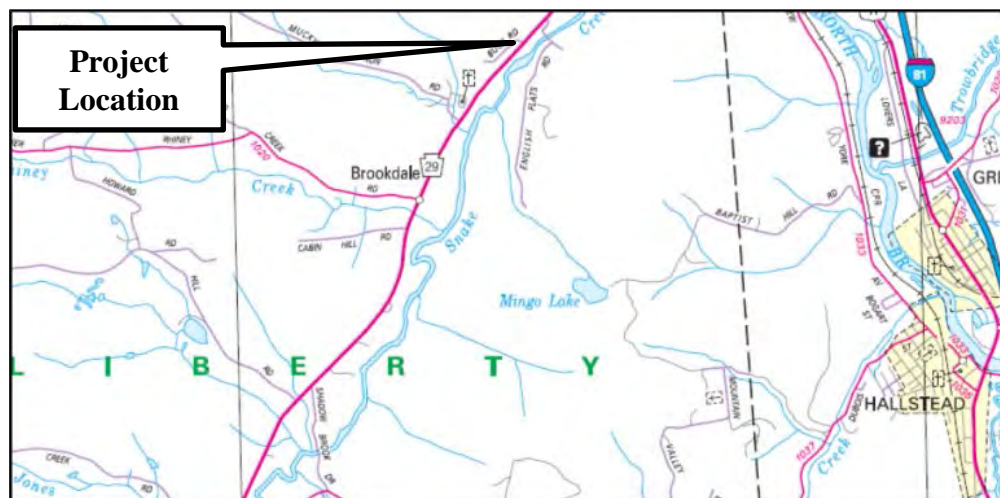
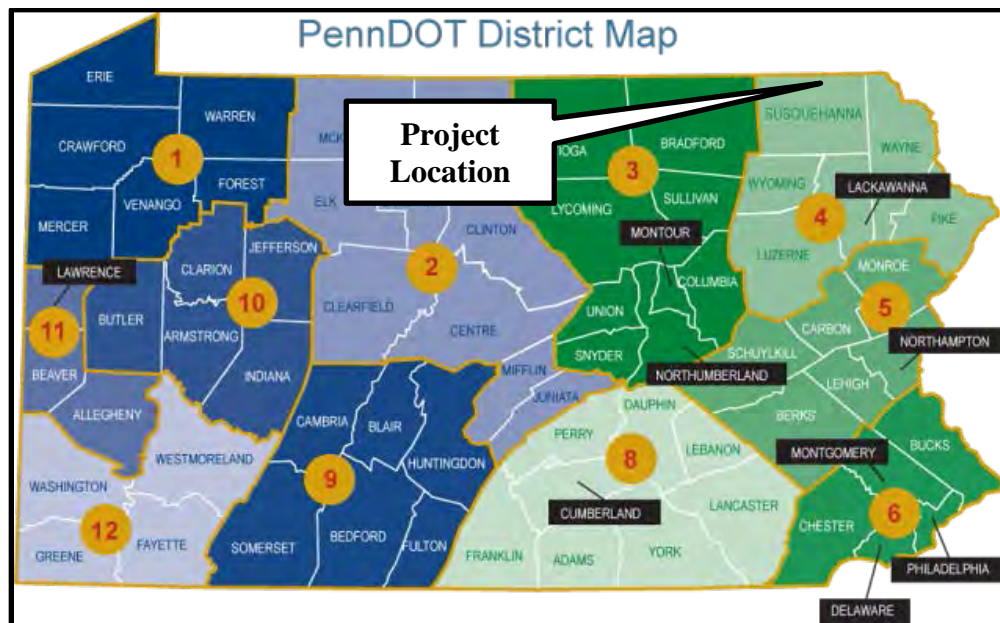
All Rights Reserved. Printed in the United States of America. No part of this publication may be reproduced or copied in any form or by any means – graphic, electronic, or mechanical, including photocopying, taping, or information storage and retrieval systems – without prior written permission of the HGS. This excludes the original author(s)

ABSTRACT

For over six decades, an active landslide has been adversely affecting the roadway on S.R. 0029 in Liberty Township, Susquehanna County, Pennsylvania near the New York State border. Movement of the slope drastically increased during and following Tropical Storm Lee and Hurricane Irene in 2011. The landslide is characterized by tension cracks, large bumps, offset guard rail, a significant toe bulge and hummocky ground surface. Published literature indicated the project area was underlain by glacial materials, including a glaciolacustrine deposit from the Pleistocene. Ten borings were drilled to confirm and augment historical subsurface investigations at the project site. Instrumentation, consisting of inclinometers and piezometers, were installed to monitor slope movement and groundwater levels. Geotechnical laboratory tests were completed to classify soils and estimate engineering parameters, including shear strength of the glaciolacustrine deposit. Laboratory testing included direct shear with residual measurements and triaxial shear. Inclinometer data verified the failure plane was located within the glaciolacustrine deposit. Multiple landside repair alternatives were considered to remediate the landslide. Back analyses were completed to verify soil parameters, and comprehensive slope stability analyses using the residual shear strength of the glaciolacustrine deposit were performed to evaluate remedial alternatives. Due to the size and geometry of the slide mass, an earth berm with drainage control and stream relocation was selected as the preferred remedial alternative. Distinct features of this project included a deep-seated block failure, historical movement, relatively large size of the slide mass, low residual shear strength, toe erosion, and previous attempts to remediate the landslide.

INTRODUCTION

For over six decades, an active landslide has been adversely affecting the roadway on S.R. 0029 in Liberty Township, Susquehanna County, near the New York State border. Slope movement has been on-going, as anecdotal information provided by local residents indicated that the roadway has been rough and has been repeatedly repaired for many years. Maps showing the location of the project are provided in Figures 1 and 2.



Figures 1 and 2: Project Location Maps

S.R. 0029 in this area parallels Snake Creek which flows northward into New York where it empties into the North Branch of the Susquehanna River. S.R. 0029 is a major north/south roadway in this area of the county and experiences considerable use by trucks due to Marcellus shale drilling activities, logging, and bluestone quarrying operations in the region. The landslide damaged the S.R. 0029 roadway, as large bumps, tension cracks, and rough

roadway conditions were evident through the landslide area (Photo 1). Periodic maintenance consisting of filling tension cracks with cold patch and milling/overlay of the pavement was performed in an effort to restore rideability. S.R. 0029 remained open to traffic and warning signs were installed to caution oncoming motorists of the bump and rough roadway conditions at the project site.



Photo 1: Dip/Rough Roadway Conditions Through Landslide Area

PROJECT HISTORY

PENNDOT investigated the landside by drilling borings and installing/monitoring inclinometers as far back as 2001. The claim made by the local residents that the movement was occurring over decades was substantiated in October 2001 when two borings completed through the roadway encountered up to 14 feet of bituminous concrete, confirming that significant movement took place over a long period of time within the landslide area. As the roadway displaced downward over time, PENNDOT maintenance crews repaved this stretch of roadway in an effort to maintain the vertical profile, resulting in the large accumulation of bituminous concrete encountered in the borings.

In October, 2006, a Geotechnical Engineering Report (GER) was prepared by a previous consultant, which outlined various remedial alternatives such as slope reinforcement, retaining walls, buttresses, soil nailing, stone columns, limited mobility displacement (LMD) grouting, and driven timber piles. The alternatives studied did not consider a deep seated block failure extending from the roadway to the creek downslope, but rather a circular failure in the vicinity of the roadway embankment.

Subsequent to the 2006 GER, an embankment excavation and replacement with a rock buttress was designed and constructed during the summer of 2010. The intent of the rock buttress was to provide load reduction at the top of the slope and to keep the repair area within the existing right-of-way. During construction of the rock buttress, 13 to 14 feet of pavement was exposed and confirmed the boring data collected by PENNDOT and the local resident's claims of a long history of slope movement (Photo 2).



Photo 2: 2010 Excavation of Roadway Exposing 13 to 14 feet of Pavement

Several months after the completion of the rock buttress, a slight movement was observed by PENNDOT personnel along the newly constructed pavement surface in the spring of 2011. A total of nine survey points were installed and monitored for movement from May 13 to October 11, 2011. The points indicated relatively small magnitudes of movement in the range of a tenth of a foot until Hurricane Irene and Tropical Storm Lee occurred during late August and early September of 2011, respectively. At some point during Hurricane Irene and Tropical Storm Lee, Snake Creek, located at the base of the slope, caused a large portion of the toe of the slope to be eroded, thereby causing a progressive series of soil slope failures to migrate up-slope to the roadway and an increased rate of slope movement.

Gannett Fleming, Inc. was engaged in the summer of 2012 to assist PENNDOT with additional geotechnical exploration, analysis, and design of alternatives to remediate the landslide. Table 1 below provides a timeline summary of project events and investigations.

Table 1 – Project History Summary

2001	An initial geotechnical investigation by PENNDOT was completed and determined 14 feet of bituminous concrete was present beneath the roadway surface.
2006	A GER was prepared for PENNDOT which outlined various remedial alternatives which included the following: slope reinforcement, retaining walls, soil nails, low mobility grout, and a buttress.
2010	An embankment excavation and replacement with a rock buttress was designed and constructed during the summer of 2010.
2011	In the spring of 2011, movement was observed by PENNDOT personnel along the newly constructed pavement surface. From May to October survey points were monitored and movement in the range of a tenth of a foot was recorded.
2011	Hurricane Irene and Tropical Storm Lee occurred during late August and early September of 2011, respectively, which caused Snake Creek, located at the base of the slope, to divert from its original alignment in a direction towards the toe of the roadway slope resulting in severe toe erosion and increased the rate of slope movement.
2011	Between October, 2011 and January 2012, a geotechnical investigation comprised of borings and inclinometers at five locations within the slide area was completed. Monitoring of the five inclinometers was performed by PENNDOT from November 4, 2011 through January 31, 2012.
2012	Gannett Fleming, Inc. was engaged in the summer of 2012 to assist PENNDOT with additional geotechnical exploration, analysis, and design of alternatives to remediate the landslide.

REVIEW OF AVAILABLE PUBLISHED INFORMATION

A review of available published information, including bedrock geology and surficial geology, was performed to gain an understanding of the project subsurface conditions. Based on the Pennsylvania Bureau of Topographic and Geologic Survey, the Devonian age Lock Haven (Dlh) Formation underlies the active landslide area, and the contact between the Catskill (Dck) and the overlying Lock Haven Formation is located upslope of the active landslide area (1). The Catskill Formation is a complex unit consisting of grayish-red sandstone, siltstone, and shale generally in a fining upward sequence. Gray sandstone and conglomerate are also present. The Lock Haven Formation is composed of predominantly light olive gray interbedded sandstone, siltstone, and shale. Fine grained rocks (shale and siltstone) constitute about 70 percent of the formation. A Bedrock Geology Map is shown in Figure 3.

The surficial geology at the project location consists of Wisconsin Till underlain by Glacial Lake Clays (2). A Surficial Geology Map is shown in Figure 4. The till is characterized as a poorly sorted, unstratified diamict – a nonsorted or poorly sorted, unconsolidated deposit containing a wide range of particle sizes. Material commonly ranges from clay to cobble or boulder size. Rock fragments are angular to rounded, and matrix material may be clayey, silty, or sandy depending on the local source bedrock. The till typically forms a smooth landform with a bouldery surface with no clear knob and kettle structure. The upper 3 feet is often colluviated, displaying a downslope oriented fabric. The total thickness is greater than 6 feet and typically on the order of 10 to 15 feet, but can be greater than 200 feet in some buried valleys. The underlying clay-rich proglacial lake (lake formed by damming of a moraine or ice dam during the retreat of a melting glacier or by meltwater trapped against an ice sheet) sediments are mostly varves, alternating thin layers of silt and clay. Each layer is usually less than one inch thick.

EXISTING GEOTECHNICAL DATA

PENNDOT provided geotechnical data from subsurface exploration programs conducted in 2001, 2006, and 2011. The subsurface explorations were initiated and performed by PENNDOT, District 4-0, and other consulting firms working for the District. The three subsurface programs included eleven (11) borings, where inclinometers were installed in nine (9) borings to monitor slope movement and determine the location of the failure plane. A total of six (6) piezometers were installed to monitor groundwater conditions in and around the slide mass. A battery of geotechnical laboratory tests was also completed. A review of the boring logs indicates that the subsurface conditions generally consisted of three soil strata overlying sandstone and shale bedrock. The surficial soils were generally composed of an upper glacial till consisting of gravelly clay, and clayey gravel; a lacustrine or glacial lake clay deposit comprised of alternating layers of silt and clay with localized zones of fine sand and gravel; and a very dense lower glacial till comprised of gravel with silt and clay.

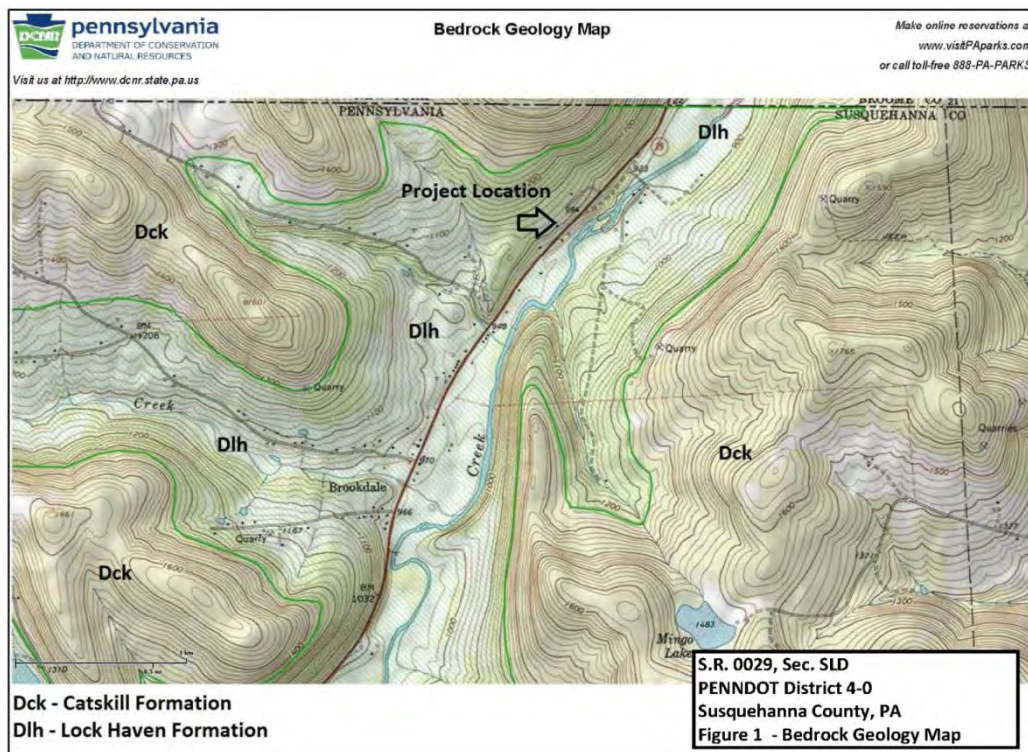
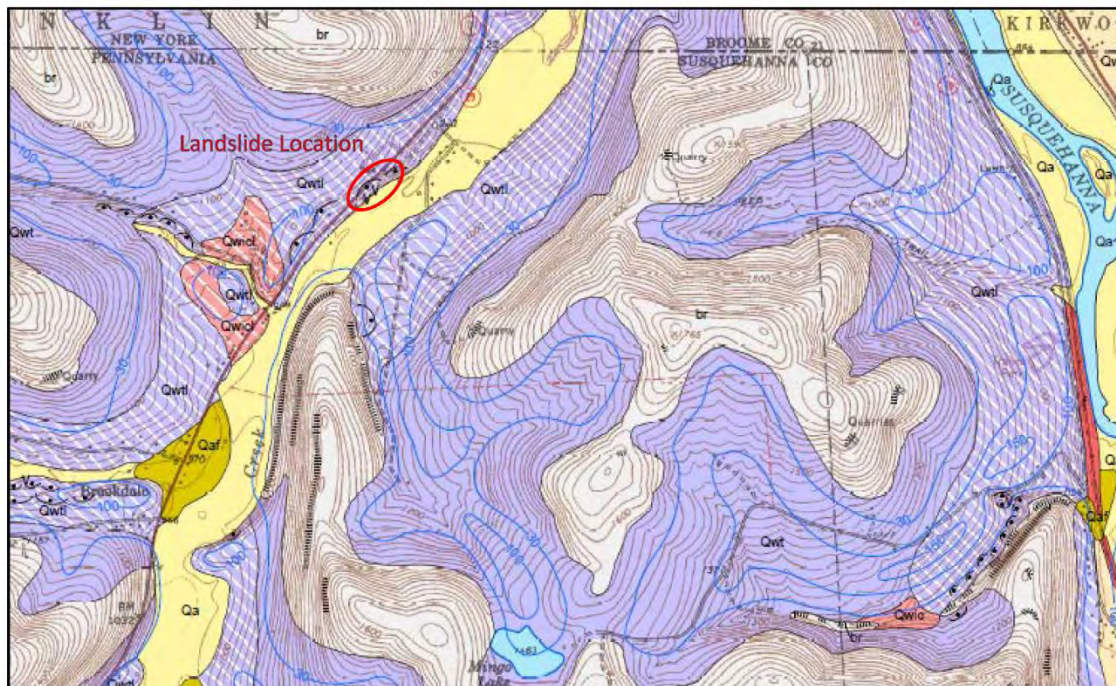


Figure 3: Bedrock Geology Map

2012 GEOTECHNICAL EXPLORATION

Gannett Fleming, Inc. initiated a subsurface exploration program for PENNDOT in 2012 to gain additional information at the site. A total of ten (10) geotechnical borings were drilled at the project site to better define the subsurface conditions, collect soil samples for laboratory testing, and for installation of inclinometer casing and piezometers in the area of the landslide between September and November of 2012. A boring location plan showing all borings drilled at the site since 2001 is shown in Figure 5 and a typical subsurface cross section, developed at Station 16+68 (Section A-A) from historical and recent borings is shown in Figure 6.

The boring logs indicate relatively consistent subsurface conditions that correspond with the available published soil and geology literature. Top of rock is relatively flat lying, and consistently located at about elevation 895 to 897 feet based on borings which encountered bedrock. The bedrock encountered was classified as interbedded medium gray to bluish gray shale and sandstone which is consistent with lithology of the Lock Haven Formation. The top of the overlying lower glacial till is also very consistent at an elevation of approximately 910 feet. The lower glacial till is comprised of very dense, grayish brown to reddish gray, gravelly clay with sand, clayey gravel with sand, and clayey gravel. Split spoon refusal was often met during Standard Penetration Testing in this unit.



(Modified from Braun, 2009)

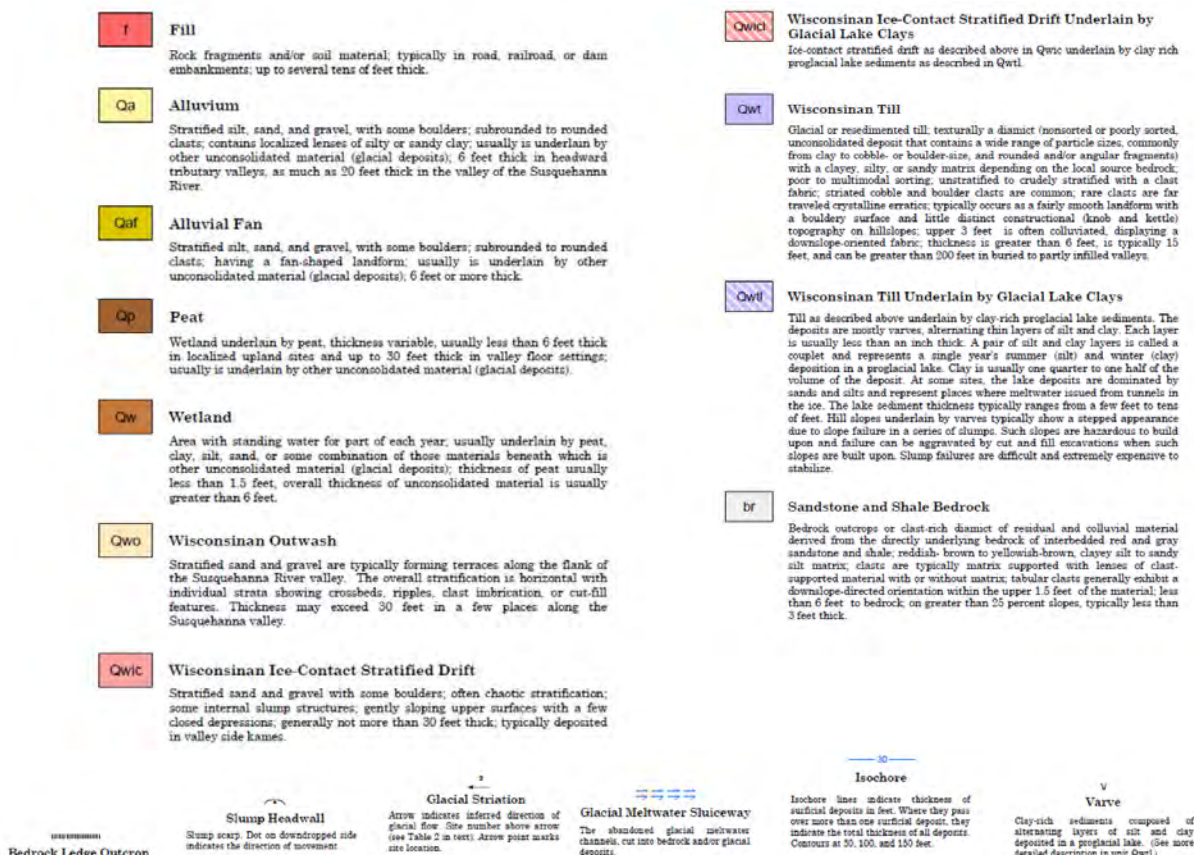
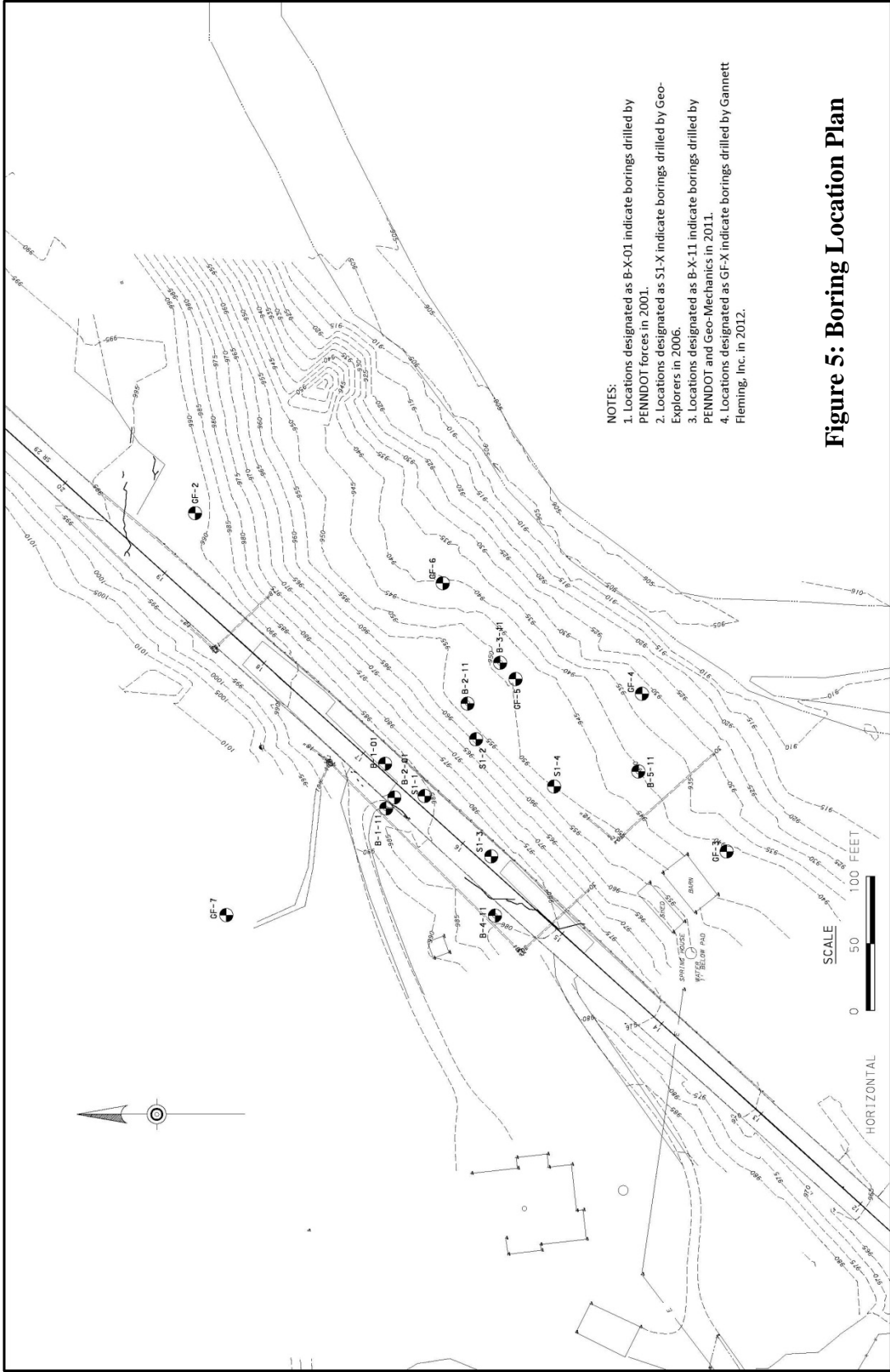


Figure 4: Surficial Geology Map



- NOTES:
1. Locations designated as B-X-01 indicate borings drilled by PENNDOT forces in 2001.
 2. Locations designated as S1-X indicate borings drilled by Geo-Explorers in 2006.
 3. Locations designated as B-X-11 indicate borings drilled by PENNDOT and Geo-Mechanics in 2011.
 4. Locations designated as GF-X indicate borings drilled by Gannett Fleming, Inc. in 2012.

Figure 5: Boring Location Plan

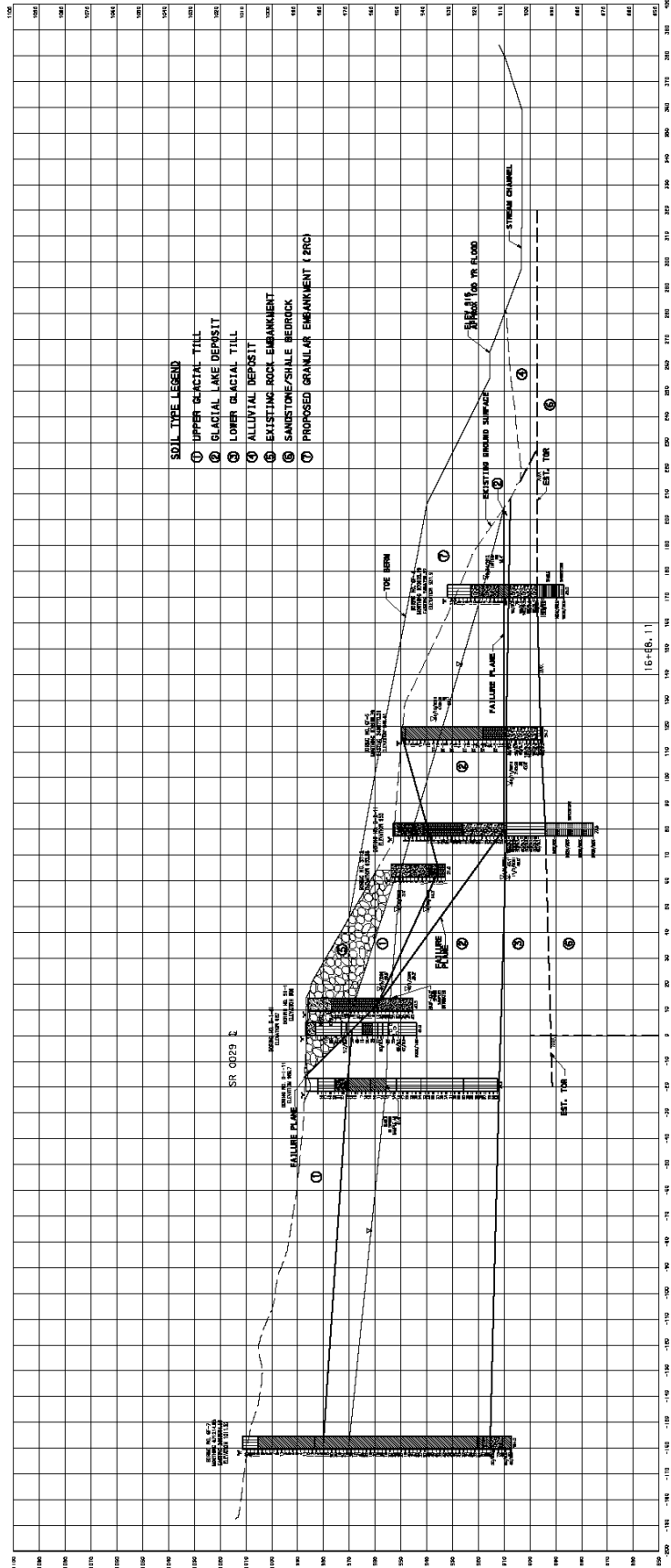


Figure 6: Typical Subsurface Cross Section

Overlying the lower till is a gray to grayish brown lacustrine or glacial lake clay deposit. The borings confirmed the presence of alternating intervals or couplets of silt and clay sized particles, often termed varves, as shown in Photo 3. The glacial lake clay was typically moist and ranged from stiff to very hard. Localized rounded to subrounded gravel fragments were also identified.

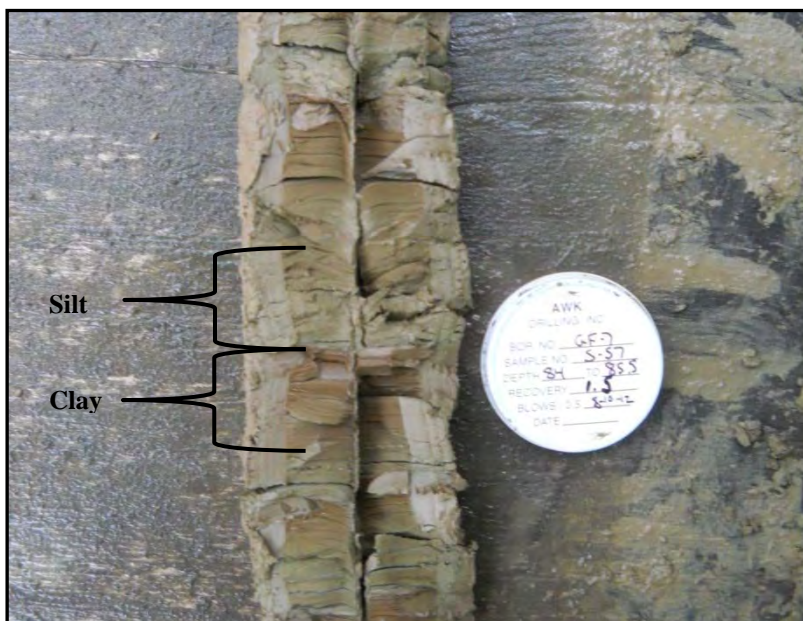


Photo 3: Varved Lake Clay Sample Encountered in GF-7

Above the glacial lake clay is an upper glacial till deposit comprised primarily of brown to gray clayey gravel, gravelly clay, and gravelly silt. The contact between the upper till and the underlying glacial lake clay deposit varied from boring to boring, particularly within the landslide mass. In GF-7, located above the crown of the landslide, the contact was well-defined and was encountered at elevation 983 feet for a clay thickness of 28 feet. In GF-2, located near the right flank of the landslide, the contact between the clay and upper till was encountered at elevation 967 feet for a clay thickness of 24 feet. In borings GF-4, -5, and -6, located within the main body of the landslide, the upper till varied from 1.5 feet in GF-5 to 16 feet in GF-6. The upper glacial till was 29 feet thick in GF-3, located near the left flank of the landslide.

INSTRUMENTATION

During the 2012 subsurface investigation inclinometer casing was installed in 5 borings. Three of the inclinometers were installed within the active landslide and the remaining two located outside the active landslide. These inclinometers, together with the inclinometers installed by PENNDOT in 2001, 2011, and a previous consultant in 2006, were very successful in identifying the location of the failure plane. The inclinometer readings consistently showed that the movement of the slide mass was within the glacial lake clay layer, just above the lower glacial till. Table 2 below lists the inclinometers and the elevation of the failure plane at each instrument. Figure 7 presents a typical plot of the inclinometer readings taken over a four month time period in a direction perpendicular to the head scarp of the landslide.

Table 2 – Summary of Failure Plane Elevations

Boring/Inclinometer ID	Installation Date	Approximate Failure Plane Elevation (ft)	Material Description (USCS)
B-1	2001	962.6	ml
S1-1	2006	960	cl-ml
S1-3	2006	952	cl-ml
B-2	2011	910	cl-ml
B-3	2011	910.2	cl-ml
B-5	2011	909	cl-ml
GF-2	2012	946	cl
GF-4	2012	909	cl
GF-6	2012	925.2 (Upper) 912.0 (Lower)	cl

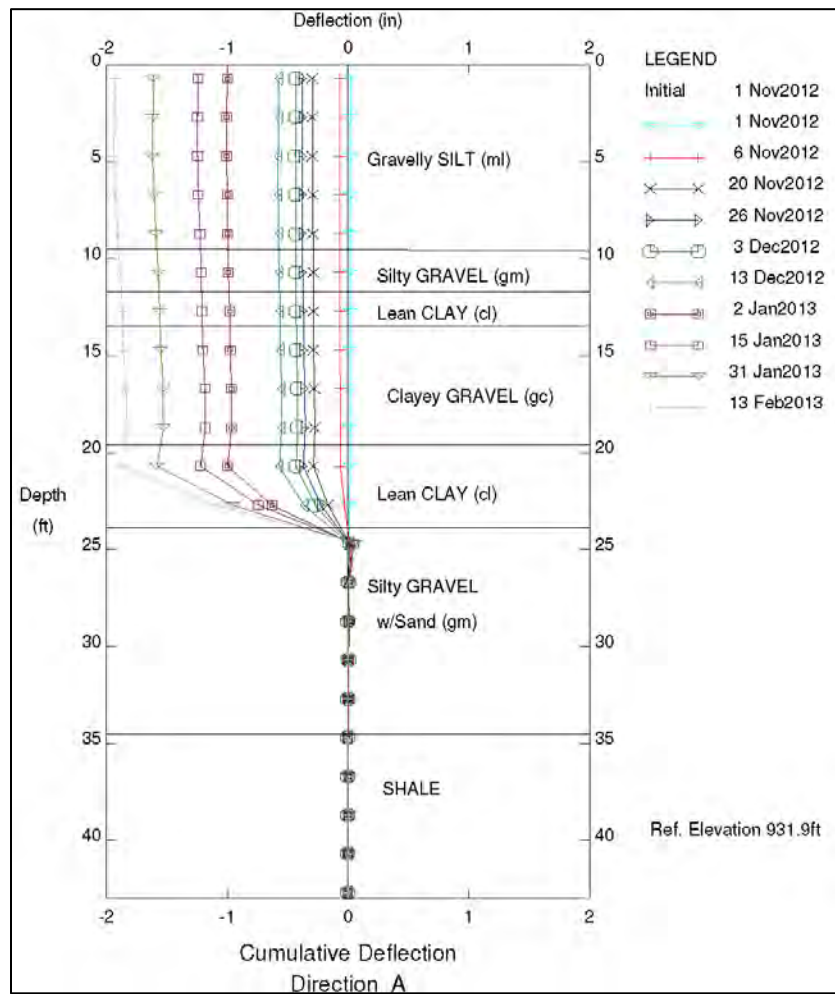


Figure 7: Typical Inclinometer Plot

Standpipe (Casagrande) piezometers were constructed in five borings located throughout the landslide area to monitor long-term groundwater fluctuations at the site. Automated transducers were installed in the aforementioned piezometers to monitor long term groundwater levels for slope stability analysis.

LABORATORY TESTING

Since the existing geotechnical data provided by PENNDOT indicated that the slope failure was located within the glacial lake clay deposit, the majority of laboratory testing performed for final design was focused on the engineering properties of the clay and silt material. Tests performed included sieve and hydrometer analysis, Atterberg limits, natural moisture content, specific gravity, direct shear (peak and residual), consolidation, and triaxial shear (consolidated-undrained with pore pressure readings). A summary of laboratory test results is presented in Table 3. Historical laboratory test results, obtained by others, are also shown in Table 3 for comparison.

The soil index testing completed focused on the glaciolacustrine deposits in which the failure plane(s) are located. These soils generally classified as inorganic silts and clays with low plasticity (CL, ML, and CL-ML). The natural moisture content of the glaciolacustrine material ranged from 14.9 to 25.8 percent, liquid limits ranged from 25 to 37 percent and dry unit weights ranged from 103.8 pcf to 112.6 pcf.

Eight direct shear tests were performed to estimate the peak shear strength of the glaciolacustrine soils. Based on the eight tests completed the peak shear strength ranged from 18.5 to 31.1 with an average of 24.6 degrees. The results are presented in Table 3.

Movement along a shear plane in fine-grained soils results in reorientation of the soil particles and very often a significant reduction in the shear strength of the material along the shear plane. The residual shear strength was considered particularly important to the slope stability analyses and remediation design for this project because of the long history and significant magnitude of slope movement at the site. Seven residual shear tests were performed to estimate the residual shear strength of the glaciolacustrine soils where the landside failure plane was located. The residual shear strength values ranged from 10.8 degrees to 17.5 degrees and are summarized in Table 3. These results are similar to other testing results of Wisconsin age glacial lake clay deposits in northern Pennsylvania tested by Gannett Fleming. Based on the results of the direct shear testing the residual shear strength is significantly less than the peak shear strength.

Table 3 – Summary of Geotechnical Laboratory Testing Results

Boring	Sample	Depth (ft)	Material Description	USCS	Direct Shear			Triaxial Shear	
					Peak Strength (deg)	Cohesion (psf)	Residual Strength (deg)	Peak Strength (deg)	Cohesion (psf)
Laboratory Analysis Completed by PENNDOT and other Consultants									
B-1	BAG	16-19	sandy CLAY with gravel	CL	-	-	-	-	-
B-1	BAG	25-29.5	sandy CLAY with gravel	CL	-	-	-	-	-
B-1	BAG	41-61	clayey SAND with gravel	SC	-	-	-	-	-
B-2	BAG	36-45	silty CLAY with sand	CL	-	-	-	-	-
B-3	BAG	10.5-12	silty CLAY	CL	-	-	-	-	-
B-3	ST	21-23	lean CLAY	CL	29.9	72	-	-	-
B-4	BAG	12-15	sandy CLAY	CL	-	-	-	-	-
B-4	ST	24-26	silty CLAY	CL-ML	-	-	-	-	-
B-5	ST	18-20	lean CLAY	CL	26.9	316	-	-	-
Laboratory Analysis Completed by Gannett Fleming, Inc. Laboratory									
GF-3	S-16	22.5-24	gravelly CLAY	-	-	-	-	-	-
GF-5	ST-2	14-16	SILT	ML	28.8	-	15.2	-	-
GF-5	ST-3	17.5-19.5	lean CLAY	CL	23.1	-	14.7	-	-
GF-5	ST-4	22.5-24.5	lean CLAY	CL	23.9	-	17.5	-	-
GF-5	ST-6	29.5-31.5	silty CLAY	CL-ML	31.1	-	29	-	-
GF-5	ST-7	34.5-36.5	lean CLAY	CL	26.2	-	14.5	-	-
GF-5	ST-7 (2)	34.5-36.5	lean CLAY	CL	23.2	930	-	-	-
GF-6B	ST-1	20.5-22.5	lean CLAY	CL	18.5	-	12.2	-	-
GF-6B	ST-2	28-30	SILT	ML	22	-	10.8	-	-
GF-5	ST-1 to 3	10.5-19.5	silty CLAY	CL	-	-	-	21.9	166

One triaxial shear (consolidated undrained with pore pressure measurement) test was performed on a sample from where the majority of the landslide failure plane was located. The test was performed to estimate the peak shear strength of the glacial lake clay where the orientation of the failure plane was somewhat perpendicular to the varves, rather than parallel to the varves as obtained through the direct shear testing. The test result indicated the peak effective shear strength of the clay and silt stratum was 21.9 degrees with a cohesion of 166 psf.

LANDSLIDE TRIGGER MECHANISMS

As with most landslides, it is likely that more than one factor existed that triggered the landslide. Although some of the triggering mechanisms presented below are based on speculation, information exists to substantiate the perceived trigger(s).

The principle cause to the landslide was continual erosion of the toe of the slope by Snake Creek particularly during high flow events. A secondary cause was most likely the low shear strength, and particularly, the low residual shear strength of glacial lake deposited silt and clay material encountered at the site. The majority of the defined failure plane was located within this stratum. In addition, published mapping of the surficial geology indicated the lake clay deposit and overlying till were susceptible to slope instability as scarps were mapped at the project site.

Another factor suspected to have contributed to the slope instability was the presence of surface drainage pipes emptying directly onto the slope and localized seeps throughout the hillside.

LANDSLIDE REMEDIATION ALTERNATIVES

Landslide remediation alternatives considered included: no-build, structural elements, and upslope drainage control with an earth berm and stream relocation. A no-build alternative was considered, but would not remediate the landslide. The landslide would continue to slump during periods of wet weather and high water events in Snake Creek as additional material at the toe of the slope was eroded. Periodic maintenance would still be required to maintain traffic on S.R. 0029, the existing roadway depression would continue to grow, and winter maintenance at the depressed area would be extremely difficult. A safety risk to the traveling public would still be present. Structural elements including driven piles, drilled-in piles, and drilled shafts were also considered. Several rows of structural elements were required along with a cap wall to connect the elements and the slope needed to be reconstructed and protected at the toe. Due to the high cost of providing a viable structural element remediation alternative, this alternative was not selected for the project.

Earth berms are commonly used to remediate landslides, require little to no maintenance and are not considered to have a finite design life. Therefore, the recommended remediation alternative for this project was to relocate Snake Creek, towards its historical alignment, approximately 70 feet away from the existing toe and provide an earth berm at the toe of the landslide. The relocation of the creek involved coordination with, and approval from, the Susquehanna County Conservation District (SCCD), the Pennsylvania Department of Environmental Protection (PADEP), the Pennsylvania Fish and Boat Commission (PFBC), the U.S. Army Corps of Engineers (USACE), and the U.S. Fish and Wildlife Service (USFW). Some major considerations during the permitting process included wetland mitigation since the proposed berm encroached on existing wetlands, accommodation of fish passage during low flow periods, and preparation of an Aids to Navigation Plan (ATON) since the stream can be used recreationally by canoes. Because the relocation of the stream was towards its historical alignment and within the boundaries of its former channel, obtaining approvals from the required agencies was not a major stumbling block for the berm alternative.

In conjunction with the earth berm, a drainage system comprising of a series of trench and blanket drains will also be installed to intercept seepage and groundwater from the existing rockfill roadway embankment before it saturates the soil slide mass. To minimize overland flow of water, roadway drainage will be diverted to the south and prevented from discharging into the landslide area. A detailed discussion of earth berm design is provided below.

EXISTING SLOPE STABILITY ANALYSES

The computer software program GSTABL7 was used to perform the slope stability analyses for the project. The slope stability analyses were performed to evaluate the soil parameters selected for use in the stability model and to validate the model through back calculation. The back calculation model would ultimately become the basis for designing the remediation. A cross-section at Station 16+68.11 (Section A-A), as shown in Figure 6, was analyzed for the project and slope stability analyses were performed for the existing condition and several earth berm configurations. This location was selected because it was located near the middle of the landslide, mapped tension cracks were present throughout the slope, the section was representative of the landslide area, and subsurface data was extensive.

Data obtained from the borings and inclinometers confirmed the failure plane of the landslide was located in the glacial lake clay deposit. The residual strength of this material was used in the slope stability analyses due to the significant past activity of the landslide and the ongoing movement. The laboratory test results for residual shear strength of the silt stratum varied from 10.8 to 17.5 degrees with an average value of 14.2 degrees, not considering the test result from sample GF-5 (ST-6). The test result from this sample was not considered representative due to a piece of gravel in the sample, which adversely affected the test. The residual shear strength values were considerably lower than the peak shear strength values for the glacial lake clay. Since the landslide had a long history of movement, the residual shear strength was considered more appropriate for use in determining the existing factor of safety of the slope and for designing the remediation. Peak shear strength values would have produced higher factors of safety in the stability analyses and lead to an under-designed remediation.

The results of the residual shear testing were further evaluated using statistical analyses. The 33rd percentile strength is a method of interpretation described by the U.S. Army Corps of Engineers in EM 1110-2-1902 such that two-thirds of the test data are above the selected failure envelope and one-third are below. This evaluation resulted in a 33rd percentile value of 13.7 degrees. As a result, a residual shear strength parameter for the glacial lake clay was conservatively selected as 13.0 degrees. Some cohesion was considered in the glacial lake clay for the analyses, as discussed in the paragraph below.

Since the slope was actively moving, was significantly eroded at its toe by Snake Creek during recent high flow events, and it was not known when the slope was last stable (i.e. F.S. \geq 1.0), determination of soil strength parameters by means of a back analysis to compare with laboratory results was not considered practical. As an alternative, an existing conditions analysis using a residual shear strength value of 13.0 degrees was used for the analyses, assuming no cohesion. A stability run using these parameters resulted in a F.S. of less than 0.6 for the modeled section. Such a low factor of safety was considered unrealistically low, even for the failing slope, considering the relatively consistent rate and long history of the movement. In

order to create a more reasonable model, 250 pounds per square foot (psf) of cohesion was included in the shear strength of the glacial lake clay deposit. The addition of cohesion to the model was justifiable because the varved clay and silt was overconsolidated due to past glacial loading. The over consolidation ratio (OCR) of 2.4 determined by consolidation testing verified that the material was overconsolidated. The shear strength of overconsolidated clay typically includes some cohesion. Results of the existing condition analysis stability run utilizing 250 psf of cohesion resulted in a F.S. of 0.9, which was assumed to be a realistic factor of safety for the moving slope condition.

Multiple iterations for both sliding block and circular types of failures were evaluated to find a failure plane that closely matched the depth of the failure plane identified by the inclinometers. Various initiation and termination points were evaluated to determine the most critical factor of safety of each run. The GSTABL7 model and the results of the existing slope analysis are shown in Figure 8.

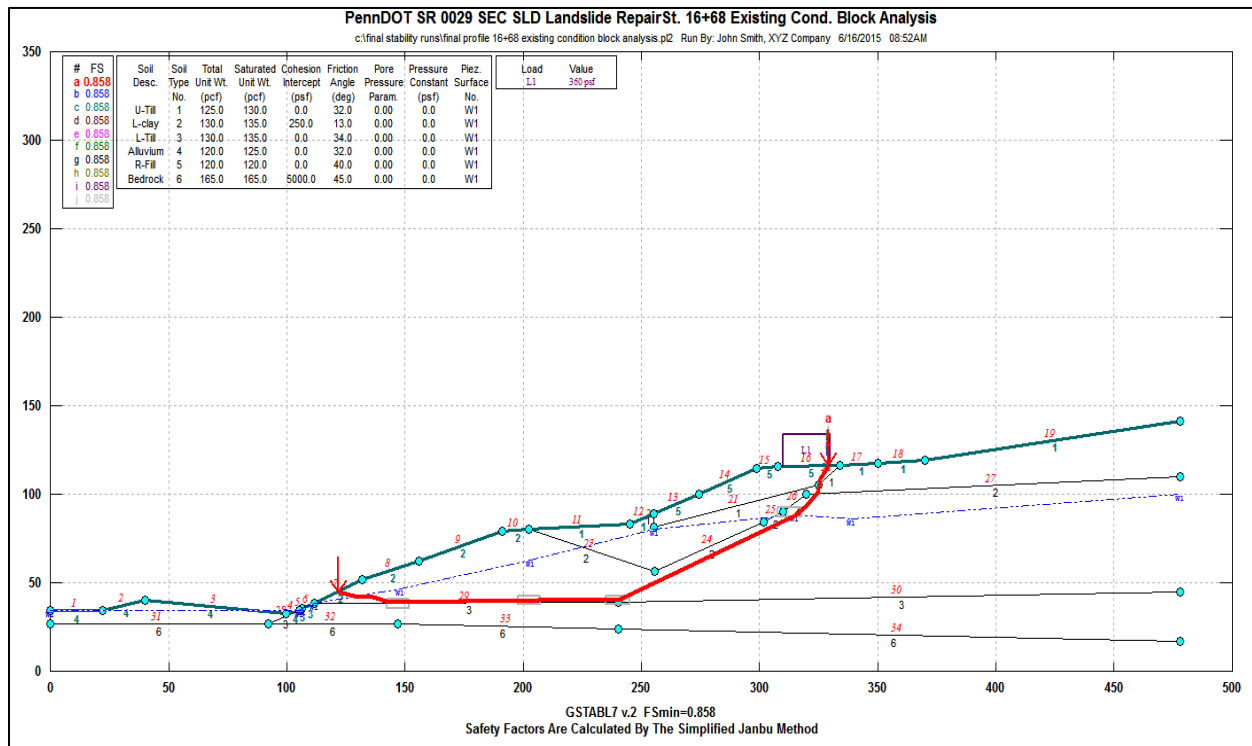


Figure 8: GSTABL7 Plot of Existing Conditions Analysis

The various subsurface strata used in the stability analyses and are shown below:

- Upper Glacial Till - clayey gravel (GC), gravelly clay (CL), and gravelly silt (ML)
- Glacial Lake Deposit - clay (CL), silty-clay (CL-ML) and silt (ML)
- Lower Glacial Till - gravelly clay with sand (CL), clayey gravel with sand (GC), and clayey gravel (GC)
- Alluvial Deposit
- Existing Rock Fill
- Bedrock

The top of bedrock was used in the existing conditions analysis as a limiting boundary so that failure surfaces did not extend below the top of bedrock. The soil parameters for the upper and lower glacial till units and alluvium were determined based on laboratory test results, in-situ SPT results, and published empirical data. Groundwater levels obtained from the piezometers installed at the site were used to model the groundwater table. The soil and bedrock rock parameters, presented in Table 4, were used in the stability analyses.

Table 4 – Summary of Soil Strength Parameters

Soil Description	Moist Unit Weight (pcf)	Saturated Unit Weight (pcf)	Cohesion (psf)	Friction Angle (deg)
Existing Rockfill	120	120	0	40
Upper Glacial Till	125	130	0	32
Residual Strength Clay-Silt	130	135	250	13
Peak Strength Clay-Silt	130	135	250	22
Lower Glacial Till	130	135	0	34
Alluvium	120	125	0	32
Bedrock	165	165	5000	45
Earth Berm	125	130	0	34

REMEDIAL EARTH BERM ANALYSES

Earth berm configurations consisting of varying berm widths, heights, and slope angles were analyzed in GSTABL7 to determine the ideal berm configuration. The soil and rock parameters used in the earth berm analyses were consistent with the soil parameters used for the existing conditions analyses. The soil parameters used in the analyses for the earth berm material were values typically used in stability analyses for PENNDOT embankments constructed of material that meets the requirements of PENNDOT specifications for granular borrow material (3). A live load traffic surcharge of 360 psf was included in the analyses along the S.R. 0029 roadway at the top of the slide mass. In addition, stability analyses to model the 100-year flood elevation of Snake Creek were performed to investigate various design conditions. The soil parameters used in the analyses are presented in Table 4.

The subsurface profile, failure plane and groundwater levels used in the earth berm analyses were consistent with the models used for the existing conditions analyses and were based on boring information and instrumentation data obtained from the inclinometers and piezometers installed at the site. A summary of the results of the slope stability analyses performed for the representative cross section at Station 16+68.11 is presented in Table 5, and the GSTABL7 plot for the critical analysis is shown in Figure 9.

Table 5 –Summary of Slope Stability Analyses at Station 16+68.11

Station	Analysis Condition	Factor of Safety
16+68.11 (Section A-A)	Existing Condition – No cohesion – Block analysis	0.63
	Existing Condition – 250 psf cohesion – Block analysis	0.86
	Existing Condition – 250 psf cohesion – Circular analysis	1.13
	Pile Alternate – 250 psf cohesion – Circular analysis	0.94
	Toe Berm – 250 psf cohesion – Normal Water - Block analysis	1.43
	Toe Berm – 250 psf cohesion – Normal Water - Circular analysis	1.56
	Toe Berm – 250 psf cohesion – 100-year flood - Block analysis	1.43
	Toe Berm – 250 psf cohesion – 100-year flood - Circular analysis	1.56

The results of the stability analyses were presented to PENNDOT during a progress meeting in January of 2013 and it was determined that the earth berm in conjunction with the relocation of Snake Creek was the preferred remedial design because it provided an acceptable factor of safety and was a more reliable solution than other alternatives considered. The stability of the earth berm was assessed and the results indicated the factor of safety was greater than the required factor of safety of 1.3. The GSTABL7 analysis modeling the normal water surface elevation in Snake Creek resulted in the lowest factor of safety.

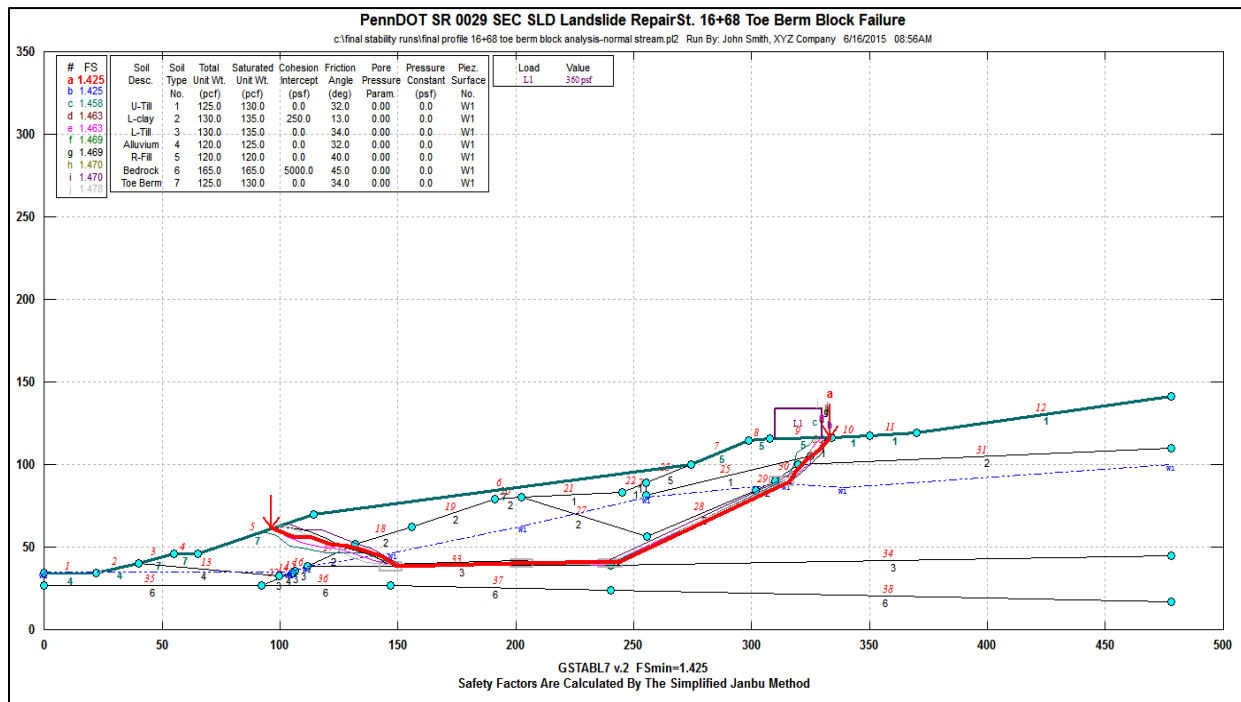


Figure 9: GSTABL7 Plot of Critical Toe Berm Analysis

LANDSLIDE REMEDIATION

The landslide remediation consists of the relocation of Snake Creek, armoring of the relocated stream banks, constructing a toe berm, installing surface and subsurface drainage features, restoring the grading on the upper portion of the slope, and reconstructing the roadway. The stream banks of relocated Snake Creek have 3H:1V side slopes to the approximate 100-year flood elevation of 915 feet, where a 10-foot wide bench is provided on the sloped side of the creek. An earth berm with an initial 2H:1V slope will be placed from Elevation 915 to 940 feet. At Elevation 940 feet the slope of the berm will flatten to between 3H:1V to 6H:1V, up to elevation 970 feet, and extend onto the existing rock roadway embankment. To protect the earth berm from erosion during future flood events, a 10-foot thick rock veneer constructed of rip rap is provided on the face of the berm. The stream banks will consist of native material excavated from the stream bed. A typical cross section of the berm and stream relocation is included as Figure 10.

Based on the amount of seeps that were observed within the project limits during site reconnaissance, and the nearly continuous wet soil conditions in localized areas of the landslide, seeps during construction of the earth berm were a concern. Aggregate chimney drains and underdrain pipes are provided to collect and control water from the seeps and direct it to exit points lower on the slope, where it will be outlet onto the rock veneer. Additionally, considering that the existing roadway embankment in the vicinity of the slide is constructed of rock, a trench drain along the toe of the existing embankment is provided. The trench drain will collect any water that travels through the rock embankment from the upslope side of the S.R. 0029 roadway. Lateral outlet pipes are provided at minimum 100-foot intervals along the trench drain, and extend to the berm slope to outlet.

Surface drainage along the S.R. 0029 roadway will be enhanced by relocating two drainage pipes that outlet in the vicinity of the landslide on the downslope side of S.R. 0029. Roadway drainage and water from an intermittent stream located on the upslope side of S.R. 0029 will be collected in pipes and removed from the landslide area to prevent it from saturating the slope. The water will be outlet to the south of the landslide area. Additionally, a concrete curb and inlets will be provided along the edge of the S.R. 0029 roadway to prevent water from flowing downslope.

The remediation includes reconstruction of the S.R. 0029 roadway through the landslide area. Tension cracks were documented in many locations within the roadway throughout the landslide area and the head scarp is located just off the shoulder of the roadway. To mitigate the potential for reflective cracking in the reconstructed roadway, overexcavation below the pavement subgrade and placement of alternating layers of biaxial geogrid and coarse aggregate subbase will be provided. A roadway reconstruction detail is included as Figure 10.

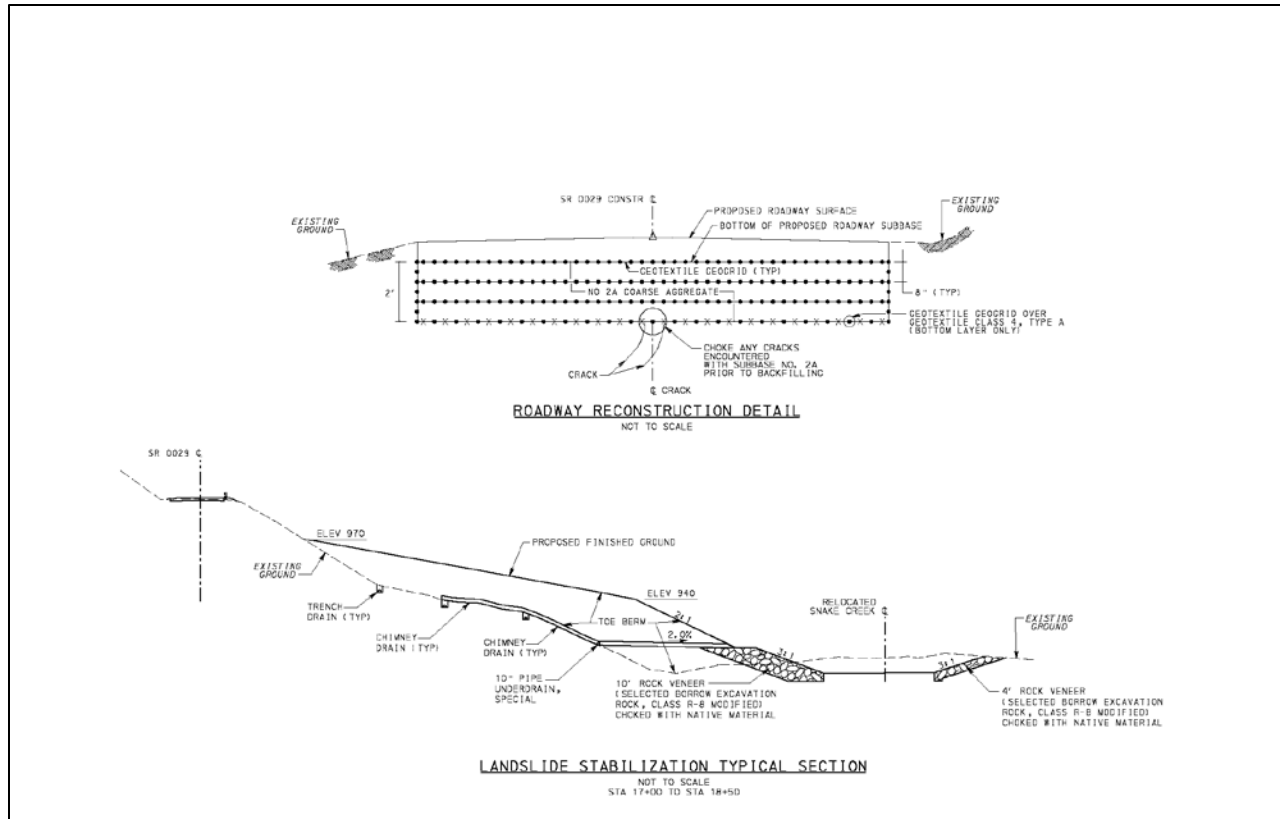


Figure 10: Landslide Stabilization Typical Section and Roadway Reconstruction Detail

CONSTRUCTION PROGRESS

The project was advertised for bids on September 25, 2014 and was awarded to Latona Trucking, Inc. on October 10, 2014. The low bid price for the project was \$3.3 million. Construction began in the winter of 2014 to install temporary access roads to the stream and to the toe of the landslide, and to divert Snake Creek to its new location; however, poor weather and high water conditions delayed the contractor's progress through the winter of 2014 and the spring of 2015. The contractor has since successfully relocated Snake Creek to its new alignment and has begun to place the new rock buttress at the toe of the slope. The construction will progress from the bottom of the slope to the top to enhance the stability of the slope as the new embankment is placed. Construction is expected to be completed by the winter of 2015.

REFERENCES

- (1) Pennsylvania Department of Conservation and Natural Resources, Bureau of Topographic and Geologic Survey, *PAMAP*, 2012.
- (2) Braun, Duane D., Pennsylvania Bureau of Topographic and Geologic Survey, *Surficial Geology of the Franklin Forks 7.5 Minute Quadrangle, Susquehanna County, Pennsylvania and Broome County, New York*. Open File Report 09-03.0, 2009.
- (3) Pennsylvania Department of Transportation, Publication 408, *Construction Specifications and Standard Provisions*, 2011.

Investigation, Design and Mitigation of a Landslide in Newport, Vermont

Jay R. Smerekanicz, P.G.

Golder Associates Inc.
670 North Commercial St., Ste. 103
Manchester, NH 03101
(603) 668-0880
jay_smerekanicz@golder.com

Jeffrey D. Lloyd, P.E.

Golder Associates Inc.
670 North Commercial St., Ste. 103
Manchester, NH 03101
(603) 668-0880
jlloyd@golder.com

Mark S. Peterson, P.E.

Golder Associates Inc.
174 South Freeport Road, Ste. 20
Freeport, ME 04032
(207) 865-4024
mpeterson@golder.com

Peter C. Ingraham, P.E.

Golder Associates Inc.
670 North Commercial St., Ste. 103
Manchester, NH 03101
(603) 668-0880
pingraham@golder.com

Christopher C. Benda, P.E.

Soils and Foundations Engineer
Vermont Agency of Transportation
Program Development/Materials and Research
2178 Airport Road, Unit-B
Berlin, VT 05641-8628
(802) 828-6910
Chris.Benda@state.vt.us

Acknowledgements

The author(s) would like to thank the individuals/entities for their contributions in the work described:

Chad Allen, P.E. – Vermont Agency of Transportation
Dr. Don De Groot – University of Massachusetts, Amherst

Disclaimer

Statements and views presented in this paper are strictly those of the author(s), and do not necessarily reflect positions held by their affiliations, the Highway Geology Symposium (HGS), or others acknowledged above. The mention of trade names for commercial products does not imply the approval or endorsement by HGS.

Copyright Notice

Copyright © 2015 Highway Geology Symposium (HGS)

All Rights Reserved. Printed in the United States of America. No part of this publication may be reproduced or copied in any form or by any means – graphic, electronic, or mechanical, including photocopying, taping, or information storage and retrieval systems – without prior written permission of the HGS. This excludes the original author(s).

ABSTRACT

Shortly after new embankment construction for Route 191 in Newport, Vermont in 1971, a slow-moving landslide developed, requiring the Vermont Agency of Transportation (VTrans) to periodically maintain the roadway with pavement shimming, guard rail repair, and culvert replacement. Initial investigations and mitigation in the 1970's included borings and drains, but slope movement was not reduced. Removal of 4 ft of pavement shim in 1986 indicated 3.2 in/yr of vertical movement from 1971-1986. VTrans installed piezometers and inclinometers in the 1980's to further delineate the landslide depth and extent, leading to installation of a stability berm near the suspected landslide toe to slow movement. After movement continued, additional deep inclinometers installed in 2007-2008 further downslope indicated the slide extent was much greater than suspected, and that artesian groundwater pressures exist deep in the slide mass. The deep inclinometer installations relieved deep groundwater pressure and slowed movement, indicating hydrogeology plays an important factor in landslide movement and hence mitigation.

VTrans conducted a comprehensive geologic, hydrogeologic and geotechnical investigation in 2012-2013 to collect data and evaluate several mitigation approaches, with the goal of selecting a suitable remedy to slow or stop landslide movement. The investigation included field reconnaissance geologic mapping; an extensive subsurface investigation program, including sonic and conventionally drilled test borings; extensive geotechnical laboratory testing; well, piezometer and automated inclinometer instrumentation; and hydrogeologic testing. Field and laboratory data were used to refine the site geologic and hydrogeologic 3-D models; and to develop a calibrated numerical groundwater model to support geotechnical stability analyses, remedial design development, and construction cost estimating.

Basal glacial sediments of the slide (alternating clayey silts, sandy silts and silty sands), which are key in evaluating remedial alternatives, exhibited high overconsolidation ratios, very stiff to hard consistency when undisturbed, high plasticity, and folded varves. One geologic interpretation of the origin of these sediments is deposition by a pre-Pleistocene glacial advance, and subsequent burial by the last ice sheet. Sonic cores indicate several previous slip planes/zones exist, defined by slickensides and folded varves, indicating slumping or ice grounding deformed the sediments. The slip planes contributing to the current movement may occupy some of these historical failure planes, and residual shear strengths at these zones likely govern behavior. Pumping tests indicate hydrogeologic connectivity exists between the lowermost coarser sediments and overlying coarser sediments separated by clayey silts, suggesting the silty clay units are discontinuous, but act as semiconfining units.

Groundwater and slope stability models simulating several groundwater withdrawal options including passive and active groundwater extraction indicate landslide movement can be slowed or even halted. However physical constraints, such as right-of-way, groundwater chemistry and treatment, and permitting, must be evaluated to design, construct and operate a permanent groundwater extraction system.

INTRODUCTION

Slope movements at an embankment fill constructed as part of the Route 191 connector between Interstate 91 and the town of Newport, Vermont have been the subject of investigations, mitigation construction and monitoring by the Vermont Agency of Transportation (VTrans) for over 40 years since the roadway was constructed in 1971 (Figure 1). Mitigation measures, subsurface investigations and stability analyses completed over the 20 year period from 1971 to about 1991 concluded that continuous slope movements were the result of embankment fill loads and groundwater pressure effects on a circular slip surface extending from the uphill side of the roadway to the downslope toe of the embankment fill inclusive of an overall slope length of about 200 feet. Mitigation measures constructed in 1991 based on this hypothesis were ineffective. Based on monitoring data, additional subsurface investigations and stability analyses completed over the subsequent 20 year period from 1991 to 2011, the roadway slope movements are now believed to be part of a much larger non-circular slide mass extending up to 120 feet below ground surface and inclusive of an overall slope length of roughly 600 feet. Moreover, the mechanisms causing slope movements are now believed to include a complex combination of geologic stratigraphy, groundwater conditions, and soil strength characteristics, all of which have bearing on an effective mitigation plan to monitor and preferably arrest future slope movements.

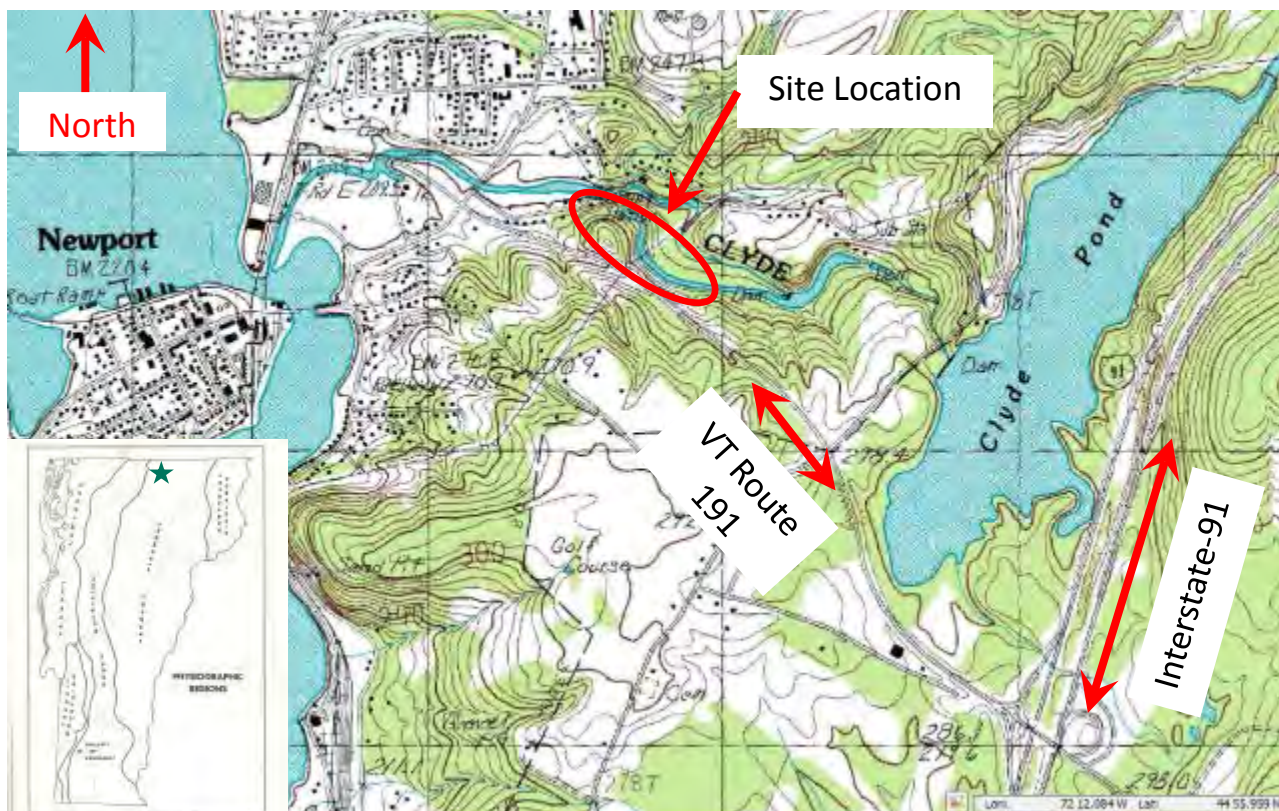


Figure 1 - Site location map.

In 2011 VTrans evaluated mitigation alternatives including: 1) removal of the counter berm placed in 1991; 2) excavation of embankment fill and replacement with lightweight fill; 3)

reinforcement with piles or drilled shafts; and 4), drainage to reduce groundwater pressures acting on the slide mass. Also in 2011 VTrans engaged Civil Engineering Associates, Inc. (CEA) of South Burlington, Vermont to assess soil strength behavior as a possible contributing cause to the slope movements. The results of these evaluations indicated that reducing groundwater pressures would probably be the most effective means of stabilizing the slide mass; however, developing cost effective measures to sufficiently reduce groundwater pressures would require further evaluation, and additional laboratory testing was warranted to better understand the strength behavior of the site soils and related risks to long term roadway stability.

In March 2012 Golder was requested to assist VTrans in developing a plan for managing future slope movements using a phased approach. The first task included reviewing the extensive records of site and project information, and performing a preliminary reassessment of slide mass stability. The second task consisted of developing a plan for sustainable long-term monitoring coupled with recommendations for additional site investigations and testing considered necessary to fill data gaps, develop design plans in the future to mitigate slope movements, and manage risk. The third task involved implementation of an extensive field investigation and laboratory investigation, detailed geologic and geotechnical modeling, and evaluation of potential mitigation techniques.

Review of reports and data prior to 2012 indicated the site has been logically investigated over the years and the approaches to mitigating slope movements were reasonable given the understanding of the subsurface conditions at the time the measures were developed. The condition of the pre-2012 instrumentation was poor due to a lack of discrete screened intervals in piezometers, and excessive deflection of inclinometer casings that reduces their potential life for longer term monitoring or automation going forward. However, data from the pre-2012 inclinometers provided valuable insight concerning slide mass behavior because: 1) they showed the location of discrete horizontal displacements indicating the base of the slide mass is located up to about 120 feet below ground surface; and 2) the rate of displacement at the inclinometers decreased significantly since borings drilled in October 2009 near the banks of the Clyde River encountered and apparently provided some relief of artesian water pressures. The deep-seated base of the slide mass indicates the scale of the slide mass geometry that should be considered to understand existing stability conditions and evaluate mitigation alternatives. Correlations between slope movements, precipitation/snowmelt and relief of artesian pressures beneath a portion of the slide mass provide a clear indication of the significant influence that hydrogeologic conditions have on slope movements.

EXISTING CONDITIONS

Geology

Late Pleistocene (Wisconsin) glaciation (14 to 24 thousand years ago) modified all of New England. The continental glaciation formed north of New England and advanced to the south. As the glaciers advanced, some of the material picked up by the glaciers was deposited directly on bedrock surfaces at the base of the glacier as dense, relatively fine-grained glacial till (lodgement till). In most areas, when the glacial front retreated to the north, the soil and boulder-sized particles carried in the body and on the surface of the glacier formed a new mantle of less

dense glacial till (ablation till) deposited directly on the lodgement till or exposed bedrock surfaces. Meltwater streams removed the glacial till and further modified the landscape, forming well sorted (poorly graded) deposits of silts, sands and gravels in the river valleys and other fluvial environments.

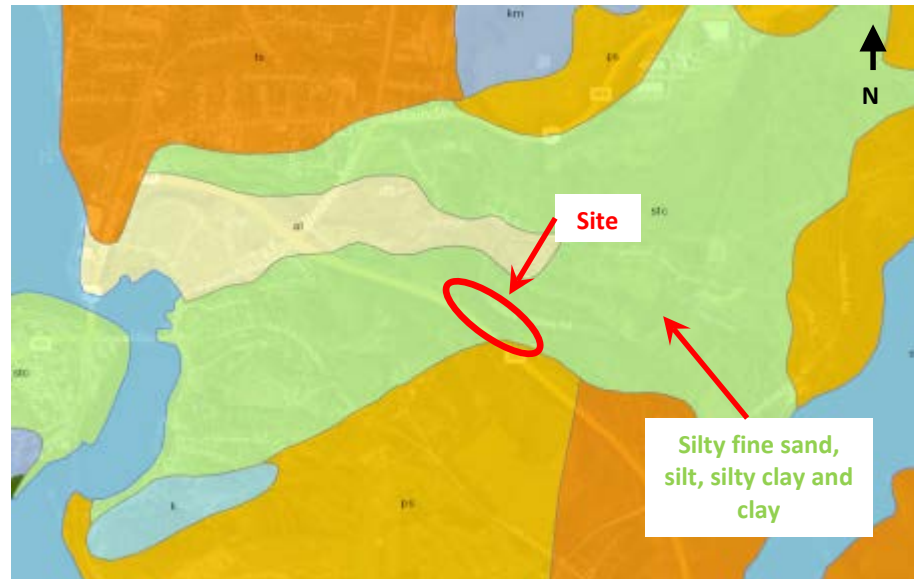


Figure 2 - Surficial geologic map.

In areas such as northeast Vermont, glacial lakes dammed by ice-contact deposits formed in some topographically low areas, including the Lake Memphremagog basin. These lakes deposited sediments consisting of clays, silts, and fine sands on the slopes of submerged regional hillsides (Figure 2). In some areas, the till materials may have been eroded during glacial retreat and prior to glaciolacustrine sedimentation, especially in topographically steep areas. As floating ice melted in the lakes, cobbles and boulders contained in the ice were also deposited within these fine-grained sediments as dropstones. Regional mapping indicates the project area is covered by silt, silty clay and clay from glacial Lake Memphremagog, deposited during a late stage of the lake when the lake shore was just above the site elevation (Stewart and MacClintock, 1969; Doll, Stewart and MacClintock, 1970).

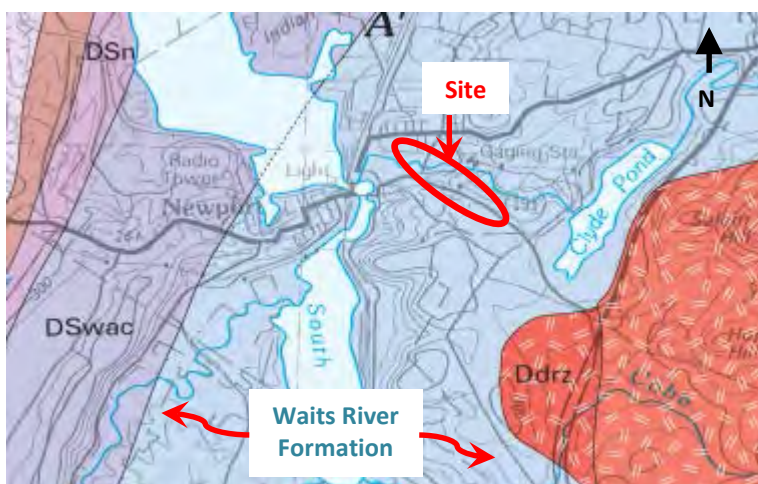


Figure 3 - Bedrock geologic map.

The project area lies within the Carbonaceous Phyllite and Limestone member of the Lower Devonian and Upper Silurian Waits River Formation (Ratcliffe et al., 2011), previously mapped as the Silurian-aged Barton River Formation (Doll, 1951) (Figure 3). The lithology of this member consists of a dark-gray to silvery-gray, lustrous, carbonaceous muscovite-biotite-quartz (\pm garnet) phyllite containing abundant beds of punky-brown-weathering, dark-bluish-gray micaceous quartz-rich limestone in beds ranging from about 1 ft to 30 ft thick.

Project Description

From 1969 to 1971 VTrans constructed the Route 191 connector roadway between Interstate 91 and Newport. In the early stages of construction an embankment fill was placed on the side of a 2.5 horizontal to 1 vertical (2.5H:1V) slope at the approximate location shown on Figure 1. The fill embankment was approximately 1,000 feet (ft) long and up to roughly 35 ft thick. Subsurface conditions underlying the fill embankment generally include about 170 ft of glaciolacustrine deposits of silty sands layered with at least two distinct clay strata overlying bedrock.

Shortly after construction was completed in 1971, embankment settlement was observed, and an underdrain was placed along the uphill side of the fill to collect and discharge surface water. Continued road settlements led to the installation of horizontal drains at the toe of a portion the embankment fill in 1973. From 1973 to 1989 road settlements (and pavement shimming) continued at an average rate of about 3 to 4 inches per year. Based on further VTrans investigations and evaluations, a stabilizing berm (i.e., a “counterberm”; Figure 4) and additional horizontal drains were constructed in 1991 at the toe of the embankment fill slope to stabilize slope movements and reduce or stop road settlements.

Over the subsequent 15 year period (1991 to 2006) road settlements (and pavement shimming) continued to occur (Figure 5). VTrans estimated that by 2006 the aggregate road settlement since original construction was about 8 ft. From 2006 to 2009 VTrans conducted further site investigations and installed instrumentation to monitor and assess the movements of a larger potential slide mass than had previously been considered. Inclinometer data from this period indicated the base of the slide mass was located up to



Figure 4 - Counterbalance berm (“counterberm”) installed in 1991 (March 23, 2012).



Figure 5 - View to northwest showing pavement shims at headscarp crossing of roadway. Note depression in roadway and stressed guardrail (October 31, 2006).



Figure 6 - Inclinometer near landslide toe installed in 1989 with artesian groundwater flow through pressure relief tube (~800 mL/min) (March 22, 2012).

about 120 ft below ground surface and possibly extended laterally to the Clyde River at the base of the valley roughly 600 ft north of Route 191. During the installation of two inclinometers adjacent to the Clyde River in late 2009, significant artesian water pressures were encountered in confined sand layers underlying the site producing heads above ground surface of at least 11 ft as measured during drilling (Figure 6). The reduction of artesian pressures at the inclinometer boreholes resulted in lower hydraulic heads in monitoring wells near the roadway indicating hydraulic connectivity across the site. Deep seated slope movements have slowed since 2009 when the artesian pressures were relieved at the two inclinometer boreholes.

Project History

A chronology of key events is listed below (A-Baki and Batchelder-Adams, 1989; Allen and Benda, 2011; CEA, 2011). Refer to Figure 2 for locations of referenced information.

Date	Event Description
1969-1971	Original embankment construction
1971	April: first sign of slope movement; 5 inches of separation at 30-inch diameter culvert traversing beneath roadway within embankment fill. June: installed underdrain system at toe of upslope embankment slope.
1973	Installed 17 horizontal drains
1974	1.5 ft of settlement measured since 1971 construction (average of 6 in/yr).
1971-1976	Roadway pavement settlements average 4 inches per year
1986	Operations removed 4 ft of pavement (average = 3.2 in/yr for 15 year period 1971-1986).
1989	VTrans subsurface investigation, evaluation and report ² . Failure surface identified about 10 to 25 ft below original ground surface beneath embankment fill.
1991	Counter berm construction and more horizontal drains added.
1996	Sinkhole developed at 30-inch diameter culvert due to 8 ft of vertical separation. Culvert was replaced.

1996-2011	Numerous pavement leveling operations. Culvert location still experiencing significant deformation.
2006-2009	VTrans subsurface investigations including additional borings, instrumentation, laboratory testing and a culvert inspection survey. Culvert deformation measured at about 8 inches.
2006-2011	Inclinometer data indicates base of slide mass located up to 120 ft below ground surface (bgs) at counterbalancing berm and extends to base of slope near Clyde River
2011	VTrans evaluations of stability and mitigation alternatives presented at ASCE conference ³ . Groundwater lowering identified as preferred mitigation alternative
2012	Inspection of 30-inch diameter culvert indicates additional deformation.
2013-2014	Focused geologic, hydrogeologic and geotechnical subsurface investigation, detailed geotechnical laboratory testing program, and installation of automated instrumentation system with web based data management.
2014-2015	Mitigation alternatives evaluation and final design

Explorations Prior to 2013

VTrans completed subsurface explorations in 1966 prior to embankment construction and during three periods after construction: 1971 to 1974, 1989, and 2006 to 2009. During the third investigation, VTrans installed instrumentation to monitor and assess movement of a larger potential slide mass than had previously been considered. Inclinometer data from this period indicate the base of the slide mass is located up to about 120 ft below ground surface and probably extends laterally to the Clyde River at the base of the valley roughly 600 ft north of Route 191. During installation of two inclinometers down slope and adjacent to the Clyde River in late 2009, significant artesian water pressures (greater than 11 feet above ground surface) were encountered in confined sand layers at depth. To seal the inclinometer casing with grout under artesian conditions, makeshift pressure relief tubes were installed to bleed off pressure. Subsequent measurements of lower hydraulic heads in monitoring wells near the roadway (1 to 2 ft) indicate some hydraulic connectivity across the site. The relief of artesian pressures at the down slope inclinometers resulted in lower hydraulic heads in monitoring wells near the roadway (1 to 2 ft), indicating some hydraulic connectivity across the site.

The site instrumentation in place prior to 2013 included manual inclinometers and standpipe piezometers, both of which required traveling to the site to collect data. To collect and analyze site data more efficiently, VTrans requested the installation of automated instrumentation systems that can be read remotely – to both limit the need to travel to site and to continuously monitor the slope and provide notification if displacements accelerate or exceed a critical threshold. Some of the pre-2013 inclinometer casings approached total displacements large enough to prevent an inclinometer probe from passing through the zone of deformation or have little remaining deformation capability, rendering them incapable of accommodating long term deformations during ongoing monitoring. These inclinometer casings were abandoned and/or replaced during the 2013 field program.

STABILITY ANALYSES COMPLETED PRIOR TO THE 2013 INVESTIGATION

1989 Analyses

Evaluations of slope stability completed in 1989 (A-Baki S. and Batchelder-Adams, 1989) used existing ground surface topography and interpreted subsurface conditions in a slope stability model, and soil strength parameters were varied until a factor of safety (FS) of about 1.0 was obtained. The resulting slip surface configuration and soil strengths were compared to instrumentation/ laboratory data to assess reasonableness, and the model was then used to assess mitigation alternatives. The initial stability analysis indicated that, based on a localized failure surface assumed to be located about 10 ft below the original ground surface underlying the embankment fill, a friction angle of 18 degrees was determined for the upper layer of “loose to medium dense gravelly silty glacial till.” The size of the counterberm constructed in 1991 was based on this analysis.

2011 Analyses

Stability analyses completed in 2011 (Allen and Benda, 2011) reviewed the stability of three cross sections oriented perpendicular to Route 191. Non-circular slip surfaces were analyzed and correlated to the depths where lateral displacements were measured by the inclinometers for the large slide mass extending from Route 191 to the Clyde River. The critical slip surface identified for each section was located predominantly through the lower very stiff to hard clay layer with an assigned residual friction angle of 12.8 to 13.8 degrees. Movement direction was suspected to be roughly perpendicular to the roadway, i.e., to the northeast. Groundwater pressures were assumed to be hydrostatic based on a ground water surface located approximately at the ground surface (pre-fill). This model was used to evaluate mitigation alternatives that would increase the long term FS to 1.3 or greater. The only alternative found to meet these criteria required permanently lowering the groundwater table to 75 ft below the Route 191 alignment.

2012 Analyses

The 2012 analysis was similar to previous analyses in that a back-analysis was conducted to develop a model simulating soil strength parameters that result in a FS of 1.0 (Figure 7). The model was then used to evaluate remedial measures to improve the FS for long term stability, including lowering the groundwater elevation (Figure 8). The analysis varied from the initial studies due to differences in the orientation, interpreted soil profile, soil strengths and groundwater pressures. Review of inclinometer data indicated that the slide is moving in a north-northeasterly direction towards the bend in the river, possibly following the trough of a bedrock surface depression. Due to the long term nature of the movements this subsequent analysis concluded that drained residual strength parameters were appropriate to assess existing conditions. Analyses were conducted using the 2-dimensional Slide software package (RocScience Inc., 2015).

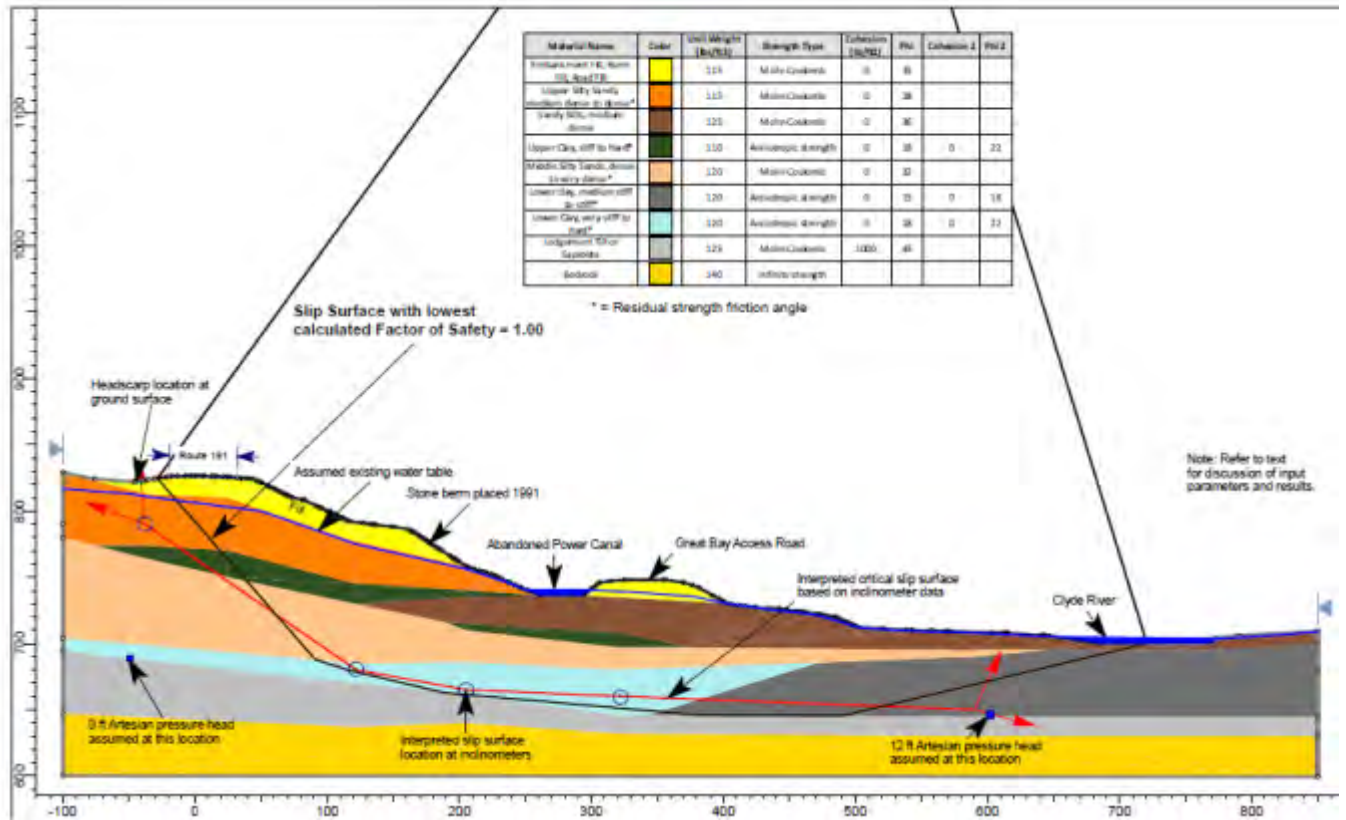


Figure 7 – 2012 stability analysis of ambient groundwater conditions.

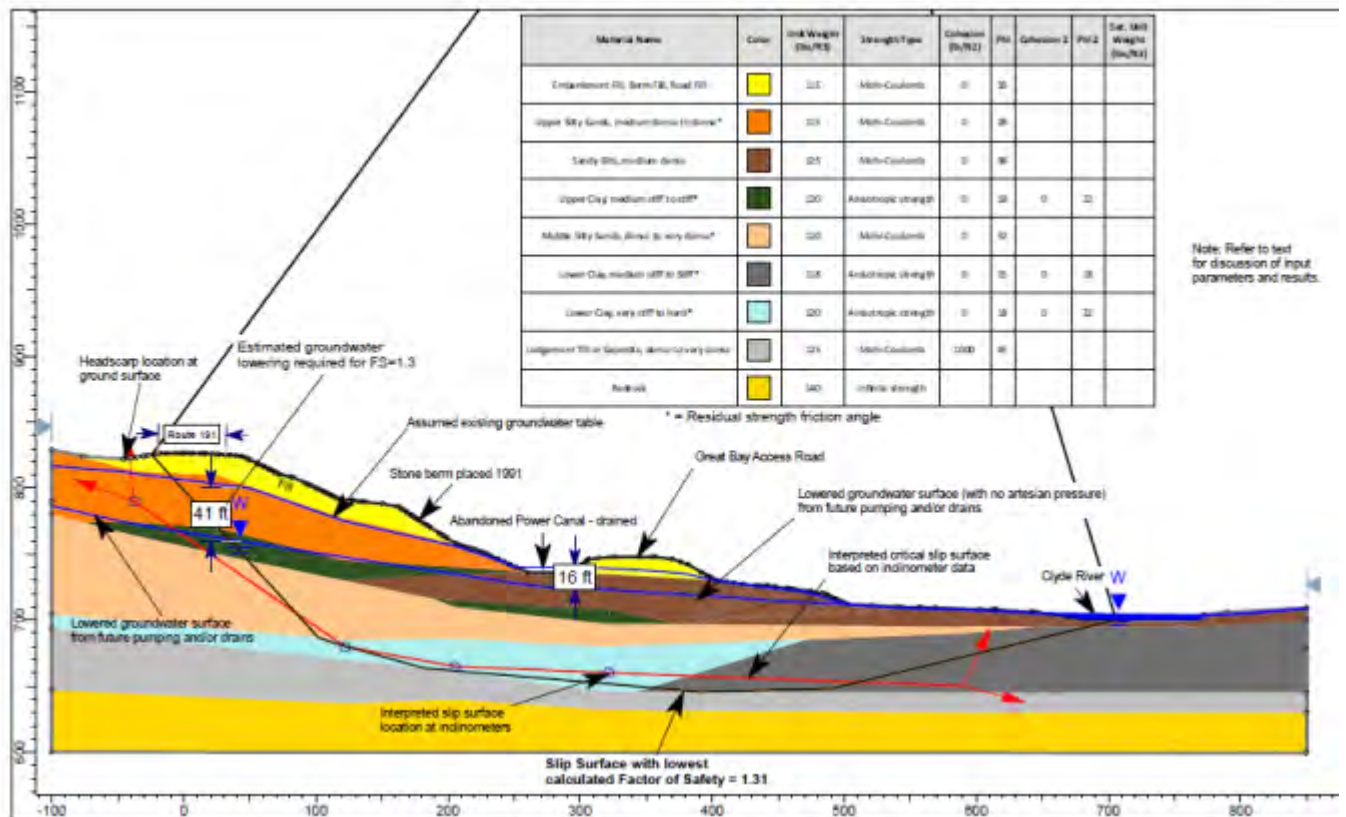


Figure 8 – 2012 stability analysis of lowered groundwater levels.

2013 INVESTIGATION

In summer 2013 VTrans completed a site investigation program using both sonic and drive and wash drilling methods. The program included soil and rock sampling, in-situ testing, installation of an automated instrumentation system, and a field pumping test. A site investigation location map, including the cross section parallel to inferred slide movement is presented in Figure 9.

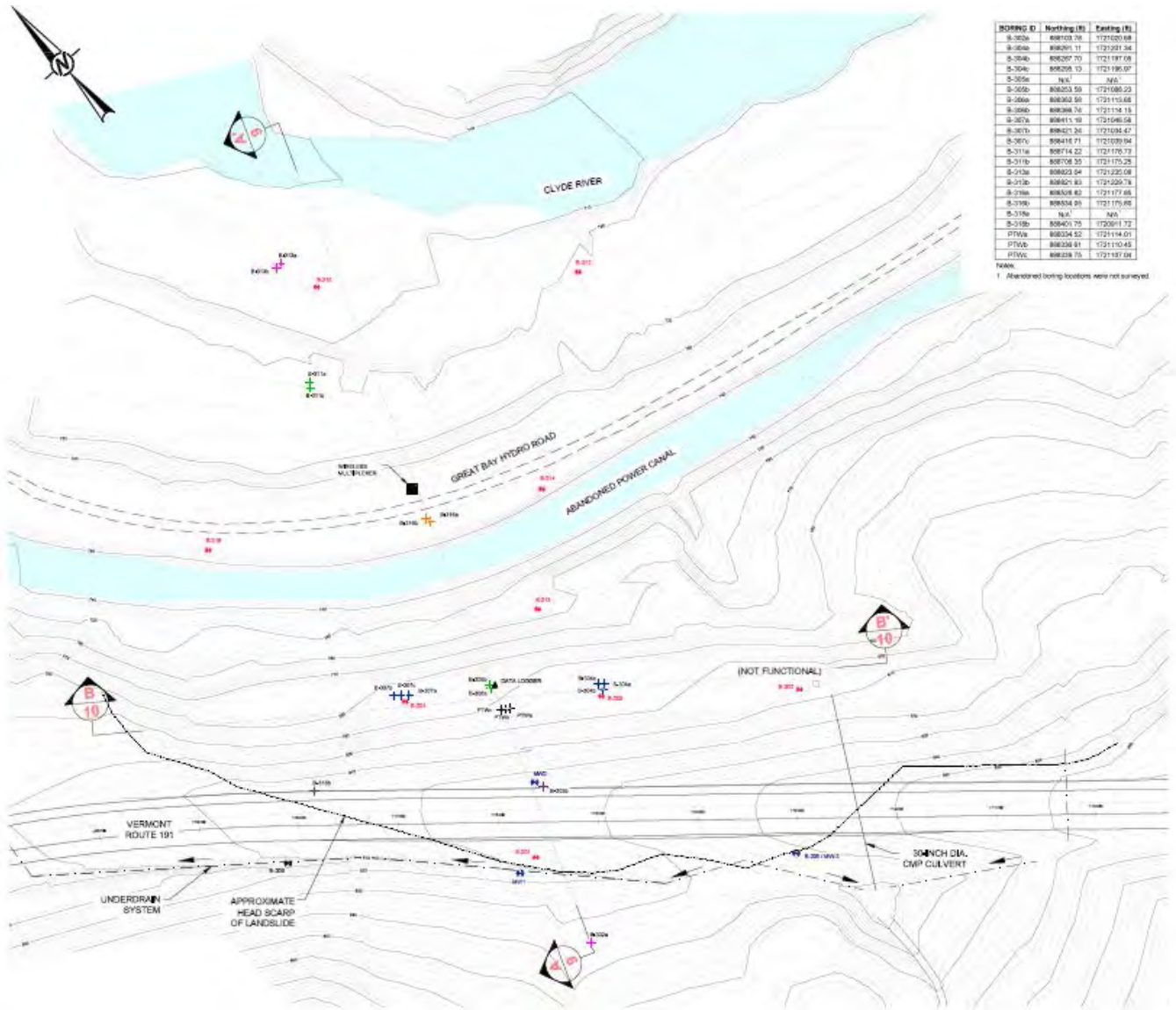


Figure 9 – Site investigation map.

Sonic Geotechnical Drilling

Between June 3 and June 21, 2013 Boart Longyear Environmental and Infrastructure of Little Falls, Minnesota (now Cascade Drilling L.P.), completed 12 borings to depths ranging from 36 to 176 ft below ground surface (bgs) using a Boart Longyear 600T track mounted sonic drill rig (Figure 10). Eight of the borings were advanced to bedrock and included 5 ft of advancement into bedrock and recovery of disturbed rock core. The remaining four borings were advanced to a predetermined depth solely to install monitoring wells. All boreholes were advanced with a 4-inch diameter core barrel and a 6-inch diameter override casing using sonic methods. In general, the core barrel was advanced



Figure 10 - Drilling test borings on the counter berm using a track-mounted sonic drilling rig (June 2013).



Figure 11 - Logging sonic drill continuous core samples of the overburden (June 2013).

dry to a depth of 5 to 20 ft below the bottom of the hole, and then the 6-inch override casing was advanced to the bottom of the core barrel using water to flush the annulus between the casing and core barrel. The core barrel was then withdrawn and the soil core vibrated out using the sonic head into roughly 5 foot lengths of soil bagged in a plastic sleeve (Figure 11). The core barrel was then advanced further into the hole. The core barrel was typically advanced dry to preserve the structure of the soil, however water was used in some boreholes to preserve bedrock core that generally disintegrates into a powder when drilling without water. Continuous disturbed soil samples were logged for the entire depth of each borehole and representative samples were collected from each borehole for index testing. Standard Penetration Test (SPT) using standard tooling was employed for the conventionally drilled borings.

At four test boring locations a greater borehole diameter was required to accommodate instrumentation or the well casing being installed. To achieve this, once the 6-inch casing had reached final depth, an 8-inch diameter override casing was advanced around the 6-inch casing using water to flush the annulus between the 8-inch casing and 6-inch casing. After the 8-inch override casing was advanced to the desired depth the 6-inch casing was fully removed and the instrumentation or well casing was installed.

Drilling rates for the sonic borings were notably higher than conventional drilling. One sonic boring was completed with 6-inch casing to 176 ft in approximately 10 rig hours. The sonic drill was able to complete the full scope of their work in 15 days on site for an average rate of about 92 ft per day. This average rate included 1,388 ft of drilling, well and inclinometer

casing installation, well development of the three pumping test wells, moves between holes, limited brush clearing, and relocation of the drill rig and support equipment from the upper part of site down to the lower portion of the site below the abandoned power canal.

Conventional Geotechnical Drilling

Between June 10 and July 25, 2013, New Hampshire Boring of Londonderry, New Hampshire completed 10 borings to depths ranging from 40 to 183 ft bgs using rubber-tired ATV and track mounted drill rigs (Figure 12). Most of the borings were started with 4-inch diameter (HW) casing, generally driven to 10 to 60 ft bgs into very dense soil and then completed with an open hole below using drilling mud when advancing below the bottom of the casing. SPT sampling was generally conducted at 5-foot intervals except when targeting specific layers, where the sample interval was decreased at the discretion of the field engineer/geologist. Samples were generally collected using a 2 inch diameter split spoon sampler with a rope and cathead pulley system in accordance with ASTM D1586. For encountered conditions where the 2 inch split spoon had low recovery, a 3 inch diameter split spoon sampler was used to improve sample recovery. Twelve undisturbed Shelby tube samples were collected following ASTM D1587 methods.



Figure 12 - Drilling conventional geotechnical borings on shoulder of roadway (June 2013).

Multiple in-situ vane shear tests were attempted in deposits where cohesive soils were encountered. No vane tests were completed because the very stiff and varved deposits encountered prevented the vane from being advanced by hand to the test depth.

Test Well Installation

To conduct pumping and slug tests, eight 2-inch diameter PVC observation wells and three 4-inch diameter PVC pumping wells were installed at various locations. Vibrating wire piezometers were later installed into two of the wells and connected to the automated instrumentation system for long-term ground water monitoring.

Instrumentation Installation

A remotely-accessible automated instrumentation system was installed to monitor slope movement and groundwater conditions. The system includes:



Figure 13 - Installation of inclinometer casing with sonic rig (June 2013).

- Two ShapeAccelArray inclinometer arrays (SAAs) manufactured by Measurand, Inc. of Fredericton, New Brunswick, Canada;
- Two In-Place-Inclinometer (IPI) arrays;
- Seventeen Vibrating-Wire (VW) piezometers;
- One VW barometer;
- A tipping bucket rain gauge; and
- Two CR1000-based dataloggers manufactured by Campbell Scientific Inc. of Logan Utah.

With the exception of the two SAAs and their interface boards, the instrumentation system components were supplied by Geokon, Inc. of Lebanon, New Hampshire.



Figure 14 - Installation of SSA inclinometer (June 2013).

Inclinometers

During the field program, both drilling subcontractors completed borings that were used for the instrumentation program (Figure 13). In four of the borings, 3.34-inch outside-diameter ABS plastic inclinometer casing supplied by Geokon was installed 5 ft into bedrock and grouted in place using the same grout mix design used for the piezometers and monitoring wells. Two inclinometer casings contain In-Place-Inclinometer arrays to automatically monitor slope movement. The other two inclinometer casings are reserved for traditional manual inclinometer measurements on a periodic basis to assess slope movements. One-inch gray Schedule 40 PVC electrical conduit was used as casing for the two SAA inclinometers (Figure 14).

Piezometers

Vibrating-wire piezometers were installed in seven borings. All of the piezometers were attached to the outside of inclinometer casing, SAA casing, or a sacrificial PVC grout tube, so that the piezometer could be placed at the specified depth. The borehole was then completely grouted from bottom to top at one time using the same grout mix design as the inclinometers and monitoring wells. One piezometer each was lowered to the bottom of two monitoring wells. Piezometer installation depths were identified during the field program based on the continuous soil cores logged in the sonic borings. Generally the piezometers were located in predominantly sandy zones and an effort was made to install the deepest piezometer in the lower sand and gravel layer above the bedrock surface. One deep piezometer was placed in a one-foot zone where the driller observed high groundwater pressures while drilling. To help identify whether multiple aquifers exist, all of the piezometers were installed in a multi-level configuration where they are separated in elevation by intermediate silt and clay layers. Use of fully grouted boreholes without sand packs around the piezometers was intended to prevent communication between instruments in the same borehole.

Dataloggers, Multiplexer, Automated Data Retrieval Equipment and Signal Cable

To provide remote monitoring capability the 2013 site investigation included installation of a solar powered remote monitoring system, utilizing cellular communication (Figure 15). Shallow cable trenches were excavated between the boring locations and a datalogger for locations south of the abandoned power canal and between the borings and a wireless multiplexer on the north side of the canal. Communication cables for the instruments were directly buried in the trenches and backfilled. To cross Route 191 with a communication cable, VTrans cut into the asphalt and installed a 1.5 inch electrical conduit across the road prior to the start of the field program. The top of each instrumented boring was fitted with a lightning protection board or terminal board in a weatherproof enclosure that allows the various separate instrument cables to be combined into a larger multipair cable that is run to the datalogger or wireless multiplexer. This also allowed the trenching and installation of the communication cables to be performed prior to completion of the borings and before the removable instruments (SAAs and IPIs) were installed.



Figure 15 - Remote data collection and cellular communication system with solar panel power source.

The datalogger and the wireless multiplexer were mounted to plywood panels supported by pressure-treated wood posts set into the ground. After installing the plywood panels, 2-inch galvanized steel pipe was attached to one of the posts at the main datalogger and at the wireless multiplexer to support radio modem antennas and solar panels. A copper-clad grounding rod was installed at all boring locations and at the main datalogger and wireless multiplexer for grounding the installed lightning protection.

Initial Setup

After completion of the drilling program and instrumentation installation, Geokon's Data Acquisition Systems group provided internal training and to help complete the wiring of the instruments into the dataloggers and multiplexers. Once the wiring was finished, the dataloggers were turned on and all the instruments were confirmed to be working correctly. The main datalogger that reads all of the vibrating wire instruments, the barometer, and the rain gauge, was set to a 2 hour reading cycle. The second datalogger, which reads only the two SAA inclinometers, was set to a 6 hour reading cycle

Geotechnical Laboratory Testing

Geotechnical laboratory tests were performed on soil samples collected during the subsurface investigation to assist in soil classification and establish relevant engineering



Figure 16 - Clay and silt varves exposed in sonic core sample.

properties for design (Figure 16). The testing was conducted by VTrans at their Materials and Research Laboratory in Berlin, Vermont, and by Dr. Don J. DeGroot, Sc.D, P.E., at his soil testing laboratory at the University of Massachusetts Amherst. Shelby tubes were also X-Rayed by GeoTesting Express of Acton, Massachusetts prior to being testing by Dr. DeGroot or VTrans. Laboratory work was generally performed in accordance with applicable American Association of State Highway and Transportation Officials (AASHTO) and American Society for Testing Materials (ASTM) testing procedures. The testing performed for the investigation is summarized in Table 1 below.

Table 1 - Geotechnical Testing Summary of 2013 Site Investigation

Soil Laboratory Test	Testing Procedure	Number of Tests
Grain Size Analysis sieve only	AASHTO T88, ASTM D422	52
Grain Size Analysis including Hydrometer	AASHTO T88, ASTM D422	37
Natural Moisture Content	AASHTO T265, ASTM D2216	53
Atterberg Limits	AASHTO T89 & T90, ASTM D4318	64
X-Ray	ASTM D4452 (no AASHTO test)	12
Constant Rate of Strain with unload/reload cycle	ASTM D4186 (no AASHTO test)	2
Direct Shear with residual strength	AASHTO T236, ASTM D3080	17
Hydraulic Conductivity – Flexible Wall	ASTM D5084 (no AASHTO)	12
Hydraulic Conductivity – Rigid Wall	ASTM D5856 (no AASHTO)	7

OVERBURDEN, BEDROCK AND GROUNDWATER CONDITIONS

Overburden Conditions

Overburden materials encountered in the test borings include a complex stratigraphy of fills and glaciolacustrine deposits consisting of interbedded silts, fine sands, sands and gravels, silty clays and clays. Total soil thickness is interpreted to vary from roughly 172 ft at Route 191 to about 78 ft at the Clyde River. Dropstones, consisting of ice-rafted cobbles and boulders, occur within all natural units, and are ubiquitous in the wooded surface areas of the slide not affected by roadway and development construction activities. The boulders observed on the surface are up to 6 ft or more in longest dimension.

Figure 17 presents our interpreted soil profile along a southwest to northeast section through the axis of the interpreted slide mass, parallel to our estimated direction of slide movement based on inclinometer data. The 2013 site investigation provided refinement to the site geologic/geotechnical model, including more layers and different orientations and thicknesses of major soil units.

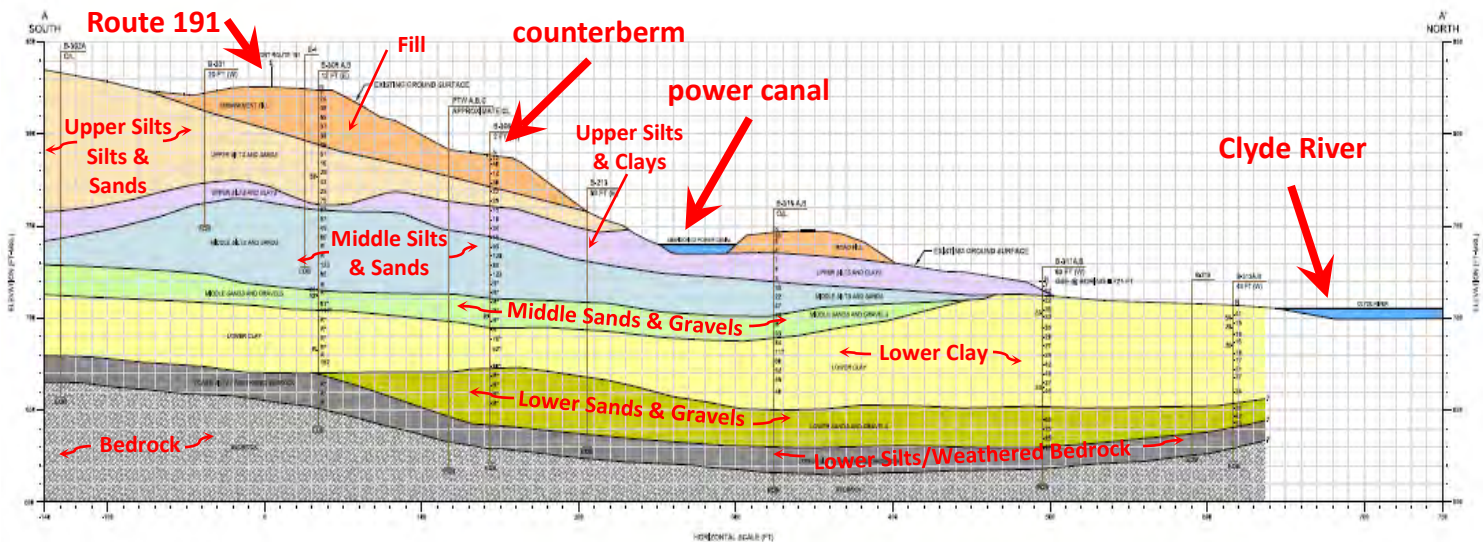


Figure 17 - Cross section parallel to landslide movement showing complex glacial geology.

Changes in soil types were generally gradual and tended to grade into and out of coarser material, consistent with glaciolacustrine and fluvial deposits. The encountered soils were grouped into distinguishable subsurface layers taking into account geological origin and engineering behavior; not all soils were encountered in all of the borings. The stratigraphic units encountered are described below in descending order.

- Fill:** Embankment fill was encountered in the borings advanced under Route 191, located on the stability berm, and next to the Great Bay Hydro Road. The fill material was observed to be reworked native material, probably from the roadway cuts immediately uphill and downhill of the site along Route 191. The fill is generally described as gray brown to dark gray brown, moist to wet, loose to dense, fine to coarse sand, some to trace silt, little to trace gravel, with layers of silt throughout (AASHTO: A-1-b to A-2-4 to A-4, USCS: SM).
- Upper Silts and Sands:** Starting at the ground surface, or at original grade in boring locations with embankment fill, a layer of gray brown to dark brown, moist, medium dense to dense, layered fine to medium sand, fine sand, and silt, with trace fine gravel and coarse sand throughout exists (AASHTO: A-2-4 to A-4, USCS: SM to ML). Total thickness of this layer ranges from 10 to 75 ft. This layer terminates at a point above the abandoned power canal.
- Upper Silts and Clays:** Below the upper silts and sands a potentially continuous layer of stiff to hard, low plasticity varved silty clay exists (AASHTO: A-6 to A-7-6, USCS: CL), ranging in thickness from 3 to 15 ft and extending from uphill above the roadway and terminating downhill.
- Middle Silts and Sands:** Underlying the upper silts and clays a layer of gray, dry to moist, very dense, layered silt, silty fine to medium sand, and clayey silt, with little to trace rounded gravel throughout exists (AASHTO: A-4, USCS: SM to ML). Occasional layers of dark gray,

fine to medium sand were also encountered in this stratigraphy. Total thickness ranges from 15 to 40 ft before tapering off near the canal.

- **Middle Sands and Gravels:** Below the middle silts and sands a separate layer of medium brown and orange brown, moist, very dense, silts, some fine sand, and some gravel, with pockets of gray, moist, very dense, fine to medium sand exists (AASHTO: A-1-b to A-2-4, USCS: SM). The thickness of this layer ranges from 10 to 15 ft before it also tapers off near the canal.
- **Lower Clay:** Underlying the middle silts, sands, and gravels a continuous layer of layered, dry to moist, very stiff to hard, generally high plasticity varved clayey silt and silty clay exists (AASHTO: A-6 to A-7-5 to A-7-6, USCS: MH, CH, and MH-CH). The orange brown and gray color of the layer changes to brown and gray towards the river. This lower clay layer was observed in all of the borings, ranging in thickness from 20 to over 60 ft. Zones of disturbance and slickensides were noted throughout (Figure 17). Folded varves and reworked zones were



Figure 17 - Folded varves exposed in sonic core.

observed in the sonic borings at the approximate depth of the failure surface identified in the historic inclinometers. In some borings, seams containing sand and gravel were encountered within the deposit. Varve thickness ranges from 0.1 to 2 inches. Zones of non-varved clay up to 5 ft thick were also encountered.

- **Lower Sands and Gravels:** Beneath the lower clay a layer of brown and gray, medium dense to very dense, fine to coarse sand, with some to little gravel and little silt (AASHTO: A-1-b to A-3, USCS: GM to SM) was encountered in all of the boring locations. Thickness of this layer ranges from 20 to 30 ft. Occasional cobbles were noted throughout.
- **Lower Silts and Weathered Bedrock:** Directly above the bedrock surface at all boring locations a layer of dark brown, moist to wet, dense, silts and silty fine sands exists (AASHTO: A-4, USCS: ML). The thickness of this layer is fairly consistent, ranging between 10 and 15 ft. Fractured and weathered bedrock was encountered along the bottom of the deposit immediately above intact bedrock.

The Lower Clay is a significant component of the geologic, hydrogeologic and geotechnical models of the slide. These sediments have high overconsolidation ratios (16 to 35), very stiff to hard, high plasticity silty clays ($N > 100$), and folded varves. One geologic interpretation of the origin of these sediments is deposition by a pre-Pleistocene glacial advance, and subsequent burial by the last ice sheet. Sonic cores indicate several previous slip planes/zones and minor faulting exist, defined by slickensides, folded varves and shear planes, indicating slumping or ice grounding deformed the sediments. Very thin, white partings in the core are not fine sand or coarse silt typical of the varves, but consist of highly plastic fine grained sediment with high liquid limit. When water is added, these partings feel “greasy,” indicating they may be smectite/montmorillonite layers of possible volcanic origin. The slip planes contributing to the current movement may occupy some of these historical failure features. The

observation of these deformation features would likely not have been possible without the use of the sonic drilling to obtain continuous, large diameter soil cores.

Bedrock Conditions

Bedrock was cored in all of the sonic borings to verify the top elevation of unweathered bedrock. Due to the nature of sonic drilling and the amount of disturbance that occurs to hard rock, the recovered bedrock core was not logged for discontinuity data. Bedrock was diamond-cored using an NQ sized rock core barrel in one boring using the conventional geotechnical drill rig. The core recovered is a medium dark to dark grey, very fine grained, fresh, strong to very strong, weakly foliated to massive, strongly calcareous, muscovite-quartz metalimestone, with trace pyrite. Discontinuities are mostly parallel with foliation, dipping 10-20 degrees and very close to moderately spaced. This lithology is consistent with the Waits River formation.

Saprolite was noted in one core log for an inclinometer boring conducted by VTrans in 1989. Saprolite, often called residual soil, is defined as soft, thoroughly decomposed rock formed in place by chemical weathering, and is characterized by preservation of structures present in the unweathered rock (e.g., bedding joints or foliation). The lower silt and weathered bedrock layer encountered in all of the 2013 borings is generally consistent with the presence of saprolite. The saprolite may have been developed from a parent interval that was highly susceptible to weathering. Saprolite is rare in New England as the multiple glacial advances typically removed the mantle of completely weathered rock; however pockets can be preserved in valleys and near the base of slopes where protection from the glacial fronts may have existed. As saprolite is generally clay rich, groundwater flow is generally restricted in saprolites.

Groundwater Conditions

Groundwater conditions as measured by the permanently installed piezometers indicate that groundwater appears to react quickly to heavy rainfall events (including the deep piezometers), although the rise in pore pressure is slight, generally less than 1 to 2 ft. The piezometer data indicate a noticeable downward gradient in water pressures exists on the uphill side of the abandoned power canal bisecting the site, and an upward gradient in water pressures at and below (north of) the canal. Artesian pressures, where the measured piezometric head elevation is above the ground surface, range from about 10 to 20 ft for the deep piezometers below the canal, and up to 24.4 ft above ground surface for the deep piezometers at the toe. The shallow piezometer at the toe of the slide appears to react to changes in the stage elevation of the Clyde River and has not exhibited artesian pressure to date. The piezometer pair adjacent to the power canal also shows a very strong upward gradient.

Conceptual Groundwater Model

The site conceptual hydrogeologic model is controlled by recharge areas, varying lithologies and regional discharge. Percolating precipitation becomes groundwater in recharge areas (i.e., the hill) southwest of Route 191, and moves generally to the northeast towards the abandoned power canal and the Clyde River through the relatively higher permeable layers within the Lower, Middle and Upper Silty Sand units (Figure 19). Precipitation is also collected

and stored by surficial soils, embankment fill and the counterberm, and during significant precipitation events, these units may act temporarily as run-off storage, and then slowly discharge to the underlying units.

Groundwater movement occurs predominantly in a primary porosity developed from the voids between sedimentary particles within bedding planes present within the overburden. Groundwater flow within the metamorphosed bedrock is secondary in nature, flowing within joints and bedding planes.

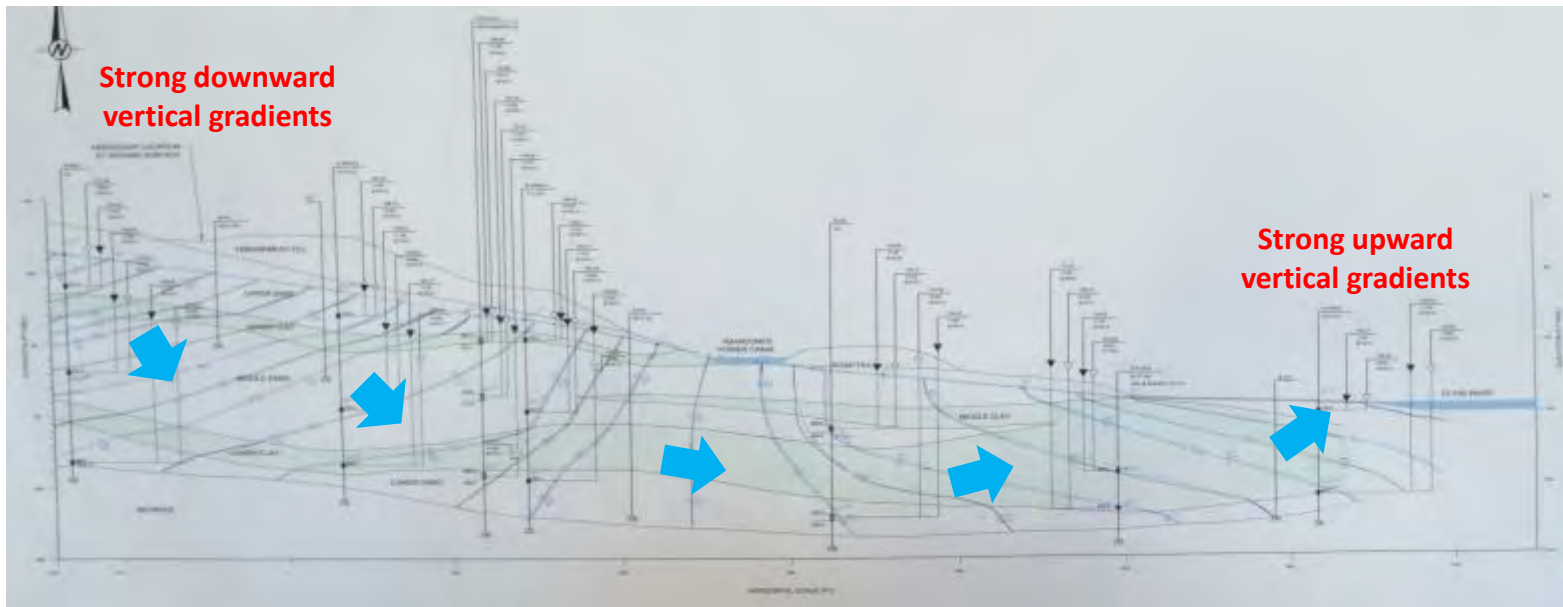


Figure 19 - Conceptual groundwater flownet along site cross section.

The Lower and Upper Clay units play an important role in groundwater flow. While these units appear to be discontinuous in some portions of the site, their thickness provides confining pressures beneath and downgradient of Route 191. Groundwater, originating as precipitation recharge southwest of Route 191, flows downward to the northeast, across the site, discharging to the Clyde River. The pressures within the Middle and Lower Silty Sands are higher than within the Upper Silty Sand, as measured by artesian conditions observed during installation of the inclinometers near the toe of the slide in 1989. This indicates an upward vertical gradient exists between the counterberm and the Clyde River. The 2013 piezometers in this area indicate artesian heads as much as 24.4 ft above the ground surface exist in this area (Figure 20). Shallower surface water, originating as precipitation, is trapped as perched groundwater on low hydraulic conductivity soils (clays and silts) within the upper soils, and is discharged as springs feeding small unnamed streams.

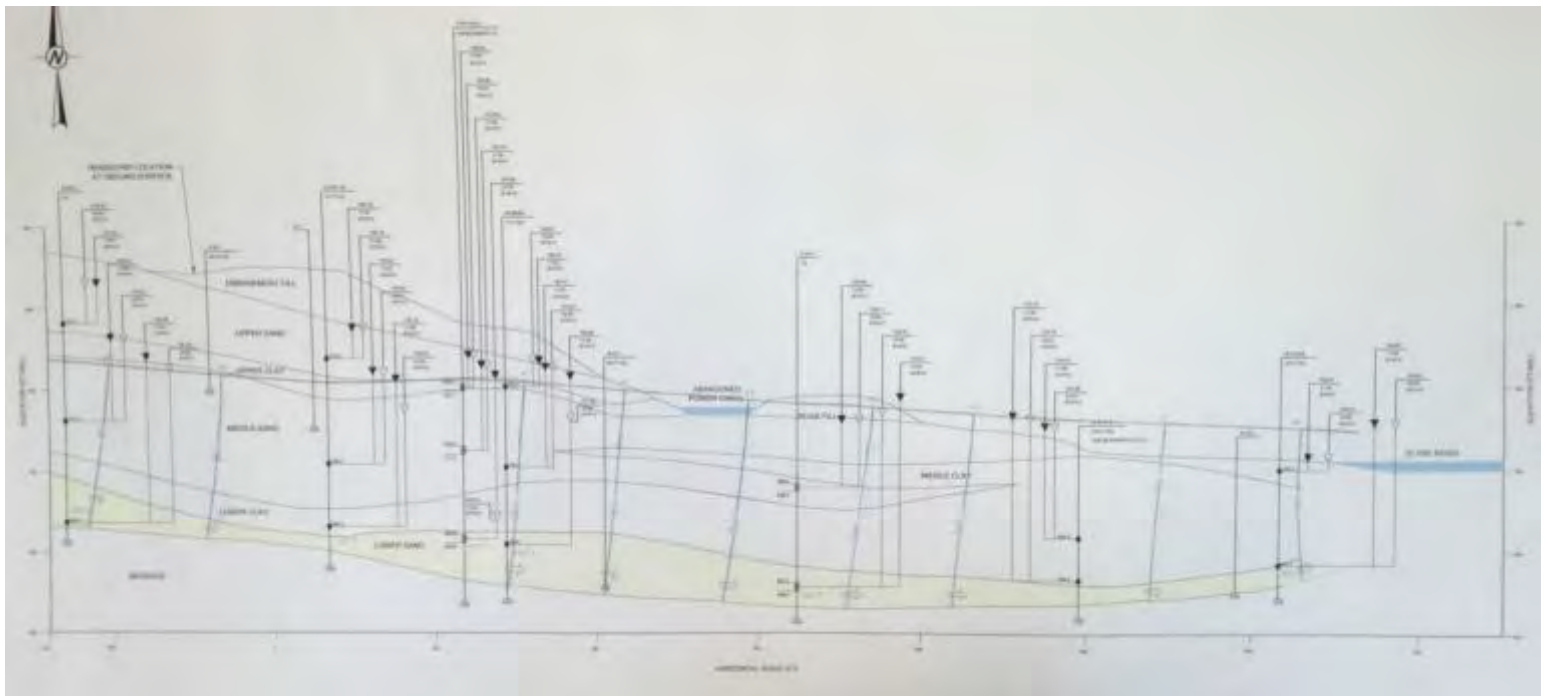


Figure 20 – Piezometric surface and groundwater flow net of Lower Sands and Gravels (yellow) under ambient conditions. Note artesian conditions exceeding 24.4 ft at toe.

The secondary porosity provided by the bedding and fracture systems control groundwater flow within the weathered and unweathered bedrock. Structurally, the bedrock strikes generally north, and dips to the east. Steeply inclined to near-vertical fractures and joints oriented west-east cut across these beds. The RQD for the weathered and unweathered bedrock range from 0 to 84 percent (average of 26 percent). However, due to the highly weathered nature of the bedrock, including development of saprolite, groundwater flow within the bedrock appears to be of minor importance.

Hydrogeologic Testing Results

The hydrogeologic field testing program indicated the sandy units have relatively low hydraulic conductivities, ranging from about $5E-03$ to $5E-05$ centimeters per second (cm/sec), with an average of about $5E-04$ cm/sec. The Lower Clayey Silt, which acts as a confining layer, has hydraulic conductivities ranging from $2E-05$ to $3E-09$ cm/sec. The testing also indicated the Lower Sands and Gravels are interconnected in varying degrees with the Middle Sands and Gravels, and to a lesser degree with the Upper Sands and Silts. The observations confirmed the excessive artesian head exhibited by the Lower Sands and Gravels exists in the lower/northern portion of the slide mass. The testing also indicated a reduction in vertical groundwater gradients occurs when pumping from the Lower Sands and Gravels, including a reduction in the artesian heads (Figure 21).

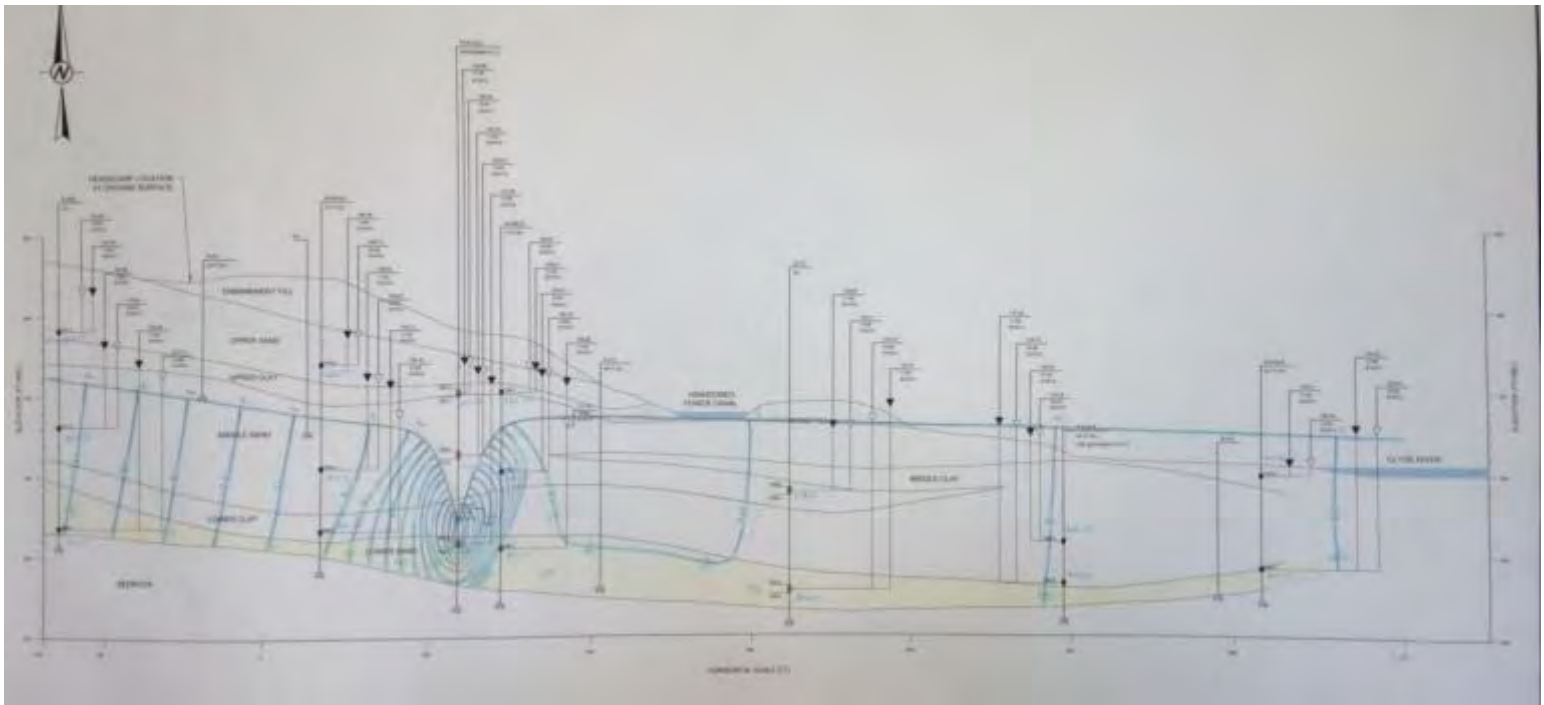


Figure 21 - Piezometric surface and flow net of lower sands and gravels unit (yellow) during pumping test showing cone of depression and reversal of local horizontal gradients.

The principal pumping test of the program included a 24-hour constant-rate pumping drawdown phase. The relatively short pumping test indicates the Lower Sands and Gravels initially behave as a confined aquifer during pumping. However, the late-time drawdown response suggests the aquifers within the slide mass may be best described as leaky confined. The 2013 borehole program verified that the Middle Silts and Sands and Upper Silts and Clays are discontinuous aquitards within the slide mass, which would confirm the leaky aquifer hypothesis.

Inclinometer Data

Typical inclinometer data (SSA and manual) are shown in Figure 22. The data collected since 2013 indicate landslide movement continues roughly at about 0.1 to 0.2 inches/year, similar to the reduced rate observed since installation of the inclinometers at the toe of the slide in 1989 which relieve artesian pressures. The data indicate that while the rate of landslide movement has slowed, movement continues, which if not mitigated, will require continued maintenance and eventual replacement of roadway infrastructure.

STABILITY AND GROUNDWATER MODEL UPDATES

To help evaluate landslide remedial design approaches, the data generated from the 2013 hydrogeologic investigation was used to construct a calibrated numerical groundwater model. The model was then used to evaluate passive/active groundwater removal scenarios (principally from the Lower Sands and Gravels), and to provide pore pressure distribution data for ambient groundwater conditions, and conditions generated by modeled remedial groundwater removal

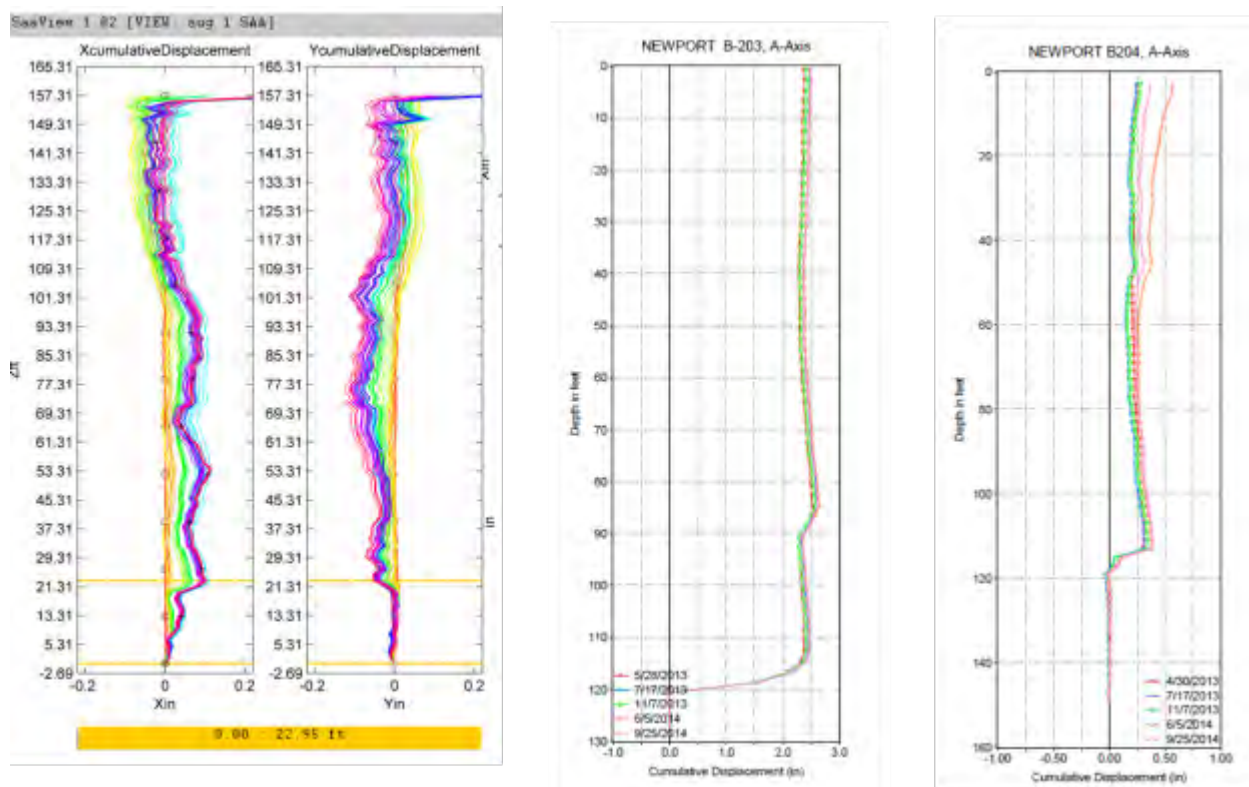


Figure 22 - SSA data (right) and manual inclinometer data (left) indicating slope movement between 0.1 and 0.2 inches/year since 2013.

systems. The pore pressure distributions were then used in slope stability models to evaluate the extent and magnitude of the effects that a lower groundwater pressure regime may have on the slide mass stability.

Stability Model Update Using 2013 Field Investigation Data

The site geologic model and the slope stability model were updated and refined using the data collected during the 2013 field exploration. Initial material properties were selected based on laboratory testing results and empirical correlations between SPT and friction angle. Clays were modeled using anisotropic drained properties, with the vertical friction angle approximately six degrees greater than the horizontal friction angle. Clay friction angles were selected using

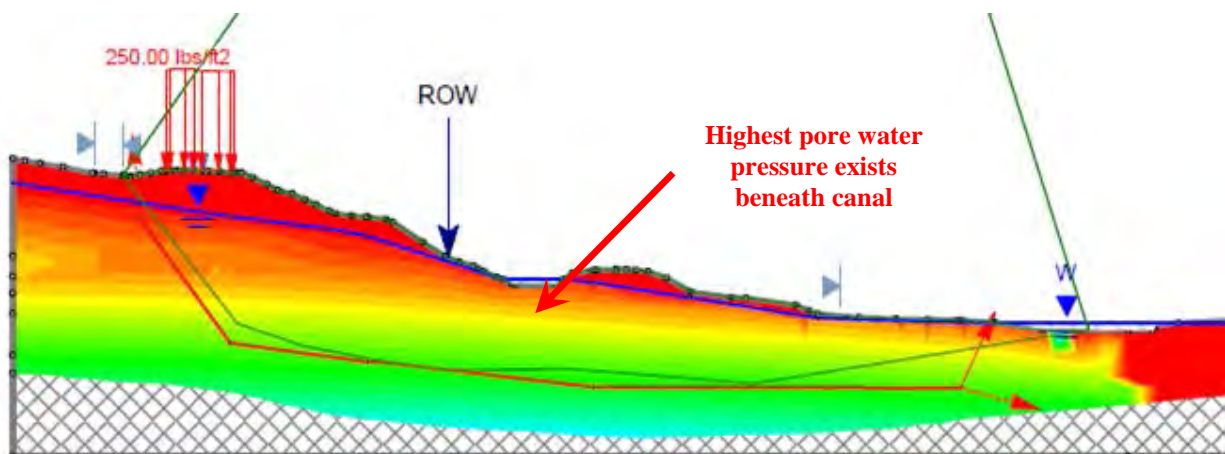


Figure 23 – Updated slope stability model of deep seated slide mass current conditions (FOS = 1.001).

the residual strength data from the extensive direct shear testing program based on the assumption that the movement of the slope to date has been sufficient to mobilize residual strengths. The lower clay layer was further divided into two units due to slightly lower strengths observed north of the abandoned power canal (the “downslope” lower clay). Granular soil layers were modeled using Mohr-Coloumb strength parameters assuming no cohesion. Once initial material properties were entered in the model, the “current” groundwater scenario was modeled and the soil properties of the lower clay unit were adjusted slightly to result in a FS of 1.001 (Figure 23). This stability model indicates the highest pore water pressure exists beneath the power canal.

The revised stability model was also used to model site conditions prior to installation of the toe inclinometers in 2009 which relieved artesian pressures in the Lower Sands and Gravels. The estimated FS for conditions prior to 2009 is 0.95, lower than the current FS. The faster movement of the landslide prior to 2009 reinforces the accuracy of the revised stability model.

Numerical Groundwater Model

The numerical groundwater model was completed using MODFLOW, published by the U.S. Geological Survey (Hill et al., 2000). This is a modular 3-dimensional finite-difference groundwater flow model that utilizes a numerical solution for the equations governing groundwater flow through porous media. The model geometry is defined by external and internal boundaries

(consisting of geologic and hydrogeologic features as well as hydraulic flow) and a grid of orthogonal blocks with a central node. The input parameters include the geologic layer thicknesses and extents, the hydraulic conductivities from the pumping test performed in 2013 and the laboratory testing, storage and porosity, and precipitation recharge measured from the on-site rain gauge. The 3-dimensional geologic modeling software platform EVS/MVS (C-Tech Development Corporation, 2014) was used to compile the geologic layer geometry for the MODFLOW model (Figure 24). Once the groundwater model was assembled, with the pre/post processor Groundwater Vistas (Environmental Solutions Inc., 2015), it was refined and calibrated to predict the “current” groundwater conditions measured on site shortly before the start of the pumping test in August 2013. Since the groundwater model is 3-dimensional, output of groundwater head pressures for use in the 2-dimensional slope stability model was accomplished using Arc GIS and an Excel spreadsheet to translate x, y, z, and head pressure from the groundwater model into x, y, and pore

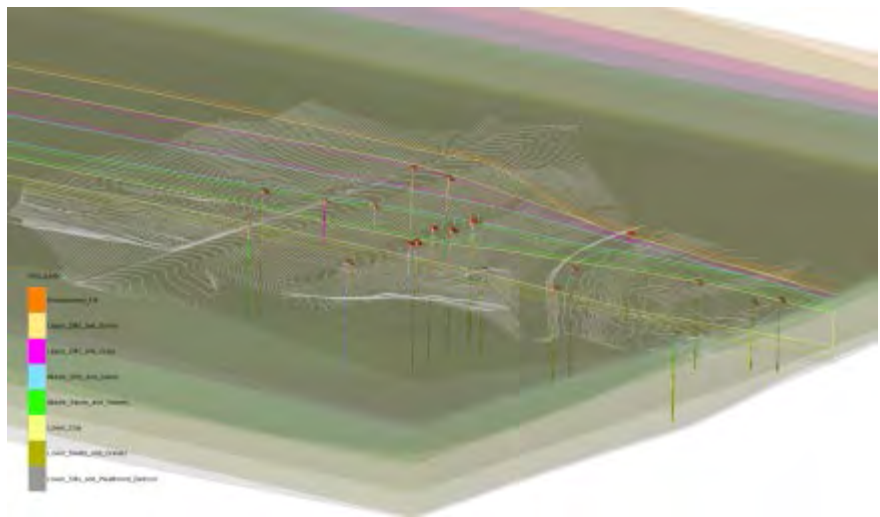


Figure 24 - Block diagram of EVS/MVS geologic model.

water pressure for use in the slope stability model. This translated data was then imported into the slope stability model using the pore water pressure grid function in Slide.

Mitigation Analyses

Using the groundwater model and the resulting groundwater pressures imported into the slope stability model, four stabilization alternatives that reduce groundwater levels were evaluated. Alternative A consists of twelve (12) passive artesian flowing wells near the river with an assumed groundwater flow of 1 gallon per minute (gpm) from each well. Alternative B replaced the twelve passive wells with three (3) active extraction wells near the river, with an assumed flow of 6 gpm each. The wells for Alternatives A and B are

assumed to be about 70 ft deep. Alternative C moved the three active wells up slope to the canal access road, and Alternative D further moved the three active wells up slope to the counter berm below Route 191, within the VTrans ROW. The depth of the wells for each alternative would need to be determined as part of final design for the system, but would increase from roughly 70 ft for Alternatives A and B, to roughly 105 ft for Alternative C, to roughly 130 ft for Alternative D. When evaluating these alternatives, only the groundwater pressures were adjusted; no changes to the topography or material properties were made. Stability analyses for these four scenarios indicated the FS ranged from 1.19 for Alternative A (12 passive wells at toe) to 1.37 for Alternative C (three active wells at the canal). All three of the active well alternatives have a higher FS than the passive well alternative, which is consistent with the ability of the active wells to decrease pressures below artesian pressure, as the passive wells of Alternative A can only reduce the water pressure to that equaling the local topographic head.

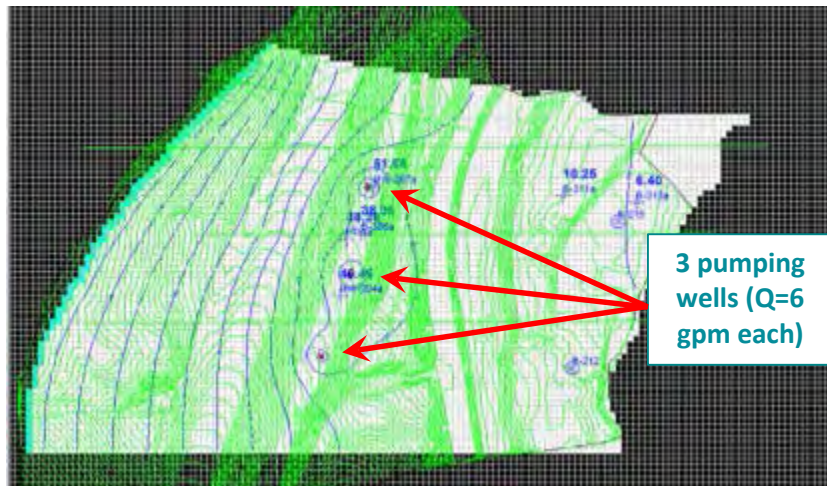


Figure 24 - Groundwater model simulating three extraction wells in lower sands and gravels on counterberm (Alternative D).

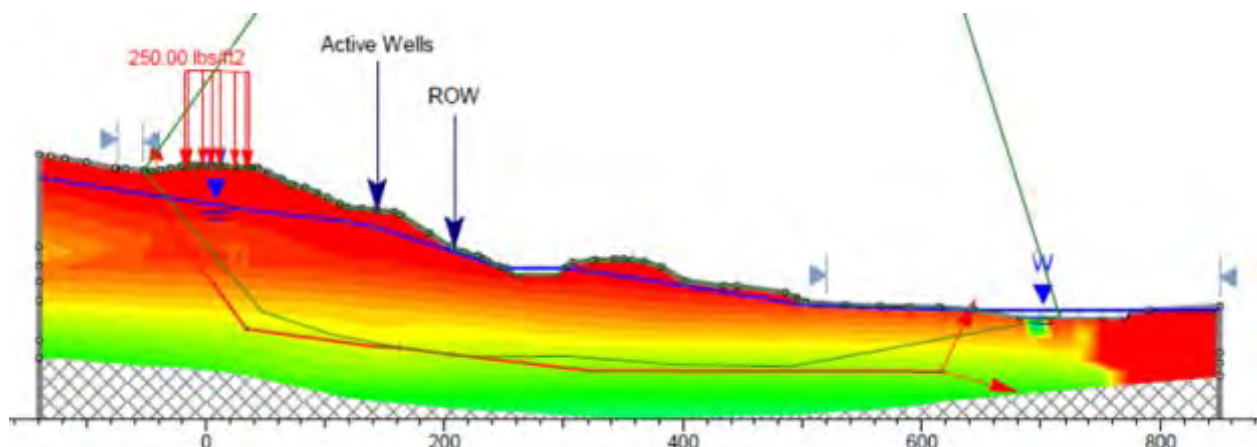


Figure 25 - Stability analysis simulating three pumping wells on the counterberm (Alternative D) (FS = 1.272).

Uncertainties with the groundwater extraction alternatives include groundwater quality and any need for treatment; environmental permitting for both construction and maintenance of the wells and discharge of the groundwater, where the groundwater will be discharged, property acquisition or easements since wells for Alternatives A through C are not located on property owned by VTrans, providing electricity to the active well locations, and long-term changes in regional groundwater extraction.

To help address the unknown groundwater quality, groundwater was sampled at six locations on March 25 and 26, 2015. The six sampling locations relate to the three alternative deep extraction well location areas being considered for slide stabilization, i.e., the counter berm, the abandoned power canal roadway, and the toe of the slope adjacent to the Clyde River. Analysis of the collected samples showed in general that the inorganic groundwater parameters sampled within the Lower Sands and Gravels exist at concentrations below the standard limits of the Vermont Groundwater Quality Standards (VGQS), and the USEPA's Maximum Contaminant Level (MCL) from the National Primary Drinking Water Regulations. Concentrations of total and dissolved Iron and Manganese were found to exceed USEPA's Secondary Maximum Contaminant Level (SMCL) at all three alternative deep extraction well locations considered for slide stabilization. These results indicate that groundwater geochemistry will need to be considered for extraction well design.

SELECTED REMEDIAL DESIGN

The remedial design approach selected by VTrans involves design, installation and operation of groundwater extraction wells placed on the existing counterberm to lower the groundwater pressures affecting the stability of the deep slide mass (Alternative D; Figure 25). Issues involving property acquisition or right-of-way, wetlands, power transmission and access to the well system present unfavorable costs and challenges for either a passive or active groundwater extraction system at the power canal or toe of the landslide. Favorable access is allowed by an existing access road from Route 191 to the counterberm, and can be used for extraction system construction, operation and maintenance. The extreme winter conditions of northern Vermont, including a design frost depth of 6.5 ft, will need to be considered for the extraction system design. A self-sufficient solar power generating system with the ability to dump excess energy onto the local power grid will be considered for pump operations during final design. Groundwater chemistry data indicate post-extraction treatment is not required according to the Vermont Department of Environmental Conservation, and groundwater can be discharged into the power canal and eventually into the Clyde River. VTrans has begun the final mitigation design for the system, which may be operational by 2017 or 2018. Following successful construction of the extraction system to lower groundwater pressures, and subsequent establishment of the cessation of landslide movement, permanent roadway infrastructure repairs can then be implemented.

CONCLUSION

The work performed by many geotechnical and geological personnel throughout the history of the project has led to a mitigation design solution with a high likelihood of success to solve a perplexing and costly problem. The success of the project required a multi-discipline approach, which identified the importance of understanding the complex hydrogeology to

provide guidance and detailed analysis of stabilization analyses. A key component of this success was the identification by VTrans early in the investigation process from difficult drilling conditions that groundwater extraction would likely play a large role in reducing or stopping landslide movement. An additional key was the use of geotechnical stability and hydrogeologic models concurrently to evaluate alternative mitigation design.

REFERENCES:

- A-Baki, S. and Batchelder-Adams, C., 1989. *Slide Remediation Report for Derby-Newport F134-3(19)*, Materials and Research Division, Vermont Agency of Transportation, November 1989.
- Allen, C. and Benda, C., VTrans, 2011. *VT-191 in Newport, VT – A Landslide Case History*, presented at American Society of Civil Engineers (ASCE) Geo-Institute Landslide Conference, Norwich University, Norwich, VT, April 23, 2011.
- Civil Engineering Associates, Inc., 2011. *Geotechnical Report, Creep Deformation Analysis, Slope Movements on Vermont Route 191 – Newport, Vermont*. Prepared for Vermont Agency of Transportation, Newport City STP 134-3(22), Contract No. PS0077. December 1, 2011.
- C-Tech Development Corporation, 2014. *Environmental Visualization Software/Mining Visualization Software*, vers. 9.52.
- Doll, C.G., 1951. *Geology of the Mephremagog Quadrangle and the Southeastern Portion of the Irasburg Quadrangle, Vermont*. Vermont Geological Survey Bulletin No. 3, 113 p.
- Doll, C.G., Stewart, D.P. and MacClintock, P., 1970. *Surficial Geologic Map of Vermont*. Vermont Geological Survey, scale 1:250,000.
- Environmental Simulations Inc., 2015. *Groundwater Vistas*, vers. 6.75 Build 8, 64-bit.
- Golder Associates Inc., 2012. *Review of Landslide Records and Analyses, Route 191 Roadway Embankment, Newport, Vermont*, VTrans Newport STP 1343(22), Contract No. PS0172, November 29, 2012, 125 p.
- Golder Associates Inc., 2014. *Geotechnical Data Report, Route 191 Roadway Embankment, Newport, Vermont*, VTrans Newport STP 1343(22), Contract No. PS0172, August 28, 2014, 758 p.
- Hill, M.C., Banta, E.R., Harbaugh, A.W., and Anderman, E.R., 2000. *MODFLOW-2000, the U.S. Geological Survey Modular Ground-Water Model - User guide to the observation, sensitivity, and parameter-estimation process and three post-processing programs*. U.S. Geological Survey Open-File Report 00-184, 210 p.
- Ratcliffe, N.M., Stanley, R.S., Gale, M.H., Thompson, P.J. and Walsh, G.J., 2011. *Bedrock Geologic Map of Vermont*. United States Geological Survey Scientific Investigations Map 3184, scale 1:100,000.
- RocScience, Inc., 2001, 2015. *Slide – 2D Limit Equilibrium Slope Stability Analysis*, Toronto, Ontario, Canada.

Stewart, D.P. and MacClintock, P., 1969. *The Surficial Geology and Pleistocene History of Vermont*. Vermont Geological Survey, Bulletin No. 31, 251 p.

**Stream Restoration to Improve Slope Stability along Park Road at
Gibsonville, Letchworth State Park, New York**

James J. Janora, CPESC, CPSWQ
McMahon & Mann Consulting Engineers, P.C.
2495 Main Street – Suite 432
Buffalo, NY 14214
716.834.8932
jjanora@mmce.net

Marc D. Kenward, P.E.
Erdman Anthony
2165 Brighton Henrietta Town Line Road
Rochester, New York 14623
585.427.8888
kenwardmd@erdmananthony.com

Paula L. Smith, P.E.
New York State Office of Parks, Recreation & Historic Preservation
One Letchworth State Park
Castile, NY 14427
585.493.3649
Paula.Smith@parks.ny.gov

Acknowledgements

The authors would like to thank Shawn W. Logan, P.E. for his thoughtful review of this manuscript and for his unequalled ability to develop design plans that clearly illustrate the intent of even the most imaginative details.

Disclaimer

Statements and views presented in this paper are strictly those of the authors, and do not necessarily reflect positions held by their affiliations, the Highway Geology Symposium (HGS), or others acknowledged above. The mention of trade names for commercial products does not imply the approval or endorsement by HGS.

Copyright Notice

Copyright © 2015 Highway Geology Symposium (HGS)

All Rights Reserved. Printed in the United States of America. No part of this publication may be reproduced or copied in any form or by any means – graphic, electronic, or mechanical, including photocopying, taping, or information storage and retrieval systems – without prior written permission of the HGS. This excludes the original authors.

ABSTRACT

A road to the historic Gibsonville settlement was originally aligned along the side of a steep valley slope in what would later become Letchworth State Park. Ongoing stream erosion at the toe and soil slope instability along the valley side prompted the park to place a culvert along the stream channel, cover the culvert with up to 20 feet of fill, and realign the road. After almost 40 years, stream hydraulics began causing erosion again, and the culvert showed signs of structural deterioration. Therefore the park determined that the culvert configuration needed to be remediated.

A slope stability analysis indicated that excavation for replacing the culvert would require a shoring system to minimize the potential for slope movement. The dense glacial soil present at the site dictated that the shoring system would require drilled soldier piles, which was deemed cost prohibitive. Furthermore, the U.S. Army Corps of Engineers preferred that an ecologically-friendly solution be implemented.

The innovative design included abandoning the culvert in-place and restoring the stream to surface flow. Elements of the design included regrading the stream valley to help slope stability, restoring a stream channel that resembled the geomorphic characteristics of nearby reference stream reaches, and building a drop structure that conveys the stream flow non-erosively to the return channel. Construction of the project was completed in 2014.

HISTORY

Within the northern portion of Letchworth State Park lie the remnants of a former hamlet known as Gibsonville. Established in 1825, Gibsonville was comprised of industrial mills, commercial buildings, and residences located along Silver Lake Outlet. By 1933, Gibsonville was converted into a Civilian Conservation Corps (CCC) camp to put unemployed men to work building Letchworth State Park (Figure 1).

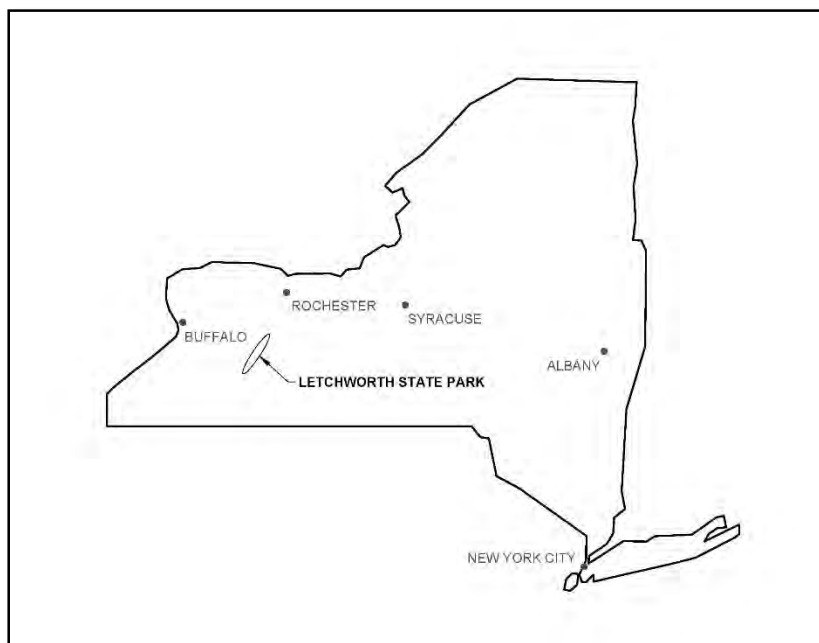


Figure 1 – Location of Letchworth State Park in New York State

The original road through Gibsonville traversed the steep slopes of an unnamed tributary valley (herein referred to as Gibsonville Creek) north of Silver Lake Outlet. Design plans dated 1937 show that the CCC realigned the road over the valley by constructing a concrete box culvert to convey Gibsonville Creek beneath a new embankment fill. The realigned road provided a smoother vertical profile, however the road was aligned parallel to Gibsonville Creek on a steep slope. This road, now known as Park Road, is the main north-south route through Letchworth State Park operated by the New York State Office of Parks, Recreation, and Historic Preservation (NYSOPRHP) (Figure 2).

In 1972, severe flooding in Gibsonville Creek during Hurricane Agnes eroded the toe of the slope parallel to the realigned Park Road. As part of the post-Agnes reconstruction efforts, NYSOPRHP decided to install a 500-foot reach of 90-inch diameter corrugated metal culvert in the bed of the stream and backfill it with upwards of 15 feet of fill. The new culvert and fill would be located approximately 500 feet upstream of the concrete box culvert that the CCC used to cross the stream under Park Road. The new culvert and fill were intended to serve as a buttress to stabilize the adjacent slope and Park Road. The stream reach between the two culverts was left in its steep valley configuration.

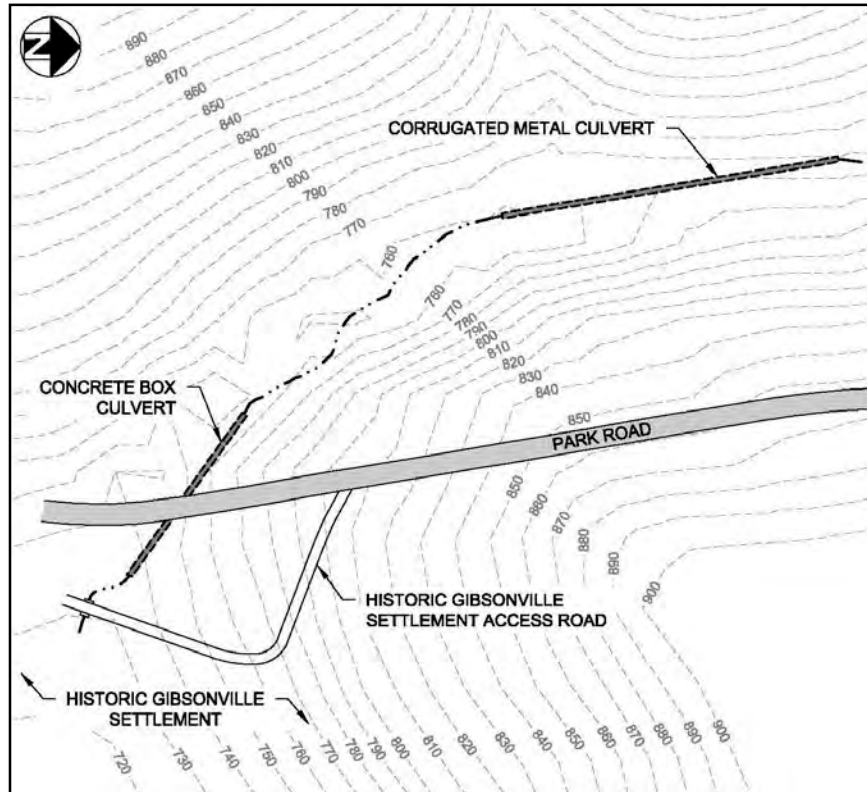


Figure 2 – Site plan view

The NYSDOT Geotechnical Engineering Bureau (GEB) developed a plan to install the corrugated metal culvert and construct the buttress. The GEB plan included cutting soil from the steep slope above Park Road and placing it as a buttress below Park Road. A slope failure was triggered during construction, at least in part because the contractor stockpiled the cut material on Park Road in advance of placing the culvert below the road. Other factors that the GEB identified as contributing to the slope failure include an abnormally high amount of precipitation during construction and excessive excavation to install the culvert pipe.

A NEW PROBLEM DEVELOPS

After 35 years in service, the corrugated metal culvert deteriorated and was approaching the end of its service life. Throughout its service life, the hydraulic conditions resulting from the culvert's installation also caused erosion and loss of pipe stability at both the inlet and outlet of the culvert (Figures 3, 4, and 5). Conversely, the slope between this culvert and Park Road did not show signs of instability, indicating that the GEB 1976 work successfully stabilized the slope following Hurricane Agnes.



Figure 3 – Culvert: Upstream End



Figure 4 – Culvert: Downstream End



Figure 5 – Dislodged End & Pipe Sections



Figure 6 – Park Road Settlement

The valley slope and Park Road adjacent to the reach of Gibsonville Creek between the corrugated metal culvert and the concrete box culvert was, however, showing signs of slope instability. The integrity of Park Road was being threatened (Figure 6) here similarly to the way the upstream reach had after Hurricane Agnes. The instability was evidenced by cracked and settled roadway pavement, together with sloughs and scarps in the slope between Park Road and Gibsonville Creek.

The design team of Erdman Anthony and McMahon & Mann Consulting Engineers, P.C. was retained by NYSOPRHP to assess the existing conditions, to develop alternatives for addressing the slope instability and the deteriorating culvert, and to prepare design plans for implementing the preferred alternative.

EXISTING CONDITIONS ASSESSMENT

Pavement Conditions

In addition to the pavement distress directly attributed to the failing slope, a wide variety of pavement distress of varying severity was prevalent in the segment of Park Road parallel to Gibsonville Creek. Classic alligator cracking was prevalent in the south bound shoulder and right edge of the travel lane, indicating the presence of wet and saturated soil conditions in the subbase or subgrade. The alligator cracking was more prevalent in the shoulder area where record plans indicated an overall thinner pavement section. Longitudinal cracking was observed in the southbound travel lane, primarily uphill from the pavement damage adjacent to the failing slope.

The most intriguing pavement distress was transverse pavement cracking. The severity of the transverse cracking tended to be light to moderate. The transverse cracking was intriguing because the transverse cracks were nearly perfectly perpendicular to the centerline and they were equally spaced. Also, some of the transverse cracks were fresh, while others had grass growing in them. It was speculated that the transverse cracking was a result of ground movement caused by, or at least exacerbated by, the presence and movement of ground water near the pavement subgrade.

Topographic Survey

Due to the steep slopes along the stream valley, laser scanning survey methods were used to gather existing topographic conditions. Fortunately, the client provided the Notice-to-Proceed early enough in the spring so that the laser scanning work could be conducted before foliage developed in the forested area. Laser scanning technology provides extremely accurate digital terrain models of existing conditions, which otherwise with conventional survey would result in much more data interpolation.

Geotechnical Exploration

An exploration program was completed in an effort to characterize the soil, to define the groundwater conditions, and to measure the depth of subsurface movement. Soil borings were advanced adjacent to the settlement along Park Road, and also in the valley bottom along the corrugated metal culvert. A total of ten soil borings were made. Two of the borings were instrumented with slope indicators and four of the borings were completed with standpipe monitoring wells.

The native soil was comprised of a thick unit of laminated fines overlying glacial till. A thin unit of laminated fines was found within the upper five to ten feet of the glacial till, at about 20 feet below the ground surface in the vicinity of the corrugated metal culvert fill area. The fill material adjacent to the corrugated metal culvert was generally clayey, and it was similar to the native glacial till found nearby. The fill beneath Park Road was granular material and it was placed on top of the upper laminated fine unit.

Wet soil was encountered in several of the valley borings near the elevation of the corrugated metal culvert. Generally, groundwater was measured within ten feet of the ground surface.

Slope movement was monitored over the course of four months, from May until September, 2012. Movement occurred from ten to twenty feet below Park Road. The magnitude of movement was generally less than ¼ inch.

Hydrologic & Hydraulic Modeling

Hydraulic modeling of Gibsonville Creek was conducted for the reach from Park Road to 200-feet upstream of the existing 90-inch culvert. The contributing drainage basin area was delineated using the *Watershed Modeling System, Version 8.4 (WMS)* and determined to be 1.22 square miles (Figure 7). The U.S. Army Corps of Engineers *Hydraulic Engineering Center's hydrology software, HEC-1*, was used to develop the hydrology for Gibsonville Creek (Table 1).

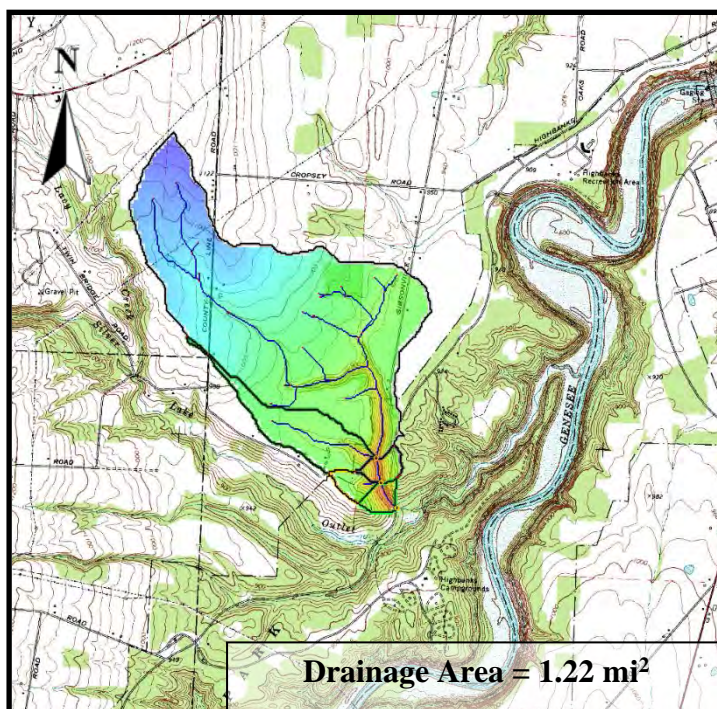


Figure 7 – Portion of the Mount Morris USGS Quadrangle showing the drainage area for Gibsonville Creek upstream of Park Road

Table 1 - HEC-1 Flows for Gibsonville Creek upstream of Park Road

Recurrence Interval (years)	24-hour Precipitation (inches)	HEC-1 Flows for Gibsonville Creek (cubic-feet / second)
1	1.87	45
2	2.15	71
5	2.64	128
10	3.08	189
25	3.78	299
50	4.42	410
100	5.16	548

The hydraulic analysis was performed using the U.S. Army Corps of Engineers *River Analysis System* program, *HEC-RAS (Version 4.1.0)*. The results (Figure 8) confirmed that for nearly all storm events analyzed, flows through the existing 90-inch culvert were supercritical, thus confirming the severe erosion that plagued both the inlet and outlet of the culvert.

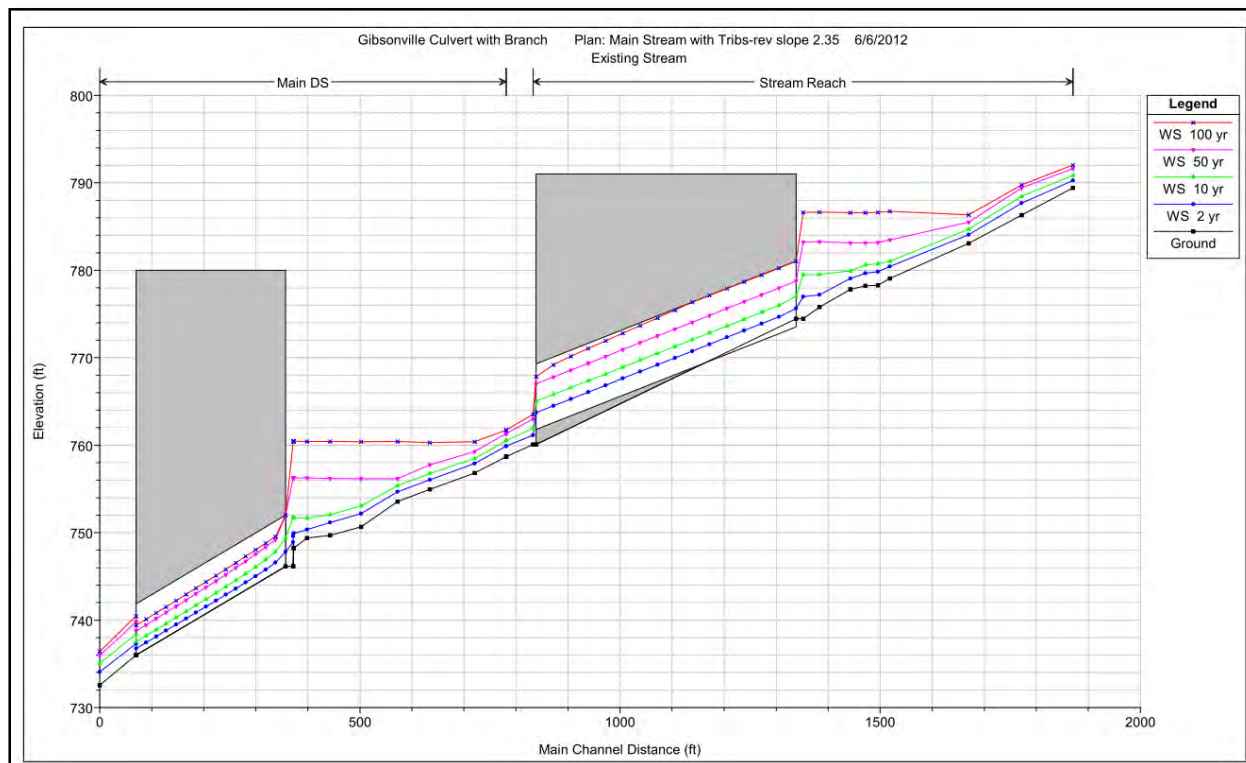


Figure 8 - HEC-RAS Water Surface Profiles – Existing Conditions

Geomorphic Assessment

A fluvial geomorphic reconnaissance was made to assess the conditions of stream reaches upstream and downstream of the site along Gibsonville Creek, and along other streams in the area. Procedures for performing reference reach assessments are described by Rosgen (1996) and Thorne et.al. (1997). The information gained from assessing these reference reaches would later dictate some of the design details when an alternative was selected.

Two distinct channel forms were identified in reference reaches during the fluvial geomorphic assessment, and they were controlled by the geologic conditions that occurred through the reaches. The two channel forms included those controlled by bedrock and those controlled by soil.

The streams in the lower, or downgradient reference reaches were incised into shale and siltstone outcrops (Figure 9). The channel profiles included flat benched areas, slopes in shale up to 45 degrees, and vertical falls below siltstone beds. There were disorganized flow paths that diverged and converged along discontinuities in the bedrock, resulting in a channel section that was significantly wider than it was deep. The sinuosity of the bedrock reaches was approximately unity, meaning that the channel length was equal to the valley length. The

bedrock reaches were devoid of sediment, except where round cobbles accumulated below the shale and siltstone falls.



Figure 9 – View of bedrock exposed in the downstream reference reaches

The streams in the upper reference reaches were incised into glacial till, silt, and sand. The streambed had cobbles and boulders that were eroded out of the till banks, and often formed lateral and medial bar deposits. The cobbles and boulders created an armor layer in the stream bed where fines had been winnowed out from the spaces between the coarser materials (Figure 10). The D_{50} particle size was estimated at $\frac{1}{2}$ inch. The channel slope was on average approximately 3%, however, the bed featured numerous step/pool features rendering the average slope not representative of the localized bed conditions. The step/pools often occurred near woody debris, where sediment accumulated above fallen trees and scour pools formed below as the stream cascaded over the woody debris steps (Figure 11). Several of the pools, where the stream velocity was low, were lined with sand and silt. The channel cross section was trapezoidal, and it was considerably wider than it was deep. The channel length was slightly longer than the valley length in the soil reaches, resulting in a sinuosity of 1.2 (ratio of channel length to valley length).



Figure 10 - View of typical bedload in upstream reference reaches



Figure 11 – View of logs forming step – pool stream structure

ALTERNATIVES EVALUATION

Two alternatives to address the deteriorated culvert were evaluated. They included replacing in-kind by installing a new culvert along the alignment and grade that was established after Hurricane Agnes, or restoring the stream by replicating the form and function of the stream system similar to Pre-Hurricane Agnes conditions. Neither alternative considered modifying the embankment layout or the culvert beneath Park Road as this would cause unacceptable disruption to visitor traffic along Park Road.

The criteria for developing the alternatives included meeting regulatory requirements, avoiding slope destabilization, and increasing the stability of the slope between the culverts.

Replace In-Kind

Replacing the culvert in-kind would require compliance with the current US Army Corps of Engineers (USACE) regulations that included restoring a stream bottom that mimics natural conditions. Such an installation would be difficult to establish and maintain because of the hydraulic conditions. Even with a larger opening, erosive flow conditions would still be prevalent at the inlet and outlet of the culvert. This would preclude the use of a culvert lining application, requiring full removal and replacement of the culvert.

Replacing the culvert in-kind would therefore require an excavation down to nearly 25 feet deep, with side slopes graded or benched to meet the valley slopes. A slope stability analysis was performed using the program Slide, manufactured by RocScience. The slope stability analysis indicated that excavation to the pre-culvert slopes, a minimum condition, could not be made without lowering the factor of safety of the slope to below one (without destabilizing the slope above). The design team determined that a shoring system would need to be constructed to allow for removal and replacement of the culvert.

This alternative did not address the stability of the valley slope between the corrugated metal culvert and the concrete box culvert beneath Park Road.

Restore the Stream

The USACE would play a role in regulating the decisions associated with restoring Gibsonville Creek to a functional riparian corridor. Their concerns included selecting an acceptable stream gradient, avoiding head cutting, width/depth ratio of the channel cross section, channel sinuosity, and habitat improvement.

Restoring the stream would require that the gradient of the channel projected above the level of the corrugated metal culvert. Furthermore, the culvert would need to be removed or filled to prevent future settlement along its alignment. Continuing the gradient through an extended valley fill downstream of the culvert would provide buttress to the adjacent valley slope. This would require a non-erosive return of the gradient down to the existing stream channel before it entered the culvert beneath Park Road. These gradients would need to be consistent with the gradients found in the reference reaches.

The channel cross section and sinuosity would need to mimic the conditions found in the reference reaches. The more important characteristic of the restored stream would be that it needed to be capable of passing the design storm flow.

Habitat improvement would be a combination of stream structures that created diversity in the bed and banks, as well as a vegetated corridor that used only rock protection to resist erosion. These conditions existed in the reference reaches and it appeared that they could be replicated along the restored stream.

Another slope stability analysis was performed. This time the analyses included both the section of the valley above the stream along the corrugated metal culvert, and the section of the valley above the extended valley fill downstream of the corrugated metal culvert. The analysis of the slope above the corrugated metal pipe indicated that excavating the stream grades would reduce the factor of safety from 1.8 to 1.6. The analysis of the slope above the extended valley fill indicated that the fill would increase the factor of safety from 1.1 to 1.3.

Selected Alternative

The decision was made to restore the stream rather than replace the culvert. The basis for the decision was partially that the cost-benefit of the shoring system needed to replace the culvert was deemed unacceptable. The shoring system would be high in cost, and it would only serve as a temporary measure during excavation. By restoring the stream, the culvert could be abandoned in place without a shoring system. The decision was also based on the understanding that restoring the stream would satisfy the regulatory requirements for the project. Taking a cue from the conditions found in the reference reaches, the alternative to raise and restore the stream bed though the valley adjacent to Park Road became a constructible and cost effective solution.

FINAL DESIGN

The stream restoration would begin approximately 200-feet upstream of the corrugated metal culvert. The stream profile (Figure 12) would carry through the valley along the culvert by cutting into the soil above the culvert, and matching the grade at the top of the culvert at its downstream end. From there, the valley would be filled with as much as 20 feet of fill, adding a buttress to the adjacent valley slope and conveying the stream on top of the fill. Beginning at a point 140 feet upstream of the concrete box culvert beneath Park Road, a grouted riprap drop structure would be constructed to bring the stream down to match the existing stream elevation.

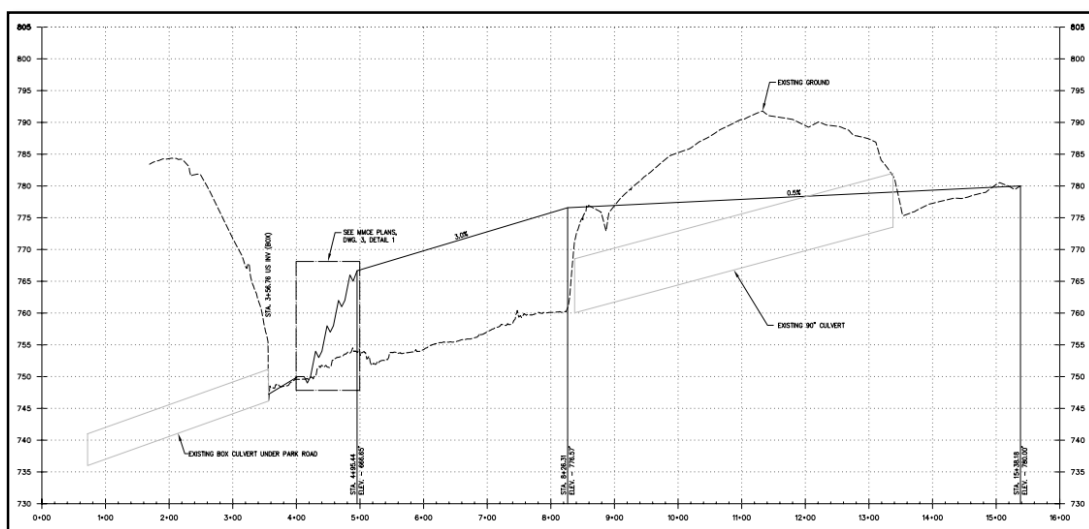


Figure 12 - Proposed Stream Profile

Stream Hydraulics

The sinuosity of the restored stream reach was designed to generally mimic the sinuosity found in the upstream reference reaches. However, the design included bends that were less abrupt than some of the meanders found in the reference reaches. This was done to avoid interaction between the stream and the buried corrugated metal culvert and to align the channel on approach to the drop structure.

The channel gradient could not exceed 0.5% along the corrugated metal culvert to avoid interaction between the stream and the buried corrugated metal culvert. Once clear of the buried culvert, the channel gradient was increased to 3.0%, similar to that found in the reference reaches. The drop structure was designed to convey the channel down 18 feet over the length of 70 feet to the existing elevation with a sequence of drops and pools to dissipate energy.

The cross section of the channel was designed as a vee to keep the width/depth ratio low, as required by the USACE, despite the wide trapezoidal channel found in the reference reaches. The sides of the channel were sloped at a ratio of 2 horizontal for every 1 vertical (2H:1V).

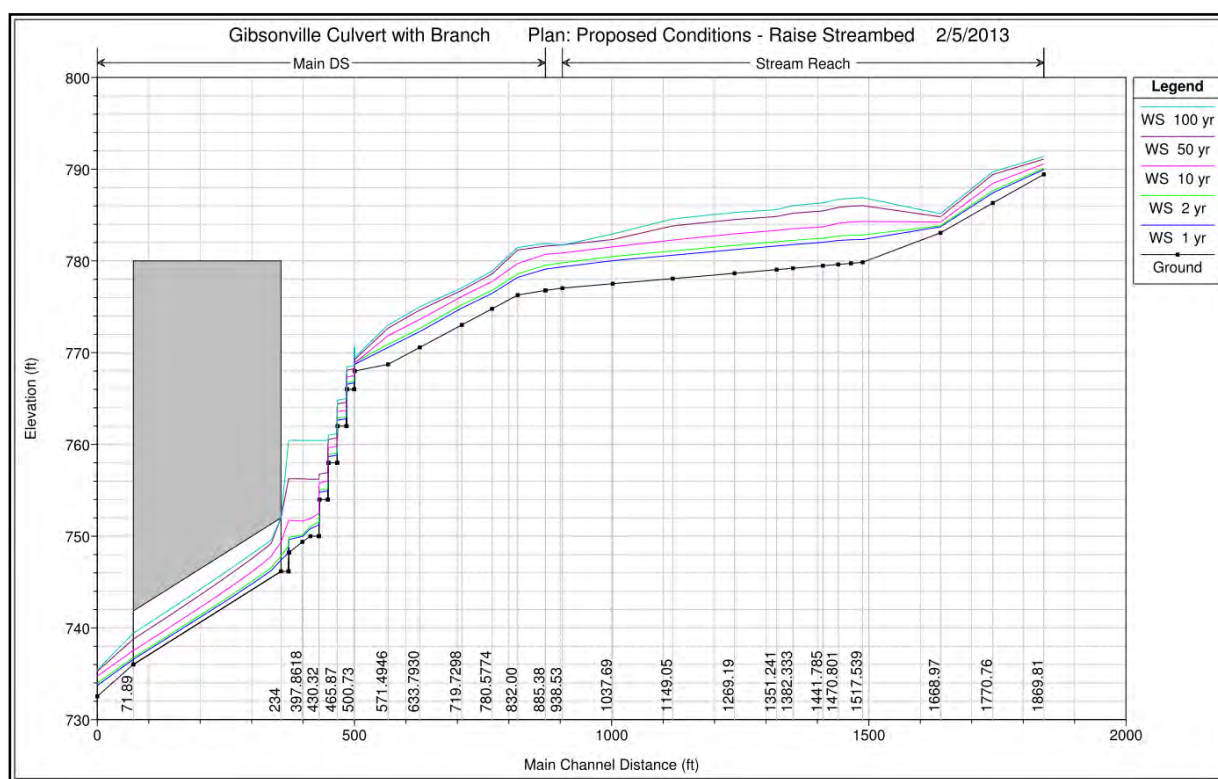


Figure 13 - HEC-RAS Water Surface Profiles – Proposed Profile

The hydraulic analysis of the proposed stream conditions demonstrated the benefits of eliminating the 90-inch culvert and the erosive conditions associated with it. Figure 13 shows the HEC-RAS water surface profiles for the proposed restored stream.

Details for Stream Stability

The design included abandoning the corrugated metal culvert in place as opposed to excavating and removing it. This posed the future threat that the pipe could collapse and cause sink holes along the stream bank. The design detailed that the culvert would be abandoned in place by filling it with controlled low-strength material. A sacrificial section of HDPE pipe was slipped through the culvert before filling it so the stream bypassed the site during construction.

Slope Stabilization

Slopes above the stream channel in the section along the abandoned culvert needed to be as steep as 2H:1V to match to existing grades outside the work limit. Knowing that it would be difficult to stabilize topsoil on that steep of a slope due to rill erosion, the design team included multiple rows of fiber rolls staked down into the subgrade soil. The fiber rolls were intended to serve as barriers to flow concentration, instead redistributing concentrated flows as sheet flow. The slopes in this section were seeded with a design mixture that was specific for steep slope applications.

The design included placing as much as 20 feet of fill in the valley bottom between the end of the corrugated metal culvert and the concrete box culvert. The valley fill was intended to provide buttress to the slopes supporting the Park Road embankment.

As in almost all slope stability problems, subsurface water needed to be controlled. The design included drainage trenches that were excavated into the native subgrade below the valley fill section of the project. The drainage trenches extended from the valley side down to the invert of the original channel and into a perforated underdrain pipe that also carried the stream bypass pipe. A contingency was built into the design that included provisions to locate additional drainage trenches at any areas where subsurface water was encountered during construction.

Channel Gradient

While the average gradient of the designed stream section between the abandoned corrugated metal culvert and the drop structure was 3.0%, wood debris features were included to disrupt the average gradient condition and enhance small scale changes in the stream bed gradient.

Stream Armoring

Stream bed and bank armoring were carefully considered during the design. The overlying intent of the project was to protect the stability of the slopes between the stream and Park Road. Knowing that erosion would inevitably occur along the restored stream, the design team developed a plan to reduce the potential for erosion in the direction of Park Road.



Figure 14 – View of log revetment

The woody debris features were oriented similarly to bendway weirs and bank attached vanes (Figure 14). These structures are commonly made of rock riprap, and are used to concentrate the thalweg at a point in the stream section that creates an advantageous scenario of erosion and deposition. The design used the woody debris bendway weirs and bank attached vanes to replicate the conditions of the woody debris found in the reference reaches as well as to serve as redirective structures.

The woody debris that was used to serve as bendway weirs and bank attached vanes was also designed to serve a longer term purpose. At each location where the woody debris weirs and vanes were constructed, the design team decided to bury additional structures upstream and away from the stream bank. The buried structures were to be oriented the same as those exposed in the stream bed, but they would not become engaged unless lateral erosion proceeded into the bank toward Park Road. Theoretically, as the lateral erosion progressed, the buried structures would redirect the erosive force onto the opposite bank.

Streambed revetment stone was placed along the channel banks to resist scour. The design team decided to use stone that mimicked the armor layer found in the upstream reference reaches. The design assumption was that the armor layer in the reference reaches was generally stable in the current stream conditions, and that transport was limited to minor reworking of lateral and medial bars. The design team also allowed that boulders resembling river rock could be placed along the channel to serve as habitat enhancement.

Strategic placement of vegetation was designed to armor the stream against erosion toward Park Road. Tree and shrub plantings were designed to be placed in rows approximately perpendicular to the stream channel. These vegetated rows were intended to serve as living dikes in the overbank areas between the stream and Park Road. In the event of overbank flow conditions, the living dikes would serve to increase the roughness, thereby reducing flow velocity and causing sediment deposition.

Micro-topographic grading in the form of vernal pools was also used to reduce the potential for erosion toward Park Road. Vernal pools were located on the overbank on the side of the stream opposite from Park Road. The vernal pools would not only add habitat to the stream corridor, but they would serve as pilot channels that could convey more overbank flow than the overbank between the stream and Park Road.

Structural fill that had high clay content was important to the integrity of the stream system. The design team identified that it could be detrimental to the stability of the downstream drop structure if surface water was capable of percolating into the embankment. Clayey structural fill with a plasticity index of at least 7% was specified as the embankment fill beneath the stream.

Grouted Riprap Drop Structure

The grouted riprap drop structure was designed to dissipate the erosive energy of the descending stream flows using grade drops, pools, and roughness (Figure 15). The drop structure was also meant to keep the stream flowing on the surface, rather than into the riprap subgrade, which could cause high pore-water pressure along the structure. The hydraulics mimicked the step/pool conditions found in the upstream reference reaches as well as the steep bedrock cascades found in the lower reference reaches.

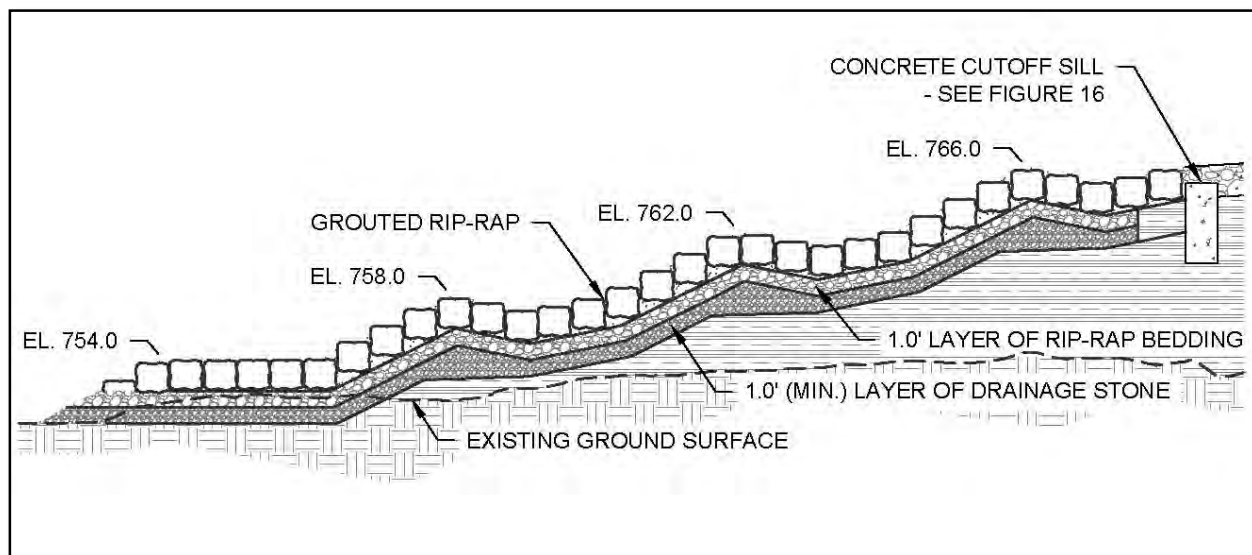


Figure 15 – Profile of the Grouted Riprap Drop Structure

The USACE expressed concern about the need for the grouted riprap drop structure, and suggested that the channel could be graded over the length of the valley to match the elevation of the existing stream. The USACE had to be convinced that leaving the channel on top of the fill for as long as practicable served the function of buttressing the adjacent valley slope. This was not an approach that the USACE was familiar with.

An important design element of the grouted riprap drop structure was that pore-water had to be minimized in the subgrade. The subgrade consisted of a granular filter between the riprap bedding and the clayey structural fill. This was identified as a potentially destabilizing feature in the event that it became saturated. The design specified that the granular filter and the riprap

bedding needed to be connected to the underdrain system. As it turned out, the USACE had the same concerns during their review of the design plans.

Lateral short-circuiting of the grouted riprap drop structure was another concern that needed to be addressed by the design. One of the most common failure mechanisms of a drop structure is that they get eroded around the end, leaving the inlet to the drop higher than the eroded channel. The design team included a steel reinforced concrete cutoff sill that extended into the valley side slopes (Figures 16 and 17). The center third of the 150 foot wide cutoff sill was designed to be three feet lower than the outer flanks of the cutoff sill. This depressed section would serve to promote a centralized spillway, rather than a spillway located near the valley side slopes.

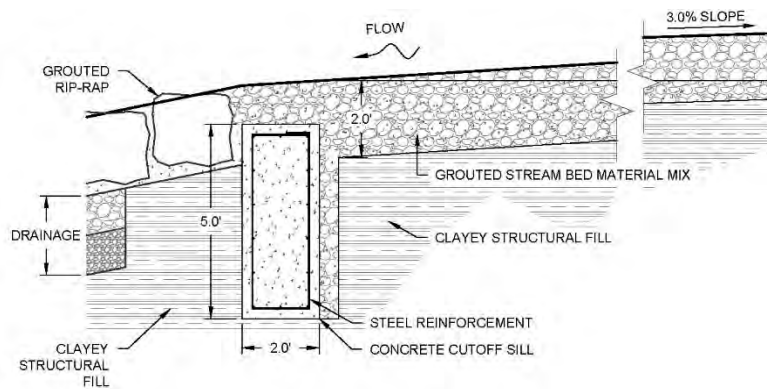


Figure 16 – Section through the concrete cutoff sill



Figure 17 – Concrete cut-off sill under construction

The inlet area above the drop structure and the outlet area below the drop structure were also identified as areas of potential scour. The design team decided to include a grouted streambed revetment pad above the concrete cutoff sill to prevent a pool from forming above the drop structure, and a grouted riprap stilling basin at the toe of the drop structure to prevent the formation of a knickpoint below the drop structure.



Figure 18 – View of the grouted riprap drop structure

Pavement Subgrade Drainage

Speculation that the transverse pavement cracking resulted from ground water in the subgrade led the design team to develop a plan to address drainage beneath Park Road. A 6-foot deep underdrain was installed off the edge of the southbound shoulder. Three-foot deep transverse underdrains were installed at 7 locations throughout the distressed area. The transverse underdrains were designed to coincide with the locations of the transverse pavement cracks. The underdrain system was conveyed to an outlet at a low point in Park Road so the water was not reintroduced onto the slope between Park Road and Gibsonville Creek.

MONITORING

The site endured extended periods of record low temperatures during January, February, and March of 2015, three months after stream construction was completed. Frozen soil was observed at depths exceeding 12 inches at a nearby project site. The subsequent thaw caused a slough along the right valley side in the cut section at Gibsonville Creek. The slough was about 150 feet long, 25 feet high, and 1.5 feet deep. The fiber rolls and topsoil in this area were displaced down the slope, and a tree fell from the forest into the stream channel.

The site experienced abnormally high rainfall in late May and early June of 2015, approximately 6 months after stream construction was completed. According to a nearby monitoring station, a severe storm event on June 14, 2015 dropped 3.4 inches of rain in 12 hours. The peak intensity of that storm resulted in 2.3 inches of rain over a 90 minute time period which suggests an extreme event based on the below data in Table 2.

The June 14th storm flow transported streambed revetment stone out of the 3% channel reach. The stone within about 3 feet of the channel invert was affected, while the stone higher on the bank was not disturbed. A large boulder that was placed in the 3% channel approximately 30 feet upstream of the drop structure was transported to the bottom of the drop structure. Several of the log revetments were scoured or undermined, however the orientations of the log revetments

concentrated the scour onto the opposite bank as intended (Figure 19). The drop structure performed well during the severe storm flows.

Extreme Precipitation Estimates (Perry, NY) Source: <http://precip.eas.cornell.edu/>

	5min	10min	15min	30min	60min	120min		1hr	2hr	3hr	6hr	12hr	24hr	48hr		1day	2day	4day	7day	10day	
1yr	0.26	0.40	0.50	0.65	0.82	1.00	1yr	0.71	0.88	1.14	1.36	1.60	1.88	2.11	1yr	1.67	2.03	2.45	2.94	3.34	1yr
2yr	0.31	0.48	0.60	0.79	1.00	1.22	2yr	0.86	1.09	1.37	1.62	1.88	2.16	2.43	2yr	1.91	2.33	2.77	3.26	3.70	2yr
5yr	0.37	0.57	0.72	0.96	1.23	1.51	5yr	1.06	1.35	1.70	2.00	2.32	2.65	3.00	5yr	2.34	2.89	3.38	3.95	4.50	5yr
10yr	0.41	0.64	0.81	1.10	1.44	1.78	10yr	1.24	1.60	2.01	2.36	2.71	3.08	3.53	10yr	2.72	3.39	3.93	4.58	5.22	10yr
25yr	0.48	0.76	0.97	1.34	1.77	2.21	25yr	1.53	2.00	2.49	2.92	3.34	3.76	4.37	25yr	3.33	4.20	4.80	5.56	6.36	25yr
50yr	0.54	0.86	1.11	1.55	2.08	2.60	50yr	1.80	2.37	2.94	3.43	3.91	4.38	5.14	50yr	3.87	4.94	5.58	6.43	7.39	50yr
100yr	0.60	0.98	1.26	1.79	2.45	3.07	100yr	2.11	2.80	3.47	4.04	4.58	5.10	6.05	100yr	4.51	5.82	6.50	7.46	8.59	100yr
200yr	0.69	1.12	1.45	2.08	2.88	3.62	200yr	2.48	3.32	4.09	4.75	5.37	5.94	7.12	200yr	5.26	6.85	7.58	8.64	9.99	200yr
500yr	0.82	1.35	1.76	2.55	3.56	4.49	500yr	3.07	4.16	5.07	5.88	6.61	7.28	8.84	500yr	6.44	8.50	9.28	10.51	12.19	500yr

Table 2 – Extreme Precipitation Estimates for Perry, NY



Figure 19 – View looking at erosion following the June 14, 2015 storm flow

CONCLUSIONS

Restoring a stream corridor to a condition that replicates the form and function of undisturbed streams in reference reaches is a state of the art technique that can be used to strategically reduce erosion and to stabilize embankment slopes. It can be beneficial on transportation projects where past activities have unintentionally increased the rates of scour along the toe of embankments, and also to sites that have experienced exacerbated erosion and scour due to a major storm event.

No two stream projects are the same. Investigations must be site specific and include the exploration of similar undisturbed stream reaches that exhibit similar geology to the project site. The design should then strive to replicate the conditions found in the reference reaches, given that sound engineering judgments translate the observations into a constructible concept. Details of the design should not be made to appease regulatory agencies unless an unbiased practitioner has considered the potential ramifications of a compromised design detail.

REFERENCES

Rosgen, Dave (1996). *Applied River Morphology*. Wildland Hydrology.

Thorne, C. R., Hey, R.D., Newson, M.D. (Eds.) (1997). *Applied Fluvial Geomorphology for River Engineering and Management*. Edited by Thorne, Hey, and Newson; John Wiley & Sons Ltd., West Sussex, England.

HEC-1 Flood Hydrograph Package, (1998). U.S. Army Corps of Engineers, Hydraulic Engineering Center.

Brunner, G.W. (2010). HEC-RAS. U.S. Army Corps of Engineers, Institute for Water Resources, Hydraulic Engineering Center.

Natural geologic controls on rockfall hazard and mitigation on the Niagara escarpment, King's Highway 403 at Hamilton, ON, Canada

Dave Gauthier

Dept. of Geological Sciences and Geological Engineering, Queen's University
Kingston, ON, Canada
613-893-4920
d.gauthier@queensu.ca

David F. Wood

David F Wood Consulting Ltd.
Sudbury, ON, Canada
705-698-0909
info@dfwood.com

D. Jean Hutchinson

Dept. of Geological Sciences and Geological Engineering, Queen's University
Kingston, ON, Canada
613-533-3388
hutchinj@queensu.ca

Stephen Senior

Ontario Ministry of Transportation
Downsview, ON Canada
416-235-3734
Stephen.senior@ontario.ca

Prepared for the 66th Highway Geology Symposium, September, 2015

Acknowledgements

We wish to thank the Ontario Ministry of Transportation for their permission to publish this case history, and the Canadian Railway Ground Hazard Research Program for sharing advances in photogrammetric analysis.

Disclaimer

Statements and views presented in this paper are strictly those of the author(s), and do not necessarily reflect positions held by their affiliations, the Highway Geology Symposium (HGS), or others acknowledged above. The mention of trade names for commercial products does not imply the approval or endorsement by HGS.

Copyright Notice

Copyright © 2015 Highway Geology Symposium (HGS)

All Rights Reserved. Printed in the United States of America. No part of this publication may be reproduced or copied in any form or by any means – graphic, electronic, or mechanical, including photocopying, taping, or information storage and retrieval systems – without prior written permission of the HGS. This excludes the original author(s).

ABSTRACT

The southern part of Ontario, Canada – adjacent to and west of Lake Ontario – is generally absent of rockfall hazard. However, the Niagara escarpment traverses this part of the Province, and in many locales it is expressed as a vertical cliff with active talus slopes. The King’s Highway 403 (four-lane, 110 km/hr design speed) climbs the escarpment along the base of one such talus slope, within the City of Hamilton. There has been a history of rockfall affecting the highway there, and a 500 kJ catchment fence was installed almost twenty years ago along a 2 km stretch. As part of a recent assessment of this catchment fence, we generated detailed 3d terrain models of the slope using oblique aerial photogrammetry (OAP). In combination with traditional fieldwork, the 3d OAP model allowed us to resolve in detail the escarpment geology and its influence on the talus slope. In this paper we report on the nature of the rockfall hazard at this site, and identify some natural geological controls on the form of the talus slope which result in natural mitigation of hazard. Specifically, we found that the talus slope is interrupted by narrow, flat benches related to very slightly protruding bedrock strata, which underlie the main rockfall-producing layer. We noted the accumulation of fallen blocks along these benches. This geological and geotechnical interpretation, and the resulting recommendations regarding the suitability of the existing catchment fence, would likely have been elusive with traditional approaches and without the very high resolution 3d terrain model.

INTRODUCTION

The southern part of Ontario, Canada around Lake Ontario is generally absent of rockfall hazard. However, the Niagara escarpment traverses this part of the Province, and in many locales it is expressed as a vertical cliff with active talus slopes. The King's Highway 403 (four-lane, 110 km/hr design speed) climbs the escarpment along the base of one such talus slope within the City of Hamilton (Figure 1). There has been a history of rockfall affecting the highway there, and a 500 kJ catchment fence was installed almost twenty years ago along a 2 km stretch of highway. As part of a recent assessment of this catchment fence, we generated detailed 3d terrain models of the slope using oblique aerial photogrammetry (OAP). In combination with traditional fieldwork, the 3d OAP model allowed us to resolve in detail the escarpment geology and its influence on the talus slope. In this paper we report on the nature of the rockfall hazard at this site, and identify some natural geological controls on the form of the talus slope which result in natural mitigation of hazard, and how the OAP model was applied.

Typically, remote-sensing methods used to study slopes and other geological features are land-based, such as LiDAR and photogrammetry (e.g. Olariu et al., 2008; Lato et al., 2009; Sturznegger and Stead, 2009; Brodu and Lague, 2012; Gigli et al., 2014). (See Andrew et al. (2013) and Abellan et al. (2013) for reviews of the applications of LiDAR techniques to rock slope problems.) In the last few years 'structure-from-motion' (SFM) photogrammetric processing has advanced to the point where in some cases the 3d terrain models generated in this way can be used in place of LiDAR or other data sources (e.g. Westoby et al., 2012; James and Robson, 2012; Fonstad et al., 2013; Hugenholtz et al., 2013). For this study we collected oblique aerial photographs suitable for SFM photogrammetry from a moving helicopter. Gauthier et al. (2015) describe the method and precision/accuracy of the techniques used here.

While not the first application of this method to rock slopes (e.g. see Gauthier et al., 2014; Gauthier et al., 2015; Kromer et al., 2015; Lato et al., 2015), the current study is unique in that the geological interpretation of the site, and the geological controls on the hazard, were identified through the photogrammetric slope model *and* traditional field investigations.

Study Area

The site is characterized by an approximately 2 km long rock face adjacent to the Highway 403 (four-lane divided, posted speed 100 km/h) right-of-way, as it descends the Niagara Escarpment, within the City of Hamilton. The highway grade essentially traverses the escarpment stratigraphy from west to east, given the horizontality of the strata. The highway grade is at crest elevation west of the site; approximately 10 m below the crest near the west project limit; and at least 30 m below the crest at the east project limits. The main crest through the site is at approximately 185 m above sea level (ASL), which is the ultimate top of the escarpment. Between the highway and the crest lies a natural rock face and talus-covered slope, with a slope angle that varies from 30-33° generally, but reaches 35° in places.



Figure 1 – Overview map showing the location of the study area, at Hamilton ON. Image courtesy of Google Earth.

While the highway in the west section is generally within 30 m horizontal of the crest, near the east project limit this increases to greater than 60 m, with the additional space occupied by a more prominent talus-covered slope below the main escarpment face.

A 500 kJ low-elongation rockfall catchment fence was installed in 1998 over the entire length of the project area.

The Niagara Escarpment is composed of differentially-weathered, Silurian-age dolostones and associated shales and sandstones, deposited in a marine environment (Hewitt, 1971). While no detailed geological mapping and interpretation was conducted as part of the current study, we recognize a number of features relevant to the rockfall problem:

- The general shape of the terrain, particularly in section, is bedrock-controlled (See Figures 2 and 3);
- The generalized stratigraphy identified across the site is expressed in the rock face and slope as intervals of differing colour, weathering, blockiness, and texture (See Figures 2 and 3);
- Rockfall may be sourced from many of the strata, but not equally by frequency, volume, or contribution to the hazard.

Figure 2 presents a basic stratigraphic interpretation for a typical section in the west part of the site. Formations and their characteristics were compiled from Hewitt (1971). The typical section in the east part of the site is identical, except with a longer talus-covered slope at the toe.

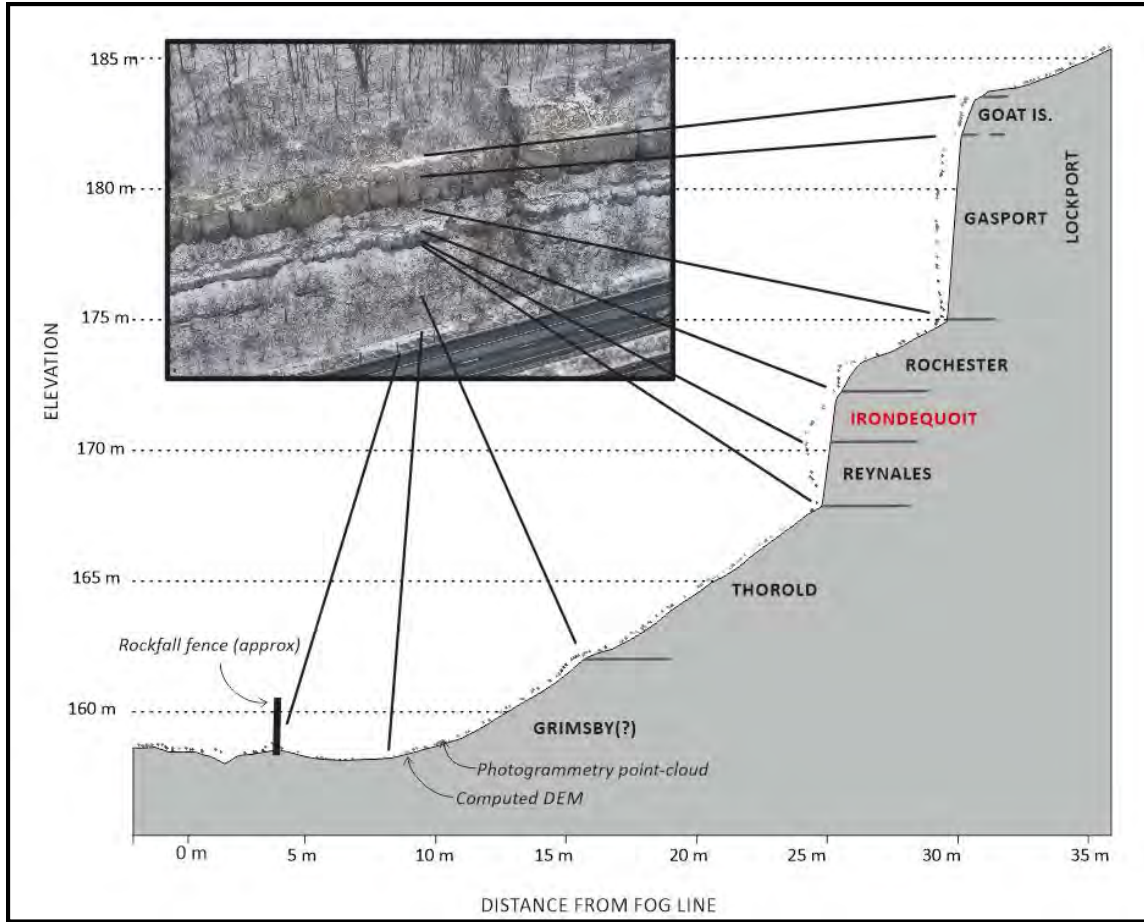


Figure 2. Idealized geological cross section showing typical geometry (DEM and point cloud) in the west section. The lower slope is mostly talus covered.

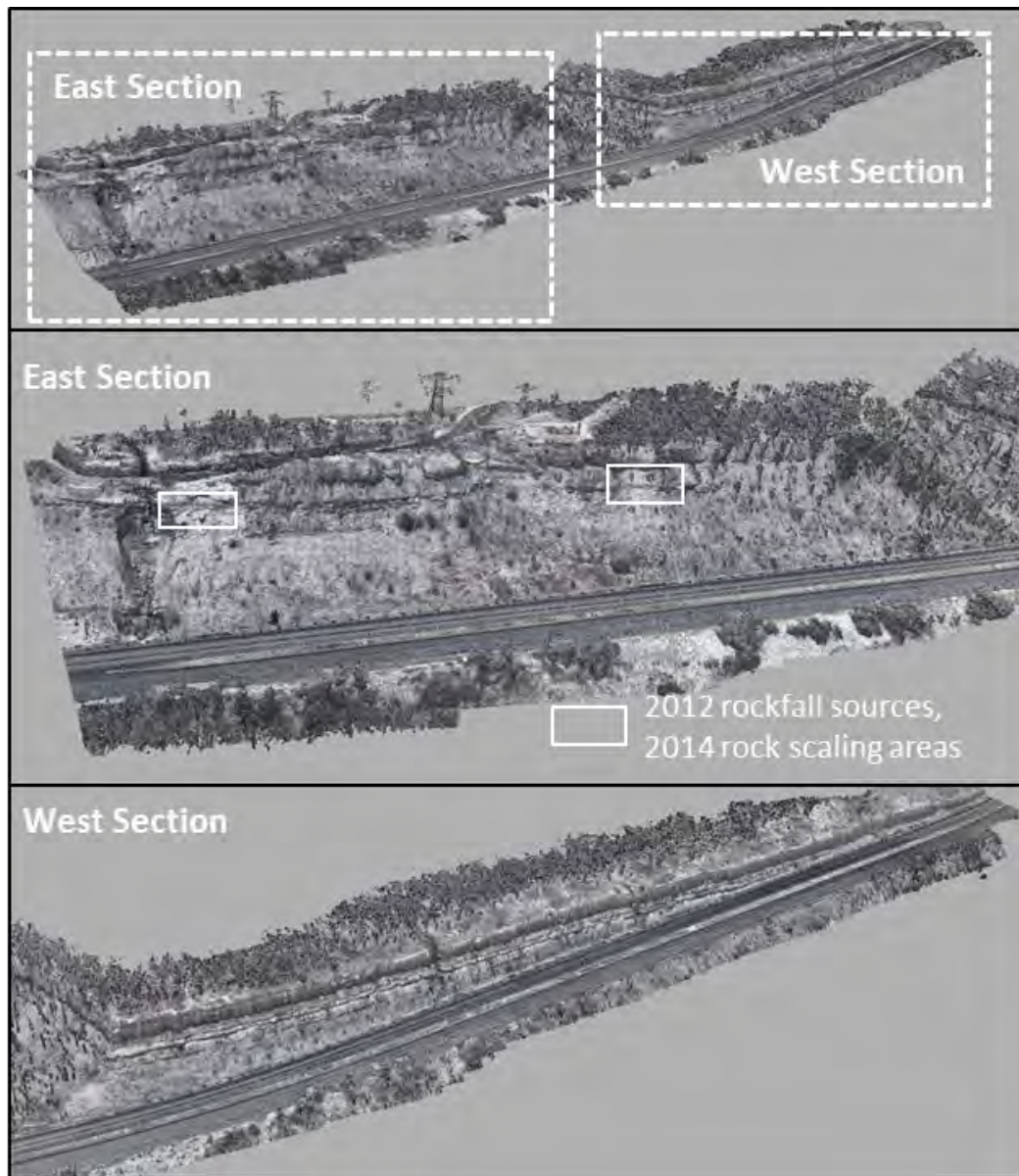


Figure 3 – Oblique view of the 3d photogrammetry model of the site, highlighting the known source areas of significant rockfalls and remediation effort.

METHODS AND DATA

In November 2014 we chartered a Robson R44 helicopter for the purposes of collecting a set of oblique aerial photographs of the study area. The intent was to use these to develop the detailed three-dimensional photogrammetric model of the slope, as well as the travelled lanes, fence and ditch, and terrain beyond the crest.

Images were collected and processed as follows:

- Camera: Nikon D5300 (GPS equipped), 24MP, DX sensor, 50 mm (75 mm eq.) lens
- 567 photos, geotagged
- Two surveys: one multipath close (438 photos), one single path wide (129 photos)
- Photogrammetric processing completed using Agisoft Photoscan Pro (V1.0)
- Alignment points culled to retain only those with reprojection error < 0.5 pixel, then optimized
- Relative error (camera GPS to aligned position) generally <10 m x,y,z
- 53 million point dense cloud generated for entire length (25% of pixels used), 185 points/m² (Figure 2)
- 95 million point dense cloud generated for west rockfall section (50% of pixels used), 815 points/m² (Figure 2)
- Meshed point cloud surface generated within Photoscan (Figure 3)

To support this study we also had access to aerial photos, terrestrial LiDAR, DEM products, and rockfall and remediation consultant's reports.

RESULTS

The idealized geological section presented in Figure 2 was partly derived based on descriptions of geological and geotechnical character of the strata, described in Hewitt (1971). With reference to observed and potential rockfall occurrence, and resulting rockfall hazard to the highway, the following is noted, working down the slope and stratigraphy from crest to highway-level:

Lockport Fm.: The Goat Island Member is highly fractured/jointed and closely bedded, and susceptible to weathering, freeze-thaw, and displacement by vegetation. Block size is typically small, and the predominant failure mode is raveling, although some larger (1 m³) disaggregation failures are possible. Deposits from these are unlikely to reach the catchment fence, rather they seem to stop on (and make up the majority of) the talus-covered sections of slope. The underlying Gasport Member is of similar character, but with a more widely spaced fracture/bedding pattern resulting in slightly larger blocks. Some raveling and discrete rockfall are possible, but block size is small and falls seem to arrest on the talus-covered slope, or may rarely reach the ditch, but with relatively low energy.

Rochester Formation: Rarely exposed in outcrop, this shale unit is typically covered with fine talus sourced from the Lockport rocks above. It is noted as susceptible to weathering elsewhere along the escarpment.

Irondequoit Formation: This is a massive, 1-2 m thick dolostone unit, with wide (1-2 m) subvertical fracturing, and no noted bedding planes. Therefore, blocks in the range of 1 – 3 m³ are common, and rarely up to 5 m³. This unit is the source of several rockfalls in 2012, some of which engaged the catchment fence.

Reynales Formation: Underlying the Irondequoit are bedded dolostones with shaley interbeds, and generally widely spaced subvertical fracturing. Block size is somewhat smaller than the

Irondequoit above, and preferential weathering and more frequent rockfall of this unit may lead to an undermining of the larger blocks above.

Thorold/Grimsby Formations: Make up the lower part of the slope, and are generally talus-covered. However, in the field a subtle bench feature is noted in some locations directly below the exposed faces of the Irondequoit and Reynales rocks (which can be seen in section at the west project limit within an eroded drainage channel; Figure 4). This is assumed to be a protrusion of the Thorold beds through the otherwise talus-covered slope (Figure 4). Lower on the slope, particularly in the east part, inspection of the photogrammetry-derived fine DEM shows other similar, but more subtle, bench features, assumed to represent similar bedrock control on the form of the slope. On further inspection these benches serve to break up the slope and provide natural attenuation for rolling blocks, both because of their shape and because of the coarser composition of the talus overlying them (due to previous rocks having stopped there).

Talus: We expect the talus to be relatively thin over bedrock benches, and thicker between them. Despite some shallow creep-like instabilities identified in the 3D model (Figure 11), the talus slope does not appear to generate hazardous rockfalls. Note – further assessment of the stability of the talus slopes was beyond the scope of this project.

In summary, the Irondequoit and Reynales Formation rocks seem to be the main drivers of the rockfall hazard within the project area, based on recent rockfall history and their potential to produce large blocks. The Thorold/Grimsby bedding protrusions into the lower talus-covered slope provide natural, geological attenuation features.

Using Rocscience's Rocfall (V5) program we conducted rockfall simulations at the source of the most hazardous rockfalls. The two-dimensional cross-sections were captured directly from the photogrammetry-derived DEM. We used observations of real events for calibration, with the goal of replicating the reach and approximate impact energy of those events. The design block was 4.5 m³, with an assumed density of 2500 k/m³, for a mass of 11,250 kg. The simulations were seeded at the known source location of the most hazardous falls, i.e. within the Irondequoit Fm. We selected conservative model parameters for the slope materials and initial conditions of the blocks. The results showed that blocks reached the catchment fence, stopped in the ditch or at its foreslope, and stopped on the talus-covered lower slope – typically at the subtle benches noted in the terrain model (Figure 5a).

Using these calibration parameters we conducted simulations at two other locations (Figure 5b,c). Both were chosen as potential worst-cases, since the slope is tallest, and least impeded by vegetation etc. In the case with similar benches in the talus, we found a similar distribution, i.e. blocks arresting on the benches, which are more pronounced and numerous than in the calibration set. In the other case, which was a section further west, where the highway is close in elevation to the source formation – and therefore the talus slope is less developed and not benched, showed most blocks reaching the ditch and catchment fence, rather than arresting on the slope.

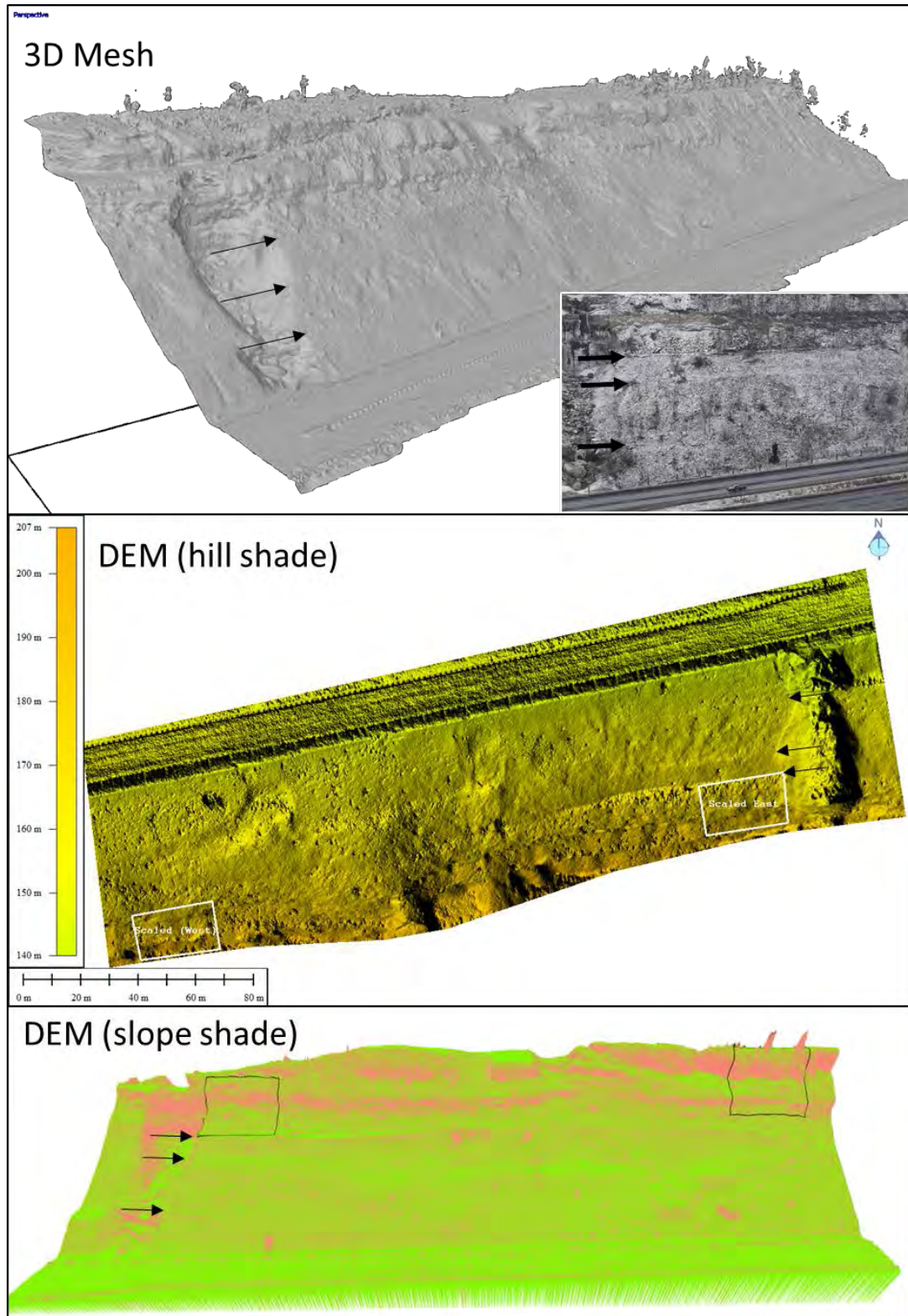


Figure 4 – Oblique view of the photogrammetry mesh surface, map-view of the hillshaded DEM, and oblique view of the slope-angle shade DEM surface, highlighting the subtle bench features in the talus slope, which are related to underlying bedrock strata and appear to arrest a certain number of falling/rolling/sliding blocks.

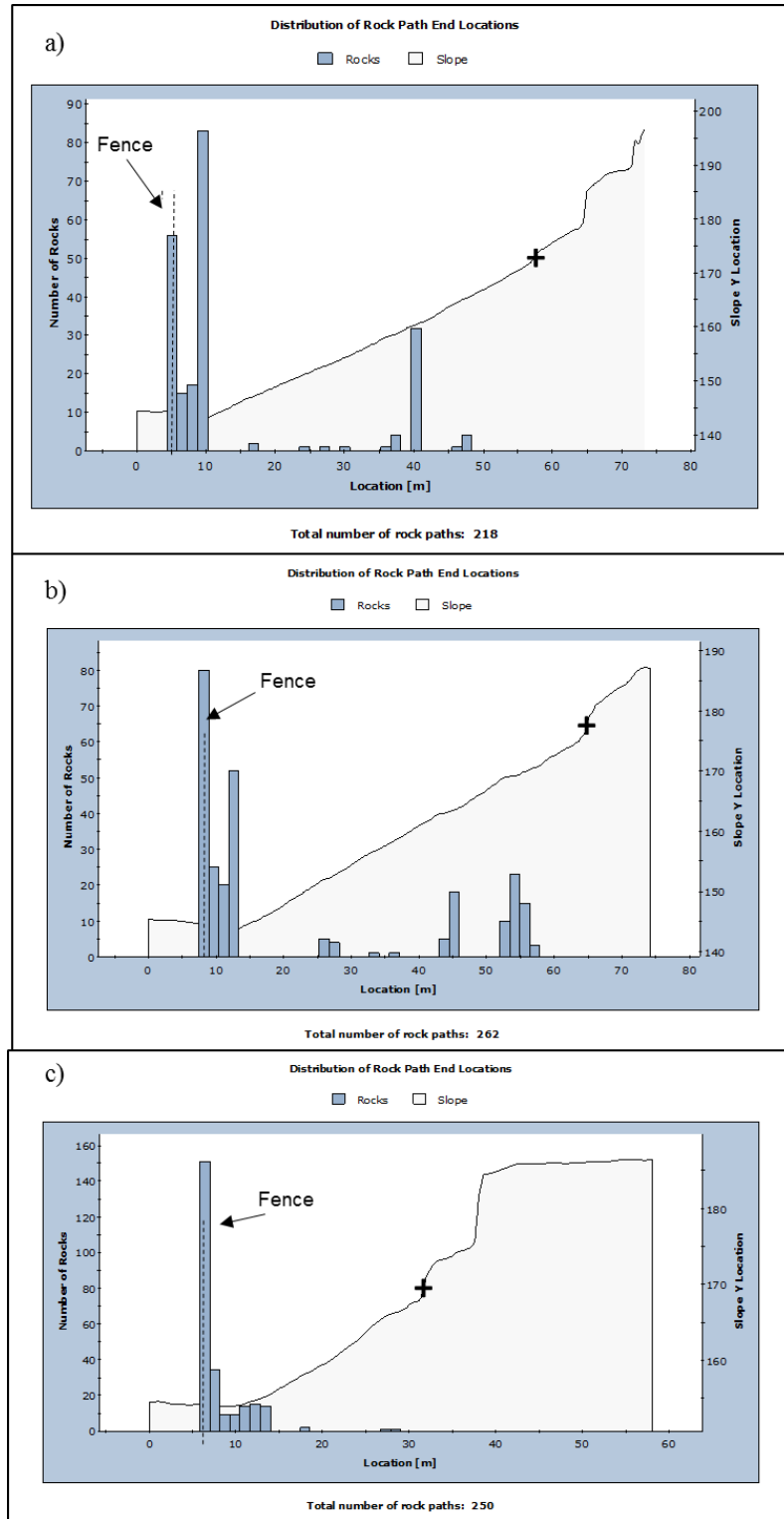


Figure 5 – Rocfall (V5) model simulation results for three sections, highlighting arrest of rolling/sliding blocks on subtle benches in talus (a, b), but not where they don't occur (c).

DISCUSSION

Our results confirm those of previous investigations, which showed that the main driver for rockfall hazard at this site is the Irondequoit Fm, given its mostly massive, but blocky texture, and the fact that it is underlain by a weathering-susceptible stratum (Reynales Fm.). Other strata on the escarpment at this location are prolific rockfall-producers, but only small blocks are generated through raveling and disaggregation-type failures, which has led to the development of the talus slope. Natural attenuation of rolling and sliding blocks, on the slope, exist in the form of subtle benches protruding through the talus-covered portions of the slope. These have demonstrated capacity (in the field and simulations) to arrest rockfall.

The main benefits of the OAP model in this study were the ability to visualize and analyze the terrain in 3D, in order to document quantitatively the existence and occurrence of the rockfall-attenuating benches in the talus slope. The level of detail available in this model (i.e. hundreds of georeferenced points per square metre) over the entire study area meant that we could review and manipulate the terrain using GIS analytical tools (e.g. Figure 4), and interpret the geological controls on the rockfall hazard similarly. In general, the possibility of generating cross-sections for rockfall simulations at any location in the study area, at any time after the field campaign, is a further benefit, since it is not always clear in the field which locations should be manually surveyed for cross-section generation. Compared to terrestrial LiDAR, the OAP data have the advantage of being fully coloured, which certainly helps with the geological interpretation. However, in this study and others we found that a properly georeferenced LiDAR dataset for at least part of the slope was invaluable for registration of the OAP data. Lastly, since the OAP model from the 2014 campaign captured the condition of the slope at that time, it could serve as a baseline for any future quantitative 3D change-detection efforts (e.g. see Gauthier et al 2014).

Given the geological controls on the rockfall hazard and natural mitigation, several strategies to augment the existing attenuation features, rather than construct new structural protection to reduce any residual risk to the travelling public, could include:

- 1) 3D or traditional Monitoring for the development of large, loose/overhanging blocks in the Irondequoit and Reynales Formations, and subsequent focused scaling/trimming efforts as required to remove the potentially hazardous blocks. This could be focused on springtime, and could include both regular engineering assessments and supplementary reviews following weather or climate events known to condition or trigger rockfall.
- 2) Padding of the ditch with coarse local material, to enhance its ability to dissipate the energy of falling or rolling blocks in the same manner as the benches on the slope
- 3) Construct catchment benches (as per the natural ones) on the talus-covered portion of the slope.

For sites not amenable to other near-field remote sensing techniques, such as LiDAR, the OAP method can provide useful data that would otherwise be unavailable, and in some cases, such as in the current study, allows for insights on the geological controls on rockfall hazard that might otherwise go unnoticed or documented.

CONCLUSIONS

In this study of rockfall hazard along the Niagara escarpment above The King's Highway 403, in Hamilton ON, we confirmed that rockfall hazard was driven almost entirely by blocks falling from a single stratum (the Irondequoit Fm), and that the talus slope below is interrupted by narrow, flat benches related to very slightly protruding bedrock strata, which underlie the main rockfall-producing layer. We noted the accumulation of fallen blocks along these benches, and measured the general profile of the slope, which currently sits at somewhat less than angle of repose due to the protruding beds and their attenuation of large rolling blocks. This geological and geotechnical interpretation was enhanced by our use of the very high resolution 3d terrain model, derived from oblique aerial photographs.

REFERENCES:

- Conference Proceedings
 - Gauthier, D., Hutchinson, D., Wood, D., and Morris, T. Rockfall source detection and volume measurement from autonomous UAV-acquired photogrammetry: A case study from a transportation corridor in northwestern Ontario, Canada. *Proceedings: GeoRegina 2014, Regina, SK, September 28-October 1, 2014.*
 - Gauthier, D., Hutchinson, J., Lato, M., Edwards, T., Wood, D., Bunce, C. On the precision, accuracy, and utility of oblique aerial photogrammetry (OAP) for rock slope monitoring and assessment. *Proceedings: GeoQuebec 2015, Quebec, QC, September 20-23, 2015.*
 - Kromer, R., Hutchinson, J., Lato, M., Gauthier, D. and Edwards, T. Early Warning of Rockfall Hazard from Remote Monitoring. *Proceedings: GeoQuebec 2015, Quebec, QC, September 20-23, 2015.*
 - Lato, M., Gauthier, D., Quinn, P., Hutchinson, J., Kromer, R., Edwards, T., Riopel, J. 3D data collection for rapid rock fall response situations. *Proceedings: GeoQuebec 2015, Quebec, QC, September 20-23, 2015.*
 - Ondercin, M., Kromer, R., and Hutchinson, D.J., 2014. A Comparison of Rockfall Models Calibrated Using Rockfall Trajectories inferred from LiDAR Change Detection and Inspection of Gigapixel Photographs. *Proc., 6th Canadian Geohazards Conference, Kingston, Ontario, 2014.*
- Federal Government Reports
 - Andrew, R., Arndt, B., and Turner, K. *Instrumentation and monitoring technology.* In: Turner, K. and Shuster, R. (eds), *Rockfall characterization and control*, Transportation Research Board, Washington, DC, pp 56-71, 2012.
 - Hewitt, D. The Niagara Escarpment. Industrial Minerals Report 35. Ontario Department of Mines and Northern Affairs. pp 68, 1971.
- Journal
 - Abellan A, Oppikofer T, Jaboyedoff M, Rosser N, Lim M, Lato M. Terrestrial Laser Scanning of rock slope instabilities. *Earth Surface Processes and Landforms*; doi: 10.1002/esp.3493, 2013.
 - Brodu, N., & Lague, D. 3D terrestrial lidar data classification of complex natural scenes using a multi-scale dimensionality criterion: Applications in geomorphology. *ISPRS Journal of Photogrammetry and Remote Sensing*, 68, 2012, pp. 121-134.
 - Fonstad, M., J. Dietrich, B. Courville, J. Jensen, and P. Carbonneau. Topographic structure from motion: a new development in photogrammetric measurement. *Earth Surface Processes and Landforms* 38 (4), 2013, pp. 421-430.

- Gigli, G., Frodella, W., Garfagnoli, F., Morelli, S., Mugnai, F., Menna, F., & Casagli, N. 3-D geomechanical rock mass characterization for the evaluation of rockslide susceptibility scenarios. *Landslides*, 11, 2014, pp. 131-140
- Hugenholtz, C., K. Whitehead, O. Brown, T. Barchyn, B. Moorman, A. LeClair, K. Riddell, and T. Hamilton. Geomorphological mapping with a small unmanned aircraft system (sUAS): feature detection and accuracy assessment of a photogrammetrically-derived digital terrain model. *Geomorphology*, 194, 2013, pp 16-24.
- James, M. R., and S. Robson. Straightforward reconstruction of 3D surfaces and topography with a camera: Accuracy and geoscience application. *Journal of Geophysical Research: Earth Surface* 117.F3, 2012, pp. 2003-2012.
- Lato, M., Diederichs, M. S., Hutchinson, D. J., & Harrap, R. Optimization of LiDAR scanning and processing for automated structural evaluation of discontinuities in rockmasses. *International Journal of Rock Mechanics and Mining Sciences*, 46(1), 2009, 194-199.
- Olariu, M. I., Ferguson, J. F., Aiken, C. L., and Xu, X. Outcrop fracture characterization using terrestrial laser scanners: Deep-water Jackfork sandstone at Big Rock Quarry, Arkansas. *Geosphere*, 4(1), 2008, pp. 247-259.
- Sturzenegger, M., and D. Stead. Close-range terrestrial digital photogrammetry and terrestrial laser scanning for discontinuity characterization on rock cuts. *Engineering Geology* 106(3), 2009, pp. 163-182.
- Westoby, M. J., Brasington, J., Glasser, N. F., Hambrey, M. J., & Reynolds, J. M. 'Structure-from-Motion' photogrammetry: A low-cost, effective tool for geoscience applications. *Geomorphology*, 179, 2012, pp 300-314.



SEA-TO-SKY HIGHWAY PROJECT

Grant A. Lachmuth, ASct, RTMgr – Senior Project Director

**GeoStabilization International
Inc.**

Canada Division

Vancouver, British Columbia,
Canada

Introduction

The Ministry of Transportation decided to make improvements to the Sea-to-Sky Highway.

The Sea-to-Sky Highway is a 95-kilometre long section of Highway 99 from West Vancouver to Whistler. Set in a mountain landscape, the highway presents complex engineering, traffic management and construction challenges. British Columbia's Ministry of Transportation (MoT) decided to make improvements to the highway between West Vancouver and Whistler to improve its safety, reliability and capacity. These improvements, completed by 2009, included highway widening and straightening, and other measures designed to reduce hazards, shorten travel times, and increase capacity of the highway.

The improvements moved MoT toward its long-term corridor objectives for the highway: to accommodate population growth, economic development in corridor communities, increasing demand for resident and visitor travel, and increased goods movement.

Any additional improvements delivered contributed to the fulfillment of MoT's long-term objectives.

In January 2003, Treasury Board approved a maximum \$600 million (\$2002) capital commitment for improvements to the highway (the Sea-to-Sky Highway Improvement Project – referred to in this document as the overall project). In a subsequent submission to Treasury Board in December 2003, MoT concluded it could provide essentially the same physical improvements at a lower capital cost – for an estimated \$600 million in as-spent dollars over the period to 2009 or for a net present cost of \$516 million (\$2005). These improvements represented a portion of MoT's long-term corridor objectives and are referred to in this document as the baseline improvements.

Improving and Operating the Highway

MoT chose a combination of design-build-finance-operate and design-build contracts to deliver the highway improvements.

Approximately two-thirds of the capital expenditure of the overall project was undertaken through a 25-year performance-based Design-Build-Finance-Operate (DBFO project) public private partnership contract between MoT and the S2S Transportation Group (S2S).

The remaining third of the capital expenditure for the improvements was procured by MoT through separate Design-Build (DB) contracts. The purpose of the DB contracts was to mitigate schedule risk by utilizing the 2004 and 2005 construction seasons, to coincide with the business planning and the competitive selection process of the DBFO project. Under the DBFO contract, S2S designed and constructed highway improvements on approximately two-thirds of the corridor, and now operate, maintain and rehabilitate the full corridor in keeping with performance standards in the contract.

Fair, Open, and Competitive Selection Process

The project had a fair, open, and competitive process.

The competitive selection process had the following features:

- disclosure of initial competitive selection process documents on the project's web site and the Partnerships BC web site;
- a proponent consultation process designed to increase proponents' understanding of the contract requirements and to encourage feedback from proponents throughout the process to improve the final contract;
- evaluation of proposals on their ability to provide the private sector portion of the baseline improvements, provide additional highway improvements and remain within an annual affordability ceiling (the AAC); the selection of a preferred proponent and limited negotiations between the proponent and MoT to reach a final contract; and
- a fairness reviewer who observed the process and determined that it was fair and unbiased.

Final Contract

The final contract between MoT and S2S is a 25-year performance-based contract designed to deliver safety, reliability and capacity improvements along the Sea-to-Sky Highway.

Contract provisions include:

- S2S provided the design, construction and financing of its portion of the baseline highway improvements;
- S2S provided additional highway improvements that are incremental to its portion of the baseline improvements;
- S2S provided operations, maintenance, and rehabilitation for the whole corridor;
- an allocation of risks between the parties, each taking responsibility for the risks they can most cost-effectively manage;
- a performance-based contract designed to protect the public interest and provide incentives to S2S to achieve the project schedule, maintain traffic flow during construction and ensure reliable service;
- the annual maximum allowable performance payments to S2S (as indicated by the AAC);
- formal dispute resolution provisions giving MoT the ability to pursue a measured response for deficiencies, up to and including contract termination; and

- MoT retained ownership of the highway.

Achieving Value for Money

MoT believes value for money for this project is demonstrated because of the additional improvements, and the anticipated user benefits that flow from them, provided in the DBFO contract.

Value for money represents the relationship between costs and benefits of a project, and includes quantitative and qualitative factors.

Cost:

Proposal evaluation usually involves some element of low price competition in which the specifications or outcomes are set and proponents provide a price. For the Sea-to-Sky DBFO project, this typical MoT process was reversed so proponent proposals would be evaluated for the additional improvements beyond the baseline they would provide at a set price. The maximum annual price that MoT estimated it would pay for the baseline highway improvements, and the operations, maintenance and rehabilitation of the whole corridor, was prescribed in the Request for Proposals (RFP) document (in the form of the annual affordability ceiling, or AAC). The expected cost of the project to the Province is \$789.8 million (NPC \$2005) over the 25-year contract. This amount includes the capital cost of MoT's DB contracts and the costs of annual payments to S2S for providing its portion of the baseline improvements and the additional improvements, and for operating, maintaining and rehabilitating the entire corridor. By comparison, MoT estimates that the NPC of the risk-adjusted public sector comparator (PSC) would be \$744.0 million (\$2005). While the cost of the DBFO contract exceeds the expected cost had MoT pursued a series of DB contracts (the PSC), MoT believes that the benefits from the additional improvements demonstrate value for money.

Benefits:

From a benefits perspective, the overall value for money proposition considers those additional highway improvements in excess of the baseline improvements to be provided by the private sector and the anticipated user benefits that will flow from them.

Additional highway improvements, beyond baseline, provided in the DBFO:

- 20 km additional passing lanes;
- 16 km additional median barrier;
- Additional highly reflective pavement markings to enhance safety;
- 30 km additional shoulder and centre-line rumble strips where most effective;
- improved lighting and roadside reflectors for additional safety;

- improved earthquake resistance and lighting on bridges;
- 10 km additional wider shoulders for improved safety and accommodation of cyclists;
- improved rock fall and debris catchment;
- additional highway straightening and improved sightlines;
- safer and more effective intersections, particularly in urban settings;
- improved signage signifying community entrances and recreational and tourism features;
- improved recreational trail facilities in Squamish; and
- improved highway maintenance response to weather conditions (three road/weather information sites).

One of the goals of any road improvement is to produce benefits for road users. MoT believes that one indication of the value for money provided by the DBFO is a calculation of the anticipated user benefits from the incremental improvements provided under the DBFO. To estimate the expected user benefits, there is a common international approach used for estimating travel time savings and safety benefits in transportation projects. By applying this approach, along with a degree of professional judgment, MoT estimates the user benefits for major transportation projects in B.C.

The sum of the expected user benefits from the incremental improvements is estimated to be \$131 million net present value (NPV) over the life of the contract. To put these in perspective, benefits provided by the baseline improvements are estimated to be \$427 million NPV over the life of the contract. In the opinion of MoT, and Partnerships BC and their advisors, the benefits resulting from the incremental improvements are in the order of 15 to 30 per cent above the expected benefits of the baseline improvements.

Also, the contract required that S2S meet standards that are comparable or equivalent to the standards applicable on other highways in B.C. The consequences to S2S for failing to meet the required standards were sufficiently significant that the overall result should be that S2S maintains the highway to a level that is, on average, higher than the maintenance level attained on other highways in B.C.

Ongoing Contract Monitoring

The contract between MoT and S2S includes provisions for ongoing monitoring designed to ensure that each phase of the construction, and the contract as a whole, was implemented as intended. For example, S2S must certify that the highway design complies with the contractual requirements. MoT continued to oversee the DBFO project, to ensure contract requirements and performance standards for safety, reliability and capacity (such as highway width, number of lanes, safety requirements, sightline requirements and signage) are appropriately met.

1. Project Background, Objectives and Partnership Structure

Background

The Ministry of Transportation decided to make improvements to the Sea-to-Sky Highway.

British Columbia's Ministry of Transportation (MoT) decided to make improvements to the highway between West Vancouver and Whistler to improve its safety, reliability and capacity. These improvements, to be completed by 2009, include highway widening and straightening, and other measures designed to reduce hazards, shorten travel times, and increase capacity of the highway.

The improvements are expected to move MoT toward its long-term corridor objectives for the highway: to accommodate population growth, economic development in corridor communities, increasing demand for resident and visitor travel, and increased goods movement. In January 2003, Treasury Board approved a maximum \$600 million (\$2002) capital commitment for improvements to the highway (the Sea-to-Sky Highway Improvement Project – referred to in this document as the overall project). In a subsequent submission to Treasury Board in December 2003, MoT concluded it could provide essentially the same physical improvements at a lower cost – for an estimated \$600 million in as-spent dollars over the period to 2009 or for a net present cost of \$516 million (\$2005). These improvements represented a portion of MoT's long-term corridor objectives and are referred to in this document as the baseline improvements. Any additional improvements delivered through the project will contribute to the fulfillment of MoT's long-term objectives.

Objectives

MoT's objectives are to achieve improved safety, reliability and capacity of the Sea-to-Sky Highway.

The primary objectives for the Sea-to-Sky Highway Improvement Project include:

Safety:

Improve the safety of the highway, primarily through improvements to the highway design.

Reliability:

Improve travel time predictability for highway users.

Capacity:

Enhance the ability of the highway to accommodate community growth and other user needs.

Project:

With the selection of Vancouver to host the 2010 Winter Olympics, to complete the highway improvements by late 2009 within the budget.

Manage Traffic:

To minimize disruption and maximize predictability for road users because the improvements are being undertaken on an operating highway with no alternate route to which traffic can be diverted.

With these objectives in mind, MoT defined a set of baseline improvements.

To achieve the objective of completion by 2009, MoT implemented measures to mitigate schedule risk.

One measure was the development of a construction and traffic management plan allowing simultaneous construction north and south of Squamish. The plan allowed for what MoT considered an acceptable level of traffic delays while enabling the project to be completed on schedule.

In addition, MoT's decision to undertake two Design-Build (DB) contracts for a portion of the overall project enabled construction during the 2004 and 2005 construction seasons. An 830-metre long "test section" south of Lions Bay was completed in August 2004 to gain more knowledge of geotechnical, constructability and traffic management issues associated with the overall project. In September 2004, under a separate DB contract, construction started on the Sunset Beach to Lions Bay section of the highway.

Concurrently, the remainder of the project underwent a business planning process to determine procurement structures that would further alleviate schedule risk.

Selection of Partnership Structure

For the remainder of the project, MoT considered public sector delivery and a number of procurement structures, including Design Build Operate (DBO) and Design Build Finance and Operate (DBFO).

The following criteria were utilized by MoT and Partnerships BC to select the delivery model, assuming the use of an effective competitive process to implement it:

- deliver the baseline improvements on time and on budget;
- deliver additional highway improvements;
- transfer appropriate risks to the private sector at appropriate prices;
- include incentives in the contract to achieve project performance objectives; maintain project schedule and budget; and address traffic management requirements;
- conduct a fair, open and competitive process; and
- achieve value for money.

Based on the criteria above, MoT and Partnerships BC considered the two most viable delivery options to be: a series of separate contracts purchased by MoT (the public sector comparator), and the other, a public private partnership using a DBFO structure. These options were developed during the business planning process.

Development of the Public Sector Comparator

The public sector comparator (PSC) represents a cost estimate of the public sector procuring a project where assets and services are purchased through a series of separate contracts. Partnerships BC was committed to the use of a PSC as it is intended to:

- inform decision makers on whether the output specifications are likely to be affordable before the project goes to market; and
- serve as a base case for estimating the range of value for money expected to be achieved in the final DBFO contract. During the development of the public sector comparator for the Sea-to-Sky Highway Improvement Project, MoT and Partnerships BC primarily gave consideration to two procurement methods for the design and construction portions of the project:
 - a series of DB contracts; or
 - a single DB contract.

MoT and Partnerships BC determined that each method had advantages and disadvantages relative to the other, and each could have been used. On the basis of the criteria above, MoT determined that MoT would have used a series of DB contracts to procure the design and construction portion of the project in the event the DBFO arrangement did not offer the potential to achieve greater value for money

Expected Benefits of the Selected Partnership Structure

The Province decided on a design-build-finance-operate (DBFO) partnership structure for the portion of the project not utilizing the DB contracts.

The Province chose a DBFO partnership structure for the remainder of the Sea-to-Sky Highway Improvement Project. In comparison to the PSC, a DBFO partnership structure adds private sector financing, integrates a wider range of services provided by the private sector and transfers additional risks to the private sector. MoT and Partnerships BC were of the view that the addition of private sector financing would provide incentive to the private sector to meet or exceed the contractual requirements, because payments from MoT would be based on performance. MoT and Partnerships BC assessed both qualitative and quantitative criteria to assist the Province in determining the appropriate competitive selection process for the project. Based upon the expectation of achieving additional highway improvements, and other advantages including management of schedule risk, a DBFO was recommended by Partnerships BC and MoT. This recommendation was accepted by Treasury Board.

Risk Management

A risk assessment to estimate the potential and cost of transferring certain risks to the private sector was conducted by members of the project team and their advisors, based on their knowledge and experience. The financial consequences and probabilities of various possible outcomes were assigned to the key project risks, utilizing methodologies such as simulations that are generally used to quantify risks.

Examples of risks that were considered to be transferable to a greater extent to the private sector using the DBFO option but, in the opinion of the project team, were less likely to be transferred in the PSC option, included:

- capital cost and construction risks – including schedule delays, latent defects³ and cost overruns;
- operating, maintenance and rehabilitation cost risks – including management of life-cycle costs;
- financial risks – including insurance risks during construction and a portion of insurance risks during the operational period; and
- traffic management risks – during construction and on an ongoing basis.

Schedule and Cost Efficiencies

Based on their experience on previous projects, the project team identified the potential for the contractor to realize schedule and cost efficiencies, resulting from:

- greater flexibility in detailed design, construction management, traffic management, and schedule achievement across the whole project when integrated by a single contracting party rather than as multiple separate contracts;
- accounting for life-cycle costs when developing design and operations and maintenance procedures;
- standardizing design elements and construction methods for structures;
- pooling geotechnical risk and recovery from poor conditions at any particular site;
- comprehensive equipment, labour and materials planning;
- improved risk distribution for the contractor across a larger portfolio of work segments; and
- pooling insurance costs.

Despite the longer competitive selection process required to develop and negotiate the DBFO, MoT believed that the financial incentives and penalties in a final contract would result in a shorter construction period and that more schedule predictability could be achieved.

2. Competitive Selection Process

The competitive selection process was designed to:

- select a qualified private sector contractor to design, build, and finance the improvements to the portion of the Sea-to-Sky Highway Improvement Project not utilizing the two DB contracts; and operate, maintain and rehabilitate the whole corridor; and

- be a fair, open and competitive process.

Annual Affordability Ceiling

MoT established an annual affordability ceiling to drive proponents to maximize scope within a fixed price.

Proposal evaluation usually involves some element of low price competition in which the specifications or outcomes are set and proponents provide a price. For the Sea-to-Sky DBFO project, this process was reversed – the maximum price that MoT was prepared to pay for the private sector portion of the baseline highway improvements and for operations, maintenance and rehabilitation of the entire corridor was prescribed in the Request for Proposals (RFP) document (in the form of an annual affordability ceiling, or AAC). To arrive at the AAC, MoT financial advisors combined the capital, operating, maintenance and rehabilitation cost inputs estimated for MoT delivery using a series of DB contracts together with the assumed financial structure for the DBFO project into a project finance model. This was done to estimate what the required annual maximum allowable performance payments from the Province would need to be to meet financial commitments typical for such a transaction. By establishing the AAC, MoT encouraged proponents to compete in terms of what additional improvements they were willing to contractually commit to for that price.

Proponent Consultation Process

The consultation process was designed to increase proponents' understanding of the contract requirements and to encourage their feedback throughout the process to improve the final contract, while maintaining competitive tension and fairness in the process.

Features of the proponent consultation process included:

- a series of meetings between the project team and each of the proponents covering a range of topics (examples include technical issues, highway design, construction schedule and traffic management, quality management, risk allocation, payment mechanism, and the contract); and
- MoT and proponents had the opportunity to exchange information, engage in dialogue, and clarify issues related to the RFP, including the form of the contract. The intention was for proponents to gain a better understanding of the project and to improve the contract.

3. The Final Contract

The final contract between MoT and the S2S Transportation Group is a 25-year performance-based contract designed to deliver safety, reliability and capacity improvements.

Profile of the S2S Transportation Group

The S2S Transportation Group (S2S) includes:

- Macquarie North America Limited is the financial advisor to S2S and is a member of the Macquarie Group, a global investment bank which invests in and develops infrastructure assets and manages infrastructure funds worldwide.
- Peter Kiewit Sons Co. is the project design/build contractor with North American experience in transportation design/build projects, and is a civil contractor with more than 60 years of building experience.
- JJM Construction Limited is a B.C. road builder and has constructed portions of the Island Highway and other rock excavation work.
- Hatch Mott MacDonald (HMM) will lead the design for Peter Kiewit Sons Co. HMM is a North American transportation consultant, having designed more than \$15 billion worth of transportation projects worldwide. HMM will be supported by ND Lea, McElhanney Engineering Services Limited and Urban Systems Limited. These firms provided approximately two-thirds of the preliminary design for the Sea-to-Sky project.
- Miller Paving is a provider of highway operations, maintenance and rehabilitation services in Canada.
- Capilano Highway Services has more than 15 years of maintenance and operations experience on the Sea-to-Sky Highway.

S2S is financing the project through two primary sources of funds - equity and senior debt. Equity is provided by Macquarie Essential Assets Partnership (MEAP), a Macquarie-managed fund focused on investing in North American infrastructure assets which has committed capital primarily from Canadian pension funds and other Canadian institutional investors. Senior debt is provided by way of arrangements between S2S and Royal Bank of Scotland and Société Générale.

Key Terms of the Performance-Based Contract

The contract is designed to protect the public interest by specifying service standards, with financial incentives to meet the standards through the use of underlying performance payments. The key terms of the contract include:

- S2S will design, construct, and finance its portion of the baseline highway improvements;
- S2S will provide additional highway improvements incremental to its portion of the baseline improvements;
- S2S will operate, maintain and rehabilitate the whole corridor;
- S2S will receive payment from MoT for fulfilling its contractual obligations, with financial incentives to achieve the project schedule, and ensure reliable service after construction is completed. These payments are comprised of availability payments, vehicle usage payments and performance incentive payments. The performance incentive payments include:

- a traffic management payment during construction, which is contingent upon adherence to the traffic management plan set out in the contract. For example, if S2S exceeds the number and duration of stoppages or closures set out in the contract, the traffic management payment will be reduced. The maximum traffic management payment is \$2.1 million per year; a payment which is earned if the safety performance of the highway exceeds the Provincial safety performance record for comparable highways. The maximum bonus in a given year is \$1 million;

▸ If S2S fails to meet the specified performance standards, MoT will be entitled to make deductions from the availability payment.

Examples include the following:

- penalties will be applied where S2S has failed to meet the operations and maintenance standards;

- deductions will be made from the maximum allowable performance payments based on the travel time delay experienced by road users; and

- deductions will be applied where sections of the highway have been unavailable;

▸ S2S will assume certain risks, such as construction schedule and budget;

▸ S2S is responsible to ensure that, at the end of the contract term, the asset meets certain conditions (e.g. that the highway's running surfaces and bridge decks meet the agreed-upon criteria). If the highway meets all the end of term requirements, the payment to S2S is \$50 million (\$2030). If the highway does not meet the requirements, the payment can be reduced by MoT's cost required to meet them. If the highway exceeds the requirements, the payment can be increased by the additional value of the highway up to a maximum of \$10 million (\$2030);

▸ MoT has the ability to monitor compliance against contractual requirements;

MoT is able to have further improvements made to the highway at its own option and cost. Latent defects in portions of the highway not constructed by S2S are not part of the future works item as MoT is obligated to repair any such defects;

▸ MoT retains ownership of the highway and S2S is granted a non-exclusive license (not ownership) for 25 years to access and use the highway and its structures for the purpose of carrying out the operations;

▸ S2S is prohibited from charging tolls;

▸ MoT has the right to perform work itself where S2S fails to do so and to offset related costs against future payments to S2S;

▸ formal dispute resolution provisions give MoT the ability to pursue a measured response to deficiencies, up to, and including contract termination;

▸ the amount payable to S2S assumes the Provincial Base Case traffic forecast. For example, in any given year, a 10 per cent variance in traffic volume (either increase or decrease) results in a 1.2 per cent change in the payments to S2S.

4. Achieving Value for Money

MoT believes value for money for this project is demonstrated because of the additional improvements, and the anticipated user benefits that flow from them, provided in the DBFO contract.

Value for money represents the relationship between costs and benefits of a project, and includes quantitative and qualitative factors. As noted earlier, for the Sea-to-Sky DBFO project, the typical MoT evaluation process was reversed so proponent proposals would be evaluated for the additional improvements beyond the baseline they would provide.

Cost:

The expected cost of the Project to the Province is \$789.8 million Net Present Cost (NPC \$2005) over the 25-year contract.⁶ This amount includes the capital cost of MoT's DB contracts and the costs of annual payments to S2S for providing its portion of the baseline improvements and the additional improvements, and for operating, maintaining and rehabilitating the entire corridor. By comparison, MoT estimates that the NPC of the risk-adjusted PSC, which excludes the additional improvements, would be \$744.0 million (\$2005). While the cost of the DBFO contract exceeds the expected cost had MoT pursued a series of DB contracts (the PSC), MoT asserts the qualitative benefits demonstrate value for money.

Cost Components

1 Capital expenditures are based on a series of design/build contracts and include other acquisition costs, such as land. The increase of \$0.1 million, from \$515.9 to \$516.0 million NPC reflects a change in the RFP evaluation date. Thus, the amount of work on highway improvements undertaken by MoT occurred over a slightly longer period of time and MoT expenditures were higher than the amount in the December 2003 PSC.

2 In addition to operations and maintenance required to keep the highway open to traffic every day, this figure includes adjustments for other MoT-incurred costs including:

- signals and lighting;
- electrical power and maintenance;
- line painting, avalanche control and weather stations;
- rock scaling; and

- a portion of annual overhead costs for management and administration of the Highways District. The net increase of \$1.8 million (from \$105.7 to \$107.5 NPC) is the difference between:
- \$31.7 million NPC increase that reflects the project team's and their technical advisors' improved understanding of the costs entailed in maintaining the highway to the baseline operations and maintenance requirements.

And

- \$29.9 million NPC decrease in assumed financing costs. In December 2003, financing for the capital expenditure and operation of the Project was a combination of the available MoT funding during the construction period and third party financing where expenditure requirements exceeded MoT's available funding. By December 2005 this financing assumption was no longer required and the PSC was adjusted accordingly.

3 Rehabilitation is the major repairs that are undertaken periodically to optimize the life-cycle of the highway. Rehabilitation costs increased by \$3.6 million (from \$32.7 to \$36.3 million NPC) to reflect additional information about the final highway inventory, increases in pavement rehabilitation costs due to rising oil prices and better specific asset condition information.

4 The risk adjustment reflects how the risks for this project (described in Chapter 3) were valued by the project team and its advisors. The risk adjustment increased by \$4.0 million (from \$38.9 to \$42.9 million NPC). This increase reflects the value assigned to the risks by the project team as they changed between December 2003 and just prior to receipt of the RFP submissions. Some risk estimates increased (schedule, contractors cost over-runs, increase in operations and maintenance costs, asset performance, complexity of procurement process, ability to resource), while others decreased (owner's cost over-runs, management of life-cycle costs, and insurance). For some risks, there was no change.

5 The competitive neutrality adjustment is made to ensure that the PSC does not reflect any competitive advantage that would simply be the result of public sector ownership. This allows a like-with-like value for money assessment. Without a competitive neutrality adjustment, the PSC may be artificially low and not reflect the full costs to government. The competitive neutrality adjustment decreased by \$21.2 million (from \$62.5 to \$41.3 million NPC) to reflect the final tax payable under S2S's corporate structure. The final amount (\$41.3 million NPC) adjusts for the tax-exempt status of public sector corporations (\$4.2 million) and the self-insurance policy of the Province (\$37.1 million).

6 MoT capital costs include MoT capital expenditures on the DB portions of the Sea-to-Sky Highway Improvement Project, contingency and all land acquisition costs. The MoT capital costs increased by \$62.1 million NPC, (from \$146.0 to \$208.1 million NPC). The increase is due to finalization of the scope of work for the DB portions, higher land acquisition costs, and transfer of responsibility for a portion of the contingency from S2S to MoT.

7 MoT will continue to have some responsibility for operations and maintenance, largely through its role in overseeing the project and contract administration costs. The NPC of the operations and maintenance costs paid for by MoT decreased by \$7.4 million NPC (from \$10.6 to \$3.2 million NPC). The decrease reflects additional responsibilities transferred to S2S in the final contract, including responsibility for operations and maintenance of the MoT DB sections as they are completed.

8 With responsibility for Sea-to-Sky Highway rehabilitation being fully transferred to S2S, MoT does not incur rehabilitation costs. MoT rehabilitation costs decreased from \$2.0 million NPC to \$0. The December 2003 calculation assumed that MoT would retain responsibility for rehabilitation of the DB sections over the term of the contract. The final agreement stipulates that S2S is responsible for rehabilitation for the whole highway.

9 The payment to S2S is for design and construction of highway improvements on approximately two-thirds of the corridor and operations, maintenance and rehabilitation of the full corridor to the performance standards in the contract. The payment to S2S over the term of the contract increased by \$48.3 million (from \$530.2 to \$578.5 million NPC). The increase was made to the AAC during the RFP process and all three short-listed teams based their submissions on the revised AAC. The revision was based upon the project team's consideration of cost pressures identified by proponents and independent information provided by technical advisors. The specific cost pressures were:

- the improved understanding of both the project team and proponents of the costs of achieving the operations and maintenance obligations required by the incentive based contract. The contract requires that S2S meet standards that are comparable or equivalent to the standards applicable on other highways in B.C. The consequences to S2S for failing to meet the required standards are sufficiently significant that the overall result should be that S2S maintains the highway to a level that is, on average, higher than the maintenance level attained on other highways in B.C.
- labour cost inflation and shortages;
- oil and fuel cost increases;
- higher than anticipated requirements for the condition of the asset at end of the contract term and rehabilitation costs; and
- no opportunity to adjust the payment over the contract term for unanticipated inflation. In the judgment of MoT and its project advisors, these changes were appropriate. As shown on page 17, the capital cost shown in the PSC did not materially change between 2003 and 2005.

Expected User Benefits

One of the goals of any road improvement project is to produce benefits for road users, such as improved safety or shorter trip times. For example, the purpose of adding a passing lane would be to improve the capacity of that section of the road and to reduce the number of collisions. MoT believes that one indication of the value for money provided by the DBFO is a calculation of the anticipated user benefits resulting from the additional physical improvements provided under the DBFO.

Road user benefits can be calculated as:

- those benefits that would be expected from the construction of the baseline improvements; and

- those benefits that result from the additional improvements that S2S will provide through its contract with the Province. The MoT project team calculated the expected road user benefits arising from the highway improvements that private sector proponents included in their proposals in response to the RFP. In this exercise, not all benefits could be quantified. For example, today's highways throughout B.C. include many features that provide for a safer highway relative to the design criteria that were not in place when the road was first constructed. Although these improvements are not specifically calculated (and thus any estimation of their value is a professional engineering judgment factor), they include things such as:

- wider shoulders, with allowance for bicycle passage;

- highways designed for larger vehicles; and

- interchanges to provide safe entrance and exit to the highway for vehicles. To estimate the expected user benefits, there is a common international approach used for estimating travel time savings and safety benefits in transportation projects. By applying this approach, along with a degree of professional judgment, MoT estimates the user benefits for major transportation projects in B.C. By applying this quantitative approach to the additional improvements obtained through the DBFO, MoT has estimated the expected benefits to be realized by road users as (all benefits are presented in net present value (NPV) terms):

1. Road improvements that result in reduced travel times and thus generate travel time savings. When people use their time to travel there is an opportunity cost equal to the value they place on the next best alternative activity.

- a. Estimated anticipated user benefits from incremental improvements: \$48 million from completion of construction in 2009 to end of contract term in 2030.

- b. Estimated benefits provided by baseline improvements over existing highway: \$279 million.

2. Safety improvements reduce accidents. Current standard values for accident costs have been derived from international research by MoT.

- a. Estimated anticipated user benefits from incremental improvements: \$74 million from completion of construction in 2009 to end of contract term in 2030.

- b. Estimated benefits provided by baseline improvements over existing highway: \$148 million.

3. Additionally, by S2S reducing road closures by 50 per cent over the road closure plan developed by MoT for the baseline improvements, savings in travel time costs will be generated by reducing the number and duration of delays incurred by road users.

- a. Estimated anticipated user benefits: \$9 million. These benefits are realized only during the 2005-2009 construction period.

The sum of the expected user benefits from the incremental improvements is estimated to be \$131 million NPV over the life of the contract. To put these in perspective, benefits provided by the baseline improvements are estimated to be \$427 million NPV over the life of the contract. In the opinion of MoT and its advisors, the benefits resulting from the incremental improvements are in the order of 15 to 30 per cent above the expected benefits of the baseline improvements. The generally accepted method for evaluating a project's costs and benefits is to compare the incremental differences between undertaking and not undertaking the project. If MoT had chosen to leave Highway 99 as is (i.e. not undertake either the DBFO or the PSC), it would still

have incurred operations, maintenance and rehabilitation (OM&R) costs. In MoT's opinion, the OM&R costs it would have incurred if it had not undertaken the project would have been similar to those of the PSC. Therefore, MoT would determine the benefits of the Sea-to-Sky Highway Improvement Project by comparing the total incremental benefits of the project to the incremental costs, which are approximated by the total costs of the DBFO less the OM&R costs of the PSC.

In summary, MoT believes value for money will be demonstrated for this project because of the additional improvements, and the anticipated user benefits that flow from them, provided in the DBFO contract.

5. Ongoing Contract Monitoring

MoT oversee the project, ensuring that contractually committed standards are met.

Under the contract terms, S2S is required to register for, and maintain the standards of, the ISO 90007 program, a program that focuses on maintaining good management standards. Penalties will be incurred by S2S for non-compliance.

Design and Construction Period

The design of the project is the responsibility of S2S, who must certify that the design complies with the contractual requirements in all respects. As well, S2S' work must pass two interim reviews by MoT (at 50 per cent design and at 90 per cent design). MoT will provide comments on submittals to ensure contractual obligations are met.

Operations

Under the terms of the contract, S2S is responsible for operating the highway and for maintenance and rehabilitation. Outcome-based specifications determine the work required by S2S, which is subject to performance auditing by both S2S and MoT. MoT retains a number of ongoing responsibilities, including integration with the provincial highway system, managing side road rehabilitation, and managing highway operations during the Olympic period in 2010.

Reference: Project Report: Achieving Value For Money – Sea-to-Sky Highway Improvement Project, Partnerships BC, December 2005

(BC, 2005)



Sea-to-Sky Highway Improvement Project

Development of Grading Requirements for Drought Weather Conditions

By

James B. Nevels, Jr., Ph.D., P.E., PLLC
Geotechnical Engineering Consultant
605 Mimosa Dr. Norman, OK 73069-8622

Introduction. In a recent case history involving longitudinal cracks that developed in two re-constructed city streets within weeks following the completion of the paving and opening up to traffic, forensic work was completed to explain the causes for the cracking. The question was asked by the City of Norman of the project geotechnical engineer, Burgess Engineering and Testing, Inc. (BETI), to explain why the newly constructed pavements developed predominantly longitudinal cracks within weeks following completion of the paving. A compounding factor in this forensic study was the fact that the geotechnical engineer requested that the explanation of the longitudinal cracking be done with minimum of testing and cost. This request necessitated the use of estimated soil properties.

In the investigative process it became apparent that construction grading practices were partly to blame for the cracking in the pavements. In the final analysis of re-constructed pavement subgrades, the concept of treating a subgrade at its equilibrium moisture content that had been covered for an extensive time period as an asset is recommended.

The paper first discusses the case history for two City streets – Himes and Johnston, followed by drought indices and then a strategy to minimize the effects of drought weather conditions in grading operations.

Site History. The site location of Johnson and Himes streets is in a housing tract known as the Sooner Homes Addition platted on December 05, 1947, see an excerpt from the 1947 plat in Figure 1. The housing addition at the time of platting was immediately south of Robinson Street and the U.S. Naval Air Base and bordered by Flood Street and the Norman Interurban Railway. The subdivision at the present time is bordered by Flood and Robinson streets and the Burlington Santa Fe Railroad tracks. The original Sooner Homes Addition consisted of a tract composed of four city streets: Hayes, Moasier, Himes and Johnston streets. The completion time of the construction of the original concrete pavement for all the subdivision streets was not recorded by the City of Norman but is believed to have been completed in the early 1950's.

BETI performed and reported a preliminary geotechnical and pavement investigation report of Hayes, Moasier, Himes and Johnston streets for the project designer, Cardinal Engineering, Inc. on November 11, 2011. Cardinal Engineering, Inc. prepared the design plans for the City of Norman, Oklahoma in August 10, 2011. The City of Norman let a contract to Shell Construction, Inc. in their street replacement program to re-construct Moasier, Himes and Johnston streets in April 2012. This pavement re-construction work took place between May

and September of 2012. The original concrete pavement of Hayes Street is still in place but has been overlaid with asphalt for several years earlier. The project site is in a residential area in the north part of the City of Norman, Oklahoma in Cleveland County. The streets of the Sooner Addition run from west to east. The lineal extent of new pavement for Himes Street is 811.42 feet and the lineal extent of the new pavement for Johnston Street is 927.28 feet. The site location of Himes and Johnston Streets in reference to arterial streets and the present day Burlington Northern Sante Fe railroad is shown in Figure 1.



Figure 1. A October 12, 2011 Google Earth view of the Sooner Homes Addition.

The street construction required the removal of the old 6 inch concrete slab pavement installed in the early 1950's. The new pavement section consisted of 6 inch asphalt pavement placed in two lifts (bottom 4 inch layer and a top 2 inch layer) underlain by a 6 inch thick hydrated lime modified subgrade base course. A detail for the pavement section for these streets is shown in Drawing No. ST 01 taken from the City of Norman Engineering Criteria for Streets, Storm Drains, Water Lines and Sanitary Sewers, Amendment No. 8b: July 11, 2006, see Figure 2.

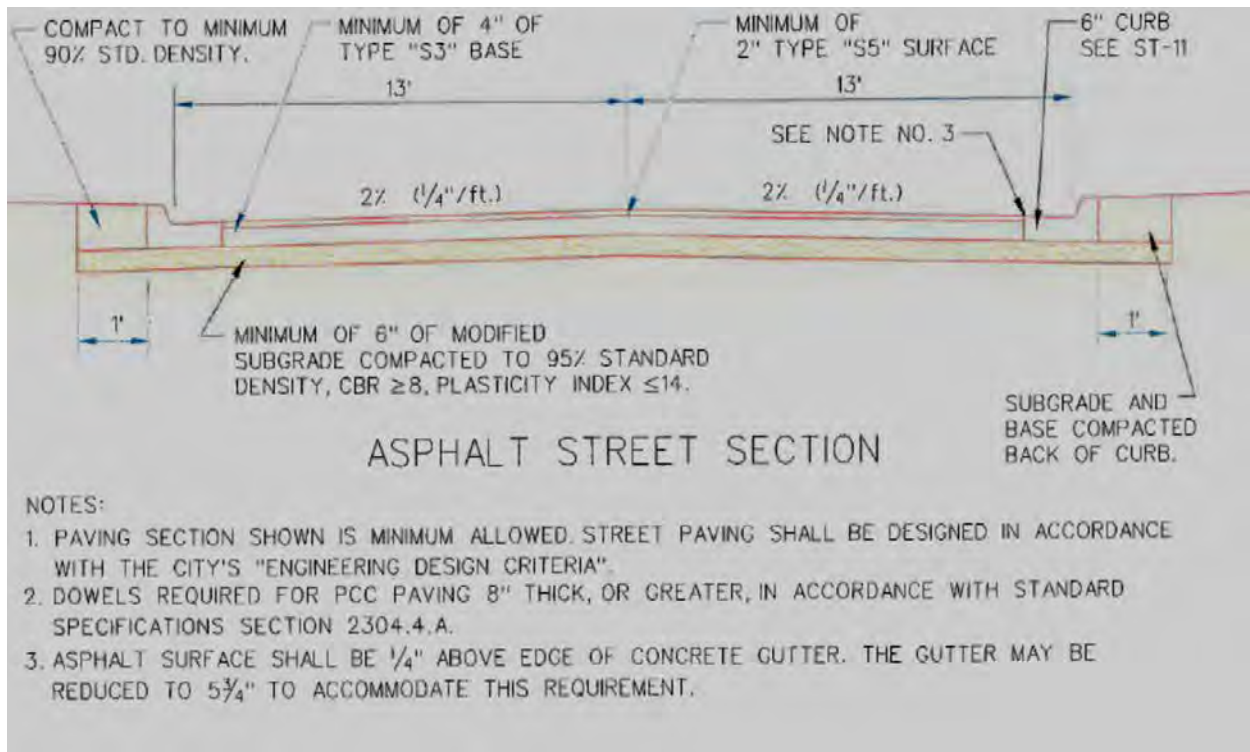


Figure 2. City of Norman Drawing No. ST 01 for asphalt pavement typical section.

The pavement is lined with 4 inch mountable concrete curb. The sequence of construction was estimated to be the following: a.) construct 6 inch thick hydrated lime modified subgrade base course, b.) install the 4 inch the integral mountable concrete curb, and c.) construct the two asphalt pavement lifts.

The design plan cross-sections developed by Cardinal Engineering indicates that the average depth to the top of the finished subgrade below the natural surrounding ground line for Himes and Johnston Streets was respectively 1.02 and 1.31 feet – relatively at a grass root grade. The design plans also show the canopy of trees that overhang Himes and Johnston Streets. Some smaller trees adjacent to the curb line where the canopies also overhang into the streets were not recorded on the design street plan views. A visual count of all trees that are influencing the pavement subgrade was made by a thorough walkout of Himes and Johnston Streets. A total of fifteen trees were counted on Himes Street and sixteen trees were counted on Johnston Street.

Pavement Distress. During and following the pavement re-construction in the spring and summer of 2012, the asphalt separated from both integral mountable concrete curbs throughout the lengths of the pavement re-construction for both Himes and Johnston Streets. The crack widths were observed to range from a 1/8 to 1/2 inch. Longitudinal cracks were also seen to develop under the canopies of the larger trees and in a few non-tree areas. In addition a

diagonal crack was observed paralleling along the side of a subsidence above an 18 inch corrugated metal pipe at approximate center line station 7+08.45.

Surface Soils. According to the current USDA Natural Resources Conservation Service (NRCS) Web Soil Survey 3.1, the mapped soil series underlying the lineal extents of both Himes and Johnson Streets are the Kirkland–Urban land–Pawhuska complex, 0 to 3 percent slopes (49) and the Bethany–Urban land complex, 0 to 3 percent slopes (59). The results of the Web Soil Survey 3.1 include the following: soil survey; the soil series extended soil information; and the Official Soil Descriptions (OSD) of the Kirkland, Pawhuska, and Bethany soil series.

An enlargement of soil map from the Web Soil Survey 3.1 is shown in Figure 3. Based on Figure 3 the Kirkland–Urban land–Pawhuska complex soil series is the predominately mapped soil unit along the lineal extents of both of these streets. The distribution of the Kirkland–Urban land–Pawhuska complex and Bethany–Urban land complex soil series is also seen in an enlarged soil map from the Web Soil Survey 3.1, see Figure 3. Based on Figure 3, the approximate percentages of the Kirkland–Urban land–Pawhuska complex and Bethany–Urban land complex are respectively 632 feet (72.34 percent) and 241.6 feet (27.66 percent) along the lineal extent for Himes Street and 620 feet (69.43 percent) and along the lineal extent for Johnston Street 273 feet (30.57 percent) for Johnston Street.



Figure 3. Web Soil Survey 3.1 for the Sooner Homes Addition.

A review of the Cleveland County Soil Survey (April 1987) indicates that the soil series along Himes and Johnston Streets have been re-correlated in the Web Soil Survey 3.0. The Doolin–Urban land–Pawhuska complex, 0 to 3 percent slopes (49) has been changed to the Kirkland–Urban land–Pawhuska complex, 0 to 3 percent slopes (49) in the Web Soil Survey 3.0. The Bethany–Urban land complex, 0 to 3 percent slopes (59) remained the same. The map unit boundaries in the Cleveland County Soil Survey sheet number 22 have essentially stayed the same as seen in the Web Soil Survey 3.1.

Subgrade Characterization. Two auger borings were used in the subgrade analysis to characterize the Kirkland and Bethany soil profiles with depth, see Figures 4 and 5 respectively.

Soil classification and index properties that were used in this subgrade soil analysis were taken from a hand auger boring in a Kirkland soil series map unit approximately 1.30 miles northeast of the Himes and Johnson Street site location. The soil profile in this non-related project was sampled on July, 27, 2008. A hand auger boring of the Bethany soil series profile was made at the end of Johnston Street in City property.

An estimate of the shrinkage limit with depth was made from Arthur Casagrande equation, $S.L. = 20 +/\- \Delta p_i$, where Δp_i is the distance above or below the A–line in the soil plasticity chart (Holtz & Kovacs 1981). The dry unit weight was estimated from the tabulated primary characterization data found in the Web Soil Survey for selected Kirkland and Bethany soil series pedons in Cleveland County wide basis (NRCS 2013). From the primary characterization data base, two Kirkland soil series data sets and four Bethany soil series were found. The soil properties in the data set that matched the depths of the hand auger boring shown in Figure 4 was selected sub-grade soil analysis. The total unit weight and shrinkage limit estimates are shown in Table 1. The specific gravity of the Kirkland soil series soil horizons with depth was estimated at 2.70.

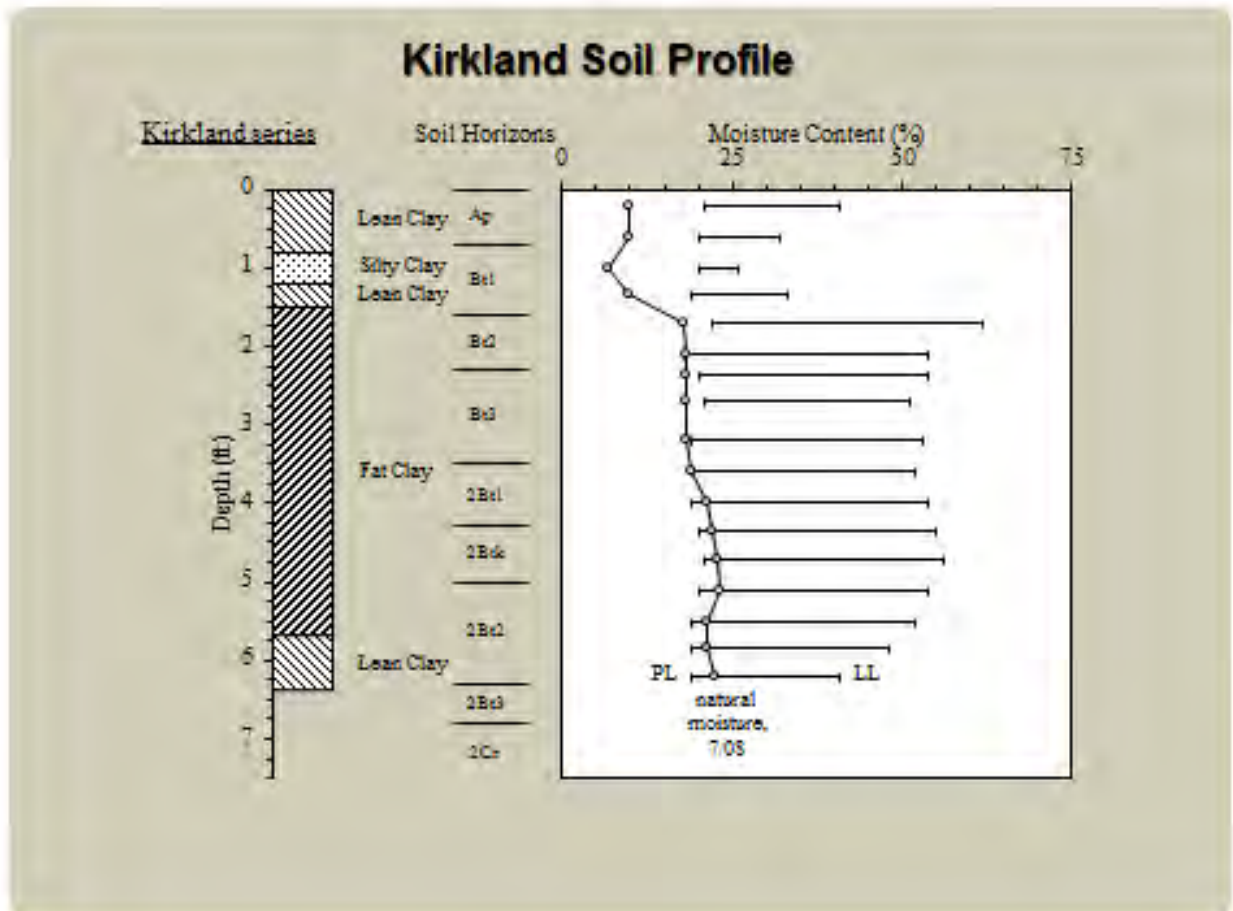


Figure 4. Kirkland soil series profile.

Table 1. Kirkland soil series shrinkage limit estimate

Horizon	Horizon Depth m	γ_d kg/m ³	M.C. %	γ_m kg/m ³	S.L. %
Ap1	0.00 – 0.12	1710	9.99	1880	*
Ap2	0.12 – 0.27	1640	9.77	1800	*
Bt1	0.27 – 0.37	1690	6.73	1800	*
Bt2	0.37 – 0.51	1860	9.68	2040	13
Bt3	0.51 – 0.67	1800	18.07	2130	10
Bt4	0.67 – 0.85	1940	18.13	2290	11
Btk1	0.85 – 1.17	1660	18.78	1970	12
Btk2	1.18 – 1.44	1880	22.08	2300	11
Btk3	1.44 – 1.74	1800	23.06	2220	11
Btk4	1.74 – 2.04	1930	22.37	2360	13
Btk5	2.04 – 2.38	1760	24.75	2200	14

* Profile was excavated to 0.4 m.

The in situ moisture contents used in the analysis were taken from eight auger borings in the BETI report. These auger borings were augered to a depth of 2.99 feet. The eight moisture content measurements were all made in the subgrade soils at 0.98 and 2.49 foot depths on Himes and Johnson Streets.

Subgrade Soils. A subgrade analysis was made for both the Kirkland and Bethany soil profiles, and analysis for the Kirkland soil series is presented, see Figure 6. The in situ moisture contents from the BETI report were observed to be very wet, close to or in excess of the plastic limit. The highest in situ moisture content at 0.98 feet was 25.7 percent, and the highest moisture content at 2.49 feet was 21.9 percent, and these values were used to establish a wet moisture profile shown in Figure 6.

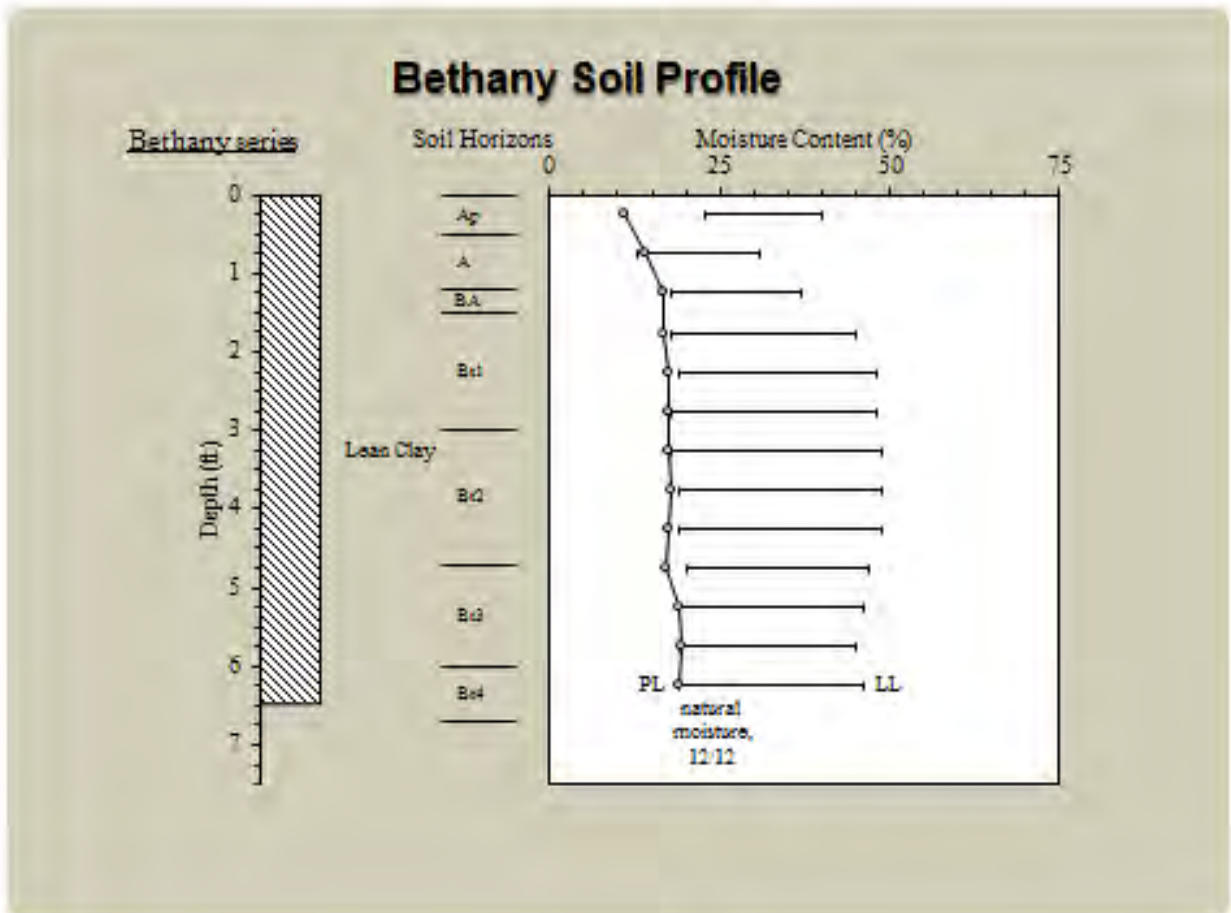


Figure 5. Bethany soil series profile.

Kirkland series

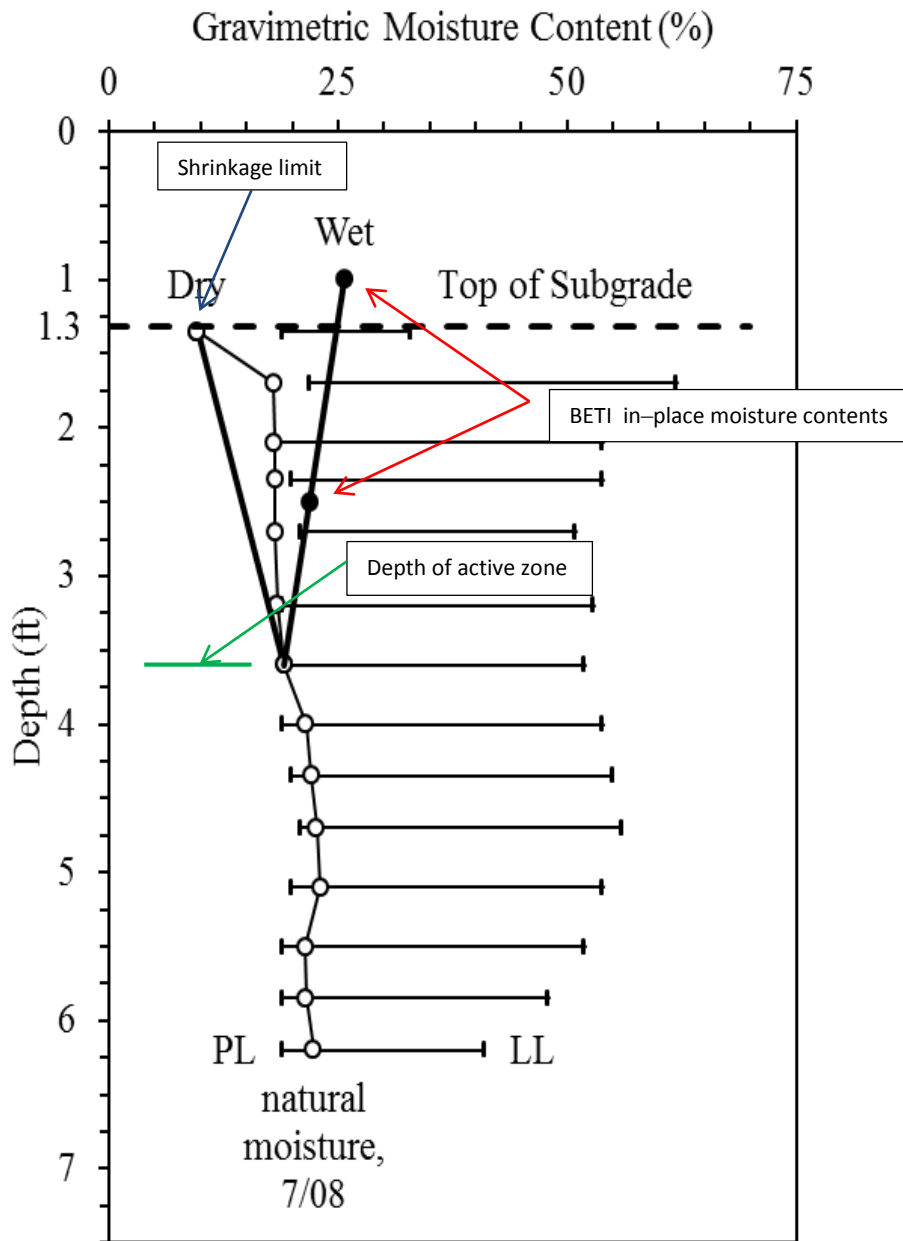


Figure 6. Estimated wet and dry moisture profiles.

The Kirkland soil moisture profile in Figure 4 was adjusted to the top of the average finished subgrade depth of 1.31 feet below the natural surrounding ground line (Johnson Street) for the soil analysis, see Figure 6. As seen in Figure 6, the wet moisture profile is extended to an intersection with the in situ moisture profile to establish the active zone at approximately 3.61 foot depth below the ground surface.

Below an active zone depth of 3.61 feet, the underlying moisture contents with depth are assumed not fluctuate much.

Observe in Figure 6 that the in situ moisture profile in Figure 4 is close to the shrinkage limit estimated in Tables 1 at the finished subgrade depth at depth of 1.31 feet. A dry moisture profile is estimated as a straight line from the shrinkage limit to the depth of the active zone at 3.61 feet. The idealized initial and final moisture profile with depth is shown in Figure 3 and this procedure is reported by Nelson & Miller (1992).

Climatic Conditions. At the time of the re-construction of Himes and Johnson Streets, the City of Norman as well as much of Oklahoma experienced a very dry year. A snap-shot of the climatic conditions was developed for an approximately 10 year period preceding and including the construction time frame for these city streets.

The Thornthwaite Moisture Index (TMI) (Thornthwaite 1948) and the designated time of construction are presented in Figure 7. Referring to Figure 7, the time of construction is in a negative TMI zone indicating a dry sub-humid climatic condition. During the construction time frame, the TMI indicates that the slight drying and wetting. Following the construction period, the TMI suggests that drying continues.

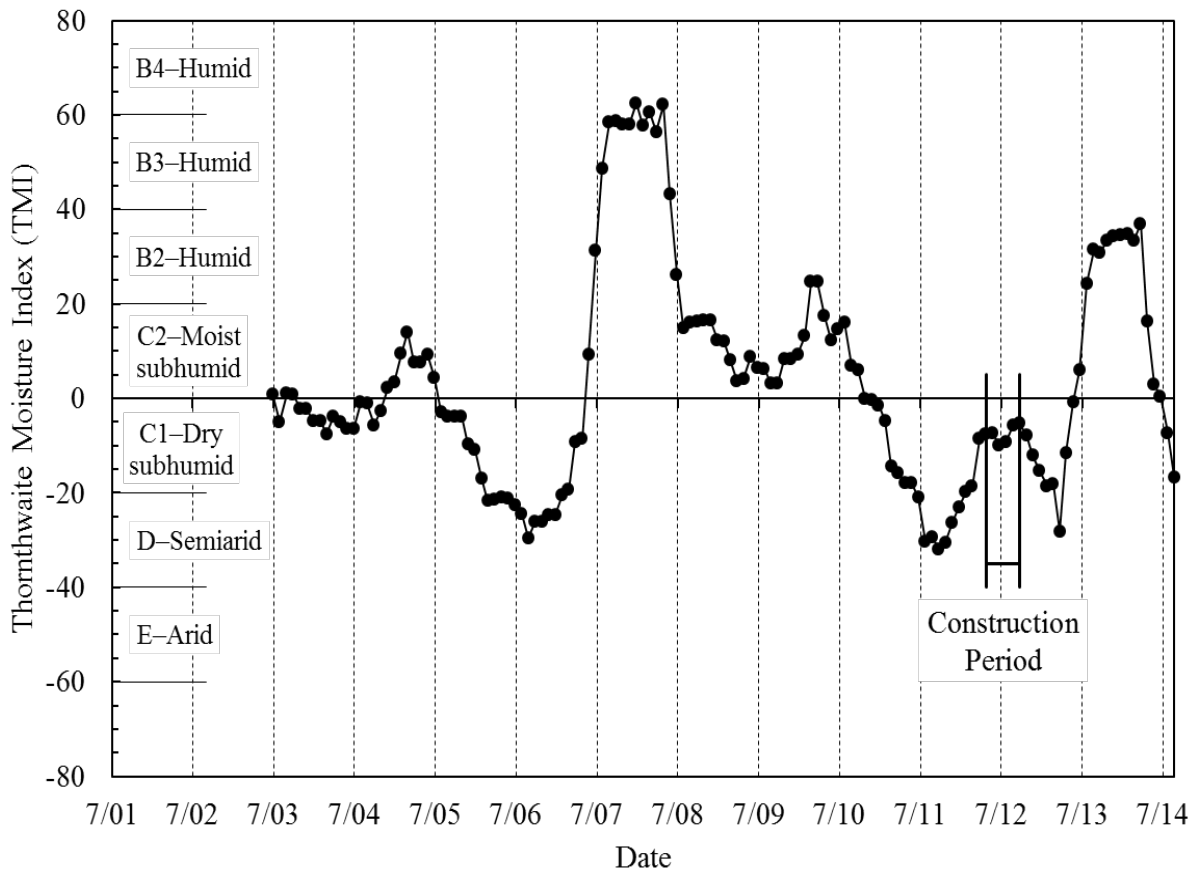


Figure 7. Thornthwaite Moisture Index (TMI) versus time at the site.

At the start of the re-construction of Himes and Johnson Streets, the subgrade soil was observed to be in a very wet state as evidenced by the BETI report subgrade moisture contents at or exceeding the plastic limit. It is assumed that the water content of the subgrade under old concrete had reached a state of equilibrium over a period of approximately 60 years. The tree root system of fifteen trees on Himes Street and sixteen trees on Johnson Street was also assumed to be in equilibrium. In recent geotechnical literature Blight (2013) points out that water at the field capacity is never constant but dynamic. The pavement construction continued while desiccation of the in-place subgrade was occurring from the root systems of the 15 trees on Himes Street and sixteen trees on Johnson Street.

Soil Moisture Deficit. The climate at the time of re-construction of Himes and Johnson Streets was in a very dry condition. In order to quantify the potential shrinkage occurring in the subgrade soil once the old concrete pavement was removed, an estimate of the soil moisture deficit was utilized. The soil moisture deficit defined by Biddle (1998) refers to the amount of water which needs to be added to a soil profile to bring it to its normal moisture content or field capacity. The soil moisture deficit (SMD) calculated for the idealized initial and final moisture profile with depth is shown in Figure 8 and presented in Table 2. The SMD is shown over a twelve-year period in Figure 8. The SMD during the re-construction period is shown in Figure 9. Here the SMD is based on an estimate of the potential evapotranspiration rather than the actual evapotranspiration.

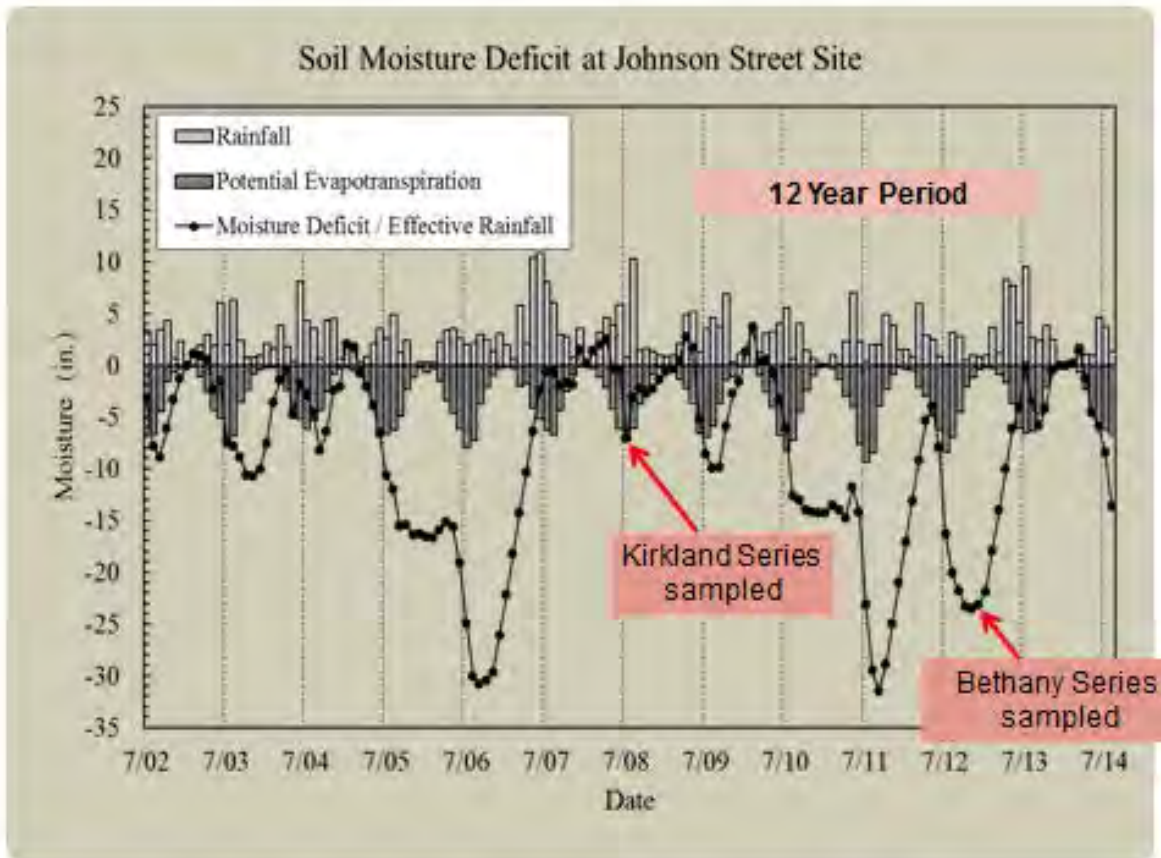


Figure 8. Soil moisture deficit versus time at site.

Table 2. Soil moisture deficit and shrinkage calculations.

Depth (m)	0.4	0.5	0.6	0.8	0.9	1.0	1.1
Dry unit weight ¹ (kg/m ³)	1860	1860	1800	1940	1660	1660	1660
Estimated dry profile, gravimetric moisture ²	9.68	11.15	12.84	14.52	15.99	17.47	19.15
Estimated dry profile, volumetric moisture ³	18.00	20.74	23.11	28.17	26.55	28.99	31.79
Estimated wet profile, gravimetric moisture ⁴	24.78	23.90	22.89	21.88	21.00	20.12	19.15
Estimated wet profile, volumetric moisture ³	46.09	44.45	41.20	42.45	34.86	33.40	31.79
Layer soil moisture deficit (mm) ⁵	28.08	23.71	18.10	14.28	8.31	4.41	0.00
Cumulative soil moisture deficit (mm) ⁶	96.89	68.81	45.10	27.01	12.72	4.41	0.00
Layer shrinkage (mm) ⁷	7.02	5.93	4.52	3.57	2.08	1.10	0.00
Cumulative shrinkage (mm) ⁸	24.22	17.20	11.28	6.75	3.18	1.10	0.00

WSF=4.0

¹AASHTO T 233-02

²Based on 7/08 moisture profile

³Gravimetric moisture times dry unit weight divided by unit weight of water

⁴Based on BETI moisture profile

⁵Difference between wet and dry volumetric moistures

⁶Summation of moisture deficits from 1.14 m (bottom)

⁷Shrinkage = SMD/WSF, where WSF=4.0

⁸Summation of layer shrinkage from 1.14 m (bottom)

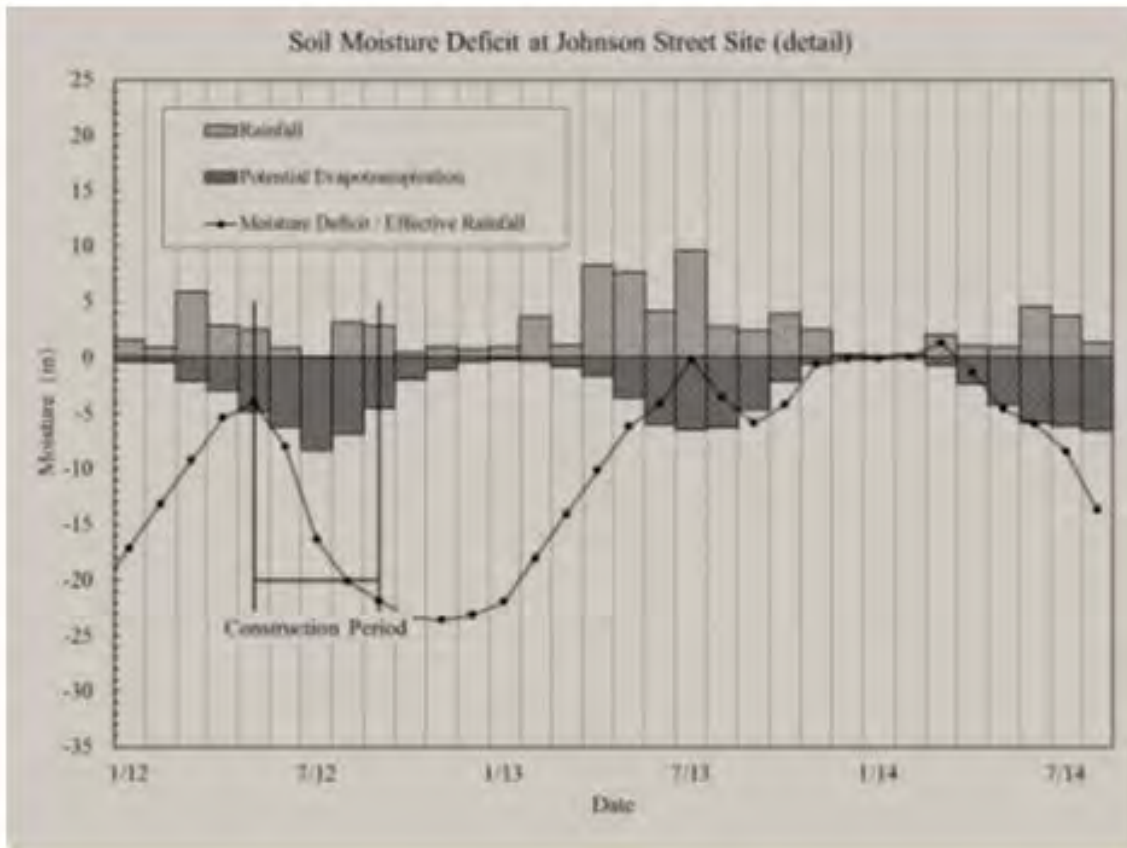


Figure 9. Soil moisture deficit during construction period.

As soil subgrade is drying out following the original pavement removal, shrinkage is assumed to occur in an isotropic state. The ratio of the SMD and vertical shrinkage is known as the water shrinkage factor (WSF). If drying in the subgrade soil is occurs while air can enter into the subgrade then the WSF can be greater than 3.

Soil Water Characteristic Curve. The soil suction change associated with the drying of the subgrade during and following the re-construction of Himes and Johnson Streets can be found from soil water characteristic curve (SWCC), see Figure 10. The SWCC used in this analysis was estimated using the Zapata fitting parameters in Fredlund and Xing equation (Fredlund et al. 2013) and is presented in metric units.

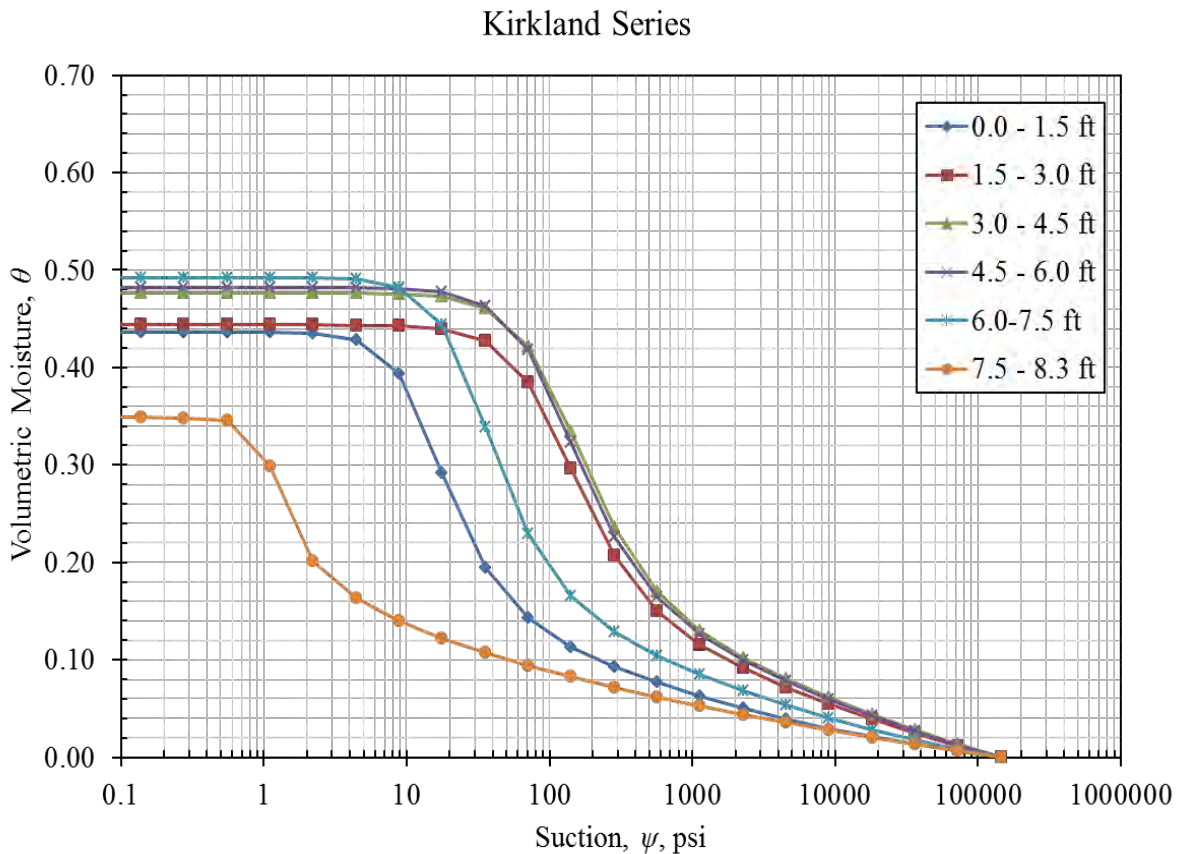


Figure 20. Soil water characteristic curves for the Kirkland soil series.

Based on the moisture contents and plasticity indices shown in Figure 4 for the depth of influence of the idealized initial and final moisture profile with depth shown in Figure 6, a SWCC was estimated between 1.39 and 3.02 feet. For the moisture contents (12 and 22 percent) a depth of 1.31 feet in Figure 6 the volumetric water contents were based on a weighted unit weight average and found to be 21.9 and 40.2 percent. From Figure 11 these volumetric water contents resulted in approximate suction increase of 195 psi.

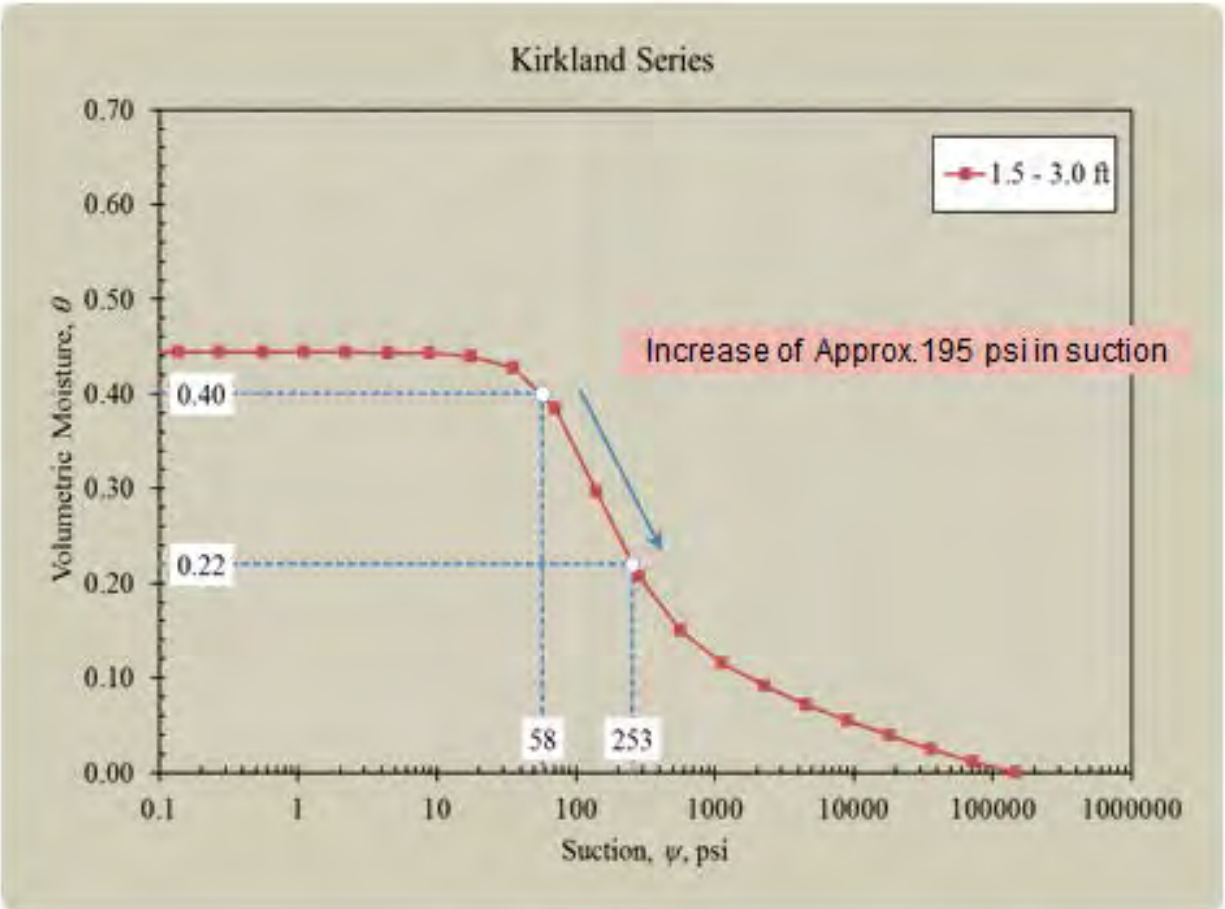


Figure 11. Soil water characteristic curves for the Kirkland soil series at 1.5 to 3.0 foot depth.

Conclusion. The conclusions reached in this case study are the following:

1. From the study of the SMD in this case history the site location is estimated to be prone to a persistent soil moisture deficit which can have adverse effects on construction.
2. The accumulation of water under the old pavement (a covered surface) was assumed to be in equilibrium but in reality is in a dynamic state of flux. Water content is being removed by the tree root systems as needed.
3. The increase in soil suction of approximately 195 psi represents a significant tensile stress and is assumed to have occurred. The prediction is approximate due to being based on the idealized initial and final moisture profiles. However, as seen in Figure 9, the SMD is continuing to decrease throughout the construction period and beyond.

Drought Indices. Common to all types of drought is the fact that they originate from a deficiency of precipitation resulting from an unusual weather pattern. There are five drought indices that are in common use by the National Drought Mitigation Center, and they are as

follows: a.) percent normal, b.) standardized precipitation index (SPI), c.) crop moisture index (CMI), d.) surface water supply index (SWAZEE), and e.) reclamation drought index.

The SPI because is significant because of the following features:

- It requires only monthly precipitation.
- It can be compared across regions with markedly different climates.
- The standardization of the SPI allows the index to determine the rarity of a current drought.
- It can be created for differing periods of 1 to 36 months.

The most important feature of the SPI with regard grading construction is that predications can be made up to 36 months in advance. The SPI is obtained by fitting a gamma or a Pearson Type III distribution to monthly precipitation values.

The SPI data can be obtained from the US Drought Monitor (droughtmonitor.unl.edu) from the National Drought Mitigation Center in Lincoln, Nebraska.

SPI drought ranges are as follows:

D0 – –0.5 to –0.7 abnormally dry

D1– –0.8 to –1.2 moderate drought

D2– –1.3 to –1.5 severe drought

D3 –1.6 to –1.9 extreme drought

D4 –2.0 or less exceptional drought

Specifications for Moisture Control. Predominately moisture control specifications for earthwork grading are found in most states to be laid down by the State Department of Transportation for State controlled construction projects. Public and private construction also tends to utilize the State Department of Transportation earthwork grading specifications. Typical grading specifications for the Oklahoma Department of Transportation are presented in Table 3. Research into modification of the moisture control with regard to drought weather conditions resulted in no significant data or information found.

OHD/ODOT Construction Specification

OHD/ODOT Construction Specification	Subsection 202 Embankment	Subsection 309 Rolling and Sprinkling	Subsection 310 Subgrade Method B	Subsection 408 Prime Coat	Comments
1954	Language	Maintain moisture content	Language	Prime Coat	
1959	Language	Maintain moisture content	Language	Prime Coat	
1967	Language	Language	Language	Prime Coat	
1976	Language	Language	Language	Prime Coat	
1988	Within 2 % of OMC	Language	Language	Prime Coat	A – 4 and A – 5 to within 3 or 4 points below OMC
1999	Within 2 % of OMC	Language	Within 2 % of OMC	Prime Coat	A – 4 and A – 5 to within 4 points below OMC
2009	Within 2 % of OMC	—	Within 2 % of OMC	Prime Coat	

Table 3. A history of the moisture control requirements of Oklahoma Highway Department/Oklahoma Department of Transportation.

Proposed Grading and Moisture Control Specifications for Drought Weather Condition. The control of the moisture loss at and immediately below the finished subgrade elevation (or grade line) is recommended to be controlled by the SPI drought index. The predication of the SPI drought range can found through US Drought Monitor (droughtmonitor.unl.edu) in advance of project grading letting, and apply the appropriate SPI medication to the grading contract. For all SPI ranges of drought apply a prime coat to seal the finish subgrade upon completion. For grading of A–6 and A–7 subgrades with SPI ranges of drought D2 through D4, compact the top two feet of the finished subgrade at 95 percent dry density and moisture content between 2 and 4 percent wet of optimum moisture content.

- D0 – Water finished grade upon completion a minimum of three times per day
- D1 – Water finished grade minimum of four times per day
- D2 – Water finished grade minimum of five times per day
- D3 – Compact finished subgrade to no less than 4 % wet of OMC. Water finish grade upon completion minimum of three times per day
- D4– Remove old pavement section in extents with minimum amount exposure to the atmosphere prior to performing grading operations and apply D3 criteria.

References:

- Biddle, P.G. 1998. *Tree Root Damage to Buildings, Volume 1*. Oxford: Willowmead Publishing Ltd.
- Blight, G.E. 2013. *Unsaturated Soil Mechanics in Geotechnical Practice*. London: CRC Press Taylor & Frances Group.
- Fredlund, D.G., Rahardjo, H., and Fredlund, M.D. 2013. *Un-saturated Soil Mechanics in Engineering Practice*. New York: John Wiley & Sons, Inc.
- Holtz, R.D. and Kovacs W.D. 1981. *An Introduction to Geotechnical Engineering*. Englewood Cliff, New Jersey: Prentice-Hall, Inc.
- Nelson, J.D. and Miller, D.J. 1992. *Expansive Soils: Problems and Practice*. New York: John Wiley & Sons, Inc.
- Soil Conservation Service (SCS) 1987. *Soil Survey of Cleveland County, Oklahoma*. Washington DC: US Department of Agriculture.
- Thornthwaite, C. W. 1948. An Approach toward a Rational Classification of Climate. *Geographical Review* 38: 55–94.

**MICROPILES IN KARST – THE NEW CENTRAL UTILITY PLANT AT
SHIPPENSBURG UNIVERSITY**

Jason M. Gardner, P.E.

Gannett Fleming, Inc.

207 Senate Avenue

Camp Hill, PA 17011

(717)-763-7211

jgardner@gfnet.com

Prepared for the 66th Highway Geology Symposium, September, 2015

Acknowledgements

The author would like to thank the following individuals/entities for their contributions in the work described:

Sara Frailey, P.E. – Gannett Fleming, Senior Geotechnical Engineer
Greg Braun – Gannett Fleming, Geotechnical Project Designer

Disclaimer

Statements and views presented in this paper are strictly those of the author(s), and do not necessarily reflect positions held by their affiliations, the Highway Geology Symposium (HGS), or others acknowledged above. The mention of trade names for commercial products does not imply the approval or endorsement by HGS.

Copyright Notice

Copyright © 2015 Highway Geology Symposium (HGS)

All Rights Reserved. Printed in the United States of America. No part of this publication may be reproduced or copied in any form or by any means – graphic, electronic, or mechanical, including photocopying, taping, or information storage and retrieval systems – without prior written permission of the HGS. This excludes the original author(s).

ABSTRACT

The new Central Utility Plant at Shippensburg University (Pennsylvania) was required to convert the University's heating system from coal to natural gas and to replace the existing cooling system. The new plant included the Plant Building and an approximately 65-foot diameter, 65-foot high Water Storage Tank. The proposed plant site is underlain by Ordovician-aged carbonate rock from the Rockdale Run Formation. Karst related features, including sinkholes, closed depressions and local intense pinnacle development are common traits of the Rockdale Run Formation. Many sinkholes have been documented on campus and within close proximity to the Plant site. A subsurface exploration program, consisting of 10 borings, was performed to evaluate subsurface conditions at the project site. Geophysical techniques, including microgravity and 2D electrical resistivity imaging, were also utilized to identify potential karst conditions at the project site. Both the borings and geophysics data showed that karst conditions were evident beneath the Water Storage Tank. Since differential settlement would be detrimental to the performance of the proposed tank, deep foundations were required to support the Water Storage Tank. Many deep foundation alternatives were considered to support the tank, but 7-inch diameter micropiles socketed into bedrock were the recommended foundation alternative. The micropile installation verified the presence of karst conditions encountered in the borings and identified in the geophysics data. A sinkhole that opened during the design phase of the project was repaired during construction.

INTRODUCTION

The new Shippensburg University's Central Utility Plant, located on the Shippensburg University Campus in Shippensburg, Pennsylvania was implemented in order to convert the existing heating system from coal to the environmentally friendly natural gas, as well as to replace the existing cooling system. The benefits of the new system include a substantial savings in operating cost as it is estimated to save the University approximately \$50 million dollars over the 30 year life cycle. In addition, the new plant is expected to reduce the carbon footprint by 68 percent when compared to the existing coal fired plant. The new Central Utility Plant includes the Plant Building and an approximately 65-foot diameter, 65-foot high Water Storage Tank. A map showing the location of the project is provided in Figure 1.

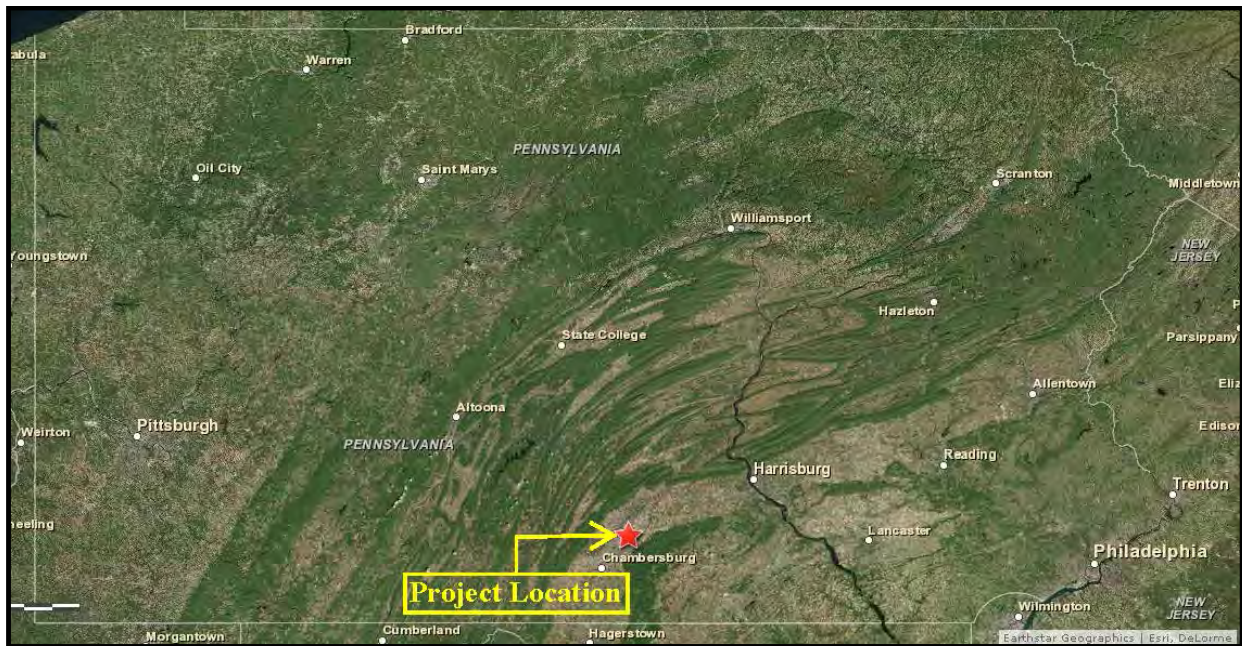


Figure 1: Project Location Map

Based on the Pennsylvania Bureau of Topographic and Geologic Survey, the project location is underlain by limestone and/or dolomite bedrock that is considered most susceptible to sinkhole development (1). A map showing the carbonate bedrock distribution in relation to the project site is provided in Figure 2.

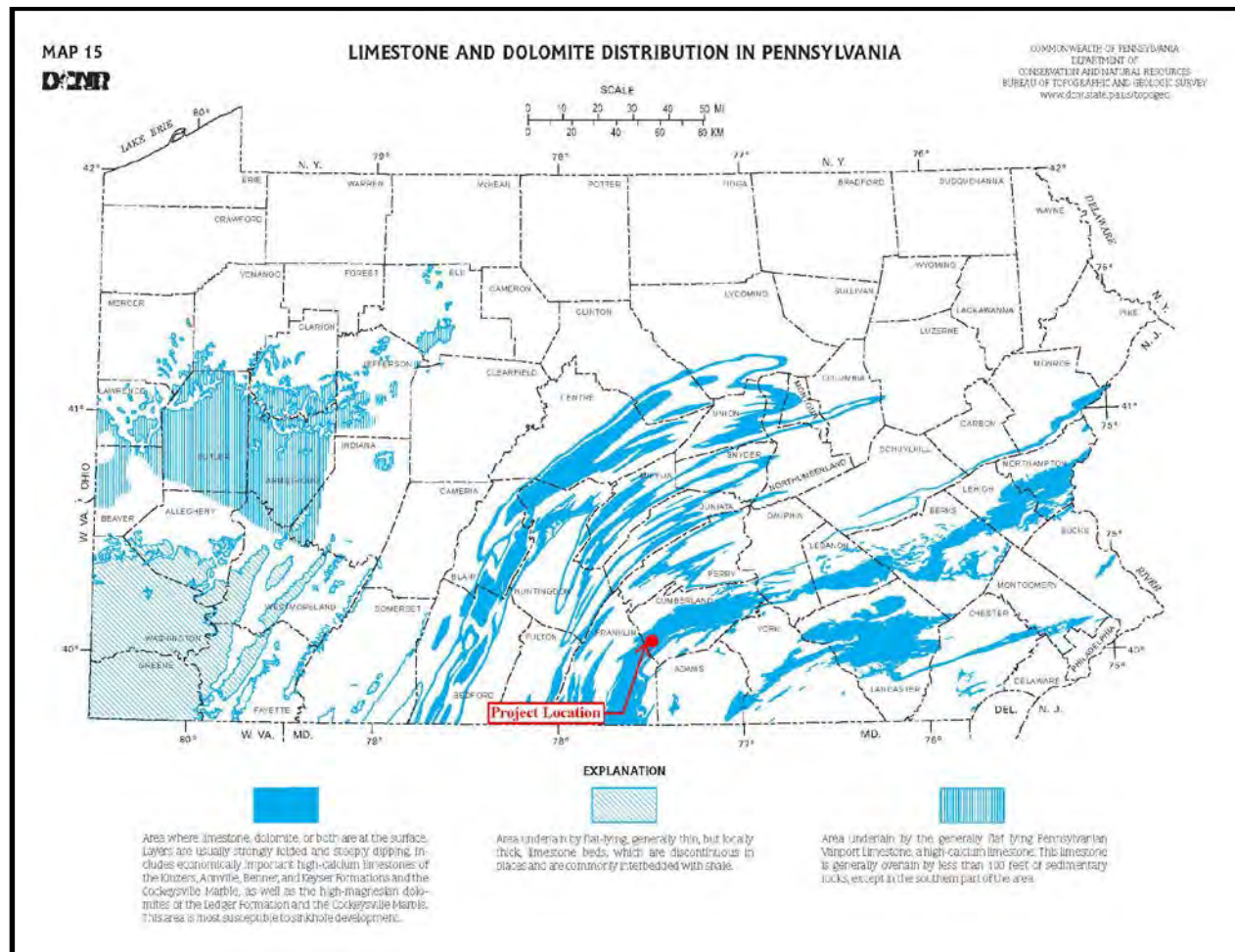


Figure 2: Limestone and Dolomite Distribution in Pennsylvania

REVIEW OF PUBLISHED GEOLOGIC LITERATURE

Based on the Pennsylvania Department of Conservation and Natural Resources, the project site is underlain by the Rockdale Run (Orr) Formation (2). The Rockdale Run Formation is Ordovician-aged carbonate bedrock consisting of very light gray, finely laminated, fine-grained limestone with dolomite interbeds, chert lenses and white quartz rosette bearing beds near the top of the formation. The fractures within the Rockdale Run Formation are typically open and steeply dipping, and the formation is moderately resistant to weathering and moderately weathered to a deep depth. The interface between soil and bedrock is characterized by local intense pinnacle development and solution openings (3).

The Pennsylvania Bureau of Topographic and Geologic Survey identified historical karst related features, in particular, closed depressions and a sinkhole in the vicinity of the Central Utility Plant site (4). A Geology Map that also includes historical karst related features is shown in Figure 3.

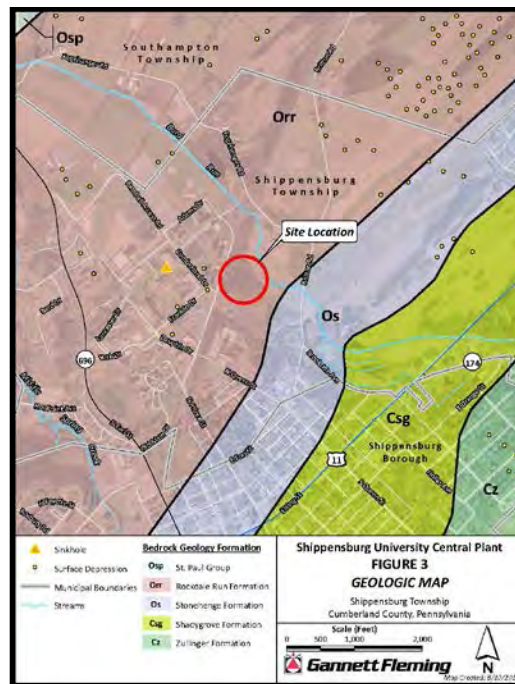


Figure 3 – Geology Map with Historical Karst Related Features

SITE RECONNAISSANCE

Site reconnaissance of the project area was performed during the design phase of the project. The proposed Central Utility Plant site was completely wooded and covered with extremely dense vegetation. Exposed bedrock was observed at the ground surface at several locations throughout the site, which is indicative of the pinnacled top of bedrock surface that was described as a common characteristic of the Rockdale Run Formation (3). Exposed bedrock at the Central Utility Plant site is shown in Photo 1. A sinkhole was observed within a natural swale that carries stormwater runoff from the adjacent developed site. The sinkhole was located approximately 100 feet from the proposed Plant building and approximately 25 feet from a proposed stormwater detention pond. The sinkhole was approximately 5 feet in diameter and approximately 5 feet in depth when observed during site reconnaissance. The sinkhole is shown in Photo 2.



Photo 1: Exposed Bedrock at Ground Surface



Photo 2: Sinkhole on Plant Site

For informational purposes, Shippensburg University provided the Geotechnical Investigation Report from a project that was located immediately adjacent to the Central Utility Plant site. Based on the report, several small sinkholes developed during construction of the access road to the site (5).

Gannett Fleming, Inc. performed geotechnical design services for a building on the Shippensburg University campus that was completed in 2007. The building is located less than

one-half mile from the Central Utility Plant Site and is also underlain by the Rockdale Run Formation. Sixteen (16) borings were conducted at the building site as part of the subsurface exploration program. The borings encountered intense local pinnacle development in the form of extremely variable depths to the top of limestone bedrock within borings located as little as 3 feet apart. The borings also encountered soil seams within the bedrock, but no voids were encountered in the borings. The local intense pinnacle development and soil filled solution features discovered in the borings are consistent with the characteristics of the Rockdale Run Formation presented in published literature. Micropile foundations socketed into limestone bedrock were utilized to support the building and multiple sinkholes opened during micropile installation (6). Examples of the sinkholes encountered during construction of the micropiles are provided in Photos 3 and 4.



Photos 3 and 4: Sinkholes Encountered During Construction of Campus Building

SUBSURFACE EXPLORATION

The subsurface exploration program conducted at the Plant Building and Water Storage Tank took place between December 2013 and March 2013 and included a total of ten (10) borings and a geophysics survey. In addition, four (4) test pits were performed to evaluate the subsurface conditions at the two stormwater detention basins and to perform infiltration testing. The boring and test pit locations are shown in Figure 4.

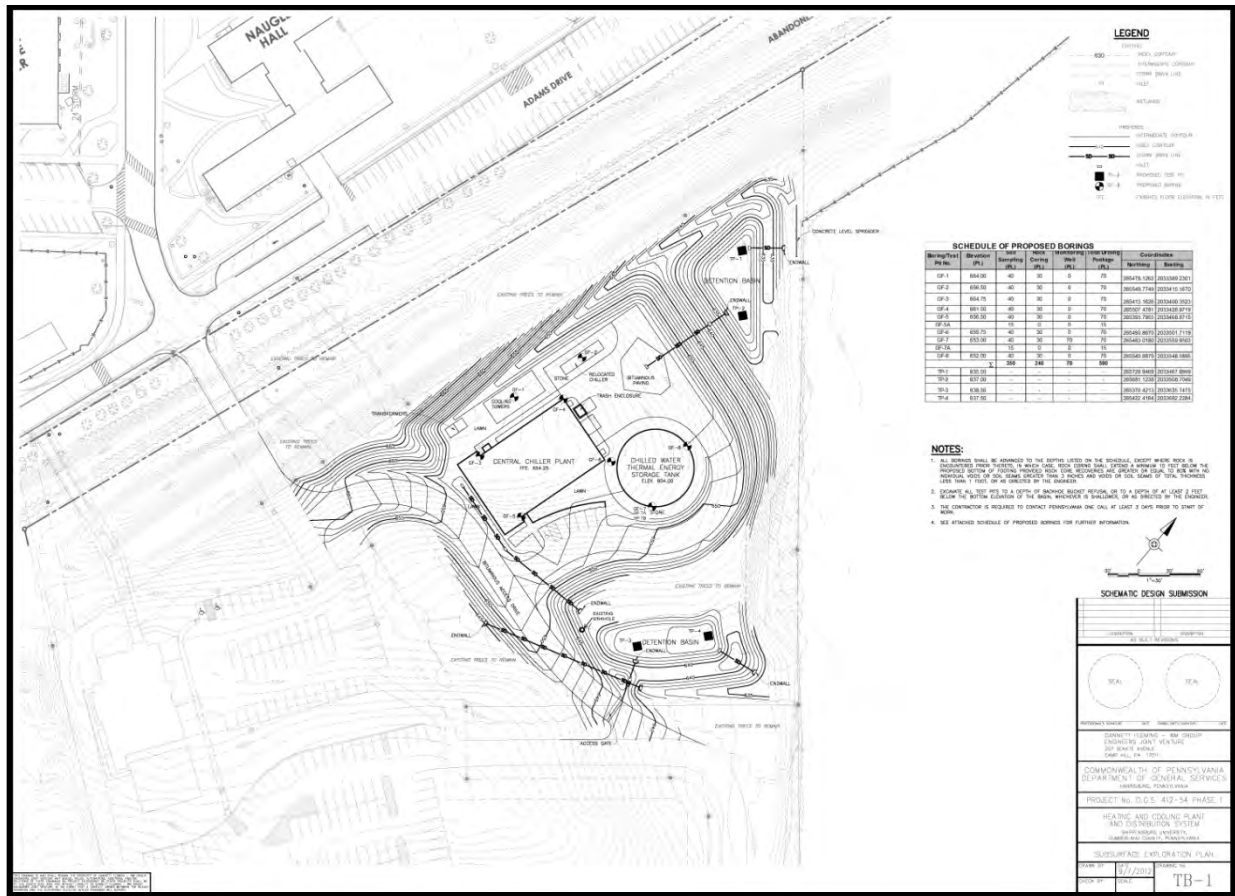


Figure 4 – Boring and Test Pit Location Plan

The borings were performed to determine the subsurface conditions and collect soil and rock samples for laboratory testing. In general, the subsurface profile encountered at the site consisted of residual soil overlying limestone bedrock. The depth to bedrock ranged from 6.0 feet to 27.1 feet in the borings. Bedrock was not cored in Boring GF-7 due to casing deviation and subsequent loss of drill casing in the borehole. In addition, a split spoon sampler was bent during Standard Penetration Testing. The variable depths to the top of bedrock, casing deviation, loss of drill tooling and bent split spoon sampler indicated that a pinnacled top of bedrock surface was evident at the Plant site. In addition to the pinnacled top of bedrock, highly weathered zones, soil seams and voids within the bedrock were encountered in five (5) borings. The highly weathered zones and soil seams ranged in thickness from 0.6 feet to 17.6 feet. One open void with a thickness of 0.5 feet was identified in Boring GF-3. The highly weathered bedrock zones as well as the soil seams and voids encountered within the bedrock, indicated that solution openings were evident at the Plant Site. Accordingly, the pinnacled top of bedrock surface and solution openings identified in the borings correlate well with the information presented in the published geologic literature (3).

A standpipe (Casagrande) piezometer was constructed in Boring GF-6 to a depth of 30 feet below ground surface during the subsurface exploration program to monitor groundwater levels at the project site. Ground water was not encountered in any subsequent readings of the piezometer.

Geophysics was utilized to identify potential karst conditions underlying the Plant Building and Water Storage Tank. Because no one geophysical technique can detect all features that may be related to karst conditions, two techniques were implemented to complement the subsurface boring data; microgravity and 2D electrical resistivity imaging. The microgravity method was utilized to detect localized changes in gravity, which for karst conditions, may be indicative of pinnacles at the top of bedrock and/or voids or solution cavities within the bedrock in karst terrain. Electrical resistivity imaging was utilized to provide more clarity regarding the location of the soil/bedrock interface and detect variations in electrical resistivity that may indicate the presence of a void, soil seam or zone of weathered or fractured rock within the bedrock.

The microgravity geophysics technique identified nine potential voids at the Central Utility Plant site. Five of the voids were located within the footprint of the Plant Building, three were located within the Water Storage Tank and one was located to the west of the Plant Building. The microgravity data suggested that the size of the potential voids was relatively small and are generally not expected to be more than about 10 feet in length or width, except for one larger, irregular shaped void located along the west side of the Plant Building that shows the potential void was as large as 30 feet long. The microgravity survey also noted that pinnacled bedrock was encountered in the footprint of both structures and that the depth to top of rock is greatest on the east side of the Water Storage Tank. The pinnacled top of rock and depth to top of rock correlated well when compared with the data obtained in the borings. The microgravity results, including the potential voids and relative location of the top of bedrock, are shown on Figure 5.

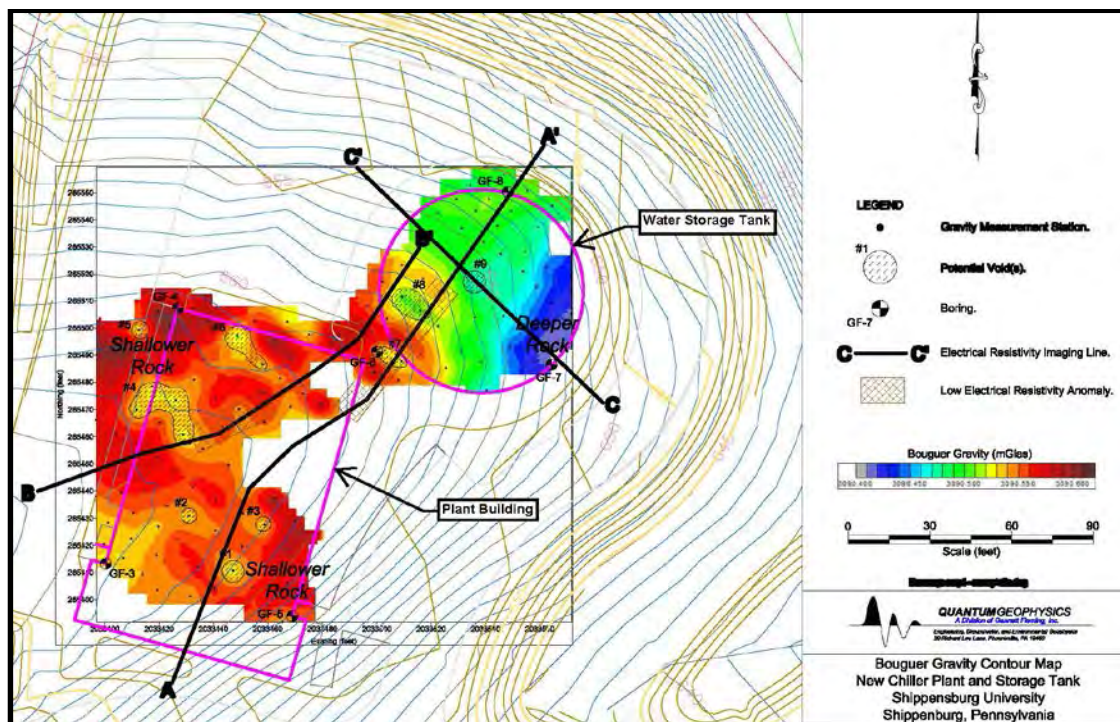


Figure 5 – Microgravity Results

The electrical resistivity imaging (ERI) technique identified two low electrical resistivity anomalies within the bedrock at depths of 30 to 50 feet below ground surface. One of the anomalies is located completely within the footprint of the Plant Building, while the other anomaly underlies the north east corner of the Plant Building and continues under the west side of the Water Storage Tank. These anomalies are generally associated with the potential voids that were identified in the microgravity survey. Boring GF-6 was located in the vicinity of a low resistivity anomaly and a potential void indicated by the microgravity survey. This boring encountered more than 20 feet of continuous rock with no voids, but highly weathered zones were encountered from 19 feet to 24.5 feet and from 29.1 feet to 29.8 feet. The ERI survey interpreted the soil/rock interface and indicated that the depth to rock is generally 6 to 8 feet below ground surface at the Plant Building, and is variable at the Water Storage Tank. These findings are consistent with the depth to rock recorded in the borings. The locations of the low electrical resistivity lines and anomalies are shown on the plan view in Figure 5 and the ERI profiles are provided in Figures 6, 7 and 8.

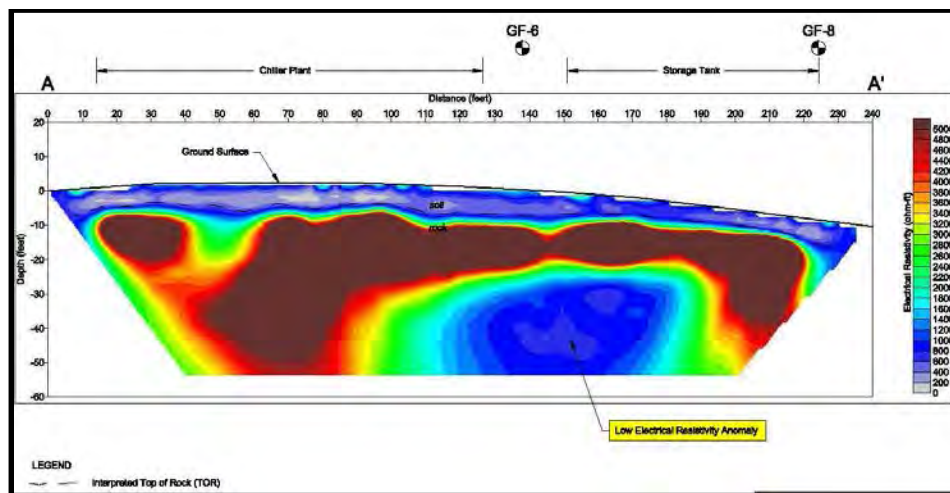


Figure 6 – ERI Line A-A' Profile

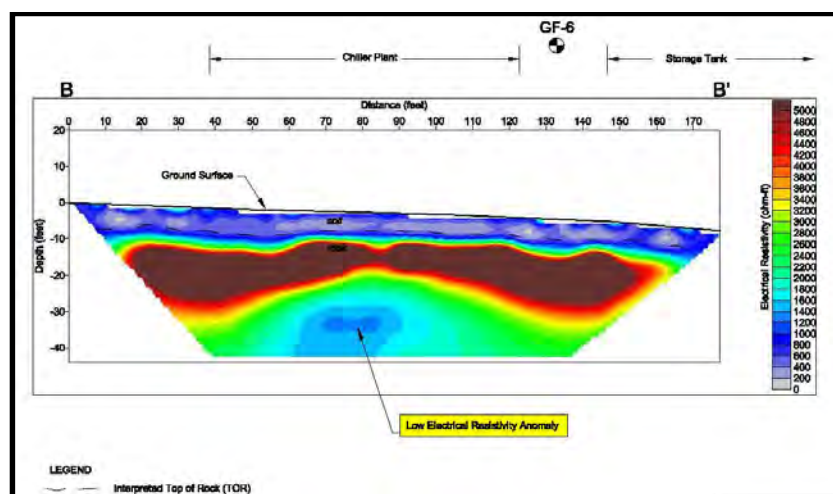


Figure 7 – ERI Line B-B' Profile

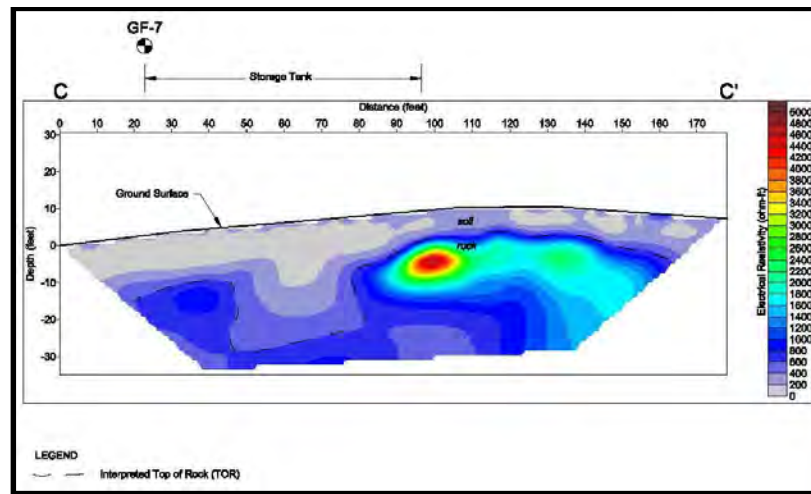


Figure 8 – ERI Line C-C' Profile

LABORATORY TESTING

Twelve rock core samples collected during the subsurface investigation were tested for unconfined compressive strength in accordance with ASTM D7012. Each of the samples was collected from core runs below the proposed bottom of footing elevation. Unconfined compressive strength test results ranged from 294.2 tons per square foot (tsf) to 1200.8 tsf and averaged 689.6 tsf. A summary of laboratory unconfined compressive strength of rock test results are shown in Table 1.

Boring	Sample Depth (ft)	Rock Type	Unconfined Compressive Strength (tsf)
GF-3	15.0'-15.6'	Limestone	391.5
GF-3	20.0'-21.0'	Limestone	1042.2
GF-4	12.0'-12.8'	Limestone	294.2
GF-4	16.1'-17.0'	Limestone	832.0
GF-5	8.5'-9.3'	Limestone	809.7
GF-5	9.7'-10.2'	Limestone	932.0
GF-5	15.6'-16.4'	Limestone	822.5
GF-6	25.0'-26.5'	Limestone	1200.8
GF-7A	25.4'-25.9'	Limestone	609.1
GF-7A	29.8'-30.4'	Limestone	415.8
GF-8	11.0'-12.0'	Limestone	489.8
GF-8	18.2'-19.0'	Limestone	435.7

Table 1: Unconfined Compressive Strength of Rock Test Results

FOUNDATION DESIGN

The foundation design of the Plant Building and Water Storage Tank considered the irregular top of rock surface characterized by pinnacles, the presence of soil seams and voids below the top of rock and the potential for future sinkhole development. The recommended foundation type for the Plant Building and Water Storage Tank was based on an evaluation of the boring and geophysics information available at the structure location. Although there is a risk of structure failure if sinkhole development occurs underneath a shallow foundation, it was determined that the risk of sinkholes at this site was considered relatively low provided minimal soil seams/voids were present in the underlying bedrock and care was taken during construction to limit the amount of surface water infiltration under/around the perimeter of the structure. Shallow foundations were recommended if the soil/rock encountered beneath the structure provides adequate bearing capacity, the applied foundation loads resulted in less than ½ inch of settlement, and minimal soil seams/voids were present in the underlying bedrock. Deep foundations were recommended if the subsurface conditions underlying a proposed structure were variable such that the applied foundation loads would cause excessive differential settlement or if significant soil seams/voids were present in the underlying bedrock.

Shallow foundations were recommended to support the Plant Building since the boring data indicated that the lightly loaded foundations were expected to be founded in limestone bedrock with minimal underlying soil seams voids. However, due to the potential voids in the bedrock identified by the geophysical investigations, isolated shallow foundations were not recommended. The recommended shallow foundation consisted of a structural slab with integral thickened footings that was designed to span an unsupported distance of approximately 15 feet in the unlikely event of future sinkhole activity underneath the structure. The unsupported distance of approximately 15 feet was believed to be appropriate since the majority of the potential voids identified in the geophysical survey were less than 10 feet wide.

At the Water Storage Tank, the borings encountered varying subsurface conditions at/below the proposed footing elevation. The subsurface conditions consisted of limestone bedrock with some weathered zones in two borings, while the other boring identified approximately 27 feet of clay and intermittent bedrock/soil seams beneath the proposed footing elevation. The geophysics data supported the boring information, as the geophysical data indicated the depth to rock varied significantly across the proposed footprint of the Tank. Shallow footings were considered as an alternative to support the proposed Tank. However, based on the varying subsurface conditions encountered in the borings and geophysics results, unacceptable differential settlement of shallow footings was expected. Furthermore, an existing sinkhole had been observed in close proximity to the proposed Water Storage Tank and future sinkhole development at the site was a significant concern based on the potential voids and low resistivity anomaly identified by the geophysics and the subsurface conditions encountered in the borings. Supporting the Water Storage Tank on shallow footings would result in a significantly greater risk of future issues with the structure due to settlement and/or ground loss due to sinkhole activity than deep foundations supported by competent rock. Accordingly, a deep foundation system that transfers the structure loads to competent limestone bedrock was recommended to support the Water Storage Tank.

DEEP FOUNDATION ALTERNATIVES

The feasible deep foundation alternatives considered to support the Water Storage Tank included: driven piles, drilled shafts and micropiles. Both driven steel pipe and H-section piles were considered to support the Water Storage Tank. Driven piles obtain their load carrying capacity from driving the pile to refusal on bedrock, and due to the pinnacled bedrock, maintaining pile alignment would likely be problematic. Additionally, with the intermittent soil/rock seams identified in the subsurface exploration program, predrilling would be required at some pile location to verify that pile tips bear on competent bedrock. Generally, predrilling through rock, particularly through highly variable limestone, is very costly. Lastly, in order to delineate locations that require predrilling, exploratory air track drilling would be required at each pile location. Based on the anticipated difficulty in installing driven piles due to pinnacled rock and the cost associated with predrilling and exploratory drilling, driven piles were considered cost prohibitive; therefore, driven piles were not recommended to support the Water Storage Tank.

Drilled shafts were considered to support the Water Storage Tank, but were not recommended. Based on design calculations, drilled shafts socketed into bedrock were required in order to carry the anticipated structure loads. Similar to driven piles, the pinnacled bedrock was expected to make drilled shaft construction very difficult. In addition, excessive rock excavation was anticipated in some areas in order to penetrate beyond any solution channels encountered below the top of bedrock such that the drilled shaft bottom and/or rock socket was entirely in rock. Furthermore, drilled shafts socketed into bedrock have extremely high load carrying capacity, but provide very little redundancy in the foundation system if future sinkhole development were to occur. Consequently, drilled shafts were considered cost prohibitive and included a higher level of risk of structure deformation if sinkhole development occurs in the future.

Micropiles, socketed into bedrock were considered the most appropriate deep foundation alternative to support the Water Storage Tank. The small diameter, drilled and grouted piles obtain their capacity from friction, opposed to the other deep foundation alternatives that obtain their capacity predominantly from end bearing. Since micropiles obtain their capacity from friction between the sides of the pile and surrounding limestone and bearing driven piles or drilled shafts have the potential to be founded immediately above a void or soil seam in the limestone bedrock that likely would not provide adequate capacity to support the structure loads, micropiles were believed to provide the least amount of risk of future foundation issues if voids or soil seams are present below the pile tip. In addition, since micropile drilling equipment easily advances through soil and rock, micropiles were the most cost effective deep foundation alternative for this project.

MICROPILE DESIGN

The micropile geotechnical and structural capacity was designed in accordance with the Federal Highway Administration's design methodology. The geotechnical capacity of micropiles is obtained from the grout to rock bond along the sidewalls of the rock socket and no end bearing is utilized. A conservative value of 150 psi was assumed for the ultimate grout to rock bond

stress. The geotechnical capacity for micropiles with varying diameters, grout compressive strength and rock socket length were analyzed to determine a feasible micropile configuration. The analyses indicated that a 7-inch diameter micropile with 4.5 kips per square inch (ksi) compressive strength grout and 6.5-foot-long rock socket had an ultimate geotechnical capacity of 250 kips. Using a factor of safety of 2.5 due to the variability of the bedrock resulted in an allowable axial geotechnical capacity of 100 kips (7). A load test was performed to further verify the bearing capacity of the limestone bedrock. Battered piles were utilized to resist lateral loads.

In order to provide verification that at least 10 feet of competent bearing material was present at the rock socket, a minimum 10-foot-long socket was recommended. Competent bearing material was defined as moderately weathered to fresh limestone with minimal soil seams. Minimal soil seams were not to exceed 6 inches for any individual seam and a total of 12 inches in thickness over a 10 foot drilled length.

The structural design, including casing thickness and sizing the reinforcement bar, was performed by the Contractor in accordance with the performance specification developed for this project. The specification required the structural capacity of the micropiles to meet or exceed the geotechnical capacity. In addition, the specification required the Contractor to advance the steel casing to the bottom of the rock socket and then withdraw the casing to a minimum of 1 foot below the top of bedrock during grouting in an effort to minimize grout loss. A typical micropile detail is shown as Figure 9.

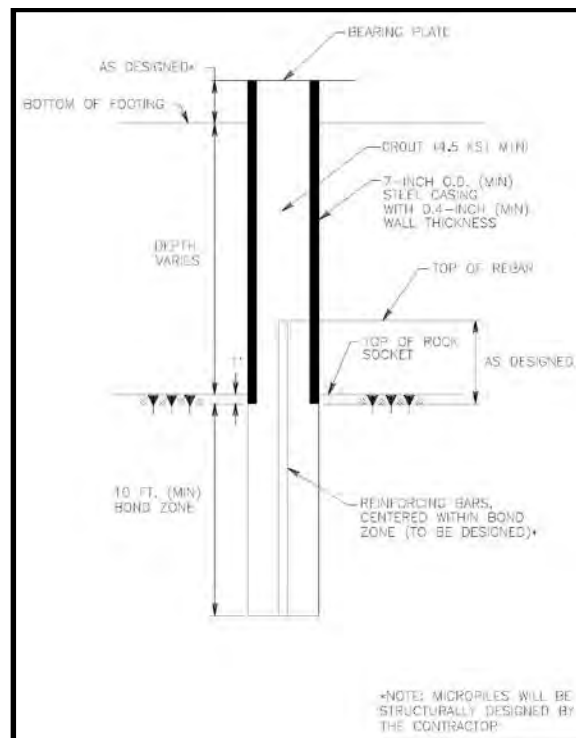


Figure 9 – Typical Micropile Detail

MICROPILE LOAD TEST

A micropile compression load test was conducted in accordance with ASTM D1143 to verify that the micropile design and construction techniques were adequate to carry design loads without excessive micropile deformation (7, 8). A steel reaction beam and sacrificial reaction micropiles were utilized along with a hydraulic jack and load cell to perform the compression load test. The micropile deformations were measured using dial indicators attached to an independent reference frame. The maximum load transferred to the test pile was 250 kips, or 2.5 times the micropile design load of 100 kips. The casing movement at the maximum test load was 0.046 inches, which was less than the expected elastic deformation of the steel casing. Based on the limited micropile deformation at the maximum test load, the micropile design and construction techniques for this project were considered satisfactory. Photo 5 was taken during the load test.



Photo 5: Micropile Load Test

MICROPILE CONSTRUCTION

Lobar, Inc. submitted the low bid to construct the structures involved with the Central Utility Plant project. Lobar, Inc. subcontracted with Nicholson Construction Company to install the 261 micropiles required to support the Water Storage Tank. Nicholson Construction Company completed micropile installation in June and July 2014. To date, the Water Storage Tank is not in service, but no foundation issues or sinkhole activity at the site have been reported. The micropile layout is shown in Figure 10.

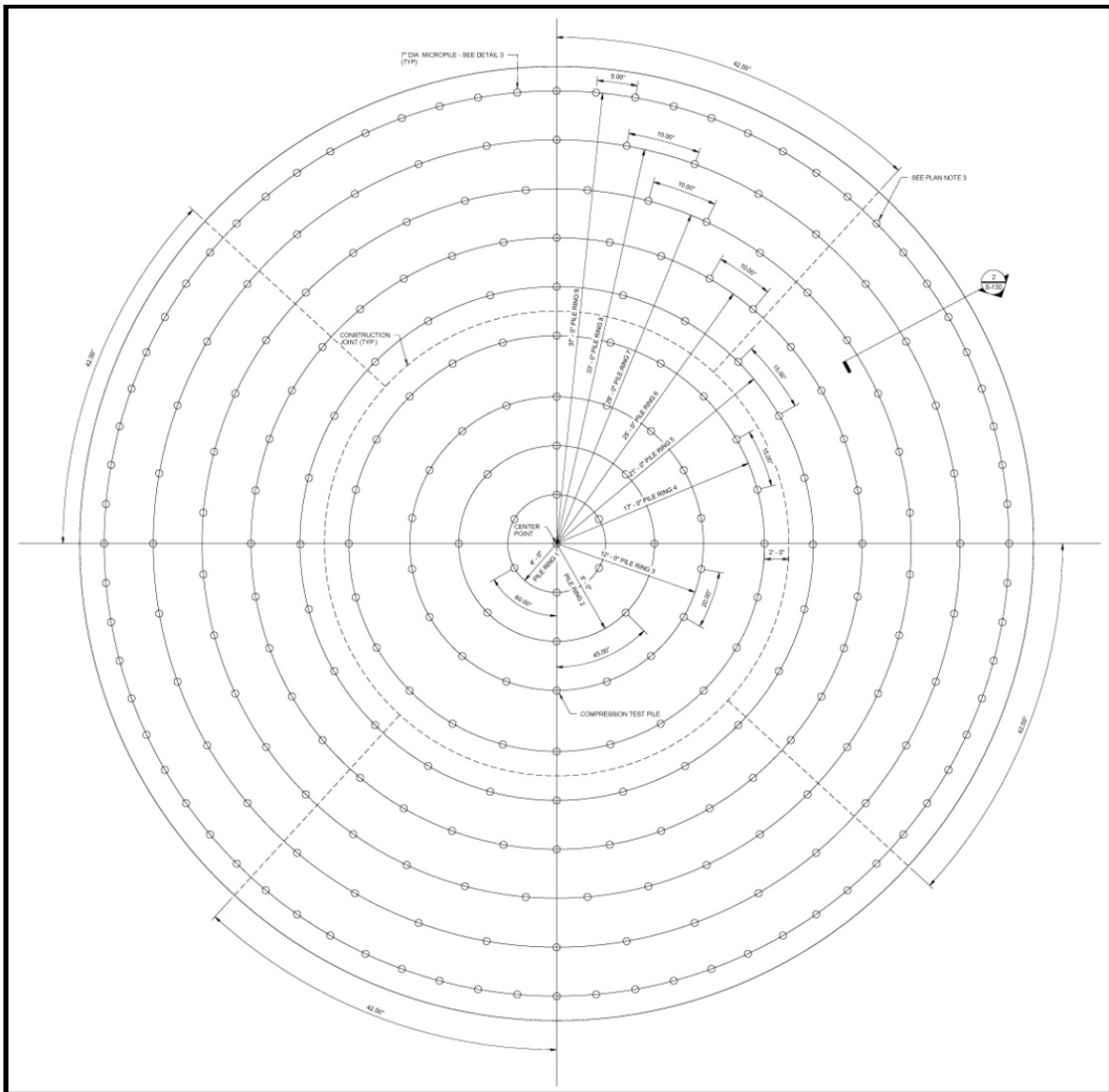


Figure 10 –Micropile Layout

Photos 6, 7 and 8 were taken during micropile construction and the completed Water Storage Tank is shown on Photo 9.



Photo 6: Micropile Installation



Photo 7: Battered Micropile Installation



Photo 8: Completed Micropiles



Photo 9: Water Storage Tank and Plant Building

The lengths of the installed micropiles corresponded well with the depth to rock identified in the geophysics and boring data. The longer micropiles were generally installed in the area of the Water Storage Tank that the Microgravity survey identified deeper rock. In addition, Boring GF-7 was drilled in this area and the depth to top of rock in this area was the deepest top of rock encountered in any of the borings.

Many soil seams were identified within the bedrock during micropile installation, but no air-filled voids were encountered. The location of the soil seams did not appear to correspond to the potential voids identified with geophysics.

SINKHOLE REPAIR

The on-site sinkhole identified within the natural swale during site reconnaissance was repaired by Lobar Inc. in July 2014. The sinkhole repair included excavation to determine the location of the sinkhole throat. The sinkhole throat was discovered and the voids in the bedrock were filled with rock fill and encapsulated with concrete. The remainder of the excavated area was backfilled with low permeability soil consisting of lean clay. A photo of the sinkhole repair is shown on Photo 10.



Photo 10: Sinkhole Repair

REFERENCES

- (1) Pennsylvania Department of Conservation of Natural Resources, Bureau of Topographic and Geologic Survey, *Limestone and Dolomite Distribution in Pennsylvania, Map 15*. Revised 2000.
- (2) Pennsylvania Department of Conservation and Natural Resources, Bureau of Topographic and Geologic Survey, *PAMAP*, August 2012.
- (3) Geyer, S.R. and Wilshusen, J.P., Pennsylvania Bureau of Topographic and Geologic Survey, *Engineering Characteristics of the Rock of Pennsylvania*, Revised 1982.
- (4) Kochanov, W.E., Pennsylvania Department of Conservation of Natural Resources, Bureau of Topographic and Geologic Survey, *Sinkholes and Karst-Related Features of Cumberland County*, OFR 8902, 1989.
- (5) Triad Engineering, Inc., *Report of Geotechnical Investigation, New Spiritual and Interfaith Chapel*, January 9, 2001.
- (6) Gannett Fleming, Inc. *Geotechnical Engineering Report for the Proposed Student Recreation Center*, August 2005.
- (7) Federal Highway Administration, *Design and Construction Reference Manual*, Publication No. FHWA NHI-05-039, December 2005.
- (8) ASTM D1143, *Standard Test Method for Deep Foundations Under Static Axial Compressive Load*, 2013.

An Improved Calculation Method to Design Flexible Facing System for Soil Nailing

Marco Cerro

Maccaferri, Inc
10303 Governor Lane Blvd.,
Williamsport, MD 21795-3116
Ph: 301-223-6910
m.cerro@maccaferri.com

Giorgio Giacchetti

OFFICINE MACCAFERRI S.p.A.
Via Kennedy 10
40069 Zola Predosa
Ph: 01139051646000
giorgio.giacchetti@maccaferri.com

Ghislain Brunet

Maccaferri, Inc
10303 Governor Lane Blvd.,
Williamsport, MD 21795-3116
Ph: 301-223-6910
gbrunet@maccaferri-usa.com

Alessio Savioli

OFFICINE MACCAFERRI S.p.A.
Via Kennedy 10
40069 Zola Predosa
Ph: 01139051646000
alsessio.savioli@maccaferri.com

Alberto Grimod

France MACCAFERRI SAS
8, rue Pierre Mechain
26901 Valence Cedex 9
Ph: 330475860919
agrimod@maccaferri.fr

Disclaimer

Statements and views presented in this paper are strictly those of the author(s), and do not necessarily reflect positions held by their affiliations, the Highway Geology Symposium (HGS), or others acknowledged above. The mention of trade names for commercial products does not imply the approval or endorsement by HGS.

Copyright Notice

Copyright © 2015 Highway Geology Symposium (HGS)

All Rights Reserved. Printed in the United States of America. No part of this publication may be reproduced or copied in any form or by any means – graphic, electronic, or mechanical, including photocopying, taping, or information storage and retrieval systems – without prior written permission of the HGS. This excludes the original author(s).

ABSTRACT

According to the experience of several Authors, under certain conditions soil nail facing systems can be developed with nails using steel mesh fabric (flexible structural facing). The goal of this system is to improve slope face stability and allow vegetation to grow.

A simple design approach was introduced a few years ago that analyzed the behavior of the mesh by comparing the maximum volume of debris that can move among the nails to the maximum volume that can be held by the mesh. Even if it took into account the real interaction between mesh and soil, the procedure was only rudimentary in solving the non linearity of the load - displacement problem. Recently, a new design approach using forces generated by the soil pushing on the mesh was proposed, considering the most unfavorable case between a two wedge analysis and a single wedge, as the slope failure mode (according to the standard BS 8006 – 2011). Concerning the mesh resistance, thanks to the library of load-displacement curves for different mesh types generated by the new UNI 11437 Standard, and the introduction of the “scale effect” that modifies nail spacing and mesh behavior accordingly, the new software overcomes the non-linearity of the problem and allows a more realistic calculation approach.

While the methodology is not perfect, it at least allows consideration of the Ultimate Limit State and the Serviceability Limit State through a simple calculation. This paper analyzes the main calculation steps and concepts implemented in the new Bios 2 software design approach which is used by Maccaferri for design of flexible facings for cut and natural slopes.

INTRODUCTION

The use of steel mesh for facing soil nailed slopes has increased considerably within the last few years. The system, known in the technical literature as Flexible Facing (Phear, 2005), has, without doubt, some advantages for its natural aesthetic appearance where it can be used to successfully stabilize slopes with vegetation. Whereas the design of the nails is well known and used in practice, the design analysis of the mesh facing is less known. In the past Giacchetti et al. (2011) suggested an initial design approach for such facings in order to improve industry understanding of the use of meshes. That approach highlighted that design has to consider the resistance as well as the deformation of the meshes, and introduced criteria for serviceability. The purposed approach – named BIOS (Best Improvement of Slopes) - was quite rudimentary since it was simply based on the comparison between volume of soil that potentially could move among the nails, and the maximum volume of soil that could deform or reach the ultimate resistance of the mesh. The present paper completely reviews the BIOS approach on the basis of better knowledge of the meshes under deformation loads.



Fig. 1 - Example of soil nailing with hexagonal mesh and steel rope panel or facing.

THE CONCEPT OF SOIL NAILING

The aim of soil nailing is to improve soil stability when there are unfavorable stability conditions. The stability is achieved by inserting reinforcement bars into the soil, which are then grouted and fixed soundly to the ground for their entire length (nailing). As the nail is not tensioned, it has a “passive” behavior and mobilizes friction forces along the entire length when there are displacements in the soil (Schlosser F. et al., 2002; Soulas R., 1991; BS 8006; Byrne, R.J et al., 1998). The frequency and the length of the nails must be calculated in accordance with the criteria suggested in many codes (example: BS 8006; EN 1997-1; Government of Hong Kong, 2008, FHWA) and specifications (example: NCHRP REPORT 701 - Lazarte, 2011). The protection of the exposed surface of the soil reinforced by the nails is obtained with a facing, the

aim of which is to retain the soil between the nails, prevent erosion phenomena and assume an aesthetic function. The facing obviously must interact with the passive action of the nails.

HOW THE FLEXIBLE FACING DOES ITS WORK

Phear (2005) and BS 8006-2 (2011) suggest that on slopes of up to approximately 60° the facing may also be made with flexible structures (Flexible Facing – wire mesh or wire mesh geocomposites); the preferential field of application of the flexible facing is on natural slopes or on relatively small excavated faces, where significant variations in the applied stresses are not expected.

Experience shows that the facing provides passive restraint (Turner, 2012) despite any construction effort: on one hand placing the mesh in continuous contact with the soil is not possible because of the surface morphology (Ferraiolo and Giacchetti, 2004), on the other hand pre-tensioning of the mesh by means of nail plates does not offer any advantage because the forces are short circuited just below the plate. (Giacchetti et al., 2011). For this reason, the flexible facing can never be considered as a structural fit to allow perfect cooperation between nails, especially when their spacing is wider than 1.5 m (5 ft). The flexible nature of the meshes means that the ground surface can deform and push on the facing, which will then allow formation of pockets of debris (Figure 2).



Fig. 2 - Large pockets of debris pushing on the facing and deforming the mesh.

Based on the author's experiences and the technical literature, the main properties of the meshes are the weight per unit area, the resistance to- and related deformability under tensile and punch testing. Various studies and laboratory tests have been carried out with regard to the behavior of the meshes using various sized samples fastened to test frames with a range of constraint conditions. (Ruegger R., & Flumm D., 2000; Bonati & Galimberti 2004; Torres et al., 2000; Muhunthan B. et al., 2005, Bertolo et. al. 2007; Bertolo et. al., 2009). The results of the research highlight that the movement of meshes subject to punching ranges from several tens of centimeters (a few inches) up to one or more meters (feet), with a non-linear development of response, the trend of which depends mainly on the combination of the mesh weave, the size of

the test sample and the type of constraint with which the sample is fixed during testing. During the initial phase of loading, large displacements have been observed in all the tests. Then the mesh starts to appreciably resist the load.

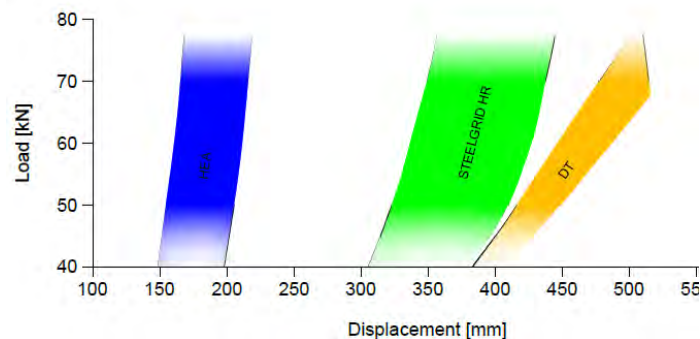


Fig. 3 Comparison between the load-displacement curves of different mesh types subject to punch tests

Given this behavior, one of the more relevant problems while in a soil nailing system consists of identifying the most cost effective mesh aimed at reducing the deflection of the facing: for example, with the stiffer meshes available on the market and according to lab experience, it is advisable to consider samples 3 x 3 m (10 x 10 ft) fastened on all sides. The doubletwist wire mesh reinforced with steel cables (Rockmesh and Steelgrid) is more deformable compared with the wire rope panel (see Fig. 3), but more rigid than the single-twist meshes with high strength wire (IUAV, 2012). The Italian Standard UNI 11437 (2012) Rockfall protection measures: Tests on meshes for slope coverage has introduced a new test method that can be used to design flexible facing, as it is the first worldwide testing guideline that describes the procedure for punch resistance testing of meshes. The standard is carried out with samples having a size of 3.0 x 3.0 m (10ft x 10ft) ±20%, restrained into a rigid frame and loaded by means of a punching device with a diameter of 1.0 m (3 ft) (see Fig. 4). This procedure is the first full scale test that allows direct comparison between different kinds of mesh (i.e.: double twist, RockMesh, ring net, HEA panel and so on) and accordingly the choice of suitable mesh types.

Since the test generates a typical graph load vs. deformation curve, a design approach considering Ultimate and Serviceability approaches for the structure is becoming possible. For example (Figure 2), a large deformation implicates conditions of potential stripping of the nails or an incipient rupture of the mesh (ultimate limit state). If the facing is slightly deformed, the pocket of debris should be removed before the mesh is irreversibly damaged (serviceability limit state).

Estimation of the deformation is not simple because the spacing between the nails could vary from the size and arrangement of the standard punch test (example: sample 3.0 m x 3.0 m (10 ft x 10 ft); with the field spacing of nails at 1.5 m x 1.5 m (5 ft x 5 ft). In that case the test carried out in accordance with UNI 11437 is not fully representative of the full scale test and real mesh behavior, and in this case a correction may be necessary. It is possible to assert that the larger the sample size, the larger the displacement will be, and also the larger the sample is, the larger the punch resistance will be. This principle is named the scale effect of meshes. The general law of the scale effect is assumed in the following simplified form referring to the coordinates of the load-displacement diagrams (Fig. 5):

$$x = x_0 \mu_x$$

$$y = y_0 \mu_y$$

where

(x, y) = generic coordinate of the scaled graphic

(x_0, y_0) = generic coordinate of the reference graphic

(μ_x, μ_y) = constants correlating the scale to the reference graphic, that depend on the mesh type.

The constants (μ_x, μ_y) are scale coefficients that correlate the mechanical behaviour of the net as a function of the sample dimensions (the distance between the nails on the jobsite application). Maccaferri has been able to get reliable values because of the large amount of data they have collected during many tests.

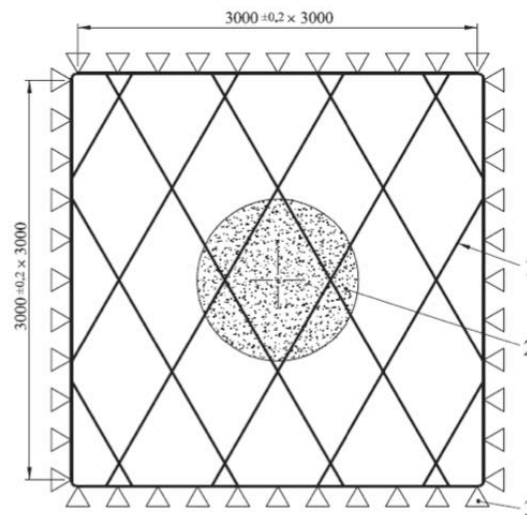


Fig. 4 Plan view of the punch test according to UNI 11437:2012. Legenda: 1 = tested mesh; 2 = punching device (1.0 m (3 ft) in diameter); 3 = perimeter constraint between the mesh and the frame.

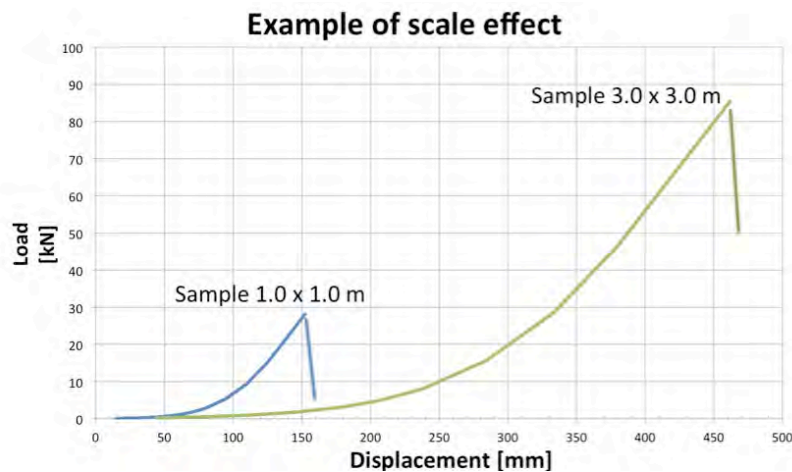


Fig. 5 Graph Displacement VS Load with the typical scale effect in the punch test

SIMPLIFIED APPROACH: BIOS

Design of the facing with BIOS

Below is a discussion of the verification of flexible structural facing by OFFICINE MACCAFERRI's software BIOS. The software analyzes only the behavior of the net, evaluating the average spacing of nails as given.

The analysis is divided into 4 steps:

1. **Short term analysis:** the stretch of the slope between two nails is analyzed, which must have a safety factor not less than 1.0. In fact, if not at equilibrium it is not possible to install the net. So the adequacy of the nail spacing in relation to the geotechnical properties of the soil is verified. If limit equilibrium is not satisfied, it is necessary to decrease the spacing between the nails. To ensure stability without the flexible structural facing, the analysis is done with two different approaches: a single wedge method and a two wedge method. The minimum value of safety factor (FS_{min}) obtained from the two methods is compared with the limit equilibrium value of 1.0; if FS_{min} is greater than this value you can proceed with the next steps.

The characteristic values of resistance of the soil have been used because the calculation concerns a temporary condition and the *geotechnical safety coefficient* $\gamma_{\phi'}$ (friction angle) and $\gamma_{c'}$ (cohesion) *are not taken into account*. If there are serious uncertainties, the designer can insert the project's resistance values, which are equal to the characteristic values conveniently reduced by the safety factors (e.g. for Eurocode 7 $\gamma_{\phi'}$ (friction angle) and $\gamma_{c'}$ (cohesion) *are both equal to 1.25*).

For the same reason, in this phase seismic loading is not taken into account.

2. **Long term analysis:** the aim of this analysis is to evaluate the load on the net facing suspended between the anchors. For this reason, in accordance with the British Standard 8006-2:2011 and CIRIA 637 procedures, the geotechnical parameters that characterize the soil have been reduced assuming that the ground conditions decay to the residual resistance (close to rupture). The parameters are defined as:

- c' (residual cohesion) = 0;
- ϕ_a' (friction angle) = residual friction angle of the soil.

Therefore the debris friction angle ϕ_a' will be equal to the residual friction angle of the soil in examination. In absence of experimental data, it is suggested to use a value equal to $\phi_a' = \phi'/2$.

The calculation procedure for the load acting on the facing is conducted, according to the BS 8006-2 procedure with reiterative analysis using the method of the two wedges (with possible seismic load). This calculation method maximizes the force acting on the net analyzing every possible geometrical configuration of the two wedges (combinations of angles ε_1 and ε_2 - see Figure 32 BS 8006-2).

3. Ultimate limit state check: the forces, calculated in the previous step, are compared with the punching resistance of the net which is obtained from standardized laboratory tests (UNI 11437: 2012) appropriately modified in order to consider the scale effect. The check is satisfied if the resistance of the net is greater than the pressure of the soil.
4. Serviceability limit state check: this analysis checks whether the deformations of the flexible facing induced by the soil are acceptable. If the forces are evaluated as excessive, a stiffer mesh type, or a narrower anchor spacing are required. The procedure is based on the graphics of punching test UNI 11437: 2012 appropriately modified because of the scale effect.

Short term analysis

The short term solution is divided in two sub-analysis; in particular two wedges are analyzed (Figure 6) and along with a one wedge (Figure 7) mechanism of failure to consider every possible collapse. The minimum value of safety factor obtained from the two methods is compared with the limit value of 1.0:

$$FS = \min(FS_{\text{ONE WEDGE}}; FS_{\text{TWO WEDGES}}) > 1.00 \quad [1]$$

Two wedges method

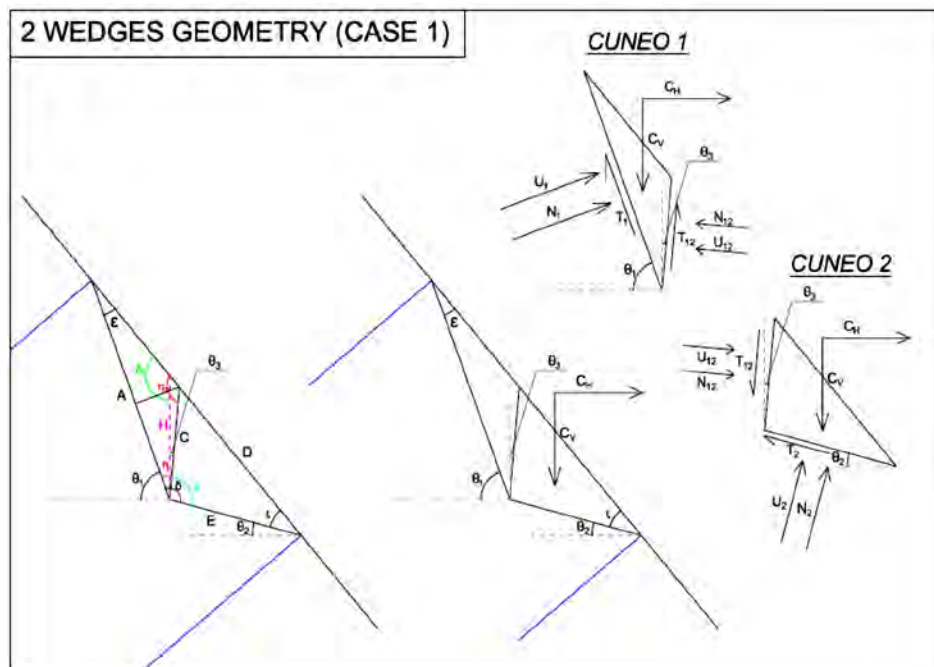


Figure 6 – Two wedges mechanism of failure

The analysis is carried out evaluating the forces acting on the two wedges faces and the value of the safety factor (FS). You get 2 equations of equilibrium to the translation (vertical and

horizontal) for each wedge, and 3 equations of the tangential stress T_i function of the safety factor:

$$\begin{cases} \sum x^{(1)} \\ \sum y^{(1)} \end{cases} \quad \begin{cases} \sum x^{(2)} \\ \sum y^{(2)} \end{cases} \quad [2]$$

$$T_1 = \frac{[c_1^I \cdot l_1 + (N_1 - U_1)\tan(\varphi_1^I)]}{FS} \quad [3]$$

$$T_2 = \frac{[c_2^I \cdot l_2 + (N_2 - U_2)\tan(\varphi_2^I)]}{FS} \quad [4]$$

$$T_{12} = \frac{[c_{12}^I \cdot l_{12} + (N_{12} - U_{12})\tan(\varphi_{12}^I)]}{FS} \quad [5]$$

The expanded system is shown below:

$$\begin{cases} N_1 \cdot \sin(\theta_1) - T_1 \cdot \cos(\theta_1) + T_{12} \cdot \sin(\theta_3) - N_{12} \cdot \cos(\theta_3) + F_{X1} = 0 \\ F_{Y1} - N_1 \cdot \cos(\theta_1) - T_1 \cdot \sin(\theta_1) - T_{12} \cdot \cos(\theta_3) - N_{12} \cdot \sin(\theta_3) = 0 \\ N_2 \cdot \sin(\theta_2) - T_2 \cdot \cos(\theta_2) - T_{12} \cdot \sin(\theta_3) + N_{12} \cdot \cos(\theta_3) + F_{X2} = 0 \\ F_{Y2} - N_2 \cdot \cos(\theta_2) - T_2 \cdot \sin(\theta_2) + T_{12} \cdot \cos(\theta_3) + N_{12} \cdot \sin(\theta_3) = 0 \\ T_1 - \frac{1}{FS} [c'_d \cdot A + (N_1 - U_1) \cdot \tan(\varphi'_d)] = 0 \\ T_2 - \frac{1}{FS} [c'_d \cdot E + (N_2 - U_2) \cdot \tan(\varphi'_d)] = 0 \\ T_{12} - \frac{1}{FS} [c'_d \cdot C + (N_{12} - U_{12}) \cdot \tan(\varphi'_d)] = 0 \end{cases} \quad [6]$$

Where:

$$c'_d = \frac{c'}{\gamma_{c'}}$$

$$\varphi'_d = \tan^{-1} \left(\frac{\tan \varphi'}{\gamma_{\varphi'}} \right)$$

a_v = average spacing between the nails

β = slope angle

γ = self-weight of the soil

r_u = pore pressure coefficient

$$\xi = \beta - \theta_2$$

$$\varepsilon = \theta_1 - \beta$$

$$\delta = \pi - \theta_1 + \theta_2$$

$$\eta = \frac{\pi}{2} - \theta_1 + \theta_3$$

$$\eta_1 = \pi - \eta + \varepsilon$$

$$\psi = \delta - \eta$$

$$\delta_1 = \pi - \varepsilon - \eta + \theta_3$$

$$E = a_v \cdot \frac{\sin(\varepsilon)}{\sin(\delta)}$$

$$A = a_v \cdot \frac{\sin(\xi)}{\sin(\delta)}$$

$$C = A \cdot \frac{\sin(\varepsilon)}{\sin(\eta_1)}$$

$$D = C \cdot \frac{\sin(\psi)}{\sin(\xi)}$$

$$H = A \cdot \frac{\sin(\varepsilon)}{\sin(\delta_1)}$$

$$h_1 = C \cdot \sin(\eta)$$

$$\text{Area}_1 = \frac{1}{2} \cdot h_1 \cdot A$$

$$h_2 = C \cdot \sin(\pi - \eta_1)$$

$$\text{Area}_2 = \frac{1}{2} \cdot h_2 \cdot D$$

$$W_1 = \gamma \cdot \text{Area}_1$$

$$W_2 = \gamma \cdot \text{Area}_2$$

$$U_1 = \frac{1}{2} \cdot \gamma \cdot r_u \cdot H \cdot A$$

$$U_2 = \frac{1}{2} \cdot \gamma \cdot r_u \cdot H \cdot E$$

$$U_{12} = \frac{1}{2} \cdot \gamma \cdot r_u \cdot H \cdot C$$

$$F_{X1} = U_1 \cdot \sin(\theta_1) - U_{12} \cdot \cos(\theta_3)$$

$$F_{X2} = U_2 \cdot \sin(\theta_2) + U_{12} \cdot \cos(\theta_3)$$

$$F_{Y1} = W_1 - U_1 \cdot \cos(\theta_1) - U_{12} \cdot \sin(\theta_3)$$

$$F_{Y2} = W_2 - U_2 \cdot \cos(\theta_2) + U_{12} \cdot \sin(\theta_3)$$

Solving the system we get a single cubic equation yielding the unknown parameter FS (safety factor):

$$A \cdot FS^3 + B \cdot FS^2 + C \cdot FS + D = 0 \quad [7]$$

The expanded equation is shown below:

$$\left\{ \frac{F_{Y1} - \left[\frac{1}{FS} (c'_d \cdot A - U_1 \cdot \tan(\varphi'_d)) \right] \cdot \sin(\theta_1) - \left[\frac{1}{FS} (c'_d \cdot C - U_{12} \cdot \tan(\varphi'_d)) \right] \cdot \cos(\theta_3) - N_{12}(FS) \cdot \left[\sin(\theta_3) + \frac{\tan(\varphi'_d) \cdot \cos(\theta_3)}{FS} \right]}{\left[\cos(\theta_1) + \frac{\tan(\varphi'_d) \cdot \sin(\theta_1)}{FS} \right]} \right\} \cdot \left[\sin(\theta_1) - \frac{\tan(\varphi'_d) \cdot \cos(\theta_1)}{FS} \right] - \left[\frac{1}{FS} (c'_d \cdot A - U_1 \cdot \tan(\varphi'_d)) \right] \cdot \cos(\theta_1) + \left[\frac{1}{FS} (c'_d \cdot C - U_{12} \cdot \tan(\varphi'_d)) \right] \cdot \sin(\theta_3) - N_{12}(FS) \cdot \left[\cos(\theta_3) - \frac{\tan(\varphi'_d) \cdot \cos(\theta_3)}{FS} \right] + F_{X1} = 0 \quad [8]$$

Where:

$$N_{12}(FS) = - \frac{(X_A + X_B)}{X_C} \quad [9]$$

$$X_A = \frac{F_{Y2} - \left[\frac{1}{FS} (c'_d \cdot E - U_2 \cdot \tan(\varphi'_d)) \right] \cdot \sin(\theta_2) + \left[\frac{1}{FS} (c'_d \cdot C - U_{12} \cdot \tan(\varphi'_d)) \right] \cdot \cos(\theta_3)}{\left[\cos(\theta_2) + \frac{\tan(\varphi'_d) \cdot \sin(\theta_2)}{FS} \right]} \cdot \left[\sin(\theta_2) - \frac{\tan(\varphi'_d) \cdot \cos(\theta_2)}{FS} \right] \quad [10]$$

$$X_B = - \left[\frac{1}{FS} (c'_d \cdot E - U_2 \cdot \tan(\varphi'_d)) \right] \cdot \cos(\theta_2) + F_{X2} - \left[\frac{1}{FS} (c'_d \cdot C - U_{12} \cdot \tan(\varphi'_d)) \right] \cdot \sin(\theta_3) \quad [11]$$

$$X_C = \cos(\theta_3) - \frac{\tan(\varphi'_d) \cdot \sin(\theta_3)}{FS} + \frac{\left[\sin(\theta_3) + \frac{\tan(\varphi'_d) \cdot \cos(\theta_3)}{FS} \right]}{\left[\cos(\theta_2) + \frac{\tan(\varphi'_d) \cdot \sin(\theta_2)}{FS} \right]} \cdot \sin(\theta_2) - \frac{\tan(\varphi'_d) \cdot \cos(\theta_2)}{FS} \quad [12]$$

$$FS = \frac{K_1 + K_2 + (W^\perp - U_1^\perp + U_2^\perp) \tan \varphi'_p}{W^{\parallel} - U_2^{\parallel}} \quad [16]$$

Where:

W^\perp (kN) Weight of wedge perpendicular to the sliding surface;

W^\parallel (kN) Weight of wedge parallel to the sliding surface;

K_1 (kN) Cohesion force acting at the top of wedge;

K_2 (kN) Cohesion force acting at the base of wedge;

U^\perp (kN) Resultant of the pressure of the water acting perpendicular to the sliding surface;

U^\parallel (kN) Resultant of the pressure of the water acting parallel to the sliding surface;

φ_d (°) Design friction angle of debris;

The minimum FS has to be found solving the equation for each value of the angle ϑ_1 ($0 < \vartheta_1 < \beta$) and selecting the safety factor with minimum value.

Long term analysis

The analysis calculates the forces acting on structural flexible facing according to BS 8006-2.

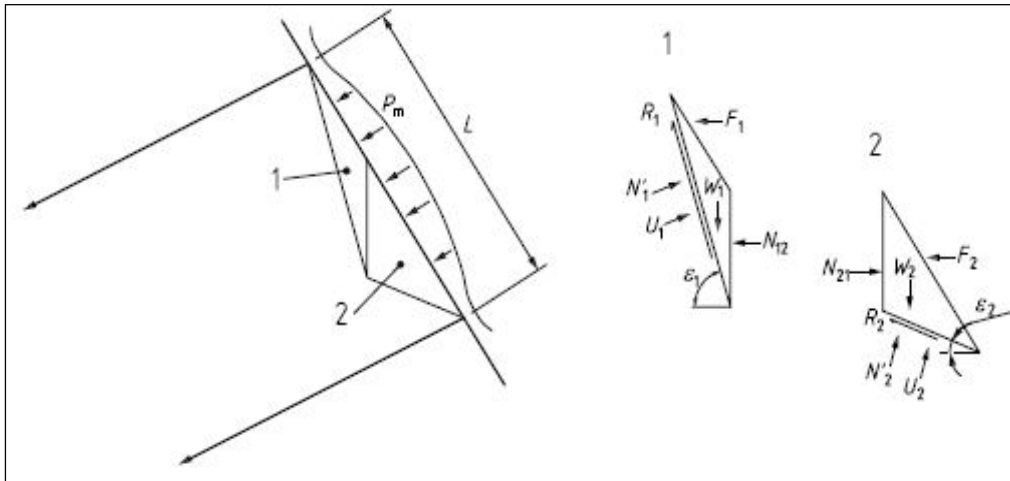


Figure 8 – BS 8006-2 Figure 32 - Calculation of design loading acting on a simple flexible facing

In the seismic case, the load acting on the net is equal to:

$$F_1 + F_2 = \frac{W_1(\tan \varepsilon_1 - \tan \varphi_a) + W_1 C_V(\tan \varepsilon_1 - \tan \varphi_a) + \frac{U_1 \tan \varphi_a}{\cos \varepsilon_1}}{1 + \tan \varepsilon_1 \tan \varphi_a} + \frac{W_2(\tan \varepsilon_2 - \tan \varphi_a) + W_2 C_V(\tan \varepsilon_2 - \tan \varphi_a) + \frac{U_2 \tan \varphi_a}{\cos \varepsilon_2}}{1 + \tan \varepsilon_2 \tan \varphi_a} + C_H(W_1 + W_2) \quad [17]$$

Where:

W_1 (kN) Weight of wedge 1;

W_2 (kN) Weight of wedge 2;

ε_1 (°) Angle at the base of wedge 1;

ε_2 (°) Angle at the base of wedge 2;

U_1 (kN) Resultant of the pressure of the water acting at the base of wedge 1;

U_2 (kN) Resultant of the pressure of the water acting at the base of wedge 2;

φ_a (°) Design friction angle of debris;

C_V Vertical seismic acceleration coefficient;

C_H Horizontal seismic acceleration coefficient;

The calculation method maximizes the force acting on the net analyzing every possible geometric configuration of the two wedges (combinations of angles ε_1 and ε_2 - see Figure 8).

This procedure is in favor of safety because it always considers the worst sliding surface from a structural point of view. In fact, in reality it may establish sliding surfaces that cause an action on the net less than that calculated.

Ultimate limit state check

The load, determined in the calculation step number 2, is increased with a safety coefficient that takes into account the uncertainties of the geotechnical model ($F_{TOT,Design} = (F_1 + F_2) \times \gamma_{DF}$).

The limit load tolerated by the net (F_{lim}) is directly estimated from the characteristic curve of the punching test.

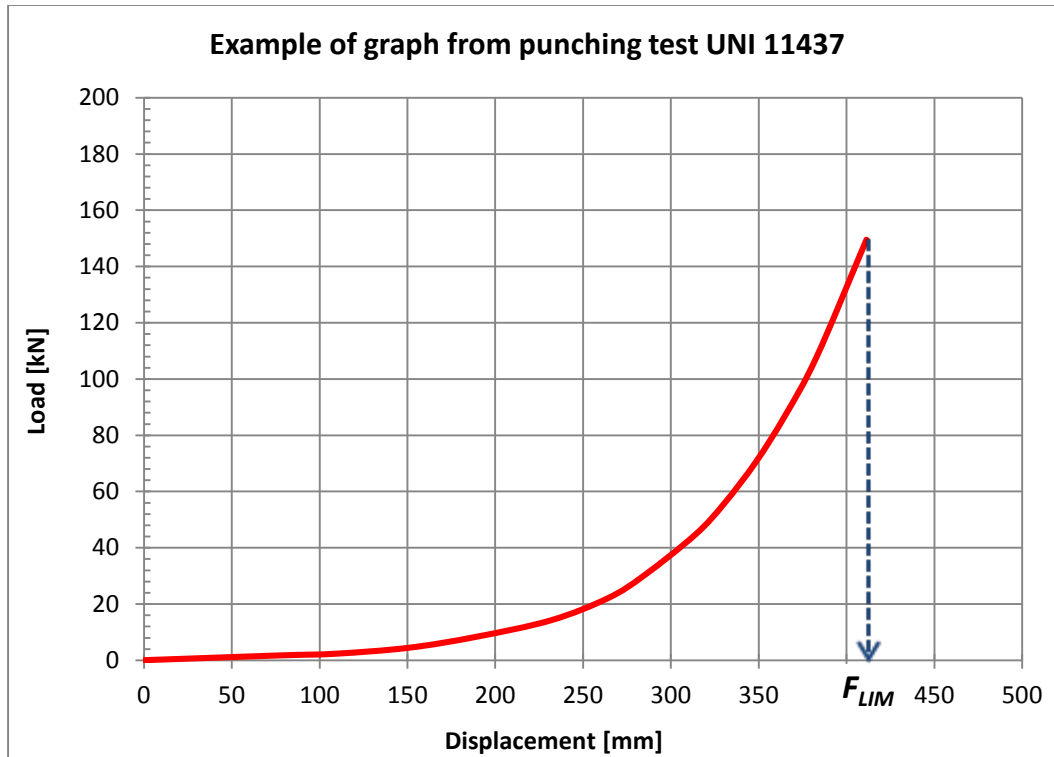


Figure 9 – Punching test graph according UNI 11437

The condition is:

$$F_{TOT,Design} < F_{lim} \quad [18]$$

Serviceability limit state check

In the serviceability limit state, the deformation of the net is checked. In fact, to permit the normal operation of the infrastructure protected by the net, we have to control deformation.

The value of deformation (Δh_d) is obtained from the characteristic graph of the punching test. This value is amplified to take into account the slope irregularities and the installation anomalies:

$$F_{TOT,Design} \cdot \gamma_{BULG} \rightarrow \Delta h_d \quad [19]$$

Where γ_{BULG} is the amplifying coefficient that takes into account the slope irregularities. This value should never be less than 1.5.

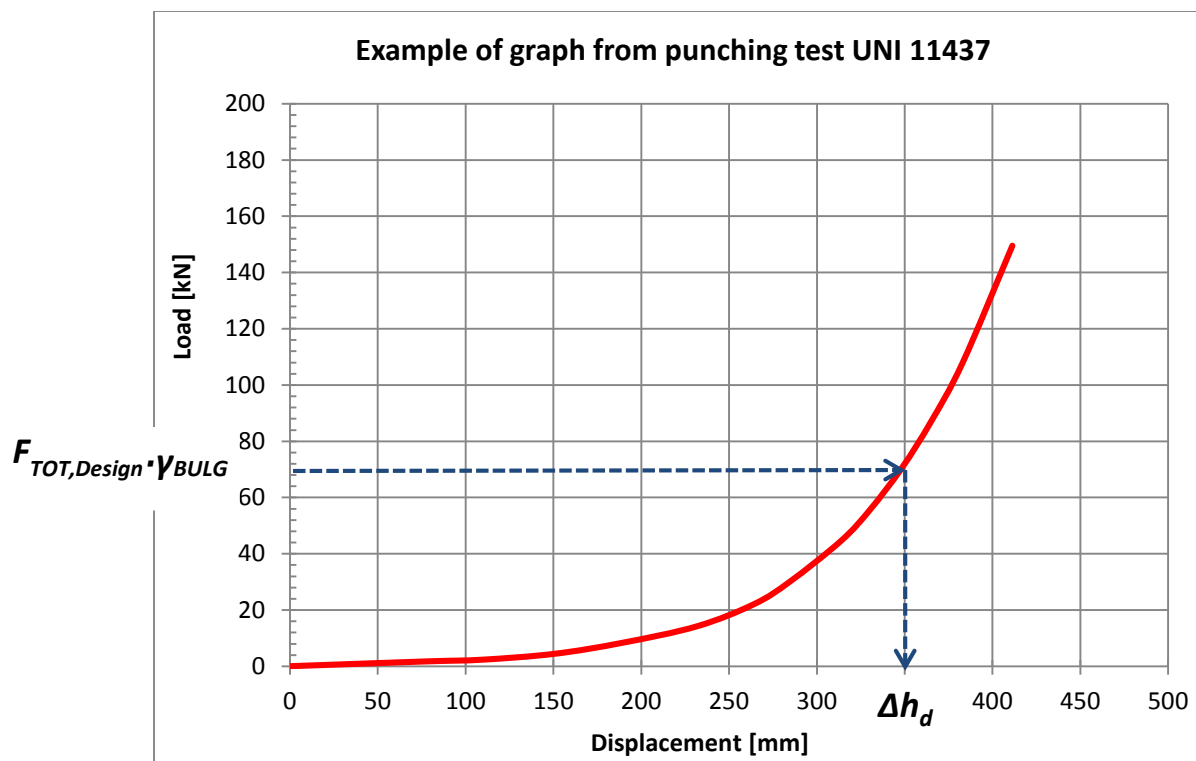


Figure 10 – Punching test graph according UNI 11437

An additional displacement value is added to Δh_d due to the assumed inaccuracy of net installation (Δh_{error}):

$$\Delta h = \Delta h_d + \Delta h_{error} \quad [20]$$

If the net is not installed to be perfectly adhering to the slope and it is not well stretched, you might have additional displacement, because the net deforms before starting its sealing function because it is loose. Recommended values of Δh_{error} range from 0.20 m (8 inches) to 0.35 m (14 inches).

The final check compares the allowable deformation with the value obtained above (Δh). The result must be that:

$$\Delta h < \textit{Limit Bulging} \quad [21]$$

When deformation exceeds the project limits, the net is not broken, but there is necessary maintenance such as emptying the net, anchor plates tightened, and cable grid installation to stiffen the flexible facing.

CONCLUSION

The design theory presented herein proposes a simplified procedure aimed at designing flexible facing with steel meshes in concert with soil nailing. The procedure is based on a limit equilibrium method and the punch tests standard UNI 11437: 2012. The procedure improves and upgrades the previous version of the BIOS software developed by Maccaferri, and allows calculating a solution where there are several unknown variables or data and represents a more sophisticated approach. Finally, the designer can choose the most effective solution among a considerable range of conditions with less time-consuming analyses. The approach highlights the fact that the fundamental property for this type of solution is the membrane stiffness of the flexible facing, while its tensile strength has limited influence because the forces at work are generally very low. However, it must be stressed that the designer's judgment is always required in order to verify the conditions in which the facing is to be applied, and identify the general geotechnical conditions that drive a successful stabilization. Further testing and development may be required to better understand the interaction between flexible facings and anchor plates.

REFERENCES:

1. Arredi F., 1978 *Note sul procedimento per blocchi dell'analisi di stabilità dei rilevati di materiali sciolti*.
2. Bertolo P., Giacchetti G. *An approach to the design of nets and nails for surficial rock slope revetment*. In Interdisciplinary Workshop on Rockfall Protection, June 23-25 2008, Morshach, Switzerland.
3. Bertolo P., Ferraiolo F., Giacchetti G., Oggeri C., Peila D., e Rossi B. *Metodologia per prove in vera grandezza su sistemi di protezione corticale dei versanti*, GEAM Geingegneria Ambientale e mineraria, Anno XLIV, N. 2, Maggio-Agosto 2007.
4. Bertolo P., Oggeri C., Peila D., 2009 – *Full scale testing of draped nets for rock fall protection*, Canadian Geotechnical Journal, No. 46 pp. 306-317.
5. Besseghini F., Deana M., Di Prisco C., Guasti G. *Modellazione meccanica di un sistema corticale attivo per il consolidamento di versanti di terreno*, Journal GEAM Geingegneria ambientale e Mineraria, Anno XLV, N. III dicembre 2008 (125) pp. 25-30 (in Italian).
6. Bonati A., e Galimberti V., 2004 *Valutazione sperimentale di sistemi di difesa attiva dalla caduta massi* – in atti “Bonifica dei versanti rocciosi per la difesa del territorio” - Trento 2004, Peila D. Editor.
7. BS 8006-2:2011 Britishstandard *Code of practice for strengthened/reinforced soils*
8. BS 8006, 1995 *Code of practice for Strengthened/reinforced soils and other fills*.
9. Byrne R.J, Cotton D., Porterfield J., Wolshlag C., e Ueblacker G., 1998 *Manual for design & construction monitoring of soil nail walls* U.S. Department of transportation – Federal Highway Administration. FHWA A-SA-96-06R – Washington D.C
10. Castro D., 2008 *Proyectos de investigación en la Universidad de Cantabria*, II Curso sobre protección contra caída de rocas – Madrid, 26 – 27 de Febrero. Organiza STMR Servicios técnicos de mecánica de rocas.
11. EN 14490: 2010 *Execution of special geotechnical works*, Soil nailing
12. EN 1997 1, 2005 Eurocode 7 *Geotechnical design - Part 1: General rules*
13. Ferraiolo F., e Giacchetti G., 2004 *Rivestimenti corticali alcune considerazioni sull'applicazione delle reti di protezione in parete rocciosa* – in atti “Bonifica dei versanti rocciosi per la difesa del territorio” – Trento 2004, Peila D. Editor.
14. Flumm D., Ruegger R. 2001 *Slope stabilization with high performance steel wire meshes with nails and anchors*, International Symposium Earth reinforcement, Fukuoka, Japan.
15. Giacchetti G., Cardinali S., Grimod A., 2014 - *Design considerations for meshes used in secured drapery systems* - RocExs 2014 - 5th Interdisciplinary Workshop on Rockfall Protection, Lecco (Italy) 29th - 31st May 2014.
16. Giacchetti G., Grimod A., Cheer D. (2011) - *Soil Nailing with flexible structural facing: design and experiences* - Proceedings of the Second World Landslide Forum – 3-7 October 2011, Rome
17. Giuseppe Dellalana : Appunti di GEOTECNICA
18. Government of the Hong Kong Special Administrative Region (GHKSAR). 2008. *Geoguide 7: Guide to Soil Nail Design and Construction*, Civil Engineering and Development Department, GHKSAR, Hong Kong.

19. IUAV , 2012 - Internal report about the test series according to UNI 11437:2012.
20. Lazarte C.A. (ed.), 2011 - *Proposed Specifications for LRFD Soil-Nailing Design and Construction*, NCHRP REPORT 701, Project 24-21
309-21351-6
Academy of Sciences - Washington, D.C.
-ISSN 0077 -ISBN 978
, Library of Congress Control Number
21. NF P94 270: 2010 *Remblais renforcés et massifs en sol cloué*
22. Phear A., Dew C., Ozsoy B., Wharmby N.J., Judge J., e Barley A.D., 2005 *Soil nailing – Best practice guidance*, CIRIA C637, London, 2005.
23. Ruegger R., e Flumm D., 2000 High performance steel wire mesh for surface *protection in combination with nails and anchors*, Contribution to the 2nd colloquium “Construction in soil and rock” – Accademy of Esslingen (Germany).
24. Schlosser F., (Chairman), 2002 *Additif 2002 aux recommandations clouterre 1991 pour la conception, le calcul, l'exécution et le controle des soustènements realises par cluage des soil*, Presses Ponts et chaussées.
Torres Vila J.A., Torres Vila M.A., e Castro Fresno D., 2000, *Validation de los modelos fisicos de analisis y diseno para el empleo de membranas flexible Tecco G-65 como elemento de soporte superficial en la estabilizacion de taludes*.
25. UNI 11437:2012 (2012) Rockfall protection measures: Tests on meshes for slope coverage.
26. Turner A.K, Schuster R.L. Editors (2012) *Rockfall Characterization and control –* Transportation Research Board, Washington D.C